
ω -Transaminases as Promising Biocatalysts for the Chiral Synthesis of β -Amino Acids

Zur Erlangung des akademischen Grades eines DOKTORS DER
INGENIEURWISSENSCHAFTEN (Dr.-Ing.)

der Fakultät für Chemieingenieurwesen und Verfahrenstechnik
des Karlsruher Instituts für Technologie (KIT)

vorgelegte

Genehmigte
DISSERTATION

von

M. Sc. Oliver Buß
aus Weinheim a. d. Bergstraße

Referent: Prof. Dr. rer. nat. Christoph Syldatk

Korreferent: Prof. Dr. rer. nat. Jürgen Pleiss

Tag der mündlichen Prüfung: 18.10.2018

Preamble

Parts of this dissertation are based on submitted manuscripts for publication or on peer-review research articles.

The publications are based on work carried out between January 2015 and July 2018 for this dissertation. Sections based on publications are marked at the beginning of each section. The text of these sections may be largely identical to the publications, but has been supplemented in parts by further information as well as illustrations.

You may never know what results come of your actions, but if you do nothing, there will be no results. (Mahatma Gandhi)

Abstract

The enzyme family of ω -transaminases (ω -TA) catalyzes a stereoselective transfer of an amino group from an amino donor to an acceptor molecule (with ketone/aldehyde function). ω -TA are of great interest for many pharmaceutical processes and synthesis strategies, as they enable the production of enantiomerically pure amino-drugs.

This thesis, which is part of the Molecular Interaction Engineering (MIE) project funded by the German Federal Ministry of Education and Research, deals with enzyme production and modification using the synthesis of β -amino acids and their degradation by microorganisms as examples. Therefore, the focus of this work was set on the transamination of β -keto acids/esters, the necessary enzyme engineering, as well as the characterization and cataloguing of the ω -transaminase family. The primary goal was to demonstrate the synthesis of the chiral cancer drug component paclitaxel (Taxol), β -phenylalanine(ester), mediated by ω -transaminases.

In summary, the following points could be achieved in this thesis:

- The β -phenylalanine converting *Variovorax paradoxus* ω -TA gene was codon optimized for expression in *E. coli* BL21, purified by fast protein liquid chromatography (FPLC) using Ni-NTA columns and thermostabilized by *in silico* guided site directed mutagenesis.
- The ω -transaminase engineering database (ω TAED) was developed as a helpful starting point for protein engineering and discovery of ω -TA.
- Functional amino acid positions in the *V. paradoxus* ω -TA were mutated and the effects on activity were investigated.
- The protein stability of ω -TA from *V. paradoxus* was improved by targeted mutagenesis (single mutation) while maintaining the enzymatic activity.
- The difficulties in the synthesis of β -phenylalanine (β -PA) by a lipase- ω -TA reaction cascade were demonstrated. Alternative synthesis methods were proposed and at least one established.
- Therefore two ω -TA for the synthesis of (*R*)- and (*S*)- β -phenylalanine ethyl ester were identified by screening an ω -TA library.
- The ω -TA 3FCR_4M showed potential for up-scaling by a factor of 200 for the synthesis of (*S*)- β -phenylalanine ethyl ester (200 mL - 30 mM product concentration).

- The degradation of β -phenylalanine by two bacteria was analyzed in detail under controlled conditions. Additionally for the first time the simultaneous degradation of both enantiomers was shown for one bacterium.

Chapter 1 introduces the importance of α - and β -amino acids and presents the various synthesis processes (chemical and enzymatic). The mode of action of the enzymatic catalyst is also described in detail. In addition, it is discussed how enzymes can be specifically modified by simulation methods in order to modify important properties such as substrate selectivity or protein stability.

This also presupposes that the enzyme family(s) are systematically catalogued and characterized in order to predict and underline properties such as enantioselectivity, substrate selectivity and to adapt reaction conditions. Therefore, a publicly available transaminase database was created which is described in **Chapter 3**. In this chapter, the evolutionary conserved amino acid positions within the two ω -TA families (fold type I and type IV) are shown and their functions are analyzed. It could also be shown that by standardizing the amino acid positions (standard numbering), the properties of certain amino acid positions can be compared and transferred between different ω -TA. As an example, a mutation study conducted at a particular ω -TA can be transferred to a second poorly characterized ω -TA (within the same family). In order to demonstrate the standardization of amino acid positions, data from the literature were compared with each other, with the result that different mutation studies (at different ω -TA) had actually mutated and investigated the same standard amino acid positions. This illustrates the need for standard numbering of amino acid positions within an enzyme family, in particular with regard to ω -TA engineering, since the large and extensive search for engineering sites within the long peptide chain of enzymes is no longer necessary.

Within the ω -TA family of (*S*)-selective enzymes, a relatively large group of β -PA converting transaminases was determined within the database. This group also includes ω -TA from *V. paradoxus* which show high activity towards this substrate. Therefore, **chapter 4** deals with the characterization, enzyme production and the targeted improvement of the protein stability of ω -TA from *V. paradoxus*. This particular ω -TA allows the conversion of β -PA under mild reaction conditions in a buffered aqueous reaction system. This enzyme should be modified for further processing by specific mutations within the protein sequence in such a manner that the protein stability and long-term activity of the enzyme will be increased. This was achieved using the FoldX protein stabilization algorithm and potentially energy-stabilizing mutations were identified and tested. The amino acid changes predicted on this basis were introduced into the gene of ω -TA by mutagenesis PCR. The activities of the resulting ω -TA variants were investigated and the resulting stabilization was analyzed using the protein melting point. The starting point of protein melting was shifted by approx. 4°C for the best variant. This increase

in thermostability allows maintaining the enzymatic activity over a longer period of time. Furthermore, this improvement can be used as a basis for further enzyme mutation experiments, as mutations often lead to a reduction in protein stability.

Based on the systematic analysis of mainly the (*S*) and (*R*)-selective ω -TA family, **Chapter 5** discusses the enzymatic synthesis of β -phenylalanine ethyl ester from the substrate ethyl 3-oxo-phenylpropanoate (β -keto ester) using mutant and natural ω -TA. It was therefore shown for the first time that ω -TA are able to convert this category of aromatic substrate. For this reason, mutation experiments were carried out for the ω -TA from *V. paradoxus*, as it converts the product, β -phenylalanine, with a high turnover rate. The amino acid positions of the ω -TA, which should have an influence on substrate selectivity, were determined and mutated by methods developed in Chapter 3. At all, the wild type enzyme showed no activity towards the β -keto ester substrate. Mainly amino acid residues within the enzyme were altered which should have an influence on the substrate binding, namely: R41, Y76, Y159 and R398. R41, for example, is an important arginine residue that binds the negatively charged carboxyl group of β -phenylalanine via its positive charge. This residue was replaced because the substrate of interest does not have a free carboxyl group, but an ester functionality. However, no activity against ethyl 3-oxo-phenylpropanoate could be detected for most variants. Only the variant R41K-R398K could be regarded as active in qualitative terms, but the activity was too low to allow a quantitative statement about the activity. Since no clearly active variant with a quantifiable turnover was found, an ω -TA library of the Bornscheuer working group (University of Greifswald) was screened. For this purpose, a chromophoric screening test was used which allows a quick selection between non-active and active transaminases. At least two transaminases with activity were detected in this screening, one (*R*)-selective, the other (*S*)-selective. These two transaminases are no longer wild type enzymes, but contain several mutations. The (*R*)-selective enzyme was determined as the transaminase ATA117, which was created for the synthesis of sitagliptin by Savile *et al.*. The (*S*)-selective ω -TA is an enzyme which was engineered by the Bornscheuer research group for the conversion of large aromatic ketones. The (*S*)-selective reaction was used in a preparative approach with an (*S*)-selective enzyme to demonstrate that the detected ω -TA also enables up-scaling. In this context, a preparative purification method using automated column chromatography was also established.

In contrast to the enzyme conversion, however, little is generally known about the degradation of β -amino acids by microorganisms. Therefore, **chapter 6** deals with the characterization of β -PA degradation by β -Proteobacteria *Paraburkholderia* PsJN and BS115. BS115 is a strain isolated from potting soil enriched with soy-peptone. Type strain PsJN, on the other hand, has

originally been isolated from plants and is closely involved with the nitrogen cycle in soil. The aim was to discover new, as yet uncharacterized ω -TA and maybe additional enzymes and to investigate the microbial resolution of the racemate as an alternative to an enzymatic resolution. This degradation process was investigated under controlled conditions in a 2.5L bioreactor and the temporal degradation and biomass formation was investigated. It could be shown that racemic β -PA is degraded stereoselectively by PsJN. During this process, (*S*)- β -PA was completely degraded while the (*R*)-enantiomer was completely retained in the fermentation medium. In contrast, the strain BS115 showed that (*R*)- β -PA was also degraded at a late stage of fermentation. However, it could be ruled out that the degradation process of (*R*)- β -PA took place via a ω -TA, so presumably the activity of an additional enzyme has been detected. The results showed that genome sequencing of the BS115 strain is probably required to more accurately characterize the monitored (*R*)- β -phenylalanine degradation.

Zusammenfassung

Diese Arbeit erörtert die Enzyme-Familie der ω -Transaminasen (ω -TA), die eine stereoselektive Übertragung einer Stickstoffgruppe von einem Amino-Donor auf ein Akzeptor-Molekül (mit Keton/Aldehyd-Funktion) katalysieren. ω -Transaminasen sind von großem Interesse für viele pharmazeutische Prozesse und Synthese-Strategien, da selbige es ermöglichen, stickstoffhaltige Wirkstoffe enantiomerenrein zu produzieren.

Die Dissertation, angefertigt im Rahmen des vom Bundesministerium für Bildung und Forschung geförderten Projektes *Molecular Interaction Engineering* (MIE), beschäftigte sich hierbei mit der Enzymherstellung und Modifikation am Beispiel der Synthese von β -Aminosäuren sowie dem Abbau selbiger durch Mikroorganismen. Im Fokus dieser Arbeit stand daher die Transaminierung von β -Ketosäuren/estern, das dafür notwendige Enzym Engineering, sowie die Charakterisierung und Katalogisierung der ω -Transaminase-Familie. Das primäre Ziel war hierbei die Synthese des chiralen Paclitaxel-Bestandteils, β -Phenylalanine(ester), durch ω -Transaminasen demonstrieren.

Zusammenfassend konnten in dieser Thesis folgende Punkte erreicht werden:

- Die Proteinproduktion und Reinigung der ω -TA aus *Variovorax paradoxus* konnte durch Codon-Optimierung sowie *Fast protein liquid chromatography* (FPLC) mittels Ni-NTA-Säulen verbessert werden und die Langzeitstabilität konnte erhöht werden
- Außerdem konnte eine ω -Transaminase-Engineering-Datenbank (ω TAED) als hilfreiche Basis für das Transaminase-Engineering etabliert werden
- Funktionelle Aminosäurepositionen in der *V. paradoxus* ω -TA wurden mutiert und die Auswirkungen auf die Aktivität untersucht
- Durch gezielte Mutagenese konnte die Proteinstabilität der ω -TA aus *V. paradoxus* unter gleichzeitigem Erhalt der Aktivität verbessert werden.
- Es konnten die Schwierigkeiten bei der Synthese von β -Phenylalanin (β -PA) durch eine Lipase- ω -TA Kaskadenreaktion erörtert und gezeigt werden. Hierbei wurden alternative Syntheseweg vorgeschlagen und analysiert
- Es wurden zwei ω -TA für die Synthese von (*R*)- sowie (*S*)- β -PA-Ethylester identifiziert durch Screening einer ω -TA Bibliothek
- Eine ω -TA (namentlich 3FCR_4M) zeigte Potenzial für eine Maßstabsvergrößerung um den Faktor 200 für die Synthese des (*S*)- β -PA-Ethylester (200 mL - 30 mM Produktkonzentration).

- Der Abbau von β -PA durch zwei Bakterien konnte unter kontrollierten Bedingungen genauer analysiert werden. Dabei wurde erstmals der simultane Abbau beider Enantiomere einer β -Aminosäure durch ein Bakterium gezeigt, wobei neben der Transaminierung noch ein weiterer, bislang unbekannter Abbaumechanismus erfolgt.

Kapitel 1 führt in die Bedeutung von α - sowie β -Aminosäuren ein und stellt die verschiedenen Syntheseverfahren (chemisch u. enzymatisch) vor. Es wird zudem die Wirkungsweise des enzymatischen Katalysators im Detail beschrieben. Außerdem wird darauf eingegangen, wie durch Simulationsverfahren Enzyme gezielt modifiziert werden können, um wichtige Eigenschaften wie Substratspezifität oder Proteinstabilität modifizieren zu können.

Dies setzt aber auch voraus, dass die Enzyme-Familie(n) systematisch katalogisiert und charakterisiert sind um Eigenschaften wie Enantioselektivität, Substratspezifität und Reaktionsbedingungen eingrenzen und vorhersagen zu können. Daher wurde in **Kapitel 3** eine öffentlich verfügbare Transaminase Datenbank erstellt und beschrieben. In dieser Thesis konnten evolutiv konservierte Aminosäurepositionen innerhalb der zwei ω -TA-Familien (Fold type I und type IV) aufgezeigt und deren Funktion analysiert werden. Dabei konnte auch gezeigt werden, dass durch Standardisierung der Aminosäurepositionen die Eigenschaften bestimmter Aminosäurepositionen zwischen verschiedenen ω -TA verglichen und übertragen werden können. Beispielsweise kann eine Mutationsstudie, durchgeführt an einer bestimmten ω -TA, auf eine zweite noch wenig charakterisierte ω -TA (innerhalb der Familie) übertragen werden. Zur Demonstration der Standardisierung von Aminosäurepositionen wurden hierfür Daten aus der Literatur untereinander verglichen, mit dem Ergebnis, dass verschiedene Mutationsstudien (an verschiedenen ω -TA) im Endeffekt die gleichen Standard Aminosäurepositionen mutiert und untersucht hatten. Dies verdeutlicht die Notwendigkeit einer einheitlichen Nummerierung der Aminosäurepositionen innerhalb einer Enzymfamilie, insbesondere im Hinblick auf ω -Transaminase-Engineering, da die große und umfangreiche Suche nach *Engineering*-Stellen innerhalb der langen Peptidkette der Enzyme entfällt.

Innerhalb der ω -TA Familie der (*S*)-selektiven Enzyme, wurde so auch eine relativ große Gruppe an β -PA umsetzenden Transaminasen bestimmt. Zu dieser Gruppe gehört unter anderem auch die ω -TA aus *V. paradoxus*, die hohe Aktivitäten gegenüber diesem Substrat aufzeigt. Daher beschäftigt sich **Kapitel 4** mit der Charakterisierung, der Enzymherstellung und der gezielten Verbesserung der Proteinstabilität der ω -Transaminase aus dem Mikroorganismus

V. paradoxus. Diese besondere ω -TA erlaubt die Umsetzung von β -PA unter milden Reaktionsbedingungen in einem gepufferten wässrigen Reaktionssystem. Dieses Enzym sollte für das weitere Vorgehen durch gezielte Mutationen innerhalb der Proteinsequenz so modifiziert werden, dass die Proteinstabilität und Langzeitaktivität des Enzyms verbessert werden sollte. Hierfür wurde der Proteinstabilisierungs-Algorithmus FoldX angewandt und potentiell energiestabilisierende Mutationen hervorgesagt und getestet. Die auf dieser Basis vorhergesagten Aminosäureveränderungen wurden durch Mutagenese-PCR in das Gen der ω -TA eingeführt. Die erhaltenen ω -TA Varianten wurden auf ihre Aktivität hin untersucht und die erhaltene Stabilisierung anhand von Proteinschmelzkurven analysiert. Hierbei zeigte sich, dass der Startpunkt der Proteinfaltung, dem Schmelzen, um ca. 4°C verschoben werden konnte. Diese Erhöhung der Thermostabilität erlaubt, über einen längeren Zeitraum die Aktivität des Enzyms in der Reaktionslösung zu erhalten. Des Weiteren kann diese Verbesserung als Grundlage für weitere Enzym-Mutationsexperimente verwendet werden, da oftmals Mutationen zu einer Absenkung der Proteinstabilität führen.

Auf Grundlage der systematischen Analyse der (*S*)-selektiven ω -TA Familie, behandelt **Kapitel 5** die enzymatische Synthese von β -Phenylalaninethylester aus dem Substrat Ethyl-3-oxo-phenylpropanoat (β -Ketoester) mit Hilfe von mutierten und natürlichen ω -Transaminasen. Es wurde erstmalig gezeigt, dass ω -TA in der Lage sind diese aromatische Substratkategorie umzusetzen. Bis zu diesem Zeitpunkt waren andere Transaminasen mit Aktivität gegenüber dem nicht chiralen β -Ketoester nicht bekannt. Es wurden daher zunächst Mutationsexperimente an der ω -Transaminase aus *V. paradoxus* durchgeführt, da selbige das Produkt mit hoher Aktivität umsetzt. Die Aminosäurepositionen der ω -TA, welche einen Einfluss auf die Substratselektivität haben sollten, wurden durch in die Kapitel 3 erarbeiteten Methoden bestimmt und mutiert. Das ursprüngliche Enzym zeigte hierbei keine Aktivität gegenüber dem β -Ketoester. Es wurden vor allem Aminosäure-Reste innerhalb des Enzyms verändert die einen Einfluss auf die Substratbindung haben sollten, namentlich: R41, Y76, Y159 sowie R398. R41 ist beispielsweise ein wichtiger Arginin-Rest der über seine positive Ladung die Bindung der negativ geladenen Carboxylgruppe des β -PA ermöglicht. Dieser Rest wurde ausgetauscht, da das Substrat keine freie Carboxylgruppe besitzt, sondern eine ungeladene Ester-Funktionalität. Es konnte jedoch für keine Variante eine Aktivität gegenüber Ethyl 3-oxo-phenylpropanoat nachgewiesen werden. Lediglich die Variante R41K-R398K konnte qualitativ als aktiv betrachtet werden, jedoch war die Aktivität zu gering um eine quantitative Aussage über die Aktivität treffen zu können. Da keine eindeutig aktive Variante gefunden wurde, die einen quantifizierbaren Umsatz aufwies, wurde eine ω -Transaminase

Bibliothek der Arbeitsgruppe Bornscheuer (Universität Greifswald) in einem Screening untersucht. Hierfür wurde ein farbgebender Screening-Test verwendet, der eine schnelle Selektion zwischen nicht aktiven und aktiven Transaminasen erlaubt. Es konnten in diesem Screening zwei Transaminasen mit Aktivität gefunden werden, eine (*R*)-selektiv, die andere (*S*)-selektiv. Beide Transaminasen sind keine natürlichen Enzyme mehr, sondern enthalten mehrere Mutationen. Das (*R*)-selektive Enzym war hierbei die Transaminase ATA117, die für die Synthese von Sitagliptin von Savile *et al.* mutiert worden war. Die (*S*)-selektive TA ist ein Enzym, welches von der Forschungsgruppe Bornscheuer mutiert worden war für den Umsatz von großen aromatischen Ketonen. Die (*S*)-selektive Reaktion wurde in einem präparativen Ansatz mit einer (*S*)-selektive TA gezeigt, um das Potential der ω -TA für ein *Up-scaling* zu untersuchen. In diesem Zusammenhang wurde auch eine präparative Reinigungsmethode mittels automatisier Säulenchromatographie etabliert.

Im Gegensatz zur enzymatischen Umsetzung ist jedoch wenig über den Abbau von β -Aminosäuren durch Mikroorganismen im Allgemeinen bekannt. Daher beschäftigt sich **Kapitel 6** mit der Charakterisierung des β -Phenylalanin Abbaus durch die β -Proteobakterien *Paraburkholderia* PsJN und BS115. BS115 ist ein Isolat, welches in Vorarbeiten aus Blumenerde isoliert wurde, die mit Sojapepton angereichert wurde. Der gut untersuchte Typenstamm PsJN dagegen wurde ursprünglich von Pflanzen isoliert und ist eng in den Stickstoffkreislauf im Boden involviert. Ziel war es zum einen, neue, noch nicht charakterisierte ω -TA sowie möglicherweise weitere Enzyme zu entdecken, zum anderen die mikrobielle Resolution des Racemats als eine Alternative zu einer enzymatischen Resolution zu untersuchen. Dieser Abbauprozess wurde unter kontrollierten Bedingungen in einem 2.5 L Bioreaktor untersucht und der zeitliche Abbau, sowie die Biomassebildung untersucht. Es konnte gezeigt werden, dass racemisches β -PA stereoselektiv durch PsJN abgebaut wird. Hierbei wurde vollständig (*S*)- β -PA abgebaut und das (*R*)-Enantiomer blieb hingegen vollständig im Fermentationsmedium erhalten. Der Stamm BS115 dagegen zeigte, dass zu einem späten Zeitpunkt der Fermentation auch (*R*)- β -Phenylalanin abgebaut wurde. Es konnte jedoch ausgeschlossen werden, dass der Abbauprozess des (*R*)- β -Phenylalanin über eine ω -TA erfolgte; folglich wurde hier die Aktivität eines bislang nicht beschriebenen Enzyms entdeckt. Die Ergebnisse zeigten, dass wahrscheinlich eine Genom-Sequenzierung des Stamms BS115 erforderlich ist, um den beobachteten (*R*)- β -PA Abbau genauer charakterisieren zu können.

Danksagung

Ich möchte allen Menschen danken, die zum Gelingen dieser Doktorarbeit beigetragen haben.

Im Besonderen danke ich Christoph Syldatk für die Möglichkeit am KIT meine Doktorarbeit machen zu dürfen und für die wissenschaftliche Förderung von Kooperationen mit den Universitäten Greifswald und Stuttgart, sowie der Technischen Universität Darmstadt.

Jens Rudat danke ich für die gute Betreuung, Diskussionen, Beratung, für die Konzeption des spannenden Forschungsthemas, sowie für die Förderung meiner Dissertation und Publikationen.

Kersten S. Rabe danke ich, der mit seinen Ideen einen Anstoß lieferte für Experimente und die Erstellung einer Publikation, sowie für die guten Diskussionen die ich mit ihm am Campus Nord * führen durfte.

Katrin Ochsenreither danke ich für ihr großes Interesse an der Fragestellung meiner Doktorarbeit, sowie für ihren Input, insbesondere für die wissenschaftliche Exkursion in die Welt der Bioinformatik.

Sven Jager danke ich für die zahlreichen Simulationen, sowie intensiven Diskussionen die zum Gelingen von mindestens zwei Publikationen beitrugen.

Jürgen Pleiss, sowie Uwe Bornscheuer danke ich für die Ermöglichung von Kooperationen über Karlsruhe hinaus, die ein Anstoß für die Erschließung von neuen wissenschaftlichen Themengebieten waren.

Moritz Voß danke ich für die gute Zusammenarbeit in Greifswald die zum Gelingen einer Publikation beigetragen hat.

Matthias Franzreb und Elisabeth Schmalbach danke ich für die gute Kooperation zur Erstellung von 3D gedruckten Enzym-Reaktoren.

Außerdem danke ich der Evonik-Stiftung, sowie der Evonik Industries AG, die mich im Rahmen des Evonik-Perspectives Programm förderte und mir Einblicke in die Welt der chemischen Industrie ermöglichte.

Ich danke auch dem BMBF für die Förderung dieser Arbeit im Rahmen des Projekts *Molekular Interaction Engineering*. In diesem Zusammenhang danke ich auch Iris Perner-Nochta und

Jürgen Hubbuch für die Organisation zahlreicher Treffen, Exkursionen, sowie einer internationalen Konferenz.

Meinen Kollegen danke ich für den guten Zusammenhalt, die angenehme Arbeitsatmosphäre sowie die große Hilfestellung bei Problemen des Laboralltags, sowie für die zahlreichen Diskussionen die einen Beitrag zum Gelingen dieser Arbeit beitrugen.

Daher danke ich Laura Krämer für die permanente und zeitintensive Instandsetzung der HPLC-Anlagen, wenn mal wieder kein Druck, ein Überdruck oder alles rot geleuchtet hat. Sowie Pascal Gorenflo, der für den enormen Nachschub an Lösungsmitteln sorgte, vor chemischen Experimenten im Labor nicht zurück schreckte und sich wagemutig in den Ring warf um die GC-Anlage in Betrieb zu halten. Ich wünsche ihm viel Erfolg bei seiner zoologischen Grundlagenforschung (*Mantis* sp.). Besonders möchte ich Delphine Muller danken für die unermüdliche Arbeit und Unterstützung im Bereich der Proteinaufarbeitung, sowie den zahlreichen Kämpfen mit den Flusschromatographie Systemen, die leider nicht immer das machten was wir wollten. Mein Dank gilt außerdem: Michaela Zwick für alle Beratungen die sich um die Fragestellung der Fermentation drehten; Werner Mandel der die Analytik überwachte; Anke Neumann die immer noch im Finanzhaushalt etwas Geld für HiWis fand; Susanne Warth und Beate Skolik die immer halfen wenn mal wieder administrative Fragestellungen aufkamen und Ulrike Engel für den Anstoß von zahlreichen kritischen Diskussionen; sowie Sandra Baumann für ihren großen Schatz an Erfahrungen.

I thank Habibu for nice discussions and conversations. I would also like to thank all doctoral students or those who have already completed their doctorates for the good time at TeBi, even if movements or equipment failures once again greatly simplified life: Christin&Sarah™, Janina▲, Johannes▲, Jens☺, Judit☺, André ☺, Fei,Stefán †, Florian☺, Caro♦, Vanessa, Julia, Sascha, Olga, Alba ☼ ☿ ☿, Aline, Teresa ✈, Rebecca🐎 und Marcus †.

Ganz besonderem Dank gilt in diesem Zusammenhang Sascha, Jens und Stefan die sich mit meinen Laborproblemen oft konfrontiert sehen „durften“ und mir gerne Input, sowie Aufmunterung zu Teil werden ließen.

Außerdem den zahlreichen Studenten, die sowohl am TeBi als auch in meinem Labor arbeiten durften/mussten: Fabian der nicht nur als Bachelorand, sondern auch als HiWi für mich arbeiten durfte: Anna, Asta, Steffi, Jessica Tien, Lara, Anika, Christina, Robin. Außerdem Nora die neue

Danksagung

Enzymreaktoren testen durfte und Peter, der feststellen musste, dass Disulfid-Brücken nicht das halten was sie versprechen.

Ich möchte auch meinen Freunden danken, die mich während meiner Promotion unterstützt haben: Tobias (alias King), Stefan (alias Dör), Max, Ralf, Sven&Caro, (die Kädings) und Michael. Einen ganz besonderen lieben Dank geht an dich Teresa ♥, dass du immer für mich da warst während der Promotion. Sowie meinen Eltern, die mich während meiner Promotion stets unterstützt und ermutigt haben. Außerdem der Familie Körber für viele ermutigende Worte.

Last but not least, möchte ich HPLC-2 danken, die als eine der dienstältesten Chromatographie Anlagen den größten Durchhaltewillen von allen zeigte. Dagegen danke ich HPLC 6 explizit nicht.

Publications

This thesis is based on four original research publications and one review article published in peer-reviewed scientific journals. All publications have been adapted, shortened or supplemented. The author contributions are stated at each publication based chapter and at the end of thesis. Furthermore references of each part are presented at the end of the particular chapter.

Publications which are part of this thesis:

The ω -Transaminase Engineering Database (ω TAED): a navigation tool in protein sequence and structure space

- Database and Engineering tool developed in cooperation with University Stuttgart- AG Prof. Pleiss (Bioinformatics) published in PROTEINS. DOI: 10.1002/prot.25477 – **Chapter 3**

FoldX as protein engineering tool: Better than random based approaches?

- Review about the protein stability engineering *in silico* tool FoldX – published in Computational and Structural Biotechnology Journal DOI: doi.org/10.1016/j.csbj.2018.01.00 – **Chapter 4**

Improvement of the thermostability of a β -amino acid converting ω -transaminase using FoldX

- Thermostabilization of transaminases in cooperation with Kersten S. Rabe (IFG-KIT)– published in ChemBioChem DOI: 10.1002/cbic.201700467 – **Chapter 4**

β -Phenylalanine ester Synthesis from Stable β -Keto Ester Substrate using Engineered ω -Transaminases

- ω -Transaminase Screening und synthesis of β -phenylalanine ester in cooperation with University Greifswald AG Prof. Bornscheuer- MDPI-Molecules – DOI: 10.3390/molecules23051211 – **Chapter 5**

Microbial Chiral Resolution of Racemic β -Phenylalanine: Fermentation of *Paraburkholderia* sp. elucidates the Participation of Two Different Enzymes

- Fermentational microbial resolution of racemic β -phenylalanine - AMB-Express DOI: 10.1186/s13568-018-0676-2– **Chapter 6**

Publications which are not part of this thesis:

Statistical Evaluation of HTS Assays for Enzymatic Hydrolysis of β -Keto Esters

- Statistical analysis and development of high-throughput hydrolase tests using β -keto acid esters as an example – in cooperation with Technische Universität Darmstadt – AG Prof. Hamacher and AG Prof. Schmitz published in PLoS ONE DOI: 10.1371/journal.pone.0146104

Neue *in silico* Methoden für die Etablierung einer Grünen Chemie

- Mini-Review published in Biospektrum (german) – DOI: 10.1007/s12268-018-0892-y

Conference talk:

O. Buß, Jens Rudat (2016) **ASYMMETRIC β -AMINO ACID SYNTHESIS WITH AN ENGINEERED ω -AMINOTRANSFERASE** – International Conference on Molecular Interaction Engineering , 15-16 June 2016, Karlsruhe, Germany.

Poster presentations:

O. Buß, S. Jager, K. Rabe and J. Rudat (2016) **ASYMMETRIC β -AMINO ACID SYNTHESIS WITH AN ENGINEERED ω -AMINOTRANSFERASE** – International Conference on Molecular Interaction Engineering , 15-16 June 2016, Karlsruhe, Germany.

O. Buß, S. Jager, K., C. Sylдатk, K. Rabe and J. Rudat (2016) **ENGINEERING an ω -AMINOTRANSFERASE TOWARDS THE SYNTHESIS OF β -AMINO ACID** - 8th International Congress on Biocatalysis, 28-1. September 2016, Hamburg, Germany

O. Buß, S.Jager, C. Sylдатk, J. Pleiss, K. Rabe and J. Rudat (2017) **IMPROVMENT OF AN ω -TRANSAMINASE TOWARDS SMARTER SYNTHESIS OF β -AMINO ACID(S) BY ENZYME ENGINEERING** - 13th International Symposium on Biocatalysis and Biotransformations, 9-13 July 2017, Budapest, Hungary

Buß O, Rudat J (2015) **β -AMINO ACID PRODUCTION BY A LIPASE/TRANSAMINASE ENZYME CASCADE_1 – SCREENING THE BEST FITTING LIPASE** - Proceedings of the Annual Conference of the Association for General and Applied Microbiology (VAAM), March 13th – 18th, Jena, Germany, ISSN 0947-0867

O. Buß, K. S. Rabe, J. Rudat (2017) **β -AMINO ACID PRODUCTION BY A HYDROLASE/TRANSAMINASE ENZYME CASCADE: INCREASING THE STABILITY OF A β -TRANSAMINASE BY DIRECTED EVOLUTION** -5th Joint Conference of the DGHM & VAAM 2017, 05.-08. March 05th – 08th, Würzburg, Germany

J. Rudat, O. Buß, S.M.-Dold, D. Litty (2018) - **β -AMINO ACID DEGRADATION BY A NEWLY ISOLATED PARABURKHOLDERIA STRAIN CLEARLY DIFFERS FROM TYPE STRAIN PSJN** - Proceedings of the **Annual** - Conference of the Association for General and Applied Microbiology (VAAM), April 15 – 18, Wolfsburg, Germany, ISSN 0947-0867

Table of contents

<u>PREAMBLE</u>	<u>I</u>
<u>ABSTRACT</u>	<u>III</u>
<u>ZUSAMMENFASSUNG.....</u>	<u>VIII</u>
<u>DANKSAGUNG</u>	<u>XII</u>
<u>PUBLICATIONS.....</u>	<u>XV</u>
<u>INTRODUCTION.....</u>	<u>1</u>
1.1) Amino acids as important chemicals and building blocks.....	2
1.1.2) Role of β amino acids as compounds active agents and as part of compounds	3
1.2) Enzymatic and chemical strategies for the synthesis of β-amino acids	8
1.3) Mechanism, function and applications of ω-Transaminases	15
1.3.2) Transaminase mechanism	18
1.3.3) Industrial applications of ω -transaminases	22
1.4) Protein engineering	33
1.4.1) The challenge of function prediction	34
1.4.1) Thermostabilization using <i>in silico</i> tools	37
1.4.2) Outlook of enzyme engineering	43
1.5) References chapter 1	44
<u>2) RESEARCH PROPOSAL.....</u>	<u>51</u>
References chapter 2	52
<u>3) ANALYSIS AND CREATION OF A SYSTEMATIC ω-TA DATABASE (ωTAED)</u>	<u>53</u>
3.1) Introduction.....	55
3.1.1) Definition and function of transaminases	55
3.2) Methods.....	59
3.3) Results	62
3.3.1) The ω -Transaminase Engineering Database (ω TAED)	62

3.3.2) Fold type I sequence analysis	66
3.3.3) Fold type IV – sequence analysis	70
3.3.4) Selectivity- and specificity-determining positions	74
3.4) Discussion.....	80
3.4.1) Understanding the substrate specificity of ω -TA	86
3.4.2) Thermostability of ω -TA	87
3.5) Conclusion.....	88
3.6) References Chapter 3.....	90
<u>4) THERMOSTABILITY ENGINEERING OF THE <i>V. PARADOXUS</i> ω-TA.....</u>	<u>97</u>
4.1) FoldX as protein stability engineering tool.....	98
4.1.1) Relevance of thermostability of proteins	99
4.1.2) Techniques for thermostabilization	100
4.1.3) Computational approaches for stability engineering	101
4.1.4) Un/folding energy algorithms	102
4.1.5) Accuracy of FoldX	112
4.1.6) The next generation of FoldX based predictions	116
4.1.7) Conclusion	117
4.2) Thermostabilization of the <i>V. paradoxus</i> ω-TA using FoldX.....	118
4.2.1) Introduction on the thermostabilization of ω -transaminases	119
4.2.3) Methods and Materials	121
4.2.5) Results and Discussion	130
4.2.6) Disulfide bond engineering	146
4.4) Conclusion.....	153
4.5) References chapter 4.....	155
<u>5) TOWARDS BIOCATALYTIC β-KETO ESTER TRANSAMINATION APPROACHES...</u>	<u>162</u>
5.1) Substrate profile engineering of <i>V. paradoxus</i> ω-TA.....	163
5.1.1) Alternative synthesis route to the lipase- ω -TA cascade reaction for the production of chiral β -PA	164
5.1.2) Engineering <i>Variovorax paradoxus</i> ω -TA	168
5.1.3) Materials and Methods	169
5.1.3) Results and Discussion	172
5.1.4) Conclusion	191
5.2) Screening of an ω-TA library towards β-keto ester converting enzymes.	192

Table of contents

5.2.1) Introduction	194
5.2.2) Material and Methods	196
5.2.3) Results and discussion	200
5.2.3.1) Screening of ω -TA library	200
5.2.3.2) Asymmetric synthesis of β -PAEE	201
5.2.4) Outlook and conclusion	209
5.3) Conclusion chapter 5	210
5.4) References Chapter 5	211
<u>6) DEGRADATION AND DERACEMIZATION OF β-PA USING DIFFERENT PARABURKHOLDERIA SPECIES.</u>	<u>214</u>
6.1) Introduction	216
6.2) Materials and methods	219
6.3) Results	223
6.3.1) Fermentation of <i>Paraburkholderia</i>	223
6.3.2) ω -TA activity test	227
6.4) Discussion	228
6.4.1) Degradation of (<i>S</i>)- β -PA by BS115 and PsJN	228
6.5) Conclusion	233
6.6) References Chapter 6	234
<u>7) CONCLUDING REMARKS</u>	<u>237</u>
7.1) Reaction conditions	238
7.2) Outlook	239
7.3) References Chapter 7	239
<u>ABBREVIATIONS AND SYMBOLS</u>	<u>240</u>
<u>LIST OF ALL REFERENCES</u>	<u>242</u>
<u>APPENDICES</u>	<u>258</u>
Chapter 4)	259
Chapter 5)	264
Chapter 6)	271

KEYWORD INDEX..... 274

Introduction

The following parts reflect the technical background with regard to the experimental section of this thesis. The aim of this thesis is the systematic analysis of the function of ω -TA as well as enzyme engineering under the objective of the synthesis of β -amino acids. In subsection **1.1.** the target molecules of this thesis are introduced, with focus on β -phenylalanine. In **1.2.**, ω -TA and reaction mechanism as well as applications are introduced **1.3** focuses on synthesis strategies to produce chiral β -amino acids. Therefore, chemical as well as enzymatic synthesis approaches are presented. In subsection **1.4** an introduction in protein engineering with focus on protein stability is given.

1.1) Amino acids as important chemicals and building blocks

Beside the (de)oxyribo-nucleic acids as molecules for saving information and as blue script for building biological systems, amino acids are the most important biofunctional carbon compounds on earth. The life we know is inconceivable without amino acids: Even the simplest biological systems need amino acids to build functional proteins. Furthermore amino acids are even found in extraterrestrial matter (e.g. meteoritic dust/rocks) and it is possible that meteors delivered these molecules to the earth [1,2]. This proves that amino acids can be found everywhere and have played a role since the beginning of the earth.

The importance of amino acids is visualized by the high demand for amino acids by world economy. The scale ranges at millions of tons, particular for food and feed industry, but also for precursors for the production of pharmaceuticals like antibiotics, sweeteners, peptide-drugs, polymers but also as agrochemicals [3–5]. The dominant group with the largest focus is L- α -amino acids. As building blocks for proteins, these molecules are omnipresent in nature, but some (micro)organisms need external L- α -amino acids, which cannot be produced by their own metabolism. These amino acids are known as essential amino acids and therefore a multibillion \$ market exists. One of the most prominent examples for chemically produced amino acids is methionine (as a racemate), which is fed in large scale to chickens to reduce the necessary amounts of feed [6]. Methionine is produced on a scale of 0.85 million tons per a [7]. As a side effect, it might be even beneficial for the immune response of chickens [8].

Beside methionine, the most prominent proteinogenic L- α -amino acids are L-threonine, L-lysine and L-tryptophan for feed industry. Moreover L-glutamate is an important flavor enhancer. These amino acids are mainly produced by fermentation processes with sugar as carbon source [8]. However, α -amino acids are not only used in the food and feed industry. L-Arginine, for example, shows manifold effects from improvement of wound healing, support of muscle growth to increased release of hormones. [9]. Although chemical synthesis routes like the Strecker-synthesis are known since 1850, later developed enzymatic and microbial processes became important for chiral processes [10]. The world-wide market for amino acids is 8 billion \$ and the two bestselling amino acids are L-glutamate/L-lysine with 3.3 and 2.2 million tons per year (Table 1). This underpins the importance of fermentative and enzymatic methods towards the world economy. The most prominent example for bioprocesses is the L-glutamate production using *Corynebacterium glutamicum* [7].

Table 1 Overview of world production of L- α -amino acids on the basis of fermentation or enzyme processes according to Sanchez *et al.*[7].

	market [\$]	volume [thousand tons]	Scale [thousand tons]	Fermentation titer [g/L]
L -glutamate	1.5 billion		3300	150
L -lysine-HCl	1.5 billion		2200	170
L -threonine	0.270 billion		30	132
L -arginine	0.150 billion		1.5	96
L -tryptophan	0.150 billion		14.0	60
L -tyrosine	0.05 billion		0.200	55
L -phenylalanine	1.0 billion		30	57

However, also non- α -amino acids gained attention as important building blocks for pharmaceuticals, artificial and protease resistant peptides and as antibiotics. The research and development is also focused on these special amino acids as well as important amines, which are synthesized using enzymes or microorganisms.

1.1.2) Role of β -amino acids as compounds active agents and as part of compounds

One of these special group of amino acids are β -amino acids, which are part of functional biomolecules. They are labeled with “ β ”, because the amine group is positioned at the second carbon atom from the carboxylic group within the molecule (see also **Figure 1.1**). A general introduction to the naming and description of β -amino acids was given by Seebach *et al.*, Juaristi *et al.* and Dold *et al.* [11–13]. These special amino acids can be utilized as single compounds for the design of bioactive ligands and other biomaterials. A particularly important example are antifungal β -amino acids, which are inhibiting the protein synthesis and cell growth e.g. of the yeast *Candida albicans* [14]. Further examples for bioactive β -amino derivatives are cispentacin (**10**), BAY 10-8888 (**12**), tilidin (**3**), oxetin (**11**), icofugipen (**1**) and oryzoxylicin (**6**). They are acting as antifungal, antibacterial or as analgetic compounds [15]. Furthermore the β -amino acid-azanindoles show potential as inhibitor against influenza polymerase (**4**) [16]. This molecule class has a promising function for the treatment of both seasonal and pandemic influenza. In addition, the β -amino acid ester-phosphodiamide compound is known as antiviral drug and acts as inhibitor for the reverse transcriptase of HI-virus (**12**)[17]. It can be concluded

that β -amino acids have great potential as active ingredients parts in respect to improved protease resistance and properties compared to α -amino acid containing active ingredients. Moreover, β -amino acids can be utilized for the production of self-assembling nanomaterials and for bioactive β -peptides [18].

β -peptides as promising drugs

Artificial β -amino-acid containing peptides form more stable secondary structures than known for proteinogenic amino acids [11]. Furthermore, single β -amino acids can protect peptides towards degradation by proteases, because evolution adapted proteases for peptides and proteins consisting of standard L- α -amino acids. Small protein-like chains, which are composed of β -amino acids, are also called peptidomimetics, because they mimic the shape and function of natural peptides. For example antimicrobial peptides must be protected against protease degradation, otherwise they will be decomposed in biological systems very fast. Therefore cyclic β -amino acids or β -amino acids as peptide building blocks are able for efficient protease protection [15].

One example for peptidomimetics is a derivative of morphiceptin (**8**) which contains β^2 and β^3 amino acids and acts as opioid drug [19]. These β^2 and β^3 peptidomimetics act as antinociceptive and antidiarrheal drugs and lower the sensation of pain [19]. As oligopeptide-modified poly(β -amino acid ester)s they can be utilized as inductors for osteogenesis to reprogram dental pluripotent-cells to stem cell like statesⁱⁱ [20]. In addition peptides of β/γ -amino acids show antimicrobial effects, especially against the pathogenic bacteria *Pseudomonas aeruginosa* and *Staphylococcus aureus* [21]. Another example is the β -PA containing pseudopeptide andrimid (**13**), which acts as inhibitor of the bacterial fatty acid biosynthesis. More precisely andrimid inhibits the bacterial acetyl-CoA carboxylase [22]. This biomolecule was originally isolated from the plant hopper *Nilaparvata lugens* [23].

β -amino acids as functional building blocks

Furthermore cyclic β -amino acids are important precursors of β -lactam antibiotics (**2**) (Scheme 1). Cyclic peptides which are containing β -amino acids are able to act as antiproliferative and cytotoxic agents, like known for jasplakinolid from the marine sponge *Jaspis johnstoni* (**5**) [24]. β -amino acids can be utilized for the production of biodegradable polymers, suitable as drug

ⁱ β^3 means the amino acid residue is next to the amino group within a peptide. Conversely, β^2 means that the amino acid residue is directly adjacent to the carboxyl group [11].

ⁱⁱ The authors refer to β -amino acid esters which have been extended with a peptide terminus as oligopeptide-modified poly (β -amino acid ester)s.

delivery systems e.g. as complex former for polynucleotide drugs [25]. Those drugs can be applied as intracellular delivery system for treatment of brain cancer [26]. Beside peptides and polymers, β -amino compounds exist also in lipopeptides like described for YM-170320, topostatin and fusaristatin [27–29]. For example YM-170320 (**7**) acts as antimicrobial substances by inhibiting the ergosterol biosynthesis in fungi [27,30]. Furthermore, the two very similar substances, **12** and **10**, also act as fungicides by inhibiting the protein synthesis [31].

β -Phenylalanine as building block of the anti-cancer drug paclitaxel

The most prominent example of β -amino acid containing biomolecule is the complex natural compound Paclitaxel with thirteen stereo centers (PT, **14**). This diterpenoid agent was discovered in *Taxus* plants (yew trees), especially in the pacific *Taxus brevifolia* and acts as medical substance against ovarian cancer. The demand on PT is currently increasing due to the expanding application possibilities. Over the years PT was tested for different kinds of cancer, e.g. brain tumor types and it was considered as one of the most important anticancer drug with a market volume of over 1 billion \$ per year [32,33]. Moreover, also further applications like treatment of heart restenosis are conceivable. PT can be used in stents to avoid restenosis, which increased the interests in PT further [34,35]. Beside the original natural compound some derivatives are found or created like Docetaxel [32]. A disadvantage of PT is the marginal availability of the complex natural compound. Only 0.01 to 0.04 % dry weight are accumulated in a yew tree, mainly in the bark [32]. To overcome these limitations, alternatives are investigated and applied like transgenic plant cell lines of *Taxus sp.* [36]. Precursor molecules can also be isolated from the *Taxus baccata* (European yew), *Taxus wallchiana* (Himalaya yew) and from the needles of the *Taxus brevifolia*. These complex natural product precursors are 10-decetylbaaccatin III and docetaxel [32,37–39]. Despite the importance of the synthesis of larger amounts of PT, some enzyme conversion steps in metabolic pathways are still unknown or uncharacterized [35].

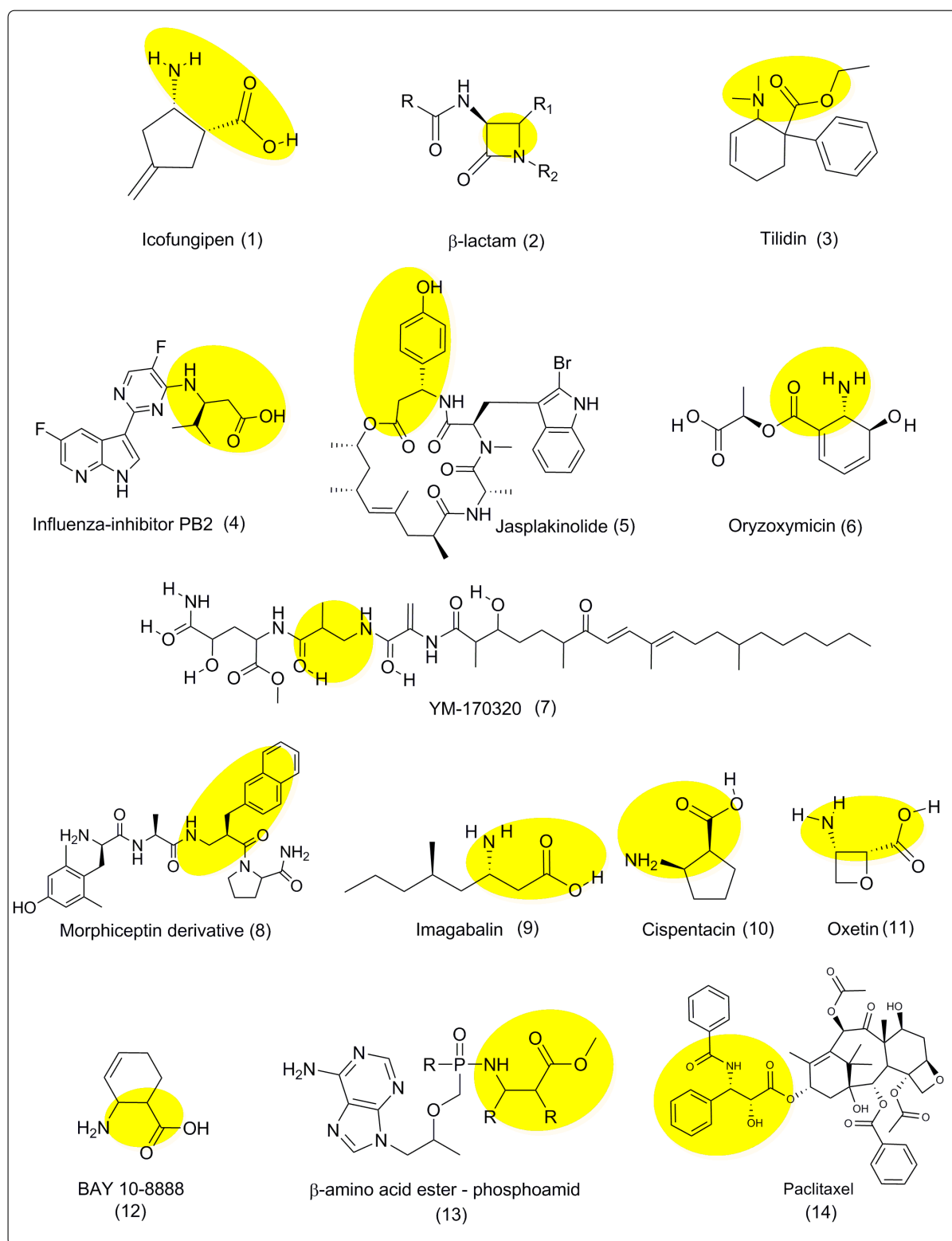


Figure 1.1 Examples of β -amino acid containing functional biomolecules or precursors for pharmaceuticals. The basic structure of the β -amino acid is highlighted in yellow.

Recently, Walker *et al.* demonstrated in a proof of concept an enzyme cascade starting with baccatin III (**15**) and β -phenylalanine (β -PA, **16**) for the synthesis of *N*-(2-furoyl)paclitaxel using four different enzymes (**Figure 1.2**). They demonstrated clearly that this reaction cascade

might by a promising strategy compared to existing processes, because baccatin III can be isolated in four times excess compared to paclitaxel from *Taxus* cell cultivations [35,40,41].

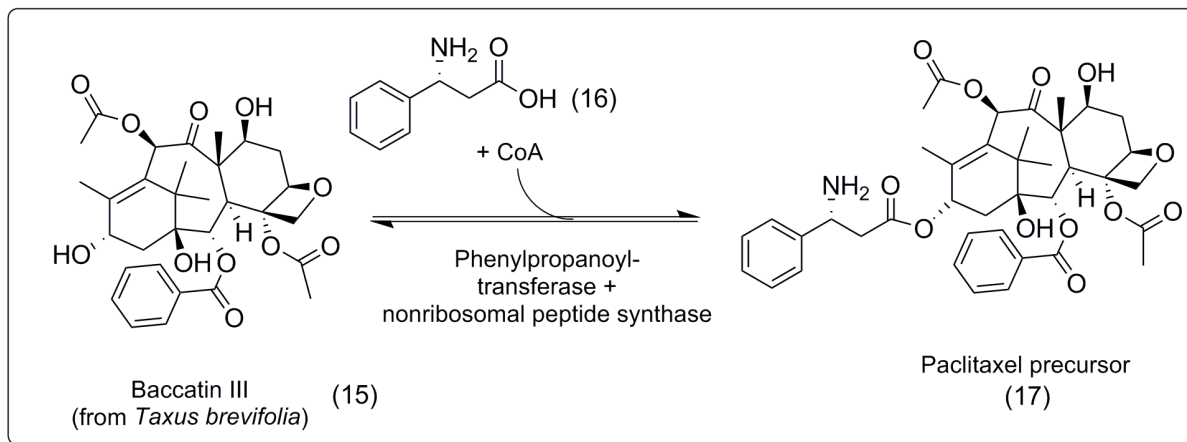


Figure 1.2 Enzymatic synthesis of **17** from **15** and **16**. Baccatin III is isolated as a paclitaxel precursor from yew species. **16** can be varied in the α and β -carbon position. The natural product from *Taxus brevifolia* carries a hydroxyl group in α -position and an aryl-residue in β -position. Note that this can also change the nomenclature from (*R*) to (*S*) and vice versa.

However, not only complex β -amino acids containing natural products show effects, also small non-cyclic β -amino acid drugs exist like Imagabalin (**9**). Imagabalin is active ingredient against general anxiety disorder and is actually tested in clinical studies by the company Pfizer [42]. This β -amino acid drug is at the same time an example for the chiral synthesis of pharmaceuticals using ω -Transaminase (ω -TA) [43], which is discussed later in chapter 1.3.

1.2) Enzymatic and chemical strategies for the synthesis of β -amino acids

The extraordinary relevance of non-canonical amino acids like β -amino acids, shown in chapter 1.1, underlines the requirement for chiral synthesis strategies with focus on highly optically pure β -amino acids, with regard to yields and atom efficiencyⁱⁱⁱ. This thesis focuses on β -phenylalanine (ester) as an example for β -amino acid synthesis using transaminases. Therefore in this chapter possibilities for β -amino acid syntheses are shown and in **figure 1.3** three main strategies are presented.

Firstly, the complete transition metal based synthesis according to the reported strategy is presented. Secondly a chemo-enzymatic strategy using the advantages of classical chemistry and kinetic resolution by lipases are shown. Thirdly, an exhaustive enzymatic synthesis using ω -TA and other enzymes in cascade approaches is presented in **figure 1.4**. For example the chemical reduction of asymmetric enamide is performed under overpressure (5-25 bar). The hydrogenation using oximes is conducted using chiral ruthenium catalysts and dichloromethane or methanol as solvent. The enantioselective ruthenium catalyst is built by large chiral phosphorus ligands, enabling the performance of enantioselective reactions. For that reason a broad spectrum exists of mono- or bi-dentate chiral ligands to synthesize differently configured products. Furthermore for enantioselective reductive amination a variety of different catalysts exist. Most strategies depend on high pressure and complex chiral ligand-metal complexes. An example is the chiral reductive amination of aromates using high pressure (69 bar) and an iridium or iron ligand [44].

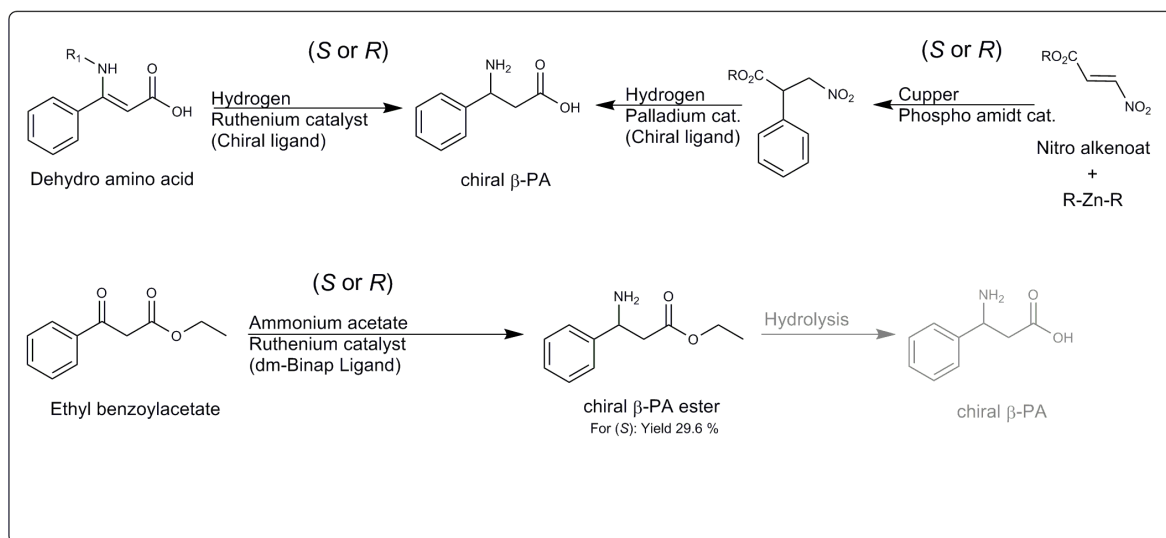
The chemical strategy for enantioselective synthesis of β -PA requires usually an (axial) chiral ligand molecules (e.g. BINAP (2,2'-bis(diphenylphosphino)-1,1'-binaphthyl) which coordinates a metal atom and reduces ketones to amines. Matsumura *et al.* demonstrated in a patent the synthesis of β -amino acid derivatives using ruthenium-dm-BINAP^{iv} as catalyst. The reaction was performed at 80 °C and under overpressure using hydrogen gas (3 MPa) resulting in diverse product yields between 7.5 % and 94 % with enantiomeric excesses between 35.8 and 93 %ee. For example the ethyl ester of (*S*)- β -PA was produced with a yield of 29 % and an enantiomeric purity of 94 %ee, but also the (*R*)-enantiomer can also be produced in this way

ⁱⁱⁱ Atom efficiency is defined as ratio between molecular mass of product(s) to the molecular mass of all substrates.

^{iv} Until now, BINAP is one of the few ligands of industrial importance. [203]

[45]. Starting with unsaturated molecules, like enamines, a rhodium/ruthenium-ligand complex can catalyze the hydrogenation of the asymmetric substrate in an enantioselective order. At the same time the catalyst itself has to be highly optically pure, otherwise no or low enantiomeric excesses will be obtained.

a) Chemical strategies



b) Chemo-enzymatic strategy

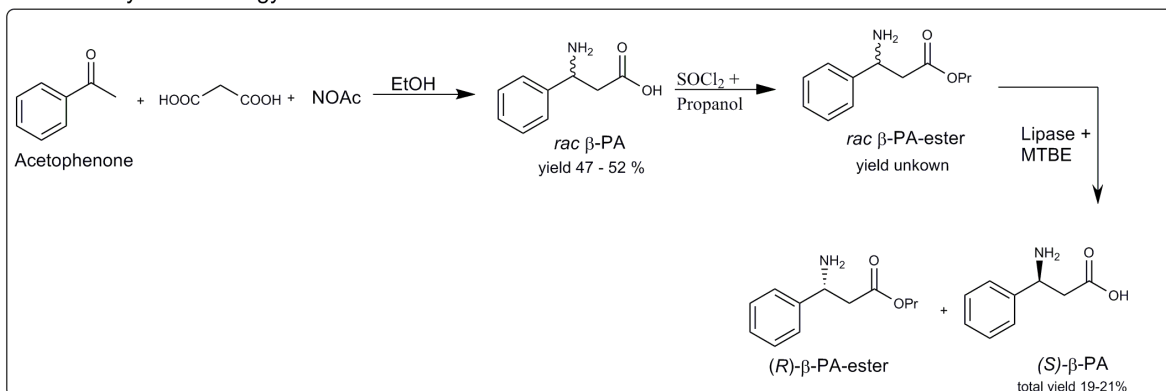


Figure 1.3 Chemical and chemo-enzymatic strategies for producing chiral (*S*) or (*R*)- β -PA. a) Chemical strategies using chiral ligands for enantioselective synthesis can be used for production of (*S*) and for (*R*)- β -PA. The amination of ethyl benzoylacetate is e.g. performed with chiral $\text{Ru}(\text{OCOCH}_3)_2(\text{R})$ -dm-binap under pressure (3 MPa) and heat [45]. b) Evonik-Degussa process using acetophenone as substrate and lipase catalyzed chiral resolution for production of (*S*)- β -PA.

Therefore the ligands are produced in enantioselective manner using chiral catalysts like esterases or lipases, which do not reduce the complexity for the complete synthesis concept [46]. Against this background, it is not surprising that Evonik-Degussa proposed a non-enantioselective process for the synthesis of *rac*- β -phenylalanine-propylester without chiral-ligand chemistry. The produced racemate is then in a second step enantioselectively hydrolyzed using an enantioselective lipase in MTBE. The disadvantage of this process is the theoretical maximal yield of 50 % (caused by kinetic resolution), because initially only the racemate is produced as intermediate (figure 1.3 (b)). In addition the efficiency of the esterification of the

rac- β -PA was not reported by the authors and might also reduce the yield of this strategy [47]. Usually, any additional reaction step reduces the practical yield and thus increases the costs.

Challenges of ω -TA catalyzed synthesis of β -PA

However, ω -TA catalyzed synthesis strategies are a promising alternative, but they have not yet been thoroughly investigated for the production of β -amino acids. Although ω -TA as sustainable catalysts for chiral syntheses can enable one-step or two-step synthesis reactions (**Figure 1.4**), but unfortunately only few ω -TA are reported to be β -PA converting enzymes so far (a general overview of transaminases can be found in chapter 1.3).

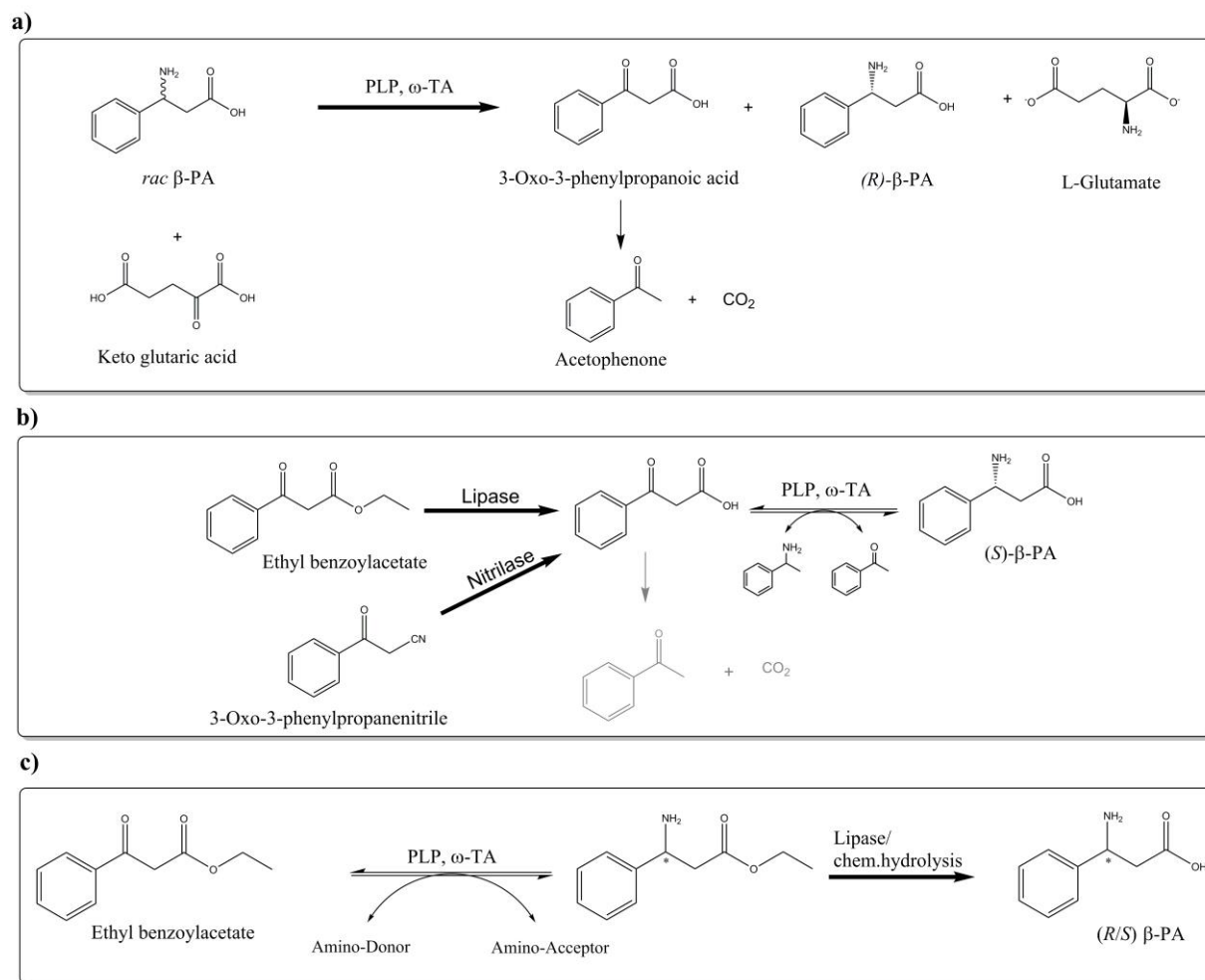


Figure 1.4 Different approaches of ω -transaminase catalyzed synthesis of β -PA. a) Chiral resolution of β -PA. b) Nitrilase and lipase-cascade reaction. c) Synthesis using β -keto ester as stable substrate.

The first ω -amino acid (non- α -amino acid) conversions were shown mainly for β -alanine and γ -aminobutyrate, which are naturally occurring amino acids [48–50]. In contrast, Yun *et al.* described in 2004 an ω -TA with an new substrat preference using *Alcaligenes denitrificans* Y2k-2, showing potential for synthesis of non-aromatic β -amino acids [51]. Three years later Kim *et al.* demonstrated that an ω -TA from *Mesorhizobium sp.* shows activity towards (S)- β -phenylalanine. Additionally they demonstrated that a lipase- ω -TA cascade reaction can

be utilized for synthesis of (*S*)- β -PA from β -keto ester substrates. After hydrolysis of the β -keto ester substrate (ethyl benzoylacetate) the instable β -keto acid is built, and finally converted by the ω -TA to the stable product β -PA. As amino donor the authors utilized 3-aminobutyric acid (β -amino acid) as reagent to shift the reaction equilibrium towards (*S*)- β -PA, because the corresponding co-product, acetoacetic acid, decarboxylates like all β -keto acids towards CO₂ and to a smaller ketone (acetone). The yield after 24 h was only 20 % but resulted in a optically pure product (> 99 % ee) [52].

Afterwards this ω -TA was fully examined by Wybenga *et al.* and the 3D structure of the enzyme was resolved. They demonstrated clearly that this enzyme is specific for binding α - and β -amino acids in the substrate binding pocket. Furthermore, it was shown that β -amino acids bind in a different manner than α -keto acceptor molecules at the substrate binding pocket. It was shown that (*S*)- as well as (*R*)- β -amino acids are converted depending on their conformation and constitution [53]. The same research group reported one year later a second ω -TA from *V. paradoxus* also with high activity towards (*S*)- β -PA [54]. After eight years the first report was given confirming that a cascade reaction from β -keto esters to β -amino acid is possible for synthesis of (*S*)- β -PA using a newly characterized ω -TA from *Polaromonas sp.* JS666. They achieved high yields by using whole cell-mixture with recombinant *E. coli* BL21 in combination with high concentrations of the amino donor 1-phenylethylamine (PEA, 150 mM). The concentration of lipase was adapted to 36 mg mL⁻¹ in combination with 20 mg mL⁻¹ of whole cell catalysts containing the (*S*)-selective ω -TA. In this highly concentrated protein-cell debris suspension they achieved yields between 26 and 99 % of product after 24 h [55]. In 2016, in a similar study with an ω -TA from *Sphaerobacter thermophilus*, they reported a maximum product concentration of 44 % of β -PA. This time they used a purified ω -TA at a concentration level of 2.5 mg mL⁻¹ (pure protein) and lowered the lipase concentration to 20 mg mL⁻¹. In a third study Mathew *et al.* exchanged the lipase towards a nitrilase (using again *Polaromonas* ω -TA). The nitrilase was used as whole-cell catalyst in a suspension with dry cell mass concentrations of 30 mg mL⁻¹ in combination with 20 mg mL⁻¹ of ω -TA resulting in a yield of 72 % for (*S*)- β -PA [56]. In 2018, Zhang *et al.* showed that the reaction cascade of a nitrilase and an ω -TA could even be optimized by a two-phase system and large amounts (in total >40 mg mL⁻¹) of lyophilized enzymes (see **Chapter 5.1.1**) [57]. Therefore, they utilized β -alanine as amino donor. These reports suggest that the reaction cascade is supported by high concentrations of protein or cell-extracts and surprisingly not inhibited by the resulting acetophenone, which was reported earlier by Shik *et al.* [58]. Additionally it has also been

reported that the ω -TA reaction rate is lowered in presence of high amino-donor concentrations of PEA [59].

Challenge of β -keto acid reactions

In view of the reported enzyme cascade reactions, the free β -keto acid is produced in all cases. However, the intermediate disintegrates very fast in aqueous solutions. The decarboxylation reaction required for this is promoted by a circular transition state (**Figure 1.5**) [60].

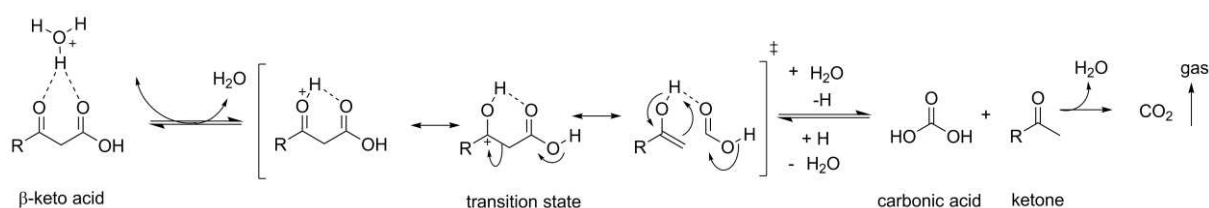


Figure 1.5 Postulated decarboxylation mechanism of β -keto acids in water according to Bach *et al.* and Hanson [60–62].

The elimination of CO₂ is supported by migrating hydrogen from β -keto oxygen to carboxyl oxygen, which leads to a cleavage of the C-C bond between carboxylic group and α -carbon atom. The decarboxylation is less favored, when the pH is physiological and additionally coulombic interactions might stabilize the β -keto acid [61]. The resulting carbonic acid can easily evaporate as carbon dioxide at standard pressure conditions. Therefore to avoid an instable β -keto acid in solution, a protected β -keto ester which cannot decarboxylate should be more beneficial. Also the reported high protein and cell concentrations of cascade reactions seem to be easily scalable to larger volumes (up to 50 g of cell dry weight per liter).

Avoiding free β -keto acids

Therefore it seems reasonable to utilize protected β -keto acid substrates to avoid large enzyme and cell concentrations. However, one of the obstacles is the low availability of ω -TA with reported activity towards β -keto ester substrates. The only enzyme with activity towards aliphatic β -keto esters was reported by Midelfort *et al.* using an engineered ω -TA from *V. fluvialis*. The ω -TA-variant was able to convert (*R*)-ethyl 5-methyl 3-oxooctanoate at high concentrations using PEA as amino donor. The enzyme concentration was reduced to 74 $\mu\text{g mL}^{-1}$ leading in a total yield of 28% of β -amino ester product. The resulting β -amino ester product can easily be hydrolyzed using a lipase or sodium hydroxide to gain the resulting β -amino acid [63]. For that reason one focus of this thesis was to engineer the β -PA converting

ω -TA from *V. paradoxus* for conversion of β -keto ester substrates avoiding free and instable β -keto acids, reported later in this work (chapter 5). A desired side effect is the easy extraction of aromatic keto-esters from the reaction medium with water immiscible^v solvents like ethyl acetate. However, it is essential to understand the function of ω -TA in order to enable efficient synthesis reactions. Therefore, the next chapter presents an overview of the reaction mechanism and applications of ω -TA. In addition, an overview of the protein-sequence-function relation is presented in chapter 3.

^v Immiscible means in this context that two liquids cannot be mixed together in all ratios.

1.3) Mechanism, function and applications of ω -Transaminases

The basic functionality of transaminases is of particular importance for understanding the synthesis strategies of possible applications and for the protein engineering.

1.3.1) The discovery and description of transaminases

Transaminases are well described enzymes for the metabolism of L-amino acids and were indirectly described by Needham *et al.* in the year 1930 during the investigation of muscle cell metabolism [64]. After several observations that muscle cells can perform transamination reactions, Braunstein, Cohen and Kritzmann showed that transaminases are the catalyst of interest [65–67]. At the beginning the German term for the reaction was used, *Umaminierung*, which was later translated to the name transaminase (Enzyme Class 2.6.1.X) according to the French and English designations [64]. These early results in enzyme research demonstrated clearly that a so called transaminase needs an amino acceptor, which was ketoglutaric acid, sulfopyruvic acid or oxaloacetic acid. Furthermore a second molecule is involved in the reaction, which is acting as amino donor. These kind of amino donors were discovered to be always an α -amino acid like cysteine, alanine, aspartate and glutamate [64]. Furthermore it was demonstrated that this class of enzymes is enantioselective towards L-amino acids and that the reaction is fully reversible [65–67]. Thereby the principle of transamination reactions was established. Braunstein suggested, that this enzyme family also requires a cofactor^{vi}, which is known today as pyridoxal-5-phosphate (PLP) and commonly known in the active form as vitamin B₆ [65]. The importance of transaminases is due to the fact that these enzymes are essential for amino acid metabolism. Several decades later Taylor *et al.* described transaminases as promising catalyst for biosynthesis according to a lack of expensive cofactor regeneration systems, rapid reaction rates and due to the relative low substrate specificity [68]. This is at the same time a shift in transaminase research from fundamental research in the field of biochemistry and metabolism towards applied researches in the field of biocatalysis.

The results of transaminase research are culminating in one of the largest enzyme engineering projects for industrial applications, Sitagliptin synthesis using a transaminase [69]. The engineered enzyme is known as a (*R*)-selective ω -TA, which means that the biocatalyst is not limited to α -amino acid substrates (**Figure 1.6**). The group of transaminases which are accepting amine molecules and are not limited towards α -amino acids are generally not

^{vi} In the biochemical context, a cofactor is understood as a non-protein molecule that participates in the reaction (e.g. vitamins/metal ions).

consistently named, but all are classified preferably with the Greek letter ω as a prefix (see also Chapter 3.4) [70,71]. The naming convention for ω derives from the possibility to convert ω -amino acids and was expanded to a common naming convention for utilizing ω - as term for every substrate, which is not an α -amino acid [72].

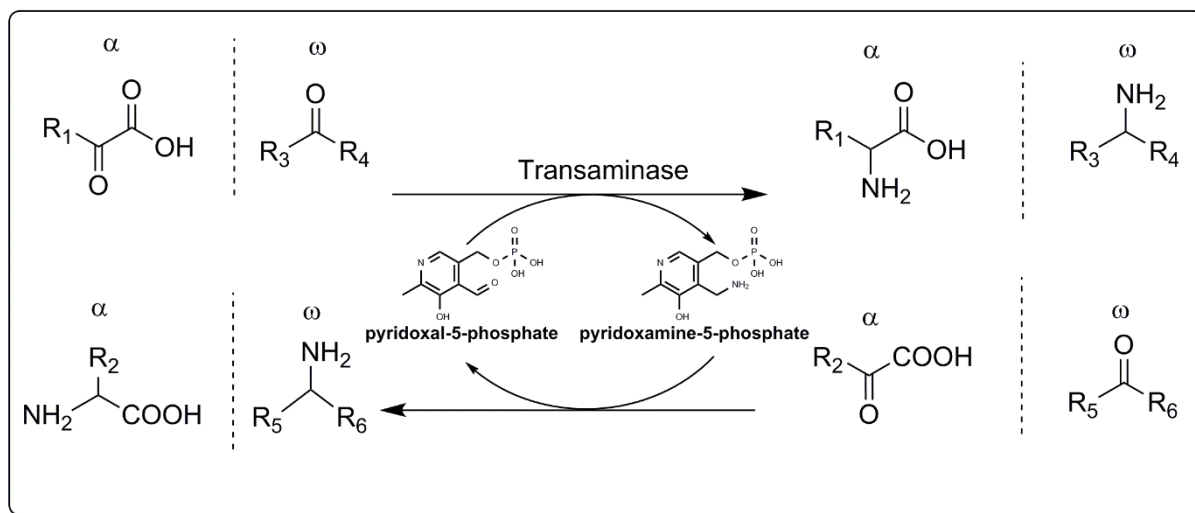


Figure 1.6 Reaction scheme of α and ω -TAs. The substrate of ω -TAs can vary between molecules with carboxylic group and without carboxylic group. α -TAs are only able to convert α -amino acids. In contrast to α -TAs the distance between carboxylic group and amino group (or acceptor position) is undefined. Moreover a carboxylic group can be completely absent. R = residue (R_{3-6}): -H, -CH₃, -COOH, -phenyl, -CH₂R, etc.)

Preferably ω -TA accept primary and secondary amino-groups, but the substrate can vary in structure, e.g. the amino donor can be *n*-butylamine, cadaverine (a C5-chain diamine), bulky bicyclic amines and many other molecule classes which are containing an amino group [73–76]. Naturally, ω - and α -TA are involved in the metabolism of amino acids, alkaloids, polyamines and amino sugars and therefore perform various transamination tasks (Reviewed by Slabu *et al.* 2017)[77].

The classification and differentiation of ω -transaminases

However, within the family of ω -TA, these enzymes are very specific to one group or subclass of substrates according to functionality and molecule size. For that reason it seems to be reasonable to sort the enzymes into groups according to their substrate preferences. Steffen-Münsberg *et al.* reviewed databases with putative enzymes and characterized ω -TA and PLP-dependent enzymes with high similarity. They demonstrated the large diversity of ω -TA within the structural Fold type I. Fold type I ω -TA and closely-related enzymes can be grouped and named after their substrate preference, similarity, or due to their reaction mechanism. The major groups are labeled as: ornithine-TA, ω -amino acid:pyruvate, ω -TA with unusual acceptor spectrum (e.g. β -PA), glutamate-1-semialdehyde transaminases, decarboxylation dependent

TA and two other groups, which have a different reaction mechanism (e.g. racemase and epimerase functions) but have a high sequence identity. Furthermore also a group of uncharacterized enzymes is named in this review, which also includes amino-sugar transaminases [78].

The close relations between enzyme classes within vitamin B₆ dependent enzymes are demonstrated at the example of two phosphorlyases, which are included according to their similarity to class III transaminase family, but surprisingly show no transaminase activity. Both enzymes, characterized by Veiga da Cunha *et al*, showed in experiments lyase activity towards *o*-phosphoethanolamine and 5-phosphohydroxy-L-lysine. It turned out, that only four key amino acids at the active site seem to be important for the change from a transaminase towards a lyase and vice versa [78,79]. This example should also be understood as an indication that the name of the uncharacterized proteins in the family of vitamin B₆ dependent enzymes is not necessarily descriptive for predicting enzyme function in protein databases. In databases these names are registered mainly according towards protein-sequence similarity and not necessarily according to protein-function.

Protein fold type as a distinguishing feature

Beside the nomenclature of transaminases, also the mentioned protein fold type of PLP-dependent enzymes can help to divide the group of ω -TA in two categories, one known as Fold type I and mostly (*S*)-selective and one known as Fold type IV and (*R*)-selective. A total of five different folding types exist within the family of PLP-dependent enzymes and therefore allows the structural classification of the same [80]. In general the group members of Fold type IV are smaller than Fold type I ω -TA, but both groups belong to the superfamily of pyridoxal-5-phosphate dependent enzymes, which includes beside transaminases also the enzyme classes of oxidoreductases, hydrolases, lyases and isomerases. Within this large enzyme family over 2700 known proteins are known [81].

Surprisingly, the functional closely related α -TA do not belong only to one fold type (Fold type I), as known for (*S*)-selective ω -TA, but are also partly member of Fold type IV. α -TA are strictly limited to α -amino acids as donor and accept only α -keto acids like pyruvate. Within the group of Fold type IV-enzymes they are specially known as branched-chain α -TA with activity to large aliphatic amino acids like L-leucin [82,83]. In contrast ω -TA show a broad amino donor substrate spectrum from α - to ω -amino acids, amino alcohols, amines and in general amino-group consisting molecules.

However, the pool of different ω -TA is growing constantly and still a general naming convention for transaminases is missing. To give the family of ω -transaminase a certain order, a database was created and the relationship of transaminases in-depth analyzed (**Chapter 3**).

1.3.2) Transaminase mechanism

In addition to classification and naming, the function of the transaminases is of interest, especially for targeted protein engineering a profound understanding is required. The mechanism of PLP-mediated transaminase reactions were investigated in detail by Kirsch *et al.* in 1984, proposed on the basis of the spatial structure, at the example of an aspartate aminotransferase from chicken heart mitochondria [84]. In addition, the energy profile of the reaction was calculated and the necessary steps to create a model were characterized. [206]. The mechanism was refined by density functional theory calculations and by visualization of

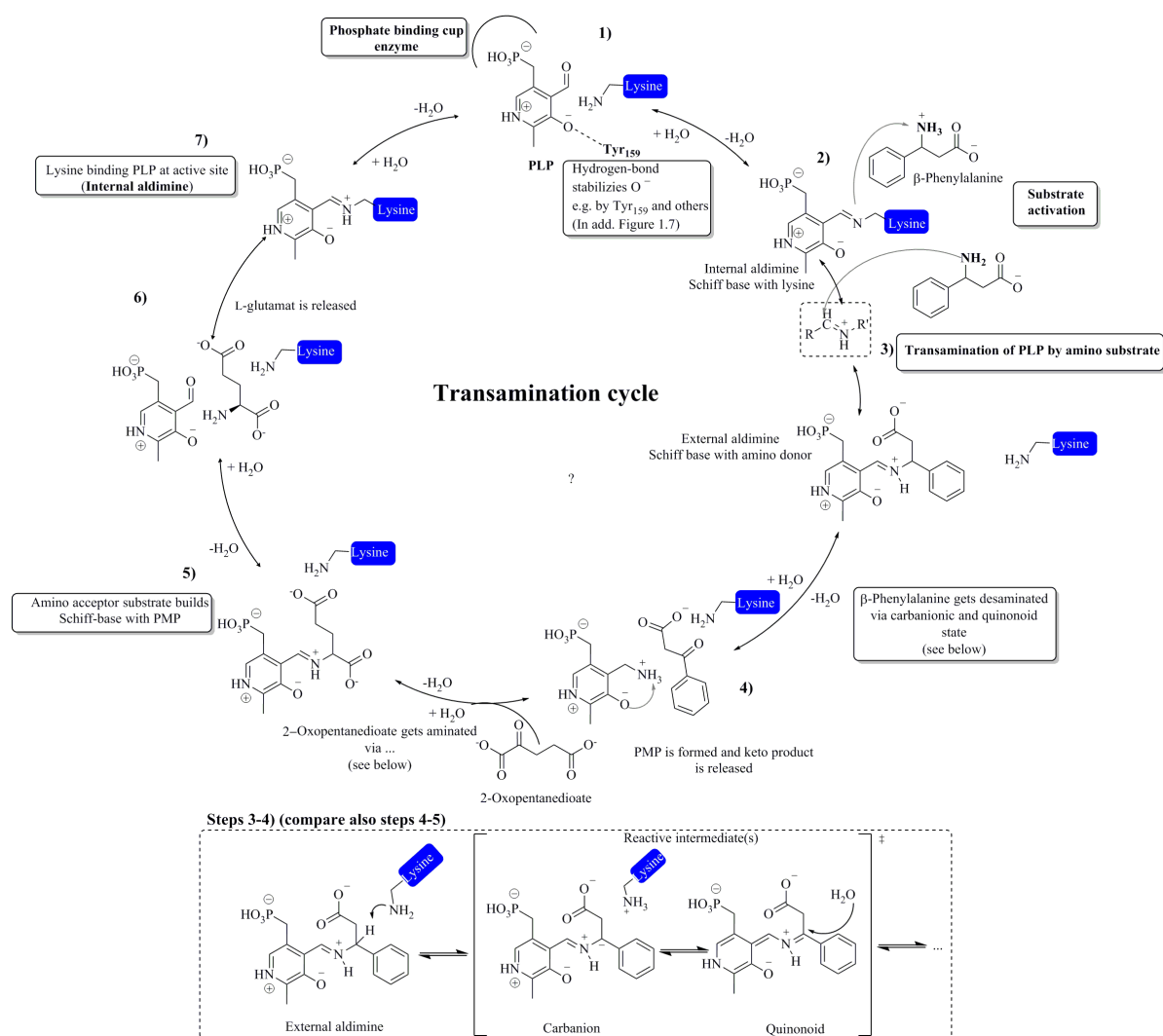


Figure 1.7 Proposed transamination cycle of two half-reactions at the example of β -phenylalanine and α -ketoglutaric acid according to Slabu *et al.*, Manta *et al.* and Dajnowicz *et al.* [77,204,205]. Active site lysine is highlighted blue. Proton transfer according to Djanowicz *et al.*. Not every intermediate state is shown in this figure.

the hydrogen atoms involved by neutron crystallography [204,205]. The studies uncovered clearly the importance of pyridoxal-5-phosphate for the reaction mechanism and furthermore functional amino acid residues of transaminase were pointed out like the catalytically-active lysine residue in the active site (**Figure 1.7**). The general reaction mechanism is closely related to other members of vitamin-B₆-enzyme family, e.g. ornithine decarboxylases, tryptophan synthases, amino acid racemases, lysine 2,3 aminomutases and more. In particular for all defined transaminase classes from I to VI the proposed reaction mechanism is valid [85]. The proposed reaction mechanism is shown using the *V. paradoxus* ω -TA as example for β -PA conversion. The detailed reaction mechanism comprises at least 17 steps and has been simplified in **Figure 1.7** [204]. The three-dimensional representation is illustrated in **Figure 1.8**. Therein the most prominent amino acid residues for active site engineering are highlighted, which are involved in binding the cofactor PLP or the cofactor-substrate complex (external aldimine) at the active site.

The reaction mechanism of transaminases is known to be a ping-pong bi-bi mechanism due to the cyclic reaction pathway using two substrates and one cofactor which is recycled after two half reactions [86]. However, this also means that the reaction equilibrium between products and substrates is usually balanced in equal parts.

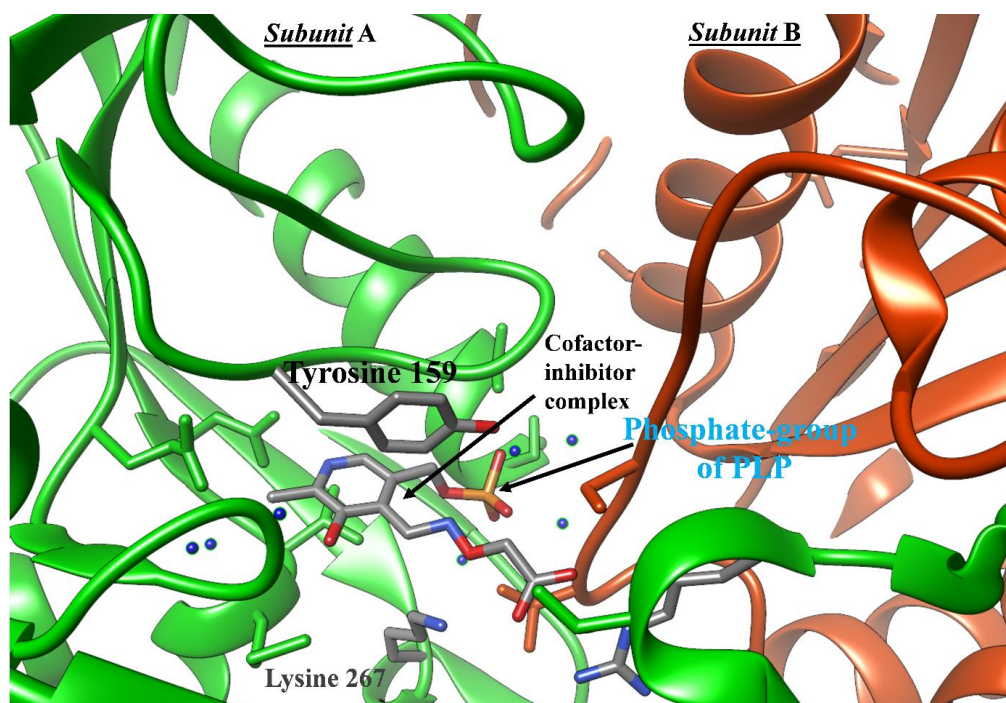


Figure 1.8 Active site of the dimeric *V. paradoxus* ω -TA as an example to describe the location of cofactor-substrate complex in ω -TAs. The prominent amino acid for binding PLP is the tyrosine 159 residue. The catalytic lysine residue 267 is located under the cofactor-substrate complex (Structure PDB-ID 4AOA). The figure was created with Chimera 1.1[87].

The transamination reaction cycle starts with bound or unbound pyridoxal-5-phosphate (PLP, **7** or **1**) which forms a covalent bond with the catalytic lysine residue (see also [77,86,88, 204,205, 206]). If PLP is bound, the cycle starts with the hydrolysis of PLP to break the imine bond between the lysine residue and cofactor (**2**). In presence of the substrate (e.g. β -phenylalanine), a reaction of carbon-aldehyde (cofactor) with the amino substrate group follows and a Schiff base intermediate is formed (like lysine-PLP aldimine). This molecule is by contrast described as external aldimine (**3**) (because no covalent bond exists anymore towards the enzyme). After deprotonating the external aldimine, a transition state is constituted known as quinonoid-carbanion intermediate. This intermediate is stabilized by resonance structures [77,88]. Afterwards the imine bond between substrate and cofactor is built (ketamine) and by addition of water the ketamine is hydrolyzed (**4**). Consequently the desaminated 3-oxo-3-phenylpropanoic acid (keto product) is released. The corresponding 3-oxo-3-phenylpropanoic acid decays on the basis of decarboxylation mechanism and therefore shifts the reaction equilibrium towards amination of the acceptor substrate, which is described as common mechanism for β -keto acids [60]. From decarboxylation experiments with aspartate and ninhydrin it is known that the formed intermediate, a β -keto acid, decarboxylates very fast [89] (see also **Figure 1.5**). In the second part of the reaction mechanism, the aminated PLP, pyridoxamine phosphate (PMP), reacts with the α -keto acid acceptor (or other acceptor molecules like aldehydes, β -keto acids etc.), which can be α -ketoglutaric acid and others (e.g. pyruvate). Analog to deamination process of β -PA the acceptor molecule gets aminated by PMP (**5**) and L-glutamate is released from the enzyme. Afterwards the reaction cycle can start again.

Special significance of PLP as catalytic cofactor

The cofactor PLP *per se* is an interesting and reactive molecule, which reduces the activation energy (E_a) of reactions. It is presumed that enzymes stabilize multiple transition states during the transamination reaction of PLP-substrate intermediates. Furthermore PLP changes the amino-group properties of the substrate and lowers the acidity of it. For example the intermediate PLP-glycine iminium ion shows a pK_a -value of 6 (pK_a (carboxyl) glycine 2.34). The cofactor substrate intermediate thus changes the protonation behaviour of the substrate molecules in the enzyme. Furthermore the phosphate-group of PLP seems to be important for transition state stabilization and for binding at the enzymatic substrate binding pocket [88,90]. The formed imine bond between the aldehyde group of the cofactor PLP and the ϵ -amine of the catalytically active lysine residue is also called internal aldimine (E-PLP, intermediary

product). This state of bound PLP seems to be also relevant with regard to the stability of the ω -TAs [91]. This also explains why the reactive vitamin B₆ has proven to be an important molecule in different enzyme classes.

As mentioned before, the cofactor is usually bound by several amino acids at the active site and particularly the phosphate-group of PLP/PMP is coordinated by a so called binding cup [92]. The aldehyde-group of PLP allows a covalent binding with the described active site lysine. In contrast to PLP, the active site's lysine seems not really to participate during the reaction, but it promotes the deprotonation of substrate and of cofactor-substrate intermediates and is located on the opposite to the PLP-coordinating tyrosine residue [92,93].

PLP enzyme binding as an indicator of enzyme stability and concentration

After release of the product, PLP gets covalently bound again by the active site lysine residue and most of the time it seems to be located at the active site. According to Cassimjee *et al.* the cofactor can even be used for quantification of active ω -TA due to an increase in light adsorption, when a PLP-enzyme bond is build. This interaction can also be utilized as an alternative for enzyme quantification compared to protein assays like Bradford or BCA-assay and to consider if the protein is functional anymore [91].

1.3.3) Industrial applications of ω -transaminases

On this account the PLP-dependent ω -TA provide the opportunity for chiral synthesis of amines and are an alternative to metal-ligand based chiral chemistry. In contrast to the already presented synthesis possibility of β -amino acids, the application possibilities of transaminases go much further (Chapter 1.2). Additionally these enzymes complement the toolbox of synthesis opportunities and can be utilized for kinetic resolution or for asymmetric synthesis approaches [94]. A prerequisite for industrial usability is the availability of transaminases and their technical formulation. In addition, it must be shown for which reactions transaminases can be used reasonably.

At this time technical ω -TA formulations are already available which can be used for semi-industrial applications in miniaturized fixed-bed reactors. Therefore an application was demonstrated by Bajić *et al.* with immobilized ω -TA in so called LentiKats[®]-encapsulations (Poly vinyl alcohol hydrogel capsules) showing a long-term activity of at least 21 days at continuous operation at RT [95]. ω -TA-LentiKats[®] were also tested at larger scale (18 L), showing a conversion rate of up to 85 % [96]. Furthermore ω -TA immobilization was shown on magnetic-poly vinyl alcohol beads in small scale, which are easy removable from liquid phases [97]. In addition to the enzyme formulation itself, the reaction applications of ω -TA are widely diversified from kinetic resolutions to asymmetric synthesis. However, the position of the chemical equilibrium is fundamentally important for all synthesis.

1.3.3.1) Reaction equilibrium

For this reason the greatest challenge of transamination reactions is to shift the reaction equilibrium towards products to reach higher space-time yields and to overcome substrate as well as product inhibition. The most prominent approach to push the equilibrium is the pyruvate(co-product)-removal system using glucose-dehydrogenase, lactate dehydrogenase (LDH) and L-alanine as amino donor. After deamination of L-alanine the corresponding pyruvate is reduced by lactate dehydrogenase to form lactic acid. This one step reaction already shifts dramatically the equilibrium [59,98](**Figure 1.9**). To inhibit the back reaction, from lactic acid to pyruvate, the expensive cofactor reduced nicotinamide adenine dinucleotide (NADH) can be regenerated by GDH using high amounts of D-glucose as driving power, whereas the complex cofactor can be recycled [99]. Alternatively, a pyruvate decarboxylase can be utilized to degrade pyruvate to CO₂ and acetic acid [100]. Such a co-product removing system is in focus of research, because most of ω -TA are able to convert the α -amino acid L/D-alanine,

which is a generally good accepted amino donor for all TA. Beside alanine, also phenylethylamine (PEA) gained attention as commonly accepted amino donor for ω -TA [58]. The corresponding co-product acetophenone (using PEA) shows an equilibrium constant K_{eq} of 10^{-3} M, this demonstrates that PEA is suitable for some amination reactions. However, a clear disadvantage is the enzyme inhibition of the ω -TA by high acetophenone concentrations [58]. Furthermore, the smallest amino donor with useful properties for transamination reactions is isopropylamine (IPA), because it converts during a reaction to acetone. The co-product acetone can then evaporate easily from the reaction mixture (e.g. under reduced pressure). For example the engineered ATA117-transaminase was adapted for accepting IPA as amino donor to produce Sitagliptin in a large scale process [69,98]. IPA and PEA are two good examples for shifting the reaction equilibrium by their corresponding product properties. This contrasts with the amino donor alanine, which requires like mentioned a coproduct removal system. Beside those three widespread amino donors, *o*-xylylenediamine (OXD) seem to be a promising substrate, because it polymerizes and precipitates after deamination [101]. The beneficial side effects are the possibility to perform large screenings with ω -TA with OXD and the second benefit is the irreversible polymerization, which pushes the reaction equilibrium towards products. Therefore the equilibrium displacement techniques are highly important for ω -TA approaches, this topic was summarized in-depth by Guo *et al.*, Dold *et al.*, and Tufvesson *et al* [76,102,103]. In **figure 1.9** an overview of the most prominent equilibrium displacement techniques is given. Donor₁ symbolizes the changeable amino donor and acceptor₂ representing the resulting co-product of Donor₁. In this reaction scheme donor₂ defines the product.

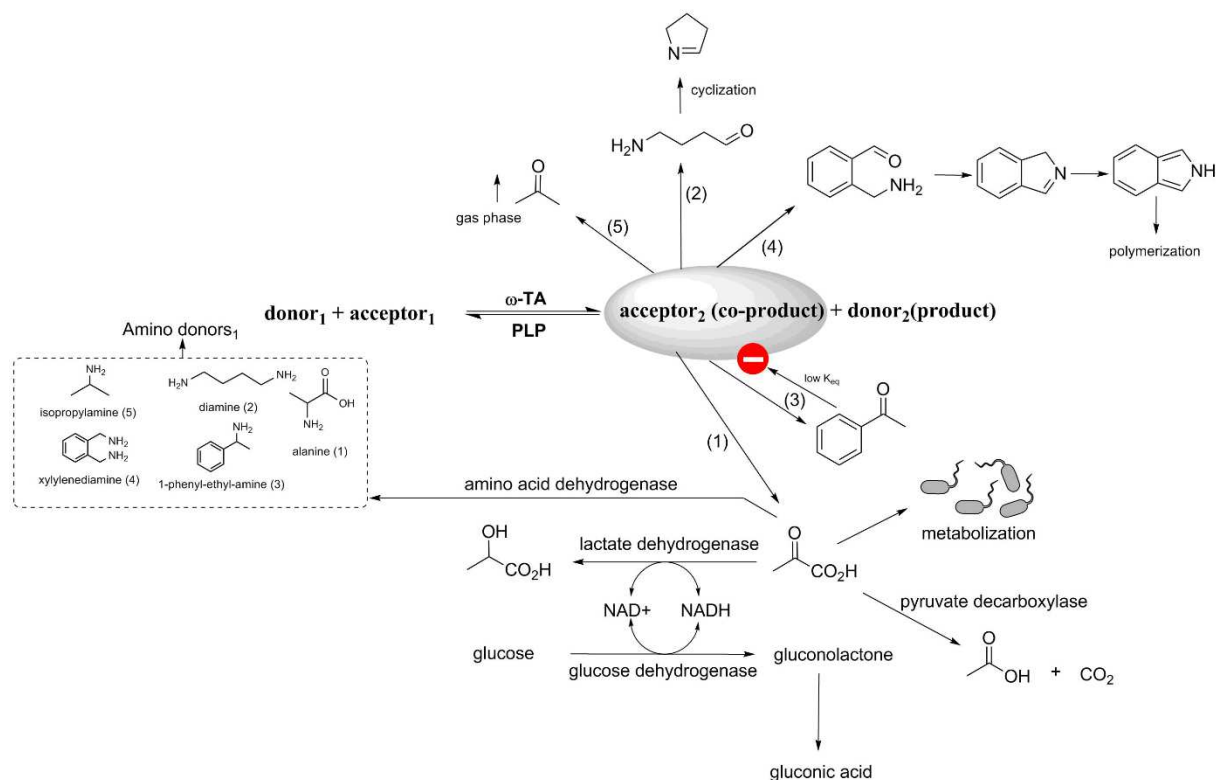


Figure 1.9 Equilibrium of prominent displacement techniques. The co-product is either removed by enzymatic reactions/metabolization (1) or continues to react autocatalytically (2,4). In addition, the co-product can either be removed by physical processes (5) (e.g. using under-pressure) or it shows a low reactivity (3) and thus prevents the back reaction [76,102,103].

In addition to the mentioned possibilities for pyruvate removal using LDH and PDC, an alternative is also amination using an amino acid dehydrogenase and ammonia, which was demonstrated by Truppo *et al.* [99]. Furthermore, also the properties of living cells can be utilized for equilibrium shifting, according to the ongoing metabolism of microorganism. For that reason, the resulting pyruvate can also be removed by an innate metabolic pathway of *E. coli*. The microorganism contains and expresses at the same time the transaminase of interest [104]. The latest application for shifting the equilibrium are aliphatic diamine(s), like putrescine, which automatically cyclize after deamination. This approach was also reported for 1,5 diketones, which undergo a spontaneous cyclization to form piperidine rings. The strategy was e.g. reported by Simon *et al.* using different lyophilized *E. coli* cells containing ω-TA, but this approach is limited in respect to the substrate(s), diketones, or to the products which are able to cyclize by itself [105].

In general every technique has its challenge, like low substrate acceptance by the most of transaminases (e.g. using putrescine), high substrate and enzyme costs, high substrate concentrations of the amino donor (e.g. IPA or L-alanine), low availability of enzymes or uncommercial substrates. Furthermore, the co-product properties might lead to interference.

For example, the deaminated co-product of OXD results in interfering precipitates caused by auto-polymerization. In general, many equilibrium shift-strategies are imaginable, but the costs and the atom economy will be pivotal for the economic efficiency of industrial processes.

In addition to the efficiency of the catalyst, the synthesis strategy is also decisive. Transaminases can be used in two synthesis strategies, one is called kinetic resolution, the other as asymmetric synthesis.

1.3.3.2) (Dynamic) Kinetic resolution

Kinetic resolution (KR) syntheses are advantageous to produce chiral products, when synthesis of a racemic educt is simple and inexpensive in relationship to the value of the chiral product. The kinetic resolution is then performed with an enantioselective (bio)catalyst to gain optically pure product.

An example of industrial scale KR was demonstrated for the synthesis of a chiral β -amino acid by Evonik-Degussa. Firstly the *rac*-amino acid is produced using a robust chemical process, afterwards the amino acid is esterified and then an enantioselective lipase separation process is applied to separate co-product and product. The racemate of β -PA is produced from benzaldehyde, succinic acid and nitroso-carboxylic acid. The intermediate product is then in a second step esterified with propanol and in a third reaction step hydrolyzed using an enantioselective lipase in a two-phase system consisting of water and MTBE (methyl-*tert*-butylether) to gain (*S*)- β -PA (see also **Figure 1.10**). The left (*R*)-enantiomer, which remained as ester, can be easily separated and hydrolyzed to the corresponding β -amino acid [47]. A general disadvantage of this strategy is the low atom efficiency, particular when only one enantiomer is demanded, because the theoretical yield is maximal 50 %. Nevertheless, also strategies were applied using ω -TA as enzymes for kinetic resolution processes, although ω -TA are more expensive and often less available than other enantioselective catalysts like the widespread lipases.

For increasing the yield, dynamic kinetic resolution (DRK) serves as approach to increase the yields, using a suitable racemase, chemically racemization or spontaneous racemization [77]. For example, analogs of PLP can be utilized for racemization, which was demonstrated on the example of L-alanine [88,106]. Most prominent examples for DKR using ω -TA are the synthesis of precursors for the synthesis of (*S*)-Ivabradine, Vernakalant and for PEA. For example Vernakalant is an antiarrhythmic drug for the treatment of atrial fibrillation in heart

[107]. Vernakalant is expected to have a market volume of \$ 1.1 billion in 2018 [108]. A second example is the drug (*S*)-Ivabradine, which is also a pharmaceutical for treatment of the heart disease like angina pectoris and sinus tachycardia [109,110].

The DKR to gain chiral Ivabradine and Vernakalant is reasonable, because the substrate can be synthesized as a racemate. Therefore, ω -TA is suitable for the enantioselective transfer of the amino group. Both examples utilize engineered transaminases, which are commercial enzymes from Codexis. Furthermore, the synthesis of a precursor of (*R*)-3-phenyl-GABA can be performed as DKR using a (*R*)-selective transaminase [111]. The substrate, 4-oxo-3-phenylbutyric acid ethyl ester, racemizes spontaneously and on this account the ω -TA can convert up to 92 % of the total substrate amount. In the most of other cases, a spontaneous racemization does not happen.

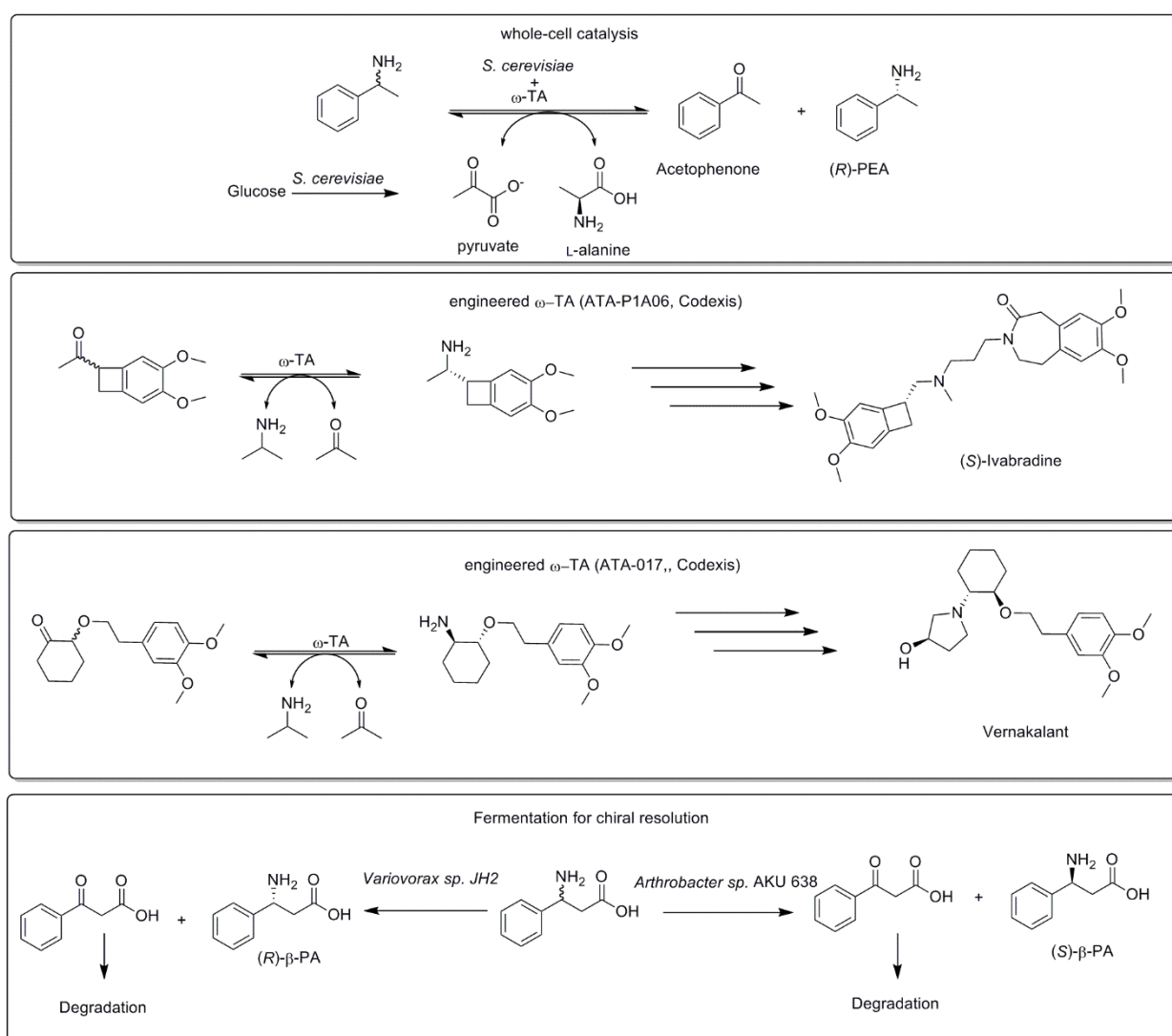


Figure 1.10 Overview of kinetic resolution-reaction examples using ω -TA or microorganism.

Moreover, also fermentation processes can be utilized for enantio-separation. The example for chiral resolution to gain optically pure (*S*)- β -PA using living cells, might not be ω -TA mediated, because the degradation pathway in *Arthrobacter sp.* AKU 638 is still unknown. However, it is presented in **Figure 1.10** as complement for KR of β -PA.

Besides the possibilities mentioned there are many approaches how a (D)KR can be carried out. The applications spread over fermentation-processes, whole-cell catalysis and enzyme reactions for chiral resolution of even small amines like 1-phenylethylamine (PEA). Mano *et al.* showed in growth studies with bacteria, that it is possible to produce chiral β -PA from racemate using two different microorganisms [112]. In **chapter 6**, an example of a fermentative KR for β -PA is therefore shown. An example for whole-cell catalysis was shown by Weber *et al.*. *Saccharomyces cerevisiae* was used for chiral separation of PEA to produce the (*R*)-enantiomer and to refill the co-substrate concentration by metabolism of *S. cerevisiae* [113]. An example for the utilization of whole-cell catalysis in *E. coli* was also given by Yun *et al.* for KR of *sec*-butylamine using overexpressed *Vibrio fluvialis* ω -TA. To shift the chemical equilibrium the pressure was reduced and the substrate concentration level was increased to 400 mM [114].

The research efforts with focus on KR also resulted in a sophisticated understanding of the equilibrium of ω -TA reactions, which is very important for realization of industrial ω -TA approaches [58]. In contrast to (D)KR, the amination of asymmetric substrates is not favored by thermodynamics, which leads to an unfavorable equilibrium with respect to product formation [114]. Other approaches of optical resolution are crystallization or chromatographic separation [115,116]. However, it is economically desired to produce a chiral and enantiomerically pure molecule than to form a racemate in the first place.

1.3.3.3) Asymmetric synthesis strategies

In general, the enzyme catalyzed asymmetric synthesis^{vii} strategies have to compete with enantioselective chemical processes. The most prominent chemical strategies are metal-catalyzed using imine- or enamine-reduction approaches. High pressure and the requirement for chiral ligands are disadvantageous for sustainable synthesis of amines. Furthermore, also strategies for removal of the metal catalyst have to be performed. The removal of metals from the reaction is very elaborate, especially when the products are considered for medical and food purposes. Moreover, starting from the ketone as asymmetric substrate, a strict chemical synthesis route requires at least a three-step reaction. Therefore enzymes seem to be ideal catalyst for amination of asymmetric ketones and a wide range of enzymes were investigated in respect of their ability to produce chiral amines, though not all strategies are asymmetric approaches. In **figure 1.11** a selection of chiral β -amino acid producing enzymes is given.

Biocatalytic strategies for enantioselective synthesis

Beside the mentioned ω -TA-catalyzed synthesis, only the engineered β -amino acid dehydrogenase and the engineered β -amino acid lyase convert asymmetric substrates to form chiral amino acids [117,118]. Most of the other strategies use chiral substrates, which are enantio-pure or racemic. For that reason the use of racemic substrates results in kinetic resolution reactions. However, also dynamic kinetic resolution is possible to produce optically pure products. An example is the utilization of the hydantoine-racemase in combination with a hydantoinase and a carbamoylase, but so far this has been realized on industrial scale only for α -amino acids [119]. Recently the enzymatic hydrolysis of dihydropyrimidine precursor for β -amino acid synthesis was demonstrated [120,121]. However, the realization of the whole enzymatic cascade is still missing.

The opportunities to use β -amino acid dehydrogenases are very limited due to the low availability of these enzymes. Until now, no wild type enzyme is described with activity towards β -keto acid(ester) substrates. Zhang *et al.* engineered for that reason a NAD(P)H dependent β -amino acid dehydrogenase from a former L-erythro-3,5-diaminohexanoate dehydrogenase. The β -keto acid conversion was demonstrated in a reaction cascade system consisting of nitrilase or lipase starting with a β -keto nitrile or β -keto ester substrate. It was described that the activity of the engineered enzyme was very low and only in the scale of mU per mg of enzyme. The cascade reactions achieved yields of 12 % and 22 %, respectively [117].

^{vii} The asymmetric synthesis is considered to be reactions that create a new stereocenter and do not produce a racemate.

The before mentioned lipase-strategy is also displayed for the resolution of racemic β -amino acid substrates. An alternative to those enzymes, is the utilization of an engineered β -amino acid lyase. This was shown for an engineered aspartase, which achieved higher activities (0.1 U per mg), but until now only the conversion of the small 3-aminobutyrate was reported [118].

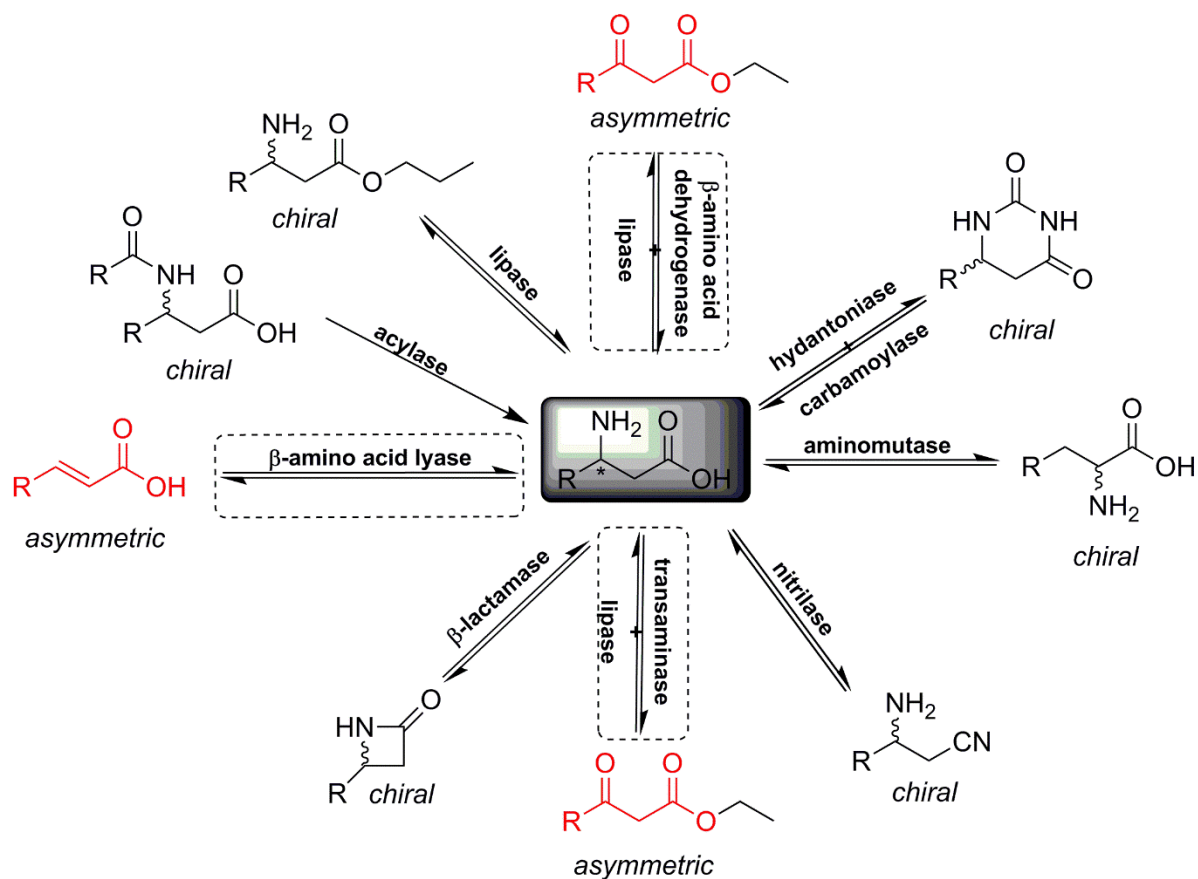


Figure 1.11 Overview of different (hypothetical) enantioselective synthesis strategies towards β -amino acid preparation. The synthesis of β -phenylalanine using hydantoniase and carbamoylase is not demonstrated in a cascade reaction until now. Figure modified, corrected and adapted from Zhang *et al.* [56,117,118,121–126].

In addition also a natural ammonia lyase –EncP– was characterized by Weise *et al.* towards activity for different arylacrylates, but the natural enzyme shows only low selectivity. However they achieved higher enantioselectivity after enzyme engineering of EncP was performed, but only for some arylacrylates-substrates [127]. In addition also the level of knowledge about β -amino acid converting lyases and aminomutases is relatively low compared to other well characterized enzymes and only little is known for the rest of enzymatic conversion strategies. So far ω -TA are the most promising enzymes for the synthesis of chiral amines and in particular for the synthesis of β -amino acids. In conclusion ω -TA are displaying many advantages compared to other enzyme-classes, with exception for lipases, because they are enantioselective and well described. In fact ω -TA are cofactor dependent, but the cofactor is recycled by every

second half reaction and ω -TA enable 100% conversion of asymmetric substrates into chiral products, unlike lipases (see **Figure 1.7**). Furthermore ω -TA shortcut the synthesis of chiral amines compared to chemical synthesis strategies. For these reasons, ω -TA are the enzymes of choice for enantioselective synthesis.

1.3.3.4) Applied enantioselective synthesis of amines

ω -TA also compete with chemical synthesis strategies. Therefore examples of prominent applications of ω -TA towards asymmetric synthesis are displayed in **Figure 1.12**. The most prominent examples, which replaced a purely chemical synthesis strategy, was demonstrated by Codexis and Merck using the engineered ω -TA ATA117_(11rd). This engineered enzyme is ideal for the amination of bulky-substrates. The best known example is the synthesis of the antidiabetic drug Sitagliptin, which is the flagship in respect of chiral amine synthesis and was discussed by a large variety of publications [69,128–132]. After engineering of the enzyme, the substrate concentration could be drastically increased to 250 g L⁻¹ and the solvent content of DMSO was increased simultaneously to 50 % (v/v). The engineered enzyme showed furthermore an increased long-term stability in respect of higher temperatures up to 50°C. This example shows that an enzymatic process can be more economical and ecological than a pure chemical process [133]. At all, the enzymatic process showed an increase in productivity of 53 % and at the same time the amount of waste was reduced by more than 19 %. The decisive factor was that the process can be carried out at standard pressure, because the transition metal catalyst was replaced by the enzyme [134]. The final chemo-enzymatic process generated sales of \$ 6 billion and is therefore also a beacon project for applied biocatalysis [135]. In addition, Besifloxacin, AZD 1480 and MK-6096 are further examples of the use of ω -TA on larger scales for production of chiral pharmaceuticals and for production of building blocks for antibiotic synthesis [136–138]. Further pharmaceutical relevant enzymatic synthesis, which are shown to be feasible at larger amounts are those of (*S*)-Ivabradine and Vernakalant.

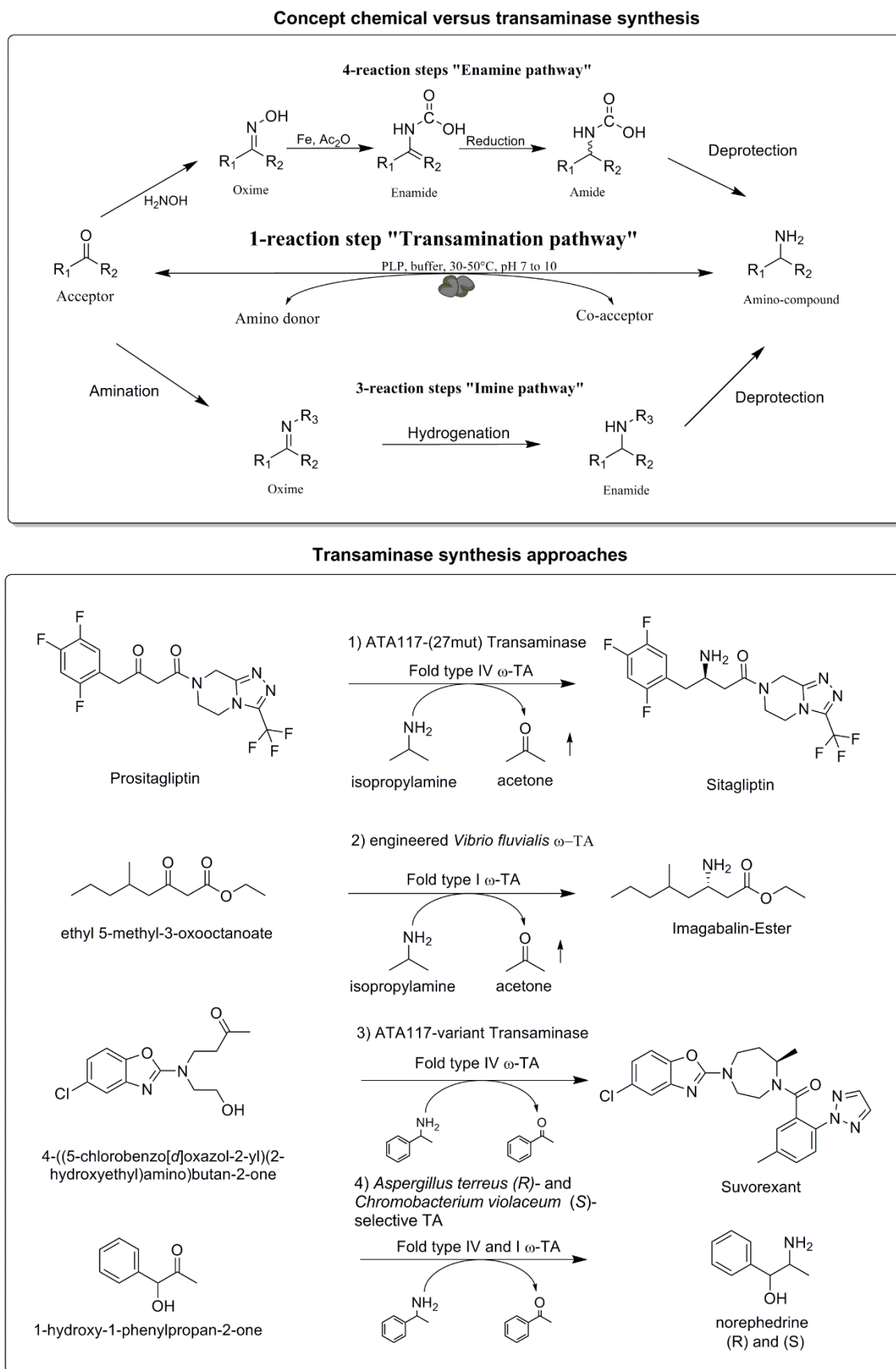


Figure 1.12 Concept and examples for using ω -TA for high valuable drug synthesis. Concept of chiral amine synthesis according to [44,47,78]. References for synthesizes: Sitagliptin [139], Imagabalin [43], Suvorexant [140,141], norephedrine [142].

A second example for asymmetric reactions of bulky ketone substrates is the synthesis of the orexin inhibitor Suvorexant. Suvorexant is used as drug for the treatment of insomnia (sleep disorder) since 2015 in USA and Japan. After transamination the Suvorexant precursor undergoes a spontaneous cyclization to the final product. In a study of Schwentner *et al.* PEA was utilized as amino donor with positive effects on the reaction equilibrium. Using the engineered and (*R*)-selective ATA117_{11rd}, they were able to reduce the number of necessary reaction steps from five to one compared to the chemical synthesis strategy [140]. Moreover the mentioned synthesis of Imagabalin is a further example for ω -TA engineering towards enzymatic processes for the production of chiral amino-drugs. Imagabalin is a phase III drug for the treatment of generalized anxiety disorder and the only example for a Fold type I engineered ω -TA using β -keto esters as substrate [43]. Until now the final technical application has not yet been published or shown. However, the smart synthesis strategy avoid the instable β -keto acids for the synthesis of β -amino acids, but until now the engineered ω -TA from *Vibrio fluvialis* displays relative low activity to β -keto esters. On the threshold of technical applicability, the research group of D. Rother demonstrated also the utility of ω -TAs for the synthesis of drugs at the example of (*R*) and (*S*)-norephedrine^{viii} synthesis using ω -TAs from *Aspergillus terreus* (Fold type IV) and *Chromobacterium violaceum* (Fold type I). The synthesis was performed in a simple one-pot reaction starting from non-chiral substrates [142].

In general, all applications are based on small amino donor molecules, such as IPA, using DMSO as a co-solvent to increase the solubility of substrates with low water solubility. The illustrated examples of drug synthesis using natural and engineered ω -TA clearly demonstrate the relevance of these family of enzymes for the synthesis of chiral amines. Furthermore it is shown that ω -TA can be utilized for industrial scale processes. On this account the focus of this work was set on the analyzation of ω -TA and furthermore the ability of chiral β -PA synthesis was investigated.

^{viii} Norephedrine is an amphetamine and it is used as an appetite suppressant and decongestant.

1.4) Protein engineering

Although function and protein structure are interdependent, the relationship between both is only understood superficially [143]. In theory, the primary sequence of the polyamide chain contains every information, which is necessary for the three dimensional folding which forms finally a structure in a minimized free energy (ΔG) state [144]. However, for theoretical calculations simplifications of reality are made, so for example the process of simultaneous translation and pre-folding is usually not considered in predictions. Whereas protein-complexes are built by independently folded monomeric units, which are interacting mainly via their surfaces with each other [145]. Since the direct prediction of protein structure and function is not feasible, many calculation methods have been established which derive functions from existing data and compare sequences in order to obtain functional information about uncharacterized proteins. A variety of such tools for sequence-function relationships were summarized by Widmann *et al.*[146]. However, in principle the procedure can be divided into three categories, depending on whether the protein structure is present, whether a target design is to be created or whether random mutations should bring the desired effects through controlled evolution (Figure 1.13).

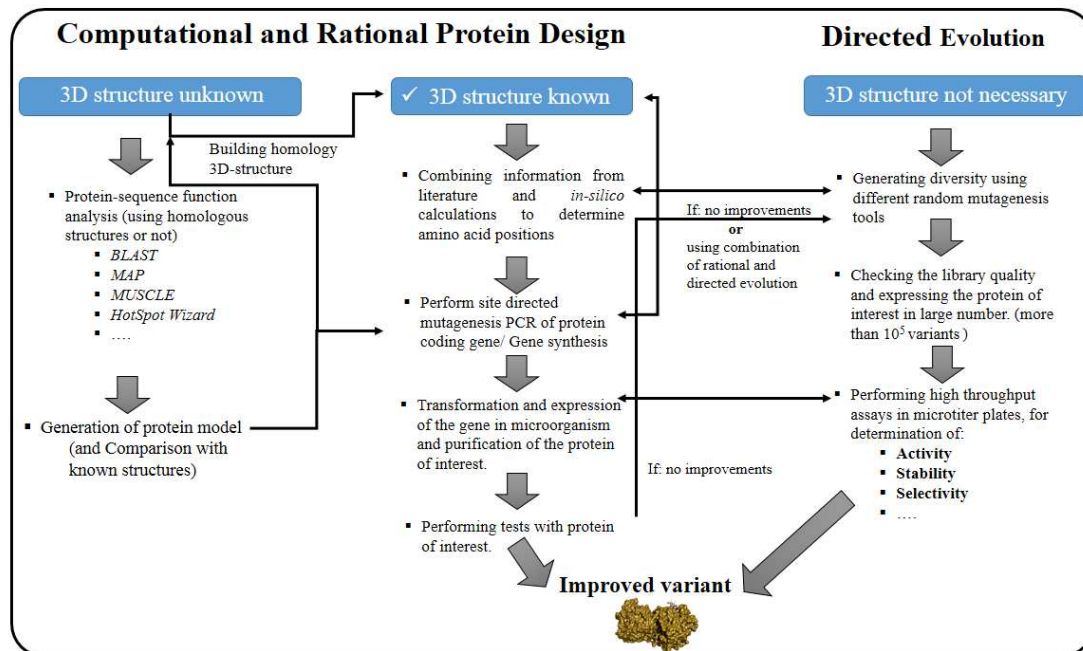


Figure 1.13 Strategy overview for enzyme engineering. For the purpose of changing the enzymatic properties, different approaches can be chosen and combined, depending on whether structure and experimental information are available or not (see also **Table 2**). For example, random mutagenesis in the context of directed evolution can help to overcome missing structure and functional knowledge. However, all approaches can be combined with each other to obtain an adapted enzyme.

In general, many variants of an enzyme still need to be investigated *in-situ*, because the prediction accuracy is too low, even though protein-function predictions currently improving. The *de novo* design of enzymes might be possible in future to create proteins with desired functions, although the number of possibility for a hypothetical protein with 300 amino acids is enormously large (20^{300}). The idea to create enzymes with desired activities by avoiding large scale libraries, would increase the attractiveness of biocatalysis [147].

1.4.1) The challenge of function prediction

Until now it is not possible to predict the structure accurately, but the knowledge about the correlation is necessary to predict the function of large biomolecules like enzymes [148–151]. Once the protein structure is dissolved, the properties of proteins can be determined with the help of various prediction tools. These and other *in-silico* strategies can help to engineer enzymes, which is an option to directed evolution experiments. The possibilities to mine enzyme information by calculations can guide enzyme designs, also known as “Rational Protein design” (RPD). RPD requires also protein structures, which are gained by X-ray crystallography or NMR to uncover the position of atoms within the polypeptide chain. The most of all protein structures are collected on the RCSB protein data bank [152]. Structure data are necessary for the majority of *in silico* tools, like for sophisticated MD-simulations and e.g. for the prediction of artificial disulfide bonds within a polypeptide chain. A summary of protein engineering tools are listed in **table 1.2**.

The displayed tools underline the diversification of prediction tools, however the majority needs protein structures as starting point. In addition, the protein structure can also be predicted, mainly using homology models for calculation. Examples for structure-prediction algorithms are CABS-fold, DCA or SHAPREN, which can be utilized to predict the structure of a protein from the amino acid sequence [153,154]. Such calculation approaches are described as *de novo modeling*. Therefore, exemplary target parameters of protein engineering are the thermostability or substrate selectivity of an enzyme. The creation of artificial disulfide bridge bonds is also a engineering goal for increasing protein stability by improving the intermolecular forces (covalent bond(s)) within the polypeptide chain [155]. One example is the Disulfide by Design 2.0 algorithm.

Table 1.2 Examples for protein function and engineering tools.

Tool	Function	Structure based	Reference
Auto-mute	Prediction of protein stability due to mutation effects	Yes	[156]
CABS-fold	Prediction of protein structure	No	[153]
CheShift	Graphic validation of protein structures	Yes	[157]
Direct coupling analysis (DCA)	Genomic sequence information for prediction of protein structures	No	[158]
Disulfide by Design 2.0	Disulfide bridge engineering	Yes	[155]
EGAD	Empirical parameter free prediction for protein design	No (only natural counterparts are necessary)	[159]
Fireprot	Prediction of protein stability due to multiple mutation effects	Yes	[160]
FoldX	Prediction of protein stability due to mutation effects	Yes	[161]
HotSpot Wizard	Prediction of hot spots for protein engineering	Yes	[162]
I-PRO	Iterative protein redesign (ligand binding)	No (parental structure needed)	[163]
I-TASSER	Prediction of structure and function	No	[149]
MAP	Directed protein evolution – tool	Not necessary	[164]
PoPMuSiC	Estimation of protein stability	Yes	[165]
PROTDES	Optimization protein folding	Yes	[166]
Rosetta Online Server	Molecular modeling-ligand binding	Yes	[167]
RosettaDesign	Design of new protein structures	Yes	[168]
SHARPEN	Protein structure prediction	No (parental structure needed)	[154]
STAR	Machine learning algorithm for design of novel proteins	No	[169]
WHAT IF	Modeling of proteins	Yes	[170]

Independent of the optimization target, also supporting tools can be utilized to short cut mutagenesis experiments. An example is the mutagenesis assistant program (MAP), which helps to identify promising engineering sites. Engineering sites are often not evolutionary conserved, which means that these amino acids can be exchanged in a protein without losing the function and stability of the protein. Amino acid positions with increased variability can be

identified as allowed engineering mutation sites and can therefore be useful to reduce the size of protein mutagenesis libraries [164]. A sophisticated prediction tool for this is HotSpot Wizard which combines evolutionary and structural information and simultaneously compares homologous protein sequences. Ultimately, this allows the quick exclusion of amino acid positions that should be preserved. The received small scale libraries contain less protein variants than necessary for classical directed evolution experiments [137].

Protein motion– molecular dynamic- simulations

However, not all predictions can be made on a pure protein sequence basis using static protein-structure data. Molecular dynamic (MD) simulations can also be used as a tool for the investigation of time-resolved structures of proteins, which can be the starting point for further calculations (e.g. prediction stability or contact probability of residues). In contrast, a static structure is only a snapshot of protein-folding on an energy minimum, this gives no indication of how a protein behaves over a longer period of time. Furthermore, also the entire protein molecule is in motion due to Brownian motion and thus in interaction with surrounding molecules (e.g. solvent molecules or other proteins) [171,172].

For example molecular dynamic simulations try to mimic the movement of the proteins in solution using theoretical force fields, which are causing movements of structural parts of proteins. This kind of simulations can be performed for prediction of protein folding and unfolding with regard to stability. However, the predictive power is limited by the short simulation time, which is mainly limited by the high computational effort. In contrast the time scale in which a protein folds can extend over very long periods of time and it also differs between proteins by a factor of one million [173]. For that reason, a trajectory is recorded normally for periods of ns to ms for gaining time-resolved coordination of amino acid residues within the protein, but therefore the simulation do not cover slow protein folding events.

Basis of MD simulations

In order to predict the mobility of the protein, a force-field is applied to the atoms of the structural model, which is based on equations of classical physical mechanics [174]. The mechanical forces are calculated according to empirical potential energy functions like adapted Lorange's or Newton's equations, which help to calculate unfolding or folding events [173,175]. Using the example of the Newton's equation, which bases on the standard equation (force is mass multiplied with movement in x,y,z coordination) the movements are predicted in a Cartesian coordinate system. The motion is described as differential r_i , which is the vector of

an atom or amino acid residue within the protein. Therefore, m_i is the mass of this atom or amino acid residue. According to this basic equation, i is the number of atom-vectors of the molecule [175].

$$m_i \ddot{r}_i = F_i \quad \text{with } \ddot{r}_i = \frac{d^2 r_i}{dt^2}$$

The so called molecular dynamic simulation is then the time resolved movement of each atom within the model. To gain trajectories (time resolved structures) the basic equations have to be integrated, which can be solved by numerical solutions. The evaluation of such motion profiles can be finally used to analyze the stability of a protein structure (shown in **Chapter 4**).

1.4.1) Thermostabilization using *in silico* tools

The thermostability of proteins depends on their environment and on intrinsic forces like bonds and interactions, but also the entropy is an essential part of stability (**Figure 1.14**). After expression of a polypeptide chain (e.g. an enzyme), the chain gets folded by it-self or will be folded by other proteins, like chaperons and rests afterwards in a local energy minimum (stable state) [176,177]. In aqueous solutions, the folded protein is permanently in balance between folding and unfolding-states. In denaturated state (partially folded states or folding intermediates) the protein-residues are disordered and the function of the protein gets lost. After complete unfolding, the protein is forming amorphous aggregates. This protein folding state is generally equal to an irreversibly inactivated protein, which loses all functions and in most of the cases a reverse folding is impossible [177,178].

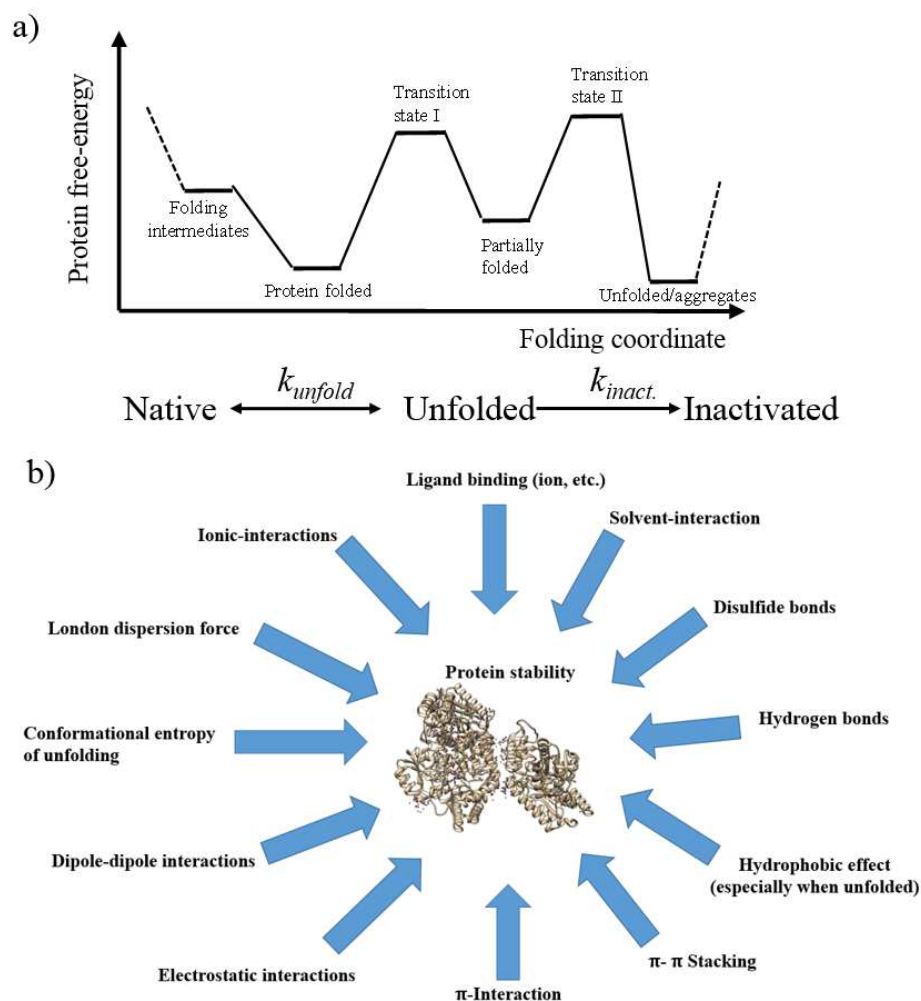


Figure 1.14 Chemo-physical forces contributing to protein stability. a) The sum of the stabilizing energies forms a local/global energy minimum (folded state) [178]. When a protein unfolds, it changes to a new energy minimum. If further denaturation occurs, the protein can be irreversibly inactivated and reaches again a new stable energy minimum. b) Influences on protein stability. (Hypothetic protein structure was visualized using Chimera 1.1)

According to the equation in **figure 1.14**, the first term is described as thermodynamic stability with the constant of unfolding (k_{unfold}). From this hypothetic unfolded state the protein can be undergo a transition to an inactivated state to form aggregates. The resistance to get inactivated is described as kinetic stability. Factors that support unfolding and denaturation of enzymes are e.g. heat, solvent-stress, ion concentrations or pH-value. The solvent (aqueous or organic) is directly responsible for protein stability and moreover the concentration of ions (salts) can be important in respect of stability [179,180]. Enzymes are naturally adapted to aqueous solutions, but some of them are also active and stable in organic solutions. An important parameter for the stability of enzymes in organic solvents is the water activity (a_w), since water molecules are elementarily important for the protein structure. The water molecules are indispensable for the structure of proteins, because they are tightly bound by the protein and build a shell around the protein, which maintains the functional structure in an organic solvent [94]. Moreover also the

pH-value has a large influence on the protein surface charge, which is important for the solubility, stability and for the intermolecular interactions of a protein. In general, proteins show the highest stability at their isoelectric point. Depending on the pH value, proteins are either protonated or deprotonated, therefore the charge of the protein also changes. Furthermore the force of repulsion (between two charged molecules/proteins) is increased [181]. In contrast to the surface, the protein core is mostly hydrophobic and stabilizes the polypeptide chain by the hydrophobic effect and other forces. This means that hydrophobic amino acid residues move away from the water and thus stabilize the folded state by formation of a hydrophobic core. The temperature of the protein containing system is very important towards the stability of the enzyme, if the temperature is increased, the energy of the protein increases and results in faster and stronger motions of protein parts (kinetic energy is increased). If these molecular kinetic energy is strong enough to expose the hydrophobic core, it will be interacting with solvent molecules and the refolding of the protein will become unlikely. The unlikely refolding is caused by the interactions of the protein backbone with water molecules (or solvent molecules) and thus prevents the formation of secondary structural elements such as helices, coils and sheets [181]. The main forces leading to the formation of a rigid enzyme are hydrogen bridge formation and the hydrophobic effect. However, hydrophobic effect seems to be the most important factor for stability [182–184]. By contrast within the protein-chain only 36 % of the stabilizing bonds are side-chain interactions, the majority are backbone interactions, which are decisive for stability [145].

Moreover, the entropy of the protein is important in regards to the stability. For example glycine residue show the highest entropy of all amino acid residues, because the degree of freedom (movement) is higher than for all other standard α -amino acids. In contrast, a proline residue shows the least entropy value, because the degree of freely selectable conformation states is lower than for all other α -amino acids [185]. Also electrostatic interactions (coulombic energy) between positive and negative charged amino acid residues are important for the stability and can act in distances of even more than 4 Å up to 6 Å (e.g. between L-glutamate and L-arginine-residues) [181,186]. Although Van-der-Waals interaction energies are quite low, the sum of all interactions contributes also to protein stability [187,188]. Furthermore the interactions with solvent molecules by Van-der-Waals forces can also stabilize proteins [187,188]. This kind of interactions can be a target for engineering experiments to increase the stability of enzymes. Therefore *in-silico* approaches like the mentioned force field algorithm FoldX are applied by exchanging amino acid residues, which is presented in detail in chapter 4. Besides the theoretical calculation of protein stability, this can also be determined experimentally by

determination of the physical melting point of proteins using circular dichroism spectra or thermal shift assays [189,190].

1.4.1.1) Protein melting point

The protein melting point (T_m) can be utilized as measure for stability, which can be detected using laboratory equipment like qPCR-devices. The T_m is the temperature at which the amount of folded and unfolded protein is equal. Moreover, the free energy change ΔG is 0 at T_m . If the stability of a protein changes, its T_m will also shift, as it describes the temperature at which the protein unfolding rate is highest. Therefore, the melting point can be also described as a function of variation of enthalpy (ΔH) between folded/unfolded state and as function of heat capacity (C_p) of the protein (known as Gibbs-Helmholtz equation) [191].

$$\Delta G(T) = \Delta H_m \left(1 - \frac{T}{T_m}\right) - \Delta C_p \left[(T_m - T) + T \ln \left(\frac{T}{T_m}\right) \right]$$

To determine the T_m value, the isolated protein is heated at a constant rate in a solution with a protein dye, such as SYPRO orange, and the shift in fluorescence intensity is recorded e.g. with a real-time PCR cycler [192]. The increase in fluorescence intensity is due to the fact that the fluorescence dye can interact with amino acid residues from the mostly hydrophobic protein core, when it gets exposed to the solvent. The fluorescence intensity of SYPRO orange is strongly quenched in presence of water [192]. In contrast, the increased number of dye-protein complex number results in drastic increase of fluorescence enhancement (increase of the fluorescence quantum yield) of up to ~500 fold [193]. After complete denaturation, the fluorescence intensity decreases again because the now emerging protein aggregates have a smaller solvent exposed surface area than the unfolded proteins. The function of denaturation can be described as a sigmoidal curve [194](**Figure 1.15**).

When the fluorescence intensity curve is plotted against the time, the inflection point marks the T_m at that equilibrium state, where the amount of unfolded and folded protein is equal [192]. The T_m is calculated by fitting the fluorescence intensity against temperature under variation of parameters of a sigmoidal function. When the parameterized function is used, the turning point (highest slope) of this function represents the T_m of the protein.

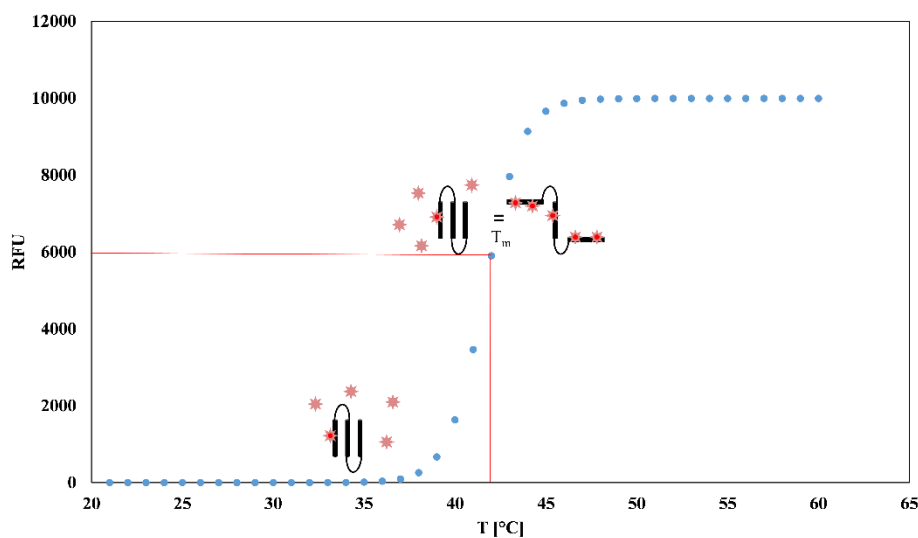


Figure 1.15 Determination of the protein melting point using thermal shift assay with protein fluorescence dye (Protein is symbolized by a black β -sheet). Not shown is the decrease of relative fluorescence intensity (RFU) after complete denaturation of the protein. The decrease is caused by protein aggregation, which reduces the protein surface again (with increasing temperature and increasing incubation time).

In addition to SYPRO orange, also the fluorescence dyes dapoxyl sulfonic acid or anilino-8-naphthalene sulfonate can be utilized [192]. The present thesis describes protein engineering applications to increase the T_m . Therefore two main approaches were performed and discussed within this thesis. As first approach for improvement of thermostability was the FoldX guided site directed mutagenesis chosen. As an alternative the disulfide bridge engineering was evaluated.

1.4.1.2) Disulfide bridge engineering

Disulfide bridges are covalent bonds, which are important for stabilization of the protein structure and therefore also the enzyme function. Proteins with disulfide bonds can be more resistant against destructive forces e.g. during industrial processes or in respect to proteolytic degradation [195–197]. Examples of proteins with natural disulfide bridges of particular importance for commercial applications are the protein products Insulin, Pectinase, Pepsin, Papain and lytic polysaccharide monooxygenases which are containing at least three disulfide bridges [195,198]. Moreover, disulfide bonds are quite beneficial for stability, because the bond between the sulfur atoms of cysteine(s) is a strong covalent bond and allows therefore the fixation of structural protein domains. Disulfide bonds are highly energy stabilizing and reduce the content of free energy between 10 kJ mol^{-1} and up to 21.7 kJ mol^{-1} [199,200]. To introduce artificial disulfide bonds, Wijma *et al.* created a disulfide-engineering algorithm, called DDD. This algorithm uses MD-simulations to gain conformational information about the protein backbone movement and analyses the distances between possible disulfide bond positions. The cut-off value for the maximal distance between cysteine-residues was defined to be maximal 7 \AA . To avoid disulfide bonds between direct neighbors (at possible disulfide sites) a minimal distance was set of 15 amino acid positions in the primary sequence. The remaining engineering sites were analyzed by conformational simulations to define the position of the introduced cysteine residue according to the dihedrals angles of the selected residues. In addition to the MD simulation itself, additional energy calculations are carried out to be able to measure the change in stability and therefore to select predicted variants. According to those tools they reduced the number of engineering sites from 28 possible engineering sites to only 17. For these sites they performed site directed mutagenesis to introduce cysteine residues. Of those 17 engineering sites, 10 were stabilizing and showed a stability improvement of 4 to 15°C according to the protein-melting point (T_m) [199]. This study demonstrated clearly that artificial disulfide bonds can drastically improve the protein stability. In earlier studies the T4-lysozyme was the subject of disulfide bridge engineering even without any MD-simulations. Improvements of up to 11°C (ΔT_m) for single disulfide bridges were achieved [201]. However, even higher stability changes were reported for multiple disulfide bridges: In T4-lysozyme a ΔT_m of $+23.4^\circ\text{C}$ was achieved by Matsumura *et al.* [202]. In contrast, it was also demonstrated that not every disulfide bond results in a stabilized protein. There exist also examples, which are reporting a decrease of protein stability [200]. Furthermore, MD-simulations and energy calculations are helpful to increase the success rate by site directed mutagenesis experiments. These artificial disulfide bonds can also be combined with stabilizing point mutants to create

enzyme variants with even higher thermostability. Wijma *et al.* demonstrated this at the example of thermostability improvement of a limone-1,2-epoxide hydrolase, which showed a ΔT_m improvement of 35°C. The enzyme activity of the wild-type enzyme was slightly higher than that of the mutants at 50°C, but at 60°C the mutants showed four times the total enzymatic activity of the wild-type (at 50°C), while the wild-type variant even lost its activity [199].

1.4.2) Outlook of enzyme engineering

In summary, the applicability of enzymes for industrial purposes is a multidimensional challenge. On the one hand, the cost-efficiency of an enzymatic process depends significantly on the long-term activity and reusability of the enzyme. A possible strategy is therefore to stabilize enzymes against external influences by targeted mutagenesis (This problem is discussed in **Chapter 4**). On the other hand, the targeted design of enzymes for specific synthesis approaches is primarily a problem based on the knowledge content of an enzyme family. For this reason, targeted protein mutation processes require a broad knowledge base (database) that enables the transfer of knowledge from literature to the target enzyme. This can be achieved in the form of protein engineering databases described in **Chapter 3** for ω -TA. Finally, such predictions have to be evaluated by experiments on the enzyme in order to finally obtain a biocatalyst with the desired properties. This is described exemplarily in more detail in **Chapter 5**. However, if such approaches do not lead to the desired success, a change in the synthesis strategy or search for new enzymes becomes necessary to solve the problem, which is exemplified in **Chapter 6**. Modern non-random-based enzyme engineering covers all these levels to ultimately obtain the desired enzyme.

1.5) References chapter 1

1. Elsila JE, Glavin DP, Dworkin JP. Cometary glycine detected in samples returned by Stardust. *Meteorit Planet Sci.* Blackwell Publishing Ltd; 2009;44: 1323–1330. doi:10.1111/j.1945-5100.2009.tb01224.x
2. Burton AS, Stern JC, Elsila JE, Glavin DP, Dworkin JP. Understanding prebiotic chemistry through the analysis of extraterrestrial amino acids and nucleobases in meteorites. *Chem Soc Rev.* The Royal Society of Chemistry; 2012;41: 5459. doi:10.1039/c2cs35109a
3. Weiner B. *New Methods towards the Synthesis of β -Amino Acids.* Rijksuniversiteit Groningen. 2009.
4. Hermann T. Industrial production of amino acids by coryneform bacteria. *J Biotechnol.* 2003;104: 155–172. doi:10.1016/S0168-1656(03)00149-4
5. Sanda F, Endo T. Syntheses and functions of polymers based on amino acids. *Macromol Chem Phys.* WILEY-VCH Verlag GmbH; 1999;200: 2651–2661. doi:10.1002/(sici)1521-3935(19991201)200:12
6. Hickling D, Guenter W, Jackson ME. The Effects of Dietary Methionine and Lysine on Broiler Chicken Performance and Breast Meat Yield. *Can J Anim Sci.* NRC Research Press Ottawa, Canada; 1990;70: 673–678. doi:10.4141/cjas90-079
7. Sergio Sanchez, Romina Rodríguez-Sanoja AR& ALD. Our microbes not only produce antibiotics, they also overproduce amino acids. *J Antibiot (Tokyo).* 2017; doi:10.1038/ja.2017.142
8. Swain BK, Johri TS. Effect of supplemental methionine, choline and their combinations on the performance and immune response of broilers. *Br Poult Sci.* Taylor & Francis Group; 2000;41: 83–88. doi:10.1080/00071660086457
9. Park SH, Kim HU, Kim TY, Park JS, Kim S-S, Lee SY. Metabolic engineering of *Corynebacterium glutamicum* for L-arginine production. *Nat Commun.* Nature Publishing Group; 2014;5: 4618. doi:10.1038/ncomms5618
10. Strecker A. Über die künstliche Bildung der Milchsäure und einen neuen, dem Glycocoll homologen Körper. *Justus Liebigs Ann Chem.* WILEY-VCH Verlag; 1850;75: 27–45. doi:10.1002/jlac.18500750103
11. Seebach D, Matthews J. β -Peptides: a surprise at every turn. *Chem Commun.* 1997; 2015–2022.
12. Juaristi E, Soloshonok VA. *Enantioselective Synthesis of β -Amino Acids.* Enantioselective Synthesis of β -Amino Acids: Second Edition. Hoboken, NJ, USA: John Wiley & Sons, Inc; 2005. doi:10.1002/0471698482
13. Dold S-M. *Enzymatic Synthesis and Microbial Degradation of β -Amino Acids via Transaminases.* Karlsruhe Institute for Technology. 2016. doi:10.5445/IR/1000067988
14. Mittendorf J, Kunisch F, Matzke M, Miltzer H, Schmidt A, Scho W. Novel Antifungal -Amino Acids : Synthesis and Activity Against *Candida albicans*. *Bioorg Med Chem Lett.* Pergamon; 2003;13: 433–436. doi:10.1016/S0960-894X(02)00958-7
15. Kiss L, Mándity IM, Fülöp F. Highly functionalized cyclic β -amino acid moieties as promising scaffolds in peptide research and drug design. *Amino Acids.* Springer Vienna; 2017;49: 1441–1455. doi:10.1007/s00726-017-2439-9
16. Farmer LJ, Clark MP, Boyd MJ, Perola E, Jones SM, Tsai A, et al. Discovery of Novel, Orally Bioavailable β -Amino Acid Azaindole Inhibitors of Influenza PB2. *ACS Med Chem Lett.* American Chemical Society; 2017;8: 256–260. doi:10.1021/acsmchemlett.6b00486
17. Vachal P, Raheem I, Guo Z, Hartingh TJ. Antiviral beta-amino acid ester phosphodiamide compounds. WO/2017/027434, 2017. Available: <https://patentscope.wipo.int/search/en/detail.jsf?docId=WO2017027434>
18. Del Borgo MP, Kulkarni K, Aguilar M-I. Using β -Amino Acids and β -Peptide Templates to Create Bioactive Ligands and Biomaterials. *Curr Pharm Des.* 2017;23. doi:10.2174/138161282366617061608301
19. Gach-Janczak K, Pieknielna-Ciesielska J, Adamska-Bartłomiejczyk A, Perlikowska R, Kruszyński R, Kluczyk A, et al. Synthesis and activity of opioid peptidomimetics with β^2 - and β^3 -amino acids. *Peptides.* Elsevier; 2017;95: 116–123. doi:10.1016/j.peptides.2017.07.015
20. Núñez-Toldrà R, Dosta P, Montori S, Ramos V, Atari M, Borrós S. Improvement of osteogenesis in dental pulp pluripotent-like stem cells by oligopeptide-modified poly(β -amino ester)s. *Acta Biomaterialia.* Elsevier; 2016: 152–164. doi:10.1016/j.actbio.2017.01.077
21. Wani NA, Gurpreet Singh, Shankar S, Sharma A, Katoch M, Rai R. Short hybrid peptides incorporating β - and γ -amino acids as antimicrobial agents. *Peptides.* Elsevier; 2017;97: 46–53. doi:10.1016/J.PEPTIDES.2017.09.016
22. Fortin PD, Walsh CT, Magarvey NA. A transglutaminase homologue as a condensation catalyst in antibiotic assembly lines. *Nature.* Nature Publishing Group; 2007;448: 824–827. doi:10.1038/nature06068
23. Fredenhagen A, Tamura SY, Kenny PTM, Komura H, Naya Y, Nakanishi K, et al. Andrimid, a new peptide antibiotic produced by an intracellular bacterial symbiont isolated from a brown planthopper. *J Am Chem Soc.* American Chemical Society; 1987;109: 4409–4411. doi:10.1021/ja00248a055
24. Bubb MR. Effects of Jaspilkinolide on the Kinetics of Actin Polymerization. An Explanation For Certain In Vivo Observations. *J Biol Chem.* 2000;275: 5163–5170. doi:10.1074/jbc.275.7.5163
25. Langer Rs, Lynn Dm, Putnam Da, Amiji Mm, Anderson Dg. Biodegradable poly (beta-amino esters) and uses thereof. 140-217-600-396-269. 2015;US: B2. Available: <https://www.google.com/patents/US9700627>
26. Rui Y, Quiñones G, Green JJ. Biodegradable and bioreducible poly(beta-amino ester) nanoparticles for intracellular delivery to treat brain cancer. *AIChE J.* 2017;63: 1470–1482. doi:10.1002/aic.15698
27. Sugawara T, Tanaka A, Tanaka K, Nagai K, Suzuki K, Suzuki T, et al. YM-170320, a Novel Lipopeptide Antibiotic Inducing Morphological Change of Colonies in a Mutant of *Candida tropicalis* pK233. *J Antibiot (Tokyo).* 1998;51: 435–438. doi:http://dx.doi.org/10.7164/antibiotics.51.435
28. Suzuki K, Nagao K, Monnai Y, Yagi A, Uyeda M. Topostatin, a novel inhibitor of topoisomerases I and II produced by *Thermomonospora alba* strain No. 1520. I. Taxonomy, fermentation, isolation and biological activities. *J Antibiot (Tokyo).* 1998;51: 991–8. Available: <http://www.ncbi.nlm.nih.gov/pubmed/9918391>
29. Shiono Y, Tsuchinari M, Shimanuki K, Miyajima T, Murayama T, Koseki T, et al. Fusaristatins A and B, Two New Cyclic Lipopeptides from an Endophytic *Fusarium* sp. *J Antibiot (Tokyo).* 2007;60: 309–316. doi:10.1038/ja.2007.39
30. Sugawara T, Tanaka A, Tanaka K, Nagai K, Suzuki K, Suzuki T, et al. pale yellowish brown. The strain produced no reproductive structures even on sterilized natural substrates. The absence of morphological characteristics implied that. 51.
31. Ziegelbauer K, Babczinski P, Schönfeld W. Molecular mode of action of the antifungal beta-amino acid BAY 10-8888. *Antimicrob Agents Chemother.* American Society for Microbiology; 1998;42: 2197–205. Available: <http://www.ncbi.nlm.nih.gov/pubmed/9736535>
32. Kundu S, Jha S, Ghosh B. *Metabolic Engineering for Improving*

- Production of Taxol. Reference Series in Phytochemistry. Springer International Publishing; 2017. pp. 463–484. doi:10.1007/978-3-319-28669-3_29
33. Malik S, Cusidó RM, Mirjalili MH, Moyano E, Palazón J, Bonfill M. Production of the anticancer drug taxol in *Taxus baccata* suspension cultures: A review. *Process Biochemistry*. Elsevier; 2011. pp. 23–34. doi:10.1016/j.procbio.2010.09.004
 34. Dwivedi N, Shah J, Mishra V, Mohd Amin MCI, Iyer AK, Tekade RK, et al. Dendrimer-mediated approaches for the treatment of brain tumor. *J Biomater Sci Polym Ed*. Taylor & Francis; 2016;27: 557–580. doi:10.1080/09205063.2015.1133155
 35. Thornburg CK, Walter T, Walker KD. Biocatalysis of a Paclitaxel Analogue: Conversion of Baccatin III to N-(2-benzoyl-2-(2-furoyl)paclitaxel and Characterization of an Amino Phenylpropanoyl CoA Transferase. *Biochemistry*. American Chemical Society; 2017;56: acs.biochem.7b00912. doi:10.1021/acs.biochem.7b00912
 36. Li S, Fu C, Zhang M, Zhang Y, Xie S, Yu L. Enhancing Taxol Biosynthesis by Overexpressing a 9-Cis-Epoxycarotenoid Dioxygenase Gene in Transgenic Cell Lines of *Taxus chinensis*. *Plant Mol Biol Report*. Springer-Verlag; 2012;30: 1125–1130. doi:10.1007/s11105-012-0436-4
 37. Talebi M, Ghassempour A, Talebpour Z, Rassouli A, Dolatyari L. Optimization of the extraction of paclitaxel from *Taxus baccata* L. by the use of microwave energy. *J Sep Sci*. WILEY-VCH Verlag; 2004;27: 1130–1136. doi:10.1002/jssc.200401754
 38. Prasain JK, Stefanowicz P, Kiyota T, Habeichi F, Konishi Y. Taxines from the needles of *Taxus wallichiana*. *Phytochemistry*. 2001;58: 1167–1170. doi:10.1016/S0031-9422(01)00305-3
 39. Witherup KM, Look SA, Stasko MW, Ghiorzi TJ, Muschik GM, Cragg GM. *Taxus* spp. Needles contain amounts of taxol comparable to the bark of *Taxus brevifolia*: Analysis and isolation. *J Nat Prod*. 1990;53: 1249–1255. doi:10.1021/np50071a017
 40. Tabata H. Paclitaxel Production by Plant-Cell-Culture Technology. Springer, Berlin, Heidelberg; 2004. pp. 1–23. doi:10.1007/b13538
 41. Bringi V, Kadkade PG, Prince CL, Roach BL. Enhanced production of taxol and taxanes by cell cultures of *Taxus* species.. U.S. 2007. p. 48pp., Cont. of U.S. Ser. No. 653,036. Available: <https://www.google.com/patents/US7264951>
 42. Birch M, Challenger S, Crochard JP, Fradet D, Jackman H, Luan A, et al. The development of a practical multikilogram synthesis of the chiral β -amino acid imagabalin hydrochloride (PD-0332334) via asymmetric hydrogenation. *Org Process Res Dev*. American Chemical Society; 2011;15: 1172–1177. doi:10.1021/op2001639
 43. Midelfort KS, Kumar R, Han S, Karmilowicz MJ, McConnell K, Gehlhaar DK, et al. Redesigning and characterizing the substrate specificity and activity of *Vibrio fluvialis* aminotransferase for the synthesis of imagabalin. *Protein Eng Des Sel*. 2013;26: 25–33. doi:10.1093/protein/gzs065
 44. Nugent TC, El-Shazly M. Chiral amine synthesis - Recent developments and trends for enamide reduction, reductive amination, and imine reduction. *Advanced Synthesis and Catalysis*. WILEY-VCH Verlag; 2010. pp. 753–819. doi:10.1002/adsc.200900719
 45. Matsumura K, Saito T. Asymmetric reductive amination of keto acid derivatives for producing amino acid derivatives. EP20040773427, 2004. Available: <https://patents.google.com/patent/EP2100875B1>
 46. Glueck DS. Catalytic asymmetric synthesis of chiral phosphanes. *Chem Eur J*. 2008;14: 7108–17. doi:10.1002/chem.200800267
 47. Grayson JI, Roos J, Osswald S. Development of a Commercial Process for (*S*)- β -Phenylalanine. *Org Process Res Dev*. American Chemical Society; 2011;15: 1201–1206. doi:10.1021/op200084g
 48. Roberts E, Ayengar P, Posner I. Transamination of gamma-aminobutyric acid and beta-alanine in microorganisms. *J Biol Chem*. American Society for Biochemistry and Molecular Biology; 1953;203: 195–204.
 49. Yonaha K, Toyama S, Yasuda M, Soda K. Purification and crystallization of bacterial ω -amino acid-pyruvate aminotransferase. *FEBS Lett*. Wiley-Blackwell; 1976;71: 21–24. doi:10.1016/0014-5793(76)80889-7
 50. Yonaha K, Suzuki K, Minei H, Toyama S. Distribution of ω -amino acid: Pyruvate transaminase and aminobutyrate: α -ketoglutarate transaminase in microorganisms. *Agric Biol Chem*. Japan Society for Bioscience, Biotechnology, and Agrochemistry; 1983;47: 2257–2265. doi:10.1080/00021369.1983.10865941
 51. Yun H, Lim S, Cho B-K, Kim B-G. omega-Amino acid:pyruvate transaminase from *Alcaligenes denitrificans* Y2k-2: a new catalyst for kinetic resolution of beta-amino acids and amines. *Appl Environ Microbiol*. American Society for Microbiology; 2004;70: 2529–34. doi:10.1128/AEM.70.4.2529-2534.2004
 52. Kim J, Kyung D, Yun H, Cho BK, Seo JH, Cha M, et al. Cloning and characterization of a novel β -transaminase from *Mesorhizobium* sp. strain LUK: A new biocatalyst for the synthesis of enantiomerically pure β -amino acids. *Appl Environ Microbiol*. American Society for Microbiology; 2007;73: 1772–1782. doi:10.1128/AEM.02119-06
 53. Wybenga GG, Crismaru CG, Janssen DB, Dijkstra BW. Structural determinants of the β -selectivity of a bacterial aminotransferase. *J Biol Chem*. 2012;287: 28495–28502. doi:10.1074/jbc.M112.375238
 54. Crismaru CG, Wybenga GG, Szymanski W, Wijma HJ, Wu B, Bartsch S, et al. Biochemical Properties and Crystal Structure of a β -Phenylalanine Aminotransferase from *Variovorax paradoxus*. *Appl Environ Microbiol*. 2013;79: 185–195. doi:10.1128/AEM.02525-12
 55. Mathew S, Jeong SS, Chung T, Lee SH, Yun H. Asymmetric synthesis of aromatic β -amino acids using ω -transaminase: Optimizing the lipase concentration to obtain thermodynamically unstable β -keto acids. *Biotechnol J*. 2016;11: 185–190. doi:10.1002/biot.201500181
 56. Mathew S, Nadarajan SP, Sundaramoorthy U, Jeon H, Chung T, Yun H. Biotransformation of β -keto nitriles to chiral (*S*)- β -amino acids using nitrilase and ω -transaminase. *Biotechnol Lett*. Springer Netherlands; 2016; doi:10.1007/s10529-016-2271-4
 57. Zhang Z-J, Cai R-F, Xu J-H. Characterization of a new nitrilase from *Hoeflea phototrophica* DFL-43 for a two-step one-pot synthesis of (*S*)- β -amino acids. *Appl Microbiol Biotechnol*. Springer Berlin Heidelberg; 2018; 1–10. doi:10.1007/s00253-018-9057-7
 58. Shin JS, Kim BG. Kinetic modeling of ω -transamination for enzymatic kinetic resolution of α -methylbenzylamine. *Biotechnol Bioeng*. Wiley Subscription Services, Inc., A Wiley Company; 1998;60: 534–540. doi:10.1002/(SICI)1097-0290(19981205)60:5
 59. Shin JS, Kim BG. Asymmetric synthesis of chiral amines with ω -transaminase. *Biotechnol Bioeng*. 1999;65: 206–211. doi:10.1002/(SICI)1097-0290(19991020)65:2
 60. Logue MW, Pollack RM, Vitullo VP. Nature of the transition state for the decarboxylation of β -keto acids. *J Am Chem Soc*. 1975;97: 6868–6869. doi:10.1021/ja00856a047
 61. Bach RD, Canepa C. Electronic factors influencing the decarboxylation of β -keto acids. A model enzyme study. *J Org Chem*. 1996;61: 6346–6353. doi:10.1021/jo960356m
 62. Hanson RW. Decarboxylation of α keto acids. *J Chem Educ*. Division of Chemical Education; 1987;64: 591. doi:10.1021/ed064p591

63. Midelfort KS, Kumar R, Han S, Karmilowicz MJ, McConnell K, Gehlhaar DK, et al. Redesigning and characterizing the substrate specificity and activity of *Vibrio fluvialis* aminotransferase for the synthesis of imagabalin. *Protein Eng Des Sel.* 2013;26: 25–33. doi:10.1093/protein/gzs065
64. Needham DM. A quantitative study of succinic acid in muscle. Glutamic and aspartic acids as precursors. *Biochem J.* Portland Press Ltd; 1930;24: 208–227.
65. Braunstein AE. The Enzyme System of Trans-Amination, its Mode of Action and Biological Significance. *Nature.* Nature Publishing Group; 1939;143: 609–610. doi:10.1038/143609a0
66. Cohen P. Transamination With Purified Enzyme Preparations (Transaminase). *J Biol Chem. A;* 1940;136: 565.
67. Kritzman Mg. The Enzyme System Transferring the Amino-Group of Aspartic Acid. *Nature.* Nature Publishing Group; 1939;143: 603–604. doi:10.1038/143603a0
68. Taylor PP, Pantaleone DP, Senkpeil RF, Fotheringham IG. Novel biosynthetic approaches to the production of unnatural amino acids using transaminases. *Trends Biotechnol.* 1998;16: 412–418. doi:10.1016/S0167-7799(98)01240-2
69. Savile CK, Janey JM, Mundorff EC, Moore JC, Tam S, Jarvis WR, et al. Biocatalytic Asymmetric Synthesis of Chiral Amines from Ketones Applied to Sitagliptin Manufacture. *Science (80-).* 2010;329: 305–309.
70. Yonaha K, Toyama S, Yasuda M, Soda K. Properties of crystalline (γ -amino acid: Pyruvate aminotransferase of *Pseudomonas* sp. f-126. *Agric Biol Chem.* Taylor & Francis; 1977;41: 1701–1706. doi:10.1080/00021369.1977.10862739
71. Huisman GW, Collier SJ. On the development of new biocatalytic processes for practical pharmaceutical synthesis. *Current Opinion in Chemical Biology.* Elsevier Current Trends; 2013. pp. 284–292. doi:10.1016/j.cbpa.2013.01.017
72. Burnett G, Yonaha K, Toyama S, Soda K, Walsh C. full-text. *J Biol Chem.* 1980;255: 428–432.
73. Slabu I, Galman JL, Iglesias C, Weise NJ, Lloyd RC, Turner NJ. n-Butylamine as an alternative amine donor for the stereoselective biocatalytic transamination of ketones. *Catalysis Today.* Elsevier; 28 Jan 2016. doi:10.1016/j.cattod.2017.01.025
74. Galman JL, Slabu I, Weise NJ, Iglesias C, Parmeggiani F, Lloyd RC, et al. Biocatalytic transamination with near-stoichiometric inexpensive amine donors mediated by bifunctional mono- and di-amine transaminases. *Green Chem. Royal Society of Chemistry;* 2017;19: 361–366. doi:10.1039/C6GC02102F
75. Weiß MS, Pavlidis I V., Spurr P, Hanlon SP, Wirz B, Iding H, et al. Protein-engineering of an amine transaminase for the stereoselective synthesis of a pharmaceutically relevant bicyclic amine. *Org Biomol Chem. Royal Society of Chemistry;* 2016;14: 10249–10254. doi:10.1039/C6OB02139E
76. Guo F, Berglund P. Transaminase Biocatalysis: Optimization and Application. *Green Chem. Royal Society of Chemistry;* 2016; 333–360. doi:10.1039/C6GC02328B
77. Slabu I, Galman JL, Lloyd RC, Turner NJ. Discovery, Engineering and Synthetic Application of Transaminase Biocatalysts. *ACS Catal.* 2017; aescatal.7b02686. doi:10.1021/acscatal.7b02686
78. Steffen-Munsberg F, Vickers C, Kohls H, Land H, Mallin H, Nobili A, et al. Bioinformatic analysis of a PLP-dependent enzyme superfamily suitable for biocatalytic applications. *Biotechnol Adv. Elsevier Inc.;* 2015;33: 566–604. doi:10.1016/j.biotechadv.2014.12.012
79. Veiga-da-Cunha M, Hadi F, Balligand T, Stroobant V, Van Schaftingen E. Molecular identification of hydroxylysine kinase and of ammoniophosphorylases acting on 5-phosphohydroxy-L-lysine and phosphoethanolamine. *J Biol Chem. American Society for Biochemistry and Molecular Biology;* 2012;287: 7246–7255. doi:10.1074/jbc.M111.323485
80. Schneider G, Käck H, Lindqvist Y. The manifold of vitamin B6 dependent enzymes. *Structure.* Cell Press; 2000. pp. R1–R6. doi:10.1016/S0969-2126(00)00085-X
81. Percudani R, Peracchi A. The B6 database: a tool for the description and classification of vitamin B6-dependent enzymatic activities and of the corresponding protein families. *BMC Bioinformatics.* 2009;10: 273. doi:10.1186/1471-2105-10-273
82. Höhne M, Bornscheuer UT. Application of Transaminases. *Enzyme Catalysis in Organic Synthesis.* Weinheim, Germany: Wiley-VCH Verlag GmbH & Co. KGaA; 2012. pp. 779–820. doi:10.1002/9783527639861.ch19
83. Höhne M, Schätzle S, Jochens H, Robins K, Bornscheuer UT. Rational assignment of key motifs for function guides in silico enzyme identification. *Nat Chem Biol.* Nature Publishing Group; 2010;6: 807–813. doi:10.1038/nchembio.447
84. Kirsch JF, Eichele G, Ford GC, Vincent MG, Jansonius JN, Gehring H, et al. Mechanism of action of aspartate aminotransferase proposed on the basis of its spatial structure. *J Mol Biol. Academic Press;* 1984;174: 497–525. doi:10.1016/0022-2836(84)90333-4
85. Mehta PK, Hale TI, Christen P. Aminotransferases: demonstration of homology and division into evolutionary subgroups. *Eur J Biochem.* 1993;214: 549–561. doi:10.1111/j.1432-1033.1993.tb17953.x
86. Lueck JD, Fromm HJ. Analysis of exchange rates for the Ping Pong Bi Bi mechanism and the concept of substrate synergism. *FEBS Lett.* No longer published by Elsevier; 1973;32: 184–186. doi:10.1016/0014-5793(73)80767-7
87. Pettersen EF, Goddard TD, Huang CC, Couch GS, Greenblatt DM, Meng EC, et al. UCSF Chimera—A visualization system for exploratory research and analysis. *J Comput Chem. John Wiley & Sons, Inc.;* 2004;25: 1605–1612. doi:10.1002/jcc.20084
88. Richard JP, Amyes TL, Crueiras J, Rios A. Pyridoxal 5'-phosphate: electrophilic catalyst extraordinaire. *Curr Opin Chem Biol. Elsevier Current Trends;* 2009;13: 475–483. doi:10.1016/J.CBPA.2009.06.023
89. Zhan Z, Gupta D, Khan AA. Kinetics and mechanism of decarboxylation of aspartic acid with ninhydrin. *Int J Chem Kinet. John Wiley & Sons, Inc.;* 1992;24: 481–487. doi:10.1002/kin.550240508
90. Denesyuk AI, Denessiouk KA, Korpela T, Johnson MS. Phosphate group binding “cup” of PLP-dependent and non-PLP-dependent enzymes: Leitmotif and variations. *Biochimica et Biophysica Acta - Proteins and Proteomics.* 2003. pp. 234–238. doi:10.1016/S1570-9639(03)00057-8
91. Cassimjee KE, Humble MS, Miceli V, Colomina CG, Berglund P. Active site quantification of an ω -Transaminase by performing a half transamination reaction. *ACS Catal. American Chemical Society;* 2011;1: 1051–1055. doi:10.1021/cs200315h
92. Eliot AC, Kirsch JF. Pyridoxal phosphate enzymes: mechanistic, structural, and evolutionary considerations. *Annu Rev Biochem.* 2004;73: 383–415. doi:10.1146/annurev.biochem.73.011303.074021
93. Wybenga GG, Crismaru CG, Janssen DB, Dijkstra BW. Structural determinants of the β -selectivity of a bacterial Aminotransferase. *J Biol Chem.* 2012;287: 28495–28502. doi:10.1074/jbc.M112.375238
94. Faber K. *Biotransformations in Organic Chemistry.* Springer Berlin

- Heidelberg; 2011. doi:10.1007/978-3-642-17393-6
95. Bajić M, Plazl I, Stloukal R, Žnidarišič-Plazl P. Development of a miniaturized packed bed reactor with ω -transaminase immobilized in LentiKats®. *Process Biochem.* Elsevier; 2017;52: 63–72. doi:10.1016/j.PROCBIO.2016.09.021
96. Stloukal R, Watzková J, Turková K. Biocatalysis: An Industrial Perspective. de Gonzalo G, Domínguez de María P, editors. The Royal Society of Chemistry; 2018. doi:10.1039/9781782629993
97. Dold S-M, Cai L, Rudat J. One-step purification and immobilization of a β -amino acid aminotransferase using magnetic (M-PVA) beads. *Eng Life Sci. Wiley-Blackwell*; 2016;16: 568–576. doi:10.1002/elsc.201600042
98. Truppo MD, David Rozzell J, Turner NJ. Efficient production of enantiomerically pure chiral amines at concentrations of 50 g/L using transaminases. *Org Process Res Dev.* American Chemical Society; 2010;14: 234–237. doi:10.1021/op900303q
99. Truppo MD, Rozzell JD, Moore JC, Turner NJ. Rapid screening and scale-up of transaminase catalyzed reactions. *Org Biomol Chem.* Royal Society of Chemistry; 2009;7: 395–398. doi:10.1039/B817730A
100. Höhne M, Kühl S, Robins K, Bornscheuer UT. Efficient asymmetric synthesis of Chiral amines by combining transaminase and pyruvate decarboxylase. *ChemBioChem.* WILEY-VCH Verlag; 2008;9: 363–365. doi:10.1002/cbic.200700601
101. Green AP, Turner NJ, O'Reilly E. Chiral amine synthesis using ω -transaminases: An amine donor that displaces equilibria and enables high-throughput screening. *Angew Chemie - Int Ed.* WILEY-VCH Verlag; 2014;53: 10714–10717. doi:10.1002/anie.201406571
102. Dold SM, Syldatk C, Rudat J. Transaminases and their Applications. *Green Biocatalysis.* Hoboken, NJ: John Wiley & Sons, Inc; 2016. pp. 715–746. doi:10.1002/9781118828083.ch29
103. Tufvesson P, Lima-Ramos J, Jensen JS, Al-Haque N, Neto W, Woodley JM. Process considerations for the asymmetric synthesis of chiral amines using transaminases. *Biotechnology and Bioengineering.* Wiley Subscription Services, Inc., A Wiley Company; 2011. pp. 1479–1493. doi:10.1002/bit.23154
104. Han SW, Shin JS. Metabolically driven equilibrium shift of asymmetric amination of ketones by ω -transaminase using alanine as an amino donor. *Biosci Biotechnol Biochem.* Taylor & Francis; 2014;78: 1788–1790. doi:10.1080/09168451.2014.930328
105. Simon RC, Grischek B, Zepeck F, Steinreiber A, Belaj F, Kroutil W. Regio- and stereoselective monoamination of diketones without protecting groups. *Angew Chemie - Int Ed.* WILEY-VCH Verlag; 2012;51: 6713–6716. doi:10.1002/anie.201202375
106. K Korn BC, Dixon JE, Bruice TC. Comparison of the Rate Constants for General Base Catalyzed Prototropy and Racemization of the Aldimine Species Formed from 3-Hydroxypyridine-4-carboxaldehyde and Alanine. *Biochemistry.* 1973;248: 599–230. Available: <http://pubs.acs.org/doi/pdf/10.1021/bi00747a031>
107. Limanto J, Ashley ER, Yin J, Beutner GL, Grau BT, Kassim AM, et al. A highly efficient asymmetric synthesis of vernakalant. *Org Lett.* American Chemical Society; 2014;16: 2716–2719. doi:10.1021/ol501002a
108. Dobrev D, Hamad B, Kirkpatrick P. Vernakalant. *Nature Reviews Drug Discovery.* 2010. pp. 915–916. doi:10.1038/nrd3323
109. Pedragosa-Moreau S, Le Flohic A, Thienpondt V, Lefoulon F, Petit AM, Ríos-Lombardía N, et al. Exploiting the Biocatalytic Toolbox for the Asymmetric Synthesis of the Heart-Rate Reducing Agent Ivabradine. *Adv Synth Catal.* 2017;359: 485–493. doi:10.1002/adsc.201601222
110. Yusuf S, Camm AJ. Sinus tachyarrhythmias and the specific bradycardic agents: a marriage made in heaven? *J Cardiovasc Pharmacol Ther.* 2003;8: 89–105. doi:10.1177/107424840300800202
111. Koszelewski D, Clay D, Faber K, Kroutil W. Synthesis of 4-phenylpyrrolidin-2-one via dynamic kinetic resolution catalyzed by ω -transaminases. *J Mol Catal B Enzym.* Elsevier; 2009;60: 191–194. doi:10.1016/j.molcatb.2009.05.006
112. Mano J, Ogawa J, Shimizu S. Microbial Production of Optically Active β -Phenylalanine through Stereoselective Degradation of Racemic β -Phenylalanine. *Biosci Biotechnol Biochem.* Japan Society for Bioscience, Biotechnology, and Agrochemistry; 2006;70: 1941–1946. doi:10.1271/bbb.60099
113. Weber N, Gorwa-Grauslund M, Carlquist M. Exploiting cell metabolism for biocatalytic whole-cell transamination by recombinant *Saccharomyces cerevisiae*. *Appl Microbiol Biotechnol.* Springer Berlin Heidelberg; 2014;98: 4615–4624. doi:10.1007/s00253-014-5576-z
114. Yun H, Cho BK, Kim BG. Kinetic resolution of (R,S)-sec-butylamine using omega-transaminase from *Vibrio fluvialis* JS17 under reduced pressure. *Biotechnol Bioeng.* Wiley Subscription Services, Inc., A Wiley Company; 2004;87: 772–778. doi:10.1002/bit.20186
115. Nohira H, Sakai K. Optical resolution by means of crystallization. *Enantiomer separation: Fundamentals and practical methods.* Dordrecht: Springer Netherlands; 2004. pp. 165–191. doi:10.1007/978-1-4020-2337-8_6
116. Yamamoto C, Okamoto Y. Resolution of enantiomers by High-Performance Liquid Chromatography. *Enantiomer Separation: Fundamentals and Practical Methods.* Dordrecht: Springer Netherlands; 2004. pp. 301–322. doi:10.1007/978-1-4020-2337-8_10
117. Zhang D, Chen X, Zhang R, Yao P, Wu Q, Zhu D. Development of β -amino acid dehydrogenase for the synthesis of β -amino acids via reductive amination of β -ketoacids. *ACS Catal.* American Chemical Society; 2015;5: 2220–2224. doi:10.1021/cs5017358
118. Vogel A, Schmiedel R, Hofmann U, Gruber K, Zangger K. Converting aspartase into a β -amino acid lyase by cluster screening. *ChemCatChem.* WILEY-VCH Verlag; 2014;6: 965–968. doi:10.1002/cctc.201300986
119. Clemente-Jiménez JM, Martínez-Rodríguez S, Rodríguez-Vico F, Heras-Vázquez FJL. Optically pure α -amino acids production by the “Hydantoine Process.” *Recent Pat Biotechnol.* 2008;2: 35–46. doi:10.2174/187220808783330947
120. Slomka C, Späth GP, Lemke P, Skoupi M, Niemeyer CM, Syldatk C, et al. Toward a cell-free hydantoine process: screening for expression optimization and one-step purification as well as immobilization of hydantoinease and carbamoylase. *AMB Express.* SpringerOpen; 2017;7: 122. doi:10.1186/s13568-017-0420-3
121. Slomka C, Zhong S, Fellinger A, Engel U, Syldatk C, Bräse S, et al. Chemical synthesis and enzymatic, stereoselective hydrolysis of a functionalized dihydropyrimidine for the synthesis of β -amino acids. *AMB Express.* Springer Berlin Heidelberg; 2015;5: 1–8. doi:10.1186/s13568-015-0174-8
122. Liljeblad A, Kanerva LT. Biocatalysis as a profound tool in the preparation of highly enantiopure β -amino acids. *Tetrahedron.* Pergamon; 2006. pp. 5831–5854. doi:10.1016/j.tet.2006.03.109
123. Groger H, Trauthwein H, Buchholz S, Drauz K, Sacherer C, Godfrin S, et al. The first aminoacylase-catalyzed enantioselective synthesis of aromatic beta-amino acids. *Org Biomol Chem.* Royal Society of Chemistry; 2004;2: 1977–8. doi:10.1039/b406380e
124. Hall BG, Salipante SJ, Barlow M. The metallo- β -lactamases fall into two

- distinct phylogenetic groups. *J Mol Evol*. Springer-Verlag; 2003;57: 249–254. doi:10.1007/s00239-003-2471-0
125. Mathew S, Bea H, Nadarajan SP, Chung T, Yun H. Production of chiral β -amino acids using ω -transaminase from *Burkholderia graminis*. *J Biotechnol*. Elsevier B.V.; 2015;196–197: 1–8. doi:10.1016/j.jbiotec.2015.01.011
126. Ogawa J, Mano J, Shimizu S. Microbial production of optically active β -phenylalanine ethyl ester through stereoselective hydrolysis of racemic β -phenylalanine ethyl ester. *Appl Microbiol Biotechnol*. Springer-Verlag; 2006;70: 663–669. doi:10.1007/s00253-005-0141-4
127. Weise NJ, Ahmed ST, Parmeggiani F, Turner NJ. Kinetic Resolution of Aromatic β -Amino Acids Using a Combination of Phenylalanine Ammonia Lyase and Aminomutase Biocatalysts. *Adv Synth Catal*. 2017;359: 1570–1576. doi:10.1002/adsc.201600894
128. Pavlidis I V., Weiß MS, Genz M, Spurr P, Hanlon SP, Wirz B, et al. Identification of (*S*)-selective transaminases for the asymmetric synthesis of bulky chiral amines. *Nat Chem*. Nature Publishing Group; 2016;8: 1–7. doi:10.1038/NCHEM.2578
129. Huisman GW, Collier SJ. On the development of new biocatalytic processes for practical pharmaceutical synthesis. *Current Opinion in Chemical Biology*. Elsevier Current Trends; 2013. pp. 284–292. doi:10.1016/j.cbpa.2013.01.017
130. Desai AA. Sitagliptin manufacture: A compelling tale of green chemistry, process intensification, and industrial asymmetric catalysis. *Angew Chemie - Int Ed*. WILEY-VCH Verlag; 2011;50: 1974–1976. doi:10.1002/anie.201007051
131. Janey JM. Development of A Sitagliptin Transaminase. *Sustainable Catalysis: Challenges and Practices for the Pharmaceutical and Fine Chemical Industries*. Hoboken, New Jersey: John Wiley & Sons, Inc.; 2013. pp. 75–87. doi:10.1002/9781118354520.ch04
132. Otte KB, Hauer B. Enzyme engineering in the context of novel pathways and products. *Current Opinion in Biotechnology*. Elsevier Current Trends; 2015. pp. 16–22. doi:10.1016/j.copbio.2014.12.011
133. Garske AL, Kapp G, McAuliffe J. *Industrial Enzymes and Biocatalysis*. Handbook of Industrial Chemistry and Biotechnology. 2017. p. 1625.
134. Malik MS, Park ES, Shin JS. Features and technical applications of ω -transaminases. *Applied Microbiology and Biotechnology*. Springer-Verlag; 2012. pp. 1163–1171. doi:10.1007/s00253-012-4103-3
135. Ferrandi EE, Monti D. Amine transaminases in chiral amines synthesis: recent advances and challenges. *World J Microbiol Biotechnol*. Springer; 2018;34. doi:10.1007/s11274-017-2395-2
136. Feng Y, Luo Z, Sun G, Chen M, Lai J, Lin W, et al. Development of an Efficient and Scalable Biocatalytic Route to (3*R*)-3-Aminoazepane: A Pharmaceutically Important Intermediate. *Org Process Res Dev*. American Chemical Society; 2017;21: 648–654. doi:10.1021/acs.oprd.7b00074
137. Frodsham L, Golden M, Hard S, Kenworthy MN, Klauber DJ, Leslie K, et al. Use of ω -transaminase enzyme chemistry in the synthesis of a JAK2 kinase inhibitor. *Org Process Res Dev*. 2013;17: 1123–1130. doi:10.1021/op400133d
138. Girardin M, Ouellet SG, Gauvreau D, Moore JC, Hughes G, Devine PN, et al. Convergent kilogram-scale synthesis of dual orexin receptor antagonist. *Org Process Res Dev*. American Chemical Society; 2013;17: 61–68. doi:10.1021/op3002678
139. Savile CK, Janey JM, Mundorff EC, Moore JC, Tam S, Jarvis WR, et al. Biocatalytic Asymmetric Synthesis of Chiral Amines from Ketones Applied to Sitagliptin Manufacture. *Science (80-)*. 2010;329: 305–309. doi:10.1126/science.1188934
140. Roland Barth, Kathrin Höferl-Prantz, Frank Richter GS. Novel Route of Synthesis for the Preparation of Suvorexant. US 20170217947 A1, 2015. Available: <https://www.google.com/patents/US20170217947>
141. Molinaro C, Bulger PG, Lee EE, Kosjek B, Lau S, Gauvreau D, et al. CRTH2 Antagonist MK-7246: A Synthetic Evolution from Discovery through Development. *J Org Chem*. American Chemical Society; 2012;77: 2299–2309. doi:10.1021/jo202620r
142. Sehl T, Hailes HC, Ward JM, Menyes U, Pohl M, Rother D. Efficient 2-step biocatalytic strategies for the synthesis of all nor(pseudo)ephedrine isomers. *Green Chem*. Royal Society of Chemistry; 2014;16: 3341–3348. doi:10.1039/C4GC00100A
143. Fersht A. Structure and mechanism in protein science. A guide to enzyme catalysis and protein folding. *Protein Science*. Cambridge University Press; 1999.
144. Anfinsen CB. Principles that Govern the Folding of Protein Chains. *Science (80-)*. American Association for the Advancement of Science; 1973;181: 223–230. doi:10.1126/science.181.4096.223
145. Cohen M, Reichmann D, Neuvirth H, Schreiber G. Similar chemistry, but different bond preferences in inter versus intra-protein interactions. *Proteins Struct Funct Genet*. 2008;72: 741–753. doi:10.1002/prot.21960
146. Widmann M, Pleiss J, Samland AK. Computational Tools For Rational Protein Engineering Of Aldolases. *Comput Struct Biotechnol J*. Research Network of Computational and Structural Biotechnology; 2012;2: e201209016. doi:10.5936/csbj.201209016
147. Huang P-S, Boyken SE, Baker D. The coming of age of de novo protein design. *Nature*. Nature Publishing Group; 2016;537: 320–327. doi:10.1038/nature19946
148. Roy A, Kucukural A, Zhang Y. I-TASSER: A unified platform for automated protein structure and function prediction. *Nat Protoc*. Nature Publishing Group; 2010;5: 725–738. doi:10.1038/nprot.2010.5
149. Yang J, Yan R, Roy A, Xu D, Poisson J, Zhang Y. The I-TASSER Suite: protein structure and function prediction. *Nat Methods*. Nature Publishing Group; 2015;12: 7–8. doi:10.1038/nmeth.3213
150. Radivojac P, Clark WT, Oron TR, Schnoes AM, Wittkop T, Sokolov A, et al. A large-scale evaluation of computational protein function prediction. *Nat Methods*. Nature Publishing Group; 2013;10: 221–227. doi:10.1038/nmeth.2340
151. Jooyoung Lee, Sitao Wu and YZ. *Ab Initio Protein Structure Prediction. From Protein Structure to Function with Bioinformatics*. Dordrecht: Springer Netherlands; 2009. pp. 3–25. doi:10.1007/978-94-024-1069-3_1
152. Rose PW, Beran B, Bi C, Bluhm WF, Dimitropoulos D, Goodsell DS, et al. The RCSB Protein Data Bank: Redesigned web site and web services. *Nucleic Acids Res*. Oxford University Press; 2011;39: D392–D401. doi:10.1093/nar/gkq1021
153. Blaszczyk M, Jamroz M, Kmiecik S, Kolinski A. CABS-fold: Server for the de novo and consensus-based prediction of protein structure. *Nucleic Acids Res*. Oxford University Press; 2013;41: W406–W411. doi:10.1093/nar/gkt462
154. Loksha I V., Maiolo JR, Hong CW, Ng A, Snow CD. SHARPEN-Systematic Hierarchical Algorithms for Rotamers and Proteins on an Extended Network. *J Comput Chem*. Wiley Subscription Services, Inc., A Wiley Company; 2009;30: 999–1005. doi:10.1002/jcc.21204
155. Craig DB, Dombkowski AA. Disulfide by Design 2.0: a web-based tool for disulfide engineering in proteins. *BMC Bioinformatics*. BioMed Central; 2013;14: 346. doi:10.1186/1471-2105-14-346
156. Masso M, Vaisman II. AUTO-MUTE: Web-based tools for predicting

- stability changes in proteins due to single amino acid replacements. *Protein Eng Des Sel*. 2010;23: 683–687. doi:10.1093/protein/gzq042
157. Martin OA, Vila JA, Scheraga HA. CheShift-2: Graphic validation of protein structures. *Bioinformatics*. Oxford University Press; 2012;28: 1538–1539. doi:10.1093/bioinformatics/bts179
158. Sulkowska JI, Morcos F, Weigt M, Hwa T, Onuchic JN. Genomics-aided structure prediction. *Proc Natl Acad Sci. National Academy of Sciences*; 2012;109: 10340–10345. doi:10.1073/pnas.1207864109
159. Pokala N, Handel TM. Energy functions for protein design: Adjustment with protein-protein complex affinities, models for the unfolded state, and negative design of solubility and specificity. *J Mol Biol*. 2005;347: 203–227. doi:10.1016/j.jmb.2004.12.019
160. Bednar D, Beerens K, Sebestova E, Bendl J, Khare S, Chaloupkova R, et al. FireProt: Energy- and Evolution-Based Computational Design of Thermostable Multiple-Point Mutants. Dokholyan N V., editor. *PLOS Comput Biol*. Public Library of Science; 2015;11: e1004556. doi:10.1371/journal.pcbi.1004556
161. Schymkowitz J, Borg J, Stricher F, Nys R, Rousseau F, Serrano L. The FoldX web server: An online force field. *Nucleic Acids Res. Oxford University Press*; 2005;33: W382–8. doi:10.1093/nar/gki387
162. Bendl J, Stourac J, Sebestova E, Vavra O, Musil M, Brezovsky J, et al. HotSpot Wizard 2.0: automated design of site-specific mutations and smart libraries in protein engineering. *Nucleic Acids Res. Oxford University Press*; 2016;44: W479–W487. doi:10.1093/nar/gkw416
163. Saraf MC, Moore GL, Goodey NM, Cao VY, Benkovic SJ, Maranas CD. IPRO: An Iterative Computational Protein Library Redesign and Optimization Procedure. *Biophys J. Cell Press*; 2006;90: 4167–4180. doi:10.1529/biophysj.105.079277
164. Wong TS, Roccatano D, Zacharias M, Schwaneberg U. A statistical analysis of random mutagenesis methods used for directed protein evolution. *J Mol Biol*. 2006;355: 858–871. doi:10.1016/j.jmb.2005.10.082
165. Dehouck Y, Kwasigroch JM, Gilis D, Rooman M. PoPMuSiC 2.1: a web server for the estimation of protein stability changes upon mutation and sequence optimality. *BMC Bioinformatics*. BioMed Central; 2011;12: 151. doi:10.1186/1471-2105-12-151
166. Suárez M, Tortosa P, Jaramillo A. PROTDES: CHARMM toolbox for computational protein design. *Syst Synth Biol*. Springer Netherlands; 2008;2: 105–113. doi:10.1007/s11693-009-9026-7
167. Lyskov S, Chou FC, Conchúir SÓ, Der BS, Drew K, Kuroda D, et al. Serverification of Molecular Modeling Applications: The Rosetta Online Server That Includes Everyone (ROSIE). Uversky VN, editor. *PLoS One*. Public Library of Science; 2013;8: e63906. doi:10.1371/journal.pone.0063906
168. Liu Y, Kuhlman B. RosettaDesign server for protein design. *Nucleic Acids Res*. 2006;34: W235–W238. doi:10.1093/nar/gkl163
169. Bauer DC, Bodén M, Thier R, Gillam EM. STAR: predicting recombination sites from amino acid sequence. *BMC Bioinformatics*. BioMed Central; 2006;7: 437. doi:10.1186/1471-2105-7-437
170. Vriend G. WHAT IF: A molecular modeling and drug design program. *J Mol Graph*. 1990;8: 52–56. doi:10.1016/0263-7855(90)80070-V
171. Blomberg C, Blomberg C. *The Physics Of Life: Physics At Several Levels*. Physics of Life. Elsevier; 2007. pp. 5–16. doi:10.1016/B978-044452798-1/50002-6
172. Erban R. From Molecular Dynamics to Brownian Dynamics. *Proceedings Math Phys Eng Sci. The Royal Society*; 2014;470: 20140036. doi:10.1098/rspa.2014.0036
173. Voelz VA, Bowman GR, Beauchamp K, Pande VS. Molecular simulation of ab initio protein folding for a millisecond folder NTL9(1-39). *J Am Chem Soc. American Chemical Society*; 2010;132: 1526–1528. doi:10.1021/ja9090353
174. Weiner SJ, Kollman PA, Case DA, Singh UC, Ghio C, Alagona G, et al. A new force field for molecular mechanical simulation of nucleic acids and proteins. *J. Am. Chem. Soc.*. 1984;106: 765–784. Available: <http://pubs.acs.org/doi/pdf/10.1021/ja00315a051>
175. Scheraga HA, Khalili M, Liwo A. Protein-Folding Dynamics: Overview of Molecular Simulation Techniques. *Annu Rev Phys Chem*. 2007;58: 57–83. doi:10.1146/annurev.physchem.58.032806.104614
176. Hartl FU. Molecular chaperones in cellular protein folding. *Nature*. Nature Publishing Group; 1996. pp. 571–579. doi:10.1038/381571a0
177. Hartl FU, Bracher A, Hayer-Hartl M. Molecular chaperones in protein folding and proteostasis. *Nature*. Nature Publishing Group; 2011;475: 324–332. doi:10.1038/nature10317
178. Chan Joo J, Je Yoo Y, Chan Joo J, Je Yoo Y. Thermostable Proteins. *Encyclopedia of Industrial Biotechnology*. Hoboken, NJ, USA: John Wiley & Sons, Inc.; 2009. doi:10.1002/9780470054581.eib562
179. Yang AS, Honig B. Structural origins of pH and ionic strength effects on protein stability. Acid denaturation of sperm whale apomyoglobin. *Journal of molecular biology*. Academic Press; 1994. pp. 602–14. doi:10.1006/jmbi.1994.1258
180. Chen S, Berglund P, Humble MS. The effect of phosphate group binding cup coordination on the stability of the amine transaminase from *Chromobacterium violaceum*. *Mol Catal. Elsevier*; 2018;446: 115–123. doi:10.1016/j.mcat.2017.12.033
181. Yoo YJ, Feng Y, Kim Y-H, Yagonia CFJ. *Fundamentals of Enzyme Engineering*. Springer Berlin Heidelberg; 2017. doi:10.1007/978-94-024-1026-6
182. Hubbard RE, Kamran Haider M. Hydrogen Bonds in Proteins: Role and Strength. *Encyclopedia of Life Sciences*. Chichester, UK: John Wiley & Sons, Ltd; 2010. doi:10.1002/9780470015902.a0003011.pub2
183. McDonald IK, Thornton JM. Satisfying Hydrogen Bonding Potential in Proteins. *J Mol Biol*. Academic Press; 1994;238: 777–793. doi:10.1006/jmbi.1994.1334
184. Pace CN, Fu H, Fryar KL, Landua J, Trevino SR, Shirley BA, et al. Contribution of hydrophobic interactions to protein stability. *J Mol Biol*. Academic Press; 2011;408: 514–528. doi:10.1016/j.jmb.2011.02.053
185. Watanabe K, Hata Y, Kizaki H, Katsube Y, Suzuki Y. The refined crystal structure of *Bacillus cereus* oligo-1,6-glucosidase at 2.0 Å resolution: structural characterization of proline-substitution sites for protein thermostabilization. *J Mol Biol*. Academic Press; 1997;269: 142–153. doi:10.1006/jmbi.1997.1018
186. Serrano L, Horovitz A, Avron B, Bycroft M, Fersht AR. Estimating the Contribution of Engineered Surface Electrostatic Interactions to Protein Stability by Using Double-Mutant Cycles. *Biochemistry*. 1990;29: 9343–9352. doi:10.1021/bi00492a006
187. Goerigk L, Reimers JR. Efficient methods for the quantum chemical treatment of protein structures: The effects of London-dispersion and basis-set incompleteness on peptide and water-cluster geometries. *J Chem Theory Comput*. American Chemical Society; 2013;9: 3240–3251. doi:10.1021/ct400321m
188. Back JF, Oakenfull D, Smith MB. Increased Thermal Stability of Proteins in the Presence of Sugars and Polyols. *Biochemistry*. 1979;18: 5191–5196. doi:10.1021/bi00590a025

Introduction

189. Greenfield NJ. Using circular dichroism collected as a function of temperature to determine the thermodynamics of protein unfolding and binding interactions. *Nat Protoc.* 2007;1: 2527–2535. doi:10.1038/nprot.2006.204
190. Ericsson UB, Hallberg BM, DeTitta GT, Dekker N, Nordlund P. ThermoFluor-based high-throughput stability optimization of proteins for structural studies. *Anal Biochem.* Academic Press; 2006;357: 289–298. doi:10.1016/j.ab.2006.07.027
191. Bedouelle H. Principles and equations for measuring and interpreting protein stability: From monomer to tetramer. *Biochimie.* Elsevier; 2016;121: 29–37. doi:10.1016/J.BIOCHI.2015.11.013
192. Niesen FH, Berglund H, Vedadi M. The use of differential scanning fluorimetry to detect ligand interactions that promote protein stability. *Nat Protoc.* Nature Publishing Group; 2007;2: 2212–2221. doi:10.1038/nprot.2007.321
193. Steinberg TH, Jones LJ, Haugland RP, Singer VL. SYPRO orange and SYPRO red protein gel stains: One-step fluorescent staining of denaturing gels for detection of nanogram levels of protein. *Anal Biochem.* Academic Press; 1996;239: 223–237. doi:10.1006/abio.1996.0319
194. Kohlstaedt M, Von Der Hocht I, Hilbers F, Thielmann Y, Michel H. Development of a ThermoFluor assay for stability determination of membrane proteins using the Na⁺/H⁺ antiporter NhaA and cytochrome c oxidase. *Acta Crystallogr Sect D Biol Crystallogr.* International Union of Crystallography; 2015;71: 1112–1122. doi:10.1107/S1399004715004058
195. Bulaj G. Formation of disulfide bonds in proteins and peptides. *Biotechnology Advances.* Elsevier; 2005. pp. 87–92. doi:10.1016/j.biotechadv.2004.09.002
196. Matsumura M, Becktel WJ, Levitt M, Matthews BW. Stabilization of phage T4 lysozyme by engineered disulfide bonds. *Proc Natl Acad Sci.* National Academy of Sciences; 1989;86: 6562–6566. doi:10.1073/pnas.86.17.6562
197. Clarke J, Fersht AR. Engineered disulfide bonds as probes of the folding pathway of barnase: Increasing the stability of proteins against the rate of denaturation. *Biochemistry.* American Chemical Society; 1993;32: 4322–4329. doi:10.1021/bi00067a022
198. Tanghe M, Danneels B, Last M, Beerens K, Stals I, Desmet T. Disulfide bridges as essential elements for the thermostability of lytic polysaccharide monooxygenase LPMO10C from *Streptomyces coelicolor*. *Protein Eng Des Sel.* 2017;30: 401–408. doi:10.1093/protein/gzx014
199. Wijma HJ, Floor RJ, Jekel PA, Baker D, Marrink SJ, Janssen DB. Computationally designed libraries for rapid enzyme stabilization. *Protein Eng Des Sel.* Horwood, New York; 2014;27: 49–58. doi:10.1093/protein/gzt061
200. Dombkowski AA, Sultana KZ, Craig DB. Protein disulfide engineering. *FEBS Letters* Jan 21, 2014 pp. 206–212. doi:10.1016/j.febslet.2013.11.024
201. Jacobson RH, Faber HR, Matthews BW. Structure of a stabilizing disulfide bridge mutant that closes the active-site cleft of T4 lysozyme. *Protein Sci.* Cambridge University Press; 1992; 46–57.
202. Matsumura M, Signor G, Matthews BW. Substantial increase of protein stability by multiple disulphide bonds. *Nature.* 1989;342: 291–293. doi:10.1038/342291a0
203. Malz RE. *Catalysis of Organic Reactions.* CRC Press; 1996.
204. Manta B, Cassimjee KE, Himo, F. Quantum Chemical Study of Dual Substrate Recognition in ω-Transaminase. *ACS Omega* 2017, 2, 890–898. doi:10.1021/acsomega.6b00376
205. Dajnowicz S, Johnston RC, Parks JM, Blakeley MP, Keen DA, Weiss KL, Gerlits O, Kovalesvsky A, Mueser T. *Nature Communications* 8:955. doi: 10.1038/s41467-017-01060-y
206. Cassimjee KE, Manta B, Himo F. *Org. Biomol. Chem.* 2015,13, 8453. doi: 10.1039/C5OB00690B

2) Research proposal

The synthesis of chiral amines is of particular interest, as 40% of all pharmaceuticals contain a stereocenter with an amine substituent in their structure [1]. In addition, amino acids as a special class of amines are of particular interest for food and feed industry, but also for the production of pharmaceuticals. The standard procedure for producing most α -amino acids is microbial fermentation. In contrast the pharmaceutically relevant chiral β -amino acids cannot be produced by fermentation, so various chemical, biocatalytical and chemo-enzymatical synthesis solutions are currently being investigated. Common enzymatic synthesis strategies bear limitations such as low solubility of substrates, instability of cascade reaction intermediates (e.g. β -keto acid) or the necessity of high enzyme concentrations. The enzyme family of ω -transaminases (ω -TA) is able to synthesize chiral amines and to convert β -amino acids such as β -phenylalanine (β -PA) and has therefore been selected as a promising group of biocatalysts. ω -TA can convert the corresponding β -keto acid into β -PA, but so far no variants have been found to convert more stable aromatic β -keto esters into corresponding β -PA-esters. Therefore, first the diversity of ω -TA was analyzed and subsequently a β -PA converting ω -TA was characterized as the starting point for enzyme engineering. Hence, this work focused on ω -TA as an alternative towards transition metal catalyzed and organocatalytic methods.

The main aims of this study are (see also **Figure 2.1**):

- The constitution of a database for ω -TA engineering in regard to literature and the investigation of its usability (**Chapter 3**)
- The improvement of (process)-stability of a selected ω -TA using an algorithm for prediction of free energy changes within the polypeptide chain (**Chapter 4**)
- Analysis of engineering sites within the ω -TA of the β -proteobacterium *Variovorax paradoxus* regarding β -phenylalanine ester synthesis (**Chapter 5.1**)
- Development of an alternative synthesis strategy for the synthesis of β -phenylalanine ester using engineered ω -TA from a protein library (**Chapter 5.2**)
- Characterization of microbial degradation and chiral resolution of *rac*- β -phenylalanine by *Paraburkholderia* PsJN in a bioreactor system (**Chapter 6**)

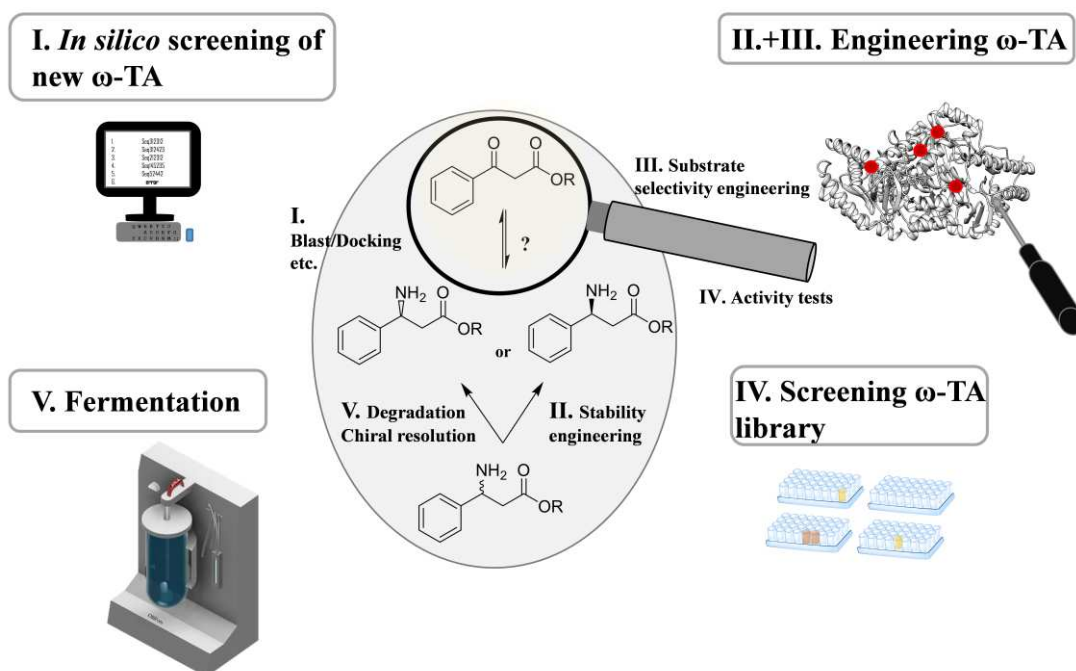


Figure 2.1 Strategy for the ω -TA catalyzed synthesis of β -phenylalanine (esters). (R= H, CH₃-, CH₃CH₂-). Enzyme structure was visualized using Chimera 1.1. The bioreactor drawing was designed using Fusion 360 (Autodesk).

Reference chapter 2)

1. Ghislieri D, Turner NJ. Biocatalytic Approaches to the Synthesis of Enantiomerically Pure Chiral Amines. *Top Catal.* Springer US; 2014;57: 284–300. doi:10.1007/s11244-013-0184-1

3) Analysis and creation of a systematic ω -TA database (oTAED)

The following chapter briefly explains the diversity of ω -TA and how to sort them into public databases like the presented oTAED database. This database collects (*S*)- and (*R*)-selective ω -TA and divides them into two superfamilies consisting of Fold type I and Fold type IV proteins. Furthermore the application of the standard-numbering tool is presented towards comparative design and engineering of ω -TA.

3) Analysis and creation of a systematic ω -TA database (ω TAED)

This chapter is mainly based on the revised version of the following publication:

The ω -Transaminase Engineering Database (ω TAED): a navigation tool in protein sequence and structure space

.

Oliver Buß^a, Patrick C. F. Buchholz^b, Maike Gräff^{cb}, Peter Klausmann^a, Jens Rudat and Jürgen Pleiss^b

^a Institute of Process Engineering in Life sciences, Section II: Technical Biology, Karlsruhe Institute of Technology, Karlsruhe Germany. ^b Institute of Biochemistry and Technical Biochemistry, University of Stuttgart, Allmandring 31, 70569 Stuttgart, Germany

Publishing details:

Accepted manuscript

Doi: [/doi.org/10.1002/prot.25477](https://doi.org/10.1002/prot.25477)

The final reviewed publication is available at PROTEINS-Wiley

© 2018 Wiley Periodicals, Inc

AUTHORS-RIGHT: *“If you wish to reuse your own article (or an amended version of it) in a new publication of which you are the author, editor or co-editor, prior permission is not required (with the usual acknowledgements).”* PROTEINS-Wiley (2018)

Authors' contribution to this publication

Oliver Buß analyzed the databank results and wrote the manuscript as first author. **Patrick C.F. Buchholz** performed the database management, created network figures and was contributed in writing of the manuscript. **Maike Gräff** was contributed in analysis of the database and in writing of the manuscript. **Patrick C.F. Buchholz** and **Maike Gräff** wrote widely parts of the methods section. **Peter Klausmann** verified protein sequences within the database, performed RMSD-analysis of described ω -TA and revised the manuscript. **Jens Rudat** supervised the work, provided administrative support and critically revised the manuscript. **Jürgen Pleiss** initiated the project, contributed to the design of the study, supervised the work and critically revised the manuscript.

3.1) Introduction

3.1.1) Definition and function of transaminases

The ubiquity of amino groups in natural products leads to a great diversity of different transaminases (TA, E.C. 2.6.1) [1]. Because the structure of the donor and the acceptor might differ and because the reaction is reversible, the enzymes accept two different amines as amino donors, which is known as dual substrate recognition [2]. As a further consequence of the reversibility of the transamination, subsequent reaction steps or product separation are required in biosynthetic applications [3]. Other members of the family of PLP-dependent enzymes include lyases, oxidoreductases, and hydrolases [4]. Because TA differ by their amine donor and acceptor scope, substrate specificity was used to assign TA to two major families. α -transaminases (α -TA) catalyze transfer of the amino group exclusively to a carbonyl group in α -position to a carboxyl group (see also chapter 1). ω -TA lack the selectivity towards α -keto substrates and have a wide spectrum of acceptor/donor molecules, e.g. α -alanine, 1-phenylethylamine, putrescine and other amines. α -TA are involved in amino acid biosynthesis, which makes them interesting enzymes for the production of D- or L-amino acids. Their limitation to α -carbonyl substrates is a disadvantage for broader application of these enzymes [5–7].

Applications of ω -transaminases

In contrast, ω -TA lack the dependence on a carboxyl group in the acceptor substrate and are therefore promising enzymes for the synthesis of a broad range of optically pure amines [15–22], such as the pharmaceuticals imagabalin and sitagliptin [23,24], rivastigmine, α -aminosteroids, mexiletine, cathine, and 3-amino-8-aza-bicyclo[3.2.1]oct-8-yl-phenyl-methanone [14,25–28] (see also chapter 1). However, considerable enzyme engineering efforts were needed to adapt enzymes to the desired substrates. In amino acid synthesis, a special focus lies on the synthesis of optically pure β -amino acids like β -PA which can be produced using lipase - ω -TA cascade reactions or racemic resolution reactions using Fold type I-(*S*)-selective ω -TA [21,29]. Non-standard amino acids might be applied in synthetic peptides or for the synthesis of the antitumor drug paclitaxel [29–31].

3) Analysis and creation of a systematic ω -TA database (oTAED)

Definitions

ω -Transaminases (ω -TA) belong to the enzyme class **E.C. 2.6.1.X**. Within this class also α -transaminases are present. For example ω -TA can be found in class 2.6.1.18 - group of β -alanine-pyruvate transaminases-. Other nomenclatures of ω -TA are: **transaminase, amine transaminase, ω -aminotransferase, α,ω -diamine transaminase, β -transaminase** and other misleading terms in protein databases. The group of (*S*)-selective ω -TA can be also found within the PLP-dependent-enzyme classification system as class III transaminase family. In contrast, (*R*)-selective ω -TA are often associated with the D-alanine transaminase family.

Fold type

Furthermore ω -TA are defined according to mainly two different Fold types of PLP-dependent enzymes. Most of the (*S*)-selective ω -TA are present within **Fold type I**, together with aspartate aminotransferases, aromatic acid aminotransferases and etc.. In contrast (*R*)-selective ω -TA are member of **Fold type IV**, together with D-amino acid aminotransferases (**DATA**), branched chain amino acid transferases (**BCAT**) and aminodeoxychorismate lyases (**ADCL**).

Concept of standard numbering

According to relocate amino acid residues in different ω -TAs a standard numbering was defined for Fold type I and Fold type IV. The standard numbering refers to a respective reference protein, the amino acid positions are then transferred to other protein sequences by alignment. If not stated otherwise, the standard positions are reported within this chapter.

Box 3.1 The nomenclature of ω -TA is not consistent within literature, therefore further information are summarized within this information box. Examples are from citations [8–14].

Like mentioned before for asymmetric synthesis, the reaction equilibrium is pushed towards the desired product by removing the co-product or by high concentrations of the amine donor or alternatively by regenerating of the co-substrate. Beside the reaction equilibrium, solvent stability of ω -TA is an important factor. Many relevant substrates exhibit low solubility in aqueous solvents. While the co-solvent DMSO is compatible with ω -TA, only few ω -TA are known to be active in organic solvents such as *tert*-butyl ether [24,32]. The most widely used ω -TA are from the microorganisms *Vibrio fluvialis*, *Chromobacterium violaceum* and *Arthrobacter citreus* [33]. The most famous amine product, sitagliptin, which is produced using ω -TA, reached in 2016 a revenue of 6 billion dollar [34]. Further applications are presented in the reviews of Guo *et al.*, Slabu *et al.* and Dold *et al.* [33,35,36].

This proves the importance for technical applications of transaminases, but there are still enzyme based limitations. To overcome the limitations of unmodified wild type ω -TA, screening, data mining, and enzyme engineering are promising strategies to develop enzymes with higher stability, broader substrate specificity and increased selectivity. While literature mining is an obvious starting point for most engineering projects, its success is limited by the lack of naming conventions and standard residue numbering of ω -TA, which makes it difficult to compare mutagenesis studies or to analyze important sequence motifs in different ω -TA groups.

Enzyme engineering of ω -transaminases

The substrate binding sites of ω -TA consist of the large O- and the small P-pocket [22], also called A and B pocket, respectively [37]. Promising mutation sites of ω -TA were reviewed recently [35]. In recent years, the aim of engineering efforts is obtaining enzymes with high activity towards bulky substrates lacking a carboxyl group [38]. In the case of *Vibrio fluvialis* ω -TA, the activity of the enzyme towards β -keto-methylester was substantially increased by only eight point mutations [23]. The most beneficial single mutation was W57F (located in the P-pocket). Palvidis *et al.* could increase activity of an (*S*)-selective ω -transaminase from *Ruegeria sp.* TM1040 (3FCR) by a factor of 8,900 [38]. The best variant was created by introducing only four mutations, Y59W, Y89F, Y152F and T231A.

The challenge of classification

Three classification schemes for TA based on biochemical function, sequence, or structure have been proposed. The functional classification divided the protein sequences into α -TA and ω -TA [23]. The sequence classification assigned TA to five different aminotransferase classes based on sequence similarity [8,39–42] or alternatively six Pfam groups based on profile hidden Markov models [43–45]. Evolutionary analysis led to a phylogenetic tree with α -TA in Pfam group I and ω -TA in Pfam group III [15,46]. Based on structure, PLP-dependent enzymes have been divided into five different fold types [42,47], with α - and ω -TA found in Fold types I and IV [42,47–49]. Fold type I (*S*)-selective ω -TA have an α - β - α -structure pattern. In contrast, Fold type IV (*R*)-selective ω -TA consisting of two domains, a two-layer ω -sandwich and an α - β -barrel pattern. TA of both Fold types form at least homodimers, and the active sites are located at the homodimer interface. Because both α - and ω -TA are found in each of the two Fold types, regioselectivity is not strictly linked to global protein structure. The substrate binding sites of Fold types I and IV are mirror images with the catalytic lysine located at the *si*- and *re*-face of PLP, respectively, resulting in the observed enantiocomplementarity of the two folds [8,50] with Fold type I (*S*)-selective ω -TA converting (*S*)-amines and (*S*)-amino acids, whereas Fold type IV (*R*)-selective ω -TA converting (*R*)-amines and (*R*)-amino acids as well as branched-chain L-amino acids [49].

The three classification schemes are used in parallel. TA are named by their stereo-preference ((*R*)/(*S*)-selective), their substrate specificity, their regioselectivity (α / ω -TA), or their Pfam group (aminotransferase class), resulting in enzyme names such as: ω -aminotransferase,

3) Analysis and creation of a systematic ω -TA database (oTAED)

(*S*)-selective aminotransferase, aromatic amino acid TA, γ -aminobutyrate TA, ω -amino acid:pyruvate TAs and class III aminotransferase [23,51–55]. A public online database on ω -TA will be a helpful tool, connecting information about mutation sites, structure data and substrate scope, thus allowing researchers the mining of uncharacterized ω -TA for the desired enzyme functions and predicting interesting mutation sites. The first public database for ω -TA screening was the B₆-database for the description and classification of vitamin B₆ dependent enzymes [4]. Höhne *et al.* and Pavlidis *et al.* demonstrated data mining as a successful strategy for *in silico* screening of (*R*)-selective TA accepting bulky substrates [14,49,56]. In contrast Calvelage *et al.* reported a systematic analysis of ω -TA (amine transaminases) according to reported reaction data and selected important selectivity and activity indicators. However, this analysis was limited to a small fraction (~500) of ω -TA and only to amine substrates [57]. To support enzyme engineering and to facilitate navigation and annotation, we established a publicly available database on ω -TA which includes sequence information and structural data. Additionally, standard numbering schemes for both Fold types were established to identify equivalent positions in homologous proteins and to compare the effects of corresponding mutations in different proteins.

3.2) Methods

Setup and clustering of the ω -Transaminase Engineering Database (oTAED)

The sequences of nine representative ω -transaminases (ω -TA) were used as query sequences against the NCBI non-redundant protein database with an E-value threshold of 10^{-10} (table 3.2) [58]. The setup of the oTAED and the clustering of the sequences was performed within the BioCatNet database system [59]. A sequence identity threshold of 98% was applied to assign sequences to proteins and a threshold of 40% sequence similarity was used to form homologous families. If the majority of sequence entries from a homologous family showed sequence lengths longer than 350 amino acids, the homologous family was assigned completely to the Fold type I superfamily. Consequently, homologous families were assigned to the Fold type IV superfamily, if most of their sequences were shorter than 350 amino acids.

All sequences within a superfamily that could not be assigned to a homologous family were collected in a separate group. Sequences shorter than 200 and longer than 550 amino acids were discarded. If available, crystal structures from the PDB repository were assigned to the sequence entries. Multiple sequence alignments and phylogenetic trees were generated using Clustal Omega [60] and can be downloaded from a WWW-accessible user interface. The oTAED is online available.

Standard numbering schemes

Standard numbering schemes were established for the two superfamilies Fold type I and Fold type IV as described previously [61]. For the respective superfamily, reference structures containing the cofactor PLP and covering the most abundant homologous families were selected (Table 3.1). For Fold type IV, a structural alignment of six reference structures was created using STAMP [62]. For Fold type I, fourteen characterized ω -TA were selected. The N-terminal region (positions 1 to 64 of PDB entry 2YKU), which was not resolved completely in all reference structures, was discarded to improve the robustness of the alignment. The multiple sequence alignment of the Fold type I reference sequences from Clustal Omega was refined manually, guided by structural superimposition [60]. From the manually optimized alignments of Fold type I and IV reference structures, profile hidden Markov models were created by HMMER (version 3) [63]. By aligning all sequences to their respective sequence profile,

3) Analysis and creation of a systematic ω -TA database (oTAED)

position numbers were transferred to Fold type I sequences from PDB entry 2YKU (ω -TA from *Mesorhizobium sp.* LUK) and to Fold type IV sequences from PDB entry 4CE5 (ω -TA from *Aspergillus terreus*).

Table 3.1 Reference structures for the standard numbering schemes of ω -transaminase superfamilies Fold Type I and Fold Type IV.

Fold Type I	Fold Type I	Fold Type IV	Fold Type IV
PDB entry	Source	PDB entry	Source
1DTY	<i>Escherichia coli</i>	3WWH	<i>Arthrobacter sp.</i> KNK168
1SZS	<i>Escherichia coli</i>	4CE5	<i>Aspergillus terreus</i>
2OAT	<i>Homo sapiens</i>	4CHI	<i>Aspergillus fumigatus</i>
2YKU	<i>Mesorhizobium sp.</i> LUK	4CMD	<i>Nectria haematococca</i>
2ZSL	<i>Aeropyrum pernix</i>	5E25	<i>Geoglobus acetivorans</i>
3A8U	<i>Pseudomonas putida</i>	5K3W	<i>Curtobacterium pusillum</i>
3DOD	<i>Bacillus subtilis</i>		
3FCR	<i>Ruegeria sp.</i> TM1040		
3I5T	<i>Rhodobacter sphaeroides</i>		
4AOA	<i>Variovorax paradoxus</i>		
4E3R	<i>Homo sapiens</i>		
4JEW	<i>Salmonella enterica</i>		
4UOX	<i>Escherichia coli</i>		
4YSN	<i>Lactobacillus buchneri</i>		

Conservation analysis

The two standard numbering schemes for Fold type I and Fold type IV sequences were used separately to analyze the amino acid composition of both superfamilies. A position was considered to be conserved in a superfamily, if a single amino acid was present in more than 70% of all sequences.

Sequence networks

Sequence networks were generated for distances between pairs of homologous sequences. To reduce the number of sequences for pairwise alignments, sequences were clustered by 30%

identity using the algorithm of USEARCH [64]. Pairwise global sequence alignments were calculated using the implementation of the Needleman-Wunsch algorithm in the EMBOSS software suite [65]. Sequence networks were created by using a cutoff of 50% pairwise sequence similarity, and the resulting networks were visualized by Cytoscape version 3.4.0 using the Prefuse force-directed layout algorithm with respect to the edge weights.

3.3) Results

3.3.1) The ω -Transaminase Engineering Database (oTAED)

The ω -Transaminase Engineering Database (oTAED) consists of two superfamilies, Fold types I and IV. The database was created using query sequences of different characterized ω -TA of Fold type I and IV (Table 3.2). The ω -TA sequences were assigned to the two superfamilies by sequence length. The oTAED includes 67,210 proteins (114,655 sequences) which were separated into 169 homologous families (HFams) based on global sequence similarity.

Table 3.2 Query sequences for the initial BLAST search to set up the ω -Transaminase Engineering Database (oTAED). Annotation according to UniProt nomenclature.

UniProt ID	Annotation	Fold type	Source organism	Reference
H8WR05	Beta-Phenylalanine Aminotransferase	I	<i>Variovorax paradoxus</i>	[22]
Q0C8G1	AT-OmegaTA	IV	<i>Aspergillus terreus</i>	[8]
A1TDP1	Multispecies: Aminotransferase IV	IV	<i>Mycobacterium vanbaalenii</i>	[66]
A1DD33	Aminotransferase, Class IV, Putative	IV	<i>Aspergillus fischeri</i>	[66]
F2XBU9	Pyruvate transaminase	I	<i>Vibrio fluvialis</i>	[67]
A0A1B4YGI6	Beta – Alanine Pyruvate Transaminase	I	<i>Mesorhizobium loti</i>	[51]
P28269	Omega Amino Acid: Pyruvate Aminotransferase	I	<i>Pseudomonas putida</i>	[68]
D5VI64	Aspartate Aminotransferase Family Protein	I	<i>Caulobacter segnis</i>	[69]
Q9I700	Aspartate Aminotransferase Family Protein	I	<i>Pseudomonas aeruginosa</i>	[10]

The database oTAED was published using the biocatnet-database platform from Pleiss's research group [59]. The tool allows researchers to identify putative ω -TA and to characterize ω -TA of interest using a standard numbering scheme for easy transfer of engineering sites between ω -TA of one Fold type. Fold type I proteins have an average length of 432 amino acids, whereas Fold type IV proteins have an average length of 297 amino acids (**Figure 3.1**). Nearly 31% of Fold type IV proteins have a length of 290 amino acids (at a bin-size of 10). The largest group of Fold type I proteins are 430 amino acids in length. Very short sequences of up to 220

amino acids occur for Fold type I, but do not have a large overall share of the size distribution. In the case these short-chain Fold type I enzymes are not only fragments. However, such short enzymes would be very interesting because shorter proteins showing less synthetic costs for the expression host and might be also evolutionary more conserved than proteins with larger lengths [70]. Fold type IV proteins with a very long length of over 500 amino acids also occur, even if their absolute number is relatively small (>40). However no proteins with lengths shorter than 270 amino acids are present within the family of Fold type IV proteins. An example for a short Fold type I protein sequence is the ornithine aminotransferase from *Trichinella spiralis* with an amino acid length of only 256 residues. However, some of those short gene bank entries might be only protein fragments, like the 220 long protein sequence (ID 1330537) of the succinylornithine transaminase from *Yersinia pseudotuberculosis* (real protein size 414, UniProt ID Q66B21). Therefore, very small protein lengths might indicate also protein fragments, which can be found within protein databases and therefore also in oTAED.

Besides the classification into HFams (homologous families), the standard numbering was also a goal of this work. For the standard numbering an ω -TA sequence was utilized as reference and an alignment was performed using a setup of 15 Fold type I ω -TA and 6 Fold type IV ω -TA structures. Therefore too similar structures were excluded, because high sequence- and structural-identities are useless in respect of creating a consensus sequence. In the following the database results of Fold type I and type IV are analyzed.

3) Analysis and creation of a systematic ω -TA database (oTAED)

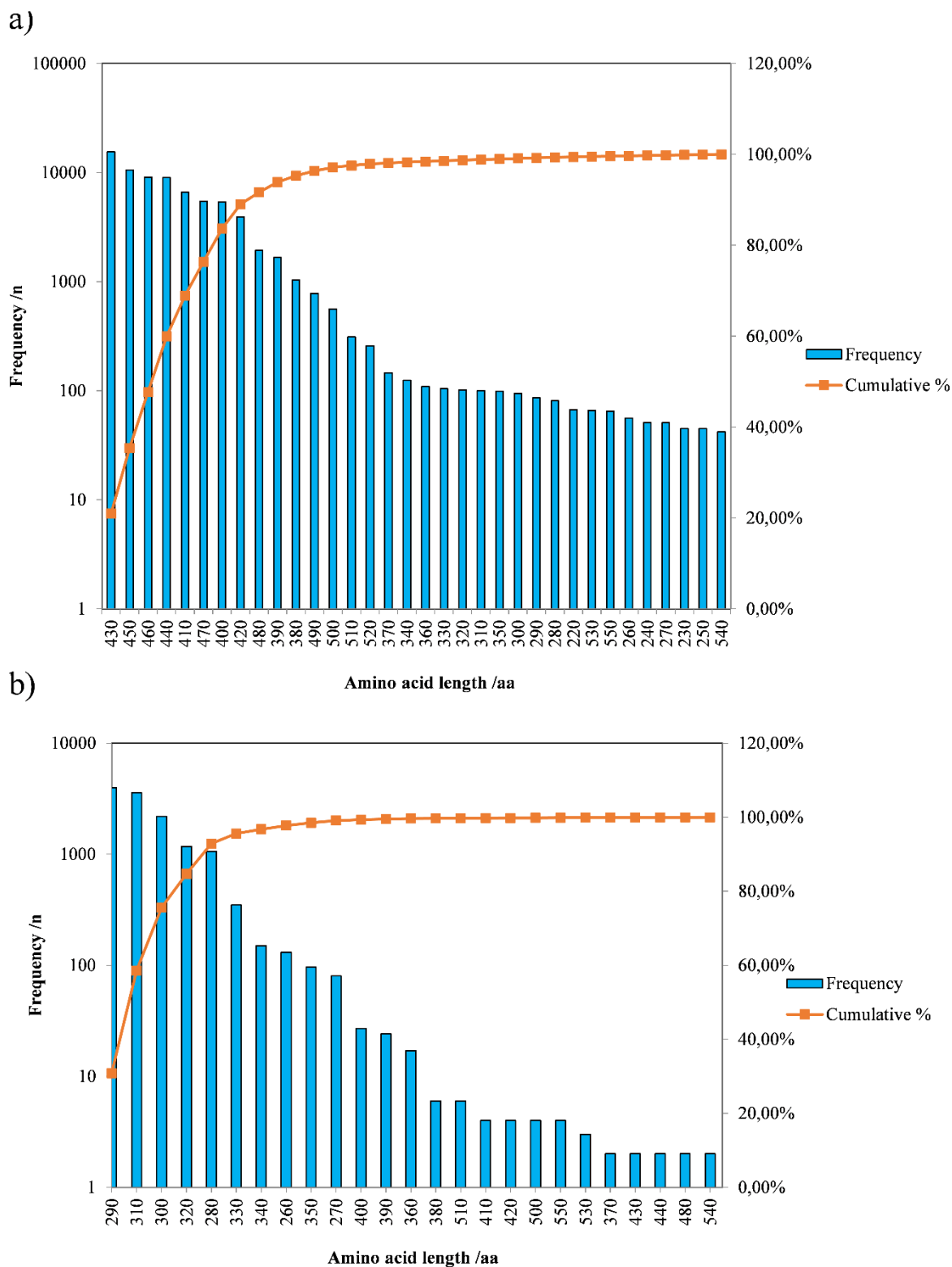


Figure 3.1 Protein length of Fold type I (a) and IV (b) (**Caution logarithmic Y-axis scaling**). Fold type IV sequences peaking in a length of 290 amino acids (~31% of all sequences). Fold type I proteins are generally larger and showing a global maximum at 430 amino acids (~21% of all sequences). The bin size was set to 10 using the total sequence FASTA-file from oTAED 1.0.1. The histogram was analyzed using Microsoft-Excel.

Characterization of Fold type I

The Fold type I superfamily consists of 101,738 protein sequences (89% of the oTAED entries), which were assigned to 124 homologous families. Most of the putative Fold type I (*S*)-selective ω -TA belong to one large homologous family (HFam 239) comprising 99,559 sequences (98% of all Fold type I sequences) and 164 structures. The discrepancy of sequence amount in regard to the amount of structures prevents the direct functional analysis of most of the sequences. However also experimentally characterized sequences can be found within the database, some of them even in combination with the protein structure.

The Fold type I family contains the previously characterized (*S*)-selective ω -TA from *Mesorhizobium* sp. LUK and *V. paradoxus* (PDB entries 4AO4 and 4AOA), which are active towards aromatic β -amino acids and were reported before in chapter 1 [11,22]. Their host organisms are soil bacteria living in symbiosis with plants for fixation of nitrogen from plant material [71,72]. A further member of HFam 239 is the ω -TA from *Rugeria* sp. TM1040 (PDB entry 3FCR) which was characterized as an (*S*)-selective ω -TA with activity towards small amino acids, 1-phenyl ethylamine (PEA), bicyclic acceptor molecules such as exo-3-amino-8-aza-bicyclo[3.2.1]oct-8-yl-phenyl-methanone and succinic semialdehyde [14,55]. Other members of HFam 239 are the ω -TA from *Chromobacterium violaceum* (PDB entry 4AH3), which exhibited (*S*)-selectivity and a broad substrate range towards amines and amino acids, as well as aldehydes and ketones as acceptor molecules [73], and an ω -TA from *Pseudomonas aeruginosa* (UniProt ID V6A7F6) with activity towards mono- and diamines. This newly characterized enzyme converts cadaverine and spermidine and catalyzes the transfer of the amino group to aromatic ketone acceptor molecules [74]. These examples demonstrate the large diversity of substrate specificities in the largest homologous family of the Fold type I superfamily.

The other homologous families consist of less than 400 sequences each (Hfam 35: 397 sequences, HFam 134: 339 sequences and eight structures). The respective proteins are often annotated as (*S*)-selective ω -TA, mostly γ -aminobutyrate aminotransferases from eukaryotic organisms.

Characterization of Fold type IV

The smaller Fold type IV superfamily consists of 12,917 protein sequences assigned to 45 homologous families (11% of the oTAED entries). It contains sequences annotated as (*R*)-

3) Analysis and creation of a systematic ω -TA database (oTAED)

selective ω -TA as well as (*R*)-selective D- α -TA (DATA). This class of enzymes is selective for D- α -amino acids like D-alanine or D-glutamate [75]. Furthermore, it contains L-branched-chain aminotransferases (L-BCAT) with activity towards aliphatic α -amino acids like valine, leucine, and isoleucine [76,77]. L-BCATs show a different enantiopreference in comparison to DATA and (*R*)-selective ω -TA, presumably caused by the reverse arrangement of the substrate in the active site [34]. Furthermore (*R/S*)-nomenclature for enzyme labeling is not stringent and allows misleading interpretations of substrate selectivity. However, the annotation in public databases such as NCBI or Uniprot is often restricted to DATA or L-BCAT [37], lacking differentiation between DATA/ L-BCAT and (*R*)-selective ω -TA. For this reason, names of Fold type I and IV are useless in the most public databases with exception of reviewed sequences.

The largest homologous family (HFam 11) includes 90% of all Fold type IV sequences and 23 annotated structures such as a branched-chain-amino-acid TA (PDB entry 4WHX) and an amino lyase with activity towards 4-amino-4-deoxychorismate (PDB entry 2Y4R) [9]. The second largest homologous family (HFam 10) contains 511 sequences and 9 structures. This HFam contains mostly ω -TA annotated as (*R*)-selective TAs, such as the ω -TA from *Arthrobacter sp.* (PDB entries 5FR9 and 3WWH) which was adapted by large site directed mutagenesis experiments for activity towards bulky substrates such as aromatic β -fluoroamines or sitagliptin [24,78], and two (*R*)-selective ω -TA from the fungi *Aspergillus fumigatus* and *A. terreus* (PDB entries 4CHI and 4CE5) showing activity towards aromatic amines [8,37,79]. The other homologous families of Fold type IV contain less than 200 sequences each.

Conserved positions of Fold type I and IV

Evolutionary conserved positions often point to structurally or functionally relevant residues, an amino acid exchange at these positions might cause drastic changes in activity as well as protein stability [80]. Therefore, these sites better be excluded in some contexts from enzyme engineering experiments [81]. Positions that are conserved but previously undescribed in literature could be investigated in future studies to elucidate their biochemical relevance. Therefore, the following overview comprises positions conserved in the sequences from the respective Fold type and is not limited to positions mentioned in literature.

3.3.2) Fold type I sequence analysis

By applying the standard numbering schemes for Fold types I, 44 conserved positions (present in more than 70% of the sequences) were identified (**Table 3.3**) with position numbers according to the ω -TA from *Mesorhizobium sp.* LUK (PDB accession 2YKU).

Table 3.3 Conserved positions in putative Fold type I (*S*)-selective ω -TA sequences with standard numbering according to the ω -TA from *Mesorhizobium sp.* LUK (PDB accession 2YKU) and their location inside the protein structure or annotated function. Positions listed here are conserved to at least 70%.

Standard position	Conserved amino acids	Location/function
7	G (88%), N (5%)	loop
12	D (81%), L (6%)	
15	G (91%)	α -turn [22]
20	D (97%)	
31	G (98%)	loop
32	H (75%), Y (18%)	
40	A (83%)	
44	Q (75%), A (10%)	
81	G (98%)	backbone hydrogen bond to PLP [22]
83	E (72%), D (10%), V (6%)	
84	A (83%), S (10%)	
88	A (85%)	
90	K (70%), R (26%)	
92	A (80%), V (8%)	
109	H (98%)	interaction with D189 [10]
110	G (99%)	loop
151	A (79%), C (9%)	
152	A (78%), C (10%), G (9%)	
156	E (97%)	hydrogen bond to PLP [82]
157	P (79%), T (7%), A (5%)	loop
160	G (82%)	loop
163	G (92%)	loop
185	L (75%), V (13%)	
186	L (71%), F (15%), M (5%)	
187	I (75%), V (20%)	
189	D (100%)	hydrogen bond to PLP [22][13]
190	E (96%)	
194	G (93%)	loop
195	G (71%), R (15%), A (8%)	loop
196	R (82%), V (8%)	
198	G (84%), L (6%)	loop
201	A (70%), G (15%), S (6%)	
209	P (93%), A (6%)	loop
210	D (99%)	salt bridge to arginine (Figure 3.2)
216	K (100%)	catalytic lysine [22]

3) Analysis and creation of a systematic ω -TA database (oTAED)

221	G (91%)	loop
223	P (88%), T (5%)	
250	T (94%), S (5%)	backbone hydrogen bond to PLP [22]
253	G (83%), A (11%)	loop
255	P (79%), A (6%)	
259	A (77%), V (5%)	
288	L (74%), I (7%), F (6%)	
302	R (77%), N (6%)	
305	G (94%)	loop

The highly conserved positions D189 and K216 were found in all sequences of Fold type I. The side chain of D189 is fixed by interacting with H109 and is involved in binding the cofactor PLP by a hydrogen bond between the carboxylic group and the pyridine nitrogen, and thus is essential for all PLP-dependent enzymes. The conserved K216 forms a Schiff base with the intermediate or with the cofactor PLP. The role of the highly conserved D210 in (*S*)-selective ω -TA is still unknown, but it might participate in a conserved salt-bridge between an α -helix and a β -strand, since in most structures an arginine or asparagine residue is found in close distance to D210 (**Figure 3.2**).

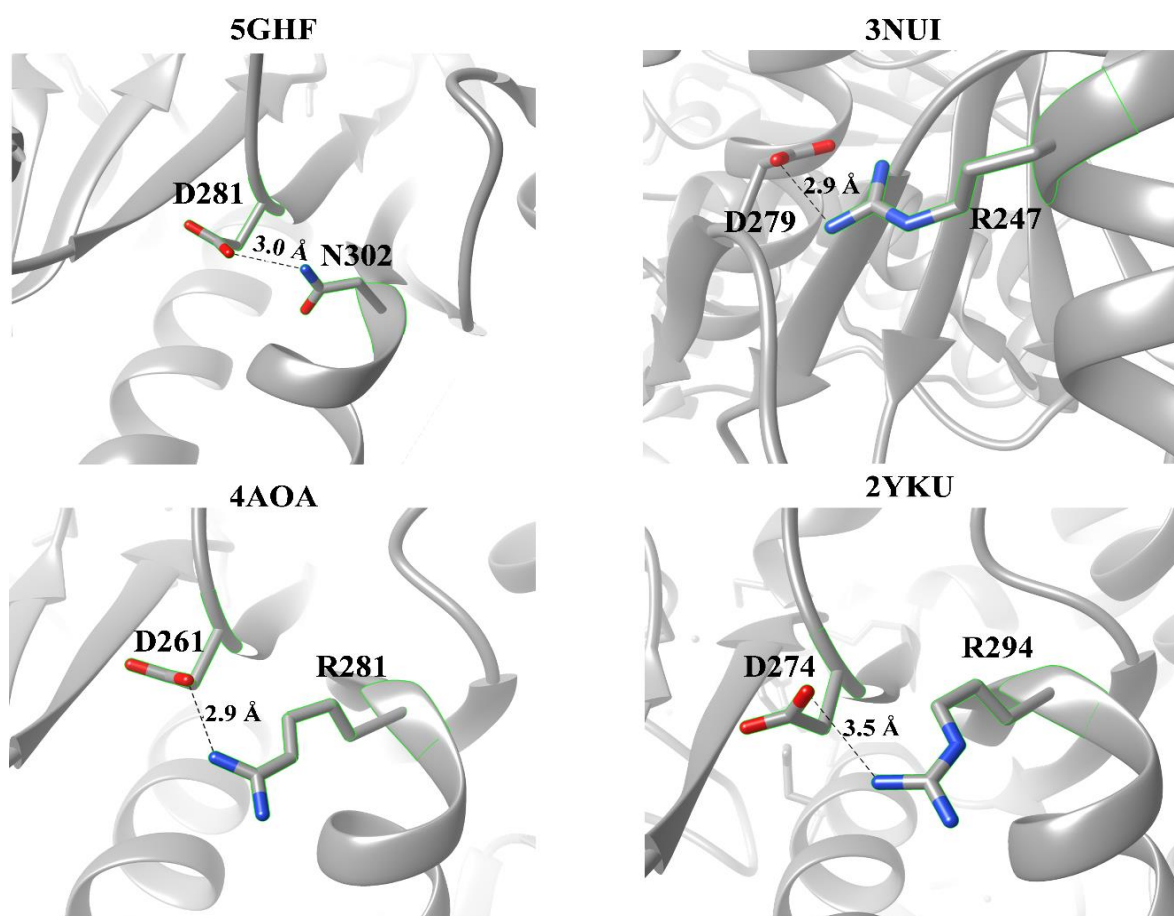


Figure 3.2 Conserved salt bridge within Fold type I ω -TA at D210. Shown for PDB structures 4AOA, 2YKU, 5GFH and 3NUI. The conserved D210 seems to be an important salt bridge starting point, but the corresponding salt bridge partner residue is not conserved, the distance between arginine/asparagine and glutamate is less than 3.5Å. The position numbers are no standard numbers. The distances were calculated using Chimera 1.1 [83].

Besides the functionally relevant positions, it is remarkable that 13 of the 44 conserved residues are glycines and 4 are prolines, most of them localized in loops (12 glycines and 2 prolines, respectively) and might therefore be involved in protein folding. For 23 conserved positions, the function is still unknown.

3.3.3) Fold type IV – sequence analysis

In contrast for Fold type IV were at least 39 conserved positions identified. Using standard numbering scheme the conserved positions were presented in table 3.4 according to the ω -TA from *Aspergillus terreus* as representative sequence (PDB accession 4CE5).

Table 3.4 Conserved positions in putative Fold IV ω -TA sequences with standard numbering according to the ω -TA from *Aspergillus terreus* (PDB accession 4CE5) annotated as in table 3.3

Standard position	Conserved amino acids	Location/function
36	G (86%)	loop
44	A (83%)	
56	G (77%), A (17%), S (5%)	loop
61	E (89%), D (9%)	salt bridge to standard position R79
68	G (82%), T (5%)	loop
76	H (98%)	
79	R (100%)	PLP binding cup [8]
80	L (84%), F (11%)	
83	S (82%), G (11%)	
109	N (73%), S (9%)	
123	G (95%)	loop
158	G (86%)	loop
180	K (88%)	catalytic lysine [8]; salt bridge to position 61
194	A (83%)	
198	G (83%)	loop
201	E (72%), D (18%)	
209	G (89%)	loop
		hydrogen bond to PLP and interaction with position 169 (R:50%, W:11%) [8]
213	E (94%)	
218	N (92%)	
220	F (76%), W (7%), Y (6%)	
222	V (73%), I (15%)	
225	G (77%), N (7%), D (5%)	loop
229	T (87%)	
230	P (78%), R (7%), H (5%)	
235	L (94%)	PLP binding cup [8]
237	G (97%)	loop
238	I (81%), V (10%)	PLP binding cup [8]
239	T (89%)	PLP binding cup [8]
240	R (90%)	

3) Analysis and creation of a systematic ω -TA database (ω TAED)

256	E (75%), V (5%)	
267	A (84%), F (7%)	
268	D (72%), E (9%)	salt bridge to position 223 (K: 51%, R: 24%)
269	E (94%)	
271	F (83%), W (7%)	
273	T (72%), S (14%), C (8%)	
281	P (84%), A (8%)	
286	D (78%), G (8%)	
293	G (76%)	loop
296	G (89%)	loop

The highly conserved position R79 is present in all sequences and is part of the conserved PLP-binding cup formed by E213, L235, I238, and T239 [8]. Furthermore a salt bridge or hydrogen bridge between standard position 61 and R79 can be observed and evolutionary allowed amino acids are glutamic acid, aspartic acid, but also threonine (Figure 3.3).

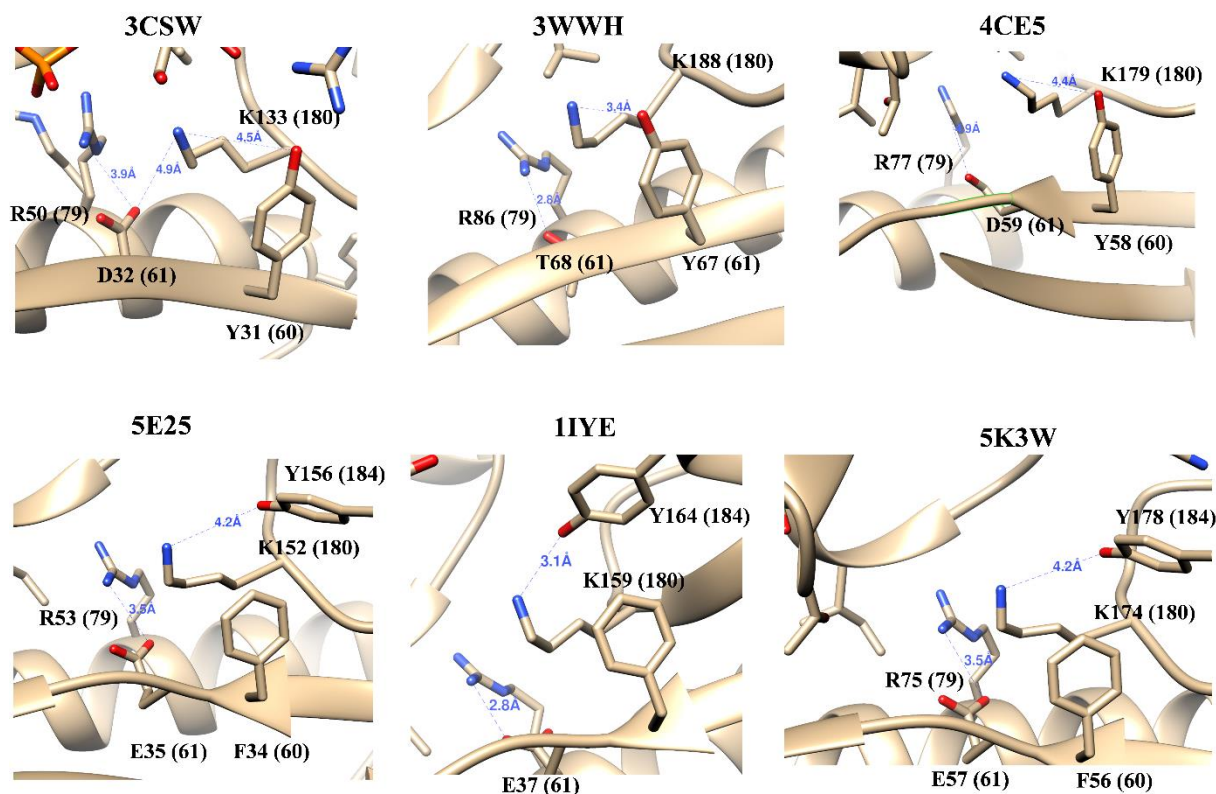


Figure 3.3 Conserved salt bridge between R79 and D/T61 within Fold type IV. Furthermore the position Y67 enables a hydrogen bridge towards K180. The coordination of K180 can be performed by standard position 184. Branched chain transaminase: 1IYE and 5E25. 3WWH, 4CE5 are known as (*R*)-selective ω -TA. 5K3W is characterized as special Fold type IV- ω -TA [49]. 3CSW is annotated as putative Fold type IV ω -TA [8]. Distances were calculated using Chimera 1.1.

3) Analysis and creation of a systematic ω -TA database (oTAED)

Moreover the non-conserved standard position Y60, is showing a hydrogen bridge towards K180 within the transaminases 3CSW, 3WWH and 4CE5. In contrast, an alignment of homologues of 4CE5 (sequence identity between 35 and 95%) showing that this position is highly conserved (Figure 3.3), but also tryptophan is an allowed alternative, which cannot be seen using the global conservation analysis of all Fold type IV members of oTAED. Furthermore standard position 61 is conserved in both conservation analysis (Table 3.4 compared to Figure 3.4) but even in small set of quite similar sequences threonine and glutamic acid are allowed as alternative amino acid residues, which are all able to build a hydrogen bridge or salt bridge to R79. The BCAT enzymes (also part of oTAED database) showing a phenylalanine at position 60 instead of a tyrosine residue. Moreover, in putative BCAT enzymes standard position 184 is evolutionary conserved as Y184 and simultaneously standard position Y60 is changed to phenylalanine, which shows that a tyrosine residue in BCAT enzymes is not necessary anymore at this position.

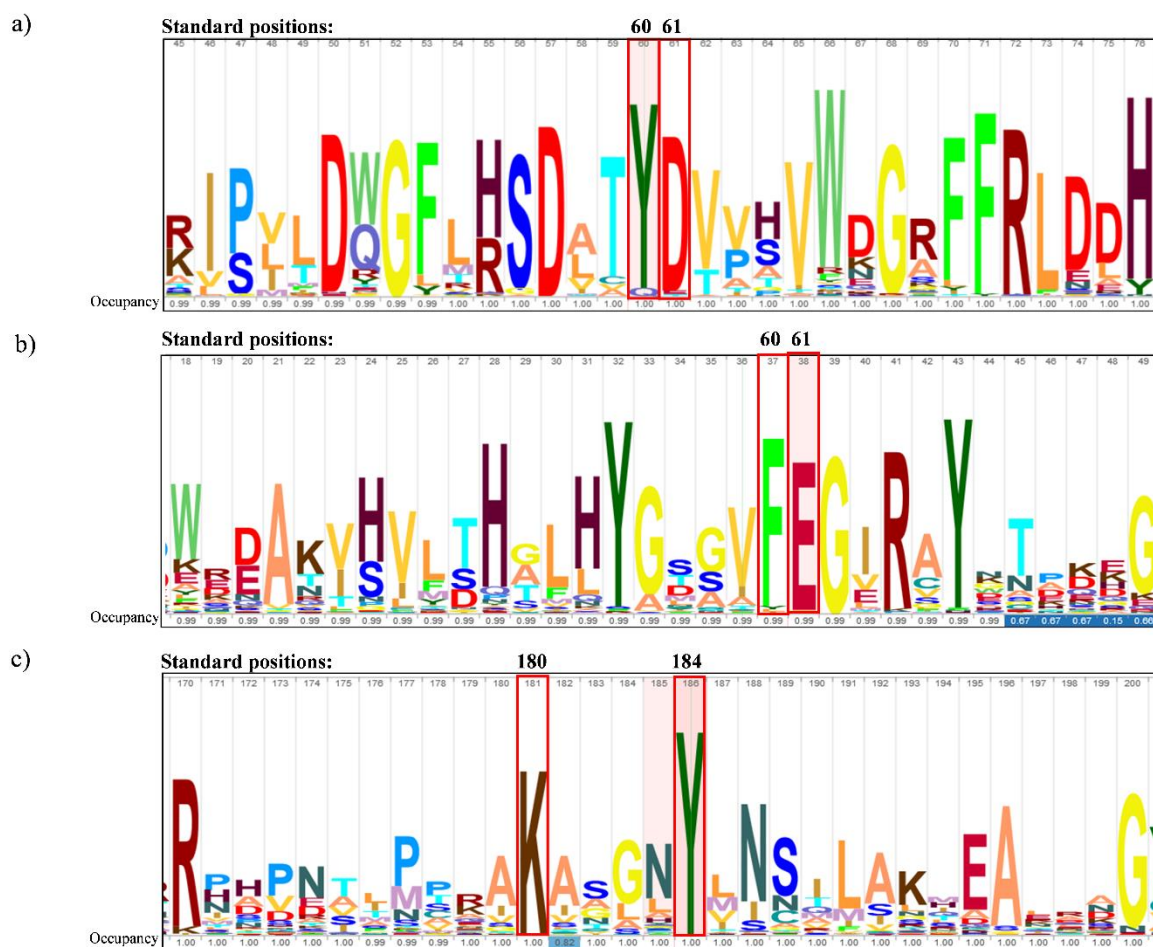


Figure 3.4 Conservation analysis of the coordinating active site tyrosine in Fold type IV. Red brackets highlighting the positions of interest. **A)** For putative ω -TA showed representative to 4CE5 (position 60 and 61). The position Y60 is highly conserved (probability 0.96), but also W60 is an evolutionary allowed residue (probability 0.04). D61 is also highly conserved (probability 0.967) and allowed alternatives are glutamic acid (0.02) and threonine (probability 0.013). **B)** Putative BCAT showed at standard position 60/61 a highly conserved F60 (probability 0.96). However also Y60, L60 and I60 are evolutionary allowed (probabilities 0.02, 0.013 and 0.007). According to A) standard position 61 is highly conserved as E61 and D61 (probability 0.98 and 0.007) but also the uncharged G61 is allowed (probability 0.013). Moreover the mentioned tyrosine residue switches to position 184 within 1IYE and homologues (putative BCATs). Standard position 184 showed to be totally conserved with a probability of 1.0. 150 sequences were utilized for creating alignments of closet related protein sequences (UniProtRef90) using ConSurf with sequential identities of 35 to 95% [84,85]. The results were visualized using Skyglign [86].

Exemplary the branched-chain transaminases 5E25 and 1IYE are analyzed. Both showing an exchange towards phenylalanine and at the same time Y60 is compensated at standard position 184 by a tyrosine residue. Y60 is also part of the motif from Höhne *et al.* [37]. This rearrangement can also be found in the structure 5K3W, which was characterized as unusual Fold type IV (*R*)- ω -TA with activity towards D-amino acids and amines [49]. This enzyme seems to be a connection point between BCAT and (*R*)-selective ω -TA. The distance between K180 and Y178 is 4 Å and between Y178 and hydroxyl-moiety of PLP only 2.6 Å, which would allow a water bridges as well as hydrophobic interactions [87]. Y178 is clearly contributed in binding PLP, which is known for Fold type I ω -TA. Furthermore only F60 might be also able to coordinate PLP by π -interactions (stacking).

Moreover E213 forms a hydrogen bond to the cofactor PLP and might form a salt bridge to R169 in some Fold type IV proteins [8]. Surprisingly the catalytically active lysine is only conserved in 88% of all sequences at Fold type IV standard position 180. As in Fold type I, the catalytic K180 might be able to form a salt bridge to the conserved E/D61, which is also aligned at R79. A further salt bridge could be present between D268 and the partly conserved K/R223. Moreover, 11 conserved glycines all of were located in loop-structures. According to Yan *et al.* they provide flexibility for enzymes and might be important for activity, which enables i.e. the adaption of the enzyme towards substrate [88,89]. For 20 conserved positions, the function is still unknown.

3.3.4) Selectivity- and specificity-determining positions

Considering that (*S*)-selective and (*R*)-selective ω -TA have a different fold, different substrate specificities, and different conserved amino acids in the substrate binding pockets, it is surprising that only one mutation can switch enantiopreference. By engineering the ω -TA of *Artherobacter citreus* (Fold type I), it was shown that a mutation at Fold type I standard position 328 from valine to alanine changes the enantiopreference from (*S*) to (*R*) for the substrate 4-fluoro-phenylacetone [90]. Other relevant positions in Fold type I are Y108 near the cofactor PLP, W26 inside the small binding pocket, and F53.1. Position F53.1 is missing in some Fold type I proteins, but was shown to have an influence in steric hindrance of bulky substrates for the ω -TA from *Chromobacterium violaceum*. [91]. With respect to the binding mechanism of substrate and cofactor of (*R*)- and (*S*)-selective ω -TA, the mechanism of binding the phosphate group of PLP via a hydrogen bond network in the phosphate-binding cup is common to both Fold types (**Figure 3.5**) [8,92,93].

The planar cofactor PLP is sandwiched between Y108 and V191 in Fold type I (*S*)-selective ω -TA and between L235 and F217 in Fold type IV (*R*)-selective ω -TA [24,94,95].

To explore which positions are involved in substrate specificity and stereoselectivity of Fold type I (*S*)-selective ω -TA, two sequence motifs at 17 sites, and 36 Fold type I standard positions were examined which have been described in literature for different ω -TA to be involved in substrate interactions (Table 3.5). The standard numbering of Fold type I revealed that many positions that have been described in different enzymes are structurally equivalent. One example is position 192, which was described in *Vibrio fluvialis* and *Pseudomonas putida* as positions 259 and 262, respectively. This position is also part of the P-pocket (small pocket) motif, and mutations at the mentioned positions to less bulky residues can allow larger substrate molecules inside the small substrate binding pocket [23,96]. It is noteworthy that multiple functional roles have been suggested in literature for the same position. Fold type I standard position 53.1 is mentioned four times in literature for three different ω -TA. Mutation of this position resulted in changing substrate specificity or inversion of enantioselectivity. Fold type I standard position 26 was mentioned seven times for six different ω -TA. The mutation from a large residue at this position to a smaller hydrophobic residue allows the conversion of larger aromatic and hydrophobic substrates. The previously described flipping R346 was described as an important site for dual substrate recognition [55,97]. It was also mentioned in a motif for the recognition of α -carboxyl binding of amino-acceptor substrate and described for the ω -TA from *Vibrio fluvialis*, *Pseudomonas sp.* strain AAC and *Silicibacter pomeroyi* [13,55]. The flipping arginine is also known for the β -phenylalanine converting ω -TA from *Variovorax paradoxus* and *Mesorhizobium sp.* LUK. For the ω -TA from *Sphaerobacter thermophilus*, which transfers an amino group to the γ -position [20], this position is a leucine, but arginines are next to this position at 346.8 and 346.13. In contrast Mathew *et al.* determined the position 0.41 (R41) as flipping arginine in *Sphaerobacter thermophilus*, which is located at the substrate binding pocket and not in the outer shell of the enzyme [20,22]. Overall, Fold type I standard position 108 seems to be an important site for the coordination of PLP, which was mentioned in literature at least four times (Table 3.5).

3) Analysis and creation of a systematic ω -TA database (oTAED)

Table 3.5 Substrate specificity-determining positions and substrate-specific sequence motifs in Fold type I (*S*)-selective ω -transaminases. Standard positions refer to position numbers of the ω -TA from *Mesorhizobium sp.* LUK (PDB accession 2YKU).

Standard position	Position	Function	Source organism	Uniprot ID	Ref.
0.19	F19W	higher activity towards β -keto esters	<i>V. fluvialis</i>	F2XB9	[23]
26	W57F				
53.1	F85A				
111	V153A				
118.1	K163F				
192	I259V				
346	R415F				
53.4	R88K				
0.20	L20	hydrophobic L-pocket	<i>C. crescentus</i> and others	P28269	[96]
0.23	(Y/W/L)23				
53.2	(Y/F)88				
108	Y152				
0.36	R36	decrease of activity towards aromatic β -amino acid	<i>S. thermophilus</i>	D1C218	[20]
0.41	R41	coordination of substrate carboxyl-group	<i>V. paradoxus</i>	H8WR05	[22]
0.41	R41	activity towards aromatic β -amino acids	<i>V. paradoxus</i>	H8WR05	[22]
0.43	(A/V/I)43				
0.50	P50				
14	D65				
15	G66				
24	(E/D/N/Q)75				
25	(Y/F/W)76				
14	G48R	improved stability; activity towards aminotetralin	<i>A. citreus</i> (alternative <i>B. megaterium</i>)	A0A1C7D1 91	[12]
26	Y60C				
118.5	Y164F				
126.5	R186S				
161	A242V				
165	A245T				
172	I252V				
175	F255I				
188	N268S				
346.9	T409R				
346.24	K424E				
346.36	V436A				

3) Analysis and creation of a systematic ω -TA database (ω TAED)

24	E75	interaction with R41	<i>V. paradoxus</i>	H8WR05	[22]
25	Y85I	shift of activity: from ornithine-TA to γ -TA	<i>Homo sapiens</i>	P04181	[98]
25	L56V	increase of activity towards	<i>V. fluvialis</i>	F2XBU9	[67]
26	W57C	branched chain substrates			
53.1	F85V				
111	V153A				
25	L57A	allows for <i>re</i> -face attack;	<i>O. anthropi</i>	A6WVC6	[99]
26	W58A	increased activity towards butyrophene			
26	W57F	opening of P-pocket	<i>V. fluvialis</i>	F2XBU9	[23]
26	W60C	increase of enantioselectivity and activity towards aromatic substrate	<i>C. violaceum</i>	Q7NWX4	[91] [100] [101]
26	W58L	opening of substrate pocket; activity towards aromatic ketons	<i>O. anthropi</i> ; <i>V. fluvialis</i>	A6WVC6	[102] [23]
26	Y59	determines size of the O-pocket	<i>Ruegeria</i> sp. TM1040	Q1GD43	[55] [56]
26	W60	determines size of the S-pocket	<i>C. crescentus</i>	P28269	Review
161	S231				ed by
192	I262				[96]
53.1	Y87	interacts with aromatic substrate in P-pocket	<i>Ruegeria</i> sp. TM1040	Q1GD43	[55] [56]
53.1	F85L	activity towards PEA and longer	<i>V. fluvialis</i>	F2XBU9	[23]
111	V153A	side chains			[94]
53.1	F85A	increase of binding pocket	<i>V. fluvialis</i>	F2XBU9	[23]
53.1	F88A	inversion of enantiopreference	<i>C. violaceum</i>	Q7NWX4	[91]
161	A231F	from (<i>S</i>) to (<i>R</i>)			[100] [101]
53.2	F92V	inhibits activity towards aromatic PEA	<i>Ruegeria</i> sp. TM1040	Q5LMU1	[55]
47	G98M	increase of stability	<i>V. paradoxus</i>	4AOA	[103]
108	Y152	coordinates PLP; prevents activity towards aromatic substrates	<i>Ruegeria</i> sp. TM1040	Q1GD43	[55] [56]
108	Y153M/S/N	switch from a α -TA to a ω -TA	<i>C. violaceum</i>	Q7NWX4	[91] [100] [101]

3) Analysis and creation of a systematic ω -TA database (oTAED)

108	Y150F	higher activity towards amino	<i>V.fluvialis</i>	<i>F2XBU9</i>	[94]
111	V153A	alcohols			
108	Y152	determines size of the small	<i>P. putida</i>	P28269	[96]
192	I262	pocket and allows only methyl residue of PEA			
111	V153A	increases size of P-pocket of ω -TA; activity towards aliphatic α -keto acids	<i>P.denitrificans</i>	A1B956	[104]
118.1	N161I	improved stability	<i>P. mandelii</i>	A0A059KS	[105]
118.5	Y164L		<i>PD30</i>	X8	
164	V228G	increase of activity towards	<i>C. crescentus</i>	Q7WWK8	[53]
220	N286A	aromatic β -amino acid			
192	I259V	tolerance for alcohol ester substrate	<i>V. fluvialis</i>	<i>F2XBU9</i>	[23]
248	V328A	Inversion of enantioselectivity from (<i>S</i>) to (<i>R</i>)	<i>A.citreus</i>	A0A1C7D1 91	[90]
251	Y331C	Increases enantioselectivity for (<i>S</i>)	<i>A.citreus</i>	A0A1C7D1 91	[90]
346	R415	flipping arginine (dual substrate recognition)	<i>V. fluvialis</i>	<i>F2XBU9</i>	[23]
346	R415F	less polarity inside P-pocket	<i>V.fluvialis</i>	<i>F2XBU9</i>	[23]
346.1	R414	flipping arginine (α -carboxyl binding site)	<i>C.crescentus</i>	P28269	[96]
346.1	R414K	loss of activity	<i>Pseudomonas</i> <i>sp. strain AAC</i>	A0A081YA Y5	[13]
346.4	P423	entrance of substrate pocket	<i>Ruegeria</i> sp.	Q1GD43	[55]
			TM1040		[56]
346.20	R416	flipping arginine (dual substrate recognition)	<i>C. violaceum</i>	Q7NWX4	[106]

In comparison to Fold type I, literature information about mutations in (*R*)-selective ω -TA in the Fold type IV superfamily is sparse, and only 17 Fold type IV standard positions were described (**Table 3.6**). Most mutation data were generated by engineering of *Arthrobacter* ω -TA for activity against prostatic gliptin. Fold type IV standard position 62 is part of the small pocket. In ω -TA from *Arthrobacter sp.* 117, the mutation of V62G increased the small pocket [24]. In ω -TA from *Nectria haematococca*, V62 was described as part of a motif which mediates specificity towards (*R*)-amines [95]. Besides that, a mutation at Fold type IV standard position 62 is proposed to increase activity towards aromatic ketone substrates [24].

Table 3.6 Substrate specificity-determining positions and substrate-specific sequence motifs in Fold type IV (*R*)-selective ω -transaminases. Standard positions refer to position numbers of the ω -TA from *Aspergillus terreus* (PDB accession 4CE5).

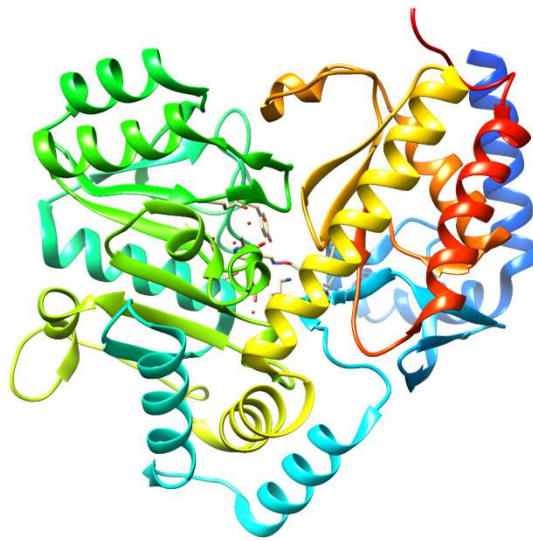
Standard position	Position	Function	Source organism	Uniprot ID	Ref.
55	H53	specificity towards (<i>R</i>)-amines	<i>Nectria haematococca</i>	C7YVL8	[95]
60	Y58				
62	V60				
55	H62A	increase of activity towards aromatic ketone substrate	<i>Artherobacter</i> 117	F7J696-1	[24]
62	V69G	increases size of small pocket	<i>Artherobacter</i> 117	F7J696-1	[24]
115	F122I				
276	A284G				
125	E125	entrance tunnel limiting the substrate size	<i>C.pusillum</i>	A0A1S4NY	[49]
147	E140			F0	
126	G136Y	increase of hydrophobic interaction with substrate	<i>Artherobacter</i> 117	F7J696-1	[24]
127	E137I				
191	V199I				
201	A209L				
128	R138	interacting with keto group of the substrate	<i>Artherobacter</i> 117	F7J696-1	[24]
130	T130M	increase of thermostability	<i>Aspergillus terreus</i>	Q0C8G1	[107]
133	E133F				
215	S223P	increases size of large pocket	<i>Artherobacter</i> 117	F7J696-1	[24]
274	T273	enantioference by limiting space in small pocket	<i>Nectria haematococca</i>	C7YVL8	[95]
275	T274				
276	A275				

3.4) Discussion

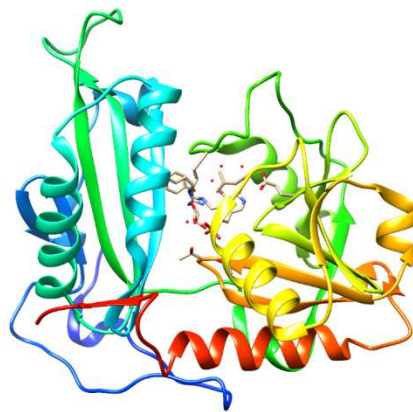
The ω -Transaminase Engineering Database (oTAED) was implemented as a public database for navigating the sequence space of the biotechnologically relevant ω -TA from Fold types I and IV. Besides the oTAED, databases have been published for Fold type IV [37] and Fold type I proteins [108]. The conserved positions in Fold type I and IV were analyzed by standard numbering schemes in the oTAED. For each Fold type, a standard numbering scheme allowed for the unambiguous comparison of structurally equivalent positions in different ω -TA described in literature. The annotation of previously identified sequence motifs and the comparison of functionally relevant positions are expected to facilitate the annotation of yet uncharacterized ω -TA [15,35,109].

Comparison of Fold types I and IV

The putative (*S*) - and (*R*)-selective ω -TA of Fold type I and IV, respectively, have different sequence lengths, different folds, and lack global sequence similarity, and are thus evolutionarily separate (**Figure 3.5**). Despite their different folds, the substrate binding sites of both Fold types consist of a large O- and a small P-pocket [22,37], and the catalytically important residues are located in the same spatial arrangement with a highly conserved catalytic lysine (standard positions 216 or 180 in Fold types I or IV, respectively) pointing to the cofactor PLP from the *si*- or *re*-face (**Figure 3.6**). Thus, in respect to the cofactor and the catalytic lysine, both active sites are mirror images to each other, which explains the observed enantiocomplementarity of Fold type I and Fold type IV (*R*)-selective ω -TA [8,110]. In contrast to Fold type I (*S*)-selective ω -TA, Fold type IV (*R*)-selective ω -TA have no reported activity towards β - or γ -amino acids [35,37,78,111,112]. Both superfamilies show activity towards alanine, which is a hint at a similar mechanism for alanine binding, which might be also a result of the small size of alanine [8,35,37]. However, IPA is also a small amino donor, but it is not accepted by a variety of ω -TA [113,114].



Fold type I
(PDB ID 4AOA)



Fold type IV
(PDB ID 3wwh)

Figure 3.5 Structure comparison of Fold type I and IV. The pattern of Fold type I consists of an $\alpha/\beta/\alpha$ pattern with the active site located at the interface of the homodimer (only monomer is shown). Fold type IV consists of two clear separated domains. Domain 1 is a two layer sandwich. Domain 2 consists of an α - β barrel. The active site is also located at the interface of the homodimer. In general Fold type IV enzymes are smaller than Fold type I members.

3) Analysis and creation of a systematic ω -TA database (oTAED)

Furthermore, it is striking that the PLP binding cup of Fold type IV is more strictly conserved than in Fold type I, which may be explained by the smaller number of currently known sequences for this superfamily. This database might be furthermore a starting point for deep machine learning to characterize sequences without experimental background, which was demonstrated to be an adequate method for prediction of enzyme function using the prediction of E.C. numbers. Such an algorithm using oTAED, might sensitive enough to separate even the different function of isozymes within the presented database [115].

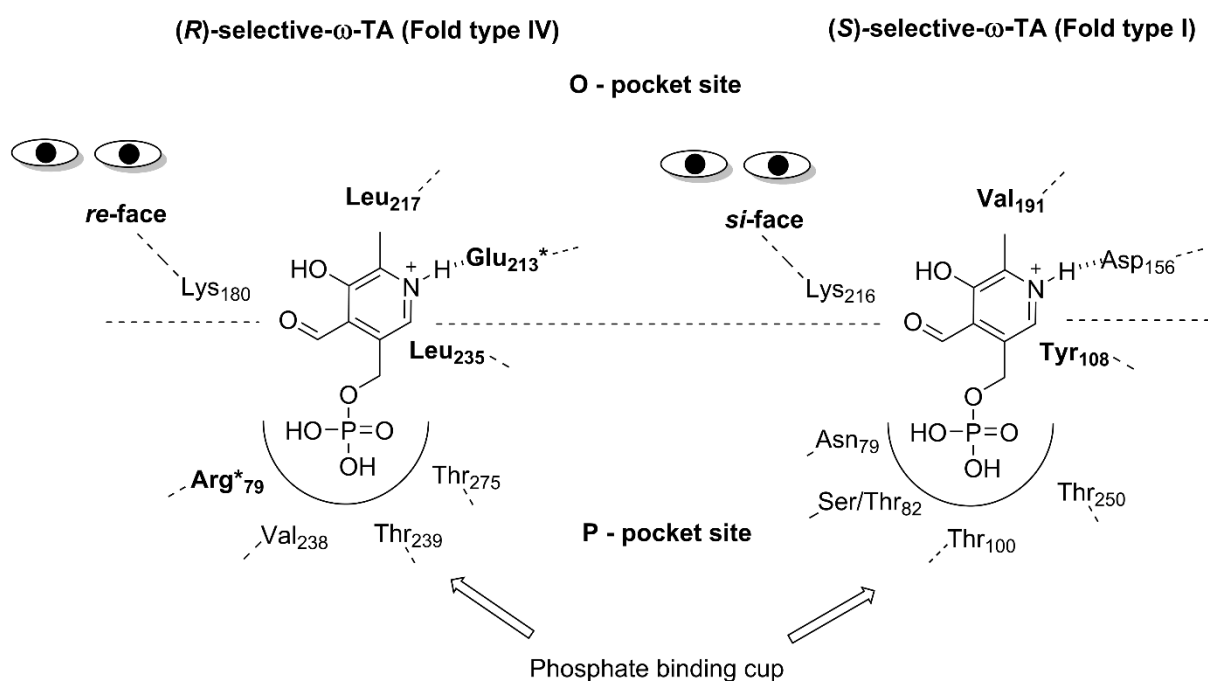


Figure 3.6 The active sites of (*R*)- and (*S*)-selective ω -TA (Fold type IV and I, respectively) as viewed from the *re*- and *si*-face, respectively. The functional residues were defined according to Lyskowski *et al.* and to Humble *et al.*[8,93]. For (*S*)-selective- ω -TA, the amino acid residues of the phosphate binding cup at position 82 are serine or threonine [11,93]. The catalytic lysine is showed as anchor point for *re* and *si*-face view.

Subsequently, Fold type I and Fold type IV enzymes are still a relatively uncharted territory with a small fraction of discovered and described enzymes. Therefore might be the standard numbering a first tool for easy comparison of important ω -TA engineering sites.

Fold type I

Using the example of putative Fold type I (*S*)-selective ω -TA, the standard numbering allows the determination of functional amino acid residues within different targets. Therefore the dual substrate recognition mechanism, which enables ω -TA to recognize quite different substrates, can be investigated. The flipping arginine at Fold type I standard positions 346 or 346.1 was predicted to mediate dual substrate recognition [2]. This position is conserved in 11,243 sequences within Fold type I, and might thus serve as indicator of ω -TA activity. α -TA are absent in the Fold type I superfamily, because sequence similarities between α -TA and (*S*)-selective ω -TA are very low [116]. However, they are functionally related, since a single mutation was sufficient to change an α -TA to an ω -TA [101]. Moreover, many enzyme families like GABA-transaminases or β -phenylalanine amine transaminases were described previously within this group [108]. The known fingerprints of sequence positions are helpful to predict catalytic function [108]. According to this fingerprint-based annotations, the largest group of ω -TA could be classified as glutamate-1-semialdehyde-aminomutases (12,667 sequences) and the second largest as β -phenylalanine transaminases (1527 sequences). In contrast, only 883 ω -TA were predicted to have catalytic activity towards synthetically relevant amines [101]. Over 11,243 sequences (11 %) contained at standard position 346 and 346.1 the mentioned flipping arginine. This shows that the flipping arginine is not only important for a sample size of tested enzymes, moreover the substrate recognition by this residue is very important. Nevertheless, in some groups are enzymes uncovered with different functions. Surprisingly the large group of glutamate-1-semialdehyde-aminomutases inhibits instead of aminomutases also ω -TA, which is misleadingly according to the title, but not unexpected when the similarity is analyzed [108]. This demonstrates also, that current motifs are not stringent enough for accurate classification. In addition Fold type I contains also 138 (0.1%) putative α -amino acid amide-racemases sequences, which were also identified by Steffen-Munsberg [108].

Fold type IV

Correspondingly, Fold type IV comprises different enzyme families with high global sequence similarity but different substrate specificity: ω -TA, 4-amino-4-deoxychorismate lyases, D-amino acid TA (DATA), and L-branched-chain amino acid TA (L-BCAT), which have been identified by specific sequence motifs (**Table 3.7**) [37,108], but could not be distinguished based on global sequence similarity [37].

3) Analysis and creation of a systematic ω -TA database (oTAED)

Relevant fingerprints of oTAED Fold Type IV standard positions as reported previously [117] for 4-amino-4-deoxychorismate lyase (ADCL), D-amino acid aminotransferases (DATA), L-branched chain amino acid aminotransferases (L-BCAT) and (*R*)-selective ω -TA. The presented position Y60 is also part of the motif for ω -TA, but not for BCAT and ADCL. Standard position 184 is not a part of this motif, but might be an important residue for differentiation of many unclassified as well as experimentally uncharacterized Fold type IV members. In addition, the catalytic lysine at Fold Type IV standard position 180 is conserved in the four subfamilies.

Table 3.7 Fingerprints of Fold type IV standard positions as reported previously for (*R*)-selective ω -TA, 4-amino-4-deoxychorismate lyase (ADCL), D-amino acid aminotransferases (DATA), L-branched chain amino acid aminotransferases (L-BCAT) and). In addition, the catalytic lysine at Fold type IV standard position K180 is conserved in the four subfamilies. [117]

Standard positions	55	60	62	64	115-	128-130
ADCL	F/Y	F	T/S	-	(V/I/L) _x (K/R)	RGY
DATA	F	Y/E/D	V	K/R	x(V/I/L)Y(V/I/L)Q	RxH
L-BCAT	Y	F/E/D	G	R/K	Y(V/I/L)R	(V/I/L)G(V/I/L)
ω -TA	H/R	Y	V/T	S/T/A/H/P	(F/Y)V(E/A/S/N/Q)	-

Interestingly, L-BCAT, 4-amino-4-deoxychorismate lyases, and DATA enzymes are highly related to (*R*)-selective ω -TA within Fold type IV and appears in our database as separate branch (**Figure 3.7**) [37]. The different substrate specificities are reflected by specific binding sites. In (*S*)-selective L-BCAT, the α -carboxyl group is bound in the small P-pocket, while in (*R*)-selective TAs it is bound in the larger O-pocket [37].

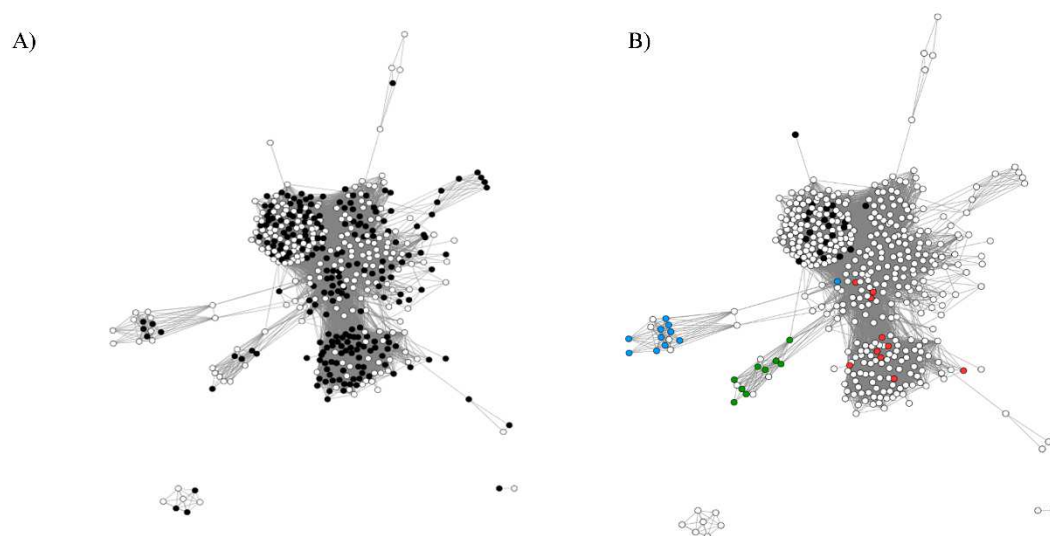


Figure 3.7 Graphical network of Fold type IV members. **A)** Putative (*R*)-selective α and ω -TA depicted in black. **B)** Putative ADCL (blue), DATA (black), L-BCAT (red) and (*R*)-selective ω -TA (green). White spots are sequences with unknown function. Classes were determined using sequence motifs from [37] and **table 3.7**. Nodes correspond to representative sequences of clusters formed by 30% identity in USEARCH. A cutoff of 50% pairwise sequence similarity is used to select the edges. The network is shown as force-directed layout, with pairs with higher similarity arranged in closer proximity (**Attention string length does not mean the evolutive distances**). Networks were designed by Patrick Buchholz.

As a consequence, L-BCAT show an opposite enantioselectivity in comparison to DATA and (*R*)-selective ω -TA [118], and were successfully engineered into ω -TA accepting large aliphatic substrates [37]. Furthermore, it is surprising that the arginine residue relevant for substrate recognition is not conserved within Fold type IV. This substrate recognition site was assigned

3) Analysis and creation of a systematic ω -TA database (oTAED)

to Fold type IV standard position 128 [119]. Therefore, Fold type IV probably includes further enzyme classes other than ω -TA or several inactive enzymes.

The sequence similarity network indicates that sequences with matching positions for potential (*R*)-selectivity did not form distinct groups, whereas sequences matching motifs for ADCL, DATA, L-BCAT, or ω -TA activity were found in different subgroups. It is, however, difficult to predict overlapping substrate scopes between different enzyme classes. Thus, enzymes marked as L-BCAT might have similar specificity towards non- α -amino acid substrates as ω -TA as shown previously [120]. In addition the standard position 60 and 184 might be important for differentiation of L-BCAT and ω -TA. Like mentioned before, position 60 is in the most of Fold type IV ω -TA conserved as tyrosine whereas a phenylalanine is positioned in most of the BCAT sequences and additionally they contain at 184 a tyrosine. This site might allow an arrangement of large aliphatic chains within the transaminases.

3.4.1) Understanding the substrate specificity of ω -TA

Substrate specificity depends on distinct amino acid residues in the substrate pockets [55]. Among them, Fold type I standard position 26 seems to be pivotal in mediating the P-pocket size. This position is relevant in ω -TA from *Chromobacterium violaceum*, *Ochrobactrum anthropi*, *Vibrio fluvialis*, *Pseudomonas putida*, *Bacillus megaterium* and *Caulobacter crescentus* mentioned in at least six publications (**Table 3.5**). The mutation from tryptophan to a smaller hydrophobic amino acid residue at Fold type I standard position 26 allowed for conversion of larger aromatic and hydrophobic substrates. Additionally, Fold type I standard position 53.1 was crucial for the conversion of large substrates, but this position is missing in some ω -TA like in the *V. paradoxus* ω -TA [91]. An exchange from a large residue like W/F to F/V/A opened the small binding pocket (P) towards larger residues and led to an inversion of enantioselectivity and a reduced activity towards 1-phenylethyl-amine, an amine donor which is accepted by all ω -TA [35,121]. However, the sequence region between 44 and 81 which is probably involved in substrate recognition showed low sequence conservation and thus could not be reliably aligned. Fold type I standard position 108 is a promising hotspot which mediates substrate recognition. This site can be exchanged with many different amino acids (Y/M/S/N/F/A) with varying effects on substrate specificity. It was expected that a smaller residue at position 108 would allow for higher flexibility of the PLP cofactor at the active site and decrease steric hindrance for bulky substrates [14]. It was even shown that this site has an influence on α - versus ω -TA activity by structural comparison of an α - with an ω -TA from *C.*

violaceum [101]. Beside the substrate specificity, also the enzyme stability is target of enzyme engineering, which can be examined using oTAED.

The residues Y60 and Y184 might be function for coordination of K180 or for coordinating of PLP via stacking. These standard positions might be hiding the same function as standard position 108 in Fold type I ω -TA, which was often engineered from tyrosine to phenylalanine.

3.4.2) Thermostability of ω -TA

Robustness of an enzyme towards harsh process conditions is often linked to its thermostability, which is therefore of major interest in enzyme design. In addition to the already mentioned method of enzyme thermostability engineering (**Chapter 1**), enzymes from thermophilic microorganisms, which are already naturally adapted to high temperatures, can be used. Furthermore, psychrophilic enzymes are interesting because of their high activity at low temperatures [122]. Until now, no psychrophilic ω -TA and only a few thermostable ω -TA are known for Fold type I [123]. Recently, three thermostable ω -TA genes from hot spring sources were found and characterized (Uniprot ID A0A1U9WZ51, A0A1U9WZ50, and A0A1U9WZ53). Further examples are ω -TA from *Thermomicrobium roseum* and from *Sphaerobacter thermophilus* [20,123]. The taxonomic sources of sequence entries in the oTAED were searched for matching entries in the BacDive database (release 27.02.2017) which comprises environmental conditions of the two domains *Bacteria* and *Archaea* [124]. For Fold type I, 2923 sequences from thermophilic, 1171 sequences from hyperthermophilic, and 2434 sequences from psychrophilic source organisms were identified. For Fold type IV, 449 sequences from thermophilic and 40 sequences from hyperthermophilic source organisms were identified. In contrast, the motifs (V/I)xLDxR and PFG(K/H)YL from Stekhanova *et al.* for thermostable ω -TA matched with only 12 sequences [125]. Sequences from extremophilic source organisms did not form separate clusters, but were distributed across the respective sequence network (**Figure 3.8**).

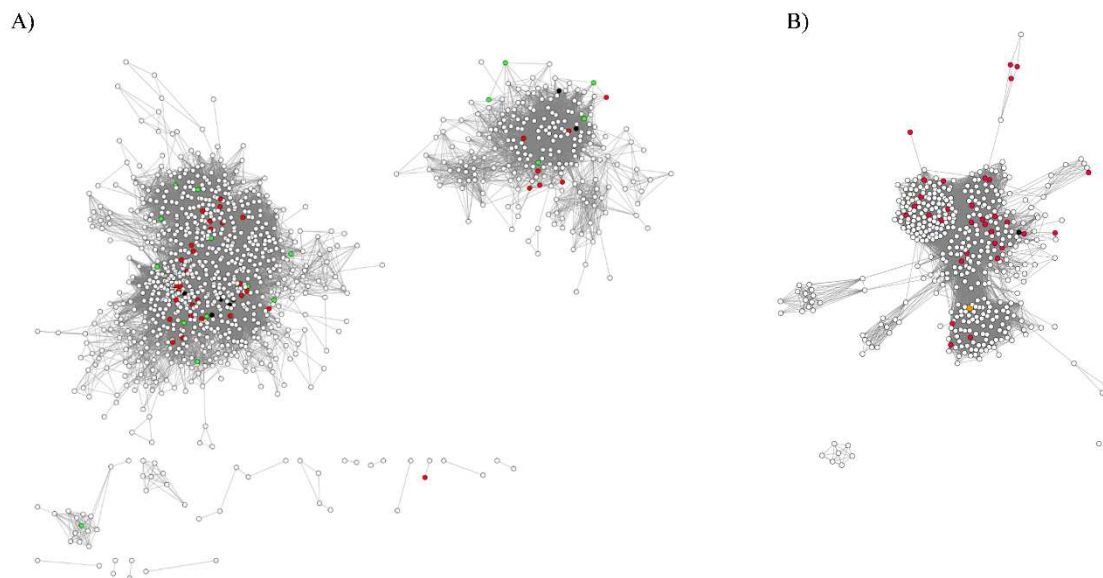


Figure 3.8 Putative ω -TA of **A)** Fold type I (A) and **B)** Fold type IV in respect to thermophile. Nodes from psychrophilic (green), thermophilic (red), and hyperthermophilic (black) sources retrieved from the BacDive database [124] and the representative node (orange) containing the motifs for thermostable Fold IV sequences (V/I)xLDxR and PFG(K/H)YL Stekhanova *et al.* 2017 are annotated[125]. The nodes correspond to representative sequences of clusters formed by 30% identity in USEARCH [64]. Network settings according to **Figure 3.8**. (Networks were designed by Patrick Buchholz)

Noteworthy, the representative node matching the motifs from Stekhanova *et al.* is not necessarily surrounded by matches from thermo- or hyperthermophilic sources.

3.5) Conclusion

The biocatnet platform allows fast comparison of engineering sites, structures and can be utilized as helpful navigation tool for orientation within Fold type I and IV ω -TA. Furthermore the results are showing, that ω -TA within both Fold types are closely related to other transaminase and to other enzyme classes. Surprisingly Fold type I α -TA are absent from database, because they differ according to their sequence significantly from ω -TA and therefore they cannot be found within the superfamily. However, the level of knowledge, especially for Fold type IV enzymes, is still relatively low. More Fold type IV ω -TA have to be uncovered and characterized to determine with higher certainty the differences between BCAT, DATA and ω -TA. Until now the nomenclature of many enzymes is doubtful within the Fold type IV family and actually no commonly accepted standard substrate exists as a reference for transaminase-activity classes. Therefore, it would be beneficial to determine standard amine-

substrate tests for classification. However, a huge amount of sequences cannot be defined by sequential fingerprints until now and in case of doubt only experimental data can verify enzyme function, but the analysis of this and other databases helps to understand the structure-sequence-function relationship and might allow in the near future directed enzyme designs.

3.6) References Chapter 3

- Jansonius JN. Structure, evolution and action of vitamin B6-dependent enzymes. *Curr Opin Struct Biol.* 1998;8: 759–769. doi:10.1016/S0959-440X(98)80096-1
- Hirotsu K, Goto M, Okamoto A, Miyahara I. Dual substrate recognition of aminotransferases. *Chem Rec.* Wiley-VCH; 2005;5: 160–172. doi:10.1002/tcr.20042
- Han S-W, Shin J-S. Metabolically driven equilibrium shift of asymmetric amination of ketones by ω -transaminase using alanine as an amino donor. *Biosci Biotechnol Biochem.* 2014;78: 1788–1790. doi:10.1080/09168451.2014.930328
- Percudani R, Peracchi A. The B6 database: a tool for the description and classification of vitamin B6-dependent enzymatic activities and of the corresponding protein families. *BMC Bioinformatics.* 2009;10: 273. doi:10.1186/1471-2105-10-273
- Cristen P, Metzler DE. *Transaminases (Biochemistry: A Series of Monographs)*. New York: John Wiley & Sons, Inc.; 1985.
- Rozzell JD. Production of L-amino acids by transamination. EP 0135846 A2, 1984.
- Breslow R, Chmielewski J, Foley D, Johnson B, Kumabe N, Varney M, et al. Optically Active Amino Acid Synthesis by Artificial Transaminase Enzymes. *Tetrahedron.* 1988;44: 5515–5524. doi:10.1016/S0040-4020(01)86057-9
- Łyskowski A, Gruber C, Steinkellner G, Schürmann M, Schwab H, Gruber K, et al. Crystal structure of an (*R*)-selective ω -transaminase from *Aspergillus terreus*. *PLoS One.* 2014;9: e87350. doi:10.1371/journal.pone.0087350
- O'Rourke PEF, Eadsforth TC, Fyfe PK, Shepherd SM, Hunter WN. *Pseudomonas aeruginosa* 4-Amino-4-Deoxychorismate Lyase: Spatial Conservation of an Active Site Tyrosine and Classification of Two Types of Enzyme. Roe AJ, editor. *PLoS One.* Humana Press Inc; 2011;6: e24158. doi:10.1371/journal.pone.0024158
- Sayer C, Isupov MN, Westlake A, Littlechild JA. Structural studies of *Pseudomonas* and *Chromobacterium* ω -aminotransferases provide insights into their differing substrate specificity. *Acta Crystallogr Sect D Biol Crystallogr.* International Union of Crystallography; 2013;69: 564–576. doi:10.1107/S0907444912051670
- Wybenga GG, Crismaru CG, Janssen DB, Dijkstra BW. Structural determinants of the β -selectivity of a bacterial Aminotransferase. *J Biol Chem.* 2012;287: 28495–28502. doi:10.1074/jbc.M112.375238
- Martin AR, DiSanto R, Plotnikov I, Kamat S, Shonnard D, Pannuri S. Improved activity and thermostability of (*S*)-aminotransferase by error-prone polymerase chain reaction for the production of a chiral amine. *Biochem Eng J.* 2007;37: 246–255. doi:10.1016/j.bej.2007.05.001
- Wilding M, Peat TS, Newman J, Scott C. A β -Alanine Catabolism Pathway Containing a Highly Promiscuous ω -Transaminase in the 12-Aminododecanate-Degrading *Pseudomonas* sp. Strain AAC. Parales RE, editor. *Appl Environ Microbiol.* 2016;82: 3846–56. doi:10.1128/AEM.00665-16
- Weiß MS, Pavlidis I V., Spurr P, Hanlon SP, Wirz B, Iding H, et al. Protein-engineering of an amine transaminase for the stereoselective synthesis of a pharmaceutically relevant bicyclic amine. *Org Biomol Chem.* Royal Society of Chemistry; 2016;14: 10249–10254. doi:10.1039/C6OB02139E
- Rudat J, Brucher BR, Sylclat C. Transaminases for the synthesis of enantiopure beta-amino acids. *AMB Express.* Springer; 2012;2: 11. doi:10.1186/2191-0855-2-11
- Koszelewski D, Tauber K, Faber K, Kroutil W. omega-Transaminases for the synthesis of non-racemic alpha-chiral primary amines. *Trends Biotechnol.* Elsevier Ltd; 2010;28: 324–32. doi:10.1016/j.tibtech.2010.03.003
- Malik MS, Park ES, Shin JS. Features and technical applications of ω -transaminases. *Appl Microbiol Biotechnol.* 2012;94: 1163–1171. doi:10.1007/s00253-012-4103-3
- Ingram CU, Bommer M, Smith MEB, Dalby PA, Ward JM, Hailes HC, et al. One-pot synthesis of amino-alcohols using a de-novo transketolase and β -alanine:pyruvate transaminase pathway in *Escherichia coli*. *Biotechnol Bioeng.* Wiley Subscription Services, Inc., A Wiley Company; 2007;96: 559–569. doi:10.1002/bit.21125

3) Analysis and creation of a systematic ω -TA database (ω TAED)

19. Tauber K, Fuchs M, Sattler JH, Pitzer J, Pressnitz D, Koszelewski D, et al. Artificial Multi-Enzyme Networks for the Asymmetric Amination of *sec* - Alcohols. *Chem - A Eur J*. WILEY-VCH Verlag; 2013;19: 4030–4035. doi:10.1002/chem.201202666
20. Mathew S, Nadarajan SP, Chung T, Park HH, Yun H. Biochemical characterization of thermostable ω -transaminase from *Sphaerobacter thermophilus* and its application for producing aromatic β - and γ -amino acids. *Enzyme Microb Technol*. Elsevier Inc.; 2016; doi:10.1016/j.enzmictec.2016.02.013
21. Mathew S, Bea H, Nadarajan SP, Chung T, Yun H. Production of chiral β -amino acids using ω -transaminase from *Burkholderia graminis*. *J Biotechnol*. Elsevier B.V.; 2015;196–197: 1–8. doi:10.1016/j.jbiotec.2015.01.011
22. Crismaru CG, Wybenga GG, Szymanski W, Wijma HJ, Wu B, Bartsch S, et al. Biochemical Properties and Crystal Structure of a β -Phenylalanine Aminotransferase from *Variovorax paradoxus*. *Appl Environ Microbiol*. 2013;79: 185–195. doi:10.1128/AEM.02525-12
23. Midelfort KS, Kumar R, Han S, Karmilowicz MJ, McConnell K, Gehlhaar DK, et al. Redesigning and characterizing the substrate specificity and activity of *Vibrio fluvialis* aminotransferase for the synthesis of imigabalin. *Protein Eng Des Sel*. 2013;26: 25–33. doi:10.1093/protein/gzs065
24. Savile CK, Janey JM, Mundorff EC, Moore JC, Tam S, Jarvis WR, et al. Biocatalytic Asymmetric Synthesis of Chiral Amines from Ketones Applied to Sitagliptin Manufacture. *Science (80-)*. 2010;329: 305–309. doi:10.1126/science.1188934
25. Fuchs M, Koszelewski D, Tauber K, Sattler J, Banko W, Holzer AK, et al. Improved chemoenzymatic asymmetric synthesis of (*S*)-Rivastigmine. *Tetrahedron*. Pergamon; 2012. pp. 7691–7694. doi:10.1016/j.tet.2012.06.031
26. Richter N, Simon RC, Kroutil W, Ward JM, Hailes HC. Synthesis of pharmaceutically relevant 17- α -amino steroids using an ω -transaminase. *Chem Commun. Royal Society of Chemistry*; 2014;50: 6098–6100. doi:10.1039/C3CC49080G
27. Koszelewski D, Pressnitz D, Clay D, Kroutil W. Deracemization of Mexiletine Biocatalyzed by ω -Transaminases. *Org Lett*. American Chemical Society; 2009;11: 4810–4812. doi:10.1021/o9101834x
28. Sehl T, Hailes HC, Ward JM, Wardenga R, von Lieres E, Offermann H, et al. Two Steps in One Pot: Enzyme Cascade for the Synthesis of Nor(pseudo)ephedrine from Inexpensive Starting Materials. *Angew Chemie Int Ed*. WILEY-VCH; 2013;52: 6772–6775. doi:10.1002/anie.201300718
29. Dold S-M, Cai L, Rudat J. One-step purification and immobilization of a β -amino acid aminotransferase using magnetic (M-PVA) beads. *Eng Life Sci*. 2016;16: 568–576. doi:10.1002/elsc.201600042
30. Arvidsson PI, Frackenpohl J, Ryder NS, Liechty B, Petersen F, Zimmermann H, et al. On the antimicrobial and hemolytic activities of amphiphilic beta-peptides. *Chembiochem*. 2001;2: 771–773. doi:10.1002/1439-7633(20011001)2:10
31. Alvin A, Miller KI, Neilan BA. Exploring the potential of endophytes from medicinal plants as sources of antimycobacterial compounds. *Microbiol Res. Urban & Fischer*; 2014;169: 483–495. doi:10.1016/j.micres.2013.12.009
32. Mutti FG, Kroutil W. Asymmetric Bio-amination of Ketones in Organic Solvents. *Adv Synth Catal*. WILEY-VCH Verlag; 2012;354: 3409–3413. doi:10.1002/adsc.201200900
33. Dold SM, Syldatk C, Rudat J. Transaminases and their Applications. *Green Biocatalysis*. Hoboken, NJ: John Wiley & Sons, Inc; 2016. pp. 715–746. doi:10.1002/9781118828083.ch29
34. Ferrandi EE, Monti D. Amine transaminases in chiral amines synthesis: recent advances and challenges. *World J Microbiol Biotechnol*. Springer; 2018;34. doi:10.1007/s11274-017-2395-2
35. Guo F, Berglund P. Transaminase Biocatalysis: Optimization and Application. *Green Chem*. Royal Society of Chemistry; 2016; 333–360. doi:10.1039/C6GC02328B
36. Slabu I, Galman JL, Lloyd RC, Turner NJ. Discovery, Engineering and Synthetic Application of Transaminase Biocatalysts. *ACS Catal*. 2017; aescatal.7b02686. doi:10.1021/acscatal.7b02686
37. Höhne M, Schätzle S, Jochens H, Robins K, Bornscheuer UT. Rational assignment of key motifs for function guides in silico enzyme identification. *Nat Chem Biol*. Nature Publishing Group; 2010;6: 807–813.

3) Analysis and creation of a systematic ω -TA database (oTAED)

- doi:10.1038/nchembio.447
38. Pavlidis I V., Weiß MS, Genz M, Spurr P, Hanlon SP, Wirz B, et al. Identification of (*S*)-selective transaminases for the asymmetric synthesis of bulky chiral amines. *Nat Chem*. Nature Publishing Group; 2016;8: 1–7. doi:10.1038/NCHEM.2578
39. Jensen RA, Gu W. Evolutionary recruitment of biochemically specialized subdivisions of Family I within the protein superfamily of aminotransferases. *J Bacteriol*. 1996;178: 2161–2171. doi:10.1128/jb.178.8.2161-2171.1996
40. Ouzounis C, Sander C. Homology of the NifS family of proteins to a new class of pyridoxal phosphate-dependent enzymes. *FEBS Lett*. 1993;322: 159–164. doi:10.1016/0014-5793(93)81559-I
41. Mehta PK, Hale TI, Christen P. Aminotransferases: demonstration of homology and division into evolutionary subgroups. *Eur J Biochem*. Blackwell Publishing Ltd; 1993;214: 549–561. doi:10.1111/j.1432-1033.1993.tb17953.x
42. Grishin N V, Phillips MA, Goldsmith EJ. Modeling of the spatial structure of eukaryotic ornithine decarboxylases. *Protein Sci*. Wiley-Blackwell; 1995;4: 1291–304. doi:10.1002/pro.5560040705
43. Rausch C, Lerchner A, Schiefner A, Skerra A. Crystal structure of the ω -aminotransferase from *Paracoccus denitrificans* and its phylogenetic relationship with other class III amino- transferases that have biotechnological potential. *Proteins Struct Funct Bioinforma*. Wiley Subscription Services, Inc., A Wiley Company; 2013;81: 774–787. doi:10.1002/prot.24233
44. Finn RD, Bateman A, Clements J, Coghill P, Eberhardt RY, Eddy SR, et al. Pfam: the protein families database. *Nucleic Acids Res*. 2014;42: D222–D230. Available: <http://dx.doi.org/10.1093/nar/gkt1223>
45. Nakai T, Okada K, Akutsu S, Miyahara I, Kawaguchi S, Kato R, et al. Structure of *Thermus thermophilus* HB8 Aspartate Aminotransferase and Its Complex with Maleate. *Biochemistry*. 1999;38: 2413–2424. doi:10.1021/bi9819881
46. Braunstein A. Amino Group Transfer. *The Enzymes*. Academic Press; 1973. p. 379. doi:10.1016/S1874-6047(08)60122-5
47. Schneider G, Käck H, Lindqvist Y. The manifold of vitamin B6 dependent enzymes. *Structure*. 2000;8: 1–6. doi:10.1016/S0969-2126(00)00085-X
48. Eliot AC, Kirsch JF. Pyridoxal Phosphate Enzymes: Mechanistic, Structural, and Evolutionary Considerations. *Annu Rev Biochem*. Annual Reviews; 2004;73: 383–415. doi:10.1146/annurev.biochem.73.011303.074021
49. Pavkov-Keller T, Strohmeier GA, Diepold M, Peeters W, Smeets N, Schürmann M, et al. Discovery and structural characterisation of new fold type IV-transaminases exemplify the diversity of this enzyme fold. *Sci Rep*. Nature Publishing Group; 2016;6: 38183. doi:10.1038/srep38183
50. Mugford PF, Wagner UG, Jiang Y, Faber K, Kazlauskas RJ. Enantiocomplementary Enzymes: Classification, Molecular Basis for Their Enantiopreference, and Prospects for Mirror-Image Biotransformations. *Angew Chemie Int Ed*. WILEY-VCH Verlag; 2008;47: 8782–8793. doi:10.1002/anie.200705159
51. Shin J-S, Yun H, Jang J-W, Park I, Kim B-G. Purification, characterization, and molecular cloning of a novel amine:pyruvate transaminase from *Vibrio fluvialis* JS17. *Appl Microbiol Biotechnol*. 2003;61: 463–471. doi:10.1007/s00253-003-1250-6
52. Han SW, Park ES, Dong JY, Shin JS. Active-site engineering of ω -transaminase for production of unnatural amino acids carrying a side chain bulkier than an ethyl substituent. *Appl Environ Microbiol*. 2015;81: 6994–7002. doi:10.1128/AEM.01533-15
53. Hwang B-Y, Ko S-H, Park H-Y, Seo J-H, Lee B-S, Kim B-G. Identification of omega-aminotransferase from *Caulobacter crescentus* and site-directed mutagenesis to broaden substrate specificity. *J Microbiol Biotechnol*. 2008;18: 48–54.
54. Clark SM, Di Leo R, Van Cauwenberghe OR, Mullen RT, Shelp BJ. Subcellular localization and expression of multiple tomato γ -aminobutyrate transaminases that utilize both pyruvate and glyoxylate. *J Exp Bot*. 2009;60: 3255. doi:10.1093/jxb/erp161
55. Steffen-Munsberg F, Vickers C, Thontowi A, Schätzle S, Meinhardt T, Svedendahl M, et al. Revealing the Structural Basis of Promiscuous Amine Transaminase Activity. *ChemCatChem*. 2013;5: 154–157. doi:10.1002/cctc.201200545
56. Pavlidis I V., Weiß MS, Genz M, Spurr P, Hanlon SP, Wirz B, et al. Identification of (*S*)-selective transaminases for the asymmetric synthesis of bulky chiral amines. *Nat Chem*. Nature Publishing Group;

3) Analysis and creation of a systematic ω -TA database (ω TAED)

- 2016;8: 1–7. doi:10.1038/NCHEM.2578
57. Calvelage S, Dörr M, Höhne M, Bornscheuer UT. A Systematic Analysis of the Substrate Scope of (*S*)- and (*R*)-Selective Amine Transaminases. *Adv Synth Catal*. Wiley-Blackwell; 2017;359: 4235–4243. doi:10.1002/adsc.201701079
58. Benson DA, Karsch-Mizrachi I, Lipman DJ, Ostell J, Sayers EW. GenBank. *Nucleic Acids Res*. John Wiley and Sons, Inc., NY; 2011;39: D32–D37. doi:10.1093/nar/gkq1079
59. Buchholz PCF, Vogel C, Reusch W, Pohl M, Rother D, Spieß AC, et al. BioCatNet: A Database System for the Integration of Enzyme Sequences and Biocatalytic Experiments. *ChemBioChem*. 2016;17: 2093–2098. doi:10.1002/cbic.201600462
60. Sievers F, Wilm A, Dineen D, Gibson TJ, Karplus K, Li W, et al. Fast, scalable generation of high-quality protein multiple sequence alignments using Clustal Omega. *Mol Syst Biol*. European Molecular Biology Organization; 2011;7: 539. doi:10.1038/msb.2011.75
61. Vogel C, Widmann M, Pohl M, Pleiss J. A standard numbering scheme for thiamine diphosphate-dependent decarboxylases. *BMC Biochem*. 2012;13: 24. doi:10.1186/1471-2091-13-24
62. Russell RB, Barton GJ. Multiple protein sequence alignment from tertiary structure comparison: Assignment of global and residue confidence levels. *Proteins Struct Funct Genet*. Wiley Subscription Services, Inc., A Wiley Company; 1992;14: 309–323. doi:10.1002/prot.340140216
63. Eddy SR. Profile hidden Markov models. *Bioinformatics*. 1998;14: 755–63. doi:doi.org/10.1093/bioinformatics/14.9.755
64. Edgar RC. Search and clustering orders of magnitude faster than BLAST. *Bioinformatics*. 2010;26: 2460–2461. doi:10.1093/bioinformatics/btq461
65. Rice P, Longden I, Bleasby A. EMBOSS: the European Molecular Biology Open Software Suite. *Trends Genet*. 2000;16: 276–7. doi:doi.org/10.1016/S0168-9525(00)02024-2
66. Mathew S, Jeong SS, Chung T, Lee SH, Yun H. Asymmetric synthesis of aromatic β -amino acids using ω -transaminase: Optimizing the lipase concentration to obtain thermodynamically unstable β -keto acids. *Biotechnol J*. 2016;11: 185–190. doi:10.1002/biot.201500181
67. Genz M, Melse O, Schmidt S, Vickers C, Dörr M, van den Bergh T, et al. Engineering the Amine Transaminase from *Vibrio fluvialis* towards Branched-Chain Substrates. *ChemCatChem*. 2016;8: 3199–3202. doi:10.1002/cctc.201601007
68. Yonaha K, Toyama S, Kagamiyama H. Properties of the bound coenzyme and subunit structure of omega-amino acid:pyruvate aminotransferase. *J Biol Chem*. 1983;258: 2260–2265. Available: <http://www.jbc.org/content/258/4/2260.short>
69. Reyes BA, Pendergast JS, Yamazaki S. Mammalian peripheral circadian oscillators are temperature compensated. *Journal of Biological Rhythms*. 2008. pp. 95–98. doi:10.1177/0748730407311855
70. Zhang J, Yang JR. Determinants of the rate of protein sequence evolution. *Nature Reviews Genetics*. NIH Public Access; 2015. pp. 409–420. doi:10.1038/nrg3950
71. Kaneko T, Nakamura Y, Sato S, Asamizu E, Kato T, Sasamoto S, et al. Complete Genome Structure of the Nitrogen-fixing Symbiotic Bacterium *Mesorhizobium loti*. *DNA Res*. Oxford University Press; 2000;7: 331–338. doi:10.1093/dnares/7.6.331
72. Satola B, Wübbeler JH, Steinbüchel A. Metabolic characteristics of the species *Variovorax paradoxus*. *Appl Microbiol Biotechnol*. Springer-Verlag; 2013;97: 541–560. doi:10.1007/s00253-012-4585-z
73. Kaulmann U, Smithies K, Smith MEB, Hailes HC, Ward JM. Substrate spectrum of ω -transaminase from *Chromobacterium violaceum* DSM30191 and its potential for biocatalysis. *Enzyme Microb Technol*. 2007;41: 628–637. doi:10.1016/j.enzmictec.2007.05.011
74. Galman JL, Slabu I, Weise NJ, Iglesias C, Parmeggiani F, Lloyd RC, et al. Biocatalytic transamination with near-stoichiometric inexpensive amine donors mediated by bifunctional mono- and di-amine transaminases. *Green Chem*. Royal Society of Chemistry; 2017;9: 285–288. doi:10.1039/C6GC02102F
75. Tanizawa K, Masu Y, Asano S, Tanaka H, Soda K. Thermostable D-amino acid aminotransferase from a thermophilic *Bacillus* species. Purification, characterization, and active site sequence determination. *J Biol Chem*. 1989;264: 2445–2449. Available:

3) Analysis and creation of a systematic ω -TA database (oTAED)

- <http://www.jbc.org/content/264/5/2445.abstract>
76. Yvon M, Chambellon E, Bolotin A, Roudot-Algaron F. Characterization and Role of the Branched-Chain Aminotransferase (BcaT) Isolated from *Lactococcus lactis* subsp. *cremoris* NCDO 763. *Appl Environ Microbiol.* 2000;66: 571–577. doi:10.1128/AEM.66.2.571-577.2000
77. Hutson S. Structure and function of branched chain aminotransferases. *Progress in Nucleic Acid Research and Molecular Biology.* Elsevier; 2001. pp. 175–206. doi:10.1016/S0079-6603(01)70017-7
78. Cuetos A, García-Ramos M, Fischereider E-M, Díaz-Rodríguez A, Grogan G, Gotor V, et al. Catalytic Promiscuity of Transaminases: Preparation of Enantioenriched β -Fluoroamines by Formal Tandem Hydrodefluorination/Deamination. *Angew Chemie Int Ed.* 2016;55: 3144–3147. doi:10.1002/anie.201510554
79. Thomsen M, Skalden L, Palm GJ, Höhne M, Bornscheuer UT, Hinrichs W, et al. Crystallographic characterization of the (*R*)-selective amine transaminase from *Aspergillus fumigatus*. *Acta Crystallogr Sect D Biol Crystallogr.* International Union of Crystallography; 2014;70: 1086–1093. doi:10.1107/S1399004714001084
80. Fang C, Noguchi T, Yamana H. Analysis of evolutionary conservation patterns and their influence on identifying protein functional sites. *J Bioinform Comput Biol.* Imperial College Press; 2014;12: 1440003. doi:10.1142/S0219720014400034
81. Bednar D, Beerens K, Sebestova E, Bendl J, Khare S, Chaloupkova R, et al. FireProt: Energy- and Evolution-Based Computational Design of Thermostable Multiple-Point Mutants. Dokholyan N V., editor. *PLOS Comput Biol.* Public Library of Science; 2015;11: e1004556. doi:10.1371/journal.pcbi.1004556
82. van Oosterwijk N, Willies S, Hekelaar J, Terwisscha van Scheltinga AC, Turner NJ, Dijkstra BW. Structural Basis of the Substrate Range and Enantioselectivity of Two (*S*)-Selective ω -Transaminases. *Biochemistry.* American Chemical Society; 2016;55: 4422–4431. doi:10.1021/acs.biochem.6b00370
83. Pettersen EF, Goddard TD, Huang CC, Couch GS, Greenblatt DM, Meng EC, et al. UCSF Chimera - A visualization system for exploratory research and analysis. *J Comput Chem.* John Wiley & Sons, Inc.; 2004;25: 1605–1612. doi:10.1002/jcc.20084
84. Celniker G, Nimrod G, Ashkenazy H, Glaser F, Martz E, Mayrose I, et al. ConSurf: Using evolutionary data to raise testable hypotheses about protein function. *Israel Journal of Chemistry.* 2013. pp. 199–206. doi:10.1002/ijch.201200096
85. Landau M, Mayrose I, Rosenberg Y, Glaser F, Martz E, Pupko T, et al. ConSurf 2005: The projection of evolutionary conservation scores of residues on protein structures. *Nucleic Acids Res.* 2005;33: W299–W302. doi:10.1093/nar/gki370
86. Wheeler TJ, Clements J, Finn RD. Skyline: A tool for creating informative, interactive logos representing sequence alignments and profile hidden Markov models. *BMC Bioinformatics.* BioMed Central; 2014;15: 7. doi:10.1186/1471-2105-15-7
87. Petukhov M, Cregut D, Soares CM, Serrano L. Local water bridges and protein conformational stability. *Protein Sci.* Wiley-Blackwell; 1999;8: 1982–9. doi:10.1110/ps.8.10.1982
88. Yan BX, Sun Qing Y. Glycine residues provide flexibility for enzyme active sites. *J Biol Chem.* American Society for Biochemistry and Molecular Biology; 1997;272: 3190–3194. doi:10.1074/jbc.272.6.3190
89. Cheng ZQ, McFadden B a. A study of conserved in-loop and out-of-loop glycine residues in the large subunit of ribulose biphosphate carboxylase/oxygenase by directed mutagenesis. *Protein Eng.* 1998;11: 457–65.
90. Svedendahl M, Branneby C, Lindberg L, Berglund P. Reversed Enantioselectivity of an ω -Transaminase by a Single-Point Mutation. *ChemCatChem.* 2010;2: 976–980. doi:10.1002/cctc.201000107
91. Humble MS, Cassimjee KE, Abedi V, Federsel HJ, Berglund P. Key Amino Acid Residues for Reversed or Improved Enantioselectivity of an ω -Transaminase. *ChemCatChem.* 2012;4: 1167–1172. doi:10.1002/cctc.201100487
92. Denesyuk AI, Denessiouk KA, Korpela T, Johnson MS. Phosphate group binding “cup” of PLP-dependent and non-PLP-dependent enzymes: leitmotif and variations. *Biochim Biophys Acta - Proteins Proteomics.* 2003;1647: 234–238. doi:10.1016/S1570-9639(03)00057-8
93. Humble MS, Cassimjee KE, Håkansson M, Kimbung YR, Walse B, Abedi V, et al. Crystal structures of the

3) Analysis and creation of a systematic ω -TA database (ω TAED)

- Chromobacterium violaceum* ω -transaminase reveal major structural rearrangements upon binding of coenzyme PLP. FEBS J. 2012;279: 779–792. doi:10.1111/j.1742-4658.2012.08468.x
94. Nobili A, Steffen-Munsberg F, Kohls H, Trentin I, Schulzke C, Höhne M, et al. Engineering the Active Site of the Amine Transaminase from *Vibrio fluvialis* for the Asymmetric Synthesis of Aryl-Alkyl Amines and Amino Alcohols. ChemCatChem. WILEY-VCH Verlag; 2015;7: 757–760. doi:10.1002/cctc.201403010
95. Sayer C, Martinez-Torres RJ, Richter N, Isupov MN, Hailes HC, Littlechild JA, et al. The substrate specificity, enantioselectivity and structure of the (*R*)-selective amine : pyruvate transaminase from *Nectria haematococca*. FEBS J. 2014;281: 2240–2253. doi:10.1111/febs.12778
96. Park E-S, Kim M, Shin J-S. Molecular determinants for substrate selectivity of ω -transaminases. Appl Microbiol Biotechnol. Springer-Verlag; 2012;93: 2425–2435. doi:10.1007/s00253-011-3584-9
97. Hirotsu K, Goto M, Okamoto A, Miyahara I. Dual substrate recognition of aminotransferases. Chem Rec. Wiley Subscription Services, Inc., A Wiley Company; 2005;5: 160–172. doi:10.1002/TCR.20042
98. Markova M, Peneff C, Hewlins MJE, Schirmer T, John RA. Determinants of substrate specificity in omega-aminotransferases. J Biol Chem. American Society for Biochemistry and Molecular Biology; 2005;280: 36409–16. doi:10.1074/jbc.M506977200
99. Han S-W, Kim J, Cho H-S, Shin J-S. Active Site Engineering of ω -Transaminase Guided by Docking Orientation Analysis and Virtual Activity Screening. ACS Catal. American Chemical Society; 2017;7: 3752–3762. doi:10.1021/acscatal.6b03242
100. Cassimjee KE, Humble MS, Land H, Abedib V, Berglund P. *Chromobacterium violaceum* ω -transaminase variant Trp60Cys shows increased specificity for (*S*)-1-phenylethylamine and 4'-substituted acetophenones, and follows Swain–Lupton parameterisation. Org Biomol Chem. 2012;10: 5466–5470. doi:10.1039/c2ob25893e
101. Deszcz D, Affaticati P, Ladkau N, Gegel A, Ward JM, Hailes HC, et al. Single active-site mutants are sufficient to enhance serine:pyruvate α -transaminase activity in an ω -transaminase. FEBS J. 2015;282: 2512–2526. doi:10.1111/febs.13293
102. Han SW, Park ES, Dong JY, Shin JS. Mechanism-Guided Engineering of ω -Transaminase to Accelerate Reductive Amination of Ketones. Adv Synth Catal. 2015; 1732–1740. doi:10.1002/adsc.201500211
103. Buß O, Muller D, Jager S, Rudat J, Rabe KS. Improvement in the Thermostability of a β -Amino Acid Converting ω -Transaminase by Using FoldX. ChemBioChem. 2017; doi:10.1002/cbic.201700467
104. Park ES, Park SR, Han SW, Dong JY, Shin JS. Structural determinants for the non-canonical substrate specificity of the ω -transaminase from *Paracoccus denitrificans*. Adv Synth Catal. 2014;356: 212–220. doi:10.1002/adsc.201300786
105. Börner T, Rämisch S, Bartsch S, Vogel A, Adlercreutz P, Grey C. Three in One: Temperature, Solvent and Catalytic Stability by Engineering the Cofactor-Binding Element of Amine Transaminase. ChemBioChem. 2017; doi:10.1002/cbic.201700236
106. Manta B, Cassimjee KE, Himo F. Quantum Chemical Study of Dual-Substrate Recognition in ω -Transaminase. ACS Omega. 2017;2: 890–898. doi:10.1021/acsomega.6b00376
107. Huang J, Xie D-F, Feng Y. Engineering thermostable (*R*)-selective amine transaminase from *Aspergillus terreus* through in silico design employing B-factor and folding free energy calculations. Biochem Biophys Res Commun. 2017;483: 397–402. doi:10.1016/j.bbrc.2016.12.131
108. Steffen-Munsberg F, Vickers C, Kohls H, Land H, Mallin H, Nobili A, et al. Bioinformatic analysis of a PLP-dependent enzyme superfamily suitable for biocatalytic applications. Biotechnol Adv. Elsevier Inc.; 2015;33: 566–604. doi:10.1016/j.biotechadv.2014.12.012
109. Koszelewski D, Tauber K, Faber K, Kroutil W. omega-Transaminases for the synthesis of non-racemic alpha-chiral primary amines. Trends Biotechnol. Elsevier Ltd; 2010;28: 324–32. doi:10.1016/j.tibtech.2010.03.003
110. Green AP, Turner NJ, O'Reilly E. Chiral Amine Synthesis Using ω -Transaminases: An Amine Donor that Displaces Equilibria and Enables High-Throughput Screening. Angew Chemie Int Ed. WILEY-VCH Verlag; 2014;53: 10714–10717. doi:10.1002/anie.201406571
111. Mutti FG, Fuchs CS, Pressnitz D, Sattler JH, Kroutil W. Stereoselectivity of Four (*R*)-Selective Transaminases

3) Analysis and creation of a systematic ω -TA database (oTAED)

- for the Asymmetric Amination of Ketones. *Adv Synth Catal.* WILEY-VCH Verlag; 2011;353: 3227–3233. doi:10.1002/adsc.201100558
112. Wu H-L, Zhang J-D, Zhang C-F, Fan X-J, Chang H-H, Wei W-L. Characterization of Four New Distinct ω -Transaminases from *Pseudomonas putida* NBRC 14164 for Kinetic Resolution of Racemic Amines and Amino Alcohols. *Appl Biochem Biotechnol.* Springer US; 2017;181: 972–985. doi:10.1007/s12010-016-2263-9
113. Park E-S, Dong J-Y, Shin J-S. ω -Transaminase-catalyzed asymmetric synthesis of unnatural amino acids using isopropylamine as an amino donor. *Org Biomol Chem.* The Royal Society of Chemistry; 2013;11: 6929. doi:10.1039/c3ob40495a
114. Iwasaki A, Matsumoto K, Hasegawa J, Yasohara Y. A novel transaminase, (*R*)-amine:pyruvate aminotransferase, from *Arthrobacter* sp. KNK168 (FERM BP-5228): purification, characterization, and gene cloning. *Appl Microbiol Biotechnol.* Springer-Verlag; 2012;93: 1563–1573. doi:10.1007/s00253-011-3580-0
115. Li Y, Wang S, Umarov R, Xie B, Fan M, Li L, et al. DEEPre: sequence-based enzyme EC number prediction by deep learning. *BIOINFORMATICS.* 2016;0: 1–9. doi:10.1093/bioinformatics/btx680
116. Sugio S, Petsko GA, Manning JM, Soda K, Ringe D. Crystal Structure of a D-Amino Acid Aminotransferase: How the Protein Controls Stereoselectivity. *Biochemistry.* American Chemical Society; 1995;34: 9661–9669. doi:10.1021/bi00030a002
117. Höhne M, Schätzle S, Jochens H, Robins K, Bornscheuer UT. Rational assignment of key motifs for function guides in silico enzyme identification. *Nat Chem Biol.* 2010;6: 807–813. doi:10.1038/nchembio.447
118. Goto M, Miyahara I, Hayashi H, Kagamiyama H, Hirotsu K. Crystal structures of branched-chain amino acid aminotransferase complexed with glutamate and glutarate: True reaction intermediate and double substrate recognition of the enzyme. *Biochemistry.* 2003;42: 3725–3733. doi:10.1021/bi026722f
119. Skalden L, Thomsen M, Höhne M, Bornscheuer UT, Hinrichs W. Structural and biochemical characterization of the dual substrate recognition of the (*R*)-selective amine transaminase from *Aspergillus fumigatus*. *FEBS J.* 2015;282: 407–415. doi:10.1111/febs.13149
120. Boyko KM, Stekhanova TN, Nikolaeva AY, Mardanov A V., Rakitin AL, Ravin N V., et al. First structure of archaeal branched-chain amino acid aminotransferase from *Thermoproteus uzoniensis* specific for l-amino acids and R-amines. *Extremophiles.* Springer Japan; 2016;20: 215–225. doi:10.1007/s00792-016-0816-z
121. Schätzle S, Höhne M, Redestad E, Robins K, Bornscheuer UT. Rapid and Sensitive Kinetic Assay for Characterization of ω -Transaminases. *Anal Chem.* American Chemical Society; 2009;81: 8244–8248. doi:10.1021/ac901640q
122. Struvay C, Feller G. Optimization to Low Temperature Activity in Psychrophilic Enzymes. *Int J Mol Sci. Molecular Diversity Preservation International;* 2012;13: 11643–11665. doi:10.3390/ijms130911643
123. Mathew S, Deepankumar K, Shin G, Hong EY, Kim B-G, Chung T, et al. Identification of novel thermostable ω -transaminase and its application for enzymatic synthesis of chiral amines at high temperature. *RSC Adv.* The Royal Society of Chemistry; 2016;6: 69257–69260. doi:10.1039/C6RA15110H
124. Söhngen C, Bunk B, Podstawka A, Gleim D, Overmann J. BacDive—the Bacterial Diversity Metadatabase. *Nucleic Acids Res.* Oxford University Press; 2014;42: D592–D599. doi:10.1093/nar/gkt1058
125. Stekhanova TN, Rakitin AL, Mardanov A V., Bezsudnova EY, Popov VO. A Novel highly thermostable branched-chain amino acid aminotransferase from the crenarchaeon *Vulcanisaeta moutnovskia*. *Enzyme Microb Technol.* 2017;96: 127–134. doi:10.1016/j.enzmictec.2016.10.002

4) Thermostability engineering of the *V. paradoxus* ω -TA

In the following chapter the thermostability improvement of the *Variovorax paradoxus* ω -TA is demonstrated using *in-silico* predicted site directed mutagenesis. The existing different computational methods are described in chapter 4.1. to understand the function of the protein stabilization algorithm(s) with focus on FoldX. In addition, the predictive quality of FoldX has been compared with other algorithms.

The aim of this project was to increase the long-term stability and activity of the mentioned ω -TA. Furthermore this stabilized enzyme should be a starting point for further enzyme engineering experiments and enzymatic processes (chapter 4.2). Additionally covalent binding energies should be increased by introduction of artificial disulfide bonds (chapter 4.3).

4.1) FoldX as protein stability engineering tool

This section is mainly based on the publication

FoldX as protein engineering tool: Better than random based approaches?

Oliver Buß, Jens Rudat and Katrin Ochsenreither

Institute of Process Engineering in Life sciences, Section II: Technical Biology, Karlsruhe Institute of Technology, Karlsruhe Germany

Publishing details:

Computational and Structural Biotechnology Journal (Open Access)

Doi: 10.1016/j.csbj.2018.01.002

Accepted: January 20, 2018

The final article is available at <https://www.journals.elsevier.com/computational-and-structural-biotechnology-journal>

Copyright: Creative Commons Attribution (CC BY)

Authors' contribution to this publication

Oliver Buß wrote the manuscript **Jens Rudat** significantly contributed in correction and evaluation of the manuscript, **Katrin Ochsenreither** significantly contributed in correction and evaluation of the manuscript.

4.1.1) Relevance of thermostability of proteins

Increasing protein stability is a desirable goal for different life science purposes, this includes design of therapeutic proteins like antibodies, human cell biology and biotechnology. It is expected that such improvements result in lower process costs and in enhanced long-term stability of the applied proteins. Enhanced protein stability in general can be achieved due to various factors, e.g. by increasing thermostability, salt tolerance or tolerance towards organic solvents, and consequently, involves different bioinformatics approaches. The emphasis for application of proteins for medical and chemical purposes is focused on the fields of biosensors (e.g. blood sugar test strips [1]), biomedical drugs (e.g. antibodies against cancer cells [2]) or on the synthesis of complex as well as chiral substances for food (e.g. high fructose corn syrup [3]) and pharmaceutical industry (e.g. the mentioned sitagliptin) [4]. Obviously biosensors for medical use assisting to diagnose several diseases like breast cancer [5], diabetes [6] or infectious diseases [7] have to be functional and reliable for a defined period of time. It seems, for example, to be beneficial to gain more thermostable antibodies for treatment of cancer diseases [8]. Furthermore, for the synthesis processes of drugs and pharmaceutically relevant intermediates, applied enzymes have to be active and functional for long batch times to prevent drastic increases in costs per unit of product [9–12]. For industrial enzymes improved stability against heat, solvents and other relevant process parameters, e.g. acidic or basic pH, often becomes crucial [13]. In addition, improved thermostability of enzymes might prevent thermal inactivation and conformational changes at higher reaction temperature, which could in turn be beneficial to raise turnover rates and substrate concentrations [14–18]. According to the Q_{10} -rule of thumb, biological systems and enzymes tend to have a Q -factor of 2, i.e. a temperature increase of about 10 K results in doubling the reaction rate [19,20]. Contrary, stabilization also can lead to more rigid enzymes, which are less active at the same temperature, but show the same activity at elevated temperatures. This can be observed when enzymes from hyperthermophilic and mesophilic sources are compared with respect to their reaction rates [21]. A thermostabilized enzyme might be less active at a certain temperature, but longer active at higher temperatures, which allows to apply the Q_{10} -rule on the condition that the activity can be maintained for longer time periods at elevated temperatures [22,23]. However, it is also possible that a thermostabilized enzyme is not impaired in activity at moderate temperatures and is even more active at higher temperatures [24–28]. Arnold *et al.* demonstrated, that an enzyme can be simultaneously developed towards higher stability and activity [23,29–31].

Protein denaturation and degradation due to both heat and solvents are based on the same protein unfolding processes. The most important forces for protein stability, which are relevant targets for the improvement of protein stability, are intramolecular interactions, i.e. disulfide bridges, ion interactions, hydrogen bonds, hydrophobic interactions and core packings [21]. The rigidity and flexibility of proteins seem to be the key parameters [32] and both can be influenced by using immobilization techniques or enzymatic engineering in order to expand the durability of protein applications.

4.1.2) Techniques for thermostabilization

The well-known technique to immobilize proteins to gain stabilized proteins is applied for antibody to increase the thermostability [33,34]. Beside the improvement of thermostability using immobilization techniques, directed evolution is an alternative approach, but the existence of a robust high-throughput screening assay for the selected protein is an important prerequisite [10,35–40]. For enzymes, activity can be used as parameter for functionality at elevated temperatures, but for non-catalyzing proteins a more sophisticated assay or even protein purification is necessary. Furthermore, the number of necessary protein variants, created by using e.g. error prone PCR or other techniques, is mostly about 10^3 to 10^5 and even higher. However, in case of enzymes, selection might easily be performed by heating up unpurified crude extracts from cells [41]. Using this technique, protein melting temperature T_m can be improved in the best screenings by far more than 10°C [42,41,43–46]. The artificial evolution approach can result in an 140-fold increase in long-term enzymatic activity like demonstrated for the alkaline pectate lyase [47]. Also for antibodies or antibody fragments evolutionary approaches can be used [48]. For example, the protein melting temperature of a human antibody domain was improved by more than 10°C [49].

Directed evolution can be a successful strategy but might not be applicable at any time, especially when missing a high-throughput screening or protein purification for stability measurements is necessary. Therefore, this mini-review focusses on protein/enzyme engineering for thermostabilization using structure guided site-directed mutagenesis. This strategy helps to reduce screening effort and also costs, which is an issue in large screenings. Furthermore, we selected the popular FoldX algorithm and would like to answer the question: how powerful is FoldX for common protein stability improvements? FoldX is a frequently used algorithm and many studies about protein stabilization experiments are described in literature. A second reason is the user-friendliness of FoldX, because it can easily be used as plugin in the protein structure visualizer YASARA [50]. In contrast to other, command-line based *in silico*

approaches, which are without graphical interface, scientists not familiar with programming languages like python, Java, R-script and so on and hide a larger workload for these kind of approaches.

4.1.3) Computational approaches for stability engineering

Besides FoldX, several other algorithms used for site-directed mutagenesis are also known aiming at different inter- and intra-protein interactions. One target is the introduction of artificial disulfide bridges into proteins. As a covalent bond, a disulfide bridge is a strong physical force which helps to stabilize the 3D-structure within a protein chain or between monomers raising the protein melting temperature (T_m) up to 30°C, and can achieve an increase of thermal stability by more than 40% at distinct temperature levels [51–53]. However, introduction of disulfide bridges can also lower the T_m up to -2.4°C [54]. Starting with the protein structure as basis for molecular dynamic simulations and energy calculations, amino acid positions can be selected which are potentially suitable for engineering of disulfide bridges. However, these approaches need profound understanding of different prediction and calculation software, often without graphical interfaces [55]. Two examples are the algorithms for fast recognition of disulfide mutation sites FRESCO and the open access webtool “Disulfide by Design 2” (DD2), but only DD2 can be easily used with graphical interface [56–58]. Using FRESCO, a temperature improvement of 35°C was achieved due to the combination of single disulfide bridges. Jo *et al.* increased the T_m of the α -type carbonic anhydrase by 7.8°C due to an introduction of a disulfide bond efficiently predicted by DD2 [59]. Albeit the promising examples, it has to be mentioned, that the extensive FRESCO strategy cannot be understood as an end-user script, but more or less as a blue script for improving thermostability. Wijma *et al.* further improved FRESCO by integrating FoldX and Rosetta as additional energy improvement tools and combined these results with an own Dynamic Disulfide Discovery algorithm based on molecular dynamic simulations [56]. After *in silico* elimination of less stable variants, they expressed, tested and combined beneficial point mutation sites and disulfide bonds to gain two variants with drastically increased T_m of 34.6 and 35.5°C, respectively. However, this strategy is very extensive and many point mutations have to be tested and combined.

Beside the possible *de novo* design of disulfide bridges, further computational methods like helix dipole stabilization or core repacking exist. Core repacking aims only at the core region of proteins to increase hydrophobic interactions. Vlassi *et al.* showed that a reduction of hydrophobic interaction decreases the protein stability [60] and computational tools like

RosettaDesign and Monte Carlo simulations are used for the optimization process [61–63]. Adapted and automated RosettaDesign framework for repacking are available, but profound programming capabilities are needed for applying [63]. In contrast, helix dipole stabilization methods lead to improvements of molecular interactions at the end of helices, which can also result in drastically increased T_m by more than 30°C [64,65]. However, for this strategy elaborate electrostatic calculations and molecular simulations are needed to select mutation sites. Beside these strategies, consensus sequences can also help to improve protein stability using multiple sequence alignments. In so-called consensus guided mutagenesis, sequences are compared according to their amino acid frequencies to elucidate consensus sequences. Replacing amino acid residues at certain positions with the most prevalent ones often result in highly beneficial energy improvements stabilizing proteins [66][67][68][69]. Huang *et al.* demonstrated that by using consensus approach it was possible to improve the stability of the reductase CgKR1 T_{50}^{15} (temperature at which the enzyme activity is halved within 15 min) by more than 10°C [70].

4.1.4) Un/folding energy algorithms

At least 22 standalone calculation tools are described for the prediction of beneficial single and multiple point mutation sites to reduce the Gibbs free energy of proteins. The broad diversity of these standalone software was reviewed by Modarres *et al.* and beside the mentioned FoldX algorithm, other tools like PoPMuSiC, CUPSAT, ZEMu, iRDP web server or SDM were mentioned [71–74]. These calculation tools are structure or sequence dependent and use energy calculation functions or machine learning algorithms. Also databases collecting changes in protein stability (e.g. for Gibbs free energy changes and melting temperatures) are available like ProTherm (others are e.g. MODEL, DSBASE), but it should be mentioned that 70% of the logged mutations are destabilizing which leads to unintended biases [72,75]. Beside the more popular algorithms others are published like mCSM, BeAtMuSiC and ENCoM using different calculation approaches [76–78]. Moreover, it is also possible to use crystallographic data gained by X-ray analysis of protein structure. The B-factor is an indicator for the flexibility of positions within the protein. Reetz *et al.* used this factor for increasing protein stability [79].

4.1.4.1) FoldX

Considering the diversity of available algorithms, it seems to be very difficult to choose an efficient tool for protein stabilization. In this review we concentrated on the force field algorithm FoldX, which we have used by ourselves to create a more stable ω -transaminase[80].

The force field algorithm, which was originally created by Guerois *et al.* 2002, became popular as webtool in 2005 by Schymkowitz *et al.* and was refined to the currently last version FoldX 4.0 [81–83] .

The software package FoldX includes different subroutines e.g. RepairPDB, BuildModel, PrintNetworks, AnalyseComplex, stability and so on. For example the repair function of FoldX reduces the energy content of a protein-structure model to a minimum by rearranging side chains and the function BuildModel introduces mutations and optimizes the structure of the new protein variant. The energy function of FoldX is only able to calculate the energy difference in accurate manner between the wildtype and a new variant of the protein [82].

$$\Delta\Delta G = \Delta G_{\text{wildtype}} - \Delta G_{\text{variant}} \text{ [kcal mol}^{-1}\text{]}$$

FoldX is also able to calculate total energies of objects, but this function is only valid to predict, whether a problem with the structure is given or not. The total energy results are not able to predict experimental results [50,82]. The core function of FoldX, the empirical force field algorithm, is based on free energy (ΔG) terms aiming to calculate the change of ΔG in kcal mol⁻¹. This equation includes terms for polar and hydrophobic desolvation or hydrogen bond energy ΔG_{wb} of a protein interacting with solvent and within the protein chain. Increased protein rigidity works against entropy and consequently, results in entropy costs (e.g. loss of rotational entropy).

$$\begin{aligned} \Delta G = & a \Delta G_{vdw} + b \Delta G_{solvH} + c \Delta G_{solvP} + d \Delta G_{wb} + e \Delta G_{hbond} \\ & + f \Delta G_{el} + g \Delta G_{kon} + h T\Delta S_{mc} + i \Delta G_{clash} \end{aligned}$$

Furthermore the energy algorithm also addresses the free energy change at protein interfaces of oligomeric proteins. These term is mainly ΔG_{kon} which calculates the electrostatic contribution of interactions at interfaces [82]. The parameters which are important for the energy calculation were determined in laboratory experiments, e.g. for amino acid residues and explored on protein chains. Beside this distinct parameters the letters of the total energy equation, **a** to **i**, represent the weights of separate terms [82]. The algorithm works with optimal accuracy when the hypothetical unfolding energy difference of the hypothetical energy from a wild-type variant is determined in comparison to a mutated protein. For this purpose, FoldX uses the 3D structure to calculate the hypothetical unfolding energy. The algorithm was first implemented as free

available web server tool and is now a commercially available software, which can be used free of charge for academic purposes. As a prerequisite, a highly resolved crystal structure is necessary to calculate the energy changes for site-directed mutagenesis experiments. Users can also automate the calculations e.g. by using the programming code Python to calculate whole protein amino acid exchanges at every distinct position [84,85]. Furthermore, FoldX shows very good performance with respect to calculation time even on single core computers. Compared to e.g. ZEMu, FoldX needs only half the time for calculating single site mutations (calculated on one single processor) and is faster than RosettaDDG [86,74]. As mentioned earlier, it can be used with a graphical user interface as plugin tool in YASARA, which opens FoldX towards a broad community of researchers.

4.1.4.2) FoldX-Applications

FoldX was applied for different stability tests, especially when protein design was performed to predict whether distinct mutations are destabilizing. Therefore FoldX shows to be beneficial for different approaches and is not strictly limited to a distinct function. Moreover the peptides, individual domains and multi-domain proteins can be addressed for experiments [87,88]. The algorithm has been used to explain and predict stability improvements when designing solvent stable enzymes. The group of U. Schwaneberg designed a laccase with improved resistance in ionic liquids for using hardly soluble lignin lysates and increased tolerance towards high molarity of salts [89]. Beside its suitability for protein energy calculations, it is also possible to calculate the energy changes of DNA-protein interactions [90]. Furthermore, FoldX is implemented in a lot of approaches like Fireprot, FRESCO, TANGO or in combination with Voronoia 1.0. Voronoia helps to engineer protein core packing and is based on energy calculations using FoldX as force field algorithm [91,92]. The program FRESCO (Framework for Rapid Enzyme Stabilization by Computational libraries) joins Rosetta with FoldX energy calculations and combines single point mutations with disulfide predictions for drastic energy improvements of enzymes [56]. The direct alternative to FoldX is the Rosetta energy algorithm. It was shown, that Rosetta predicts other possible mutation sites than FoldX for energy improvements, but only 25% of all mutations were predicted by both algorithms for the same protein [56]. Additionally, the authors of this work excluded 52% of the selected mutations manually, e.g. excluding hydrophobic mutations on surface exposed sites and mutations to a proline residue or a proline residue to a non-proline residue. At the end around 65% of the predicted mutation sites were calculated by FoldX and thereby 35% of all predicted sites were discarded. Voronoia in combination with FoldX helps to predict and to explain why

hydrophobic interactions in the core region can have a huge impact on protein stability, as it was demonstrated for the thermophilic lipase T1 [92]. Another approach is TANGO, which helps to predict the aggregation of proteins and, in combination with FoldX, is a powerful tool for the investigation of predicted mutations regarding solubility, e.g. protective site-directed mutations for the Alzheimers' $\alpha\beta$ peptide [82,93,94]. Furthermore, FoldX can also support protein design. For engineering the zinc-finger nuclease, FoldX was used as prediction algorithm to detect if the binding energy of a distinct DNA-sequence was increased or decreased [95]. Also, FoldX can help to estimate protein-protein binding energy and resulting stabilities of protein complexes. *Szcepek et al.* redesigned the interface between dimeric zinc finger nucleases using FoldX as prediction tool [96]. After deeper *in silico* calculations, only 9.3 % of predicted variants were expressed and proved to be beneficial for stability [96]. Considering these and other experiments the performance for FoldX should be critically evaluated.

Therefore, we gathered FoldX experiments and analyzed available publications if FoldX was helpful for increasing protein stability (**Table 4.1**). In general, the amount of standalone FoldX calculations for protein stability improvement in literature is relatively low compared to approaches, which are using FoldX as an additional tool for stability calculation. Furthermore, FoldX is often only used as algorithm for explanations of the impact of mutagenesis in proteins with respect to stability or towards predictions of protein-protein or protein-DNA binding. Therefore, in table 4.1 only mutations with effects based on FoldX predictions are pointed out, even when authors used additional calculation tools. When no pre-selection of distinct protein sites are indicated, a complete calculation of every position in the protein was performed. In this case, every amino acid was exchanged with the 19 standard amino acid residues. This calculation setup results very fast in high numbers of predicted variants. One criterion for excluding many variants is to set an energy barrier for $\Delta\Delta G$ between -0.75 and -5 kcal mol⁻¹ for stabilizing mutations and for destabilizing mutations of $> + 1$ kcal mol⁻¹ in accordance to the Gaussian distribution of FoldX predictions (SD for FoldX 1.78 kcal mol⁻¹[94]) [97]. After this pre-selection a large number of variants can be excluded. Furthermore, mutations nearby active sites, proline residue mutations or variants which seem to be critical for protein structure can be also excluded. In addition to manual exclusion of variants, also MD-simulations can be performed to exclude more variants. Aiming to indicate the grade of improvement, protein melting temperature T_m or half-life activity are frequently used. The largest positive changes in stability were reached for the T1 lipase, phosphotriesterase, Flavin-mononucleotide-based-fluorescent-protein and for the haloalcohol dehalogenase ranging from 8 up to 13°C using single site mutations [98]. However, FoldX also allows prediction of destabilizing mutations,

which were performed very accurately for the thermoalkalophilic lipase with a negative ΔT_m of 10°C. Noticeably, stabilizing predictions are useful for biotechnology and are therefore mentioned in studies with biotechnological background, whereas destabilizing predictions seem to be more applicable for human disease studies [94]. Beside mere stability studies, also protein design was performed towards specific enzyme-DNA binding or antibody-antigen binding, which can reduce the size of antibody libraries for distinct antigen targets. Moreover, FoldX can also be used to adapt or to select mutations to increase stability in ionic liquids. For this, FoldX calculations were performed with increasing salt concentration during the simulations, but currently no further experiments towards ionic liquid improvement can be found. In literature also numerous examples can be found dealing with diseases caused by protein mutations. These investigations aim to prove whether human proteins are less stable with a mutation compared to the wild-type or might interact differently with other proteins [99–101].

Table 4.1 Summary of different FoldX applications for single point mutations regarding stability and ligand binding. The changes achieved i.e. T_m is listed for changes in protein melting temperature. $\Delta\Delta G$ displays the change in free energy by mutation/design of proteins. “Criteria” describes the settings for experiments. “Cut-off” means, that the authors excluded those indicated FoldX predictions (with a higher or lower $\Delta\Delta G$) from further experiments. $\Delta\Delta G$ is defined as: $\Delta\Delta G = \Delta G^{\text{fold}}(\text{mutation}) - \Delta G^{\text{fold}}(\text{wild type})$

Aim of the study	Protein/Source	Criteria	Number of tested predictions	Number of correct predictions	of Greatest impact	Resolution of crystal structure	Ref.
Enzyme stabilization	Endoglucanase (<i>Hypocrea jecorina</i>)	Cut off value < $\Delta\Delta G$ -1.75 kcal mol ⁻¹)	43	6	Stabilization ($\Delta T_m = 3.2^\circ\text{C}$)	1.62 Å	[102]
Enzyme stabilization	Phosphotriesterase (<i>Pseudomonas oleovorans</i>)	Cut off value < $\Delta\Delta G$ -0.72 kcal mol ⁻¹)	52	32	Stabilization ($\Delta T_m = 8.6^\circ\text{C}$)	2.25 Å	[103]
Enzyme stabilization	T1 Lipase (<i>Geobacillus zalihae</i>)	One mutation site was selected and exchanged against Val, Ile, Met, Phe, Trp compared to wild type	7	1	Stabilization ($+\Delta T_{\text{opt}} = 10^\circ\text{C}$)	1.5 Å	[92]
Enzyme stabilization	Thermoalkalophilic lipase (<i>Bacillus thermocatenuatus</i>)	3 sites preselected and amino acids were exchanged against Phe, Try and Trp.	9	2	Destabilizing variants ($\Delta T_m = -10^\circ\text{C}$)	2.0 Å	[104]

Enzyme stabilization	Haloalkane dehalogenase (WT and one mutant) <i>Sphingomonas paucimobilis</i>	Cut off value $< \Delta\Delta G - 0.84 \text{ kcal mol}^{-1}$ + visual inspection and MD-simulation	Less than 150	5	Stabilization ($\Delta T_m = 3^\circ\text{C}$)	0.95 Å	[105]
Enzyme stabilization	Limonene-1,2-epoxide hydrolase (<i>Rhodococcus erythropolis</i>)	Cut off ($\Delta\Delta G < -1.2 \text{ kcal mol}^{-1}$) performed additionally further pre-selection	21	6	Stabilization $\Delta T_m = 6^\circ\text{C}$	1.2 Å	[56]
Enzyme stabilization	Cellobiohydrolase (<i>Hypocrea jecorina</i>)	43 mutations selected ($\Delta\Delta G < -0.75 \text{ kcal mol}^{-1}$)	43	10	Stabilization $\Delta T_m = 0.7^\circ\text{C}$	2.35 Å	[69]
Enzyme stabilization	ω -transaminase (<i>Variovorax paradoxus</i>)	Cut off value $\Delta\Delta G < -6.5 \text{ kcal mol}^{-1}$	11	3	$\Delta T_m = 4^\circ\text{C}$	2.28 Å	[80]
Enzyme stabilization	Amine transaminase (<i>Aspergillus terreus</i>)	B-factor was used as pre-filter for FoldX predictions towards stabilization	19	6	Stabilization $\Delta T_{1/2}^{10min} = 3.5^\circ\text{C}$	1.63 Å	[106]
Enzyme stabilization	Laccase (<i>Trametes versicolor</i> and fungus PM1)	Molecular dynamic averaged structures were used for FoldX calculation	11	Standard deviation max. $\Delta\Delta G < 1 \text{ kcal/mol}^{-1}$	$\Delta T_m = 3-5^\circ\text{C}$	2.4 Å	[107]
Enzyme stabilization	Haloalcohol dehalogenase (<i>Agrobacterium tumefaciens</i>)	Cut off ($\Delta\Delta G < -1.2 \text{ kcal mol}^{-1}$) 775 mutants were predicted by FoldX and reduced using	55	29	Stabilizing $\Delta T_m = 13^\circ\text{C}$	1.9 Å	[98]

		Rosetta-dgg and MD-simulation							
Enzyme stabilization	Chalcone synthase (<i>Physcomitrella patens</i>)	Calculation of total energy $\Delta G = -63$ up to 67 kcal mol^{-1}	19	2	1 variant showed high thermal stability	Homology modeling			[108]
		Single site variant							
Enzyme stabilization	Carbonyl reductase (<i>Streptomyces coelicolor</i>)	Variants with $\Delta\Delta G < -4 \text{ kJ mol}^{-1}$ were selected	3	1	Stabilization of $\Delta T_{50}^{15} = 1.3^\circ\text{C}$	1.6 \AA			[109]
Enzyme stabilization	Peptide Amidase (<i>Stenotrophomonas maltophilia</i>)	Cut off value $\Delta\Delta G < -5 \text{ kJ mol}^{-1}$	44	6	Stabilizing $\Delta T_m = 6^\circ\text{C}$	1.8 \AA			[110]
Enzyme stabilization and comparison to other tools	Penicillin G acylase (<i>Escherichia coli</i>)	Not reported -	21	8	-	1.9 \AA			[111]
Enzyme destabilization	Triosephosphate isomerase (<i>Saccharomyces cerevisiae</i>)	Selection of all energy predictions between $\Delta\Delta G = 3 - 8.5 \text{ kcal mol}^{-1}$	23	6	No correlation between $T_{1/2}$ and $\Delta\Delta G_{\text{FoldX}}$ observed	1.9 \AA			[112]
Protein-Protein interaction prediction	SH2 domain (<i>Gallus gallus</i>)	Random sequences for binding	50,000		Area under the ROC curve 0.79 (accuracy)	FoldX can predict better than random binding events	2.1 \AA		[113]
Improvement of DNA binding	Zinc finger nucleases (<i>Homo sapiens</i>)	Cut off value $< \Delta\Delta G - 5 \text{ kcal mol}^{-1}$ predicted engineering sites	420	60 % (low binding energy)	Improved DNA binding (-13 kcal mol ⁻¹)	1.6 \AA			[95]
				95 % (high binding energy)					

			Cut off value $\Delta\Delta G$ - 10 kcal mol ⁻¹					
Protein stabilization	Anti-hVEGF antibody	(<i>Homo sapiens</i>)	Single point mutations no cut off value reported	60	40% of tested sites were more stable	Stabilization (+ ΔT_m = 2.2°C (single site))	Structure modeling	[85]
			Phe, Gln, Asn, Glu. FoldX calculation were performed 5 times and averaged for each mutation.					
Protein stabilization	Growth factor 2 (<i>Homo sapiens</i>)		Cut off ($\Delta\Delta G < -1$ kcal mol ⁻¹)	5	2	Stabilization $\Delta T_m = 3.7^\circ\text{C}$	1.6 Å	[115]
Protein stabilization	Flavin mononucleotide based fluorescent	Protein (<i>Bacillus subtilis</i>)	Cut off ($\Delta\Delta G < -1$ kcal mol ⁻¹) performed additionally further pre-selections	22	15	Stabilization $\Delta T_m = 11.4^\circ\text{C}$	Resolution under 2.2 Å	[116]
Protein stabilization	Endolysin PlyC (<i>Bacteriophage</i>)		Cut off ($\Delta\Delta G < -1$ kcal mol ⁻¹) 92 mutants were determined by FoldX and reduced by visual inspection and by Rosetta	12	3	Stabilization $\Delta T_m = 2.2^\circ\text{C}$	3.3 Å refined using Rosetta Relax	[117]

Protein stabilization	Database (known mutations)	Cut off value $\Delta\Delta G < - 1.0$ kcal mol ⁻¹	30	20	n.d	1.5 to 2.25 Å	[86]
Protein destabilization	Repair protein MSH2 (<i>Homo sapiens</i>)	Cut off value ($\Delta\Delta G > 5$ kcal/mol ⁻¹)	24	22	Destabilization of > 3 kcal mol ⁻¹	3.3 Å	[84]
Protein destabilization	<i>cblA</i> -type methylmalonic aciduria (<i>Homo sapiens</i>)	Cut off value $\Delta\Delta G$ between 3.48 to 11.15 kcal mol ⁻¹	22	22	-	2.64 Å	[118]
Investigation of proline influence on stability	fungal chimeric cellobiohydrolase Cel6A (<i>Humicola insolens</i>)	$\Delta\Delta G$ of exchanges of wild type amino acid against Pro exchange was calculated	17	57 % were predicted correctly as destabilizing 43 % as stabilizing	Destabilization $\Delta T_m = - 4^\circ\text{C}$ Stabilization $\Delta T_m = +4^\circ\text{C}$	1.3 Å	[119]
Influence of core residue substitutions on stability	Glycoside-hydrolase (<i>Neisseria polysaccharea</i>)	Settings not reported. 133 (7 sites) mutants were investigated towards stabilization or destabilization	57 (stabilizing) 76 (rest)	9 (stabilizing) 24 (destabilizing)	Stabilizing up to $\Delta T_m = 2^\circ$ -Destabilizing $\Delta T_m = - 6^\circ\text{C}$	1.4 Å	[120]
Validation of estimations using FoldX	Laccase (<i>T. versicolor</i>)	2 sites selected as targets for stability in Ionic liquid	2	2	1 variant showed stability improvement in ionic liquid	2.4 Å	[89]

4.1.5) Accuracy of FoldX

From the FoldX studies summarized in table 4.1 it can be deduced that the crystal-structure quality is crucial for accurate calculations. From a benchmark test on myoglobin mutants Kepp (2015) concluded that some protein stability predicting algorithms are extremely sensitive towards crystal structure quality and some are very robust [121]. It seems plausible that interactions are in the order of atomic resolutions and therefore the crystal structure quality has an important influence on energy calculations [107,121–123]. However, for the prediction algorithms PoPmuSic, I-Mutant 3.0 and other tools the influence of the crystal structure quality was only in the order of $0.2 \text{ kcal mol}^{-1}$ (standard deviation using different structure data of superoxide dismutase 1) [123]. According to Christensen *et al.*, FoldX belongs to the more structure sensitive methods and Kepp suggested to use only structures solved in scales of near-atomic-resolutions [107,121]. With reference to table 4.1, all cited studies were based on crystal structures with an resolution better than 3.3 \AA and an average resolution of 1.87 \AA which is nearby atomic resolution (1 \AA is approximately the diameter of an atom plus the surrounding cloud of electrons). Furthermore, also protein-protein interactions might have an influence on the prediction power, which are not addressed in some performance studies like from Tokuriki *et al.*, because only monomeric proteins were selected [124], but e.g. Pey *et al.* and Dourado *et al.* showed that also oligomers can be utilized for calculations (using extra terms: ΔG_{kon} electrostatic interaction, ΔS_{tr} translational and rotational entropy) [74,125]. The root-mean-square deviation (RMSD) in a dataset of protein complexes, with known energy impacts, was determined to be $1.55 \text{ kcal mol}^{-1}$ (for single mutants) [74]. In contrast the algorithm ZEMu addresses such mutations on interfaces better than FoldX [74].

Based on experimental results, it can be concluded that the prediction of destabilizing mutations is more accurate than prediction of stabilizing mutations. After pre-selection of experiments with the aim to increase stability, it can be concluded that the approximate success rate for mutations predicted as stabilizing (according to their negative $\Delta\Delta G$ -values) is only 29.4% (focusing on 13 single mutation experiments). For experiments with focus on detection of destabilizing mutations or for simple proof of destabilizing events, sample size is only five but the average success rate is 69%. However, with regard to the small sample size a valid statement about success rates cannot be made. It is likely that many unsuccessful experiments were not published and therefore, the real success rate might be much lower. Khan *et al.* evaluated the performance of 11 protein stability predictors by using a dataset containing more than 1,700 mutations in 80 proteins which were taken from ProTherm database. It was shown that FoldX was among the three most reliable algorithms for stability increasing cases ($\Delta\Delta G \leq$

- 0.5 kcal/mol), predicting 86 true positives, 133 false positives, corresponding to a success rate of 39.2 % for stabilizing mutations. Only Dmutant and MultiMutate were comparably successful in predicting stabilization events [101].

Compared to other results, this success rate might be higher than expected. As an example for an investigation of the performance of an adapted FoldX algorithm, laccase isoenzymes were used. The large calculation setup included 9,424 FoldX predictions per isoenzyme using an adapted algorithm. These calculations were evaluated by using molecular dynamic simulations and additional different settings within FoldX were tested. Like mentioned before, the authors remarked that FoldX needs high-resolution crystal structures of proteins and that FoldX performs well in predicting stability trends, but not in a quantitative accuracy [75]. Using the deciphering protein (DPP) as an example, Kumar *et al.* showed on the basis of 54 DPP mutants how accurate the prediction power of FoldX is compared to other tools. The study focused on destabilizing mutation events, which were described in medical data sets of DPP and concluded that the R-value (correlation coefficient) was only 0.45 to 0.53. The quality of the crystal structures in this study ranged between 1.07 and 1.93 Å [76]. Potapov *et al.* utilized for performance investigation a protein database set regarding 2156 variants in 59 proteins. The crystal structure qualities were not reported. However, they concluded that 81.4 % of T_m changes were qualitatively predicted correctly [126].

Furthermore Potapov *et al.* headlined their work for analyzing different protein stability tools “*Assessing computational methods for predicting protein stability upon mutation: good on average but not in the details*”, and proved that FoldX has potential to predict if a certain mutation is stabilizing or destabilizing, but its prediction power decreases, when $\Delta\Delta G$ is correlated with $\Delta\Delta G_{\text{experimental}}$ or with stability parameters like T_m [126]. The correlation coefficient R, plotting $\Delta\Delta G_{\text{theoretical}}$ against $\Delta\Delta G_{\text{experimental}}$ values from databases was only 0.5 (for negative and positive $\Delta\Delta G$), but it also depends on the crystal structure and on the nature of the protein [126].

4) Thermostability engineering of the V. paradoxus ω -TA

Table 4.2 Summary of different algorithms evaluated in performance tests considering prediction accuracy in comparison to experimentally investigated mutations and calculated statistical parameters. This table displays reported standard deviations of predicted true positives and true negatives. Accuracy is defined as ratio of true positives/true negatives to the total number of predictions. R-values (correlation coefficients) describe how precisely the predicted energies fit to database values.

Algorithm	Standard deviation	Accuracy range (min.-max.)	R-values
FoldX	1.0to 1.78kcal mol ⁻¹ [127]	0.38 to 0.8[128]	0.29[130] to
	[94]	Average Accuracy: 0.69 [86,103,126,129]	0.73[127]
BeatMuSiC	1.2 kcal mol ⁻¹ [76]		0.46[76]
CUPSAT	1.8 kcal mol ⁻¹ [76]	0.5 [101]	0.3[76]
I-Mutant 2.0/3.0	1.2 to 1.52 kcal mol ⁻¹ [76]	0.48[101] to 0.75[126]	0.16[76] to
	[94]		0.51[94]
PoPMuSiC	1.1 kcal mol ⁻¹ to 1.32 [76]	0.62[129] to 0.85[129]	0.51 to
	[94]		0.55[94] [76]
mCSM	3.2 kcal mol ⁻¹ [76]		0.23[76]
ENCoM	1.5 kcal mol ⁻¹ [76]		0.04[76]
Rosetta-ddG	2.3 kcal mol ⁻¹ [94]	0.71[126] to 0.76[86]	0.26 [126] to
			0.54 [94]

For better comparison, we summarized statistical parameters given for the different algorithms derived from Kumar et al, and other studies (as indicated) **in table 4.2**, but not for every algorithm we were able to find a full set of data. For example, Kumar *et al.* analyzed the predictive power of eight different tools, i.e. PoPMuSiC 3.1, BeatMuSiC, CUPSAT, I-Mutant 2.0/3.0, mCSM, ENCoM and FoldX, using the example of the human superoxide dismutase1 [73] which is involved in the motor neuron disease [131]. In this benchmark test FoldX and PoPMuSiC performed best by far. FoldX showed in this test a correlation coefficient R of 0.53 and a standard error of 1.1 kcal mol⁻¹, which was only slightly surpassed by PoPMuSiC [76]. In conclusion, the authors described FoldX as more sensitive and accurate towards difficult mutation sites but PoPMuSiC as more accurate to all kinds of mutations. Also, they demonstrated that FoldX can interpret patient data for dismutase diseases quite well with an R of 0.45 compared to other tools. Bednar *et al.* compared FoldX with Rosetta-ddG, ERIS and CUPSAT [86] and determined FoldX and Rosetta-ddG as best algorithms for improving stability. Foit *et al.* showed for the immunity protein 7 that FoldX was able to predict destabilizing mutations very well (Coefficient of determination (R²) of 0.62), but the algorithm was unable to predict the influence of stabilizing mutants. However in comparison to I-Mutant

2.0, PoPMuSiC and Eris, FoldX showed a better performance for prediction of destabilizing mutagenesis events (R^2 -values of : 0.34, 0.24, 0.3) [132]. Tian *et al.* and by Broom *et al.* determined the R-value of FoldX with known true positives and true negatives to be 0.5 with an accuracy of 0.67 [97,127]. Ayuso-Tejedor *et al.* determined R-value with 0.20 to 0.29 for the corresponding mutants against predicted negative $\Delta\Delta G$ -values [130]. In contrast, by investigating 582 mutants of seven proteins, R was 0.73 with a standard deviation of 1.02 kcal mol⁻¹ [133]. The best result was a correlation coefficient of 0.73 for a lysozyme structure [126] and was increased to 0.74, when only hotspot areas were chosen for prediction. The standard deviation (1.37 kcal mol⁻¹) was in the same range of Broom *et al.* (1.78 kcal mol⁻¹) [127]. However, Tokuriki *et al.* calculated that the average $\Delta\Delta G$ for any protein is + 0.9 kcal mol⁻¹ $\Delta\Delta G$, which clearly shows, that the probability of destabilization events is much higher, which concludes that the number of stabilizing theoretical mutants is much lower [134]. Not only the number of theoretical stabilizing mutations seems to be lower, also the correlation for predicted stabilizing mutations towards real stabilization is weaker than for destabilizing mutations [56,111]. In contrast, Khan *et al.* showed for human proteins that FoldX predicts more stability increasing variants than destabilizing variants, which might be a hint that human proteins are relatively non-rigid and less thermostable compared to other protein sources or that distribution of $\Delta\Delta G_{\text{calculated}}$ against the frequency of stabilizing and destabilizing mutations is only protein depending [101]. Furthermore, the calculated $\Delta\Delta G_{\text{Foldx}}$ energies deviate from real $\Delta\Delta G$ measurements. The values can be recalculated using an experimental factor $\Delta\Delta G_{\text{experimental}} = (\Delta\Delta G_{\text{calculated}} + 0.078) 1.14^{-1}$ [134,135]. Depending on the method used to evaluate FoldX, the accuracy will be in the range from 0.38 to 0.80 [101,129]. Obviously, FoldX can predict positions which are important for stability, but the discrimination between different amino acid residues at one site is not really powerful, e.g. an exchange of lysine to glutamate did not result in any change of ΔG , but experimentally a stabilization was observed [120,128]. The summarized results in table 2 demonstrate that actually all algorithms are not able to design or predict single mutation events towards trustworthy one mutation protein designs. However, FoldX shows a good performance in most of the studies compared to other algorithms, but it is necessary to increase the number of experimental mutations above 3 to achieve probable true positive results for protein engineering experiments. A general disadvantage of FoldX and other algorithms seems to be that FoldX often predicts hydrophobic interactions but at the expense of protein solubility [94].

4.1.6) The next generation of FoldX based predictions

Due to the low accuracy of all algorithms for stabilization mutations, algorithms often are combined to find coincident predictions or to prove predictions with a second algorithm. A popular combination is FoldX and Rosetta-ddG to gain more stabilizing mutation predictions. It was shown that FoldX and Rosetta-ddG predictions overlapped only in 12 %, 15% or 25 %, respectively, which means that a good coverage of beneficial mutations can only be achieved when more than one tool is used [86,56,105]. As a consequence of low prediction accuracy, popular algorithms are continuously improved. Recently a refinement of the Rosetta energy algorithm was reported with increased accuracy and faster calculation times. This demonstrates also the continuing importance of stability prediction in the field of protein engineering, but the authors stated that it is still far away from a final gold standard in the field of energy content prediction [136].

A sophisticated approach is the freeware webtool FireProt [137]. The FireProt algorithm uses FoldX as a pre-filter to select beneficial mutations which are subsequently proved in a second round using Rosetta-ddG. Only if Rosetta-ddG also predicts these mutations as putatively stabilizing they will be used for the experimental realization of these amino acid exchanges. Furthermore, the algorithm uses a consensus analysis of the protein-sequences to predict evolutionary beneficial mutation sites towards stability. These selected sites are then evaluated for their suitability using FoldX. The algorithm is divided into three stages using different methods for crosschecking the accuracy of the calculations and combines putative beneficial mutations to gain further improvement of stability. The free webtool of FireProt allows even inexperienced users to perform protein energy calculations. Bednar *et al.* demonstrated at two examples the utility of this algorithm using the example of two enzymes and combined many mutation sites with overall improvements of ΔT_m of 21°C and 24°C for the combination of all sites [86]. However, to verify if FireProt is useful or not, more studies are necessary. Furthermore, the core function of FoldX algorithm does not simulate backbone movements of the protein, which might be a potential factor to improve FoldX [74]. The stability prediction tool of Goldenzweig *et al.* might be an alternative to the mentioned Fireprot -algorithm. Similar to Fireprot, it combines information gained in sequence homology alignments and of energy calculations using crystal structure data and Rosetta-ddG. Using the human acetylcholinesterase, an improvement in stability ($\Delta T_m = 20^\circ\text{C}$) was demonstrated and simultaneously, the expression level in *E. coli* BL21 was increased. They hypothesized, that putatively destabilizing mutations can be excluded from mutation libraries using homologous sequence alignments to prohibit certain types of amino acid exchanges [138].

4.1.7) Conclusion

The performance of FoldX depends drastically on the quality of the crystal structure and it is unclear if the protein source might have an influence on the accuracy of such algorithms. Nevertheless, FoldX seems to be more accurate for the prediction of destabilizing mutations and less accurate for the prediction of stabilizing mutations, but in both cases it was shown that FoldX is clearly better than random approaches: e.g. Christensen *et al.* described FoldX as one of the most accurate single site stability predictors and Potapov *et al.* even described the accuracy of FoldX as impressive compared to other algorithms [122,126]. The natural success rate for random mutagenesis is only ~2%, which was surpassed by most experiments [94,139]. Therefore, FoldX seems to be a promising tool for protein design, but as mentioned by Thiltgen *et al.* it can be said that FoldX cannot serve as a gold-standard for generally improving stability of proteins. Moreover, using FoldX together with other algorithms for reciprocal control of calculation results, Rosetta-ddG or PoPmuSiC as filter for true positive results will most probably increase the accuracy and the success rate of thermostability engineering [86,127,140]. In general the accuracy can be improved additionally, when mutation outliers are eliminated or additional MD-simulations are performed [82]. FoldX was used successfully in different approaches (**Table 4.1**) aiming from enzyme stabilization towards predictions of protein-protein interactions (especially for drug design) or for the prediction of disease-associated mutant proteins, making FoldX a versatile tool for life science [80,141–143]. The progress in protein stability prediction is striking, however up to now no *in silico* calculation can fully spare experimental procedures, although the existing tools can reduce the amount of lab experiments significantly.

4.2) Thermostabilization of the *V. paradoxus* ω -TA using FoldX

This chapter is based on the modified pre-peer reviewed version of the following publication. Furthermore unpublished experiments regarding disulfide bond engineering were included:

Improvement of the thermostability of a β -amino acid converting ω -transaminase using FoldX.

Oliver Buß^a, Delphine Muller^a, Sven Jager^b, Jens Rudat^a and Kersten S. Rabe^c

^a Institute of Process Engineering in Life sciences, Section II: Technical Biology, Karlsruhe Institute of Technology, Karlsruhe Germany. ^b Computational Biology Technische Universität Darmstadt, Schnittspahnstraße, 64287 Darmstadt. ^c Institute for Biological Interfaces I, Karlsruhe Institute of Technology (KIT), Hermann-von-Helmholtz-Platz 1, 76344 Eggenstein-Leopoldshafen, Germany

Publishing details:

Published: 9 November, 2017

The final peer-reviewed publication is available at

<http://onlinelibrary.wiley.com/doi/10.1002/cbic.201700467/abstract>

Author-Rights: “*This is the pre-peer reviewed version of the following article: [O. Buß, D. Muller, S. Jager, J. Rudat, K. S. Rabe, ChemBioChem 2018, 19, 379.], which has been published in final form at doi.org/10.1002/cbic.201700467. This article may be used for non-commercial purposes in accordance with Wiley Terms and Conditions for Self-Archiving.*”

Authors' contribution to this publication

Oliver Buß carried out the major experimental, conceived and wrote the manuscript **Delphine Muller** expressed and purified variants of the ω -TA. **Sven Jager** performed MD-simulations of the ω -TA. **Jens Rudat** supervised the work, provided administrative support and critically revised the manuscript. **Kersten S. Rabe** performed FoldX-calculations, contributed to the design of the study, supervised the work and critically revised the manuscript.

4.2.1) Introduction on the thermostabilization of ω -transaminases

The outstanding importance of ω -TA for synthesis approaches makes them a rewarding target for enzyme engineering to improve the characteristics of them. Like mentioned in chapter 1.3, there are a lot of possibilities to utilize different ω -TA for synthesis of chiral amines and amino acids. However, they differentiate in the enantioselectivity, which is accompanied by the Fold types IV (*R*) and I (*S*) of PLP-dependent enzymes [144,145]. The acceptor molecules can vary from classical α -keto acids to β -, γ - or ϵ -keto acids and even ketones and aldehydes are converted by this class of enzymes [146].

Although there is an increasing number of ω -TA being described, certain limitations concerning the substrate scope and physicochemical properties such as stability are still hampering their application. The pool of (*R*)-selective ω -TA is still much smaller than for (*S*)-selective ω -TA and especially more bulky substrates are still challenging. To overcome the latter limitation, the pharmaceutical companies Merck and Codexis performed a sophisticated directed evolution of an (*R*)-selective ω -TA to gain an enzyme with activity towards the substrate proisitagliptin. In this process the activity, solvent stability and thermostability were improved by several rounds of random and site directed mutagenesis experiments [147]. In total 27 mutations were introduced into the ω -TA, which originates from *Arthrobacter sp.* KNK 168. There are further examples for the redesign of an (*S*)-selective ω -TAs by Midelfort *et al.* and Pavlidis *et al.* [42,148] Midelfort *et al.* redesigned an (*S*)-selective ω -TA from *Vibrio fluvialis* towards higher activity to the aliphatic β -keto ester substrate, ethyl 5-methyl 3-oxooctanoate, and towards higher stability in organic solvents.

4.2.1.1) Thermostability of ω -TA

Apart from engineering the substrate scope, improving the stability of an enzyme can lead to more efficient production processes and enable the enzyme to tolerate more mutations in general. Deepankumar *et al.* have shown the incorporation of the non-canonical α -amino acid fluoro-tyrosine in an (*S*)-selective ω -TA from *Vibrio fluvialis*. The resulting enzyme showed an increase in thermostability about 2.3 fold as compared to the wild type. The experiments were performed at an incubation temperature of 50°C and the researchers observed an improved half-life time of 7.0 h in comparison to 3.0 h for the wildtype enzyme. However, the melting temperature was not reported [149]. Pannuri *et al.* utilized 5 cycles of error prone PCR and screening, resulting in an enzyme, based on an (*S*)-selective- ω -TA (CNB05-01) from *Arthrobacter citreus*, with improved stability. This was mainly due to an important exchange

4) Thermostability engineering of the *V. paradoxus* ω -TA

of a cysteine to a tyrosine residue located near the active site. T_{opt} has been enhanced from 30°C to 55°C and increased the activity about 260-fold, without compromising the enantioselectivity [150,151]. A rational thermostabilization strategy has recently been shown for the fold type IV (*R*)-selective ω -TA from *Aspergillus terreus* by calculation of $\Delta\Delta G^{\text{fold}}$, combined with the crystallography B-factor set as a pre-filter for $\Delta\Delta G^{\text{fold}}$ calculations resulting in 2.2 fold half-life improvement at 40°C with a single mutation [152].

Apart from engineering ω -TA from mesophilic sources, thermostable variants can in general also be established by screening enzymes from thermophilic organisms. The first (*S*)-selective ω -TA which was labeled as thermostable was discovered by an *in silico* screening in the thermophilic microorganism *Sphaerobacter thermophilus*. This enzyme showed a remarkable stability retaining its full activity at 60°C for at least 2 h [153]. The same research group identified and characterized a thermostable ω -TA with activity towards amines using a modified NCBI-blast search in the thermophilic microorganism *Thermomicrobium roseum*. This enzyme showed a T_m of 87°C [154]. The ω -TA lost only half of the initial activity after 12.5 h of incubation at 60°C. Ferrandi *et al.* discovered three thermostable ω -TA from hot spring metagenomes, with the best being a ω -TA from an unknown microorganism, labeled as B3-TA, with a T_m of 88°C [155]. This enzyme is very robust and shows a long-term stability at 80°C for at least 2 weeks, losing only 60 % of its initial activity under these conditions. The other two enzymes, Is3 and It6 showed a T_m of 79°C and 57°C, respectively.

In summary, up to now only five (*S*)-selective ω -TA are described exhibiting high thermostability and only one of these ω -TA from *S. thermophiles* showed activity towards *rac*- β -phenylalanine (β -PA). β -PA and derivatives thereof, could be also utilized in β -peptides, as inhibitor for peptidase IV and in drug delivery systems [158–160]. The β -PA converting ω -TA from *S. thermophiles* shows only a low activity of 3.3 U mg⁻¹ compared to ω -TA from *V. paradoxus* with a specific activity of 17.5 U mg⁻¹ at 37°C [161]. Thus the transaminase from *V. paradoxus* is an interesting candidate for enzyme engineering taking into account its high enzymatic activity and lack of data concerning thermostabilization.

The aim of this study was the optimization of the thermostability of the *V. paradoxus* transaminase (ω -VpTA) using an *in silico* approach in combination with site directed mutagenesis to generate an enzyme with a longer life time at temperatures above 50°C. The FoldX software was utilized to identify potentially stabilizing mutations in order to reduce necessary sample throughput and to avoid large enzyme libraries and the corresponding need

for a high throughput screen [162]. FoldX can be used to calculate the change in free energy caused by an amino acid substitution and to predict the change in the free energy to fold/unfold ($\Delta\Delta G$) a protein [162]. We sequentially exchanged every amino acid position in ω -VpTA against any standard α -amino acid and performed the free energy calculations. The hits with highest beneficial energy stabilization were selected for site directed mutagenesis. Variants with high activity in cell lysate were purified and characterized in detail regarding their thermostability and specific activity. Furthermore the long-term activity was studied and compared to that of the wild type enzyme.

As alternative and additional approach also disulfide bond engineering was performed. In contrast to FoldX engineering also the introduction of covalent disulfide bonds is possible. Therefore the MD-calculations of 4AOA were analyzed to detected amino acid positions which are nearby but not protein sequential neighbors.

4.2.3) Methods and Materials

Chemicals

Unless stated otherwise all chemicals were purchased from Sigma Aldrich (St.Louis, US) and Carl Roth (Karlsruhe, Germany) in analytical grade. All enantiopure β -amino acids were purchased from PepTech Corporation (Bedford, US).

FoldX Setup

In order to calculate the change in free energy of unfolding, the FoldX 3.0 algorithm was applied [162]. As starting point the PDB structure 4AOA of ω -VpTA was used [161]. The *in silico* temperature was set to 298 K. After applying the automatic RepairPDB function, all mutations were created using the FoldX-function BuildModel. In order to automate this process a script written in Python was utilized to change every single amino acid position into all standard α -amino acids possible. Other options were set to default. All resulting data for every position was ranked from lowest to highest $\Delta\Delta G$. The best nine hits showing the lowest $\Delta\Delta G$ were chosen for mutation experiments and in addition two amino acid exchanges were selected which showed a high energy benefit in the terms of the FoldX energy function and a relatively high $\Delta\Delta G$.

Mutagenesis PCR

The mutations were generated by site directed mutagenesis PCR employing a touch down PCR. 10 PCR cycles were performed decreasing the annealing temperature by 0.5°C each cycle, followed by 25 cycles at the calculated melting temperature of the primers. The utilized oligomer primers are displayed in table 4.3 and table 4.4 for mutation experiments regarding artificial disulfide bonds. PCR reaction mixture was mixed according to the protocol of the Phusion DNA polymerase (Thermo Fischer Scientific, USA) and additionally each PCR run was performed with and without of 3 % (v/v) DMSO. In order to remove the initial DNA vector template, 1 μ L of the endonuclease DpnI (NEB, USA) was added to the PCR product and the mixture was incubated for at least 1 h at 37°C. Subsequently 10 μ L of the PCR product was transformed into 90 μ L of chemical competent *Escherichia coli* XL10 Gold (Agilent Technologies, USA) cells. Single colonies were sequence verified by DNA sequencing of purified vector DNA (GATC, Germany).

Table 4.3 Oligomers for site directed mutagenesis of FoldX predicted mutations. The oligomers were ordered from Thermo Fischer Scientific. They were designed only to overlap partially.

Position	Exchange	T _m	Direction	primer-sequence
19	D to M	64°C	fw	ATCGTCGTTTTACC ATGG CAAATCCGGCAAGC
19	D to M	64°C	rv	GGTAAAACGACGATATGCATCTGCCAGTGCC
98	G to M	62°C	fw	TATTGAAGCAATGCAGAT TGGG TATTAATCTGACAG GTCAT
98	G to M	60°C	rv	CTGCATTGCTTCAATAACTGCATCACGAATTTCC
165	G to M	64°C	Fw	CATGGTGGTGTCTG ATG TTTGGTGCACGTCC
165	G to M	64°C	Rv	CAGAACACCACCATGATAACCACCGCTAAAAACAA CA
243	M to R	64°C	Fw	CTGGTTTTTGATGAAGTT CGT ACCAGTCGCCTGGC
243	M to R	63.2° C	Rv	AACTTCATCAAAAACCAGCAGTGCACCAACCTG
325	G to D	64°C	Fw	CCGGAAGCAGCC GATG CACTGGCCGAA
325	G to D	64°C	Rv	GGCTGCTTCCGGTGTAACAGTTTGGTC
345	E to F	62°C	Fw	GCACTGTGTGCAAAT TTCGGT GTTGCAATGC
345	E to F	62°C	Rv	ATTTGCACACAGTGCATTCAGACGGGC
391	E to R	61°C	Fw	TTTTTCATCTGCTGAAT AG AGATATCTATAGCAGTC CG
391	E to R	61°C	Rv	ATTCAGCAGATGAAAAACAGCAGCTGACG
392	D to K	62°C	Fw	TTTCATCTGCTGAATGAAA AG ATCTATAGCAGTCC GC
392	D to K	62°C	Rv	TTCATTCAGCAGATGAAAAACAGCAGCTGACG

4) Thermostability engineering of the *V. paradoxus* ω -TA

395	S to I	62°C	Fw	CATGGTGGTGTCTG ATC TTTGGTGCACGTCC
395	S to I	62°C	Rv	ATAGATATCTTCATTCAGCAGATGAAAAACAGCA GCTG
408	D to D	64°C	Fw	GCCTGCCGCTG GAT GATGCCGATATTGATC
408	D to D	64°C	Rv	CAG CGG CAG GCT CAG AAC AAC AAA ACC AC
420	G to E	62°C	Fw	GTGGCAGCGATT GAG AGCTTTATTGGTGGT
420	G to E	60°C	Rv	AATCGCTGCCACATAACGATCAATATCGG

4) Thermostability engineering of the *V. paradoxus* ω -TA

Table 4.4 Oligomers for site directed mutagenesis of disulfide-bond engineering sites. The oligomers were ordered from Thermo Fischer Scientific. They were designed only to overlap partially. *different variants were utilized for mutagenesis PCR. High differences between T_m of oligomer primer pairs are a result of high degree of mismatch of the mutagenesis Fw-primer.

Position	Exchange	T_m	Direction	primer-sequence
5	A to C	56 °C	Fw	ATGATGACCCATGCATGTATTGATCAGGCACTG
5	A to C	56 °C	Rv	TGCATGGGTCATATGGGTG
59	A to C	60 °C	Fw	CACGTGGTGAAGGTTGCGCACTGTGGGATGCAG
59	A to C	61 °C	Rv	ACCTTCACCACGTGCAATGGTCA
90*	D to C	61 °C	Fw	CACCGGAAATTCGTGTTGCAGTTATTGAAGCAAT*
90*	D to C	64°C	Rv	CACGAATTTCCGGTGCGCTATGACCAT
92	V to C	64°C	Fw	GGAAATTCGTGATGCATGTAATTGAAGCAATGCAG GGTG
92	V to C	64°C	Rv	TGCATCACGAATTTCCGGTGCGC
125	Q to C	67 °C	Fw	GTTTTCCGCAGATTGAATGTCTGCGTTTTACCAATA GCGG
125	Q to C	64°C	Rv	TTCAATCTGCGGAAAACGTTACAAATCAGACG
363	V to C	60°C	Fw	CCTGATGAATGCACATTTTTGTCAGGGTGATGTTCCG TAG
363	V to C	65°C	Rv	AAAATGTGCATTCATCAGGCTACCAATGCCG
388	L to C	54 °C	Fw	AGCTGCTGTTTTTTCATTGCCTGAATGAAGATATCT ATAG
388	L to C	60°C	Rv	ATGAAAAACAGCAGCTGACGCAGAC
404	S to C	62 °C	Fw	GTGGTTTTGTTGTTCTGTGCCTGCCGCTGA
404	S to C	64 °C	Rv	CAGAACAACAAAACCACGCGGACTGC
421	S to C	60 °C	Fw	CAGCGATTGGTTGCTTTATTGGTGGTCAT
421	S to C	62 °C	Rv	ACCAATCGCTGCCACATAACGATCAATATC
435	N to C	64 °C	Fw	TGCCTCGTGCTGTTAACTCGAG
435	N to C	64 °C	Rv	GCACGAGGCAGCAGGGCAC

4) Thermostability engineering of the *V. paradoxus* ω -TA

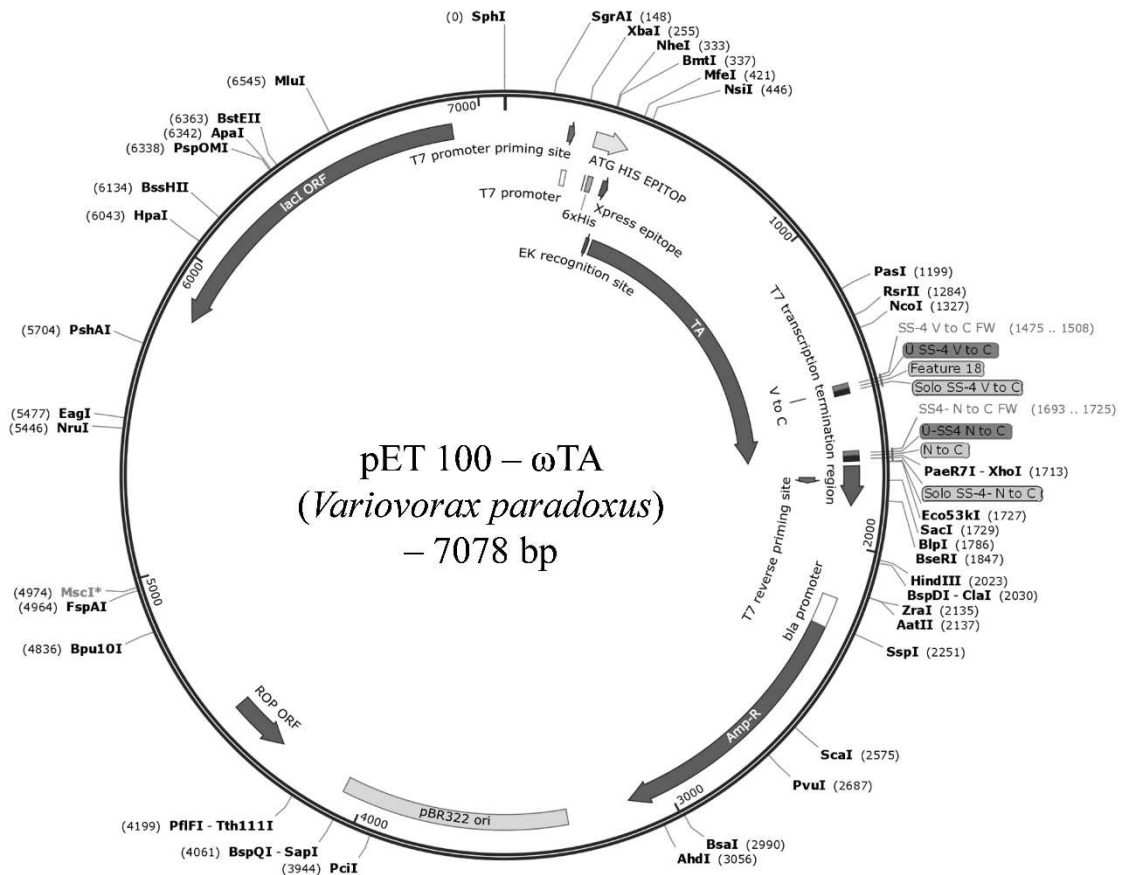


Figure 4.1 Vector map of *V. paradoxus* ω -TA with resistance gene towards ampicillin in T7-promotor system. The gene-code was codon-optimized towards *Escherichia coli* BL21 usage. For gene sequence see **appendix 8.1**

Enzyme purification

In order to express the ω -VpTA in a T7 expression system, the sequence verified plasmids were transformed into BL21 (DE3) cells. The synthetic ω -VpTA gene was ordered containing an N-terminal hexahistidine tag for purification using immobilized metal ion affinity chromatography. 1 mL of precultures grown in Luria Bertani-medium (LB) was sedimented by centrifugation in a benchtop centrifuge (Thermo Fisher Scientific, USA) at 13.300 rpm. After washing the pellet with fresh LB-medium, 1 mL was resuspended in 400 mL auto inducing medium (AIM) (Formedium, Great Britain) containing 100 μ g/mL ampicillin. Initially, the cultures were grown in an incubator (Infors, Switzerland) at a shaking rate of 120 rpm and 37°C. After 4 h, the temperature was decreased to 20°C and the incubation continued for 20 h. The protein expression is self-induced, when the D-glucose is completely consumed and the only remaining carbon source is lactose. After 24 h of incubation, the cells were collected by centrifugation at 8,000 rpm in a JA-10 rotor with a Beckman Centrifuge (Coulter-Beckman, USA). The supernatant was discarded and the cells were resuspended in 10 mL of lysis buffer (50 mM sodium phosphate, pH 7.8, 0.3 M NaCl, 10 mM imidazole and 0.1 mM of pyridoxal-5-phosphat cofactor). In order to lyse the cells, they were incubated with lysozyme for 30 min at room temperature and subsequently homogenized using ultra-sonification. The cell debris was removed by centrifugation at 49,500 g for 30 min at 4°C in a Beckman centrifuge. The purified ω -TA was obtained by Ni-NTA affinity chromatography with a 1 mL Ni-NTA column (Thermo Fisher Scientific, USA) on an ÄKTA start system (GE-Healthcare, Great Britain). In order to elute the ω -TA, a gradient ranging from 20 mM imidazole (lysis buffer) to 500 mM imidazole was applied at a flow rate of 1 mL/min. Fractions with ω -TA could be identified by visual inspection due to their slight yellow color caused by the bounded PLP, absorbing at 395nm [163]. Fractions containing the ω -TA were pooled and concentrated using centrifugal filters with a MWCO of 30 kDa (Millipore). The samples used for thermal shift assay were subjected to one freeze and thaw cycle. The purity was checked using SDS-polyacrylamide gel-electrophoresis with 12 % (v/v) acrylamide gels according to Lämmli *et al.* [164]. For determination of T_m the buffer of the ω -TA samples was exchanged to 40 mM sodium phosphate (pH 7.2). The ω -TA samples for activity testes were mixed with glycerol 20 % (v/v) and stored at -80°C. The protein concentration was determined using the Bradford assay with BSA-standard samples of known protein concentration. An adapted protocol from Zor *et al.* was used, analyzing the wavelength at 450 nm and 595 nm [165].

Activity test

The activities of ω -TA samples was tested in sodium phosphate buffered solutions (pH 7.2) containing 0.1 mM of pyridoxal-5-phosphate. The concentration of the substrate was set to 15 mM of *rac*- β PA (amino donor) and 15 mM of α -ketoglutaric acid (amino acceptor). The standard reaction temperature was set to 40°C and the mixtures were preincubated prior to starting the reaction by the addition of 10 μ L enzyme solution to 210 μ L reaction mixture. If not marked otherwise the final concentration of the ω -TA was 2.5 μ M. 50 μ L samples were collected after 15 s and 90 s and the reaction was stopped immediately by the addition to 150 μ L preheated buffer solution (99°C) with 1 mM l-leucine as internal standard. The samples were centrifuged in a benchtop centrifuge to remove all precipitates. The experiments were conducted in triplicates. To quantify the activity of the ω -TAs one unit (U) was defined as the conversion of 1 μ mol (*S*)- β -phenylalanine per min.

HPLC-analytic

Samples were analyzed via HPLC (Agilent 1200 Series, USA) with an automated precolumn derivatization protocol using *ortho*-phtaldialdehyde (according to Brucher *et al.*) [166]. A reversed phase C18 column (150 x 4.6 mm HyperClone 5 μ m, Phenomenex Inc., Germany) was operated with a mobile phase of 55 % methanol and 45 % 40 mM sodium phosphate buffer (pH 6.5) at a constant flow rate of 1 ml/min at 40°C. The elution of compounds from the column was analyzed at a wavelength of 337 nm using a UV detector. The injection volume of the samples for the derivatization mixture was set to 0.5 μ L. 7.5 μ L of the derivatization mixture were injected onto the column. A calibration was performed using defined concentrations of *rac*- β PA. β -PA was diluted in 40 mM sodium phosphate with 1 mL of L-leucine. Optically pure (*R*)- and (*S*)-enantiomers from Peptech were used to calibrate the retention times (Burlington, USA).

Thermal shift assay

Determination of T_m was conducted with 5 μ M solutions of freshly purified ω -TA in 40 mM sodium phosphate solution at pH of 7.2. SYPRO-Orange (5000 x) was used as fluorescence dye and diluted to a working solution of 200 x in buffer. 3 μ L of the dye solution were added to 27 μ L of protein solution and the fluorescence was recorded with a qPCR-cycler in transparent qPCR-strips (Eppendorf, Germany). The solution was pre-incubated for 5 min at 20°C in the cycler. A temperature gradient increasing the temperature by 0.5°C per 30 s was employed until

4) Thermostability engineering of the *V. paradoxus* ω -TA

90°C were reached. The T_m was determined at the maximal slope of fluorescence intensity against the time. Experiments were conducted in triplicates with ω -TA samples from two independent protein expressions.

Molecular dynamic simulations

All ω -TA simulations were performed using the GROMACS software suite (version 4.6.5). As protein structure we used the dimer structure of the β -phenylalanine from *V. paradoxus* with a resolution of 0.228 nm [161]. To add water molecules, we used the SPC/E model while the protein interacts through the AMBER03 force field [167]. The simulations were conducted in 0.9 % (w/v) NaCl solution. The system was first energy minimized using a conjugate gradient and equilibrated for 2 ns in the NVT-ensemble at 300 K and for 5 ns in the NpT-ensemble at 300 K, while the pressure was set to 1 bar. During the equilibration, temperature was controlled using the velocity-rescale thermostat ($\tau T = 0.1$ ps) and pressure was controlled using the Parrinello-Rahman ($\tau P = 0.5$ ps). Isothermal compressibility was set to $4.5 \times 10^{-5} \text{ bar}^{-1}$, which is the corresponding value for water [168] [169]. Production runs were performed for 100 ns. The temperature was controlled using the Nosé-Hoover thermostat ($\tau T = 1$ ps) and pressure was controlled using the Parrinello-Rahman barostat ($\tau P = 1$ ps) during the production runs. Bond lengths were constrained using the LINCS algorithm [170] [171] [172] [173]. The Lennard-Jones non-bonded interactions were evaluated using a cutoff distance of 1.4 nm. The electrostatic interactions were evaluated using the particle mesh Ewald method with a real space cutoff 1.4 nm and a grid-spacing 0.12 nm. Long-range corrections to energy and pressure due to the truncation of Lennard-Jones potential were accounted. The equations of motion were integrated using a 2 fs time step. In order to analyze structural fluctuations the root mean square fluctuation was computed (Equation 2).

$$RMSF = \sqrt{\frac{1}{t} \sum_{t_j=1}^T (x_i(t_j) - \bar{x}_i)^2} \quad (2)$$

T is defined as the duration of the simulation (time steps) and x_i the coordinates of atom x_i at time t_j .

Analysis of molecular dynamic simulations for disulfide bond engineering

For the analysis of the trajectory over 100 ns, possible contact points were filtered for the disulfide bonding engineering. Therefore the gained data were analyzed using StreamMD, StreAM-T_g algorithms to detect motifs and α -carbon atoms within the range of 9 Å with high contact probability [174,175]. Sequentially adjacent amino acid positions were excluded for further proceeding.

Calculation of free energy change

$\Delta\Delta G^{\text{unfold}}$ was calculated according to equation of Christensen and Kepp [176]. To this end the concentration of folded and unfolded protein was approximated using the fluorescence intensity at 55°C for the wild type compared to the mutants (Equation 1).

$$\Delta\Delta G = -RT \ln \left(\frac{[Mut_{folded}]}{[Wt_{unfolded}]} \frac{[Wt_{folded}]}{[Mut_{unfolded}]} \right)$$

4.2.5) Results and Discussion

The improvement of the thermostability of the ω -VpTA was carried out using FoldX guided site directed mutagenesis and disulfide bond engineering using molecular dynamic (MD) simulations.

FoldX guided enzyme engineering

Different positions within the ω -TA were analyzed by determining the melting temperature of the resulting proteins and following their reaction with *rac*- β -PA and α -ketoglutaric acid as substrates at different temperatures. After calculating $\Delta\Delta G$ -values for all 8246 possible single site mutations, we selected the eleven most stabilizing mutations with $\Delta\Delta G$ -values ranging from -30.1 to -54.3 kcal mol⁻¹. Interestingly, amongst these eleven the FoldX algorithm suggested to mutate glycine into much larger residues in four of these eleven cases at the positions 165, 325, 420 and 98. Many of the suggested mutation sites can be found at the surface of the enzyme and in a distance of more than 20 Å from the center of the enzyme, defined by the active site lysine (K267, see also Scheme 1) binding the cofactor (**Table 4.5 and Figure 4.2**). However, three proposed mutation sites were closer to the active center and M243 is the nearest amino acid residue at a distance of 5.0 Å from the catalytically center (K267).

Table 4.5 Mutation sites with the most negative $\Delta\Delta G$ as predicted by FoldX. The last two mutations (M243 and T408) were selected because they showed a predicted stabilization with a high energy benefit in parts of the whole energy equation. The distances to the active site lysine binding the cofactor (K267) were calculated using Chimera 1.1.[177]

Position	Original amino acid	Best amino acid mutation	$\Delta\Delta G$ [kcal mol ⁻¹]	Distance to K267 [Å]
165	G	M	-54.3	13.5
391	E	K	-42.9	24.5
325	G	D	-35.9	20.4
420	G	E	-35.5	26.5
19	D	M	-34.6	29.3
98	G	M	-34.2	29.1
345	E	F	-33.5	31.2
392	D	K	-30.9	21.5
395	S	I	-30.1	13.2
408	T	D	-11.7	21.2
243	M	R	-9.5	5.0

The variants were generated in a codon optimized ω -VpTA gene using touch down PCR with mismatch primers and expressed in *E. coli* BL21. In order to reduce the number of proteins which had to be purified, the enzymatic activity was preliminary checked in the lysate of small expression cultures. M243R, G325D and G420E showed no or low activity in the lysate towards (S)- β -PA and were thus excluded from further studies. M243R might be too close to the catalytically active lysine and also introduces a positive charge into the substrate pocket.

4) Thermostability engineering of the *V. paradoxus* ω -TA

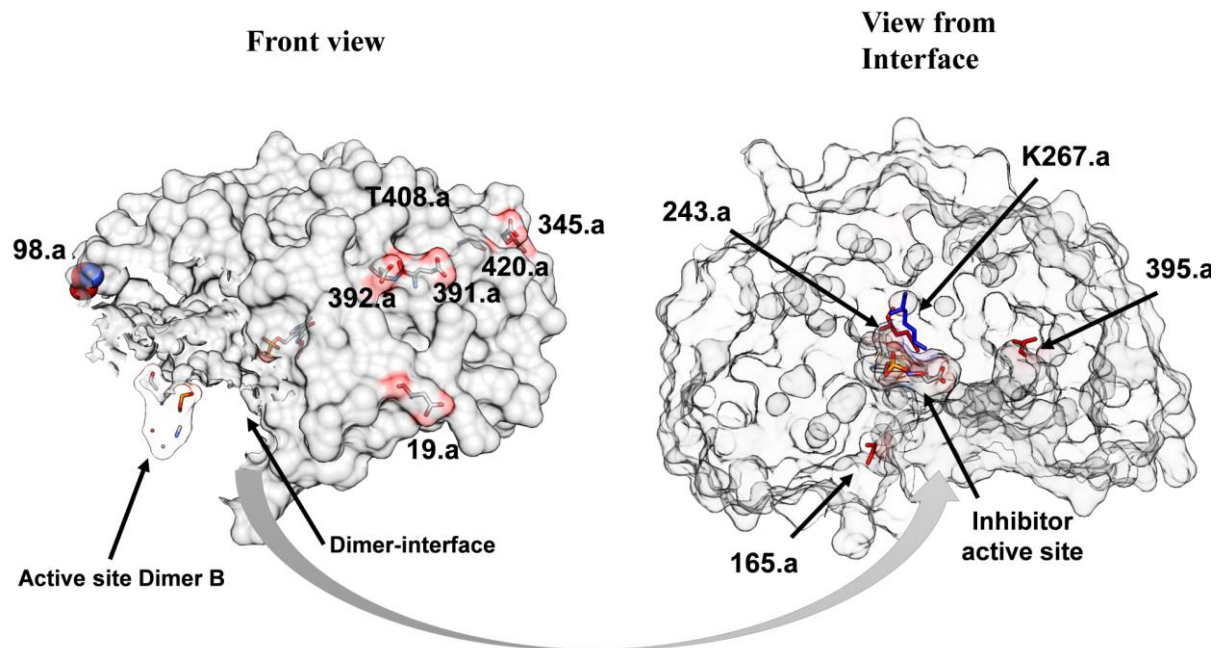


Figure 4.2 Locations of the eleven mutations predicted to be most stabilizing. Only one monomer of the dimeric *V. paradoxus* ω -TA is shown (PDB ID 4AOA)[161]. Only one monomer (chain A) is shown, note that the interface area is about one quarter of the whole protein surface (4,400 Å²). The solvent accessible parts of the mutation sites are colored in red and the two active sites are visualized by 4'-deoxy-4'-acetylamino-pyridoxal-5'-phosphate from the crystal structure. The active site lysine K267 is colored in blue. The structure is rotated 90° to show the interface site on the right side of the figure.

For the efficient expression of ω -VpTA, it was shown that the auto-induction medium provided the highest yields of the product. The clear advantages of the auto-induction medium are that higher cell densities can be achieved, metabolizing at the beginning only D-glucose (without induction), and the expression strain starts by it-self the expression by ingestion of lactose at the given time. The *E. coli* culture defines by it-self the starting point of the expression in contrast to IPTG induced protein expression, the expression rate increases slowly [178]. For therapeutic protein expression of interferon α using auto-induction medium results in higher protein yields and furthermore lowering the temperature of expression results in more soluble protein yields [178]. In addition fermentation processes in bioreactors and high throughput screenings are simplified and protein expression is tighter controlled [179,180].

All other of the hexa-histidine-tagged variants were expressed and purified using immobilized metal ion affinity chromatography (IMAC). Variants with low protein yield in *E. coli* BL21 resulted in a low grade of purity and were also excluded. For the experiments two independent protein expressions were performed and the quality and purity controlled using SDS-PAGE (**Figure 4.3**) shows an example of expression and purification). The ratio of the variant proteins versus other protein impurities was too high for the determination of the melting temperatures in those cases. An average T_m was calculated based on data determined using a thermal shift

assay with SYPRO-orange as protein-binding fluorescence dye in a classical qPCR-cycler system (exemplary shown in **Figure S2**).

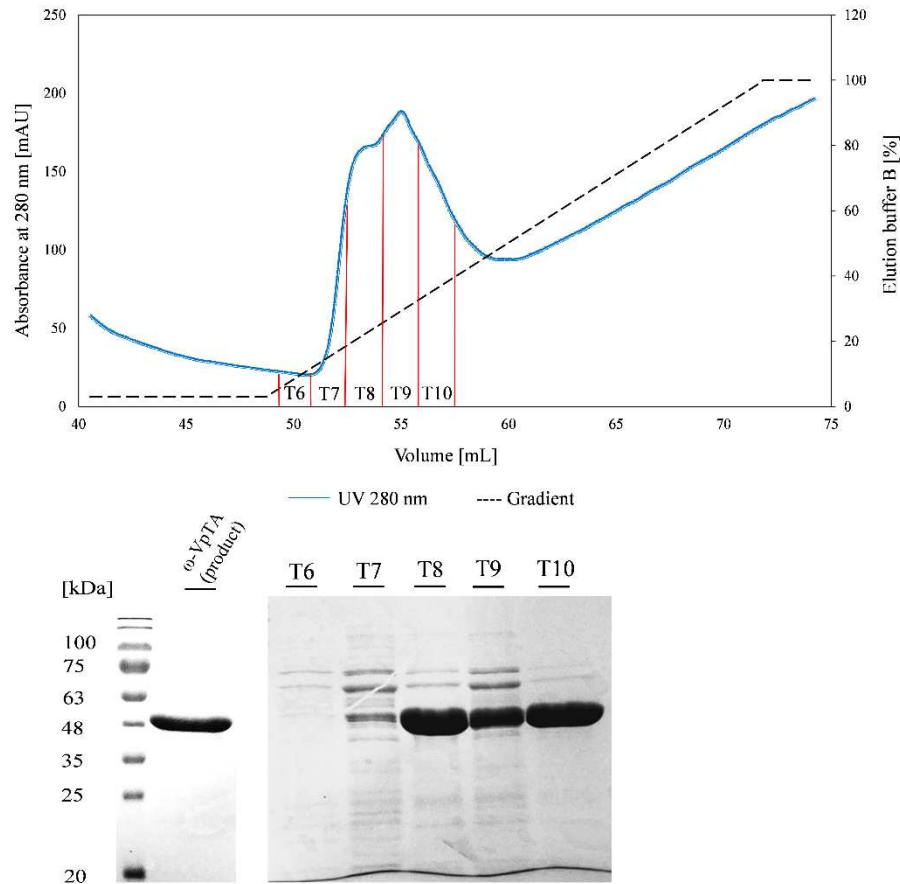


Figure 4.3 Purification of wild-type ω -VpTA by Ni-NTA affinity chromatography. Fractions 6 to 9 show slight contaminations of *E. coli* BL21 proteins. Fraction 10 is considered pure for the purpose of this work. The gradient starts at 15 mM of imidazole and reaches 500 mM at 100 %. After filtration via 30 kDa centrifugal filter a pure enzyme product is obtained.

Of the five enzyme variants analyzed, the G98M mutation showed the highest increase in T_m of + 4°C in comparison to the wildtype enzyme. The mutations at E345F and D392K also showed an increase of the T_m of + 0.9°C and + 1.4°C respectively. However, the experimental error in these cases was in the same range as the change. As can be seen from the comparison of experimental T_m and theoretical $\Delta\Delta G$ -values in Table 2. Additionally, we combined the second and third best variant with G98M to gain an additional increase in T_m . However, no significant improvement could be achieved, which also suggests that the improvement for the single site variants was not significant. In order to analyze the effect of the mutations on the specific enzyme activity all selected variants were compared to the wild type enzyme (**Table 4.6**).

4) Thermostability engineering of the *V. paradoxus* ω -TA

Table 4.6 Experimental thermostability analysis of FoldX predicted ω -VpTA variants. The measurement was conducted in triplicates and expression of every variant was performed twice. Standard deviation is determined between different expression setups.

Variant	Location	T _m [°C]	Δ T _m [°C]	Standard deviation
Wild type		55.3	0	0.2
G165M	Loop (active site)	56.0	+0.7	0.2
E391K	Loop (surface)	54.3	-1.0	0.1
G98M	α -helix (interface)	59.3	+4.0	0.7
E345F	α -helix (surface)	56.2	+0.9	1.0
D392K	Loop (surface)	56.7	+1.4	1.0
G98M+E345F		58.8	+3.5	0.5
G98M+D392K		59.4	+4.1	0.7

In order to analyze whether the mutations introduced compromised the specific activity of the mutant enzymes, the reaction catalyzed by all variants was analyzed (**Figure 4.4**). The reactions were carried out at 40°C with 15 mM *rac*- β -PA and 15 mM of the amino acceptor substrate α -ketoglutarate, which was shown to be the best substrate for the (*S*)-selective ω -TA from *V. paradoxus*. [161].

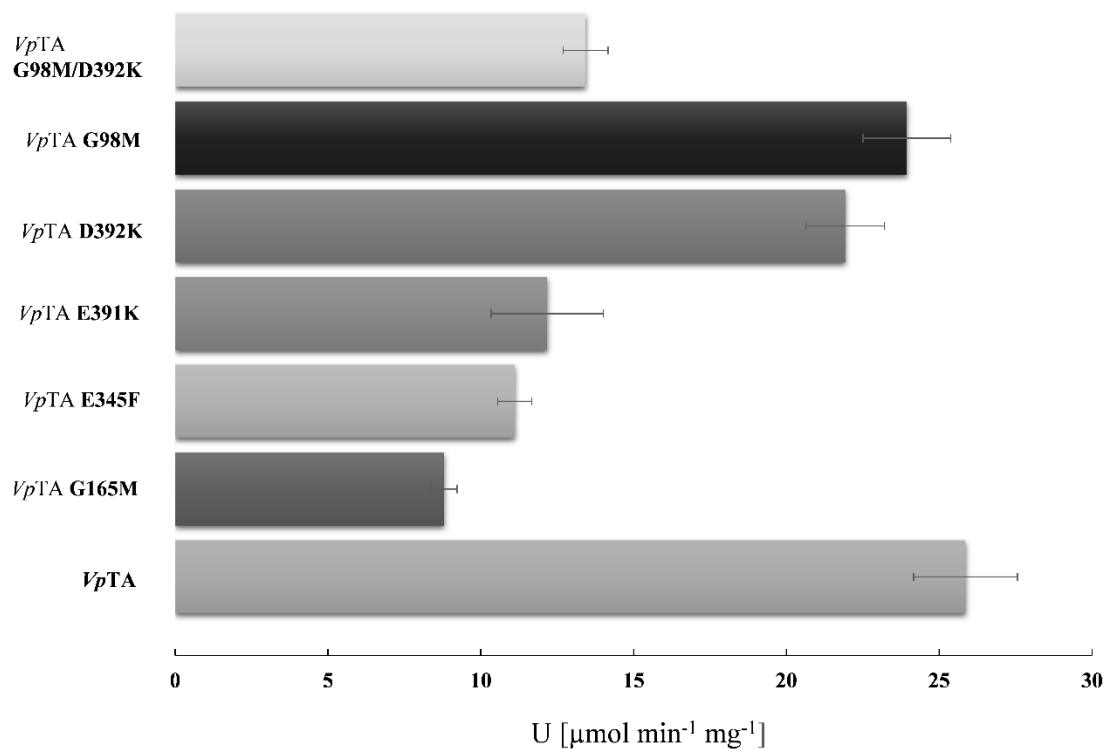


Figure 4.4 Comparison of specific enzyme activity of selected mutant variants against wild type ω -TA. The reaction mixture contained 15 mM of *rac*- β -PA and 15 mM α -ketoglutarate. The activity was measured at 40°C in 40 mM sodium phosphate buffer (pH 7.2) and determined between 15 and 90 seconds.

The specific activity of the wildtype ω -TA under these conditions was determined to be 26 U mg⁻¹, which fits well with the results of Crismaru *et al.* They determined a specific activity of 17.5 U mg⁻¹ at 30°C and 33 U mg⁻¹ at 50°C for the conversion β -phenylalanine. Our most thermostable variant G98M showed a slightly lower specific activity of 24 U mg⁻¹, followed by D392K with 22 U mg⁻¹. All other variants were clearly less active than the wild type enzyme. The mutation G165M showed the lowest activity, possibly due to the relatively close proximity to the active site (compare Table 4.5). Based on these results, the variants G98M, D392K and their combination were selected to be further investigated regarding heat stability and compared to the wild type enzyme (**Figure 4.5**). The enzymes were incubated at defined temperatures

4) Thermostability engineering of the *V. paradoxus* ω -TA

(50, 55, 60 and 65°C) in buffer solution for 20 min. After incubation, samples of the variants were retrieved and the activities were determined at 40°C with *rac*- β -PA as substrate.

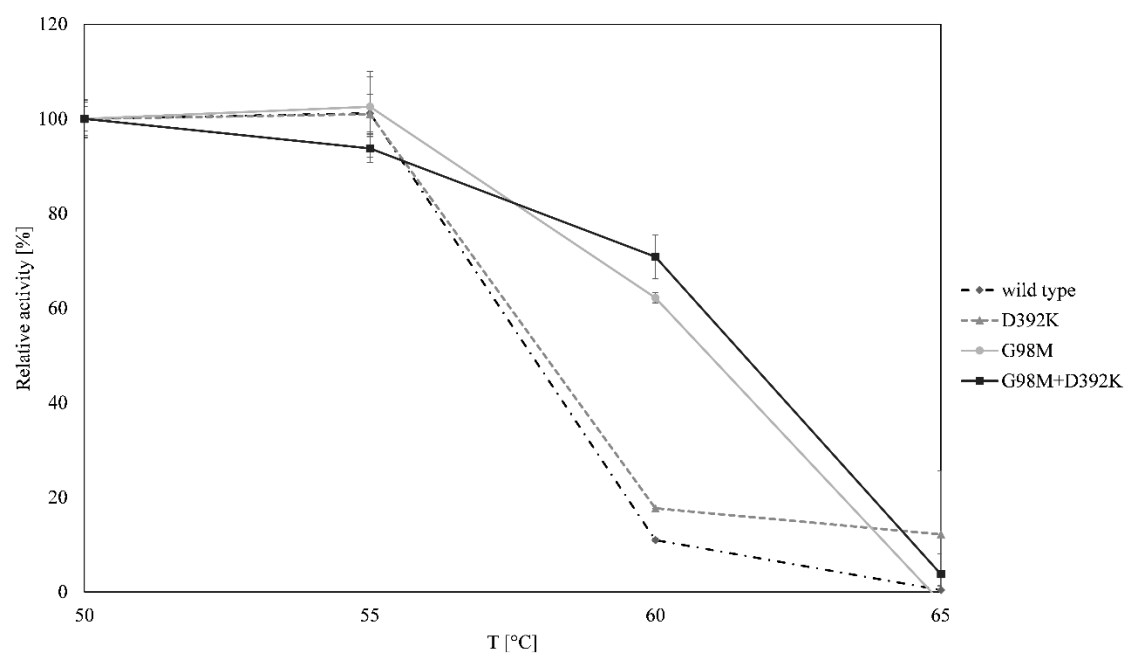


Figure 4.5 Enzyme activity of the best ω -TA variants and the wild type after preincubation at 50, 55, 60 and 65°C. 4 μ M of the purified enzyme variants were preincubated for 20 min and the subsequently employed to convert *rac*- β -PA at 40°C.

In accordance to the data from the determination of T_m (**Table 4.6**), the preincubation activity test showed that the wild type rapidly loses activity at temperatures above 55 °C. However, at this temperature the variants G98M and the double mutant G98M D392K retained a relative enzymatic activity of 62 % and 70 % respectively, as is reflected by the higher T_m of 59.3°C and 59.4°C. The single mutation D392K showed a behavior comparable to the wild type. At 65°C no variant showed any significant remaining activity, which is in agreement with the T_m experiments. Since 55°C has been described as the temperature optimum of ω -VpTA the long-term stability of the wild type and our best mutant G98M at this incubation temperature was investigated (**Figure 4.7**) [161]. While after 30 min at this temperature the remaining activity of the wild type enzyme is only 20 %, our best variant G98M retains 80 % of its activity for 30 min and still shows about 50% of the initial activity after 1.5 h of incubation.

The quite long retention of the activity over the time shows that the mutation site G98M is very beneficial for the stability of the enzyme. The improvement of $\Delta\Delta G$ calculated based on T_m (ΔT_m of 4°C) measurements was ~ 15 kcal mol⁻¹ [176]. In contrast calculations using PoPMuSiCv3.1 resulting in a $\Delta\Delta G$ of only -0.3 kcal mol⁻¹ [181]. Additionally HoTMuSiC was used for calculation resulting in a predicted neutral stability-change (ΔT_m -0.08 °C) [182]. This

would allow reactions at 55°C with higher total turnovers of β -PA without decrease of optimum activity. By contrast the only known thermostable β -PA converting ω -TA from *Sphaerobacter thermophiles* shows higher stability up to even 60°C, but a more than 80 % lower activity of 3.3 U mg⁻¹ at 37°C and no absolute activity was given for 60°C [153]. It is also worth mentioning that the variant G98M has a pH dependency of its activity comparable to the wild type enzyme (**Figure 4.6**). In accordance with Crismaru *et al.* we could determine a broad pH activity of ω -VpTA from pH 5 to pH 9 but not above pH 9 [161].

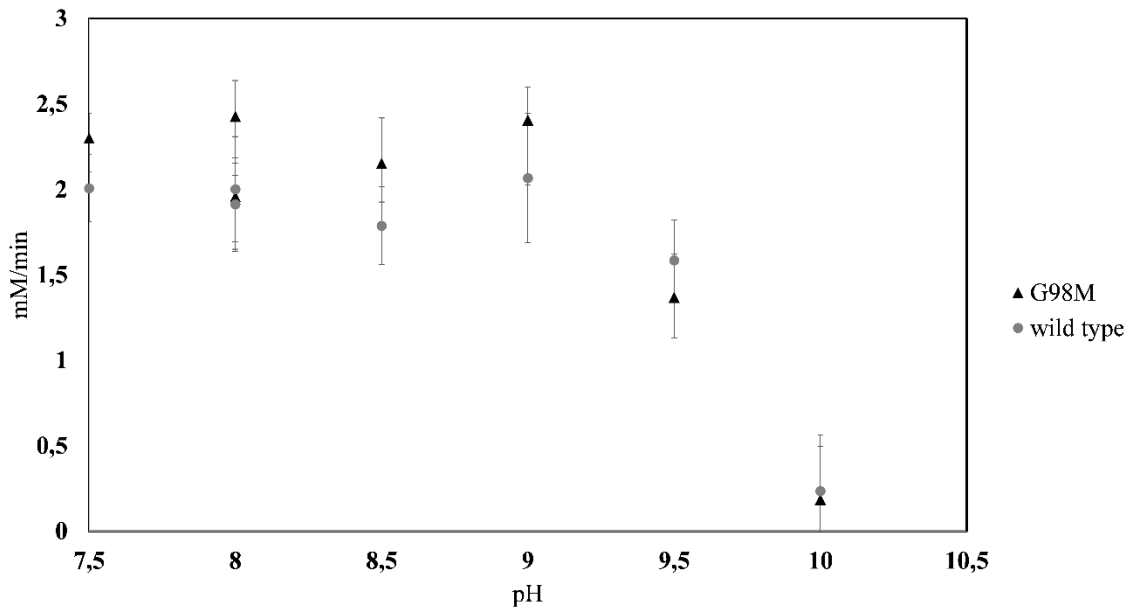


Figure 4.6 pH-dependent activity profile of the wild type ω -VpTA and G98M. The activity is described as mM min⁻¹ towards conversion of (*S*)- β -PA. For pH 7.5 and pH 8.0 40 mM sodium phosphate was used. From pH 8.0 to pH 10 40 mM TRIS buffer was used. pH 8 was measured in TRIS as well as sodium phosphate buffer.

Wild type and G98M are constantly active between pH 7.5 and pH 9.0. At pH 9.5 the activity is reduced around 40 % and at pH 10 both showing only activity within the limits of standard error. Furthermore, the size of the standard error did not allow a statement, whether wild type or G98M is more active at higher pH-levels. In general most ω -TA are described for activity in slightly alkaline medium (pH 7.0 to 9.0) [153,161,183,184], this might be reasoned by the properties of the amino-moiety. The amino-moiety is normally protonated under neutral or acidic conditions, but the higher the pH, the less amino-moieties are protonated, which could have an influence on the reaction between PLP and amino donor. For example L-alanine shows a pK_a-value of the amino group of 9.87 [185].

4) Thermostability engineering of the *V. paradoxus* ω -TA

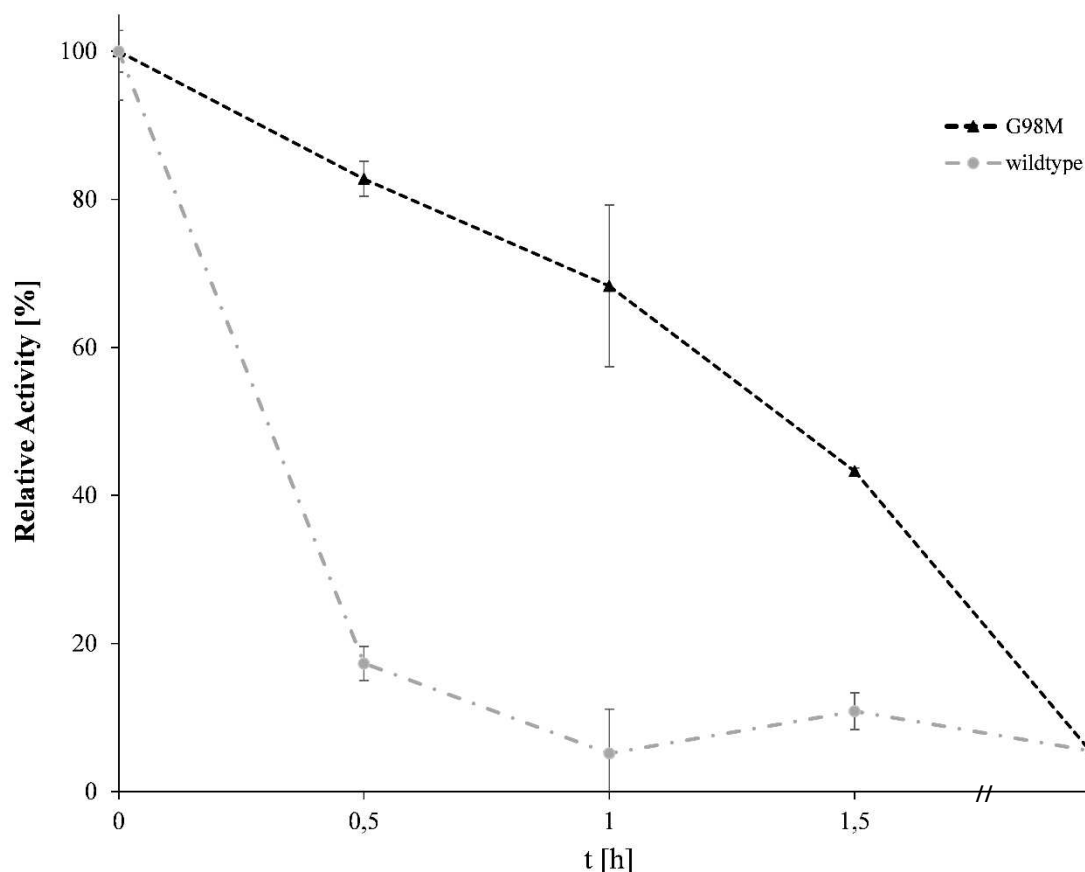


Figure 4.7 Time-activity correlation for the analysis of enzyme stability over a period of time. The ω -VpTA wild type was compared to G98M. The reaction was carried out with 15 mM of *rac*- β -PA and 15 mM α -ketoglutarate as substrates at 40°C. 4 μ M of enzyme solution was incubated in a PCR cycler to prevent condensation of water at the reaction tube lid and incubated in 40 mM sodium phosphate at pH 7.2 for a defined time.

Furthermore, the solvent stability is also an important aim of stabilization. The thermostabilization can also increase the enzyme stability in solvents, which could not be proofed with certainty by the demonstrated experiments, but it was shown the first time that the ω -VpTA is active also above 40% of DMSO. The activity of mutant and wild type showed to be equivalent to each other at every DMSO content, but with a slight tendency to higher activities for G98M (**Figure 4.8**). The co-solvent is important for increasing the solubility of many hydrophobic substrates.

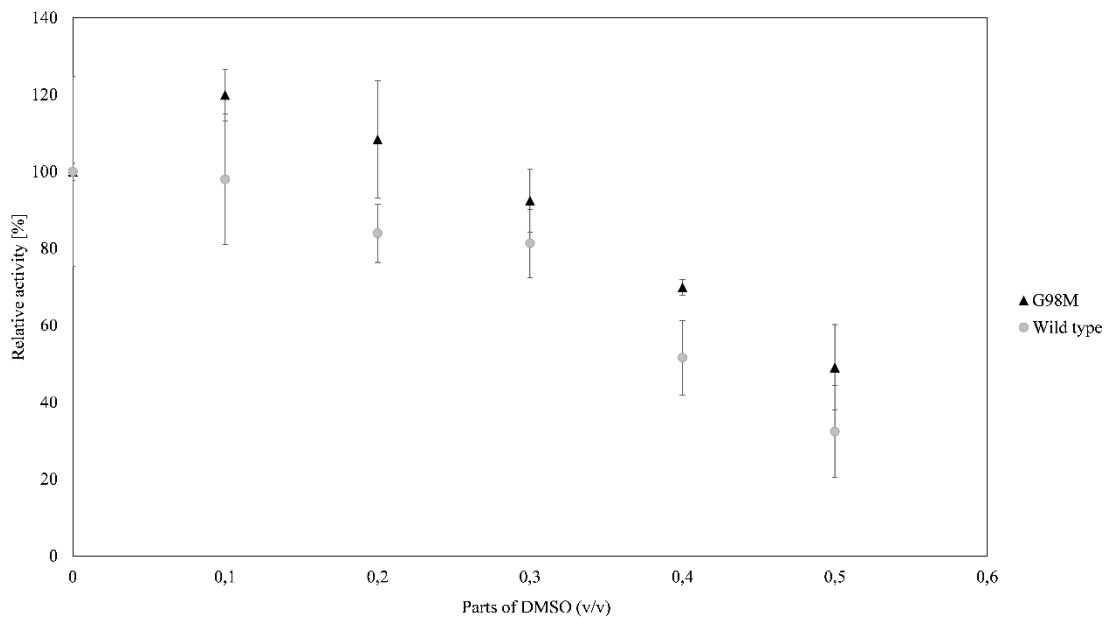


Figure 4.8 Dependence of enzyme activity on DMSO content in the reaction batch. DMSO is a general enzyme compatible solvent and can be mixed with water. For this the 2.5 μ M of ω -VpTA wild type and of G98M were compared. The reaction was carried out as mentioned before at 40°C.

The solubility of aromatic amino acids is also a function of the temperature and the higher solvent concentrations and higher DMSO concentrations allows to solve higher amounts of substrate, which is important to yield higher space time yields [186,187]. According to synthesis strategy for β -PA from 3-oxo-3-phenylpropanoic esters (oPP), by cascade reactions, a higher solubility of the substrate would be highly recommended because of the low solubility of oPP (~ 2 mM) in buffer [188]. The instable intermediate, have to converted very fast, because it shows a high decarboxylation rate [189,190].

In summary, it was clearly demonstrated that FoldX calculations can minimize experimental effort for directed mutagenesis experiments, especially when no suitable high throughput screening assay is available. On the other hand, it is known that FoldX libraries contain many predicted sites which even destabilize proteins or have no influence on stability [191]. To enhance the prospects of FoldX, Komor *et al.* performed their predictions using a sophisticated approach to gain a consensus sequence by comparisons of calculations with closely related enzymes to increase the stability [192]. Using this strategy, the thermostability was increased for the fungal cellobiohydrolase I by 2.1°C via single mutation and the authors could show that 24 % of their selected FoldX predictions were stabilizing [192]. We also found that

4) Thermostability engineering of the *V. paradoxus* ω -TA

approximately 20 % of the predicted mutant proteins, which were expressed, resulted in a stabilization. The quality of FoldX is further discussed in chapter 4.1

Our best $\Delta\Delta G$ prediction, G165M, showed a 3.3 fold reduced enzymatic activity and an only slight improvement of the T_m , stressing the importance of experimental evaluation of the theoretical data. For this specific mutation the distance to the catalytically active K267 is 13.5 Å, but only 5.0 Å to Y159. Y159 is important for the coordination of the cofactor PLP at the active site and can be found in many (*S*)-selective ω -TAs at the same position at amino acid residue ~150 [144,148,161,193]. Such important sides are not automatically excluded by FoldX and have to be selected manually. Mentioned in chapter 4.1, the low correlation of $\Delta\Delta G_{\text{FoldX}}$ to $\Delta\Delta G_{\text{Real}}$ is known for FoldX, which can be seen at the example of the two mutation sites G165M and for E391K which showing both a large discrepancy between prediction and experimental measurement. The results of these experiments conform, that FoldX is able to predict stability trends, but not with high precision. More particularly, FoldX seems to be unable to predict accurately high $\Delta\Delta G$ -values, but this might be also a result of low crystal-structure qualities [78,123,126,134,135]. Also it should be mentioned that the general standard error FoldX is known to be only between 1.0 and 1.7 kcal mol⁻¹, which is compared to high theoretical $\Delta\Delta G$ of G165M and E391K very low [127]. Additionally a conservation analysis should be performed to avoid nonfunctional proteins by excluding highly conserved amino acid positions. Also other algorithm might be utilized like FireProt or Rosetta-ddG (see **chapter 4.1**).

Our best variant, G98M, is located close to the only point of symmetry of the dimer (position 92) at the end of an α -helix, which is oriented parallel to the same α -helix in chain B. The protein Interface allows stabilization by interaction with other monomers or ligands, which can also stabilize, the own protein stability. For the activity of ω -TA, the interface is quite important, because relevant amino acid residues, for coordination of PLP or substrate, are from a second monomer [149,194,195]. The interaction between two subunits is often mediated by hydrophobic interactions [196–198]. As an example, the exchange of glycine towards methionine might be support such hydrophobic interactions directly or indirectly. Furthermore the side chain of M98 is known to interact with oxygen atoms. This can be explained by the weak dipole of M, which makes M at the same time an acceptor for hydrogen bonds. M is also known for hydrophobic interaction with residues at short distances [199]. The distance of interaction with non-hydroxyl oxygen atoms is often within 4.0 Å. Also well-known are interactions of the sulfur atom with aromatic amino acids at a very similar distance range of 3.6

Å [200]. To identify possible points of interaction of the G98M mutation and gain insight into the structural reasons for the thermostabilization, we calculated the rotamers of M98 based on the 4AOA structure and assessed the distances to the neighboring amino acids rotamers with the highest probability in an area of 6.5 Å (**Figure 4.9**). In this range no aromatic residue can be found, excluding the stabilization via this interaction. Only the oxygen containing E94 is in a short distance of 5.8 Å and this might lead to the formation of a hydrogen bond between E94 and M98 [200]. The chain B residue R55 is in a distance of 5.7 Å. The closest neighboring amino acid would be A54 (chain B) with 3.7 Å. In addition, a hydrophobic interaction with residues around M98 (magenta colored) would be possible.

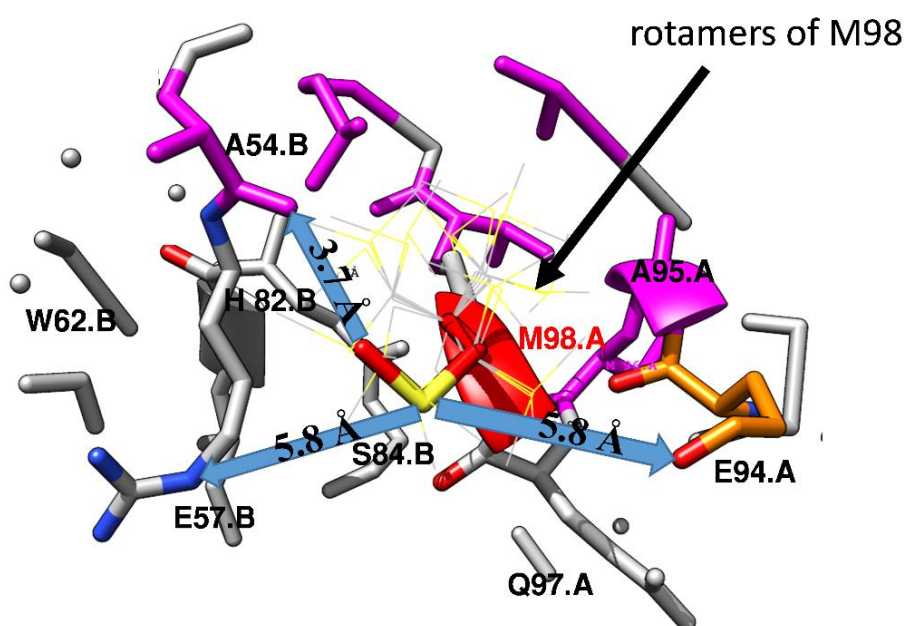


Figure 4.9 The mutation site M98 is oriented towards residue A54. The conformation of the rotamers of G98M were predicted and visualized with Chimera 1.1 [177]. Only the most likely ones (probability > 0.2) are displayed as green-yellow sticks. The most likely one is showed in red. The interacting E94 is showed in orange and R55 in blue-grey. In general hydrophobic residues are colored magenta and charged residues are orange.

To further elucidate the molecular basis for the stabilization of ω -VpTA, a molecular dynamic simulation was performed using the structure 4AOA of the wild type enzyme. One measure for the macromolecular flexibility and movement of amino acid residues is the root-mean-square fluctuation (RMSF)-value, which is a very sensitive parameter for comparison of distance of the atom positions during a trajectory [201]. Low RMSF-values means rigid parts of the protein, high values stands for flexible parts. According to the calculated RMSF-values G98M is

4) Thermostability engineering of the *V. paradoxus* ω -TA

positioned in an environment which seems to be a highly flexible part of the enzyme (**Figure 4.10**). Also the mutation site G165M, which was the best FoldX energy hit, is a highly flexible residue in the simulation. Flexible residues as target for potential stabilizing mutations are a promising approach which has been evaluated by several groups [191,201]. According to the Wood-barrel theory, these residues are more important for stability than residues in rigid parts of the protein [202]. One approach to describe flexible residues is the B-factor, also known as Debye–Waller factor, represents the thermal motion of the atoms or residues within a protein structure and is determined by X-ray scattering of the protein crystals[203,204]. Huang *et al.* pre-selected mutation sites for an enzyme stabilization, guided by the B-factor as a parameter for the dynamic mobility of parts of the enzyme and identifying one single mutation with an T_m improvement of 5°C.

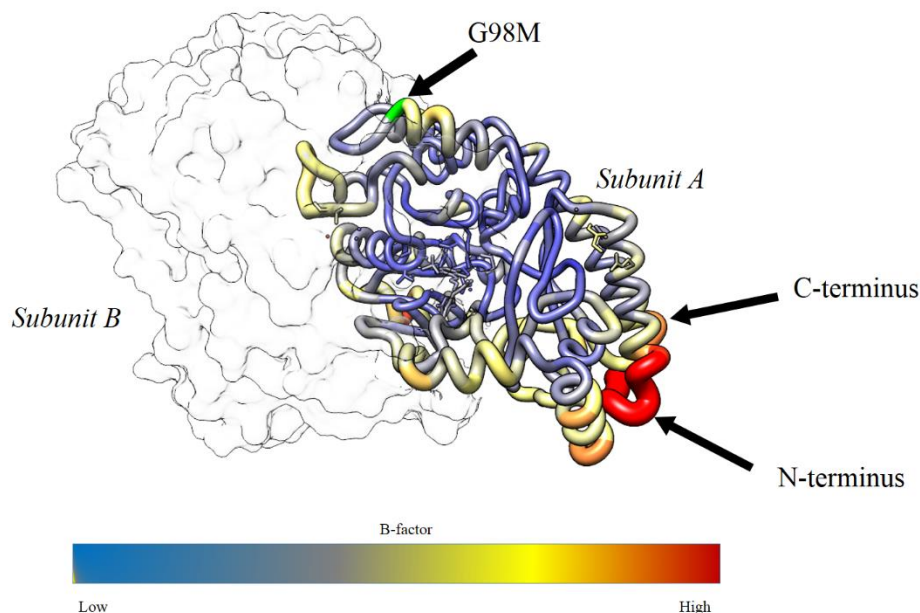


Figure 4.10 B-Factor as measure for movement of 4AOA. The mutated residue G98M is located at the interface between subunit A and B. Subunit B is displayed with a transparent surface. High flexibility (High-B factor value) is colored in red, blue represents rigid parts of the protein.

Additionally they selected some sites with minor improvements. The prediction success rate for the (*R*)-selective ω -TA from *Aspergillus terreus* was 21 % and a control experiment without pre-selection was missing, but only the comparison could show if the pre-selection can lead to an more robust approach [152]. The B-factor of crystal structures might be an interesting indicator to detect regions within the protein with higher flexibility, but for the pre-selection of mutations it has to be taken into account that flexibility can also be important for the activity of an enzyme as in case of substrate induced conformational changes or surface activations. In the case of the VpTA, MD-calculation clearly show, that the stabilizing position G98 and the non-

beneficial position G165 are both located at highly flexible parts within the amino acid sequence. An MD-simulation can predict further flexible parts, which are not shown by B-factor[191]. In the present study, no clear correlation between B-factor and energy stabilizing mutation was observed, because G98M is according to the B-factor a structure part with low flexibility. Only the N- and C- terminus of the ω -TA showing a high structural variation, which is known for many other proteins [205]. However, the α -helix next to G98M seems to be slightly more flexible than other residues and structural elements. For that reason G98M might function as structural element, which is stabilizing the following α -helix and lowers the flexibility of the loop in front of the α -helix. This could therefore have a global impact on protein instability. The RMSF-plot shows, that globally a change in flexibility can be observed, which might be a result of stabilization of only one-structural part of the protein (**Figure 4.11**).

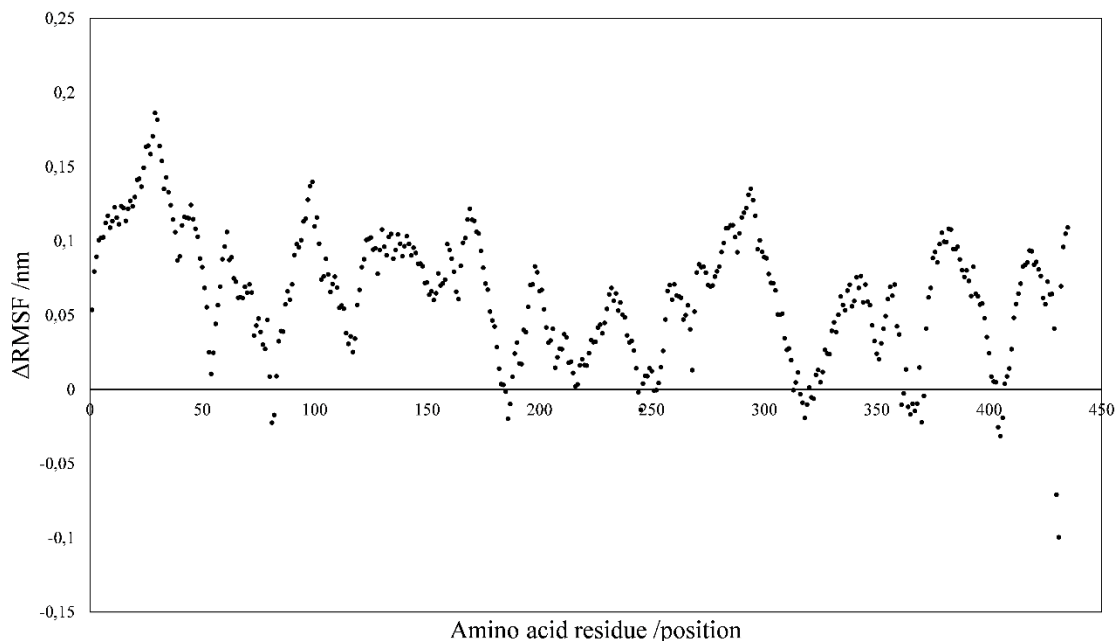


Figure 4.11 Difference of amino acid residue flexibility of WT compared to G98M at 333 K (59.85 °C) using dimeric MD-simulation over 100 ns. The simulation was performed in sodium phosphate solution at neutral pH. The amino acid position are shown for one monomer (PDB 4AOA). The positive difference of RMSF is a hint that the variant is globally more rigid than the wild type enzyme. ($\Delta\text{RMSF} = \text{RMSF}_{\text{wildtype}} - \text{RMSF}_{\text{G98M}}$)(see also **Figure S3**)

FoldX predicted mutations, which were predicted to have a large energy benefit, but which were showing only slightly or no energy benefit, can be found in areas with a low flexibility of 0.15 nm. The theory that a pre-selection by RMSF-calculation or by comparison to B-factor is highly recommended and should be further investigated.

4) Thermostability engineering of the *V. paradoxus* ω -TA

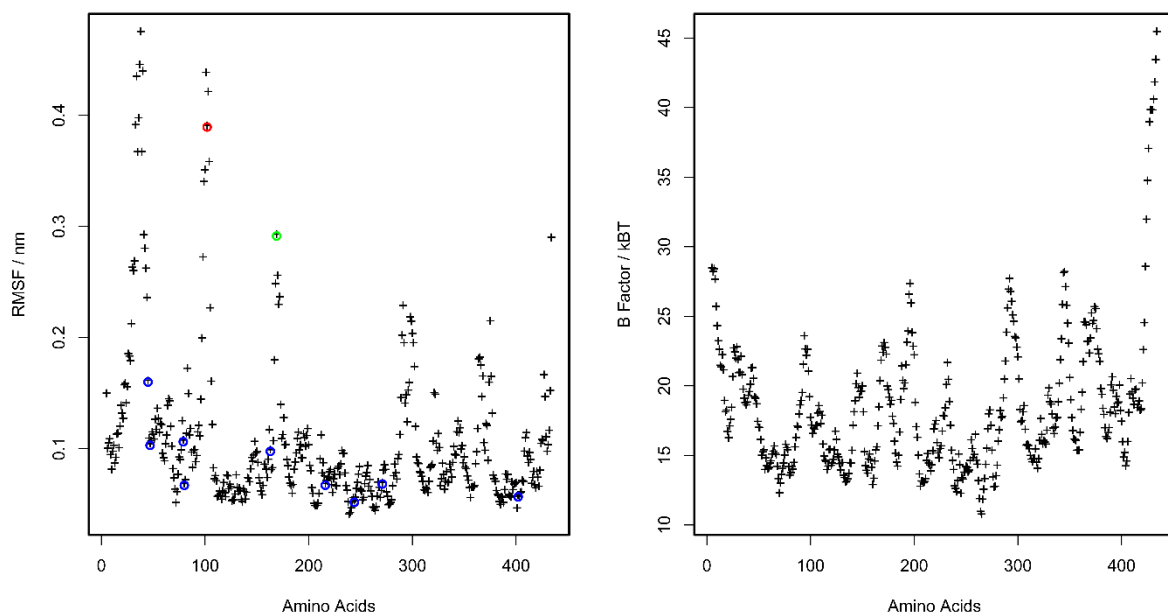


Figure 4.12. Monomeric MD-simulation of ω -VpTA to show regions with high flexibility as compared to the B-Factor. (Left) MD-simulation for the monomer. (Right) B-factor of crystal structure for one monomer (according to PDB ID: 4AOA [161]). The red and green circles highlight the residues G98 and G165 respectively. Blue circles indicate the mutated residues with low impact on thermostability according to the experimental data.

For example the FoldX predicted mutation E391K, which showed a decrease of the T_m , is even in a very rigid region with an RMSF value under 0.1 nm (**Figure 4.12**), which shows that FoldX predictions do not correlate necessarily with flexibility. G98M is situated in a region at the monomer-monomer interface, which is showing a high flexibility and is at the same time a FoldX predicted site for energy improvement. Since the monomer-monomer interaction is crucial for the enzymes' activity but cannot be calculated easily, a mutation at this site might give rise to an additional benefit in the binding energy.

However, the stability improvement might also be caused by a global effect on the protein flexibility, changing the fluctuation of the whole protein. To investigate such an effect we performed MD-simulations based on the dimeric protein and compared the global flexibility of the wildtype and the G98M variant.

The simulation showed clearly, that the global flexibility of the whole protein, shown as Δ RMSF (wild type to G98M) value for each position, was reduced, when glycine 98 was exchanged to methionine, especially when the temperature was increased to 333K (59.85°C).

At this temperature the wild type enzyme starts to unfold and the mutant retains folded. All the effects described here can contribute to the observed gain in thermostability.

This demonstrates that the prediction and explanation of (de)stabilization effects is multi-dimensional and can be explained using many approaches. The interactions of amino acid residues can be explained by direct physical interactions with other residues at the short distance, but changes in stability could also be derived from a global context, which cannot be predicted using FoldX calculations. However, since FoldX cannot generate covalent bonds that can cause major changes in protein instability, disulfide-bonding engineering was also carried out as an alternative approach.

4.2.6) Disulfide bond engineering

Disulfide bridges as stabilizing covalent bonds have long been known as enzyme engineering object of proteins. Crosslinking via disulfide bonds makes proteins and enzymes more resistant against environmental and destructive forces [206]. Therefore molecular dynamic simulations of 100 ns were performed of ω -VpTA and residues with high contact probability were selected (**Figure 4.13**). The most of all amino acid residues showing no contact-probabilities towards far-away neighbors (more than 7 amino acid positions).

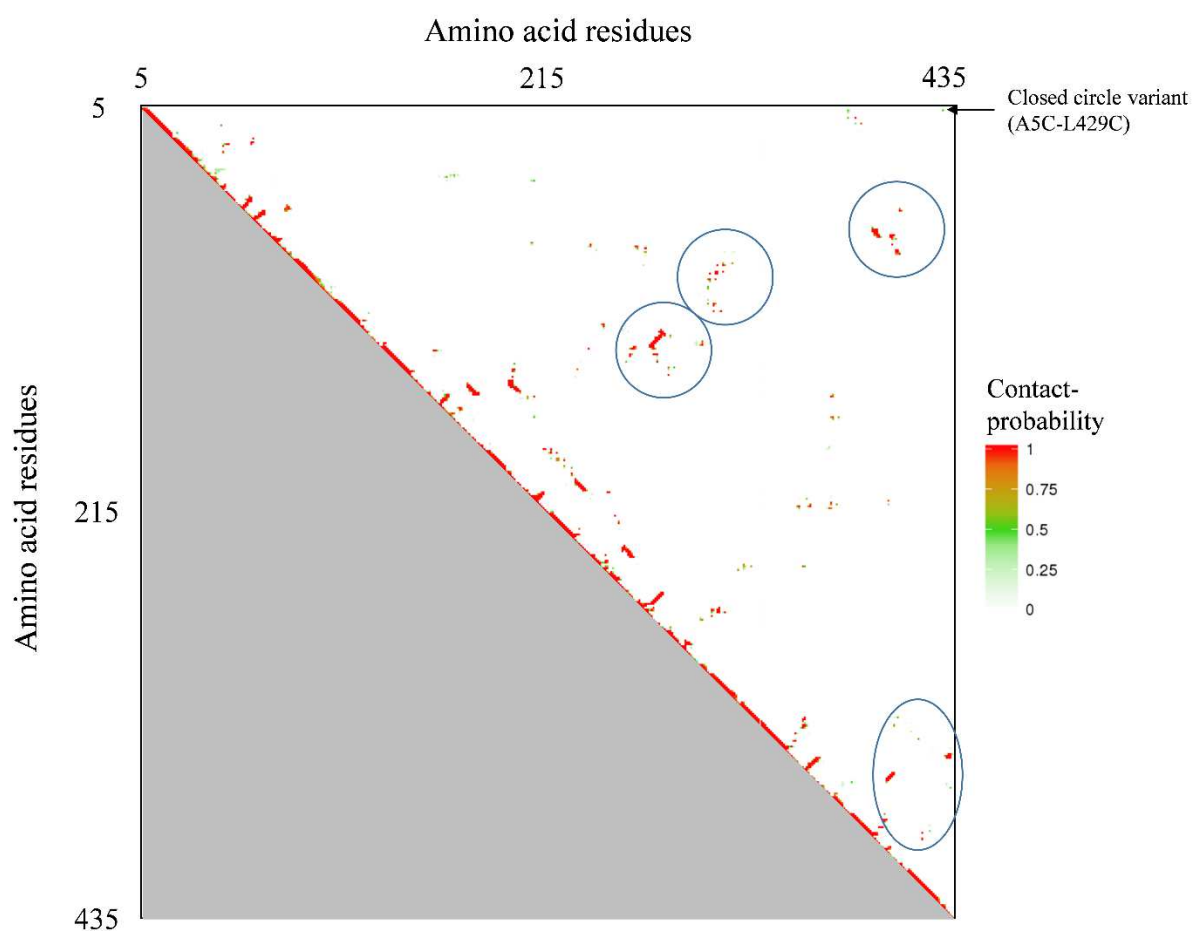


Figure 4.13 Contact probabilities within the ω -TA dimer subunit. Red-pixel means high contact probability, for this reason the diagonal is mainly red (contact residues to itself or to direct neighbors). Green means a probability of 0.5 (only a few interactions). Sites which are not directly adjacent and have at least a probability > 0.5 were selected for directed mutagenesis. In circles hot spots for contact are highlighted. In circles hot spots for contact are highlighted.

This is expected, because only direct neighboring amino acid residues getting mainly in contact. For disulfide bridges between secondary structures are amino acid residues from interest, which are separated by at least 7 amino acid positions. Furthermore these sites were ranked according to evolutionary allowed exchanges using multiple sequence alignments. In total seven sites

were selected for mutagenesis experiments (**Figure 4.15**). Furthermore also an amino acid with intermolecular contact was chosen, namely D92 and in addition also D90 next to it was selected. Interestingly D90 is naturally exchanged against cysteine in the protein sequence of *Sinorhizobium medicae/meliloti* (WP_024312421 and UniProt ID A0A222GPX9). Therefore this site could be a point with high probability for a natural occurring disulfide bond. The gene is recommended for Fold type I aspartate aminotransferase family protein (or as glutamate-1-semialdehyde 2,1-aminomutase) with high sequence identity towards *V. paradoxus* ω -TAs (> 50%) and is therefore a promising approach for site directed mutagenesis. In general the distances between the backbone's α -atoms were between 6.6 and 9.7 Å (static) and during the simulation in the range up to 9 Å. This is also the distance between naturally occurring cysteine residues of disulfide bonds in the reduced state [207,208]. The distance between the terminal atoms (sulfur atom) should be around 2 to 3 Å for formation of a disulfide bond [209]. However, the positions of amino acid residues are generally not static at room temperatures and the whole enzyme is in motion (like shown in **Figure 4.13** and **4.14**), especially secondary structures are moving, which could be observed during MD-simulations.

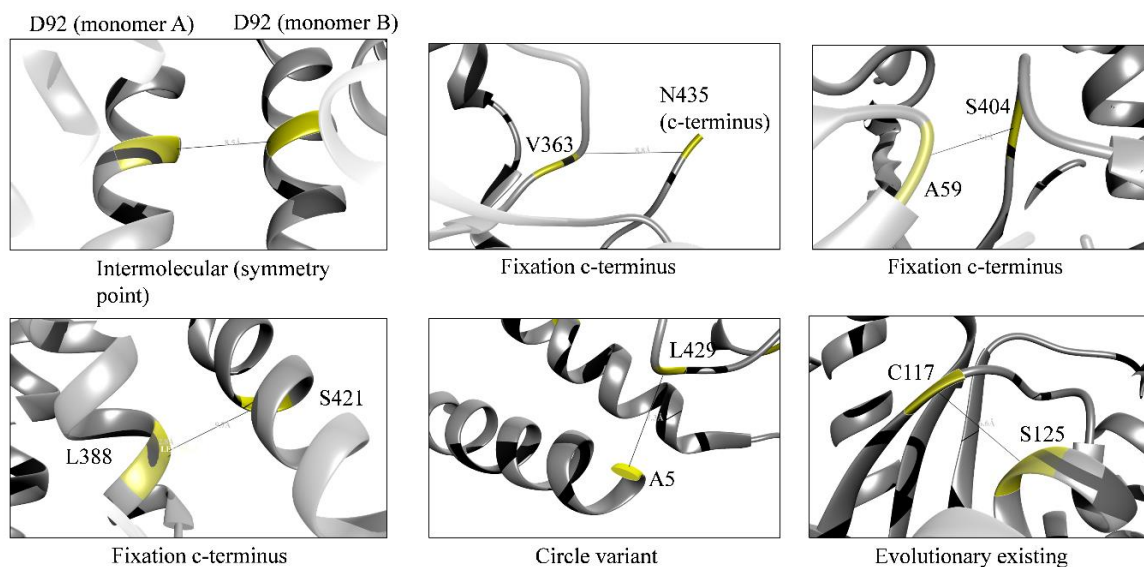


Figure 4.14 Putative sites for disulfide bridge engineering. These sites were determined according to evolutionary existing exchanges and according to their contact probability during MD-simulations over 100 ns. The shown sites were successfully expressed and tested according to their melting point.

The mutations selected mainly on the basis of the simulation, with the exception of D90, were all successfully mutated (**Table 4.5**). Using different DNA-oligomers and PCR mutagenesis strategies did not result in a successful amino acid exchange at position 90. Furthermore beside general problems of mutated proteins i.e. loss of stability, solubility and functionality, the

protein expression of disulfide bridges containing proteins is challenging, because most expression strains like *E. coli* BL21 do not show oxidizing conditions within their cytoplasm. For this reason the expression was not only performed in standard *E. coli* BL21 but also in *E. coli* SHuffle strain which shows oxidative conditions within its cytoplasm. *E. coli* Shuffle (USA, NEB), original K12-strain, is able to form disulfide bridges within heterologously expressed proteins, because an important protein (trxB gor) in the cytoplasmic reductive pathways is suppressed. Furthermore this strain contains a disulfide bond isomerase, which supports the formation of disulfide bonds [210]. The authors of this study also recommend to utilize autoinduction for protein expression, which has been done for protein expressions. In contrast as an alternative also the *E. coli* strain Origami B (DE) (Germany, Merck-Millpore) was tested. This strain is a mutant of BL21, which is recommended for expression of eukaryotic protein as well as proteins with disulfide bonds but showed no expression at all.

Table 4.7 Disulfide-bridge engineering. The variants were expressed in *E. coli* BL21. Shown in brackets after several months' incubation at -80°C. The expression was conducted in auto induction LB-medium at 37°C for 6 h, followed by 20°C for 20 h. Melting points were determined using 5 μ M of protein.

Variant	Expression	Distance between bridge α -C-atoms (backbone)	Activity	Stability change	T _m [°C]
A59C + S404C	Successful	7.1 Å	Yes	No improvement	55
D90C	No (mutagenesis failed)	-	-	-	-
D92C	Successful	8.5 Å	Yes	no improvement (After 8 months at -80°C, also no changes)	54.5 (55°C, 68 °C)
L388C + S421C	Successful	9.7 Å	No	Strong precipitation	-
V363C + 435C	Successful	8.8 Å	No	Slow precipitation	55
C117 + S125C	Successful	6.6 Å	Yes	Loses PLP binding capacity	54.5
A5C + L429C	Successful	7.3 Å	Yes	no improvement (after 8 months at -80°C improvement)	55 (58°C, 68°C)

The in *E. coli* BL21 expressed disulfide variants showed no improvement according to their melting point. The second tested expression host, *E. coli* SHuffel, produced generally less ω -TA than BL21. Furthermore the temperature of the expression culture had to be reduced at the beginning (lag-phase and beginning of log-phase) from 37°C to 30°C, followed by 20 h of incubation at 20°C. The expressed variants L388C +S421C and V363C + N435C showed reduced solubility and were sensitive towards low temperatures (> -20 °C). Especially when they were expressed inside the less reductive *E. coli* Strain SHuffle, they showed drastically reduced stability in sodium phosphate buffer. However, a general disadvantage of this strain was the reduced yield of expressed protein compared to BL21. Therefore the purity was reduced, because the ratio of *E. coli* host proteins to target protein was increased (**Figure 4.16**).

Formation of disulfide bridges at -80°C ?

The tested variants did not show any improvement in protein stability compared to the wild-type. Surprisingly two variants, expressed in BL21, showed a shifted and a second melting point after incubation at -80°C in 25 % glycerol for 8 months. The second melting point was 10 °C higher than known for the wild type (see **Table 4.7**). It is generally known that glycerol increases the stability of proteins, and therefore the variants were compared to the purified wild type ω -TA, which was incubated also in 25 % (v/v) of glycerol for at least 8 months. The final concentration of glycerol was 5 % (v/v) for all samples. The measurements, which were performed in this mixture showed a melting point of 58°C (for wild type), which is 3°C higher than known for tests without glycerol. Therefore glycerol might be the reason for the shift of the first melting point but the resulting second melting point of the disulfide variants might be caused by a different folding state of the ω -TA as well as a result of formed disulfide bridges. A deeper analysis of the reason for the change in the melting point during storage was not carried out. Since the storage time for a repetition of the experiment was too long.

***E. coli* SHuffle expression of disulfide bridge variants**

However, the successful expression of ω -VpTA variants in *E. coli* SHuffle resulted in hardly predictable melting curves with many local minima. The purification and expression was shown by SDS-PAGE (**Figure 4.15**).

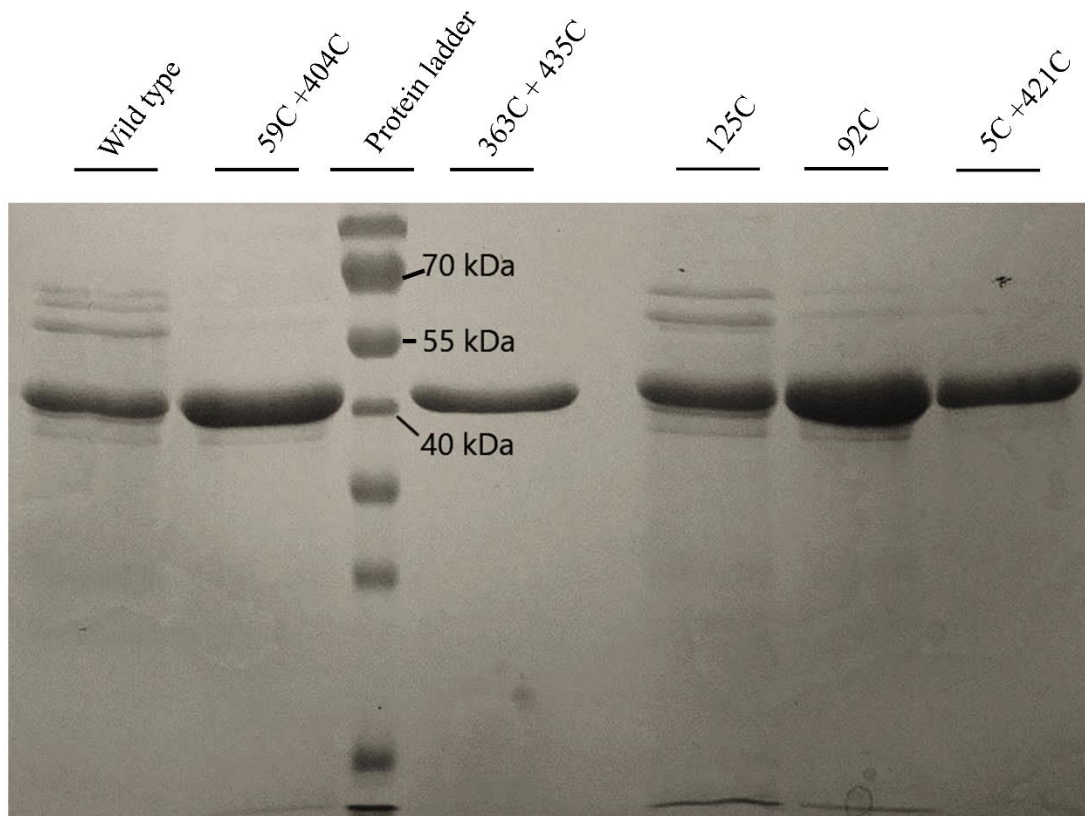


Figure 4.15 Purification of disulfide mutants of ω -VpTA. The variants were expressed in *E. coli* SHuffle and purified using Ni-NTA chromatography. The gel-picture was captured by Peter Klausmann [211].

The variants 5C+429C and 125C showed clear melting curves (only one minimum), but without a hint for an increase of thermostability. On the contrary, they even showed a deterioration of the melting point (53.5 °C). The variants 59C and 404C showed in contrast no clear T_m points. Moreover the derivation of the melting curve function showed several minima and therefore no determination of a single T_m was possible (**Figure 4.16**).

4) Thermostability engineering of the V. paradoxus ω -TA

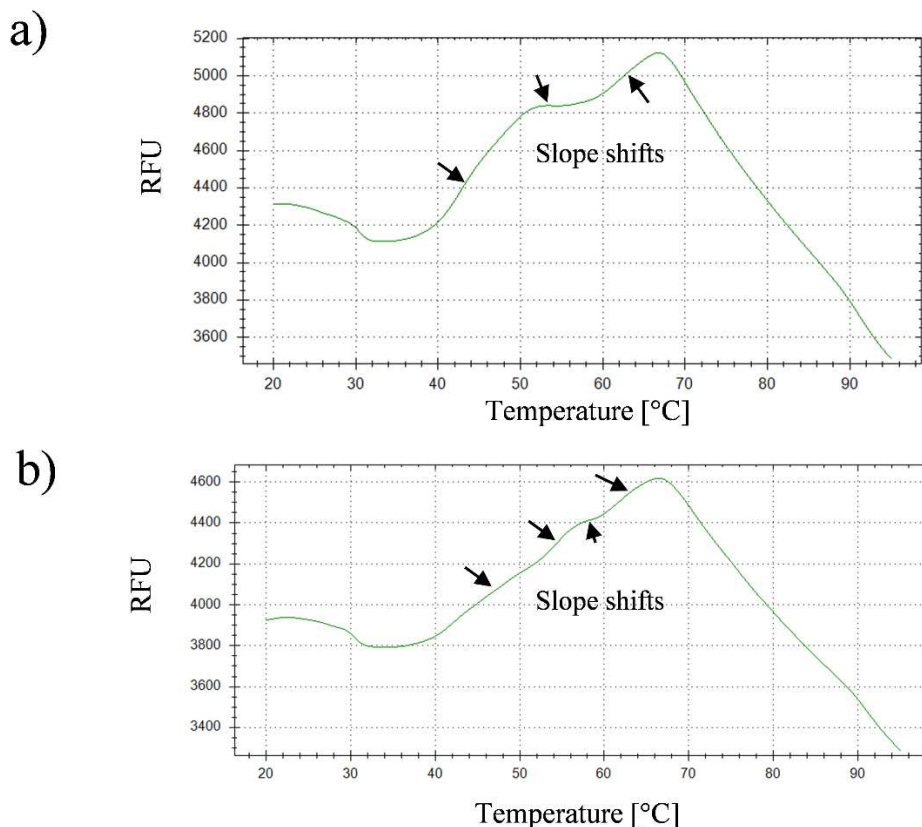


Figure 4.16 Melting curves of different disulfide engineering variants. The second derivation of the curves did not show one clear turning point, in contrast more than one maximum can be determined for the slope. Therefore T_m could not be determined. a) 59+404 b) 92. In appendix **Figure S4** unequivocal curves for 125C and 5C+429C are showed as contrast example. Different turning points can be a result of protein contaminations or of different folding states of the ω -TA.

This can also be a hint, that different energy states of the enzyme are present. However, protein precipitations were observed at high protein concentrations and at lower temperatures. This might be an additional hint for disulfide bridges, which, conversely, could have reduced the solubility of the protein. Therefore it cannot be ruled out that disulfide bonds may have formed. The protein stability determination using thermal shift assay did not prove to be the method of choice for determining whether disulfide bonds were formed.

Furthermore those variants were investigated using SDS-PAGE. The enzyme samples were denatured using non-reducing SDS-sample buffer, without 2-mercaptoethanol, resulting in no clear difference compared to reduced samples. Even at higher contents of polyacrylamide (18%) a shift of the protein bands was not observed, which would be expected when a disulfide bond is present. Summarizing no improvements of protein stability could be clearly shown. Summarizing no improvements of protein stability could be clearly showed.

Whether disulfide bonds form or not can depend on many factors. For example the disulfide forming cysteine residues might be not solvent exposed and oriented towards the core region

of the ω -TA; in this case, an oxidation of the cysteine residues would be less likely. However, the variant 5-429 shows to be surface and solvent exposed at the N and C-terminus of ω -VpTA, but did also not result in a clearly stabilizing disulfide bond. Furthermore a disulfide bond do not have necessarily have to increase the protein melting temperature, even many destabilizing disulfide bonds are reported [212]. Calculations for the (de)stabilization effect of disulfide bridges showed that entropy could be adversely affected and thus paradoxically a disulfide bond within the protein could have a destabilizing effect (Reviewed by [213]). Perhaps a disulfide bridge that have no effect on the structure could change the hydration shell of the protein and could therefore have a negative effect on stability [214]. On the other hand, Matsumura *et al.* suggested that disulfide bridges within rigid proteins might be destabilizing [215]. This corresponds to the theory that a disulfide destabilizes the protein in a region that finally begins to unfold in an unfolding process [216].

Moreover until now no disulfide bonds have been reported within Fold type I ω -VpTA, therefore general ω -TA properties might be able to avoid the formation of disulfide bonds (So far, there are no theories on this). In contrast, for Fold type IV ω -TA Xie *et al.* reported the engineering of stabilizing disulfide bonds within *Aspergillus terreus* ω -TA. The most stabilizing disulfide bond was located at the surface of the ω -TA and resulted in an increase of 5.5 °C at T_{50}^{10} (temperature at which 50 % of the activity is remained after 10 min of incubation) [217]. Moreover their MD-simulations could not confirm a great change in flexibility and stability of the investigated mutant compared to the wild type enzyme. Furthermore they utilized only *E. coli* BL21 for expression of disulfide mutants, which is not recommended for expression of disulfide bond consisting proteins. Furthermore, Xie showed no further evidence that a disulfide bridge was actually present. Therefore it might be possible, that the resulting variants are only proteins with improvement refolding capabilities at T_{50}^{10} .

4.4) Conclusion

In this work a ω -VpTA variant with an improved T_m of $\Delta 4^\circ\text{C}$ was created by FoldX and site directed mutagenesis. The FoldX predicted improvement of $-34 \text{ kcal mol}^{-1}$ $\Delta\Delta G^{\text{unfold}}$ was considerably lower than for the experimentally determined $\Delta\Delta G^{\text{unfold}}$ of $-15 \text{ kcal mol}^{-1}$ for the single site mutant G98M. This also shows that FoldX does not calculate the true energies, but only determines them on an arbitrary scale that only applies to the comparison of FoldX energy units. (within one calculation setup). However, the best ω -VpTA variant showed a similar activity compared to the wild type enzyme, but had an at least 3 fold increase half-life time at the reaction temperature optimum of 55°C. The variant G98M can thus be used as starting point

4) Thermostability engineering of the *V. paradoxus* ω -TA

for further random mutagenesis experiments and for screening towards new substrate specificities. For these reasons, this variant could be used as a more efficient enzyme for chiral resolution of *rac*- β -PA (improved long-term stability). In contrast, disulfide bridge engineering was not successful and it could not be established as a supplement method, but further activity tests and long-term incubation tests could show whether disulfide bridges were actually formed.

In future experiments the possibilities of more sophisticated computational approaches should be investigated to generate small smart enzyme libraries for the generation of thermostable enzymatically active proteins. However, the data presented here as well as in other studies emphatically underline the need for experimental confirmation of the bioinformatics-predictions. Computer-aided predictions are already a useful tool, but new techniques such as deep-machine learning could improve the chances of success of these methods

4.5) References chapter 4

1. Newman JD, Turner APF. Home blood glucose biosensors: A commercial perspective. *Biosensors and Bioelectronics*. Elsevier; 2005. pp. 2435–2453. doi:10.1016/j.bios.2004.11.012
2. Capdevila J, Elez E, Macarulla T, Ramos FJ, Ruiz-Echarri M, Taberero J. Anti-epidermal growth factor receptor monoclonal antibodies in cancer treatment. *Cancer Treatment Reviews*. W.B. Saunders; 2009. pp. 354–363. doi:10.1016/j.ctrv.2009.02.001
3. Bhosale SH, Rao MB, Deshpande V V. Molecular and industrial aspects of glucose isomerase. *Microbiol Rev. American Society for Microbiology*; 1996;60: 280–300.
4. Pollard DJ, Woodley JM. Biocatalysis for pharmaceutical intermediates: the future is now. *Trends Biotechnol.* 2007;25: 66–73. doi:10.1016/j.tibtech.2006.12.005
5. Mittal S, Kaur H, Gautam N, Mantha AK. Biosensors for breast cancer diagnosis: A review of bioreceptors, biotransducers and signal amplification strategies. *Biosens Bioelectron*. Elsevier; 2017;88: 217–231. doi:10.1016/j.bios.2016.08.028
6. Yoo E-H, Lee S-Y. Glucose Biosensors: An Overview of Use in Clinical Practice. *Sensors. Molecular Diversity Preservation International*; 2010;10: 4558–4576. doi:10.3390/s100504558
7. Sin ML, Mach KE, Wong PK, Liao JC. Advances and challenges in biosensor-based diagnosis of infectious diseases. *Expert Rev Mol Diagn*. Taylor & Francis; 2014;14: 225–244. doi:10.1586/14737159.2014.888313
8. Willuda J, Honegger A, Waibel R, Schubiger PA, Stahel R, Zangemeister-Wittke U, et al. High Thermal Stability Is Essential for Tumor Targeting of Antibody Fragments. *Cancer Res*. 1999;59.
9. Klein-Marcuschamer D, Oleskowicz-Popiel P, Simmons BA, Blanch HW. The challenge of enzyme cost in the production of lignocellulosic biofuels. *Biotechnol Bioeng*. Wiley Subscription Services, Inc., A Wiley Company; 2012;109: 1083–1087. doi:10.1002/bit.24370
10. Sheldon RA, van Pelt S. Enzyme immobilisation in biocatalysis: why, what and how. *Chem Soc Rev. Royal Society of Chemistry*; 2013;42: 6223–6235. doi:10.1039/C3CS60075K
11. Yazbeck DR, Martinez CA, Hu S, Tao J. Challenges in the development of an efficient enzymatic process in the pharmaceutical industry. *Tetrahedron Asymmetry*. Pergamon; 2004. pp. 2757–2763. doi:10.1016/j.tetasy.2004.07.050
12. Woodley JM. Protein engineering of enzymes for process applications. *Curr Opin Chem Biol*. Elsevier Ltd; 2013;17: 310–316. doi:10.1016/j.cbpa.2013.03.017
13. Salihu A, Alam MZ. Solvent tolerant lipases: A review. *Process Biochemistry*. Elsevier; 2015. pp. 86–96. doi:10.1016/j.procbio.2014.10.019
14. Peterson ME, Daniel RM, Danson MJ, Eisenthal R. The dependence of enzyme activity on temperature: determination and validation of parameters. *Biochem J. Portland Press Ltd*; 2007;402: 331–337. doi:10.1042/BJ20061143
15. Daniel RM, Peterson ME, Danson MJ, Price NC, Kelly SM, Monk CR, et al. The molecular basis of the effect of temperature on enzyme activity. *Biochem J. Portland Press Limited*; 2010;425: 353–360. doi:10.1042/BJ20091254
16. Jones HBL, Wells SA, Prentice EJ, Kwok A, Liang LL, Arcus VL, et al. A complete thermodynamic analysis of enzyme turnover links the free energy landscape to enzyme catalysis. *FEBS J*. 2017;284: 2829–2842. doi:10.1111/febs.14152
17. Reyes BA, Pendergast JS, Yamazaki S. Mammalian Peripheral Circadian Oscillators Are Temperature Compensated. *J Biol Rhythms*. Sage PublicationsSage CA: Los Angeles, CA; 2008;23: 95–98. doi:10.1177/0748730407311855
18. Rejasse B, Maugard T, Legoy MD. Enzymatic procedures for the synthesis of water-soluble retinol derivatives in organic media. *Enzyme Microb Technol*. Elsevier; 2003;32: 312–320. doi:10.1016/S0141-0229(02)00289-2
19. Laidler KJ, Peterman BF. Temperature effects in enzyme kinetics. *Methods Enzymol*. 1979;63: 234–57.
20. Wolfenden R, Snider M, Ridgway C, Miller B. The temperature dependence of enzyme rate enhancements. *Journal of the American Chemical Society*. American Chemical Society; 1999. pp. 7419–7420. doi:10.1021/ja991280p
21. Vieille C, Zeikus GJ. Hyperthermophilic enzymes: sources, uses, and molecular mechanisms for thermostability. *Microbiol Mol Biol Rev. American Society for Microbiology*; 2001;65: 1–43. doi:10.1128/MMBR.65.1.1-43.2001
22. Daniel RM, Danson MJ, Eisenthal R. The temperature optima of enzymes: a new perspective on an old phenomenon. *Trends Biochem Sci*. 2001;26: 223–5.
23. Salazar O, Cirino PC, Arnold FH. Thermostabilization of a Cytochrome P450 Peroxygenase. *ChemBioChem*. WILEY-VCH Verlag; 2003;4: 891–893. doi:10.1002/cbic.200300660
24. Han ZL, Han SY, Zheng SP, Lin Y. Enhancing thermostability of a Rhizomucor miehei lipase by engineering a disulfide bond and displaying on the yeast cell surface. *Appl Microbiol Biotechnol*. 2009;85: 117–126. doi:10.1007/s00253-009-2067-8
25. Takagi H, Takahashi T, Momose H, Inouye M, Maeda Y, Matsuzawa H, et al. Enhancement of the thermostability of subtilisin E by introduction of a disulfide bond engineered on the basis of structural comparison with a thermophilic serine protease. *J Biol Chem*. 1990;265: 6874–6878.
26. Kim J, Grate JW, Wang P. Nanostructures for enzyme stabilization. *Chemical Engineering Science*. Pergamon; 2006. pp. 1017–1026. doi:10.1016/j.ces.2005.05.067
27. Carninci P, Nishiyama Y, Westover a, Itoh M, Nagaoka S, Sasaki N, et al. Thermostabilization and thermoactivation of thermolabile enzymes by trehalose and its application for the synthesis of full length cDNA. *Proc Natl Acad Sci U S A*. 1998;95: 520–4. doi:10.1073/pnas.95.2.520
28. Korkegian A, Black ME, Baker D, Stoddard BL. Computational Thermostabilization of an Enzyme. *Science*. 2005;308: 857–860. doi:10.1126/science.1107387
29. Miyazaki K, Arnold FH. Exploring nonnatural evolutionary pathways by saturation mutagenesis: rapid improvement of protein function. *J Mol Evol*. 1999;49: 716–720. doi:10.1007/PL00006593
30. Miyazaki K, Wintrodde PL, Grayling RA, Rubingh DN, Arnold FH. Directed evolution study of temperature adaptation in a psychrophilic enzyme. *J Mol Biol*. 2000;297: 1015–26. doi:10.1006/jmbi.2000.3612
31. Giver L, Gershenson A, Freskgard PO, Arnold FH. Directed evolution of a thermostable esterase. *Proc Natl Acad Sci U S A*. 1998;95: 12809–13.
32. Karshikoff A, Nilsson L, Ladenstein R. Rigidity versus flexibility: the dilemma of understanding protein thermal stability. *FEBS J*. 2015;282: 3899–3917. doi:10.1111/febs.13343
33. Lee GM, Palsson BO. Immobilization can improve the stability of

4) Thermostability engineering of the *V. paradoxus* ω -TA

- hybridoma antibody productivity in serum-free media. *Biotechnol Bioeng.* Wiley Subscription Services, Inc., A Wiley Company; 1990;36: 1049–1055. doi:10.1002/bit.260361010
34. Radadia AD, Stavis CJ, Carr R, Zeng H, King WP, Carlisle JA, et al. Control of Nanoscale Environment to Improve Stability of Immobilized Proteins on Diamond Surfaces. *Adv Funct Mater.* WILEY-VCH Verlag; 2011;21: 1040–1050. doi:10.1002/adfm.201002251
35. Dold S-M, Cai L, Rudat J. One-step purification and immobilization of a β -amino acid aminotransferase using magnetic (M-PVA) beads. *Eng Life Sci.* 2016;16: 568–576. doi:10.1002/elsc.201600042
36. Dinger A, Telefoncu A. Improving the stability of cellulase by immobilization on modified polyvinyl alcohol coated chitosan beads. *J Mol Catal B Enzym.* Elsevier; 2007;45: 10–14. doi:10.1016/j.molcatb.2006.10.005
37. Li D, He Q, Cui Y, Duan L, Li J. Immobilization of glucose oxidase onto gold nanoparticles with enhanced thermostability. *Biochem Biophys Res Commun.* Academic Press; 2007;355: 488–493. doi:10.1016/j.bbrc.2007.01.183
38. Matsumoto M, Ohashi K. Effect of immobilization on thermostability of lipase from *Candida rugosa*. *Biochem Eng J.* Elsevier; 2003;14: 75–77. doi:10.1016/S1369-703X(02)00138-9
39. De Cordt S, Vanhoof K, Hu J, Maesmans G, Hendrickx M, Tobback P. Thermostability of soluble and immobilized α -amylase from *Bacillus licheniformis*. *Biotechnol Bioeng.* Wiley Subscription Services, Inc., A Wiley Company; 1992;40: 396–402. doi:10.1002/bit.260400309
40. Liu BL, Jong CH, Tzeng YM. Effect of immobilization on pH and thermal stability of *Aspergillus ficum* phytase. *Enzyme Microb Technol.* Elsevier; 1999;25: 517–521. doi:10.1016/S0141-0229(99)00076-9
41. Lülldorf N, Vojcic L, Hellmuth H, Weber TT, Mußmann N, Martinez R, et al. A first continuous 4-aminoantipyrene (4-AAP)-based screening system for directed esterase evolution. *Appl Microbiol Biotechnol.* 2015;99: 5237–5246. doi:10.1007/s00253-015-6612-3
42. Midelfort KS, Kumar R, Han S, Karmilowicz MJ, McConnell K, Gehlhaar DK, et al. Redesigning and characterizing the substrate specificity and activity of *Vibrio fluvialis* aminotransferase for the synthesis of imigabalin. *Protein Eng Des Sel.* 2013;26: 25–33. doi:10.1093/protein/gz065
43. Lauchli R, Rabe KS, Kalbarczyk KZ, Tata A, Heel T, Kitto RZ, et al. High-Throughput Screening for Terpene-Synthase-Cyclization Activity and Directed Evolution of a Terpene Synthase. *Angew Chemie Int Ed.* WILEY-VCH Verlag; 2013;52: 5571–5574. doi:10.1002/anie.201301362
44. Giver L, Gershenson A, Freskgard PO, Arnold FH. Directed evolution of a thermostable esterase. *Proc Natl Acad Sci U S A.* National Academy of Sciences; 1998;95: 12809–13. doi:10.1073/PNAS.95.22.12809
45. Lehmann M, Wyss M. Engineering proteins for thermostability: The use of sequence alignments versus rational design and directed evolution. *Current Opinion in Biotechnology.* Elsevier Current Trends; 2001. pp. 371–375. doi:10.1016/S0958-1669(00)00229-9
46. Eijssink VGH, GÅseidnes S, Borchert T V., Van Den Burg B. Directed evolution of enzyme stability. *Biomolecular Engineering.* Elsevier; 2005. pp. 21–30. doi:10.1016/j.bioeng.2004.12.003
47. Zhou C, Ye J, Xue Y, Ma Y. Directed evolution and structural analysis of alkaline pectate lyase from the alkaliphilic bacterium *Bacillus* sp. strain N16-5 to improve its thermostability for efficient ramie degumming. *Appl Environ Microbiol.* 2015;81: 5714–5723. doi:10.1128/AEM.01017-15
48. Wörn A, Plückthun A. Stability engineering of antibody single-chain Fv fragments. *J Mol Biol.* Academic Press; 2001;305: 989–1010. doi:10.1006/jmbi.2000.4265
49. Famm K, Hansen L, Christ D, Winter G. Thermodynamically Stable Aggregation-Resistant Antibody Domains through Directed Evolution. *J Mol Biol.* Academic Press; 2008;376: 926–931. doi:10.1016/j.jmb.2007.10.075
50. Van Durme J, Delgado J, Stricher F, Serrano L, Schymkowitz J, Rousseau F. A graphical interface for the FoldX forcefield. *Bioinformatics.* Oxford University Press; 2011;27: 1711–1712. doi:10.1093/bioinformatics/btr254
51. Bunting KA, Cooper JB, Tickle IJ, Young DB. Engineering of an intersubunit disulfide bridge in the iron-superoxide dismutase of *Mycobacterium tuberculosis*. *Arch Biochem Biophys.* Academic Press; 2002;397: 69–76. doi:10.1006/abbi.2001.2635 S0003986101926359 [pii]
52. Dehnavi E, Fathi-Roudsari M, Mirzaie S, Arab SS, Ranaei Siadat SO, Khajeh K. Engineering disulfide bonds in *Selenomonas ruminantium* β -xylosidase by experimental and computational methods. *Int J Biol Macromol.* Elsevier B.V.; 2017;95: 248–255. doi:10.1016/j.ijbiomac.2016.10.104
53. Kabashima T, Li Y, Kanada N, Ito K, Yoshimoto T. Enhancement of the thermal stability of pyroglutamyl peptidase I by introduction of an intersubunit disulfide bond. *Biochim Biophys Acta - Protein Struct Mol Enzymol.* Elsevier; 2001;1547: 214–220. doi:10.1016/S0167-4838(01)00185-6
54. Matsumurat M, Beckett WJ, Levitr M, Matthewstl BW. Stabilization of phage T4 lysozyme by engineered disulfide bonds (thermostability/lysozyme/protein structure). *Biochemistry.* 1989;86: 6562–6566. doi:10.1073/pnas.86.17.6562
55. Dombkowski AA, Sultana KZ, Craig DB. Protein disulfide engineering. *FEBS Lett.* Federation of European Biochemical Societies; 2014;588: 206–212. doi:10.1016/j.febslet.2013.11.024
56. Wijma HJ, Floor RJ, Jekel PA, Baker D, Marrink SJ, Janssen DB. Computationally designed libraries for rapid enzyme stabilization. *Protein Eng Des Sel.* 2014;27: 49–58. doi:10.1093/protein/gzt061
57. Dombkowski AA. Disulfide by Design™: a computational method for the rational design of disulfide bonds in proteins. *Bioinformatics.* Oxford University Press; 2003;19: 1852–1853. doi:10.1093/bioinformatics/btg231
58. Craig DB, Dombkowski AA. Disulfide by Design 2.0: a web-based tool for disulfide engineering in proteins. *BMC Bioinformatics.* BioMed Central; 2013;14: 346.
59. Jo BH, Park TY, Park HJ, Yeon YJ, Yoo YJ, Cha HJ. Engineering de novo disulfide bond in bacterial α -type carbonic anhydrase for thermostable carbon sequestration. *Sci Rep.* Nature Publishing Group; 2016;6: 29322. doi:10.1038/srep29322
60. Vlassi M, Cesareni G, Kokkinidis M. A correlation between the loss of hydrophobic core packing interactions and protein stability 1 | Edited by A. R. Fersht. *J Mol Biol.* Academic Press; 1999;285: 817–827. doi:10.1006/jmbi.1998.2342
61. Leaver-Fay A, Tyka M, Lewis SM, Lange OF, Thompson J, Jacak R, et al. ROSETTA3: an object-oriented software suite for the simulation and design of macromolecules. *Methods Enzymol.* NIH Public Access; 2011;487: 545–74. doi:10.1016/B978-0-12-381270-4.00019-6
62. Akasako A, Haruki M, Obatake M, Kanaya S. Conformational stabilities of *Escherichia coli* RNase HI variants with a series of amino acid substitutions at a cavity within the hydrophobic core. *J Biol Chem.* American Society for Biochemistry and Molecular Biology; 1997;272: 18686–93. doi:10.1074/JBC.272.30.18686
63. Borgo B, Havranek JJ. Automated selection of stabilizing mutations in

4) Thermostability engineering of the *V. paradoxus* ω -TA

- designed and natural proteins. *Proc Natl Acad Sci.* 2012;109: 1494–1499. doi:10.1073/pnas.1115172109
64. Lee TM. Computationally-Guided Thermostabilization of the Primary Endoglucanase from *Hypocrea jecorina* for Cellulosic Biofuel Production Thesis by. Thesis. 2014;2014. doi:10.7907/Z9S180G0
65. Marshall S a, Morgan CS, Mayo SL. Electrostatics significantly affect the stability of designed homeodomain variants. *J Mol Biol. Academic Press;* 2002;316: 189–99. doi:10.1006/jmbi.2001.5326
66. Steipe B, Schiller B, Plickthun A, Steinbacher S. Sequence Statistics Reliably Predict Stabilizing Mutations in a Protein Domain. *J Mol Biol. Academic Press;* 1994;240: 188–192. doi:10.1006/jmbi.1994.1434
67. Wang Q, Buckle AM, Foster NW, Johnson CM, Fersht AR. Design of highly stable functional GroEL minichaperones. *Protein Sci. Cold Spring Harbor Laboratory Press;* 1999;8: 2186–2193. doi:10.1110/ps.8.10.2186
68. Anbar M, Gul O, Lamed R, Sezerman UO, Bayer EA. Improved thermostability of *Clostridium thermocellum* endoglucanase Cel8A by using consensus-guided mutagenesis. *Appl Environ Microbiol. American Society for Microbiology;* 2012;78: 3458–64. doi:10.1128/AEM.07985-11
69. Komor RS, Romero PA, Xie CB, Arnold FH. Highly thermostable fungal cellobiohydrolase i (Cel7A) engineered using predictive methods. *Protein Eng Des Sel.* 2012;25: 827–833. doi:10.1093/protein/gzs058
70. Huang L, Xu JH, Yu HL. Significantly improved thermostability of a reductase CgKR1 from *Candida glabrata* with a key mutation at Asp 138 for enhancing bioreduction of aromatic α -keto esters. *J Biotechnol. Elsevier B.V.;* 2015;203: 54–61. doi:10.1016/j.jbiotec.2015.02.035
71. Parthiban V, Gromiha MM, Schomburg D. CUPSAT: prediction of protein stability upon point mutations. *Nucleic Acids Res. Oxford University Press;* 2006;34: W239–W242. doi:10.1093/nar/gk1190
72. Modarres HP, Mofrad MR, Sanati-Nezhad A. Protein thermostability engineering. *RSC Adv. Royal Society of Chemistry;* 2016;6: 115252–115270. doi:10.1039/C6RA16992A
73. Panigrahi P, Sule M, Ghanate A, Ramasamy S, Suresh CG. Engineering proteins for thermostability with iRDP web server. *PLoS One.* 2015;10: 1–20. doi:10.1371/journal.pone.0139486
74. Dourado DFAR, Flores SC. A multiscale approach to predicting affinity changes in protein-protein interfaces. *Proteins Struct Funct Bioinforma.* 2014;82: 2681–2690. doi:10.1002/prot.24634
75. Bava KA, Gromiha MM, Uedaira H, Kitajima K, Sarai A. ProTherm, version 4.0: thermodynamic database for proteins and mutants. *Nucleic Acids Res. Oxford University Press;* 2004;32: 120D–121. doi:10.1093/nar/gkh082
76. Kumar V, Rahman S, Choudhry H, Zamzami MA, Sarwar Jamal M, Islam A, et al. Computing disease-linked SOD1 mutations: deciphering protein stability and patient-phenotype relations. *Sci Rep. Springer US;* 2017;7: 4678. doi:10.1038/s41598-017-04950-9
77. Dehouck Y, Kwasiogoch JM, Rooman M, Gilis D. BeAtMuSiC: Prediction of changes in protein-protein binding affinity on mutations. *Nucleic Acids Res.* 2013;41: 333–339. doi:10.1093/nar/gkt450
78. Frappier V, Chartier M, Najmanovich RJ. ENCoM server: Exploring protein conformational space and the effect of mutations on protein function and stability. *Nucleic Acids Res.* 2015;43: W395–W400. doi:10.1093/nar/gkv343
79. Reetz MT, Carballeira JD, Vogel A. Iterative saturation mutagenesis on the basis of b factors as a strategy for increasing protein thermostability. *Angew Chemie - Int Ed.* 2006;45: 7745–7751. doi:10.1002/anie.200602795
80. Buß O, Muller D, Jager S, Rudat J, Rabe KS. Improvement of the thermostability of a β -amino acid converting ω -transaminase using FoldX. *ChemBioChem.* 2017; doi:10.1002/cbic.201700467
81. Guerois R, Nielsen JE, Serrano L. Predicting changes in the stability of proteins and protein complexes: A study of more than 1000 mutations. *J Mol Biol.* 2002;320: 369–387. doi:10.1016/S0022-2836(02)00442-4
82. Schymkowitz J, Borg J, Stricher F, Nys R, Rousseau F, Serrano L. The FoldX web server: An online force field. *Nucleic Acids Res. Oxford University Press;* 2005;33: W382–W388. doi:10.1093/nar/gki387
83. Grulich M, Brezovský J, Štěpánek V, Palyzová A, Marešová H, Zahradník J, et al. In-silico driven engineering of enantioselectivity of a penicillin G acylase towards active pharmaceutical ingredients. *Journal of Molecular Catalysis B: Enzymatic. Elsevier;* 2016. doi:10.1016/j.molcatb.2016.11.014
84. Nielsen S V., Stein A, Dinitzen AB, Papaleo E, Tatham MH, Poulsen EG, et al. Predicting the impact of Lynch syndrome-causing missense mutations from structural calculations. *PLoS Genet.* 2017;13: 1–26. doi:10.1371/journal.pgen.1006739
85. Wang S, Liu M, Zeng D, Qiu W, Ma P, Yu Y, et al. Increasing stability of antibody via antibody engineering: Stability engineering on an anti-hVEGF. *Proteins Struct Funct Bioinforma.* 2014;82: 2620–2630. doi:10.1002/prot.24626
86. Bednar D, Beerens K, Sebestova E, Bendl J, Khare S, Chaloupkova R, et al. FireProt: Energy- and Evolution-Based Computational Design of Thermostable Multiple-Point Mutants. *Dokholyan N V., editor. PLOS Comput Biol. Public Library of Science;* 2015;11: e1004556. doi:10.1371/journal.pcbi.1004556
87. Bhaskara RM, Srinivasan N. Stability of domain structures in multi-domain proteins. *Sci Rep. Nature Publishing Group;* 2011;1: 40. doi:10.1038/srep00040
88. Bhaskara RM, De Brevern AG, Srinivasan N. Understanding the role of domain-domain linkers in the spatial orientation of domains in multi-domain proteins. *J Biomol Struct Dyn. Taylor & Francis;* 2013;31: 1467–1480. doi:10.1080/07391102.2012.743438
89. Liu H, Zhu L, Bocola M, Chen N, Spiess AC, Schwaneberg U. Directed laccase evolution for improved ionic liquid resistance. *Green Chem.* 2013;15: 1348. doi:10.1039/c3gc36899h
90. Alibés A, Serrano L, Nadra AD. Structure-based DNA-binding prediction and design. *Methods Mol Biol. Humana Press, Totowa, NJ;* 2010;649: 77–88. doi:10.1007/978-1-60761-753-2_4
91. Wahab RA, Basri M, Rahman MBA, Rahman RNZRA, Salleh AB, Chor LT. Engineering catalytic efficiency of thermophilic lipase from *Geobacillus zalihae* by hydrophobic residue mutation near the catalytic pocket. *Adv Biosci Biotechnol. Scientific Research Publishing;* 2012;3: 158–167. doi:10.4236/abb.2012.32024
92. Wahab RA, Basri M, Rahman RNZRA, Salleh AB, Rahman MBA, Chor LT. Manipulation of the Conformation and Enzymatic Properties of T1 Lipase by Site-Directed Mutagenesis of the Protein Core. *Appl Biochem Biotechnol. Springer-Verlag;* 2012;167: 612–620. doi:10.1007/s12010-012-9728-2
93. Fernandez-Escamilla A-M, Rousseau F, Schymkowitz J, Serrano L. Prediction of sequence-dependent and mutational effects on the aggregation of peptides and proteins. *Nat Biotechnol.* 2004;22: 1302–1306. doi:10.1038/nbt1012
94. Broom A, Jacobi Z, Trainor K, Meiering EM. Computational tools help improve protein stability but with a solubility tradeoff. *J Biol Chem.*

4) Thermostability engineering of the *V. paradoxus* ω -TA

- 2017;292: 14349–14361. doi:10.1074/jbc.M117.784165
95. He Z, Mei G, Zhao C, Chen Y. Potential application of FoldX force field based protein modeling in zinc finger nucleases design. *Sci China Life Sci. Science China Press*; 2011;54: 442–449. doi:10.1007/s11427-011-4159-9
 96. Szczepek M, Brondani V, Büchel J, Serrano L, Segal DJ, Cathomen T. Structure-based redesign of the dimerization interface reduces the toxicity of zinc-finger nucleases. *Nat Biotechnol. Nature Publishing Group*; 2007;25: 786–793. doi:10.1038/nbt1317
 97. Tian J, Wu N, Chu X, Fan Y. Predicting changes in protein thermostability brought about by single- or multi-site mutations. *BMC Bioinformatics. BioMed Central*; 2010;11: 370. doi:10.1186/1471-2105-11-370
 98. Arabnejad H, Dal Lago M, Jekel PA, Floor RJ, Thunnissen A-MWH, Terwisscha van Scheltinga AC, et al. A robust cosolvent-compatible haloalcohol dehalogenase by computational library design. *Protein Eng Des Sel*. 2016;30: 175–189. doi:10.1093/protein/gzw068
 99. Parker AS, Zheng W, Griswold KE, Bailey-Kellogg C. Optimization algorithms for functional deimmunization of therapeutic proteins. *BMC Bioinformatics*. 2010;11: 180. doi:10.1186/1471-2105-11-180
 100. Li M, Simonetti FL, Goncarenco A, Panchenko AR. MutaBind estimates and interprets the effects of sequence variants on protein-protein interactions. *Nucleic Acids Res*. 2016;44: W494–W501. doi:10.1093/nar/gkw374
 101. Khan S, Vihinen M. Performance of protein stability predictors. *Hum Mutat*. 2010;31: 675–684. doi:10.1002/humu.21242
 102. Lee TM. Computationally-Guided Thermostabilization of the Primary Endoglucanase from *Hypocrea jecorina* for Cellulosic Biofuel Production Thesis by. Thesis. 2014;2014.
 103. Luo XJ, Zhao J, Li CX, Bai YP, Reetz MT, Yu HL, et al. Combinatorial evolution of phosphotriesterase toward a robust malathion degrader by hierarchical iteration mutagenesis. *Biotechnol Bioeng*. 2016;113: 2350–2357. doi:10.1002/bit.26012
 104. Timucin E, Sezerman OU. The conserved lid tryptophan, w211, potentiates thermostability and thermoactivity in bacterial thermoalkalophilic lipases. *PLoS One*. 2013;8: 1–17. doi:10.1371/journal.pone.0085186
 105. Floor RJ, Wijma HJ, Colpa DI, Ramos-Silva A, Jekel PA, Szymański W, et al. Computational library design for increasing haloalkane dehalogenase stability. *ChemBioChem*. 2014;15: 1660–1672. doi:10.1002/cbic.201402128
 106. Huang J, Xie DF, Feng Y. Engineering thermostable (R)-selective amine transaminase from *Aspergillus terreus* through in silico design employing B-factor and folding free energy calculations. *Biochem Biophys Res Commun. Elsevier Ltd*; 2017;483: 397–402. doi:10.1016/j.bbrc.2016.12.131
 107. Christensen NJ, Kepp KP. Accurate stabilities of laccase mutants predicted with a modified FoldX protocol. *J Chem Inf Model*. 2012;52: 3028–3042. doi:10.1021/ci300398z
 108. Rahman RNZRA, Zakaria II, Salleh AB, Basri M. Enzymatic properties and mutational studies of chalcone synthase from *Physcomitrella patens*. *Int J Mol Sci. Molecular Diversity Preservation International*; 2012;13: 9673–9691. doi:10.3390/ijms13089673
 109. Li M, Zhang ZJ, Kong XD, Yu HL, Zhou J, Xu JH. Engineering *Streptomyces coelicolor* carbonyl reductase for efficient atorvastatin precursor synthesis. *Appl Environ Microbiol*. 2017;83: 1081–1091. doi:10.1128/AEM.00603-17
 110. Wu B, Wijma HJ, Song L, Rozeboom HJ, Poloni C, Tian Y, et al. Versatile Peptide C-Terminal Functionalization via a Computationally Engineered Peptide Amidase. *ACS Catal*. 2016;6: 5405–5414. doi:10.1021/acscatal.6b01062
 111. Polizzi KM, Chaparro-Riggers JF, Vazquez-Figueroa E, Bommarius AS. Structure-guided consensus approach to create a more thermostable penicillin G acylase. *Biotechnol J*. 2006;1: 531–536. doi:10.1002/biot.200600029
 112. Sullivan BJ, Nguyen T, Durani V, Mathur D, Rojas S, Thomas M, et al. Stabilizing proteins from sequence statistics: The interplay of conservation and correlation in triosephosphate isomerase stability. *J Mol Biol*. 2012;420: 384–399. doi:10.1016/j.jmb.2012.04.025
 113. Sánchez IE, Beltrao P, Stricher F, Schymkowitz J, Ferkinghoff-Borg J, Rousseau F, et al. Genome-Wide Prediction of SH2 Domain Targets Using Structural Information and the FoldX Algorithm. *Rost B, editor. PLoS Comput Biol. Public Library of Science*; 2008;4: e1000052. doi:10.1371/journal.pcbi.1000052
 114. Jónsdóttir LB, Ellertsson B, Invernizzi G, Magnúsdóttir M, Thorbjarnardóttir SH, Papaleo E, et al. The role of salt bridges on the temperature adaptation of aqualysin I, a thermostable subtilisin-like proteinase. *Biochim Biophys Acta - Proteins Proteomics. Elsevier B.V.*; 2014;1844: 2174–2181. doi:10.1016/j.bbapap.2014.08.011
 115. Dvorak P, Bednar D, Vanacek P, Balek L, Eiseleova L, Stepankova V, et al. Computer-Assisted Engineering of Hyperstable Fibroblast Growth Factor 2. *bioRxiv*. 2016; 1–35. doi:10.1101/100636
 116. Song X, Wang Y, Shu Z, Hong J, Li T, Yao L. Engineering a More Thermostable Blue Light Photo Receptor *Bacillus subtilis* YtvA LOV Domain by a Computer Aided Rational Design Method. *PLoS Comput Biol*. 2013;9. doi:10.1371/journal.pcbi.1003129
 117. Heselpoth RD, Yin Y, Moulton J, Nelson DC, Y. Z. L. C. et al. Increasing the stability of the bacteriophage endolysin PlyC using rationale-based FoldX computational modeling. *Protein Eng Des Sel. Oxford University Press*; 2015;28: 85–92. doi:10.1093/protein/gzv004
 118. Plessl T, Bürer C, Lutz S, Yue WW, Baumgartner MR, Froese DS. Protein destabilization and loss of protein-protein interaction are fundamental mechanisms in *cblA*-type methylmalonic aciduria. *Hum Mutat*. 2017;38: 988–1001. doi:10.1002/humu.23251
 119. Wu I. Engineering Thermostable Fungal Cellobiohydrolases. *California Institute of Technology*. 2013.
 120. Daudé D, Topham CM, Remaud-Siméon M, André I. Probing impact of active site residue mutations on stability and activity of *Neisseria polysaccharaea* amylosucrase. *Protein Sci*. 2013;22: 1754–1765. doi:10.1002/pro.2375
 121. Kepp KP. Towards a “Golden Standard” for computing globin stability: Stability and structure sensitivity of myoglobin mutants. *Biochim Biophys Acta - Proteins Proteomics. Elsevier*; 2015;1854: 1239–1248. doi:10.1016/j.bbapap.2015.06.002
 122. Christensen NJ, Kepp KP. Stability mechanisms of laccase isoforms using a modified FoldX protocol applicable to widely different proteins. *J Chem Theory Comput*. 2013;9: 3210–3223. doi:10.1021/ct4002152
 123. Kepp KP. Computing Stability Effects of Mutations in Human Superoxide Dismutase 1. *J Phys Chem B. American Chemical Society*; 2014;118: 1799–1812. doi:10.1021/jp4119138
 124. Tokuriki N, Stricher F, Schymkowitz J, Serrano L, Tawfik DS. The Stability Effects of Protein Mutations Appear to be Universally Distributed. *J Mol Biol. Academic Press*; 2007;369: 1318–1332. doi:10.1016/j.jmb.2007.03.069
 125. Pey AL, Stricher F, Serrano L, Martinez A. Predicted Effects of Missense

4) Thermostability engineering of the *V. paradoxus* ω -TA

- Mutations on Native-State Stability Account for Phenotypic Outcome in Phenylketonuria, a Paradigm of Misfolding Diseases. *Am J Hum Genet.* Cell Press; 2007;81: 1006–1024. doi:10.1086/521879
126. Potapov V, Cohen M, Schreiber G. Assessing computational methods for predicting protein stability upon mutation: Good on average but not in the details. *Protein Eng Des Sel.* 2009;22: 553–560. doi:10.1093/protein/gzpz030
127. Broom A, Jacobi Z, Trainor K, Meiering EM. Tradeoff between protein stability and solubility Computational tools help improve protein stability but with a solubility tradeoff. doi:10.1074/jbc.M117.784165
128. Modarres P. *Modeling and Engineering Proteins Thermostability.* Ecole Polytechnique Federale de Lausanne. 2015.
129. Fleming N, Kinsella B, Ing C. Predicting Protein Thermostability Upon Mutation Using Molecular Dynamics Timeseries Data. bioRxiv. 2016; 78246. doi:10.1101/078246
130. Ayuso-Tejedor S, Abián O, Sancho J. Underexposed polar residues and protein stabilization. *Protein Eng Des Sel.* 2011;24: 171–177. doi:10.1093/protein/gzq072
131. Valentine JS, Doucette PA, Zittin Potter S. Copper-Zinc Superoxide Dismutase And Amyotrophic Lateral Sclerosis. *Annu Rev Biochem. Annual Reviews;* 2005;74: 563–593. doi:10.1146/annurev.biochem.72.121801.161647
132. Foit L, Morgan GJ, Kern MJ, Steimer LR, von Hacht AA, Titchmarsh J, et al. Optimizing Protein Stability In Vivo. *Mol Cell.* Cell Press; 2009;36: 861–871. doi:10.1016/J.MOLCEL.2009.11.022
133. Benedix A, Becker CM, de Groot BL, Caffisch A, Böckmann RA. Predicting free energy changes using structural ensembles. *Nat Methods.* Nature Publishing Group; 2009;6: 3–4. doi:10.1038/nmeth0109-3
134. Tokuriki N, Stricher F, Ferrano L, Tawfik DS. How protein stability and new functions trade off. *PLoS Comput Biol.* 2008;4: 35–37. doi:10.1371/journal.pcbi.1000002
135. Sánchez IE, Tejero J, Gómez-Moreno C, Medina M, Serrano L. Point Mutations in Protein Globular Domains: Contributions from Function, Stability and Misfolding. *J Mol Biol.* 2006;363: 422–432. doi:10.1016/j.jmb.2006.08.020
136. Alford RF, Leaver-Fay A, Jeliakov JR, O’Meara MJ, DiMaio FP, Park H, et al. The Rosetta All-Atom Energy Function for Macromolecular Modeling and Design. *J Chem Theory Comput.* American Chemical Society; 2017;13: 3031–3048. doi:10.1021/acs.jctc.7b00125
137. Musil M, Stourac J, Bendl J, Brezovsky J, Prokop Z, Zendulka J, et al. FireProt: web server for automated design of thermostable proteins. *Nucleic Acids Res.* 2017;45: W393–W399. doi:10.1093/nar/gkx285
138. Goldenzweig A, Goldsmith M, Hill SE, Gertman O, Laurino P, Ashani Y, et al. Automated Structure- and Sequence-Based Design of Proteins for High Bacterial Expression and Stability. *Mol Cell.* Cell Press; 2016;63: 337–346. doi:10.1016/j.molcel.2016.06.012
139. Bromberg Y, Rost B, Kruglyak L, Nickerson D, Schmitt A, Schuchhardt J, et al. Correlating protein function and stability through the analysis of single amino acid substitutions. *BMC Bioinformatics.* 2009;10: S8. doi:10.1186/1471-2105-10-S8-S8
140. Thiltgen G, Goldstein RA. Assessing Predictors of Changes in Protein Stability upon Mutation Using Self-Consistency. *PLoS One.* 2012;7. doi:10.1371/journal.pone.0046084
141. Bakail M, Ochsenbein F. Targeting protein–protein interactions, a wide open field for drug design. *Comptes Rendus Chim.* Elsevier Masson; 2016;19: 19–27. doi:10.1016/J.CRCL.2015.12.004
142. Schubert B, Schärfe C, Dönnies P, Hopf T, Marks D, Kohlbacher O. Population-specific design of de-immunized protein biotherapeutics. arXiv. 2017;1706.09083. Available: <http://arxiv.org/abs/1706.09083>
143. Yue WW. From structural biology to designing therapy for inborn errors of metabolism. *J Inherit Metab Dis.* Springer Netherlands; 2016;39: 489–498. doi:10.1007/s10545-016-9923-3
144. Wybenga GG, Crismaru CG, Janssen DB, Dijkstra BW. Structural determinants of the β -selectivity of a bacterial Aminotransferase. *J Biol Chem.* 2012;287: 28495–28502. doi:10.1074/jbc.M112.375238
145. Pavkov-Keller T, Strohmeier GA, Diepold M, Peeters W, Smeets N, Schürmann M, et al. Discovery and structural characterisation of new fold type IV-transaminases exemplify the diversity of this enzyme fold. *Sci Rep.* Nature Publishing Group; 2016;6: 38183. doi:10.1038/srep38183
146. Rudat J, Brucher BR, Syltatk C. Transaminases for the synthesis of enantiopure beta-amino acids. *AMB Express.* 2012;2: 11. doi:10.1186/2191-0855-2-11
147. Savile CK, Janey JM, Mundorff EC, Moore JC, Tam S, Jarvis WR, et al. Biocatalytic Asymmetric Synthesis of Chiral Amines from Ketones Applied to Sitagliptin Manufacture. *Science.*(80) 2010;329: 305–309. doi:10.1126/science.1188934
148. Pavlidis I V., Weiß MS, Genz M, Spurr P, Hanlon SP, Wirz B, et al. Identification of (S)-selective transaminases for the asymmetric synthesis of bulky chiral amines. *Nat Chem.* Nature Publishing Group; 2016;8: 1–7. doi:10.1038/NCHEM.2578
149. Deepankumar K, Shon M, Nadarajan SP, Shin G, Mathew S, Ayyadurai N, et al. Enhancing thermostability and organic solvent tolerance of ω -transaminase through global incorporation of fluorotyrosine. *Adv Synth Catal.* 2014;356: 993–998. doi:10.1002/adsc.201300706
150. Martin AR, DiSanto R, Plotnikov I, Kamat S, Shonnard D, Pannuri S. Improved activity and thermostability of (S)-aminotransferase by error-prone polymerase chain reaction for the production of a chiral amine. *Biochem Eng J.* 2007;37: 246–255. doi:10.1016/j.bej.2007.05.001
151. Pannuri S, Kamat SV, Garcia ARM. Thermostable Omega-Transaminases. EP1819825, 2010.
152. Huang J, Xie DF, Feng Y. Engineering thermostable (R)-selective amine transaminase from *Aspergillus terreus* through in silico design employing B-factor and folding free energy calculations. *Biochem Biophys Res Commun.* 2017;483: 397–402. doi:10.1016/j.bbrc.2016.12.131
153. Mathew S, Nadarajan SP, Chung T, Park HH, Yun H. Biochemical characterization of thermostable ω -transaminase from *Sphaerobacter thermophilus* and its application for producing aromatic β - and γ -amino acids. *Enzyme Microb Technol.* Elsevier Inc.; 2016; doi:10.1016/j.enzmictec.2016.02.013
154. Mathew S, Deepankumar K, Shin G, Hong EY, Kim B-G, Chung T, et al. Identification of novel thermostable ω -transaminase and its application for enzymatic synthesis of chiral amines at high temperature. *RSC Adv.* Royal Society of Chemistry; 2016;6: 69257–69260. doi:10.1039/C6RA15110H
155. Ferrandi EE, Previdi A, Bassanini I, Riva S, Peng X, Monti D. Novel thermostable amine transferases from hot spring metagenomes. *Applied Microbiology and Biotechnology.* Springer Berlin Heidelberg; 29 Jun 2017: 1–17. doi:10.1007/s00253-017-8228-2
156. Wani MC, Taylor HL, Wall ME, Coggon P, McPhail AT. Plant antitumor agents. VI. Isolation and structure of taxol, a novel antileukemic and antitumor agent from *Taxus brevifolia*. *J Am Chem Soc.* American Chemical Society; 1971;93: 2325–2327. doi:10.1021/ja00738a045
157. Lanen SG Van, Dorrestein PC, Christenson SD, Liu W, Ju J, Kelleher NL, et al. Biosynthesis of the β -Amino Acid Moiety of the Eneidiyne Antitumor

4) Thermostability engineering of the *V. paradoxus* ω -TA

- Antibiotic C-1027 Featuring β -Amino Acyl-S-carrier Protein Intermediates. *J Am Chem Soc. American Chemical Society*; 2005;127: 11594–11595. doi:10.1021/JA052871K
158. Jiang YK. Molecular docking and 3D-QSAR studies on beta-phenylalanine derivatives as dipeptidyl peptidase IV inhibitors. *J Mol Model. Springer-Verlag*; 2010;16: 1239–1249. doi:10.1007/s00894-009-0637-4
159. Karle IL, Gopi HN, Balaram P. Peptide hybrids containing alpha - and beta-amino acids: structure of a decapeptide beta-hairpin with two facing beta-phenylalanine residues. *Proc Natl Acad Sci U S A. National Academy of Sciences*; 2001;98: 3716–3719. doi:10.1073/pnas.071050198
160. Parween S, Misra A, Ramakumar S, Chauhan VS. Self-assembled dipeptide nanotubes constituted by flexible β -phenylalanine and conformationally constrained α , β -dehydrophenylalanine residues as drug delivery system. *J Mater Chem B. Royal Society of Chemistry*; 2014;2: 3096–3106. doi:10.1039/c3tb21856b
161. Crismaru CG, Wybenga GG, Szymanski W, Wijma HJ, Wu B, Bartsch S, et al. Biochemical properties and crystal structure of a β -phenylalanine aminotransferase from *Variovorax paradoxus*. *Appl Environ Microbiol.* 2013;79: 185–195. doi:10.1128/AEM.02525-12
162. Schymkowitz J, Borg J, Stricher F, Nys R, Rousseau F, Serrano L. The FoldX web server: an online force field. *Nucleic Acids Res. Oxford University Press*; 2005;33: W382–W388. doi:10.1093/nar/gki387
163. Cassimjee KE, Humble MS, Miceli V, Colomina CG, Berglund P. Active site quantification of an ω -Transaminase by performing a half transamination reaction. *ACS Catal. American Chemical Society*; 2011;1: 1051–1055. doi:10.1021/cs200315h
164. Laemmli U. Slab gel electrophoresis: SDS–PAGE with discontinuous buffers. *Nature.* 1979;227: 680–685.
165. Zor T, Selinger Z. Linearization of the Bradford Protein Assay Increases Its Sensitivity: Theoretical and Experimental Studies. *Anal Biochem.* 1996;236: 302–308. doi:10.1006/abio.1996.0171
166. Brucher B, Rudat J, Syldatk C, Vielhauer O. Enantioseparation of Aromatic β^3 -Amino acid by Precolumn Derivatization with *o*-Phthaldialdehyde and *N*-Isobutyryl-L-cysteine. *Chromatographia. Vieweg Verlag*; 2010;71: 1063–1067. doi:10.1365/s10337-010-1578-x
167. Berendsen HJC, Grigera JR, Straatsma TP. The missing term in effective pair potentials. *J Phys Chem. ACS Publications*; 1987;91: 6269–6271. doi:10.1021/j100308a038
168. Bussi G, Donadio D, Parrinello M. Canonical sampling through velocity rescaling. *J Chem Phys. American Institute of Physics*; 2007;126: 14101. doi:10.1063/1.2408420
169. Parrinello M, Rahman A. Polymorphic transitions in single crystals: A new molecular dynamics method. *J Appl Phys. American Institute of Physics*; 1981;52: 7182–7190. doi:10.1063/1.328693
170. Nosé S. A molecular dynamics method for simulations in the canonical ensemble. *Mol Phys. Taylor & Francis Group*; 1984;52: 255–268. doi:10.1080/00268978400101201
171. Hoover WG. Canonical dynamics: Equilibrium phase-space distributions. *Phys Rev A. American Physical Society*; 1985;31: 1695–1697. doi:10.1103/PhysRevA.31.1695
172. Parrinello M, Rahman A. Polymorphic transitions in single crystals: A new molecular dynamics method. *J Appl Phys. American Institute of Physics*; 1981;52: 7182–7190. doi:10.1063/1.328693
173. Hess B, Bekker H, Berendsen HJC, Fraaije JGEM, others. LINCS: a linear constraint solver for molecular simulations. *J Comput Chem.* 1997;18: 1463–1472. doi:10.1002/(SICI)1096-987X(199709)18:12
174. Jager S, Schiller B, Babel P, Blumenroth M, Strufe T, Hamacher K. StreAM- SST_gSS T g : algorithms for analyzing coarse grained RNA dynamics based on Markov models of connectivity-graphs. *Algorithms Mol Biol.* 2017;12: 15. doi:10.1186/s13015-017-0105-0
175. Schiller B, Jager S, Hamacher K, Strufe T. Stream - A stream-based algorithm for counting motifs in dynamic graphs. *Lecture Notes in Computer Science (including subseries Lecture Notes in Artificial Intelligence and Lecture Notes in Bioinformatics).* Springer, Cham; 2015. pp. 53–67. doi:10.1007/978-3-319-21233-3_5
176. Christensen NJ, Kepp KP. Accurate Stabilities of Laccase Mutants Predicted with a Modified FoldX Protocol. *J Chem Inf Model. American Chemical Society*; 2012;52: 3028–3042. doi:10.1021/ci300398z
177. Pettersen EF, Goddard TD, Huang CC, Couch GS, Greenblatt DM, Meng EC, et al. UCSF Chimera - A visualization system for exploratory research and analysis. *J Comput Chem. John Wiley & Sons, Inc.*; 2004;25: 1605–1612. doi:10.1002/jcc.20084
178. Studier FW. Protein production by auto-induction in high-density shaking cultures. *Protein Expr Purif. Academic Press*; 2005;41: 207–234. doi:10.1016/J.PEP.2005.01.016
179. Mayer S, Junne S, Ukkonen K, Glazyrina J, Glauche F, Neubauer P, et al. Lactose autoinduction with enzymatic glucose release: Characterization of the cultivation system in bioreactor. *Protein Expr Purif. Academic Press*; 2014;94: 67–72. doi:10.1016/j.pep.2013.10.024
180. Jia B, Jeon CO. High-throughput recombinant protein expression in *Escherichia coli*: current status and future perspectives. *Open Biol. Royal Society Journals*; 2016;6: 160196. doi:10.1098/rsob.160196
181. Dehouck Y, Kwasigroch JM, Gilis D, Rooman M. PoPMuSiC 2.1: a web server for the estimation of protein stability changes upon mutation and sequence optimality. *BMC Bioinformatics. BioMed Central*; 2011;12: 151. doi:10.1186/1471-2105-12-151
182. Pucci F, Bourgeois R, Rooman M. Predicting protein thermal stability changes upon point mutations using statistical potentials: Introducing HoTMuSiC. *Sci Rep. Nature Publishing Group*; 2016;6: 23257. doi:10.1038/srep23257
183. Guo F, Berglund P. Transaminase Biocatalysis: Optimization and Application. *Green Chem. Royal Society of Chemistry*; 2016; 333–360. doi:10.1039/C6GC02328B
184. Wang B, Land H, Berglund P. An efficient single-enzymatic cascade for asymmetric synthesis of chiral amines catalyzed by ω -transaminase. *Chem Commun. Royal Society of Chemistry*; 2013;49: 161–163. doi:10.1039/C2CC37232K
185. Beyer H, Walter W. *Lehrbuch der Organischen Chemie.* Stuttgart: Hirzel Verlag; 1991.
186. Lu J, Lin Q, Li Z, Rohani S. Solubility of L-phenylalanine anhydrous and monohydrate forms: Experimental measurements and predictions. *J Chem Eng Data.* 2012;57: 1492–1498. doi:10.1021/je201354k
187. Needham TE. The solubility of amino acids in various solvent systems. *Open Access Diss.* 1970; 1–95. Available: http://digitalcommons.uri.edu/oa_diss/159/
188. Buß O, Jager S, Dold S-M, Zimmermann S, Hamacher K, Schmitz K, et al. Statistical Evaluation of HTS Assays for Enzymatic Hydrolysis of β -Keto Esters. Oberer M, editor. *PLoS One. CRC Press*; 2016;11: e0146104. doi:10.1371/journal.pone.0146104
189. Logue MW, Pollack RM, Vitullo VP. Nature of the transition state for the decarboxylation of beta.-keto acids. *J Am Chem Soc. ACS Publications*;

4) Thermostability engineering of the *V. paradoxus* ω -TA

- 1975:97: 6868–6869.
190. Mathew S, Bea H, Nadarajan SP, Chung T, Yun H. Production of chiral β -amino acids using ω -transaminase from *Burkholderia graminis*. *J Biotechnol.* Elsevier B.V.; 2015;196–197: 1–8. doi:10.1016/j.jbiotec.2015.01.011
191. Wijma HJ, Floor RJ, Jekel PA, Baker D, Marrink SJ, Janssen DB. Computationally designed libraries for rapid enzyme stabilization. *Protein Eng Des Sel.* Oxford University Press; 2014;27: 49–58. doi:10.1093/protein/gzt061
192. Komor RS, Romero PA, Xie CB, Arnold FH. Highly thermostable fungal cellobiohydrolase I (Cel7A) engineered using predictive methods. *Protein Eng Des Sel.* U.S. Energy Information Administration, Washington, D.C; 2012;25: 827–833. doi:10.1093/protein/gzs058
193. Genz M, Vickers C, van den Bergh T, Joosten HJ, Dörr M, Höhne M, et al. Alteration of the donor/acceptor spectrum of the (*S*)-amine transaminase from *Vibrio fluvialis*. *Int J Mol Sci.* 2015;16: 26953–26963. doi:10.3390/ijms161126007
194. Humble MS, Cassimjee KE, Håkansson M, Kimbung YR, Walse B, Abedi V, et al. Crystal structures of the *Chromobacterium violaceum* ω -transaminase reveal major structural rearrangements upon binding of coenzyme PLP. *FEBS J.* 2012;279: 779–792. doi:10.1111/j.1742-4658.2012.08468.x
195. Martinez del Pozo A, van Ophem PW, Ringe D, Petsko G, Soda K, Manning JM. Interaction of pyridoxal 5'-phosphate with tryptophan-139 at the subunit interface of dimeric D-amino acid transaminase. *Biochemistry.* American Chemical Society; 1996;35: 2112–2116. doi:10.1021/bi9522211
196. Brender JR, Zhang Y, Vakser I, Kellogg E, Stephany J, Baker D. Predicting the Effect of Mutations on Protein-Protein Binding Interactions through Structure-Based Interface Profiles. Jernigan RL, editor. *PLOS Comput Biol.* Public Library of Science; 2015;11: e1004494. doi:10.1371/journal.pcbi.1004494
197. Morrow JK, Zhang S. Computational prediction of protein hot spot residues. *Curr Pharm Des.* 2012;18: 1255–1256. doi:10.2174/138920012799362909
198. Jones S, Thornton JM. Protein-protein interactions: A review of protein dimer structures. *Prog Biophys Mol Biol.* 1995;63: 31–65. doi:10.1016/0079-6107(94)00008-W
199. Huang J, Xie DF, Feng Y. Engineering thermostable (*R*)-selective amine transaminase from *Aspergillus terreus* through in silico design employing B-factor and folding free energy calculations. *Biochem Biophys Res Commun.* 2017;483: 397–402. doi:10.1016/j.bbrc.2016.12.131
200. Pal D, Chakrabarti P. Non-hydrogen Bond Interactions Involving the Methionine Sulfur Atom. *J Biomol Struct Dyn.* 2001;19: 115–128. doi:10.1080/07391102.2001.10506725
201. Smith LJ, Daura X, van Gunsteren WF. Assessing equilibration and convergence in biomolecular simulations. *Proteins Struct Funct Genet.* Wiley Subscription Services, Inc., A Wiley Company; 2002;48: 487–496. doi:10.1002/prot.10144
202. Chen J, Yu H, Liu C, Liu J, Shen Z. Improving stability of nitrile hydratase by bridging the salt-bridges in specific thermal-sensitive regions. *J Biotechnol.* 2013;164: 354–362. doi:10.1016/j.jbiotec.2013.01.021
203. Debye P. Interferenz von Röntgenstrahlen und Wärmebewegung. *Ann Phys.* WILEY-VCH Verlag; 1913;348: 49–92. doi:10.1002/andp.19133480105
204. Waller I. Zur Frage der Einwirkung der Wärmebewegung auf die Interferenz von Röntgenstrahlen. *Zeitschrift für Phys.* Springer-Verlag; 1923;17: 398–408. doi:10.1007/BF01328696
205. Smith DK, Radivojac P, Obradovic Z, Dunker AK, Zhu G. Improved amino acid flexibility parameters. *Protein Sci.* Wiley-Blackwell; 2003;12: 1060–1072. doi:10.1110/ps.0236203
206. Bulaj G. Formation of disulfide bonds in proteins and peptides. *Biotechnology Advances.* Elsevier; 2005. pp. 87–92. doi:10.1016/j.biotechadv.2004.09.002
207. Zhou NE, Kay CM, Hodges RS. Disulphide bond contribution to protein stability: positional effects of substitution in the hydrophobic core of the two stranded alpha-helical coiled-coil. *Biochemistry.* 1993. pp. 3178–3187.
208. Villafranca JE, Howell EE, Oatley SJ, Xuong NH, Kraul J. An Engineered Disulfide Bond in Dihydrofolate Reductase. *Biochemistry.* 1987;26: 2182–2189. doi:10.1021/bi00382a017
209. Dombkowski AA. Disulfide by Design: A computational method for the rational design of disulfide bonds in proteins. *Bioinformatics.* Oxford University Press; 2003;19: 1852–1853. doi:10.1093/bioinformatics/btg231
210. Lobstein J, Emrich CA, Jeans C, Faulkner M, Riggs P, Berkmen M. SHuffle, a novel *Escherichia coli* protein expression strain capable of correctly folding disulfide bonded proteins in its cytoplasm. *Microb Cell Fact.* BioMed Central; 2012;11: 753. doi:10.1186/1475-2859-11-56
211. Klausmann P. Disulfide-bond Engineering of an (*S*)-selective omega-Transaminase to Enhance its Thermostability (Master Thesis). Karlsruhe Institut of Technology. 2017.
212. Dombkowski AA, Sultana KZ, Craig DB. Protein disulfide engineering. *FEBS Letters* Jan 21, 2014 pp. 206–212. doi:10.1016/j.febslet.2013.11.024
213. Betz SF. Disulfide bonds and the stability of globular proteins. *Protein Science.* Wiley-Blackwell; 1993. pp. 1551–1558. doi:10.1002/pro.5560021002
214. Zapun A, Bardwell JC, Creighton TE. The reactive and destabilizing disulfide bond of DsbA, a protein required for protein disulfide bond formation in vivo. *Biochemistry.* 1993;32: 5083–92.
215. Matsumura M, Becktel WJ, Levitt M, Matthews BW. Stabilization of phage T4 lysozyme by engineered disulfide bonds. *Proc Natl Acad Sci.* 1989;86: 6562–6566. doi:10.1073/pnas.86.17.6562
216. Ramakrishnan V, Srinivasan SP, Salem SM, Matthews SJ, Colón W, Zaki M, et al. Geofold: Topology-based protein unfolding pathways capture the effects of engineered disulfides on kinetic stability. *Proteins Struct Funct Bioinforma.* 2012;80: 920–934. doi:10.1002/prot.23249
217. Xie DF, Fang H, Mei JQ, Gong JY, Wang HP, Shen XY, et al. Improving thermostability of (*R*)-selective amine transaminase from *Aspergillus terreus* through introduction of disulfide bonds. *Biotechnology and Applied Biochemistry.* 17 Jul 2017. doi:10.1002/bab.1572

5) Towards biocatalytic β -keto ester transamination approaches

This following chapter reports experiments aiming to the synthesis of β -amino acid ester in an asymmetric manner using engineered ω -transaminases. The subsection 5.1) describes an engineering approach to change the substrate selectivity towards aromatic β -amino acid esters. The following subsection 5.2) reports the screening of an ω -TA library to indicate engineered and wild type ω -TAs.

5.1) Substrate profile engineering of *V. paradoxus* ω -TA

In the following chapter the engineering of the *V. paradoxus* ω -TA is documented using information gained by OTAED (chapter 3) and by literature analysis. Therefor the key amino acid residues were identified and mutated. The aim of this project was to create a ω -TA with activity towards the β -keto ester ethyl 3-oxo-3-phenylpropanoate for synthesis of β -phenylalanine.

5.1.1) Alternative synthesis route to the lipase- ω -TA cascade reaction for the production of chiral β -PA

The asymmetric synthesis of β -amino acids is still challenging and different approaches are trying to solve these challenges. ω -TA catalyzed reaction are challenging until now, because instable β -keto acids have to be utilized, which decarboxylate fast in aqueous solutions [1,2]. An alternative would be the utilization of β -keto ester substrates, which do not undergo spontaneous decarboxylation, but currently no adequate β -keto ester active ω -TAs are available for this purpose. Therefore alternatives were established by Kim *et al.* and Mathew *et al.* (see also chapter 1)

5.1.1.1) Disadvantage of established cascade reactions

Both groups reported as an alternative approach cascade reactions using lipase/nitrilase (starting with asymmetric nitrile substrate) and β -PA-converting ω -TA with different yields of (*S*)- β -PA product [3–5]. However, this strategy has the major disadvantage that the unstable β -keto acid forms during the reaction and the keto acid must therefore be reduced directly to the corresponding amino acid as well as that the activity of ω -TA nitrilase/lipase must be adjusted. As reported in **chapter 1**, the enzyme concentrations of lipase or nitrilase are unfortunately quite high (**Table 5.1**).

Table 5.1 Advantages and disadvantages of a lipase- ω -TA cascade reaction for the synthesis of β -PA.

Advantages	Disadvantages
✓ One-pot reaction	✗ Undefined lipase formulation (with at least protease activity)
✓ Relative high product concentrations	✗ High lipase (up to 30 mg mL ⁻¹) and ω -TA concentrations (> 2.5 mg mL ⁻¹)
✓ Lipase commercially available	✗ Reaction mixture is more a suspension than a solution
	✗ Instable intermediate is formed (β -keto acid)
	✗ Difficult product purification
	✗ Reaction cascade cannot be spatially separated (e.g. for flow-cell-reactors)
	✗ Upscale might a problem (high enzyme concentrations necessary)

Furthermore, some uncertainties arise from the work of Mathew *et al.*, since the aromatic β -keto ester was hydrolyzed with the mentioned lipase concentration within 3 h, but the reaction time was more than 24 h. Within the first hour most of the ester should be hydrolyzed towards the free β -keto acid. In parallel, the transaminase reaction starts with whole-cell extracts or purified ω -TA. However, the exact enzyme activity is unknown for this part of the reaction, as the unstable β -keto acid cannot be used as a pure substance for activity tests. For this reason, Mathew *et al.* determined the activity of the ω -TA using the proper product (β -PA). But this reverse reaction is not valid for calculation of the activity for synthesis reaction constants. Starting from β -PA as substrate, the resulting product (β -keto acid) is naturally removed from the equilibrium. Therefore the reaction equilibrium is shifted by the ongoing decarboxylation of the β -keto acid. Another as yet unanswered question is what happens to β -keto acid intermediate. The accumulating intermediate β -keto acid will at least in part decarboxylate before it can be converted by an ω -TA [1,2,5]. Although it would be conceivable to lower the temperature of the reaction solution to slow down decarboxylation, this would also reduce at the same time the ω -TA activity. Additionally, the lyophilized lipase from *Candida rugosa* (L8525 Sigma-Aldrich), which was utilized by Mathew *et al.*, also exhibits proteolytic activity (0.001 U/mg), which might cause degradation of proteins over the time and results in an increase of amino acids contaminations, like α -PA. Overall, it is very difficult to characterize the reaction in detail and adapt it for a possible application. In addition, the group of Hyungdon Yun is the only one having reported an ω -TA containing enzymatic cascade strategy as highly successful in an aqueous reaction systems. In contrast, Zhang *et al.* demonstrated in 2018 in a two phase reaction, with a newly characterized nitrilase and an ω -TA, that the reaction from β -keto nitrile to β -PA is possible using high enzyme concentrations (concentration in water phase 30 mg mL⁻¹ of ω -TA powder and 20 mg mL⁻¹ of nitrilase powder) [6]. In contrast, within this thesis in unpublished preliminary experiments, using the ω -VpTA (1.2 mg mL⁻¹ purified) and *Candida rugosa* lipase (CRL, 20 mg mL⁻¹) the obtained yields ranged only between 7.2 and 16 %, which was already reported by Kim *et al.* in 2007 [3]. However, lower concentrations of CRL (1 mg mL⁻¹) resulted in no product formation. Furthermore nearly 50 % of the decarboxylation product, acetophenone, was obtained. Moreover, in the reports of Mathew *et al.* no preparative synthesis and purification of the product was carried out, therefore it is not possible to indicate product yields for this type of reaction strategy.

Disadvantage of whole-cell extracts

As an alternative, this research group also reported the use of whole extracts as biocatalysts for cascade reactions. In total the reported protein and cell concentration was about 50 mg mL^{-1} , which causes the challenge that amino acid contaminations can also be introduced into the reaction mixture by whole-cells. For example 100 mg of *E. coli* cells can result in 299 to 1549 μg of intracellular free α -amino acids depending on the used *E. coli* strain. At least 0.25 up to 1.5 % of cell dry weight are free amino acids [7]. Therefore it cannot be excluded that e.g. α -phenylalanine interacts during analysis and complicates the purification of β -PA.

5.1.1.2) Alternative reaction towards β -amino esters

For these reasons, an alternative synthesis strategy would be interesting in order to avoid some limitations in the reaction process. An alternative would be the synthesis of β -phenylalanine esters, which could be extractable (using an organic solvents) and avoiding at the same time the usage of two enzymes (**Figure 5.1**). In addition, β -amino esters are soluble in organic solvents and can be used for further chemical reactions or modifications, because in many cases the β -amino acid is not the desired product but mostly only an intermediate. If necessary, the free acid can easily be obtained from the ester with the help of a lipase. Midelfort *et al.* engineered the (*S*)-selective ω -TA from *V. fluvialis* for the conversion of an aliphatic β -keto ester substrate (ethyl 5-methyl 3-oxooctanoate). In this large mutation study, they showed that synthesis seems to be possible in principle. Further it was *inter alia* demonstrated that low transaminase concentrations (72 to $74 \mu\text{g mL}^{-1}$) were already sufficient for the determination of enzymatic activities. But for scale up experiments they used whole-cells to convert at least 1 g of substrate.

5) Towards biocatalytic β -keto ester transamination approaches

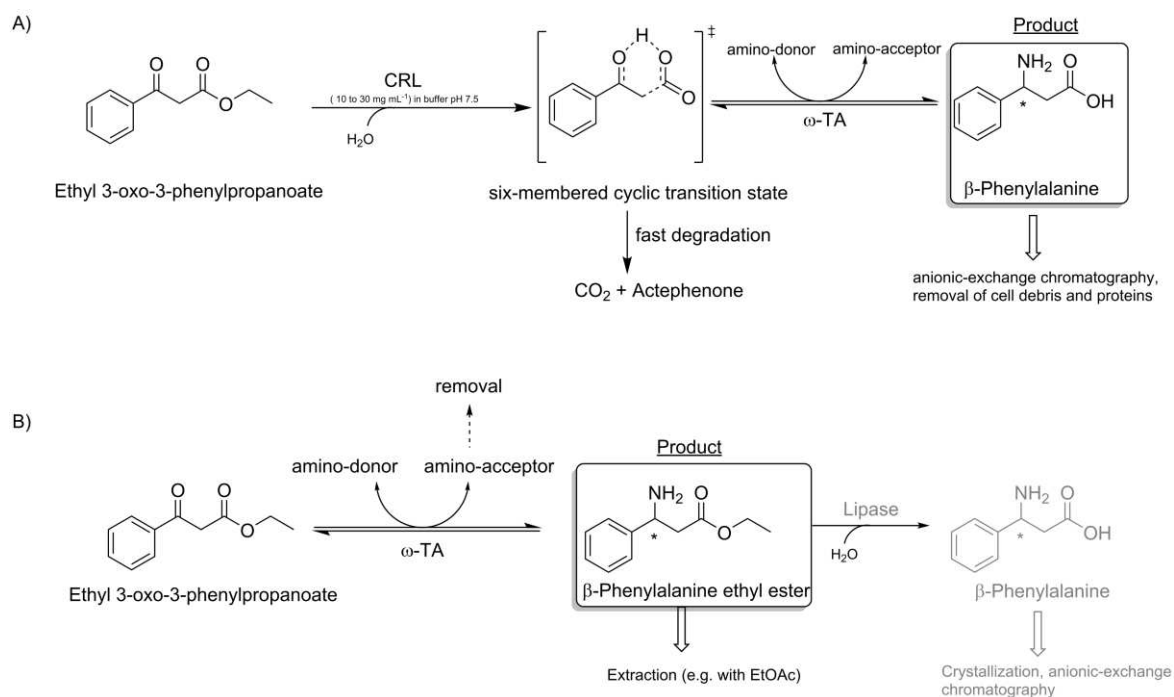


Figure 5.1 Synthesis and purification of chiral β -phenylalanine (ester). **A)** Strategy according to Mathew *et al.* The intermediate is able to degrade to carbon dioxide and acetophenone by a six-membered cyclic transition state or by a stepwise mechanism [8,9]. The resulting enol-product of the decarboxylation underlies a keto-enol tautomerization reaction to acetophenone. **B)** Alternative synthesis strategy to avoid an intermediate degradation.

Finally, after product isolation with methyl *tert*-butyl ether, they have achieved a yield of 28% [10]. In contrast Mathew *et al.* did not report a product yield (isolated product) for the cascade reaction towards β -PA.

Table 5.2 Postulated advantages and disadvantages for synthesis of β -amino acid esters using ω -TA.

Advantages	Disadvantages
✓ One-step reaction to get amino function	✗ No ω -TA with activity for aromatic β -keto esters reported (therefore screening or engineering necessary)
✓ Product extraction with organic solvents (e.g. EtOAc, Methyl <i>tert</i> -butyl ether)	✗ Hydrolysis of the β -keto ester can still lead to decarboxylation (e.g. if contaminations of hydrolases are present)
✓ Spatially separable reaction cascade possible (with lipase to gain β -amino acids)	✗ Other unforeseeable disadvantages (i.g. low activities, purification challenges)
✓ Higher substrate stability	
✓ Upscale might be easier (if only one enzyme is used)	

Moreover the strategy of Midelfort *et al.* simplifies the product isolation and in a second step the β -amino ester can be hydrolyzed enantioselectively using a lipase (**Table 5.2**).

5.1.2) Engineering *V. paradoxus* ω -TA

It has not been reported whether the *V. fluvialis* ω -TA is able to convert aromatic β -amino acids or esters. Therefore the ω -TA from *V. paradoxus* was selected as a starting point, because this enzyme shows high activity towards conversion of β -phenylalanine (33 U mg⁻¹ at 30°C, for the reverse reaction unknown) and moreover a crystal structure is available to investigate the enzyme function at a molecular level. In pre-tests, the ω -VpTA showed no direct conversion of β -keto ester substrates. Therefore amino acid residues were selected within ω -VpTA analyzing knowledge from literature database in respect of described engineering sites at the substrate binding pockets from Fold type I ω -TA. Furthermore the docking of the imino-intermediate (Substrate + PLP) was simulated with the wild type structure and the sequence tolerance of the selected engineering sites was investigated.

5.1.3) Materials and Methods

ROSIE-Ligand docking

For calculation of the binding energy the Rosetta-online server (ROSIE) was utilized. For this the crystal structure of 4AOA (resolution 2.26 Å) was utilized and with ChemBio3D Ultra (version 14.0, PerkinElmer) the 3D structure of the intermediate was built (aldimine of β -phenylalanine ethyl ester and PLP) and implicit hydrogens were added [11]. Ligand structure conformers were generated using the tool BCL [12]. The ligand docking was performed according to the manual of ROSIE and all values were set to be default. The number of conformers of the ligand was set to 200. The 3D-coordinates (X/Y/Z) of the intermediate (inhibitor) molecules was determined using Chimera 1.1[13]. The resulting intermediate-enzyme structures were ranked according to the binding energy and due to arrangement in the substrate binding pocket.

Mutagenesis PCR

For performing site-directed mutagenesis the Q5-site-directed mutagenesis Kit from NEB was utilized and the experiments performed according to the user manual. The mutagenesis PCR was performed with pET- ω -TA gene from *V. paradoxus*. The oligomers were designed using the NEB-base changer tool of NEB. The mutagenesis DNA-oligomers were produced by Thermo-Fischer.

Table 5.3 Oligomer mismatch primer for site directed mutagenesis PCR of position R41, Y76, Y159 and R398. *using PCR strategy from chapter 4

Position	Exchange	T _m	Direction	primer-sequence
41	R to S	60°C	fw	TGCAAATAGC ca AGCGTTCTGTTTTATG
41	R to S	60°C	rv	CCAGGCATATAACGTGCC
41	R to K	60°C	fw	TGCAAATAGC aaa AGCGTTCTGTTTTATG
41	R to K	60°C	rv	CCAGGCATATAACGTGCC
41	R to A	60°C	Fw	TGCAAATAGC gcc AGCGTTCTGTTTTATG
41	R to A	60°C	Rv	CCAGGCATATAACGTGCC
76	Y to F	61°C	Fw	TATTGCAGAG ttc ACCGCAGGCG
76	Y to F	61°C	Rv	AAATCTGCATAACGATGACCATC
76	Y to S	62°C	Fw	GATTTTATTGCAGAGTCTACCGCAGGCGTTTATG*
76	Y to S	62°C	Rv	CATAAACGCCTGCGGTAGACTCTGCAATAAAATC*
76	Y to A	61°C	Fw	TATTGCAGAG tca ACCGCAGGCG
76	Y to A	61°C	Rv	AAATCTGCATAACGATGACCATC

5) Towards biocatalytic β -keto ester transamination approaches

159	Y to F	60°C	Fw	TAGCGGTGGT ttc CATGGTGGTG
159	Y to F	63°C	Rv	AAAACAACAATTTTACGACGAC
159	Y to S	63°C	Fw	TAGCGGTGGT tca CATGGTGGTG
159	Y to S	62°C	Rv	AAAACAACAATTTTACGACGACC
398	R to L	57°C	Fw	TAGCAGTCCG ctg GGTTTTGTTG
398	R to K	57°C	Fw	TAGCAGTCCG gaa GGTTTTGTTG
398	R to S	57°C	FW	TAGCAGTCCG gag GGTTTTGTTG
398	R to	57°C	Rv	TAGATATCTTCATTCAGCAG

Enzyme purification

Methods for the production and purification of the ω -TA variants from *V. paradoxus* are described in chapter 4.

Activity tests

The activity of enzyme variants were tested using different amino donors and amino acceptors according to table 5.4. The reactions were performed for 24 h at 30°C using 2 μ M of purified ω -VpTA and 0.1 mM of PLP (otherwise mentioned). For poorly water soluble substrates different contents of DMSO were used. The conversion was determined using HPLC, like described in section 4). The reactions were performed in 220 μ L and started by addition of enzyme solution. For PA-KG, samples were taken after 15 and 90s and after 5 min. Samples of PE-KG, AB-KG and AL-KG were taken after 7 min and 21.5 h, because very slow consumption rates were expected.

Table 5.4 Activity test solutions using 50 mM sodium phosphate buffer pH 7.2.

Short cut	Amino donor	Amino acceptor	Co-solvent
PA-KG	15 mM <i>rac</i> β -PA	15 mM α -keto glutarate	-
PE-KG	40 mM PEA	15 mM α -keto glutarate	10 % (v/v) DMSO
AB-KG	40 mM 3-amino butyric acid	15 mM α -keto glutarate	10 % (v/v) DMSO
AL-KG	40 mM L-alanine	15 mM α -keto glutarate	10 % (v/v) DMSO
PE-EOPP	40 mM PEA	15 mM ethyl-3-oxo- phenylpropanoate	10 % (v/v) DMSO

HPLC analysis

For HPLC analysis see chapter 4. Exemplary chromatograms of the different amino donors are presented within the **Figure S8**.

5.1.3) Results and Discussion

Before ω -VpTA engineering was performed, it was tested, whether the enzyme is able to use other substrates than β -amino acids as amino donors. It was shown, that PEA and L-alanine are accepted amino donor substrates for amination of α -ketoglutarate. However for L-alanine a co-product removal system was necessary, consisting of 250 mM of L-alanine and lactate dehydrogenase (USA, Megazyme) starting with 1 mM of the reduction equivalent NADH. This result is of particular importance: first, no activity for non- β amino acids has been reported before and secondly because it is desirable for the synthesis of β -phenylalanine (esters) to use non- β amino acids as amino donor source. PEA and alanine are commonly used amino donors for ω -TA reactions. In addition, both tests could be used as a basis for the development of screening assays.

5.1.3.1) Analysis of engineering sites

The wildtype ω -VpTA shows no activity towards β -phenylalanine ethyl ester (β -PAEE) or to the corresponding β -keto ester substrate at all. Until now the capability to convert β -PA as ethyl ester was never reported for transaminase reactions and only one example for conversion of an aliphatic β -keto esters is described [14]. Therefore little is known about the binding of aromatic β -keto esters within ω -TA and in order to gain insights the binding was investigated using *in-silico* binding energy calculations.

The binding probability was investigate using the Rosetta based ligand docking calculation tool (ROSIE-ligand docking), which includes also the conformation of the binding amino acid residues [11]. The arbitrary binding energies were calculated using the intermediate (aldimine), because this reaction-step is the result of the reaction of aldehyde moiety with the amino group of β -PAEE. This intermediate occupies the most of the substrate pocket space and has to fit inside the substrate binding pocket during the reaction cycle. Clashes with amino acid residues would result in weaker binding energies. To get an insight whether binding is possible at all, the binding event was simulated. The binding was ranked in comparison to the inhibitor relative binding energy of 4'-deoxy-4'-acetylamino-pyridoxal-5'-phosphate (DAPP). Therefore the inhibitor coordination was utilized, which is known from X-ray structure analysis of ω -VpTA (PDB ID 4AOA).

Binding of β -PAEE

In general, inhibitors are quite similar to transition states of substrates and therefore inhibit the reactivity of enzymes, because they fit generally well within the substrate binding pocket [15,16]. To analyze whether the binding calculation was performed accurately, the calculated structure was compared to the crystal structure coordination of DAPP. The binding energy of DAPP was -16.2 Rosetta energy units (REU, on an arbitrary scale) and is in accordance with the 4AOA structure. The best binding energy hit of the β -PAEE-PLP intermediate was shown to be -11.4 REU, which 30% less of binding energy than compared to DAPP (**Figure 5.2**).

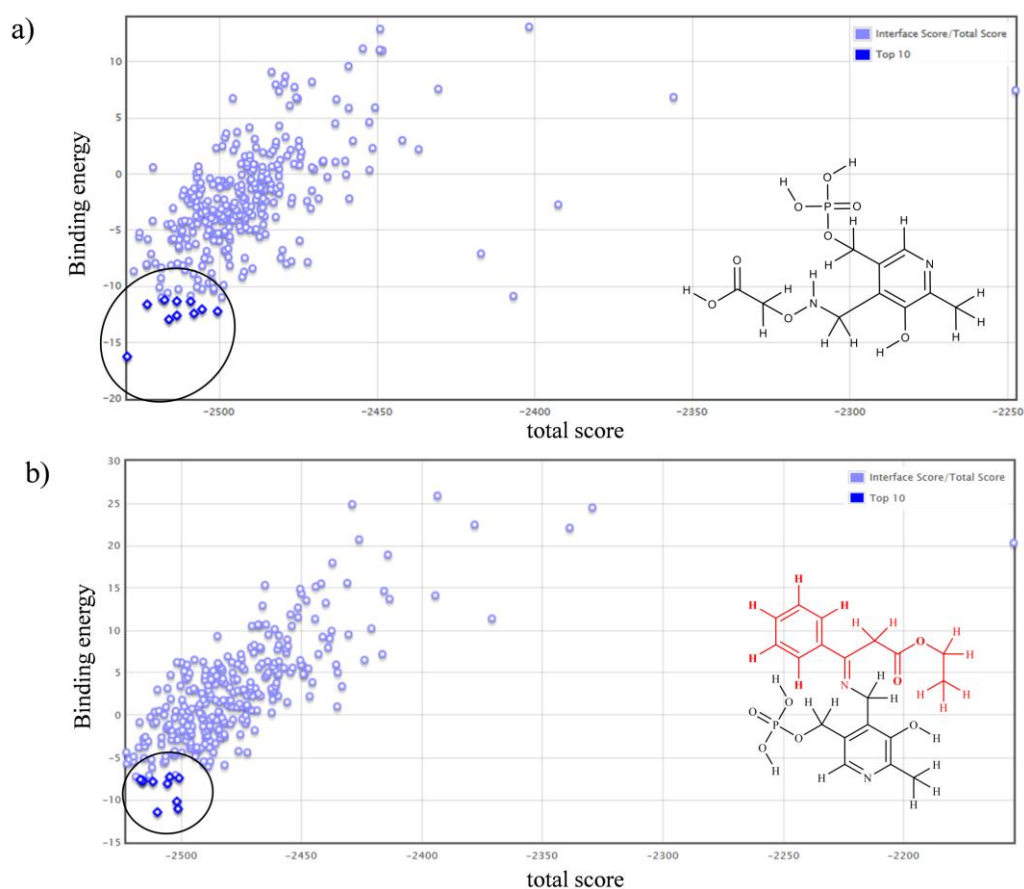


Figure 5.2 Ligand-docking in the *V. paradoxus* ω -TA using Rosetta. 200 conformational structures were tested for the docking **A)** Docking of inhibitor in 4AOA, best energy hit showed similar coordination compared to crystal structure with 4AOA. **B)** Docking of hypothetical β -phenylalanine-ethyl ester-PLP intermediate in 4AOA. (Docking was performed using ROSIE docking server [11]). The binding energies are presented on **an arbitrary scale** (Rosetta Energy Units).

Furthermore also other conformers were analyzed using visual inspection. The second and third best β -phenylalanine ethyl ester-PLP intermediates (PEEP) were oriented in different angles or fitted badly in the substrate binding pocket (clashes or orientation to substrate entrance channel).

Hence, the most important amino acid residues and position of the ligand of the original 4AOA-structure of the DAPP-calculations and of PEEP-calculations were displayed in **figure 5.3**. The intermediates were quite similar oriented within the binding pocket, but the position of the pyridine ring of PEEP was slightly shifted towards the larger binding pocket (O-pocket) of the ω -VpTA. The aldimine bond of PEEP is located 5.0 Å away from the closest hydrogen of the ϵ -amino moiety of amino acid residue lysine 267. The distance from the nitrogen atom of the pyridine ring to the coordinating amino acid residue Y159 is 9.2 Å which is 3.8 Å further than determined for the distance of the DAPP pyridine nitrogen (5.4 Å) to Y159.

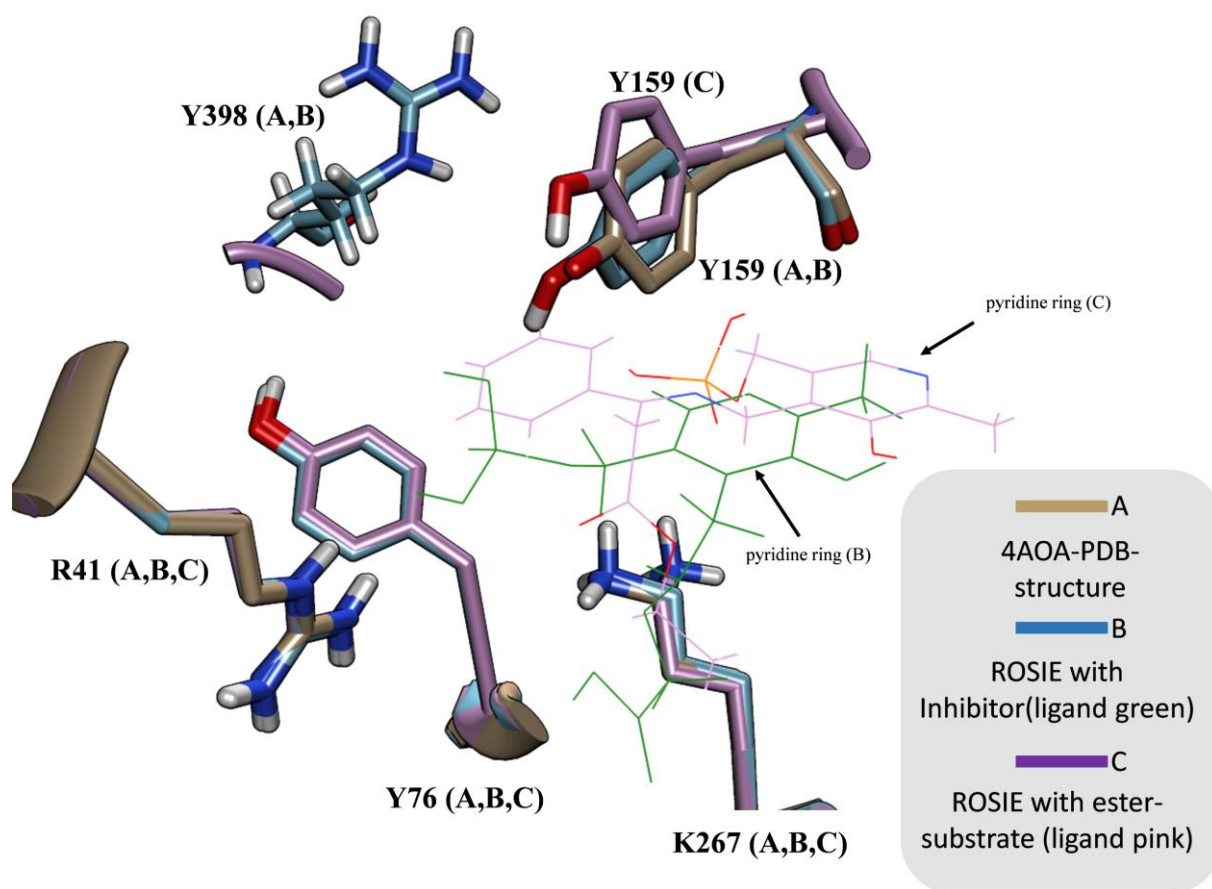


Figure 5.3 Substrate-intermediate binding showed with target substrate β -phenylalanine-ethyl-ester compared to inhibitor. Structure **A** (brown) is shown as visualization of the crystal structure PDB-ID 4AOA in combination with the inhibitor 4'-deoxy-4'-actylamino-pyridoxal-5'-phosphate (not shown). Structure **B** (blue) is the result of the simulation using ROSIE, the 4AOA structure (without inhibitor) and 4'-deoxy-4'-actylamino-pyridoxal-5'-phosphate (green). The inhibitor ligand of structure A and B fits quite well. Structure **C** shows the docking with the target substrate (PLP- β -phenylalanine-ethyl-ester-intermediate). The docking was performed using ROSIE-software. The arbitrarive binding energies are displayed in Figure 5.2.

Furthermore also the amino acid residues are reoriented slightly, especially Y159 (movement $\Delta\text{\AA}$ 3.3). On the one hand the differences and the lower relative binding energy are

an indication for the inhibition of the binding of β -PAEE, on the other hand it shows that a binding at least possible.

In contrast using the example of the α -phenylalanine ethyl-ester-PLP intermediate, the clashes are so strong that Y159 is clearly reoriented (**Figure 5.4**). Moreover, also R41, an amino acid residue which coordinates the carboxylic moiety of β -PA is reoriented to avoid a clash with the intermediate [17]. However, these are only hints, that the binding of β -PAEE is possible, although unfavorable. Also the structure quality of 4AOA has to be taken into account, because the crystal structure resolution of 4AOA is only 2.2 Å. The suspicion, that β -PAEE might be able to bind inside the substrate pocket, though less affine, is interesting in regard of further engineering experiments aiming to expand the substrate binding pocket and to avoid electrostatic barriers.

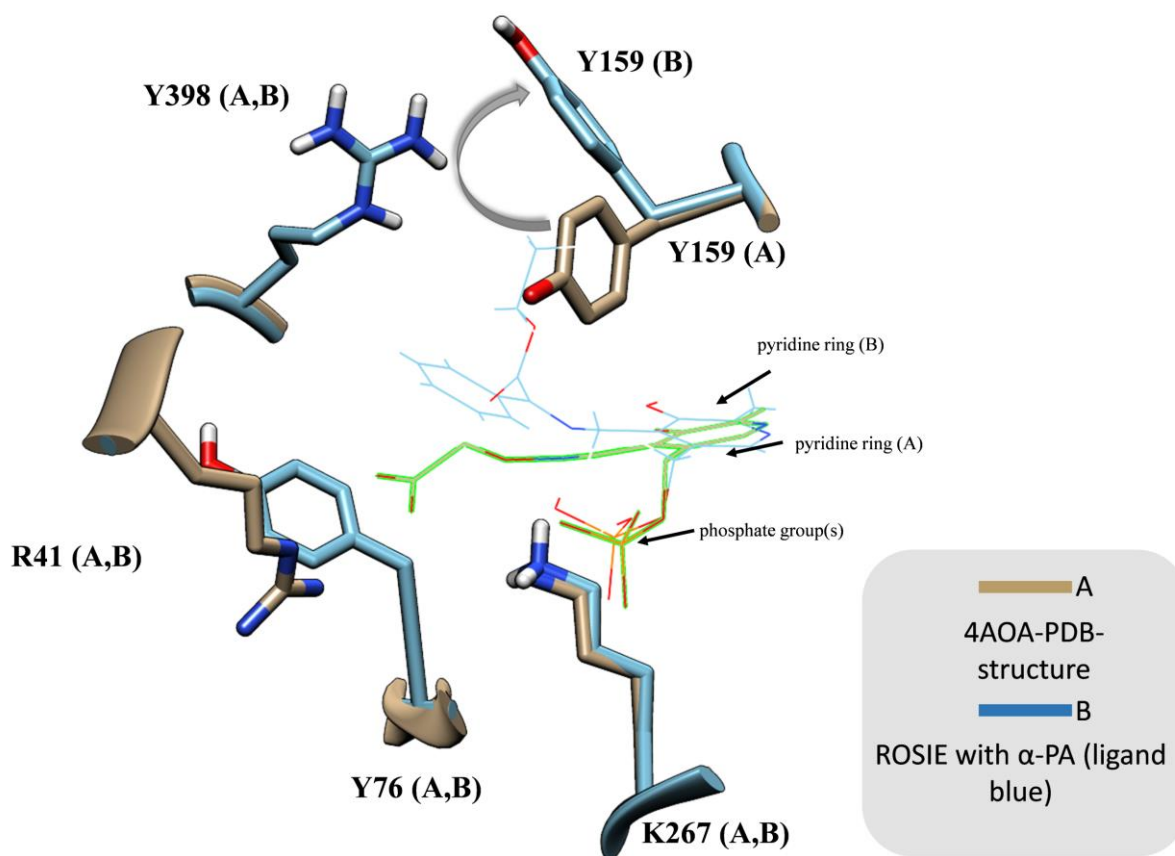


Figure 5.4 α -L-phenylalanine-ester-intermediate (blue) binding causes rearrangement of PLP coordination residue Y159. The ethyl moiety is oriented towards Y159(A), which results in a movement of Y159(B). This demonstrates, that small changes in substrate structure cause rearrangements of intermediates on the cost of binding energy. The position of the inhibitor is shown in green.

To identify engineering sites, the results from other Fold type I (*S*-selective) ω -TA engineering experiments were analyzed to identify putative interesting sites within ω -VpTA. Furthermore

also residues were taken into account which have been described to have a special function (i.e. change in specific activity, substrate interaction).

Identification of engineering sites

As already shown in chapter 3, all ω -TA engineering experiments were summarized and analyzed using the standard numbering scheme from oTAED. Sites of interest were relocated in ω -VpTA (PDB ID 4AOA) and additionally promising sites were analyzed. Weiß *et al.* showed in experiments with the ω -TA from *Ruegeria sp.* TM1040 that the residue Y59, Y87 and Y152 are highly important to generate activity for bulky substrates like exo-3-amino-8-aza-bicyclo[3.2.1]oct-8-yl-phenyl-methanone [18]. Furthermore Midelfort *et al.* demonstrated at the example of the ω -TA from *Vibrio fluvialis* that the residues W57F and R414 are important towards β -keto ester activity using the aliphatic ester substrate ethyl-3-oxohexanoate [19]. Moreover Pavlidis *et al.* reported that Y153 in *Ruegeria sp.* and Y152 in *Mesorhizobium loti* are important residues for activity towards bulky chiral amines. In addition it was reported, that Y153 coordinates the PLP at the active site and an exchange of tyrosine to phenylalanine decreases the polarity and stabilizes at the same time PLP at the active site. The lower polarity is important for the conversion of bulky and less charged substrates [20].

Selection of mutation sites

Those reports also highlighted that Y59 and W57 are prominent sites for increasing the activity towards bulky substrates. Furthermore Y87, also located in the small binding pocket (P-pocket), is limiting the space and mutations towards phenylalanine provide more space caused by the missing hydroxyl moiety and decrease the polarity in the P-pocket. Mutations towards smaller hydrophobic residues led to drastic decrease of ω -TA activity [20]. To identify those and other residues the oTAED standard numbering scheme (see **Table S1**) was used for transferring the engineering onto 4AOA (**Chapter 3**).

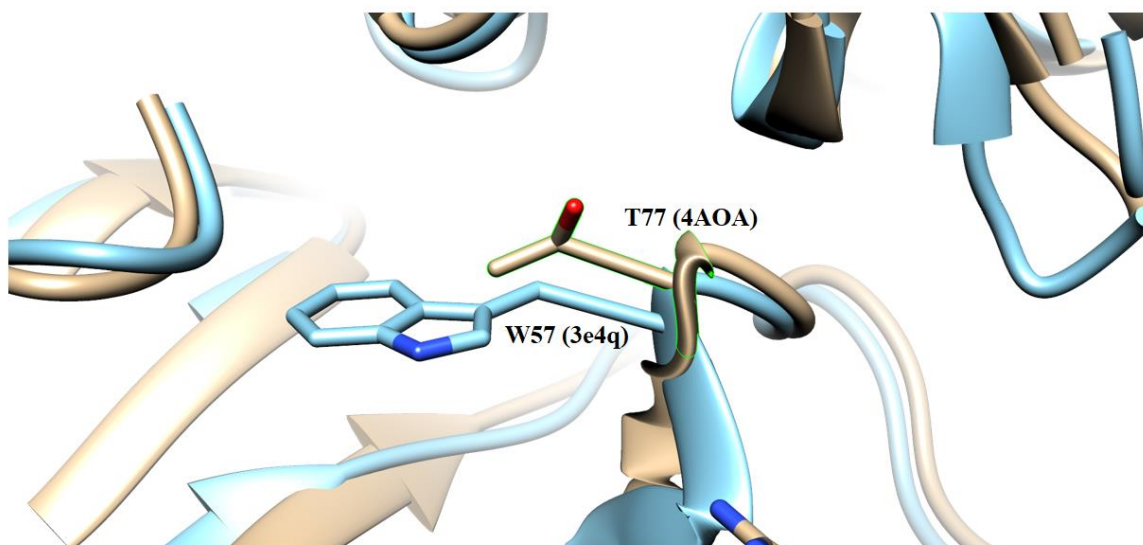


Figure 5.5 Space limiting position W57 of *V. fluvialis* ω -TA is in *V. paradoxus* a less space extensive threonine residue. The PDB structures 4AOA and 3E4Q were utilized for structurally matching. The structures were matched using Chimera 1.1 [13].

The sequence identity of both sequences is 24.87 % and the calculation of structural identity resulted in a Δ RMSD of 1.13 (of 193 pruned pairs) and in total 6.9 Å (of 394 pairing residues). Relocating W57 inside of 4AOA resulted in detection of T77 inside *V. paradoxus* ω -TA. T77 and W57 show an RMSD of 1.4 Å, which is quite similar, but the threonine residue of 4AOA is less space extensive than W57, therefore T77 should not be space limiting inside the P-pocket (**Figure 5.5**). Furthermore the engineered variant W57F of *V. fluvialis*, which is not less space-saving than threonine, showed activity against the aliphatic ethyl ester substrate tested by Midelfort *et al.*. Moreover in *V. fluvialis* a loop structure is present, which is shifted within *V. paradoxus* and cannot be relocated at the same position (**Figure 5.6**).

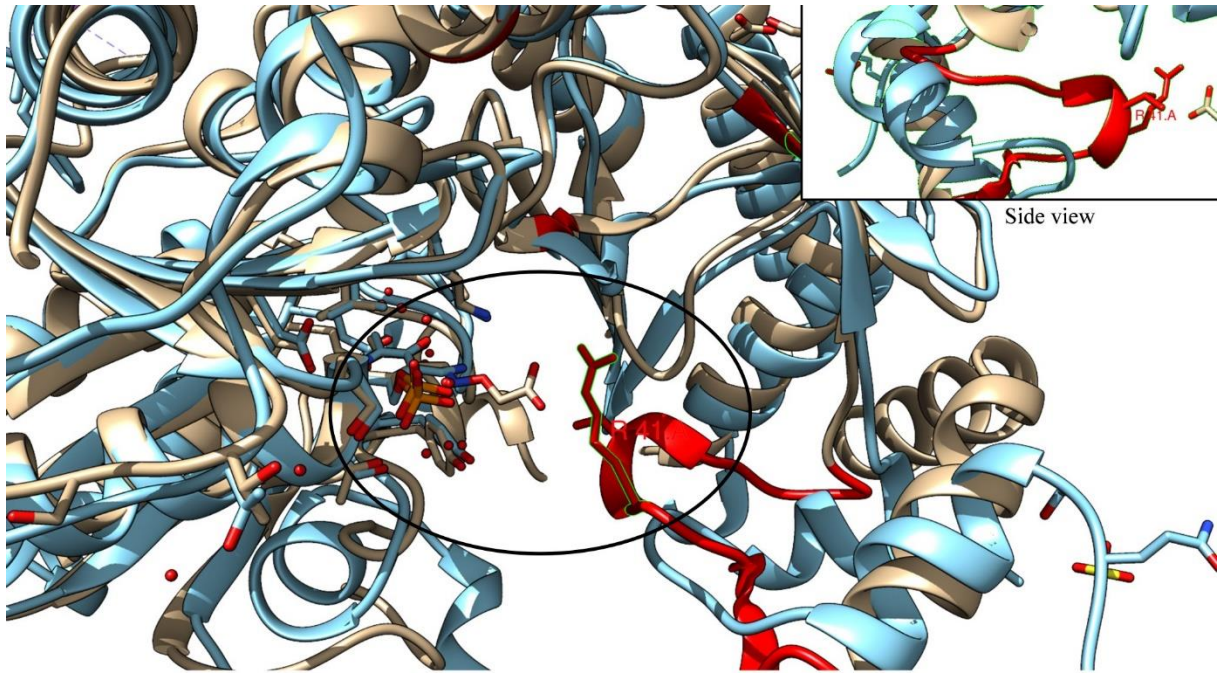


Figure 5.6 Superimpose of the structures of *V. fluvialis* (blue) and *V. paradoxus* ω -TA (brown). The main structural difference between both ω -TA is located at the P-pocket site. At this structural element of *V. paradoxus* (red) R41 can be found, which is absent in *V. fluvialis*. The structures were matched using Chimera 1.1 [13].

Especially in the side view is it obvious that the loop of *V. paradoxus* ω -TA is oriented differently in the small substrate binding pocket (P-pocket) and is arranged deeper inside the pocket than by *V. fluvialis*. The substrate binding carboxyl-moiety R41 can be relocated at the protrusion (inside 4AOA) [17]. Furthermore the sequence homology in this part is very low and therefore not alignable. Overall, T77 might have an influence on the hydrophobicity, but was excluded for the first engineering experiments.

Taken together the results of the *V. fluvialis* engineering experiments can only be used to a limited extent, but they show that beside W57 also the flipping arginine is important towards activity of ester substrates [14]. In the following only the residues R41 (substrate binding residue), Y71 (limiting space within P-pocket), Y159 (coordinating cofactor) and R398 (putative flipping arginine) were selected for further site directed mutagenesis experiments (showed in **Figure 5.7**). The expected effects are outlined in the next section.

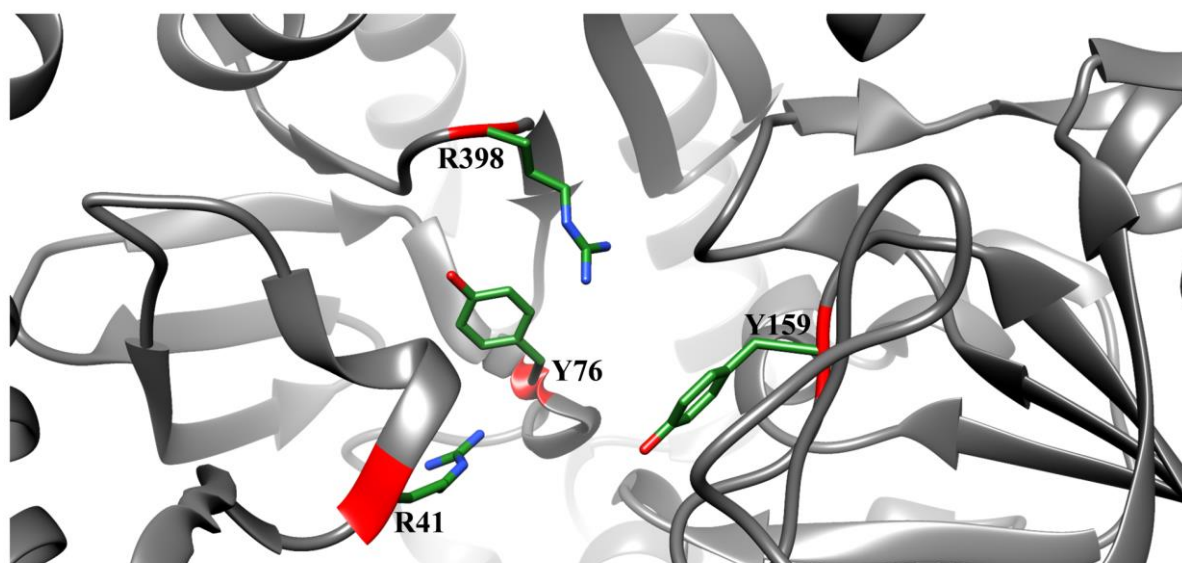


Figure 5.7 ω -VpTA engineering sites with suspected influence on β -keto ester activity. Figure was created using Chimera 1.1.

The residue R41 was mutated to L-serine, L-lysine and L-alanine. L-Lysine was chosen as smaller but positively charged amino acid residue and alanine as short and hydrophobic residue, which reduces the polarity at the P-pocket. L-Serine was selected as amino acid residue, which is smaller and able to form hydrogen-bonds, which might be necessary for the structure keeping of 4AOA, because R41 forming a salt bridge to E75. Therefore also E75 was mutated to alanine and to serine and combinations of R41 with E75 were created.

Moreover Y76 was exchanged against L-serine, L-phenylalanine and L-alanine. L-Serine was selected as residue, because it maintains the hydroxyl function of the L-tyrosine residue but less space consuming. In contrast L-phenylalanine reduces the polarity at the P-pocket side due to the lacking of the hydroxyl moiety and alanine is the smallest, but hydrophobic residue and able to enlarge the binding pocket.

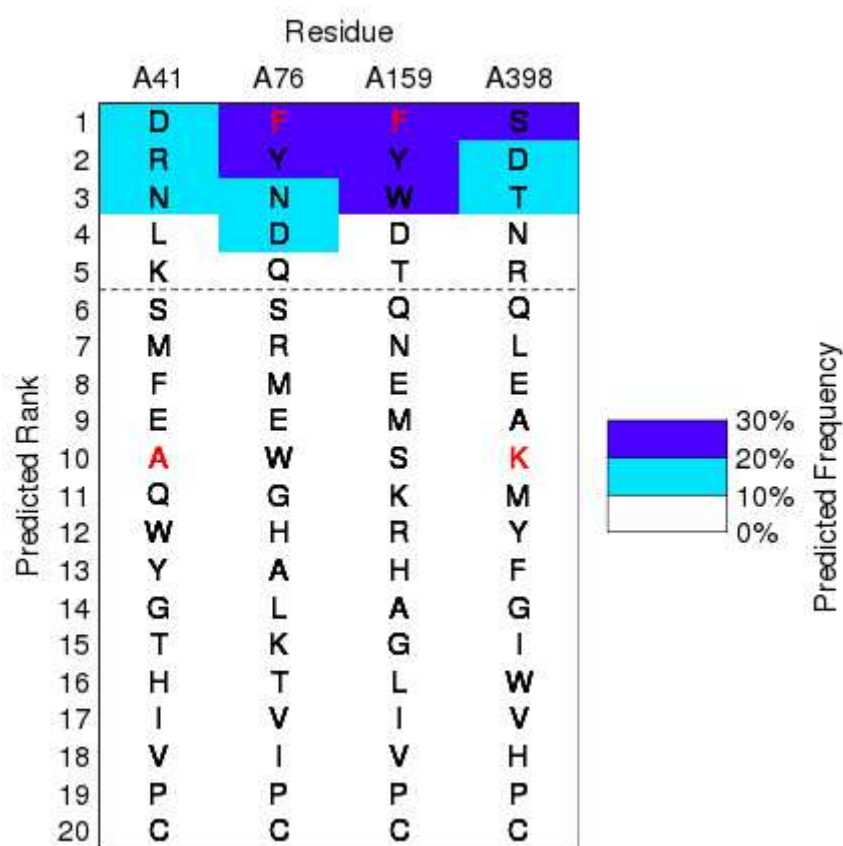
Y159 was exchanged against L-phenylalanine and L-alanine. It is well known that a mutation to L-phenylalanine increases the activity towards bulky substrates of ω -TA, which causes a polarity reduction and increases the flexibility of the cofactor PLP. This enables the intermediate to have room for movements within the substrate binding pocket [21].

Furthermore the putative flipping L-arginine (R398) [19,22], reported in **chapter 3**, was exchanged against L-leucine, L-serine and L-lysine. The exchange to lysine was reported with the complete loss of activity towards charged substrate [23]. Therefore it might be interesting

5) Towards biocatalytic β -keto ester transamination approaches

to investigate, if uncharged substrates like β -keto esters will be converted. Moreover, the conservation of these mentioned amino acid residues was analyzed in respect of evolutionary allowed or forbidden exchanges. Therefore the ROSIE tool –sequence tolerance- was utilized to investigate amino acid exchanges, which might be able to influence stability or function of 4AOA. Conserved amino acids within protein sequences often hide fundamental protein functions regarding to stability and function.

Table 5.5 Sequence tolerance of 4AOA at the positions R41, Y76, Y159 and R398. The table was created using the sequence tolerance tool of the Kortemme lab [24,25]. The dashed line marks 10 % of sequence frequency. The blue and purple field showing the predicted frequency, that a residue can be observed at a distinct position according to the stability of them.



R41 is mostly permuted against L-asparagine, L-glutamic acid, but also in some cases (less than 10% frequency) also mutations to L-leucine and L-lysine seem to be allowed. The residue Y76 is in the majority of variants a L-phenylalanine or L-tyrosine, but also an L-arginine, L-glutamate or even a L-glutamine residue are likely. The PLP coordinating residue Y159 is also allowed to mutate to L-phenylalanine, which was reported in literature, interestingly also L-tryptophan, L-glutamate and L-threonine are rarely permuted but they are allowed exchanges. The putative flipping L-arginine is in the most of the cases a serine residue and only in approx. 10 % of cases an L-arginine. Also the predicted frequency shows that L-serine is clearly favored, but it could be a hint that R398 is an important residue for at least

β -phenylalanine transaminases (compare to **chapter 3.3**). As previously described, are 11,243 Fold type I proteins with flipping arginine, which are 11 % of all oTAED entries. This confirms also the results of ROSIE sequence tolerance analysis. This position might have an influence on the substrate class of Fold type I enzymes.

Sequence analysis of the ω -TA family members with high similarity to VpTA

The evolutionary conservation of the ω -VpTA is shown in **figure 5.8**, which highlights that in particular the active site and some residues inside of helices are highly conserved (**dark purple**).

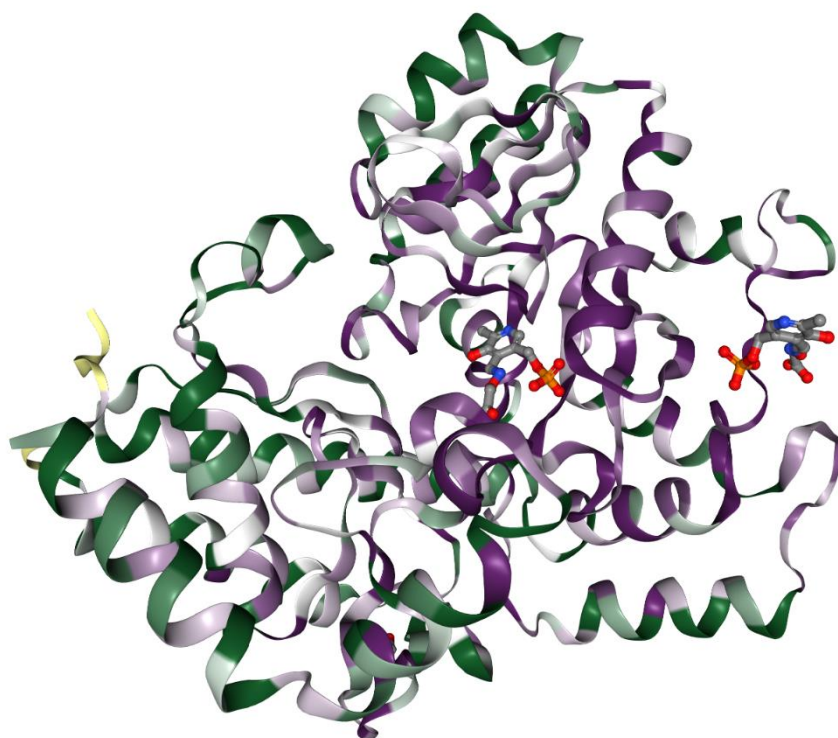


Figure 5.8 Conservation of amino acid residues of 4AOA. Highly conserved residues are shown in dark purple, conserved residues in white medium and highly variable residues in green. The frequency was calculated using ConSurf server using the PDB structure 4AOA [26,27]. The inhibitors of both subunits are displayed. The right inhibitor indicates the position of the active site of the second subunit.

Furthermore the relatives of 4AOA (35 and 95% sequence identity) were assembled for creating conservation analysis by ConSurf-protocol. The homologues sequences were collected from UniProt reference cluster UNIREF90 [26–28]. The next relatives to the ω -TA from *V. paradoxus* originate from quite different species. The closest relatives are exemplarily listed: *Variovorax* sp. CF313 (ID J3CA53), *Elioraea tepidiphila* (ID UPI000369FBA1), *Paraburkholderia phymatum* (ID B2JW91), *Phialocephala scopiformis* (ID A0A194X0V1),

5) Towards biocatalytic β -keto ester transamination approaches

Bosea lupine (A0A1H7T9F8), *Magnaporthe oryzae* (ID L7I9P9) and from *Claophialophora psammophila* CBS 110553 (ID W9WU23) (Figure 5.9).

It was not surprising that *Variovorax* contain ω -TA with a high grade of similarity, but it was not expected that also *C. psammophila*, an asexual yeast-like fungi and *E. tepidiphila*, an α -proteobacteria, are showing quite similar protein sequences [29,30]. This relatives have in common a gap, compared all other sequences, of approximately 14 amino acid positions. This gap is located in 4AOA at the position R168 and A169. More than 130 sequences are showing four or twelve amino acid residues at this area in the alignment. This evolutionary deletion is located in a distance of 17.6 Å to the active site and located at the substrate entrance of 4AOA.

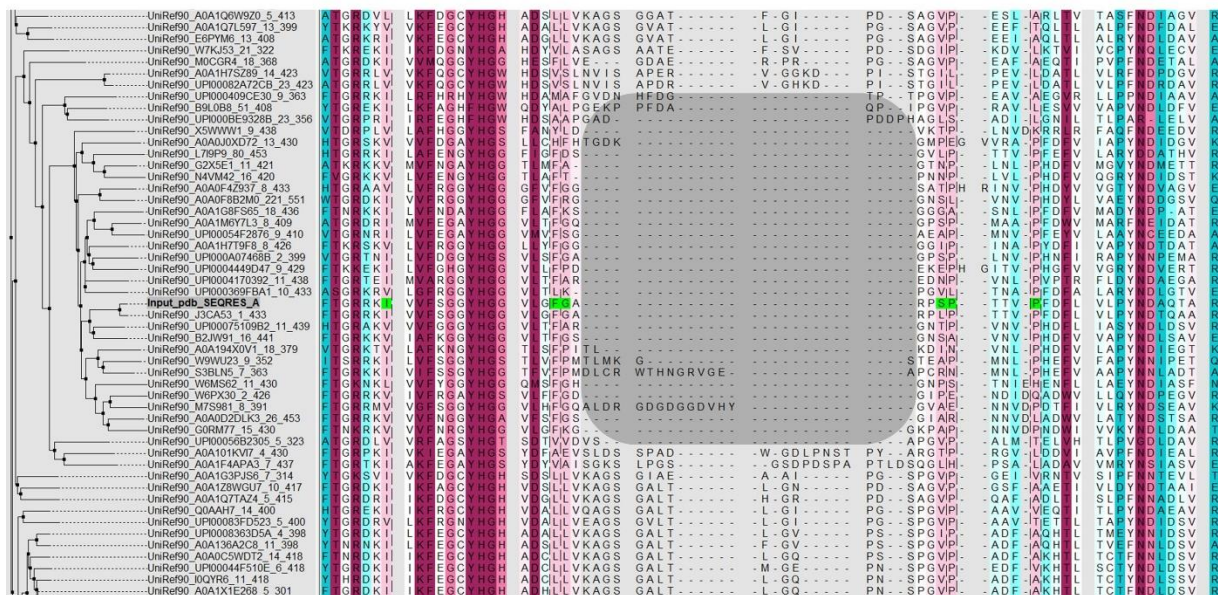


Figure 5.9 4AOA alignment for conservation analysis. 4AOA and close relatives showing a gap within the sequence alignment between positions 168 and 169 (grey box). This gap could be characteristic at substrate entrance for β -PA converting ω -TA. Purple color (high conservation), blue (medium conservation) no color (no conservation) and points indicating gaps. The sequence ID are UniProt shortcuts: Seed sequence was 4AOA (Input_pdb). The alignment was visualized using Chimera 1.1 [13].

The function of this part is not reported, but the location close to the substance entrance of the ω -TA might be important for the movement of aromatic substrates into the active site. An alignment is hardly interpretable by visual inspection, therefore the mentioned engineering positions were analyzed using the graphical interpreter Skylign [31]. The created alignment (**Figure 5.9**) was utilized and each position of interest was analyzed.

In most of the cases the PLP-binding residue Y159 is clearly conserved as tyrosine (probability 0.987), but an exchange to phenylalanine is also allowed (probability 0.013). However, no other amino acid residues are permitted at this position and the neighboring positions are strictly a histidine (H160) and next to it a glycine (G161). Moreover the carboxyl-moiety coordinating position R41 is strictly conserved as arginine within the small pool of close relatives, but compared to a larger set of less homologue sequences R41 gets variable to other amino acid residues (**table 5.5**). This is an additional hint that R41 is especially important for β -PA converting ω -TAs, but is lacking in different (*S*)-selective ω -TA like in *V. fluvialis* [17,32,33]. Furthermore the second arginine residue, which was selected as engineering site R398, is not conserved (probability 0.178) and can be exchanged against several different amino acids. Also Y76 is not conserved (probability 0.156) and the sequential entropy shows clearly that tryptophan (probability 0.725) and phenylalanine (probability 0.094) are allowed, but also other non-aryl amino acid residues are occurring like histidine and methionine.

5) Towards biocatalytic β -keto ester transamination approaches

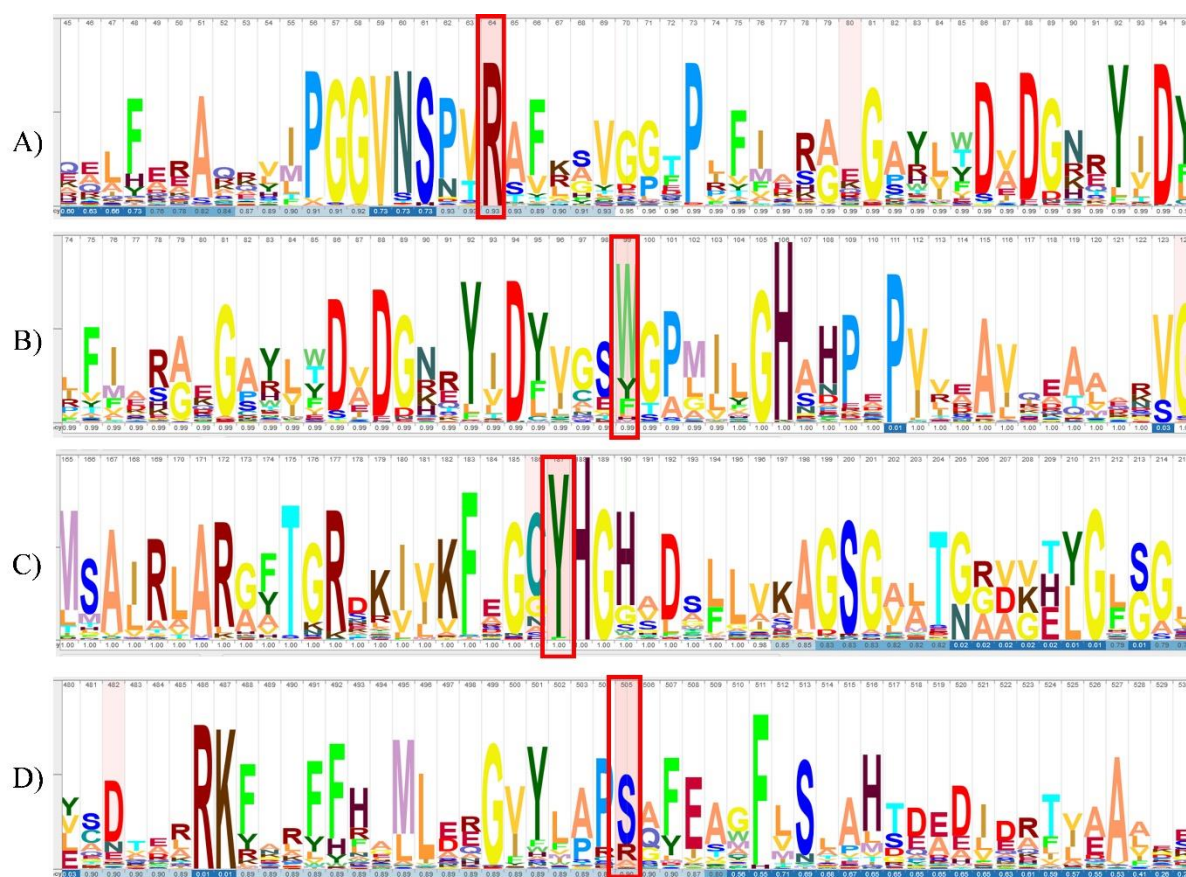


Figure 5.10 Conservation of engineered positions within 150 homologues sequences. Red bracket amino acid position of interest: **A) R41**: probability 1.0, is highly conserved no other residues found. **B) Y76**: probability 0.156, most frequent amino acid W. **C) Y159**: probability 0.987, conserved but F is allowed. **D) R398**: probability 0.178, other occurring amino acids are S, A, L, Y. Large letters symbolizes the frequency compared to other amino acid residues at this position. The higher the letter, the more the relative entropy of the amino acid position [34]. Alignments were performed using the visualization tool Skylign [31].

It is notable that R41 is the only strictly conserved residue in the presented engineering concept. Likewise this means that a change of R41 will cause a change in enzyme properties, because otherwise this position would show higher sequence entropy. Besides, the exchanges Y76F, Y159F and R398S exist in nature and those positions are not strictly conserved. Nonetheless, also not naturally occurring amino acid exchanges were performed at these positions to investigate the influence.

5.1.3.2) Creation and activity tests of selected engineering sites

All mentioned mutations were created using site directed mutagenesis PCR with mismatching DNA-oligomers. The resulting variants were sequence analyzed to identify whether the amino acid exchange was successful. The exchanges were performed as single site mutations and combinations were built of R398 and to Y76.

All variants were successfully expressed, but some variants like Y159A, showed no binding of PLP, which is reasonable with regard to binding mechanism of PLP. The assumption is that useful exchanges lead to enzyme variants which are losing their activity towards the charged substrates like β -PA and α -glutamic acid. Therefore the variants were using different amino donors and different acceptors. Finally also the acceptor ethyl-3-oxo-phenylpropanoic acid was tested. The results are reported in table 5.6.

β -PA conversion – test of initial activity

The wild type enzyme shows activity towards different amino donor substance like 3-amino butyrate and slightly towards L-alanine and PEA. However, the highest enzymatic activity can be seen with β -PA. This can also be explained by the decarboxylation of the resulting β -keto acid and is comparable to the results of Crismaru *et al.* 2013 [17]. Therefore the reaction time of β -PA tests were only 90 s and all other reaction mixtures were performed for at least 21.5 h due to the low activity of the ω -VpTA. Beside the mentioned wild type substrate β -PA, also the low *rac*-3-amino-butyric acid activity, which was reported by Crismaru *et al.*, was confirmed for the wild type variant and for Y76F. The variants Y76A/S, R41S/A, E75S and Y76F + R398K lost their former activity towards the reference substrate β -PA (**Table 5.6**).

R41 as important residue for β -phenylalanine binding

Furthermore Crismaru *et al.* performed also activity tests using the variant R41A resulting in a non-active ω -VpTA towards β -phenylalanine, which is also observed in this activity test. However, R41A showed activity towards non- β -phenylalanine substrates which might be a hint that R41 is particularly important for the conversion of this β -amino acid.

5) Towards biocatalytic β -keto ester transamination approaches

Table 5.6 Specific transamination activity (U mg^{-1}) of different ω -VpTA variants against different amino acceptor and amino donors. U was defined as $\mu\text{mol min}^{-1}$ of amino donor substrate turnover. The reaction mixture contents and reaction conditions are showed in **table 5.2**. The standard variation (\pm) is calculated from two independent reactions. Black filled fields showing no activity. *determined after 90 s. \blacklozenge determined after 21.5 h. (slow reactions)

	PA-KG*	PE-KG \blacklozenge	AB-KG \blacklozenge	AL-KG \blacklozenge	PE-EOPP \blacklozenge
Wild type	10.2 \pm 0.2	0.03 \pm 0.002	0.25 \pm 0.02	0.016 \pm 0.04	0.02 \pm 0.0006
R41S	0	0.05 \pm 0.007		0.029 \pm 0.021	
R41K	0.83 \pm 0.11				
R41A	0	0.053 \pm 0.047	0.016 \pm 0.010	0.029 \pm 0.055	0.038 \pm 0.019
E75S	0				
R41S + E75S	0				
R41K+ E75S	0				
R41A+ E75A	0	0.11 \pm 0.037			
Y76S	0	0.27 \pm 0.008		0.011 \pm 0.009	0.037 \pm 0.009
Y76F	13.6 \pm 1.33	0.03 \pm 0.004	0.30 \pm 0.003		0.041 \pm 0.004
Y76A	0				0.015 \pm 0.003
Y159F	15.0 \pm 5.8	0.03 \pm 0.003			0.022 \pm 0.002
Y159A	1.8 \pm 0.09	0.003 \pm 0.002			0.017 \pm 0.002
R398K	1.3 \pm 0.013	-	-	-	
R41K+R398K	0.41 \pm 0.001	-	-	-	0.017 \pm 0.004
Y76F+R398K	0	-	-	-	

Beside the substrate binding mechanism, the salt bridge between R41 and E75 seems to be very important for the functionality of ω -VpTA. The salt-bridge was postulated as a characteristic motif for β -amino acid converting ω -TA and the interaction might be important for the orientation of R41, which can be underlined by the presented results, because no variant with a double mutation at R41 and E75 displayed activity [17]. The only exception is R41A-E75A, which is showing activity towards the aromatic amino-donor PEA. This position seems also to be important for β -keto ester activity. A short non-polar residue, at position 41, like L-alanine might be beneficial for binding molecules absent of a free carboxylic-group (i.e. amines and amino esters). In addition also a hydrophobic interaction as well as aromatic π - π stacking of the substrate might be necessary for β -amino acid substrates, because 3-amino butyric acid shows only low activity and Crismaru *et al.* reported that the small β -amino acids, like β -alanine cannot

be converted, but the more hydrophobic amino acid β -leucine can be transaminated using ω -VpTA [17].

Substrate coordinating Y76

The amino acid residue Y76 seems to fulfill two functions. The first function might be the binding of aromatic substrates, like β -PA or PEA. The variant Y76F showed activity towards all substrates with the exception of L-alanine, which could be expandable by a lower binding energy due to the loss of the hydroxyl-moiety. Furthermore the residues Y and F may function as important intramolecular interaction point with other residues, which stabilizes the structural arrangement of the P-pocket, because Y76A causes a loss in activity towards all substrates with the exception of EOPP. The smaller residue might be able to rearrange EOPP within the binding pockets and enables more space within the P-pocket. This theory can be supported by the finding, that Y76S is able to convert EOPP, PEA and L-alanine but not β -PA.

The flipping arginine R398

Concluding R398 might inhibit the binding of EOPP (lacking of a free β -carboxyl moiety) as flexible binding residue within 4AOA [17]. Consequently R398 was mutated to the amino acids K, L and S. It was therefore investigated whether R398 is indispensable for the turnover of β -PA with α -ketoglutarate. It was found that R398L was no longer able to convert the standard substrates, whereas the variants R398S and R398K showed a low residual activity (**Figure 5.11**). It can therefore be assumed that the binding of α -ketoglutarate takes place via R398, since no interaction with R398 has been reported for the binding of β -PA [17]. Furthermore all R398 variants showed low activities towards PEA and EOPP (0.006 to 0.018 U mg⁻¹).

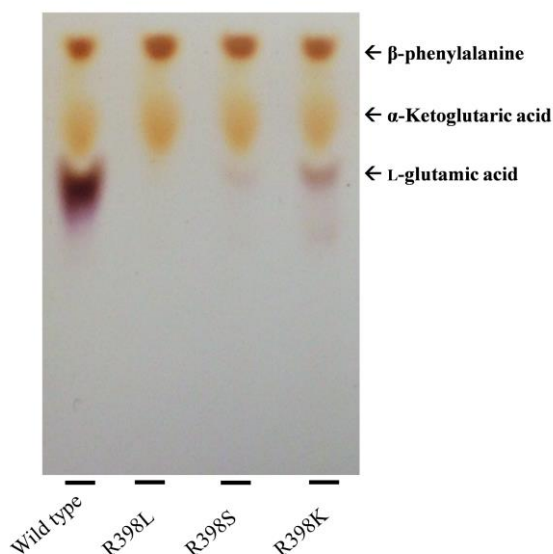


Figure 5.11 Influence of R398-variants on β -PA conversion. The conversion of the substrate β -PA was observed and L-glutamic acid detected on TLC plates. The reaction samples were analyzed after 5 min of reaction time. Therefore the activity was tested with 0.1 mg mL^{-1} of enzyme at 40°C . Reaction mixture: 15 mM *rac* β -PA, 15 mM α -ketoglutaric acid, 0.2 mM PLP in 50 mM NaPP (pH 7.2).

This finding supports also the assumption, that α -ketoglutaric acid is differently bound by ω -VpTA. More precisely it was reported that R398 enables an alternative binding mechanism for example for the mentioned α -ketoglutaric acid [32]. The PLP-binding residue 159 can be successfully exchanged to phenylalanine, which was shown for the ω -TA from *Ruegeria sp.* TM1040 by Pavlidis *et al.* [21]. The exchange of Y159A shows also, that the activity decreases drastically, when no π - π stacking stabilizes the PLP-substrate-intermediate. At all the created variants showed that non- β -PA activity is very low compared to the wild type, which suggests that the binding mechanism is highly optimized for β -PA, α -ketoglutaric acid and pyruvate. A further binding amino acid residue might inhibit the binding of non-charged β -ketones.

False positive activity?

Amino acid exchanges R41A, Y76S and Y76F showed the largest effect in the reaction system with PEA and with the β -keto ester as acceptor molecule. It can be assumed that the change in PEA concentration is not an immediate indication of activity, since the wild-type also shows a background activity of at least 0.02 U per mg . The decrease in PEA concentration could be due to the first half transamination reaction of the PLP-PMP reaction cycle (see **chapter 1**) in which the amino donor reacts together with PLP to PMP. However, if PMP cannot transfer its amino group to an acceptor, PMP⁹ remains in the reaction batch. Since the concentration of PLP was

⁹ PMP shows lower adsorption at 395 nm and therefore reaction solution is less yellow than PLP [59]

0.2 mM, very small activities could be attributed to this reaction, which would not be evidence of real activity. This theory is supported, by the observation that the yellow reaction solution (yellow indicates PLP) was converted into a colorless solution by precipitation of the enzyme at the same time, because PMP is colorless [35].

Alternative activity determination

As an alternative to the determination of the amino donor, the product, β -amino ester, was quantified. However, the disadvantage is that the expected amount of product produced by the engineered enzyme can be very small and therefore the quantification might be challenging. Therefore gas chromatography (GC) method was performed. But even with GC it could not be determined clearly whether a product was created since the quantification limit was ~ 0.25 mM (The estimated concentration was approx. 0.15 mM.).

Nonetheless, the variant R41K-R398K may have shown product formation, when using the amino donor *o*-xylylenediamine (OXD) (**Figure 5.12**). The resulting product concentration, is nearby, but lower than the quantification limit of 0.25 mM. The variant R41K-R398K showed a possible product peak during the analysis by GC, which however was slightly shifted in time but was not present in comparable chromatograms of negative controls.

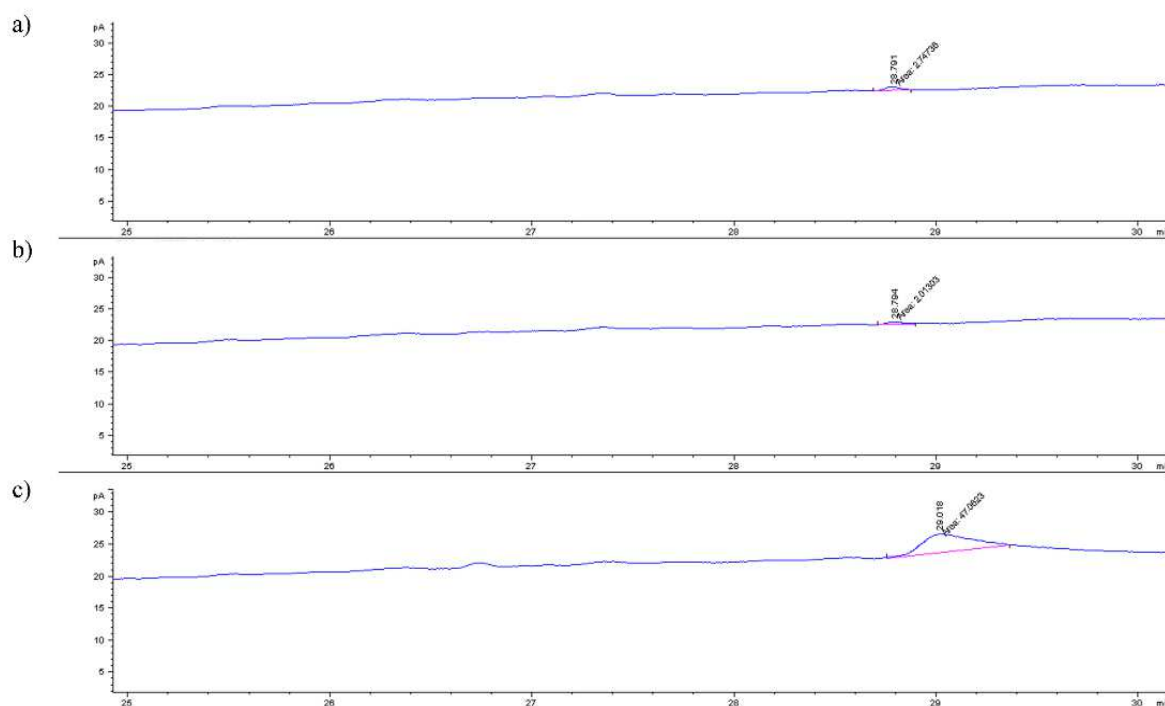


Figure 5.12 Putative product formation of ω -VpTA variants using OXD as amino donor. The experiments were performed at 40°C. a) Y76F-R398K b) R41K-R398S c) R41K-R398K.

5) Towards biocatalytic β -keto ester transamination approaches

The Y76F-R398K and R41K-R398K variants also showed smaller measurement signals at the edge of the detection limit. However, it is unclear for Y76F-R398K and for R41K-R398K, whether they aminate the β -keto ester substrate, because of the small signal intensity, but the retention times are comparable to the standard. Thin layer chromatography was also performed, but no product formation could be observed with this method. More certainty could result from a TLC or GC-MS analysis. However, it is also clear that the possible enzymatic activity is very low and further mutagenesis experiments have to be carried out to increase the product yield.

Influence of amino acid exchange on protein stability

Mutations that could be useful for the conversion of a new substrate could have a negative effect on protein stability. Especially the position R398 was therefore examined in detail, as mutations at this position have a strong influence on the activity. First experiments using R398 variants showed, that precipitations were obtained after incubation at 40°C during 24 h of incubation in 15 % DMSO containing solutions. Therefore, all tested and expressed variants of R398X are displayed in **table 5.7**. In contrast the wild type enzyme showed stability over 24 h of incubation time and retained as yellow (PLP binding) ω -TA in solution. Especially the variant R398L showed a reduced stability in the reaction mixture and it is therefore difficult to determine whether the functionality was destroyed as well as the stability was negatively affected, since no activity was observed in relation to β -PA (**Figure 5.12**). This was also indicated by FoldX calculations using 4AOA. In contrast, the variants R398K and S showed an increase in stability according to FoldX. However, calculations by HoTMuSiC showed that all R398 variants were destabilizing.

Table 5.7 Stability calculations of R398 variants. Firstly the 4AOA structure was energy minimized using the FoldX repair function. For calculations the Yasara plugin of 4.0 FoldX was utilized [36]. ΔT_m was calculated using the algorithm HoTMuSiC and PoPMuSiCv3 within dezyme online server [37].

Variant	$\Delta\Delta G_{(\text{FoldX})}$	$\Delta\Delta G_{(\text{PoPMuSiC})}$	$\Delta T_m (\text{HoTMuSiC})$
R398K	-0.44 kcal mol ⁻¹	0.88 kcal mol ⁻¹	-0.4 °C
R398L	0.02 kcal mol ⁻¹	- 0.04 kcal mol ⁻¹	-1.16 °C
R398S	-0.11 kcal mol ⁻¹	0.67 kcal mol ⁻¹	-0.85 °C

Furthermore, the PoPMuSiC algorithm also predicted that lysine and serine will increase the energy content of the protein, but leucine seems to be an energy neutral exchange according to FoldX and PoPMuSiC. On the other hand HoTMuSiC predicts a destabilization for R398L of 1.2 °C (T_m), which is confirmed by the weak but positive $\Delta\Delta G_{(\text{FoldX})}$ value. This example shows

once again that the prediction accuracy is too low (compare to **chapter 4**). The energy calculation shows at least that this residue is not involved e.g. in an important salt bridge(s).

5.1.4) Conclusion

In this study a promising variant was found, R41K-R398K, but it has to be demonstrated whether the enzyme variant has improved properties. In addition, more extensive experiments should be conducted to determine whether the enzyme is active or not, by varying the reaction conditions and by using more sensitive analytical techniques. Therefore, this part of the work can be understood as an initial basis which has shown that the chosen amino acid residues have an influence on the activity, but also on the stability. In particular, it was shown that R398 could indeed be the suspected flipping arginine residue, as all three mutations at this position resulted in a drastic decrease in activity compared to the original substrate. Furthermore, the elemental importance for the binding of the carboxyl moiety of β -PA could also be shown by mutations at position R41. Both arginine positions seem to be very important for the recognition of substrates.

Challenges and Outlook

ω -VpTA mutants that may show activity could be used for further random mutagenesis experiments. However, random mutagenesis requires a large number of variants, therefore it is also a challenge to perform larger screenings in high-throughput scale without any positive control. A second challenge is the stability of the β -keto ester substrate, as it has proved to be unstable in experiments with crude cell extracts. Furthermore, the question of chemical equilibrium remains. Therefore it would be beneficial to force a shift of the equilibrium by using co-product removal systems or special amino donors (e.g. OXD). However, since it could not be clearly proven whether OXD is accepted as a substrate by the wild type ω -VpTA, the usefulness of screening on this basis is still questionable for the time being. As an alternative to a large mutagenesis study, several already engineered and wild-type transaminases of fold type I and IV were investigated in a small scale ω -TA screening in (next subchapter, **chapter 5.2**).

5.2) Screening of an ω -TA library towards β -keto ester converting enzymes.

In the following subchapter an ω -TA library, containing engineered and wild type (*S*) and (*R*) ω -TA from different sources of microorganism (fungi and bacteria), were investigated using *o*-xylylenediamine as screening agent to detect enzymes with activity towards β -keto ester substrate. The aim was the enzymatic synthesis of 3-amino-3-phenylpropanoic acid ethyl ester (β -amino acid ester).

This chapter was adapted from the following manuscript:

Screening of an ω -transaminases library towards β -keto esters activity as novel substrate β -amino acid synthesis.

Oliver Buß^a, Moritz Voß^b, André Delavault, Pascal Gorenflo, Christoph Syldatk^a, Uwe Bornscheuer^b and Jens Rudat^a

^a Institute of Process Engineering in Life sciences, Section II: Technical Biology, Karlsruhe Institute of Technology, Karlsruhe Germany. ^b Department of Biotechnology and Enzyme Catalysis, University of Greifswald, Institute of Biochemistry, Felix-Hausdorff-Str. 4, 17487 Greifswald, Germany

Publishing details:

Published on 18 May 2018 in *Molecules* (MDPI)

Doi: 10.3390/molecules23051211

Authors' contribution to this publication

Oliver Buß wrote the manuscript as first author, designed, performed experiments and was wrote the manuscript. **Moritz Voß** revised and edited the manuscript. **André Delavault** performed flash chromatography and analyzed NMR data. **Pascal Gorenflo** performed gas chromatography experiments. **Uwe T. Bornscheuer** and **Christoph Syldatk** initiated and supervised the project. **Jens Rudat** revised the manuscript and contributed to the conception of the experiments.

5.2.1) Introduction

Like mentioned before transaminases (TA) are promising enzymes for the synthesis of chiral amines, amino acids and amino alcohols. The pyridoxal-5-phosphate (PLP) dependent transamination mediates the transfer from an amino donor group onto an acceptor substrate. Aldehydes, ketones, keto-acids or keto-esters can serve as acceptor substrate [14,38]. As an alternative to complex enzyme engineering (chapter 5.1.) natural resources of wild type ω -TA and already available engineered ω -TA were tested towards activity for β -keto ester as donor molecules.

β -amino acid esters as alternative target

β -PA esters are relevant for the synthesis of nitrogen-containing heterocyclic compounds, e.g. for synthesis of β -lactams, aminophenylpropanoic acid-terminated polyoxyethylene esters, nicotinamide derivatives for treatment of respiratory and allergic diseases, (*S*)-dapoxetine (reaction with LiAlH_4 , and for synthesis of putative anti-amnesiant agents) [39–44].

The first example of an ω -TA mediated transamination of a β -keto ester was reported by Midlefort *et al.*. They demonstrated that the synthesis of Imagabalin, a chiral β -amino acid containing drug for diabetes treatment, is possible from the β -keto ester precursor employing an engineered variant of the fold type I (*S*)-selective ω -TA from *Vibrio fluvialis* [14]. To our knowledge, such a synthesis was never reported for aromatic β -amino acid ester, β -PA or rather α -hydroxy- β -phenylalanine containing natural substance paclitaxel (Taxol) [45]. Until now, different ω -TA based methods for the synthesis of optical pure β -PA, like chiral resolution or enzyme cascade reactions were reported (**chapter 1.2**) [5,46,47]. Thereby, the synthesis from the stable asymmetric β -keto ester is favored for chiral synthesis of β -PA ester, since the corresponding β -keto acid is not stable in water and underlies decarboxylation. An approach to circumvent the decarboxylation is the creation of a reaction cascade starting from the β -keto ester using a lipase for the hydrolysis of the ester and an ω -TA for the direct conversion of the instable β -keto acid intermediate. These alternative enzymatic synthesis methods for the preparation of β -PA were already presented in **chapter 1** and **5.1** (mostly Mathew *et al.*) [4,33,48].

To avoid critical cascade intermediates, the direct transamination of the stable aromatic β -keto ester would be beneficial and result in the chiral β -PAEE, which can be chemically or enzymatically hydrolyzed to β -PA. The only obstacle for this efficient biocatalytic approach is the lack of known ω -TA with activity towards β -keto esters. An exception is the engineered

ω -TA variant from *V. fluvialis* with activity towards the aliphatic β -keto ester Imagabalin precursor [14]. In general the displayed method could allow the enantioselective synthesis of β -PAEE and simplifies the purification using extraction methods. Furthermore, the strategy could also improve the atom efficiency (amino donor/acceptor ratio) compared to existing β -PA asymmetric strategies.

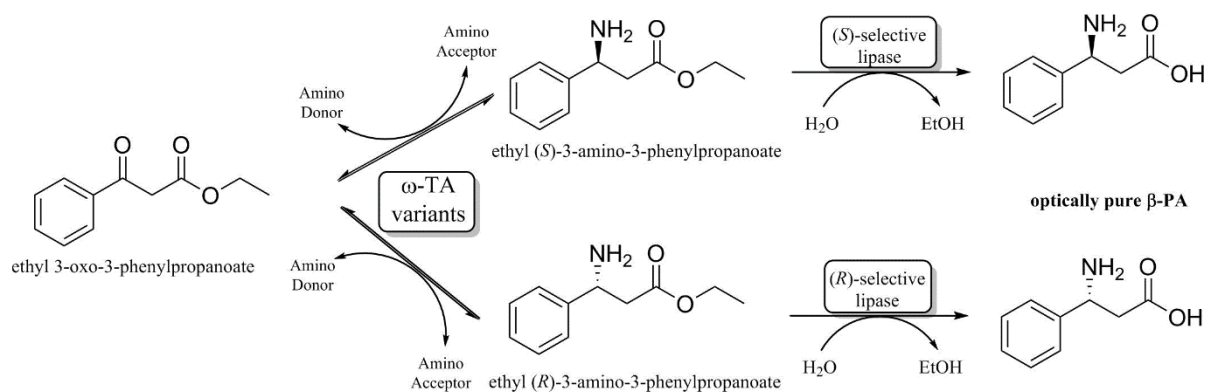


Figure 5.13 Synthesis strategies to chiral β -PA or β -PAEE starting with the β -keto ester substrate EOPP (β -KE). β -PAEE could be isolated, using solvent extraction or used in a second enzymatic step using lipase. This step would increase the optical purity and will additionally improve the product purification.

To enable the proposed direct synthesis of β -PAEE by amination of the stable β -keto ester, a screening of an ω -TA library (Group of U. Bornscheuer) was performed to identify variants converting ethyl-3-oxo-3-phenylpropanoate. The selected library contained ω -TA from Fold type I and IV of PLP-dependent enzymes to identify variants with (*R*)- and (*S*)-selectivity. Several wild type transaminases were analyzed as well as engineered variants from *Silicibacter pomeroyi* (PDB ID: 3HMU), *Rhodobacter sphaeroides* (PDB ID: 3I5T), *Ruegeria sp.* TM1040 (PDB ID: 3FCR) and *V. fluvialis* (PDB ID: 4E3Q). Also, the engineered ω -TA from *Codexis* (ATA117 11Rd; PDB ID 3WWJ) was included in the screening (see **Table S2**). For the screening the amino donor *o*-xylylenediamine (OXD) was utilized, because it showed promising acceptance by several ω -TA and serves as smart amino donor, since OXD shifts the equilibrium towards the products by polymerization of the formed isoindole co-product [49]. The formed polymer results in clearly visible precipitate, indicating conversion in the screening [49]. After a screening of ω -TA variants was performed, the hits were analyzed in respect of yield and optical purity. It was also examined whether a synthesis on a larger scale is possible.

5.2.2) Material and Methods

Materials

All chemicals were purchased from Sigma-Aldrich or Carl Roth in highest purity grade (>99%), otherwise the compounds are indicated.

Protein-expression and purification

All ω -TA for large scale expression were included in pET vector systems. The enzymes were expressed in the *Escherichia coli* (*E. coli*) BL21 strain using auto-induction-medium LB-broth with trace elements (Formedium, UK) and purified using Ni-affinity chromatography according to Buß *et al.* 2017 [50].

High throughput screening

For screening the ω -TA library *E. coli* BL21 strains were used containing pET and pGASTON plasmids with resistance genes against kanamycin and ampicillin. The concentration of kanamycin was 50 $\mu\text{g mL}^{-1}$ and for ampicillin 100 $\mu\text{g mL}^{-1}$ in the medium for growing and expression. The cells were precultured in 0.2 mL LB-medium overnight at 30 °C, 700 rpm in 96-microtiter plates (MTP). From this preculture 20 μL were transferred to inoculate 96-deepwell plates filled with 960 μL TB-medium and appropriate antibiotics. The plates were sealed with oxygen permeable membranes (Rotilabo-cling film, Carl-Roth, Germany). The cells were incubated at 37 °C for 6 h at 700 rpm and the expression was induced by the addition of 0.5 mM IPTG or 0.2 % rhamnose. The cultures were incubated at 26 °C for 20 h at 700 rpm. For harvesting, the cells were settled at 5.000 g for 20 min at 4 °C in a robotic centrifuge (Rotanta 460-Robotic, Hettich GmbH, Germany). The cell pellets were resuspended in 50 mM HEPES buffer pH 7.5 with 0.1 mM PLP for washing the pellets. After centrifuging the pellets at 4.500 rpm for 20 min at 4 °C, the pellets were resuspended for lysis in 50 mM HEPES buffer pH 7.5 with 0.1 mM PLP and 1 mg/mL lysozyme and incubated at 30 °C for 90 min at 700 rpm. The cell debris was sedimented at 4 °C and 5,000 g for 20 min. The supernatant was carefully transferred in a clean 96-well plate. 50 μL of cell free supernatant was transferred to 150 μL of reaction mixture. The final mixture contained 50 mM HEPES buffer pH 7.5, 5 mM of *o*-xylylenediamine, 7.5 mM of ethyl-3-oxo-3-phenylpropanoate (>95% purity, Sigma-Aldrich), 1 mM PLP and 10 % (v/v) dimethyl sulfoxide (DMSO). The reactions were performed in 96-well MTPs at 30 °C and 120 rpm overnight.

TLC-(MS) analysis

For the thin layer chromatography, 100 μ L samples were taken from enzymatic synthesis mixture and extracted with 200 μ L of ethyl acetate (EtOAc). The extraction was performed at shaking rate of 2.000 rpm for 5 minutes in a ThermoMixer (Germany, Eppendorf) and phases were separated by centrifugation at 13.000 rpm in benchtop centrifuge (Germany, Eppendorf). To analyze the synthesis mixture, a mobile phase consisting of acetone: *tert*-butyl ether, acetate and water (45:25:20:10) was used. For observation of reaction process samples of 10 μ L were spotted on standard silica TLC plates (Sigma-Aldrich) and stained with 0.5% ninhydrin-solution. For determination of product mass, a synthesis sample was spotted 15-times on TLC the plate, separated and analyzed using a thin-layer-chromatography mass spectrometer with electron spray ionization (expression CMS, Advion). Samples were taken directly from TLC-plate using Plate Express-TLC-plate reader and methanol for solubilization. The samples were compared to a β -phenylalanine methyl ester as reference substance. For blanking the MS-signal a TLC spot without substrate/product were taken and subtracted from sample measurements.

HPLC analysis

For HPLC analysis see chapter 4 methods section.

Enzymatic synthesis

Enzymatic synthesis of the β -phenylalanine ethyl ester (β -PAEE) was performed in a 1 mL scale consisting of 50 mM HEPES buffer (pH 7.5), containing 10 to 30% (v/v) of DMSO, 1 mM of pyridoxal-5-phosphate, 10 mM of ethyl-3-oxo-3-phenylpropanoate and different amounts of different amino donors. The concentration of the amino donors and support systems are mentioned in results section. In general, 0.2 mg mL⁻¹ of purified ω -TA were used in the reaction mixture. The temperature was set to 30 °C at 500 rpm shaking rate. 75 μ L from samples were taken at different times and directly stopped using heat (99 °C), 1 M NaOH and subsequently neutralized with 1 M HCl for further analysis using HPLC. A second sample was taken of 75 μ L and extracted using 100 μ L EtOAc to isolate the β -PAEE. For extraction, the sample were shaken at 2,000 rpm for 5 min and analyzed using TLC-(MS).

Design of experiments

For investigation of the influence of solvent content of DMSO in the reaction medium and for optimization of substrate concentration a design of experiments was performed using

5) Towards biocatalytic β -keto ester transamination approaches

Design-Expert 8 with 11 experiments for each selected ω -TA. Three center points were chosen for the experiment setup. At the same time the concentration of β -KE were varied from 10 to 50 mM, the concentration of OXD from 10 to 100 mM and the content of DMSO (v/v) was tested in the range from 10 to 30% (v/v). The response was defined as yield of β -PAEE using GC analysis.

Gas chromatography (GC)-analysis

GC-analysis was performed in order to monitor the β -PAEE concentration. Therefore, β -PAEE-standard (Sigma-Aldrich) was first solved in 50 mM HEPES-buffer (pH 7.5 according to enzyme synthesis) and a dilution series was mixed. The samples were extracted with 1:1 (v/v) of EtOAc. The two-phases were mixed according to the extraction for TLC experiments. GC-analysis was performed using a 6850N Network GC system from Agilent employing a DB-wax column (30 m (length), 0.25 mm (diameter), 0.25 μ m (film)) and flame ionization detection. 2 μ L of sample were injected (split ratio 10:1) at a temperature of 250 $^{\circ}$ C (injector temperature). The separation was achieved using an oven temperature gradient of 40 to 250 $^{\circ}$ C (8 $^{\circ}$ C/min). The flow rate was set to 0.6 mL min⁻¹. β -PAEE was detected at a retention time of 28 min.

Determination of water activity

Water activity a_w was tested using an AquaLab 4TE device (METER, USA) with a chilled mirror dew point sensor. The measurements were performed at room temperature and buffer solutions with different DMSO content were compared.

Large scale synthesis of (*S*)-phenylalanine ethyl ester and product purification

For production on a larger scale (200 mL), 30 mM OXD (0.82 g) and 30 mM β -KE (1.15 g) were solved in an aqueous 30% (v/v) DMSO solution. The pH was adjusted to 7.5 with a 100 mM HEPES buffer and 1 mM PLP was added. The reaction was started by adding 20 mg of purified 3FCR_4M. The reaction process was monitored by thin layer chromatography (solvent: 40% n-hexane, 40% EtOAc, 10% acetic acid, 10% MeOH). The pH value was monitored by pH measuring strips. The reaction was performed in a 500 mL round bottom flask at a rotary evaporator at 150 rpm and 30 $^{\circ}$ C under standard pressure. After 48 h, the reaction was stopped by EtOAc extraction using 3 times 150 mL of solvent. The solvent was filtrated to remove dark precipitate and the filtrate was dried using anhydrous MgSO₄. The extraction solvent was subsequently evaporated at the rotary evaporator and the product was solved in 5 mL EtOAc containing 5% MeOH and 10% acetic acid. The purification was performed using

MPLC (Reveleris Prep., BÜCHI Labortechnik AG, Switzerland). For separation, a Reveleris PureFlash 4g column and a flow rate of 15 mL min⁻¹ was used. As method, the liquid injection was selected and a gradient of *n*-hexane and EtOAc (5% MeOH and 10% acetic acid) was used as follows: 50% for 3.1 min, 50 to 100% EtOAc in 3.1 min, 100% holding for 3.1 min. To elute β -PAEE a gradient starting with EtOAc and MeOH was performed starting with 95% of EtOAc. Within 6.3 min the concentration of methanol was increased to 100%. Peaks were observed using an evaporative light scattering detector and fractions collected. The fractions containing β -PAEE were again evaporated and freeze dried to remove acetic acid. The product was analyzed using TLC, HPLC (optical purity) and by NMR.

Analytical NMR data of (*S*)-phenylalanine ethyl ester

(*S*)-ethyl 3-amino-3-phenylpropanoate (**2**) acetate salt as brown solution.

¹H NMR (Methanol-*d*₄, 300 MHz) δ (ppm): 1.17 (3H, t, ³*J* = 9 Hz, CH₂CH₃), 4.57 (1H, dd, ³*J* = 9 Hz, ²*J* = 15 Hz, CHCH₂CO), 4.72 (1H, dd, ³*J* = 6 Hz, ²*J* = 15 Hz, CHCH₂CO), 5.68 (2H, q, ³*J* = 9 Hz, CH₂CH₃), 6.27 (1H, t, ³*J* = 6 Hz, CHNH₂), 8.97-9.06 (5H, m, C₆H₅), 9.53 (2H, br s, NH₂).

¹³C NMR (Methanol-*d*₄, 300 MHz) δ (ppm): 14.36 (CH₂CH₃), 39.61 (CHCH₂CO), 52.94 (CHNH₂), 62.24 (CH₂CH₃), 128.42, 130.25, 130.40, 130.86 (C₆H₅), 171.23 (CO).

5.2.3) Results and discussion

5.2.3.1) Screening of ω -TA library

The ω -TA containing library was screened towards the β -keto ester substrate EOPP in the colorimetric *o*-xylylenediamine (OXD) assay. The screening was performed in 96-well MTP format, enabling the simultaneous analysis of various ω -TA variants. *E. coli* BL21 strains containing the expression plasmids pET and pGASTON were used for this purpose. The plasmids contained ω -TA fold type I and IV genes. The analyzed ω -TA variants are summarized in appendix (**Table S2**), including the 29 different ω -TAs. The concentration of the amino donor OXD was 5 mM in the screening assay. The plates were in total 24 h incubated and the cell lysate was utilized for activity tests. After starting the reaction by addition of ω -TA lysate solution, a strong staining was observed within the first hours for variants from *Ruegeria sp.* TM1040 ω -TA (3FCR). The staining was clearly visible after and resulted in dark precipitations after 24 h of incubation. In addition, the engineered Fold type IV ω -TA ATA117 11Rd from Codexis showed a slight staining. Beside those two variants, also ω -TA from *Silicibacter pomeroyi* (3HMU) showed a slightly change in color. However, it is known that only strong changes and precipitations are an indicator for enzymatic activity and therefore 3FCR variants and ATA117 11Rd were selected for further characterizations (**Figure 5.14**) [51,52].

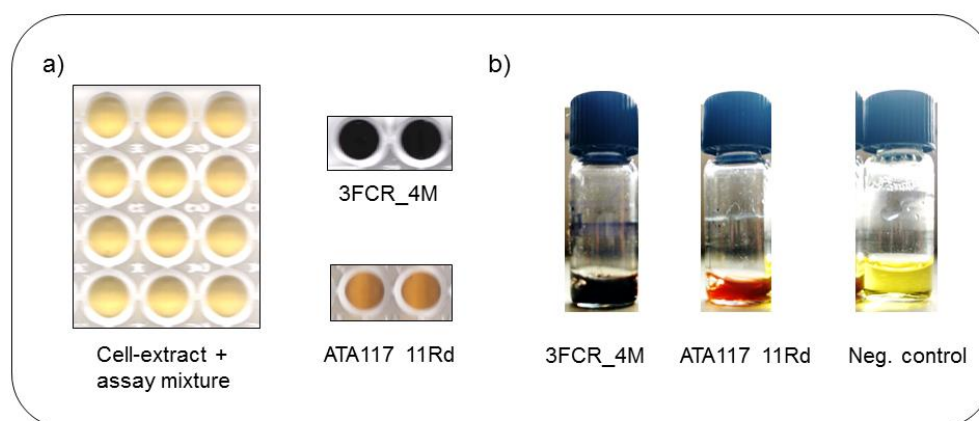


Figure 5.14 Screening for β -PAEE producing ω -TA. A) OXD was used as screening agent in 96-well plate screening. High activities resulting in dark precipitates. Yellow indicates that no or low activity is present. Brown and orange color are unclear, whether activity is present. Cell-extract mixed with assay ingredients are displayed as negative control. B) Result of 1 mL scale experiments after 24 h at 30 °C.

The variant of 3FCR contains four mutations and were chosen as promising enzyme for the synthesis of (*S*)-enantiomer of β -phenylalanine ethyl ester (β -PAEE) and for the synthesis of

(*R*)-enantiomer the engineered ATA117 with 27 mutations was selected. The 3FCR was firstly engineered by Pavlidis *et al.* towards the conversion of bulky chiral amines and afterwards by Weiß *et al.* for the conversion of bicyclic amines, which widen the small binding pocket of the enzyme [18,21]. The engineered aminotransferase ATA117 11Rd, harboring 27 mutations, from a homolog of an enzyme from *Arthrobacter sp.* KNK168 was designed by Savile *et al.* towards the conversion of the bulky substrate prositagliptin [53]. Furthermore, ATA117 belongs to the (*R*)-selective Fold type IV of PLP-dependent enzymes in contrast to the (*S*)-selective fold type I enzyme 3FCR.

5.2.3.2) Asymmetric synthesis of β -PAEE

The selected ω -TA variants were expressed in larger scale and purified using Ni-NTA chromatography. To find the best possible amino donor for this reaction, *o*-xylylenediamine (OXD), phenylethylamine (PEA), alanine and isopropylamine (IPA) tested. PEA shows a wide spread acceptance for all ω -TAs as amino donor and the corresponding acetophenone is less favorable by ω -TAs as amino acceptor. The corresponding acetophenone of PEA is not well accepted as ketone substrate and inhibits the reverse reaction, but on the other hand a clear disadvantage is the inhibition of the ω -TA by higher acetophenone concentrations [54]. Beside those three widespread amino donors, *o*-xylylenediamine (OXD) is a promising substrate, because it is able to polymerize after deamination and precipitates [51]. For that reason, the reaction is naturally shifted towards the products. Furthermore, L-alanine was utilized in an enzyme cascade reaction system consisting of glucose-dehydrogenase (GDH) and lactate dehydrogenase (LDH) to shift the equilibrium towards products [55].

Beside those amino donors also the asymmetric IPA was tested. The solubility of the β -keto ester substrate is only 2 mM in aqueous solutions, for that reason the DMSO concentration was increased to 30 % (v/v) to solubilize 10 mM of β -keto ester and to reduce slightly the water activity a_w to protect the β -keto ester [56]. The a_w -value of DMSO-HEPES solution was determined to be 0.966 (30% v/v), 0.980 (20% v/v) and 0.998 for pure HEPES-buffer. The pH of 7.5 in reaction mixture is a compromise between ester stability and ω -TA activity. The most ω -TA performing best at slightly alkaline conditions between pH 7.5 and 9, but in contrast the stability of ester substrate is under slightly acidic conditions higher. An equimolar ratio of OXD

5) Towards biocatalytic β -keto ester transamination approaches

was chosen, because by the law of mass action the equilibrium constant is very high caused by polymerization and precipitation of the resulting co-product of OXD. The reactions were performed in 1 mL scale at 30 °C with 1 mM of pyridoxal-5-phosphate and samples were taken after 1 h and 24 h. For (*R*)-selective ATA117 11Rd D/L-alanine instead of L-alanine were used. The reaction process was observed using TLC due to monitor β -PAEE formation (**Figure 5.15**).

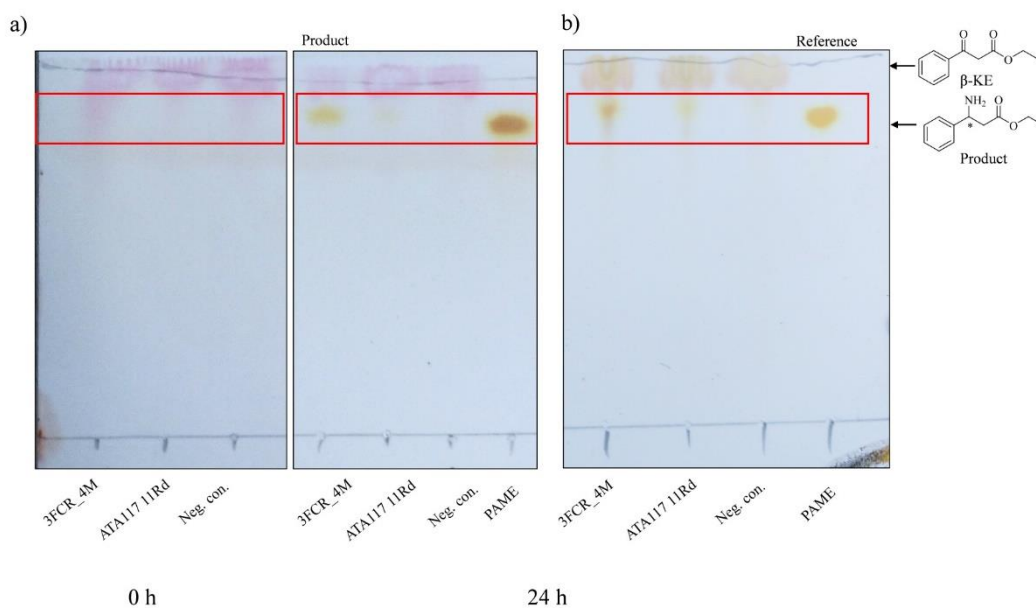


Figure 5.15 β -PAEE synthesis using alanine—GDH-LDH-NADH-regeneration system (a) and OXD (b). a) The reaction mixture conducted of 90 U ml⁻¹ of lactate dehydrogenase, 0.3 mg ml⁻¹ of D-glucose dehydrogenase and 250 mM of L-alanine respectively rac alanine for ATA117 11Rd. For both enzymes a slightly yellow spot is observed. b) 10 mM OXD were utilized as amino donor and a fast change in color was be observed.(PAME = β -phenylalanine **methyl ester**)

For identification of the product spot TLC-MS was used, as reference product the β -phenylalanine methyl ester β -PAME (R_f 0.83) was tested, which can be clearly identified on TLC-plates as slightly yellow spot after development using ninhydrin solution. The product spot β -PAEE showed an R_f value of 0.87 and running on the high of PEA and β -PA in TLC. However, PEA and β -PA are showing a purple colored spot after staining and additionally the mass is unique for β -PAME or β -PAEE. The β -keto ester substrate showing a quite similar mass, but showing a different running performance in TLC. Furthermore the variant 3FCR_4M_59L was tested, which was active but showed no improvement in comparison to 3FCR_4M and was therefore also excluded from further experiments. However, according to TLC analysis 3FCR_4M produced the expected product using L-alanine as amino donor and

pyruvate removal system (GDH-LDH). After 24 h samples were analyzed using EtOAc as extraction agent and analyzed the sample by TLC-MS. The product spot was determined to have a mass of 194.2 g mol^{-1} , which is in positive mode of the MS exactly the molecular weight plus one proton (**Figure 5.16**).

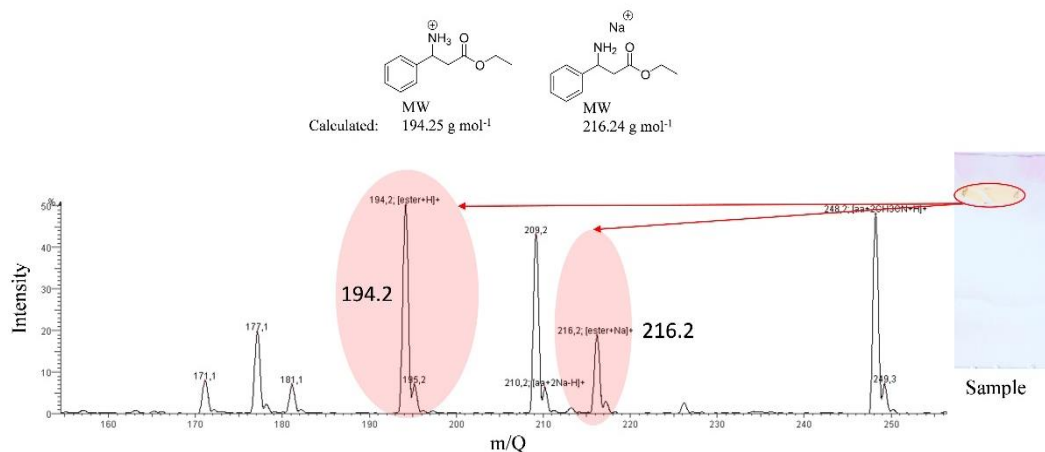


Figure 5.16 TLC-MS analysis of β -PAEE. β -PAEE was synthesized using 3FCR 4M. The resulting MS signals 194.2 (plus proton) and 216.2 (plus sodium) were identified as expected molecular weight signals for β -PAEE. TLC-MS measurements were verified using β -PAME standard.

For validation of the results pure β -PAME standard was used for TLC-MS analysis. The mass of β -PAME was determined as 180.1 g mol^{-1} , which is also the molecular mass plus one proton. On this account it can be concluded, that the yellow spot is a result of the reaction of ninhydrin with β -PA esters. Afterwards we performed experiments with PEA, IPA and OXD using TLC as mentioned.

Small scale synthesis

The end concentrations of 1 mL scale reactions were calculated using HPLC analysis after 24 h in respect of β -PA concentration. The enzyme concentration was set to 0.2 mg ml^{-1} (Table 5.). IPA was not converted with β -KE substrate at any time, but surprisingly the amino donor led to hydrolysis of the ester resulting in conversion of AP to PEA by ATA117_{11Rd} as well as with IPA-concentrations of 200 and 400 mM of IPA. Since IPA acts as a weak base (pK_s 10.6), it may have supported the hydrolysis of the β -keto ester and led to a shift in the pH value, especially at high concentrations. However, PEA showed no shift in the pH of the buffered reaction mixture, although the lower concentration of PEA could be the reason for this. The concentration of IPA in all reported reaction mixtures is generally high, since the affinity of the transaminases is used as low, which could ultimately also pose a problem for pH-sensitive

5) Towards biocatalytic β -keto ester transamination approaches

reactions (because it is a weak base). In contrast to IPA, product concentrations could be measured with PEA, alanine and OXD (**Table 5.3**).

Using the amino donor PEA, the product concentrations showed to be relative low. After HPLC-analysis the reaction resulted in a relative product concentration of 0.8 % for 3FCR_4M. In contrast only a slight increase was determined for ATA117_{11Rd}, but the resulting product amount was below quantification limit. However, OXD led to a relative product concentration of 31.8% with an optical purity of >99%*ee* using 3FCR_4M. Furthermore, ATA117_{11Rd} was able to convert also the β -KE using OXD to produce. The widespread pyruvate removing system, containing LDH-GDH-NAD and D-glucose with alanine as amino donor led to relative product concentrations of 5.8% for 3FCR_4M and no detectable product amounts for ATA117_{11Rd}.

Table 5.2 Analysis of optical purity and β -PA concentration after hydrolysis with NaOH. Different amino donors were tested. The reactions mixture contained 1 mM PLP, 10 mM β -KE and variable concentrations of amino donors in 30% (v/v) DMSO solution and 50 mM HEPES (pH 7.5). The conversion was determined after 24 h. n.d. = no detectable conversion.

Amino donor	3FCR -4M		ATA117 _{11Rd}	
	% <i>ee</i> (S)	Relative product concentration	% <i>ee</i> (R)	Relative product concentration
α -PEA (50 mM)	99 %	0.8 %	n.d.	< 0.5 %
Alanine (250 mM)*	99 %	5.8 %	n.d.	0 %
OXD (10 mM)	99 %	31.8 %	92 %	12.5 %

*GDL-LDH pyruvate removal system (see also Figure 5.15)

Nevertheless, a very small product spot could be identified by TLC analysis but could not be quantified by HPLC (see also **Figure 5.15**). Hereinafter, different concentrations of OXD were tested to increase the maximal yield of β -PAEE.

Up-scaling for (S)- β -PAEE production

The substrate and solvent concentration was varied for statistical test design (design of experiments). Therefore the reactions were performed in 200 μ L scale and samples taken after 24 h using both ω -TAs. The samples were quantified using GC (non-chiral) to detect the resulted ester-product, but the variation of DMSO, OXD and β -KE (substrate) did not increase the yield. However, it could be at least demonstrated that β -PAEE was extractable by EtOAc using GC for detection. The highest yield, for EtOAc extracted β -PAEE, was achieved for 3FCR_4M with 2.9 mM using 55 mM of OXD, 25 mM of β -KE and 20 % (v/v) of DMSO.

Using the ATA117_{11Rd} the highest yield was only 0.8 mM of β -PAEE. ATA117_{11Rd} was therefore not used for a larger 200 mL (30 mM) approach, since the yield of β -PAEE was generally many times lower than for 3FCR_4M. The reaction was followed by TLC measurements and after no increase in product concentration was observed, the synthesis was stopped after 48 hours. β -PAEE was subsequently purified using flash chromatography. For this purpose, a preparative chromatography method was developed on an ordinary silica column to separate the substrate from the product. However, the reaction product first had to be filtered because the by-product isoindole polymerizes further and forms larger amounts of precipitations (**Figure 5.17**).

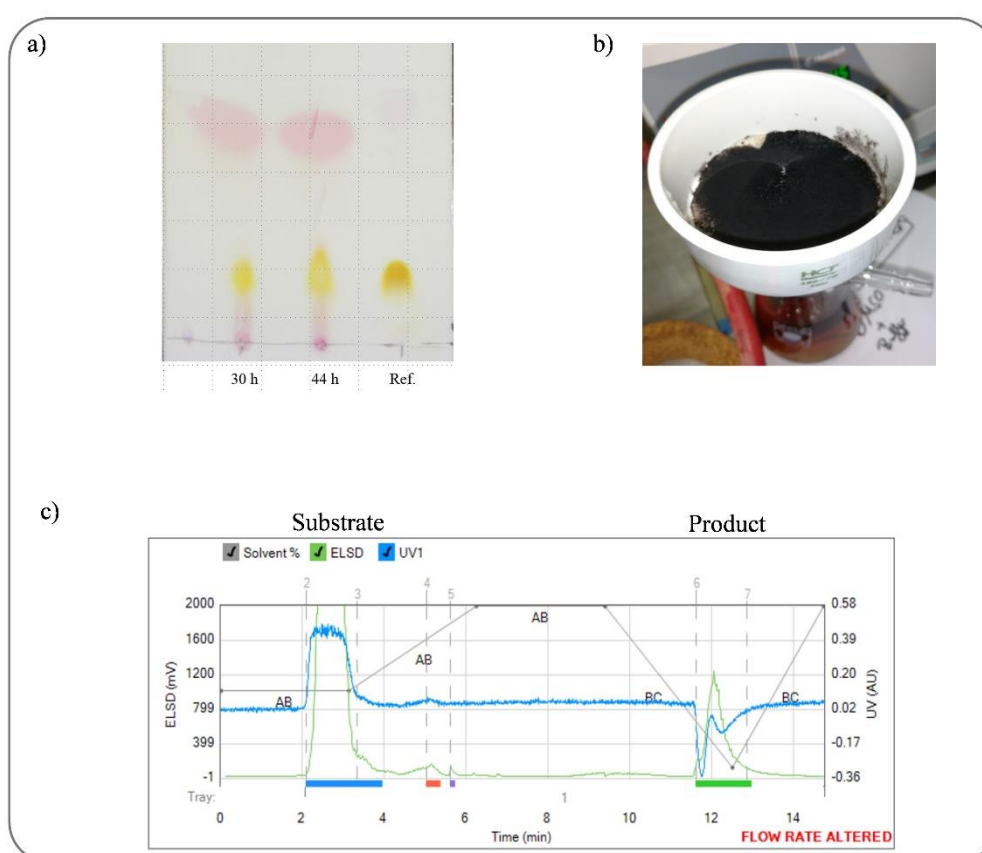


Figure 5.17 Synthesis of β -PAEE on a 200 mL scale. The reaction was performed with 3FCR_4M at 30°C for 48 h in a constantly rotated round flask. a) TLC-analysis of reaction samples (pink β -ketoester/yellow β -PAEE). b) Filtration of the reaction mixture after 48 h. c) Chromatogram of the processing of the reaction product using a solvent gradient mixed out of hexane, EtOAc, methanol and acetic acid. The product was detected by an evaporative light scattering detector (ELSD).

HPLC analysis showed that the enantiomeric purity was above 99%ee of the (*S*)- β -PAEE. In summary this is the first example of aromatic β -keto ester reduction using engineered ω -TA. However the product yield of (*S*)- β -PAEE was only about 104 mg, which are only 10 percent by mass of the substrate originally used. But this quantity was sufficient at least for the analysis

5) Towards biocatalytic β -keto ester transamination approaches

by ^{13}C and ^1H -NMR (see section Materials and Methods). In addition to the reaction equilibrium itself, the reason for the low turnover may be that the substrates (or intermediates) bind poorly to the active center of the enzymes.

Docking analysis ATA117

Albeit the turnover seems to be generally low, especially ATA117_{11Rd} showed a relative low product formation, which is not only due to the reaction equilibrium. For a more detailed analysis, the binding energies of the substrate/product in ATA117_{11Rd} were analyzed and compared with the binding energy of a known inhibitor molecule (**Figure 5.18**).

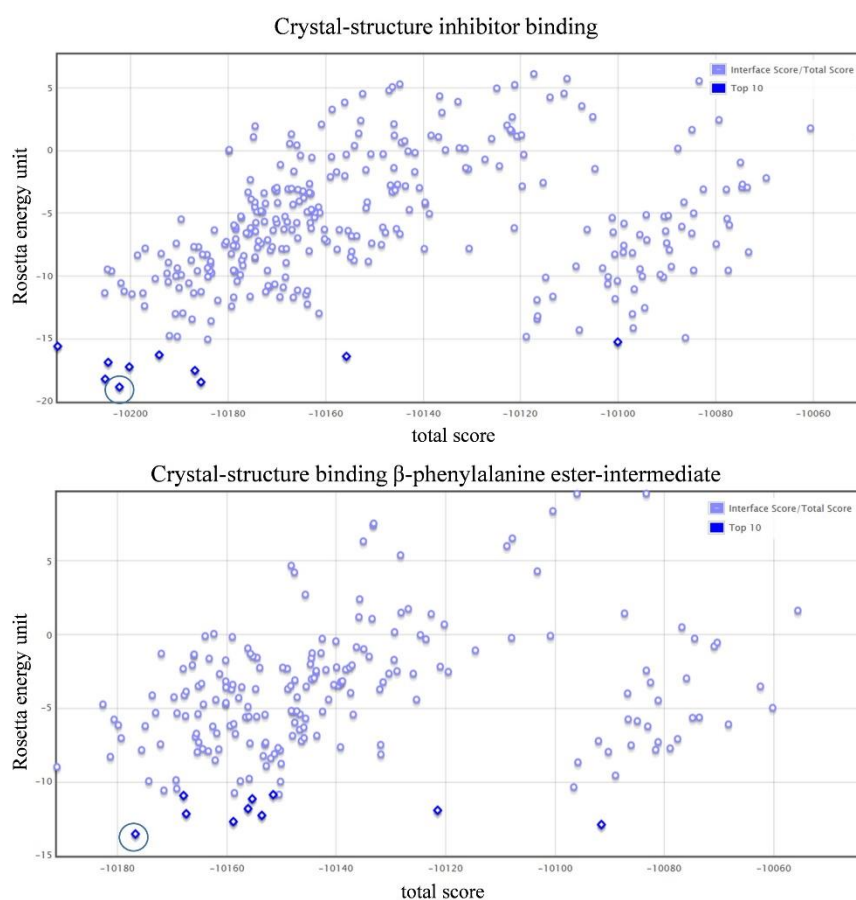


Figure 5.18 Binding energy plot of intermediate compared to inhibitor in ATA117_{11Rd} (PDB ID 5FR9). At the top binding of the inhibitor from the crystal structure 5FR9. Bottom binding of the β -amino acid intermediate in 5FR9. At least 200 rotamers were calculated. The total score is an indicator of whether the calculated bond is reasonable. The calculations were performed using ROSIE-ligand docking and PDB-structure 5FR9. Relatively low REU values are an indicator for the binding of the intermediate (in relation to the binding energy of the inhibitor).

An explanation would be that the binding energy within ATA117_{11Rd} seems to be lower for the substrate(intermediate). For this purpose, the binding energy for the substrate was calculated, using crystal structure (PDB ID 5FR9) using Rosetta-Energy calculation algorithms (*In-silico* tool ROSIE). The inhibitor showed a binding energy of nearly 19 REU (Rosetta Energy Unit).

Typically the binding energies are between -3 and -10 kcal mol $^{-1}$ [58], but Rosetta is only able to calculate energies on an arbitrary scale. For this reason, it is essential to evaluate the binding energy on the basis of a reference substrate or inhibitor, which was done.

In difference the binding energy $\Delta G_{\text{binding}}$ is 5.4 REU compared to β -keto ester intermediate. This means that the bond of substrate is may be less strong. Furthermore, also the position of the inhibitor compared to the substrate-intermediate is slightly shifted. To conclude that it was only a calculation error of the algorithm, the calculated position of the inhibitor was compared with the crystal structure data. The calculated inhibitor-position superimposed nearly perfect with the position in the crystal-structure. In contrast the β -phenylalanine-PLP-intermediate is shifted within the substrate binding pocket, compared to the inhibitor (**Figure 5.19**).

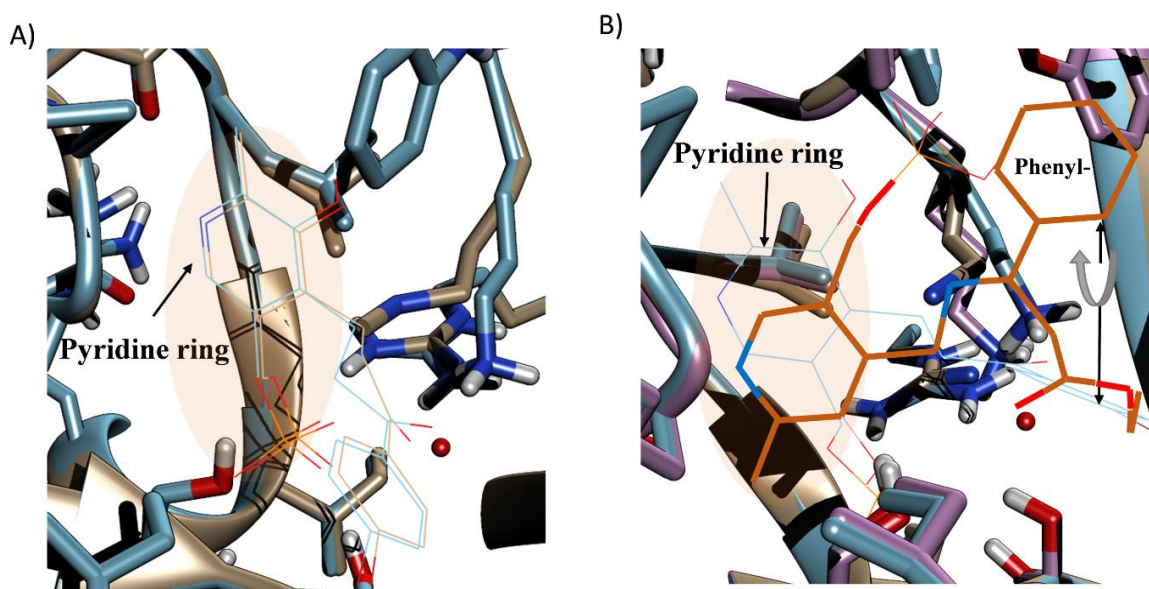


Figure 5.19 Substrate-intermediate docking in ATA117_{11Rd}. A) Comparison of ROSIE-calculation and crystal-structure inhibitor position. The inhibitor binds with 18.8 REU at the congruent position compared to the experimental determined position (thin blue and brown lines). Therefore the calculation was used as validation for substrate docking. B) The β -phenylalanine-PLP intermediate resulted in weaker binding (13.5 REU, thick brown) and is turned and shifted compared to the inhibitor position. The Phenyl-moiety is oriented between Y61, Y67 and W192. For calculations the substrate docking tool ROSIE-Ligand was utilized. (Homology structure of ATA117_{11Rd} was created by IV. Pavlidis)

However the lower activity of ATA117_{11Rd} for the β -keto ester might be reasoned by lower binding energies compared to 3FCR_4M. Within ATA117 the ethyl-residue of β -keto ester intermediate is oriented in a large pocket. However, the phenyl-moiety of the intermediate lies between three aromatic amino acid residues (Y61, Y67 and W192). Compared to inhibitor orientation (with an aryl-group), the position is occupied by the ethyl residue, thus placing the aromatic ring in a pocket full of tyrosine and tryptophan residues, which allows π - π interactions, where the hydroxyl groups of Y61/67 may be too polar for the aromatic ring of the

5) Towards biocatalytic β -keto ester transamination approaches

substrate/product. In addition, W192 can be protonated and thus carry a positive charge. In addition, the mentioned amino acid residues limit the space within the binding pocket. The pocket could be expanded by replacing it with phenylalanine or other hydrophobic residues (e.g. leucine or alanine). In contrast, the binding energy in 3FCR_4M was also calculated and compared with ATA117_{11Rd}.

Docking analysis 3FCR_4M

The calculated binding energy of the substrate intermediate in 3FCR_4M was slightly lower (-16.3 REU) than in the binding of the intermediate and ATA117. The orientation also matches the expected position of the reference bulky substrate ketone (diaryl-ketone intermediate) within 3FCR_4M (Figure 5.20).

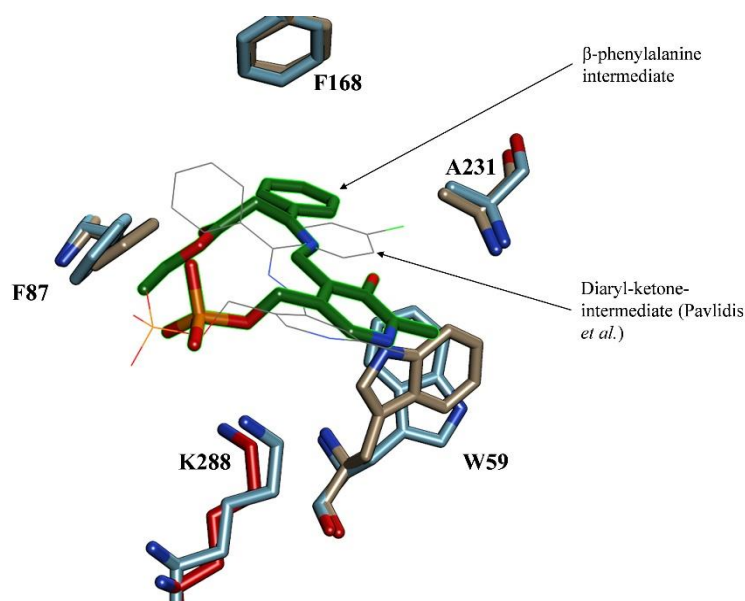


Figure 5.20 Hydrophobic-aromatic substrate pocket allows binding of β -phenylalanine-ester. The substrate-intermediate was docked into a calculated 3FCR_4M structure. The structure was calculated by Pavlidis *et al.* and shows binding of a diaryl-ketone. The β -phenylalanine-ethylester-intermediate showed to be located in the same manner and was docked into the substrate binding pocket using ROSIE-ligand. The engineered amino residues are shown within the figure.

However, like mentioned before the 3FCR_4M variant was engineered for bulky ketones without polar or hydrophilic side groups, which is why the substrate binding pocket might not be optimally suited for the polar β -keto esters. The enhanced 3FCR variant, 3FCR_4M, contains the mutations Y59W, Y87F, Y152F and T231A, which are beneficial for binding the cofactor-substrate intermediate and expansion the small binding pocket (also known as P-pocket). The

residue Y87F belongs to the small binding pocket and increases the hydrophobicity and expand the space. Y59F and T213A in combination increasing the activity towards amines and bulky substrates [21]. In addition, it has been shown that bulky diaryl ketones can be converted with 3FCR_4M, so that it is likely that the position of the ethyl ester intermediate appears reasonable. A reason for the better binding, compared to ATA117_{11Rd}, might be the high hydrophobicity of the 3FCR_4M substrate pocket, which is a result of exchanges of tyrosine-residues against non-polar aromatic phenylalanine-residues. Furthermore, the space-consuming threonine residue was replaced by a small hydrophobic alanine residue [21]. Moreover it is also possible that a tyrosine at position F87 could have a positive effect, as this amino acid residue could form a hydrogen bond to the carboxyl group of β -keto ester/intermediate.

Comparison to another β -keto ester converting ω -TA

These amino acid positions were also investigated in another transaminase engineering experiment. An important amino acid position can be also relocated, using the numbering scheme ω TAED [58], in the engineered *V. fluvialis* ω -TA from Midelfort *et al.* at W57F, which showed to be elementary important for the conversion of the ester substrate ethyl 3-aminohexanoate [14]. Therefore W59 seems to be unbeneficial for conversion of the β -keto/amino esters within 3FCR_4M. Moreover, it might be beneficial to mutate the flipping arginine of 3FCR towards phenylalanine as shown for the engineered *V. fluvialis* ω -TA. This mutation alone increased the activity of the enzyme towards the aliphatic β -keto ester substrate about 20-fold.

5.2.4) Outlook and conclusion

In summary, ω -TAs have never been engineered towards aromatic β -KE, so this work should be considered as proof of concepts. However some amino acid residues within Fold type I ω -TA can be remarked as putative important for β -KE activity. It is therefore also clear that the enzyme- and reaction properties must first be improved before further reaction scale up is sought.

However, the synthesis of β -keto acids or esters can be conducted using asymmetrical substrates and the engineered 3FCR_4M and ATA117 11Rd. Since these enzymes have not been particularly designed for the conversion of ester substrates further engineering could increase yields and avoid expensive amino donors, like OXD or expensive co-product removal systems (e.g. LDH-GDH-pyruvate removal system). In this context, the immobilization of these enzymes could also be important.

5.3) Conclusion chapter 5

The targeted mutagenesis of the ω -TA from *Variovorax paradoxus* could not be realized. Further targeted mutations as well as directed evolution should be carried out in order to enable the conversion of aromatic β -keto esters. However, the mutations of the arginine residues seem to be important for the change in substrate specificity and showed also a large change in activity. Nevertheless, this also shows that enzyme engineering can be both time and resource intensive, in particular to introduce targeted mutations into the protein by PCR, and to perform enzymatic tests or large-scale screenings of random mutagenesis enzyme libraries. Therefore, it is recommended to test already characterized and existing ω -TAs as described in chapter 5.2 in order to reduce costs and shorten the enzyme engineering process. A combination of enzyme engineering and enzyme screening could therefore be an efficient method to obtain ω -TAs with the desired properties as quickly as possible. The two ω -TAs identified by the screening could be found quickly, but both enzymes do not appear to be adapted for the reaction. Therefore, these two enzymes provide a starting point for further enzyme engineering. This demonstrates that enzyme engineering is an iterative process until the properties are adapted to the process conditions and parameters.

5.4) Reference Chapter 5

1. Logue MW, Pollack RM, Vitullo VP. Nature of the transition state for the decarboxylation of β -keto acids. *J Am Chem Soc.* 1975;97: 6868–6869. doi:10.1021/ja00856a047
2. Rudat J, Brucher BR, Syltatk C. Transaminases for the synthesis of enantiopure β -amino acids. *AMB Express.* 2012;2: 11. doi:10.1186/2191-0855-2-11
3. Kim J, Kyung D, Yun H, Cho BK, Seo JH, Cha M, et al. Cloning and characterization of a novel β -transaminase from *Mesorhizobium* sp. strain LUK: A new biocatalyst for the synthesis of enantiomerically pure β -amino acids. *Appl Environ Microbiol.* American Society for Microbiology; 2007;73: 1772–1782. doi:10.1128/AEM.02119-06
4. Mathew S, Nadarajan SP, Sundaramoorthy U, Jeon H, Chung T, Yun H. Biotransformation of β -keto nitriles to chiral (S)- β -amino acids using nitrilase and ω -transaminase. *Biotechnol Lett.* Springer Netherlands; 2016; doi:10.1007/s10529-016-2271-4
5. Mathew S, Jeong SS, Chung T, Lee SH, Yun H. Asymmetric synthesis of aromatic β -amino acids using ω -transaminase: Optimizing the lipase concentration to obtain thermodynamically unstable β -keto acids. *Biotechnol J.* 2016;11: 185–190. doi:10.1002/biot.201500181
6. Zhang ZJ, Cai RF, Xu JH. Characterization of a new nitrilase from *Hoeflea phototrophica* DFL-43 for a two-step one-pot synthesis of (S)- β -amino acids. *Applied Microbiology and Biotechnology.* Springer Berlin Heidelberg; 10 May 2018: 1–10. doi:10.1007/s00253-018-9057-7
7. Mandelstam J. The free amino acids in growing and non-growing population of *Escherichia coli*. *Biochem J.* Portland Press Ltd; 1958;89: 103–110.
8. Zhong F, Yao W, Dou X, Lu Y. Enantioselective Construction of 3-Hydroxy Oxindoles via Decarboxylative Addition of β -Ketoacids to Isatins. *Org Lett.* American Chemical Society; 2012;14: 4018–4021. doi:10.1021/ol301855w
9. Aziz HR, Singleton DA. Concert along the Edge: Dynamics and the Nature of the Border between General and Specific Acid-Base Catalysis. *J Am Chem Soc.* 2017;139: 5965–5972. doi:10.1021/jacs.7b02148
10. Midelfort KS, Kumar R, Han S, Karmilowicz MJ, McConnell K, Gehlhaar DK, et al. Redesigning and characterizing the substrate specificity and activity of *Vibrio fluvialis* aminotransferase for the synthesis of imagabalin. *Protein Eng Des Sel.* 2013;26: 25–33. doi:10.1093/protein/gz065
11. Lyskov S, Chou FC, Conchúir SÓ, Der BS, Drew K, Kuroda D, et al. Serverification of Molecular Modeling Applications: The Rosetta Online Server That Includes Everyone (ROSIE). Uversky VN, editor. *PLoS One.* Public Library of Science; 2013;8: e63906. doi:10.1371/journal.pone.0063906
12. Kothiwale S, Mendenhall JL, Meiler J. BCL::Conf: small molecule conformational sampling using a knowledge based rotamer library. *J Cheminform.* Springer; 2015;7: 47. doi:10.1186/s13321-015-0095-1
13. Pettersen EF, Goddard TD, Huang CC, Couch GS, Greenblatt DM, Meng EC, et al. UCSF Chimera - A visualization system for exploratory research and analysis. *J Comput Chem.* John Wiley & Sons, Inc.; 2004;25: 1605–1612. doi:10.1002/jcc.20084
14. Midelfort KS, Kumar R, Han S, Karmilowicz MJ, McConnell K, Gehlhaar DK, et al. Redesigning and characterizing the substrate specificity and activity of *Vibrio fluvialis* aminotransferase for the synthesis of imagabalin. *Protein Eng Des Sel.* 2013;26: 25–33. doi:10.1093/protein/gz065
15. Wolfenden R. Transition State Analog Inhibitors and Enzyme Catalysis. *Annu Rev Biophys Bioeng.* 1976;5: 271–306. doi:10.1146/annurev.bb.05.060176.001415
16. Lienhard GE. Transition State Analogs as Enzyme Inhibitors. *Annu Rep Med Chem.* Academic Press; 2004;7: 1–19. doi:10.1016/S0065-7743(08)60818-0
17. Crismaru CG, Wybenga GG, Szymanski W, Wijma HJ, Wu B, Bartsch S, et al. Biochemical Properties and Crystal Structure of a β -Phenylalanine Aminotransferase from *Variovorax paradoxus*. *Appl Environ Microbiol.* 2013;79: 185–195. doi:10.1128/AEM.02525-12
18. Weiß MS, Pavlidis I V., Spurr P, Hanlon SP, Wirz B, Iding H, et al. Protein-engineering of an amine transaminase for the stereoselective synthesis of a pharmaceutically relevant bicyclic amine. *Org Biomol Chem.* Royal Society of Chemistry; 2016;14: 10249–10254. doi:10.1039/C6OB02139E
19. Midelfort KS, Kumar R, Han S, Karmilowicz MJ, McConnell K, Gehlhaar DK, et al. Redesigning and characterizing the substrate specificity and activity of *Vibrio fluvialis* aminotransferase for the synthesis of imagabalin. *Protein Eng Des Sel.* 2013;26: 25–33. doi:10.1093/protein/gz065
20. Pavlidis I V., Weiß MS, Genz M, Spurr P, Hanlon SP, Wirz B, et al. Identification of (S)-selective transaminases for the asymmetric synthesis of bulky chiral amines. *Nat Chem.* Nature Publishing Group; 2016;8: 1–7. doi:10.1038/NCHEM.2578
21. Weiß MS, Pavlidis I V., Spurr P, Hanlon SP, Wirz B, Iding H, et al. Protein-engineering of an amine transaminase for the stereoselective synthesis of a pharmaceutically relevant bicyclic amine. *Org Biomol Chem.* Royal Society of Chemistry; 2016;14: 10249–10254. doi:10.1039/C6OB02139E
22. Manta B, Cassimjee KE, Himo F. Quantum Chemical Study of Dual-Substrate Recognition in ω -Transaminase. *ACS Omega.* 2017;2: 890–898. doi:10.1021/acsomega.6b00376
23. Wilding M, Peat TS, Newman J, Scott C. A β -Alanine Catabolism Pathway Containing a Highly Promiscuous ω -Transaminase in the 12-Aminododecanate-Degrading *Pseudomonas* sp. Strain AAC. Parales RE, editor. *Appl Environ Microbiol.* 2016;82: 3846–56. doi:10.1128/AEM.00665-16
24. Smith CA, Kortemme T. Structure-based prediction of the peptide sequence space recognized by natural and synthetic PDZ domains. *J Mol Biol.* 2010;402: 460–474. doi:10.1016/j.jmb.2010.07.032
25. Smith CA, Kortemme T. Predicting the tolerated sequences for proteins and protein interfaces using rosettabackrub flexible backbone design. Uversky VN, editor. *PLoS One.* 2011;6: e20451. doi:10.1371/journal.pone.0020451
26. Landau M, Mayrose I, Rosenberg Y, Glaser F, Martz E, Pupko T, et al. ConSurf 2005: The projection of evolutionary conservation scores of residues on protein structures. *Nucleic Acids Res.* 2005;33: W299–W302. doi:10.1093/nar/gki370
27. Celniker G, Nimrod G, Ashkenazy H, Glaser F, Martz E, Mayrose I, et al. ConSurf: Using evolutionary data to raise testable hypotheses about protein function. *Israel Journal of Chemistry.* 2013. pp. 199–206. doi:10.1002/ijch.201200096
28. Suzek BE, Wang Y, Huang H, McGarvey PB, Wu CH. UniRef clusters: A comprehensive and scalable alternative for improving sequence similarity searches. *Bioinformatics.* Oxford University Press; 2015;31: 926–932. doi:10.1093/bioinformatics/btu739
29. Albuquerque L, Rainey FA, Nobre MF, da Costa MS. *Elioraeta tepidiphila*

5) Towards biocatalytic β -keto ester transamination approaches

- gen. nov., sp. nov., a slightly thermophilic member of the Alphaproteobacteria. *Int J Syst Evol Microbiol.* 2008;58: 773–778. doi:10.1099/ijs.0.65294-0
30. Badali H, Prenafeta-Boldu FX, Guarro J, Klaassen CH, Meis JF, De Hoog GS. *Cladophialophora psammophila*, a novel species of Chaetothyriales with a potential use in the bioremediation of volatile aromatic hydrocarbons. *Fungal Biol. Elsevier;* 2011;115: 1019–1029. doi:10.1016/j.funbio.2011.04.005
31. Wheeler TJ, Clements J, Finn RD. Skyglin: A tool for creating informative, interactive logos representing sequence alignments and profile hidden Markov models. *BMC Bioinformatics. BioMed Central;* 2014;15: 7. doi:10.1186/1471-2105-15-7
32. Wybenga GG, Crismaru CG, Janssen DB, Dijkstra BW. Structural determinants of the β -selectivity of a bacterial aminotransferase. *J Biol Chem.* 2012;287: 28495–28502. doi:10.1074/jbc.M112.375238
33. Mathew S, Nadarajan SP, Chung T, Park HH, Yun H. Biochemical characterization of thermostable ω -transaminase from *Sphaerobacter thermophilus* and its application for producing aromatic β - and γ -amino acids. *Enzyme Microb Technol. Elsevier Inc.;* 2016; doi:10.1016/j.enzmictec.2016.02.013
34. Mackay DJC. *Inference, and Learning Algorithms.* Cambridge University Press; 2003. doi:10.1017/S026357470426043X
35. Campanini B, Bettati S, Di Salvo ML, Mozzarelli A, Contestabile R. Asymmetry of the active site loop conformation between subunits of glutamate-1-semialdehyde aminomutase in solution. *Biomed Res Int. Hindawi;* 2013;2013: 353270. doi:10.1155/2013/353270
36. Schymkowitz J, Borg J, Stricher F, Nys R, Rousseau F, Serrano L. The FoldX web server: An online force field. *Nucleic Acids Res. Oxford University Press;* 2005;33: W382–8. doi:10.1093/nar/gki387
37. Pucci F, Bourgeas R, Rooman M. Predicting protein thermal stability changes upon point mutations using statistical potentials: Introducing HoTMuSiC. *Sci Rep. Nature Publishing Group;* 2016;6: 23257. doi:10.1038/srep23257
38. Guo F, Berglund P. *Transaminase Biocatalysis: Optimization and Application.* Green Chem. Royal Society of Chemistry; 2016; 333–360. doi:10.1039/C6GC02328B
39. Takayama T, Shibata T, Shiozawa F, Kawabe K, Shimizu Y, Hamada M, et al. Preparation of partially saturated nitrogen-containing heterocyclic compounds, and PHD2 inhibitors, EPO formation promoters, and antianemic agents containing the heterocyclic compounds. *WO 2014021281 A1; WO 2014021281 A1,* 2014.
40. Guizzetti S, Benaglia M, Bonsignore M, Raimondi L. Trichlorosilane-mediated stereoselective synthesis of β -amino esters and their conversion to highly enantiomerically enriched β -lactams. *Org Biomol Chem. The Royal Society of Chemistry;* 2011;9: 739–743. doi:10.1039/c0ob00570c
41. Xiong Y, Luo Y, Li Z. Method for preparing aminophenylpropanoic acid-terminated polyoxyethylene acid or activated ester, and application thereof. *CN 102964588,* 2013.
42. Crawforth JM, Glossop PA, Hamper BC, Huang W, Mantell SJ, Neal BE, et al. Preparation of nicotinamide derivatives for the treatment of allergic and respiratory conditions. *WO 2009153721,* 2009.
43. Rodríguez-Mata M, García-Urdiales E, Gotor-Fernández V, Gotor V. Stereoselective chemoenzymatic preparation of β -amino esters: Molecular modelling considerations in lipase-mediated processes and application to the synthesis of (S)-dapoxetine. *Adv Synth Catal. WILEY-VCH Verlag;* 2010;352: 395–406. doi:10.1002/adsc.200900676
44. Leflemme N, Freret T, Boulouard M, Dallemagne P, Rault S. Synthesis and preliminary in vivo evaluation of new 2-Aryl-6-methyl-1,2-dihydro-1H-pyridin-4-ones and 2-Aryl-6-methylpiperidin-4-ols, as potential anti-amnesiant agents. *J Enzyme Inhib Med Chem. Taylor & Francis;* 2005;20: 551–556. doi:10.1080/14756360500212266
45. Wani MC, Taylor HL, Wall ME, Coggon P, McPhail AT. Plant antitumor agents. VI. The isolation and structure of taxol, a novel antileukemic and antitumor agent from *Taxus brevifolia*. *J Am Chem Soc.* 1971;93: 2325–7.
46. Grayson JI, Roos J, Osswald S. Development of a Commercial Process for (S)- β -Phenylalanine. *Org Process Res Dev. American Chemical Society;* 2011;15: 1201–1206. doi:10.1021/op200084g
47. Li D, Cheng S, Wei D, Ren Y, Zhang D. Production of enantiomerically pure (S)- β -phenylalanine and (R)- β -phenylalanine by penicillin G acylase from *Escherichia coli* in aqueous medium. *Biotechnol Lett. Springer Netherlands;* 2007;29: 1825–1830. doi:10.1007/s10529-007-9480-9
48. Mathew S, Bea H, Nadarajan SP, Chung T, Yun H. Production of chiral β -amino acids using ω -transaminase from *Burkholderia graminis*. *J Biotechnol. Elsevier B.V.;* 2015;196–197: 1–8. doi:10.1016/j.jbiotec.2015.01.011
49. Green AP, Turner NJ, O'Reilly E. Chiral Amine Synthesis Using ω -Transaminases: An Amine Donor that Displaces Equilibria and Enables High-Throughput Screening. *Angew Chemie Int Ed. WILEY-VCH Verlag;* 2014;53: 10714–10717. doi:10.1002/anie.201406571
50. Buß O, Muller D, Jager S, Rudat J, Rabe KS. Improvement of the thermostability of a β -amino acid converting ω -transaminase using FoldX. *ChemBioChem.* 2017; doi:10.1002/cbic.201700467
51. Green AP, Turner NJ, O'Reilly E. Chiral amine synthesis using ω -transaminases: An amine donor that displaces equilibria and enables high-throughput screening. *Angew Chemie - Int Ed. WILEY-VCH Verlag;* 2014;53: 10714–10717. doi:10.1002/anie.201406571
52. Slabu I, Galman JL, Lloyd RC, Turner NJ. Discovery, Engineering and Synthetic Application of Transaminase Biocatalysts. *ACS Catal.* 2017; aescatal.7b02686. doi:10.1021/aescatal.7b02686
53. Savile CK, Janey JM, Mundorff EC, Moore JC, Tam S, Jarvis WR, et al. Biocatalytic Asymmetric Synthesis of Chiral Amines from Ketones Applied to Sitagliptin Manufacture. *Science.* 2010;329: 305–309. doi:10.1126/science.1188934
54. Shin JS, Kim BG. Kinetic modeling of ω -transamination for enzymatic kinetic resolution of α -methylbenzylamine. *Biotechnol Bioeng. Wiley Subscription Services, Inc., A Wiley Company;* 1998;60: 534–540. doi:10.1002/(SICI)1097-0290(19981205)60:5
55. Koszelewski D, Lavandera I, Clay D, Rozzell D, Kroutil W. Asymmetric synthesis of optically pure pharmacologically relevant amines employing ω -transaminases. *Adv Synth Catal.* 2008;350: 2761–2766. doi:10.1002/adsc.200800496
56. Buß O, Jager S, Dold S-M, Zimmermann S, Hamacher K, Schmitz K, et al. Statistical Evaluation of HTS Assays for Enzymatic Hydrolysis of β -Keto Esters. Oberer M, editor. *PLoS One. CRC Press;* 2016;11: e0146104. doi:10.1371/journal.pone.0146104
57. Purich DL, Purich DL. Active Sites and their Chemical Properties. *Enzyme Kinetics: Catalysis & Control. Elsevier;* 2010. pp. 53–169. doi:10.1016/B978-0-12-380924-7.10002-X
58. Buß O, Buchholz PCF, Gräff M, Klausmann P, Rudat J, Pleiss J. The ω -transaminase engineering database (ω TAED): A navigation tool in protein sequence and structure space. *Proteins Struct Funct Bioinforma. Wiley-Blackwell;* 2018;86: 566–580. doi:10.1002/prot.25477
59. Cassimjee KE, Humble MS, Miceli V, Colomina CG, Berglund P. Active

5) Towards biocatalytic β -keto ester transamination approaches

site quantification of an ω -Transaminase by performing a half transamination reaction. ACS Catal. American Chemical Society; 2011;1: 1051–1055. doi:10.1021/cs200315h

6) Degradation and deracemization of β -PA using different *Paraburkholderia* species

In addition to the targeted design of enzymes, as well as guided evolution and database mining new enzymes can be found using screening of microorganism. The strain *Paraburkholderia* sp. BS115 was discovered by J. Rudat in potting soil in respect of β -amino acid converting enzymes . In the following part the degradation of the newly isolated and the already discovered strain is compared with regard to the degradation of β -amino acids.

This chapter is widely based on the following manuscript.

Chiral β -phenylalanine degradation by a newly isolated *Paraburkholderia* strain BS115 and type strain PsJN

Oliver Buß, Sarah-Marie Dold, Pascal Obermeier, Delphine Muller, Dennis Litty, Jens Grüninger and Jens Rudat.

Institute of Process Engineering in Life sciences, Section II: Technical Biology, Karlsruhe Institute of Technology, Karlsruhe Germany.

Publishing details:

Published on 21 Sep. 2018, AMB-Express

doi: 10.1186/s13568-018-0676-2

Authors' contribution to this publication

Oliver Buß: Performance of the experiments, HPLC analysis, data evaluation and advisory of the lab work. Writing the manuscript as first author. **Sarah Dold:** Substantial performance of the experiments with *Paraburkholderia* BS115 and HPLC analysis. **Jens Grüninger:** Substantial supporting of the experiments with *Paraburkholderia* PsJN. **Pascal Obermeier:** Performance of the fermentation with *Paraburkholderia*. **Delphine Muller:** Performance of precultures and supporting by preparation of medium. **Dennis Litty:** Performance of cell-free activity tests using BS115 lysate. **Jens Rudat:** Isolation of BS115, performance of microscopy and staining, substantial contribution to the conception of manuscript and of the experiments as well as advisory of the lab work. Critically revising of the final manuscript version.

6.1) Introduction

The catabolism of proteinogenic L-alpha-amino acids (L- α -AA) is in-depth understood and part of undergraduates' biochemical education [1]. All other amino acids have long been rendered "unnatural", which at least began to change for D-configured α -AA.

D- α -amino acids

Bacteria have long been known to be a rich source of D- α -aa which are therefore abundant in soil and fermented food [2]. The role of these special amino acids and their metabolism in mammals has also been elucidated [3]. The bacterial synthesis mechanisms of D- α -AA and their incorporation in non-ribosomal peptides are now well-understood [4]. Degradation preferably happens via oxidation to the corresponding α -keto acid (α -KA) and is carried out by D-amino acid oxidases, the first of which being discovered as early as 1935 [5]. D- α -AA are part of the peptidoglycan layer of microorganism and the most important amino acids are D-glutamate and D-alanine [4]. These D - α -AAs are synthesized by racemases and D -AA aminotransferases [6] [7][8]. Besides this both enzymes, also epimerases and dehydratase/dehydrogenase can catalyze reactions towards D-AA [9][10]. However, in some cases the enzymes for these reactions are still unknown.

Role of β -, γ -, ϵ -amino acids in organism

Furthermore not only L- α and D- α -AA are present in nature and reactions towards amino acids with amino groups in other positions than α -position are possible, leading to β -, γ -, ϵ - and other constitutional isomers of amino acids. ϵ -amino acids have e.g. a special significance in the biosynthesis pathway of β -lactams in actinomycetes and are converted by lysine γ -aminotransferases [11]. The most popular γ -AA is γ -aminobutyric acid (GABA), an important neurotransmitter which is degraded by aminobutyric acid (ω -)transaminase to succinic semialdehyde [12]. The γ -AAs are even in the focus of research for artificial bioactive molecules and occurring as parts of many natural compounds. The polypeptide Dolastatin is a prominent example of a γ -AA containing drug in cancer research [13,14]. A known drug is for example the muscle relaxant (-)baclofen, which is a derivative of γ -aminobutyric acid [15]. The synthesis of non-natural γ -AA from γ -keto acids using an ω -transaminase (ω -TA) has been reported recently [14].

By contrast, only minor insight is gained into the degradation of β -amino acids (β -AA). With the exception of β -alanine and β -aminoisobutyric acid which constitute key intermediates in several metabolic pathways, β -AA are not as abundant in nature as their α -configured

counterparts. β -alanine can be metabolized by mammalian organism [16] and is involved in pantothenate metabolism [17], finally becoming a component of the key metabolite coenzyme A (CoA). β -alanine is also linked with histidine by carnosine synthase to the dipeptide carnosine which is abundant in skeletal muscles as well as the central nervous system of most vertebrates [18]. Since β -alanine appears as the rate-limiting precursor, this β -AA has become a popular supplement in athlete diet with a documented increase in exercise performance like high intensity cycling [19]. Using the KEGG-pathway tool for analyzing the degradation of β -alanine, it can be shown that a transaminase reaction is forming malonate-semialdehyde which is further converted to malonate and finally enters the fatty acid biosynthesis as malonyl-CoA [20]. The synthesis of β -AA and their incorporation into natural compounds has been extensively reviewed by Kudo [21]. Microorganisms appear to be quite routinely affected with β -AA. Thus a deeper understanding of degradation mechanisms promises (A) an insight into defense mechanisms of microorganisms affected with these natural compounds (B) environmental aspects referring to the persistence of β -AA in soil and water (C) pharmacokinetics of these natural compounds when used as a drug, e.g. cytostatics containing aromatic β -AA. Focused on the mentioned β -phenylalanine (β -PA) as an example for chiral β -AA synthesis an approach might be the synthesis of the racemic β -PA using classical chemistry, i.e. by reaction of benzaldehyde with malonic acid and ammonium acetate, the produced racemate can be optical purified by kinetic resolution using an enantioselective transaminases and fermentation processes might be an alternative to isolated enzymes [22–24]. Such deracemization approaches are showed e.g. for secondary aryl alcohols using whole-cell biocatalysts [15]. Furthermore, the investigation of the β -PA degradation process could lead to a deeper understanding of the biochemical pathways. This chapter is focused on the isolated *Paraburkholderia sp* as whole cell biocatalyst in respect of enantiomeric resolution of the chiral β -phenylalanine.

In a previous study enrichment cultures with aromatic β -PA as sole nitrogen sources were cultivated [25]. From a variety of soil samples different bacteria capable to grow with β -PA as sole nitrogen source were investigated. Transamination was found to be the predominant initial degradation step, using cell extracts and fractions thereof gained by ammonia phosphate precipitation degradation only occurred when a suitable amino acceptor was additionally applied (preferably α -ketoglutarate or pyruvate) as well as the well-known transaminase cofactor pyridoxal phosphate (PLP). Until today, the microbial degradation of *rac*- β -PA has only once been documented by Mano *et al.* in 2006 and to the best of our knowledge these experiments have never been continued. However, further metabolization of the desaminated

6) Degradation and deracemization of β -PA using different *Paraburkholderia* species

(*S*)- β -PA (and thereby created β -keto acid, β -KA) in the degrading microorganism remained as uncertain as the fate of the (*R*)- β -AA. Here we report the degradation of racemic β -PA by the newly isolated *Paraburkholderia* strain BS115 and the *Paraburkholderia* type strain *P. phytofirmans* PsJN. The degradation of racemic β -phenylalanine using BS115 as fermentation strain was analyzed previously in the doctoral thesis of S.M. Dold [27]. In contrast this chapter is focused on the comparison of the results in regard to the β -PA degradation capabilities of the *P. phytofirmans* PsJN strain. In addition, the degradation behavior of both strains was investigated with chiral (*R*) and (*S*)- β -PA.

6.2) Materials and methods

Chemicals

All amino acids and chemicals were purchased from Sigma Aldrich (St.Louis, US) and Carl Roth (Karlsruhe, Germany) in analytical grade. All enantiopure amino acids were purchased from PepTech Corporation (Bedford, US).

Bacterial strains

Paraburkholderia BS115 was isolated by enrichment culture from garden soil spiked with soy peptone due to its high content of aromatic amino acids [25]. The strain was identified by the culture collection DSMZ (Deutsche Stammsammlung für Mikroorganismen und Zellkulturen GmbH) as *P. phytofirmans*. Cultures of the strain were deposited at the DSMZ designated as DSM 103130 *P. phytofirmans* (BS115). *P. phytofirmans* PsJN was also delivered by DSMZ (DSM 17436).

Fermentation process

The sterile minimal medium M1 contained 100 mM D-glucose and 10 mM of *rac*- β -PA, 5.8 mM KH_2PO_4 , 4.1 mM $\text{NaHPO}_4 \cdot 2 \text{H}_2\text{O}$, 1 mM $\text{MgSO}_4 \cdot 7 \text{H}_2\text{O}$, 0.5 mM $\text{CaCl}_2 \cdot 2 \text{H}_2\text{O}$ and 0.01 mM $\text{FeCl}_2 \cdot 4 \text{H}_2\text{O}$. Additionally the vitamins pyridoxal-5-phosphate (PLP) and cobalamin were added to the mixture in concentrations of 1 μM and 1 nM, respectively. The vitamins, β -phenylalanine and FeCl_2 were sterile filtrated separately while all other compounds were autoclaved. The sterile compounds were then mixed. The fermentation process was optimized for maximal growth rate in a small scale bioreactor system without pH regulation.

The fermentation of PsJN and BS115 was performed in a benchtop reactor (vessel volume 2.5 L; Minifors, Infors-HT, Switzerland) with a working volume of 1 L in minimal medium M1. The system was equipped with a pH probe (Mettler-Toledo, USA) and a Pt-100 temperature probe. The temperature was set to 30° C and the stirrer speed was adjusted to 120 rpm at the beginning. For mixing and disruption of gas bubbles a standard Rushton stirrer (diameter 46 mm) was used. The pH-value and pO_2 content were not controlled during the reaction. The aeration rate was set to 1 L/min. The experiment was conducted in a triplicate. The precultures were grown in a 100 mL shake flask in the minimal medium at the same temperature and inoculated from a glycerol stock. The precultures were cultivated in a rotary shaker (Infors-HT, Switzerland) at 120 rpm. The bioreactors were inoculated with the precultures to an optical density at $\text{OD}_{600\text{nm}}$ of at least 0.1.

Dry cell mass measurement

10 mL of the cultures were centrifuged at 6.000 g for at least 10 min at 4°C. The pellets were washed with HPH_2O (high-purity water, type I ISO 3696). After this, the cell pellets were dried overnight at 60°C in a drying oven.

Glucose assay

The concentration of d-glucose was measured by an enzymatic glucose-assay from R-Biopharm AG (Darmstadt, Germany). According to the manufacturer's assay protocol volumes were down-scaled to 96-well microtiter plates (scale 1:20). 5 μL of the sample was mixed with 100 μL HPH_2O and 50 μL of solution 1. 10 μL of 1 to 10 diluted suspension 2 was pipetted to the mixture. The adsorption at 340 nm of the incomplete mixture was measured in an epoch plate reader system before and after suspension 2 was added to the mixture. Also after 5 and 10 min the adsorption was measured. The measurement was calibrated by a D-glucose dilution series from 0.01 to 1 g/L.

Enzyme activity assay

Both strains were cultivated for at least 3 days at 120 rpm and 30°C in 100 mL minimal medium in shake flasks, the final OD_{600} was 3.4 for BS115 and 3.1 for PsJN. The cells were harvested by centrifugation at 8.000 rpm in Beckman Coulter (Brea, USA) centrifuge (JA-10 rotor) and lysed by incubation with 1 mg mL^{-1} lysozyme (Fluka) for 15 min at room temperature. Pellets were resuspended in 5 mL 40 mM ice cold sodium phosphate buffer (pH 7.2) and sonicated for 5 min with 30 sec pulsations at 50% amplitude. The cell lysate was clarified by centrifugation at 50.000 g for 30 min at 4°C (Beckman Coulter). The cell free supernatants were used for testing the enzyme activity of both strains: 100 μL of lysate were added to 100 μL of reaction solution. The consumption rate was normalized by the protein concentration (standard Bradford test) of both lysates [28]. The activity test solution contained 15 mM of *rac*- β -PA and 15 mM α -ketoglutaric acid (amino acceptor). Additionally, 0.1 mM of the cofactor PLP was added to the solution. The solution was buffered by 40 mM sodium phosphate and adjusted at 7.2 with HCl. The reaction temperature was set to 30°C and samples were taken at various points. The samples were diluted with preheated sodium phosphate buffer (40 mM, 1 mM L-leucin, pH 7.2) and incubated at 99°C for 5 min to stop the reaction. L-leucin was used as internal standard for HPLC analysis.

Quantification of β -PA by HPLC

The samples of the fermentation process were centrifuged for at least 5 min at 13.000 rpm in a bench top centrifuge (Eppendorf, Germany) and used for quantification of β -PA and AP. The so collected supernatant was used for HPLC analysis (Agilent 1200 Series) by automated precolumn derivatization with *ortho*-phthaldialdehyde and IBLC [29]. A reversed phase C18 column (150 x 4.6 mm HyperClone 5 μ m. Phenomenex Inc., Aschaffenburg, Germany) was used. The mobile phase was a mixture of 55% methanol and 45% of 40 mM sodium phosphate buffer (pH 6.5). The flow rate was set to 1 ml/min and the column temperature to 40°C. Detection was carried out by light absorption at 337 nm. The injection volume of the samples for the derivatization mixture was set to 0.5 μ L. The total injection volume of the derivatization mixture was 10 μ L. Calibration was performed using *rac*- β -PA (0 to 15 mM). To determine (*R*)- and (*S*)-enantiomers we used optically pure β -PA standards from Peptech (Burlington, USA).

Quantification of Acetophenone (AP) by HPLC

For analysis of AP the same HPLC method as mentioned before, but without derivatization. According to β -PA quantification, samples were centrifuged for at least 5 min at 13.000 rpm in a bench top centrifuge. AP was measured at 245 nm and 5 μ L sample was injected. Also a different C18 column was used (Kinetex 5 μ m EVO C18 150 x 4.6 mm).

Quantification of D-glucose by HPLC

For quantification of D-glucose in PsJN samples, HPLC was used. This was necessary, because samples showed an interaction with the enzymatic assay. Glucose concentration was measured using HPLC-system with RI-detector system (Agilent 1100 series) adapted from Buchholz et al., 2014 [30]. Briefly, samples (S) were precipitated by 4 M NH_3 in combination with 1.2 M MgSO_4 in ratio of 0.87 (S): 0.039 (NH_3): 0.087 (MgSO_4), incubated for a few minutes at RT and centrifuged at 17.000 g in benchtop centrifuge. The supernatant was mixed 1:1 with 0.1 M H_2SO_4 and was again incubated at RT for at least 20 min and centrifuged at 17.000 g for 15 min. 10 μ L of the supernatant were injected on a Rezex ROA-organic acid H^+ column (300 x 7.8 mm, Phenomenex). The mobile phase consisted of 5 mM H_2SO_4 solution with a flow rate of 0.4 ml/min. The temperature was set to 50°C for the column and 32°C for RI-detector. For calculation of the d-glucose concentration, a calibration curve was measured from 0.01 g/L to 0.5 g/L.

Data analysis

The maximal growth rate μ and substrate-consumption were fitted using a sigmoidal equation with three variable parameters to the optical density/dry-cell mass of the cell cultures and to the concentration of β -PA during the fermentation with data analysis software Sigma Plot (San Jose, USA) adapted to Dörsam *et al.* [31]. The parameters a and b were defined as variables for the sigmoidal equation fit using Sigma Plot. x_0 can be interpreted as half maximum of biomass production or as the half amount of the consumed β -PA and is the inflection point of the function. The variables are x and $f(x)$. The cultivation time was defined as x in hours. The corresponding $f(x)$ was defined as optical density, dry cell mass or the concentration of β -PA [mM].

$$f(x) = \frac{a}{1 + e^{-\frac{x-x_0}{b}}}$$

After fitting of the function against the measured values, the maximal rates were determined by calculating the slope using numeric differentiation with Excel (Microsoft, USA).

6.3) Results

Both strains BS115 and PsJN were able to grow in minimal medium containing β -PA as sole nitrogen source in 1 L scale experiment. The fermentation process was started by inoculation of β -PA induced precultures.

6.3.1) Fermentation of *Paraburkholderia*

The main fermentation process of BS115 is illustrated in **figure 6.1** a. The lag phase of the culture was observed between 0 h and 12 h. After this incubation period the culture was growing with maximal growth rate (12 h -21 h) until (*S*)- β -PA was almost completely consumed. After the preferred enantiomer was depleted, growth continued at a considerably slower rate. The stationary phase was reached 48 h after inoculation. The total consumed amount of (*R*)- β -PA was 2.5 mmol after 50 h of fermentation. In contrast the AP concentration increased with progressing fermentation and peaked at 4.5 mmol, when (*S*)- β -PA was almost fully consumed thereby nearly matching the consumed concentration of (*S*)-PA. Thereafter the AP concentration substantially decreased until the stationary growth phase was reached (Appendix S. Figure X).

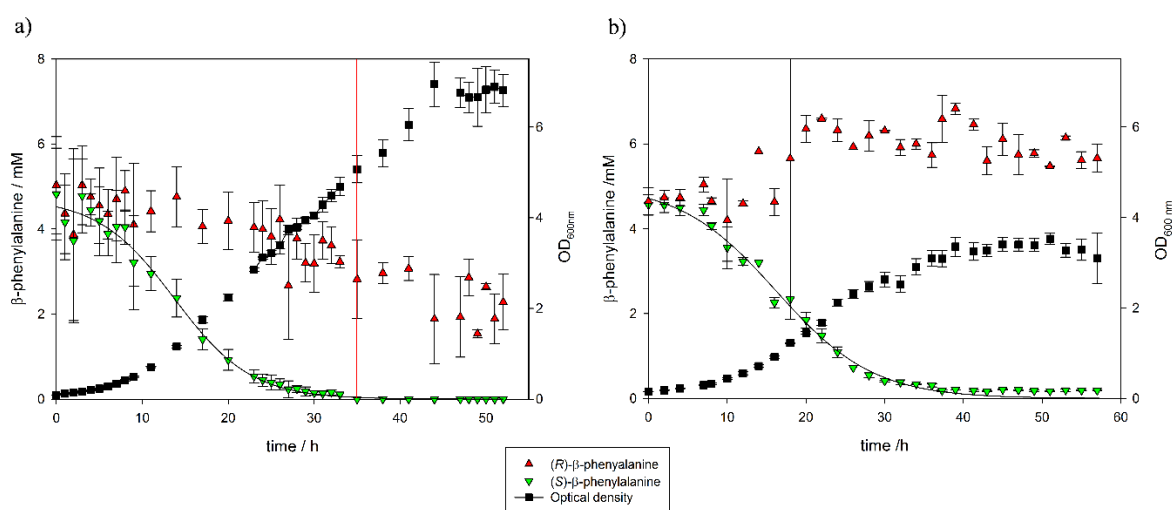


Figure 6.1 Degradation of *rac*- β -phenylalanine by *Paraburkholderia* sp. in a 2.5 L bioreactor. The fermentation was conducted in triplicate at 30°C in 1L minimal medium M1. a) BS115 b) PsJN. The red line indicates > 1% (*S*)- β -PA.. The experiments of BS115 were performed by Sarah Dold [27].

Growth resulted in a maximal optical density of 7.0, resembling a dry cell mass (DCM) concentration of 1.8 g/L at the end of the fermentation. The oxygen concentration before inoculation was set to 100 % and dropped during the process to a minimum of 80 %. While centrifuging fermentation samples for analytical purposes, the formation of a slime layer was observed when (*S*)- β -PA was fully consumed, which reproducibly happened at each

6) Degradation and deracemization of β -PA using different Paraburkholderia species

fermentation. The extracellular capsule built by BS115 was visualized by negative contrasting with Chinese ink (**Figure S11**).

After 24 h the pH-level dropped from pH 7.0 to pH 6.0, then remained constant for 20 hours, but decreased in the last 10 h to a final pH of 3.5 (**Figure S13**). The remaining concentration of D-glucose inside the reactor was 27 ± 1.6 mM and total amount of consumed d-glucose was 73 mM. The ratio between consumed carbon to consumed nitrogen (C: N) was calculated as 14.6 mM per 1 mM of (*S*)- β -PA.

The fermentation process of PsJN to characterize β -PA degradation was also investigated. Furthermore PsJN was used as control strain, to exclude that the degradation of (*R*)- β -PA is only an unspecific effect during the fermentation process e.g. by adsorption of the amino acid to bacterial cell envelopes or due to other reasons.

The fermentation parameters were maintained according to the BS115 fermentation. The degradation of the (*S*)-enantiomer was almost complete after 38 h, which is in total 5 mM of β -PA (**Figure 6.1**). During the whole fermentation no degradation of (*R*)- β -PA was observed. The AP concentration increased during the process to a maximum of 1.6 mM after 35 h (**Figure 6.2**). After 50 hours a slow decrease of the AP concentration in the medium to 0.8 mM was determined. In addition, we also observed only a slight capsulation of the microorganism with increasing fermentation time, which was not observed in shake flask experiments.

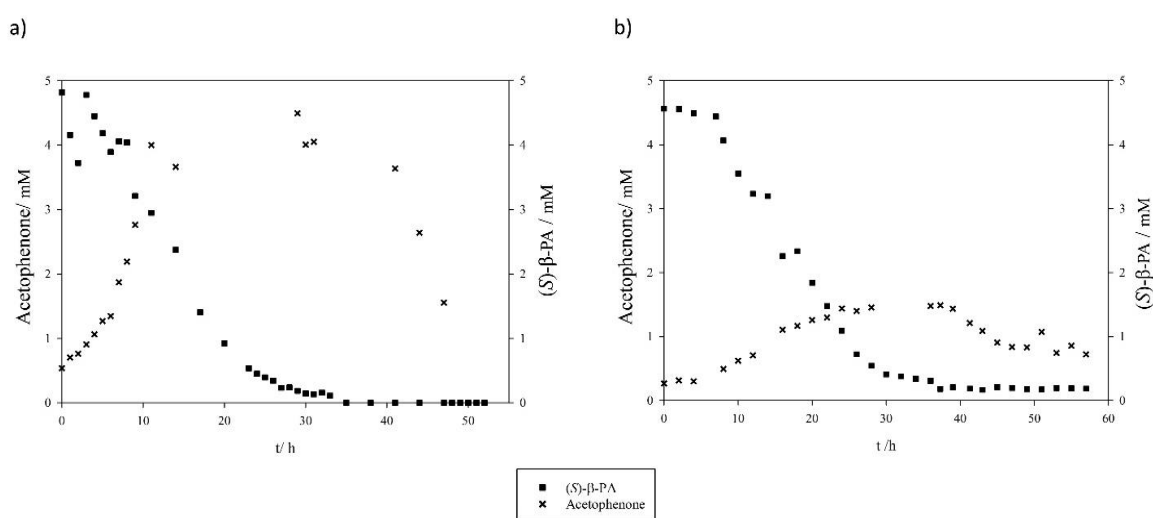


Figure 6.2 Acetophenone content during fermentation process in comparison to (*S*)- β -PA concentration. AP concentration rises inversely proportional to (*S*)- β -PA degradation and decreases after (*S*)- β -PA depletion. A) BS115 fermentation B) PsJN fermentation.

The total amount of consumed (*S*)- β -PA was three times higher than the maximal concentration of AP in the medium. The OD_{600nm} reached a maximum of 3.3 which is half the OD₆₀₀ reached in the BS115 fermentation. The oxygen concentration decreased to a minimum of 70 %. In contrast to BS115, the pH-value dropped from neutral (pH 7) to pH 5, instead of pH 3.5. The d-glucose concentration could not be determined by glucose assay, caused by an inhibition or unknown interaction of the enzymatic assay with the supernatant of the fermentation medium. Therefore, we determined the concentration of d-glucose by HPLC. The remaining concentration of glucose inside the fermentation medium was 21.9 mM \pm 2.5 mM after 50 h, which is 5 mM less than for BS115. The molar ratio of consumed carbon to nitrogen source was 15.6 per 1 mM (*S*)- β -PA. The DCM peaked after 50 h of cultivation at the concentration of 0.9 g/L, which is only half as much as for BS115.

Table 6.1 Characterization of *Paraburkholderia* sp. fermentation process. The calculations are based on the mean values of three independent fermentations

	Max. growth rate μ_{\max} [1/h]	Max. volumetric growth rate rx [g/(L h)]	Max. volumetric consumption rate $Q_{(S)\text{-PA}}$ [mM/h]	Max. specific consumption rate $q_{(S)\text{-PA}}$ [mmol/(g h)]	t_d [h]
<i>Paraburkholderia phytofirmans</i> PsJN	0.14	0.036	0.21	-2.1	4.95
<i>Paraburkholderia</i> sp. BS115	0.23	0.063	0.26	-1.3	3.0

Within the two day fermentation using BS115 the DCM level of 2 g/L is clearly higher compared to PsJN, but in respect of the produced biomass in ratio to the depleted glucose amount the $Y_{x/s}$ -value of 0.15 is rather low. Surprisingly a consumption of the (*R*)-enantiomer of β -PA was shown for BS115 but the growth was limited although neither (*R*)- β -PA nor glucose was fully depleted. The remaining concentration of glucose was 27 \pm 1.6 mM and the oxygen concentration of 80% can be ruled out as limiting factor for further growth. The conversion rates of β -PA and the growth rate μ and volumetric growth rate rx were compared in Table 1. The μ_{\max} was determined for PsJN after 17.9 h of cultivation with 0.14 h⁻¹, which is equate to a doubling time (t_d) of 4.95 h. Strain BS115 reached its maximum at 27.0 h of cultivation time with 0.23 h⁻¹.

6) Degradation and deracemization of β -PA using different Paraburkholderia species

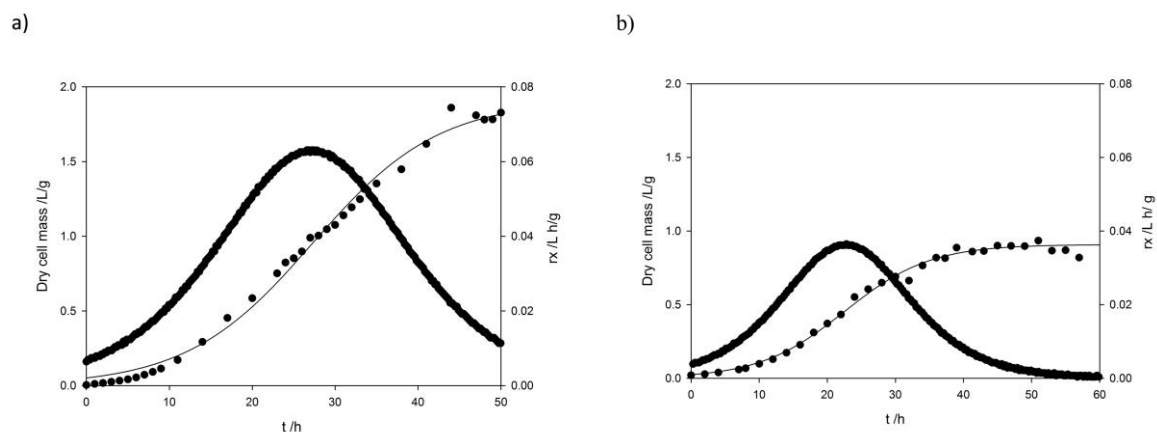


Figure 6.3 Dry cell mass building rate of a) BS115 and b) PsJN. The dry cell mass data points were fitted with a 3 parameter sigmoid function with an R^2 of 0.99. This function was used to calculate the slope ($\Delta DCM/\Delta t$).

During fermentation BS115 grew 1.6 times faster than PsJN on β -PA. (**Figure 6.3**). The $Q_{(s)\text{-PA}}$ rate was calculated to be 0.26 mM h^{-1} for BS115 after 14.2 h (**Figure 6.4**). The $Q_{(s)\text{-PA}}$ rate of PsJN was slightly lower with 0.21 mM h^{-1} after 16.2 h of cultivation time. In addition the $q_{(s)\text{-PA}}$ was determined for both strains, which is correlated to the biomass concentration. On the other hand BS115 had a specific $q_{(s)\text{-PA}}$ rate which is slightly lower with $0.74 \text{ mmol g}^{-1} \text{ h}^{-1}$ compared to PsJN with $0.88 \text{ mmol g}^{-1} \text{ h}^{-1}$ (Figure 6.4).

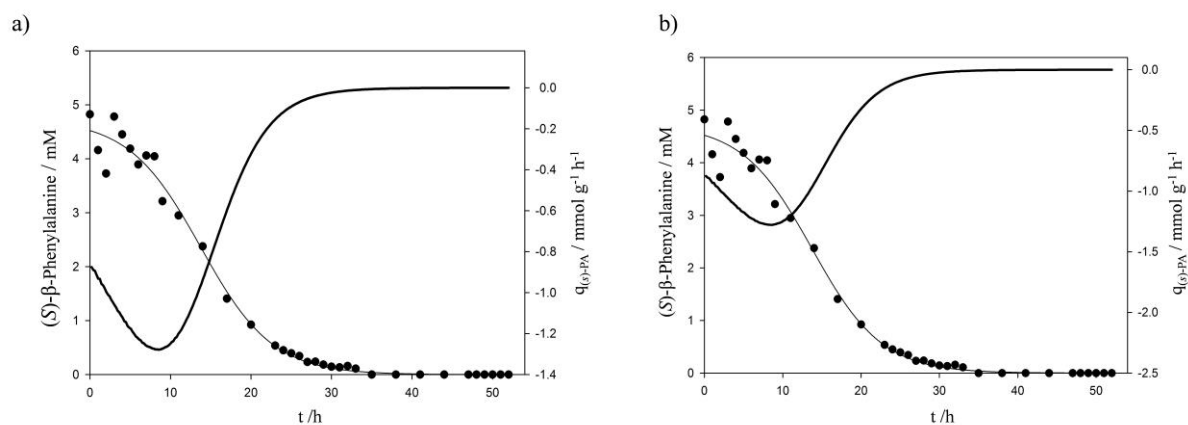


Figure 6.4 Decrease rate of (*S*)- β -PA. Bold line – $q_{(S)\text{-PA}}$. Points with line – concentration of (*S*)- β -PA in bioreactor. a). BS115 b) PsJN.

PsJN produced less biomass but the cells converted (*S*)- β -PA more efficiently. PsJN started to convert with maximal specific consumption rate, whereas BS115 reached its maximal consumption rate after 8 h of cultivation time. In contrast to (*S*)- β -PA, the consumption rate of (*R*)- β -PA could not be fitted for BS115, caused by the high variances and inconstant decreasing rate between 25 and 50 h of cultivation. The volumetric production rate Q_{AP} of AP reached a maximum of 0.07 mM h^{-1} for PsJN after 10.8 h of fermentation. After several hours the AP concentration decreased with a much slower with a Q_{AP} rate of 0.01 mM h^{-1} . Initially, the BS115 Q_{AP} rate was faster than calculated for PsJN, with 0.34 mM h^{-1} .

6.3.2) ω -TA activity test

The β -PA degrading activity of both strains were tested with cell free lysate from BS115 and compared to PsJN lysate. The temperature was set to 30°C according to the cultivation temperature of BS115 and PsJN. For the transamination reaction 0.1 mM of the ω -TA cofactor molecule PLP and selected α -ketoglutarate as acceptor molecule was added due to the compatibility towards well characterized β -phenylalanine transaminases [24,31]. The final concentration of applied protein in the reaction mixture was 0.47 mg/mL for PsJN and 0.95 mg/mL for BS115. The concentration of *rac*- β -PA in the lysate-reaction mixture was determined at different times, to recognize slow and fast conversions as well as long-term effects (**Figure S12**). After 24 h both lysates showed only activity for (*S*)- β -PA and a complete conversion of the (*S*)-enantiomer. The transaminase activity at the beginning of the reaction was considerably higher for PsJN lysate than for BS115. The specific activities of both

preparations were calculated between samples of 15 s and 1 h and varied between 35 ± 5 mU/mg for PsJN and 8 ± 4 mU/mg for BS115. In total, the amounts of the obtained lysate activity was 1.25 U and 0.32 U in 100 mL cell culture at an OD₆₀₀ of 3.1.

6.4) Discussion

6.4.1) Degradation of (*S*)- β -PA by BS115 and PsJN

Both *Paraburkholderia* strains BS115 and PsJN were able to grow with (*S*)- β -PA as sole source of nitrogen. The metabolization of the N-source most likely occurs via a transaminase reaction in which the amino group of (*S*)- β -PA is transferred to an α -keto acid. Although α -ketoglutarate has been shown to be the most suitable *in vitro* amino acceptor, the *in vivo* application of other molecules like pyruvate is also possible.

Deracemization of β -PA has only once been reported so far: The only comparable fermentation example from Mano *et al.* showed that the soil bacterium *Variovorax sp.* JH2 is able to convert (*S*)-selective 61 mM of β -PA within 8 days [26]. They achieved a maximal degradation rate of 0.26 mM h^{-1} towards (*S*)- β -PA, which is comparable to the uptake rates of PsJN and BS115. The opportunity to utilize bacterial strains for chiral resolution of *rac*- β -PA should be tested in further experiments in larger scales and at higher concentration levels, to prove whether a microbial process might be able to compete with established industrial deracemization processes as known from Evonik-Degussa using lipases [32]. Yeast cells have successfully been used for the chiral resolution of alcohols and more recent examples document the microbial resolution e.g. of DL-glyceric acid [33–35].

The rapid degradation of the (*S*)-enantiomer, in contrast to the (*R*)-enantiomer, resulted in a reduction of the pH-value by metabolizing almost half of the D-glucose. According to this, the final pH value of 3.5 is most likely to be limiting. In addition it could be seen that during BS115 fermentation the pH-value stagnated at a constant value of five for several hours before it dropped to 3.5. A total consumption of the (*R*)-enantiomer might be possible, if the fermentation process was pH regulated. The fermentation parameters quantified are valuable for using the strains as whole cell biocatalyst for chiral resolution of *rac*- β -PA for lab scale chiral resolution experiments and lead the assumption, that BS115 is able to convert (*R*)- β -PA by a mechanism unknown so far. The lowering of the pH value indicates that either an organic acid is formed or a previously buffering substance has been absorbed by BS115. A possible explanation for this could also be that when switching from (*S*) to (*R*)-enantiomer degradation, the resulting β -

keto acid production stops for a while, and its restart ultimately lowers the pH-value. The decomposing β -keto acid also forms CO_2 , which could acidify the medium but is likely to be driven out over time by the supply of fresh air.

By-product analysis

The proposed transamination of (*S*)- β -PA leads to the corresponding β -keto acid 3-oxo-3-phenylpropanoic acid. However, this molecule has never been detected in medium as it spontaneously decarboxylates to AP as has been shown in previous studies [24,36]. AP on the other hand was shown to emerge in parallel to the degradation of (*S*)- β -PA, peaking for both strains after about 30h when (*S*)- β -PA is depleted. Progress of AP formation rate and (*S*)- β -PA degradation rate are nearly identical for both strains which is strong evidence for the proposed transamination mechanism (**Figure 6.5**). In BS115, even the molar concentrations of emerging AP and metabolized (*S*)- β -PA are close to identical. So it is most likely that after transamination the corresponding β -keto acid decarboxylates and the emerging AP is excreted.

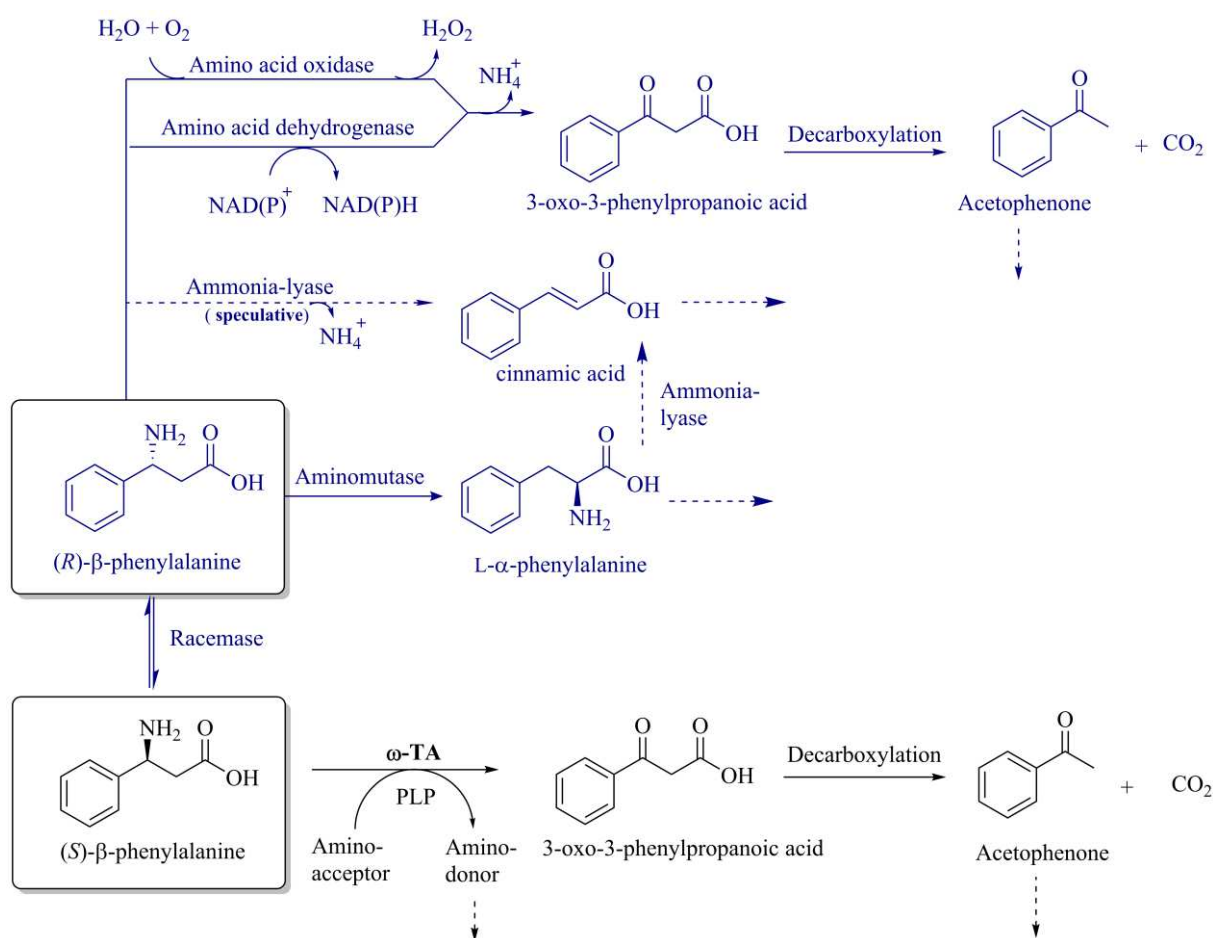


Figure 6.5 Putative degradation mechanisms for conversion of β -PA. In grey: putative degradation mechanisms of (*R*)- β -PA and (*S*)- β -PA. In black: identified degradation pathways of (*S*)- β -PA.

6) Degradation and deracemization of β -PA using different *Paraburkholderia* species

After depletion of (*S*)- β -PA, AP concentration in the medium notably decreases. Substantial evaporation of the volatile AP can be excluded from control experiments (data not shown). A reuptake of AP is possible, but from the data at hand it cannot be stated whether AP serves as additional carbon source or as amino acceptor without further metabolization which would also lead to the observed depletion. Rehdorf *et al.* showed in *Pseudomonas putida* strain JD1, that a Baeyer-Villiger monooxygenase converts 4-hydroxy AP to phenyl-acetate. Finally, phenyl-acetate is further degraded via a β -keto adipate metabolic pathway. At the same time, the enzyme is also able to convert AP [37]. This metabolic pathway releases acetic acid, which should lower the pH value of the fermentation medium. This is supported by the fact that at the very time when acetophenone decreases drastically (after 40 h), also the pH value of BS115 fermentation decreases from 6 to 4 (**Figure S13**).

Further experiments with a different *Paraburkholderia* strain demonstrated that AP can be reduced by a carbonyl reductase [38], which might serve as an evidence for further metabolization inside the cells. It is also known that *Burkholderia* sp. expresses a reductase which is able to reduce 2-aminoacetophenone to 2-amino-1-phenylethanol [39]. The same reductase might also be able to convert AP. Furthermore PsJN is known to degrade even more complex aromatic biomolecules like the plant hormone indole-3-acetic acid by a rather complex degradation pathway to catechol [40]. So a bacterial metabolization of AP as a reason for its decrease is most likely.

Superior growth of BS115

Although both strains clearly metabolize (*S*)- β -PA via the same mechanism, BS115 reaches a final OD₆₀₀ twice as high as that of PsJN under identical growth conditions. According to 16S-rDNA sequencing, both strains show >99% identity, so the basic metabolism might not differ too much and maybe only one additional enzyme makes up the severe difference in growth. However, it is also possible that different enzymes from other microbial sources are integrated in BS115 genome via horizontal gene transfer, especially when the strain was exposed to extraordinary amino sources in soil. Since the PsJN cultures obviously reaches the stationary phase when (*S*)- β -PA is depleted although sufficient amounts of d-glucose are still at hand, a growth stop can be explained by the inability of this strain to use the (*R*)-enantiomer as nitrogen source; (*R*)- β -PA remains completely unconsumed during the whole fermentation. A growth inhibition by other factors like toxic metabolites is unlikely since the closely related strain

BS115 very probably faces similar but even stronger stress conditions (e.g. ongoing acidification, depletion of other nutrients than N-source).

Moreover, BS115 shows a quite similar cell dry mass per depleted (*S*)- β -PA minus depleted (*R*)- β -PA. In total BS115 built 1.82 g of biomass per liter and consumed 7.72 mM of *rac*- β -PA, that is a ratio of 4.3 g/(mM(β -PA)). In contrast PsJN built only 0.82 g L⁻¹ (ratio 5.9 g/(mM(β -PA))) and was at the same time more efficient in using only (*S*)-PA. So we postulate at least one additional enzyme in BS115 which allows the metabolization of (*R*)- β -PA as additional N-source and potentially also as additional C-source, leading to a better growth and to the formation of considerably more cell dry mass from the same medium.

Degradation of (*R*)- β -PA by BS115

Several options of amino acid metabolization are identified and well investigated (see also introduction section), and most of these also seem conceivable for the degradation of (*R*)- β -PA. Since activity has only been observed in growing cells, a cofactor-dependent mechanism is likely. Moreover, an additional transaminase would have been detected under the given conditions, and also a side activity of the identified (*S*)- β -PA can be excluded: (*R*) and (*S*)- ω -TAs show only low sequence identities and can clearly be differentiated by protein fold types [41,42]. A transamination of (*R*)- β -PA would have led to the formation of AP, but on the contrary the concentration of AP decreased. Several (*R*)-selective ω -TAs have been described for the ability to convert and synthesize (*R*)-configured amines. However, activity towards aromatic or bulky β -AAs were only observed for (*S*)-selective ω -TAs [36,43,44] and no (*R*)-PA converting transaminase has been reported until now [45–48]. Only Mano *et al.* investigated an (*R*)-selective strain, *Arthrobacter sp.* AKU 638, which is suitable for chiral resolution to gain the optical pure (*S*)- β -PA. However, this degradation process is very slow and took 13 days of fermentation and in contrast to BS115 they did not recognize any depletion of the (*S*)-enantiomer at the same time [26]. Oxidative deamination has been suggested, but until now, the mechanism for the degradation of (*R*)- β -PA in *Arthrobacter sp.* AKU 638 is uncovered. .

In fact, the metabolism of (*R*)- β -PA has only been reported for microorganism with assured aminomutases or ammonia lyases genes [48–50]. The activity of aminomutases is described as quite low which might explain the rather slow degradation of (*R*)- β -PA using BS115 [51]. Also several amino acid oxidases exist with high activity towards several amines [52,53], but as yet amino acid oxidases with activity towards β -PA have not been published. Analogously no wildtype β -amino acid dehydrogenase is known; the only example of a dehydrogenase with

6) Degradation and deracemization of β -PA using different Paraburkholderia species

activity towards β -PA is an engineered enzyme from the amino acid fermenting bacterium *Candidatus cloacamonas* [54].

However, PA-racemases have been described for the racemization between l and d- α -PA in bacteria [55] and for plants the *Taxus* (yew) PA aminomutase is known to use α -phenylalanine as substrate to produce (*R*)- β -PA [56]. Wu *et al.* showed that a PA mutase from *Taxus chinensis* can be utilized for chiral separation of *rac*- β -PA. The corresponding α -PA is then degraded to cinnamic acid using an α -PA ammonia lyase from *Rhodospiridium toruloides*. The reported reaction time for chiral resolution was quite long with more than 48 h using 2 mM of substrate [57]. Apart from this also β -tyrosine aminomutase is known from *Oryzae sativa* with high enantioselectivity towards (*R*)- β -PA [58]. So a slow enzymatic racemization of (*R*)-PA to (*S*)-PA and further metabolization of the latter by BS115 appears at least possible; but no bacterial racemase with such an activity is known until now.

Hypothetical degradation pathway for (*R*)- β -PA

Recently Csuka *et al.* reported that *Pseudomonas fluorescens* R124 encodes three different class I lyase like enzymes, namely an ammonia-lyase, an aromatic 2,3 aminomutase and a histidine ammonia-lyase [59]. The authors describe, that under nitrogen limitation, *P. fluorescens* is able to integrate new genes by horizontal gene transfer to overcome limitations. Therefore BS115 might be adapted towards special nitrogen limitations, even when the genome is quite similar to PsJN. For this reason it might be possible that BS115, in the presence of (*S*)- β -PA, expresses an ammonia-lyase which could convert (*R*)- β -PA to cinnamic acid which could further metabolized in catabolism and might be additionally a reason for lowering the pH-value. *Pseudomonas* strains can metabolize cinnamic acid to *o*-hydroxyphenylpropionic acid and to 2,3-dihydroxyphenylpropionic acid [60]. BS115 might be able to regenerate NAD(P)⁺ by this way using an NADP oxidoreductase. In high concentrations cinnamic can also be reduced by NADH using fumarate reductase or by an oxygen-sensitive 2-enoate reductase [61,62]. An oxygen-sensitive enzyme would also give an explanation why the activity is hard to detect in crude extracts without further protective measures.

This assumption is supported by growth experiments on enantiopure (*R*) and (*S*)- β -PA as nitrogen sources, as BS115 is only able to degrade (*R*)- β -PA in the presence of (*S*)- β -PA and not when added as sole N-source (**Figure 6.6**). The experiments showed that (*S*)- β -PA was completely converted, whereas the (*R*)-enantiomer as sole nitrogen source remained untouched

even after a cultivation duration of 70 h (Figure 5a). On the other hand, the (*R*)-enantiomer was substantially degraded in the presence of (*S*)- β -PA (Figure 6.6 b). Only 40 % of 10 mM (*R*)-enantiomer retained within the cultivation medium after 70 h. Therefore (*S*)- β -PA serves as nitrogen source and (*R*) might only serve as additional carbon source or as electron acceptor, if cinnamic acid as intermediate is produced.

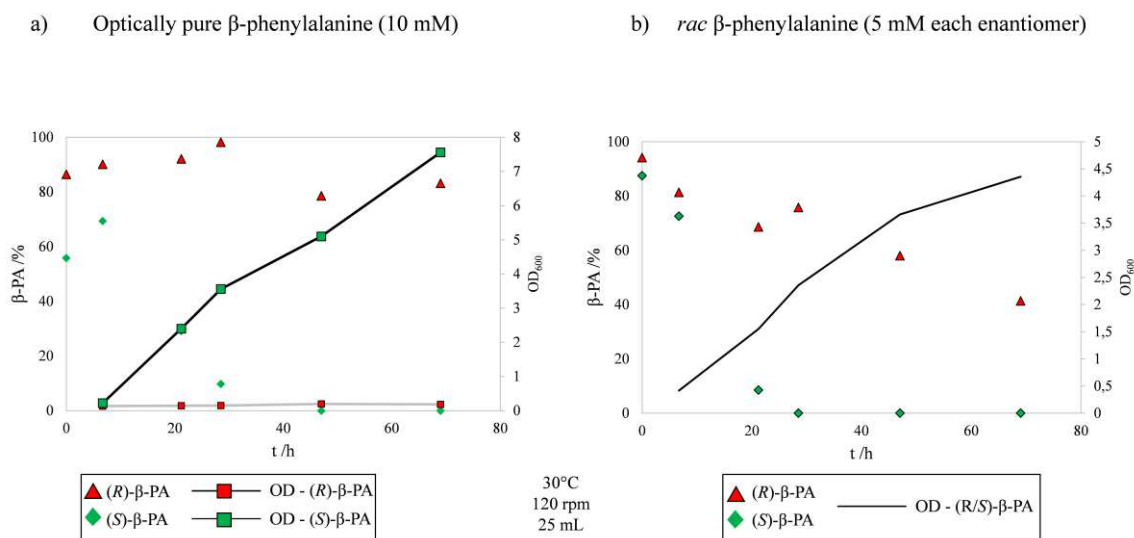


Figure 6.6 Conversion of (*R*)- β -PA in presence of the (*S*)-enantiomer (b) and no conversion as sole nitrogen source (a). The experiment was performed using optically pure β -PA in minimal medium. BS115 was pre-cultivated on (*R/S*)- β -PA for three days in shaking-flasks.

All of the above discussed potential pathways and metabolization steps using the addressed different enzymes are also summarized in figure 6.5. These results also confirm the report from Mano *et al.*, that no activity can be detected in cell-free lysate of an *Arthrobacter sp.* AKU 638 strain for (*R*)- β -PA consumption. Furthermore, the reported very slow degradation, might hint to a similar mechanism using the same enzyme as in BS115.

6.5) Conclusion

We characterized the degradation of racemic β -PA by a three days fermentation of two *Paraburkholderia* strains PsJN and BS115 in a 2.5 L-benchtop fermenter in 1 L medium. PsJN exhibited strict (*S*)-selectivity and therefore can be utilized as whole cell biocatalyst to obtain (*R*)- β -PA in high optical purity by chiral resolution. The spontaneous decarboxylation of the emerging β -keto acid to acetophenone, for the first time documented over the whole degradation process, shifts the equilibrium irreversibly towards the desired direction. To gain industrial

6) Degradation and deracemization of β -PA using different Paraburkholderia species

relevance a high cell density fermentation has to be developed with medium conditions allowing much higher substrate concentrations, maybe using fed batch approaches.

By contrast, BS115 also metabolizes (*R*)- β -PA by a so far unknown mechanism. Today, the possibilities to synthesize (*R*)-configured aromatic amines and amino acids are limited by the availability of (*R*)-selective enzymes; so far, only few plant enzymes are known for the synthesis of (*R*)- β -PA [63]. So the investigation of the (*R*)- β -PA degradation process in BS115 might not only lead to a deeper understanding of the biochemical pathways of β -AA but to novel approaches for the chemoenzymatic synthesis of this highly relevant substance class.

6.6) References Chapter 6

- [1] Voet D, Voet JG. Biochemistry. Wiley; 2011.
- [2] Brückner H, Hausch M. Gas chromatographic detection of D-amino acids as common constituents of fermented foods. *Chromatographia* 1989;28:487–92. doi:10.1007/BF02261066.
- [3] Ohide H, Miyoshi Y, Maruyama R, Hamase K, Konno R. D-Amino acid metabolism in mammals: Biosynthesis, degradation and analytical aspects of the metabolic study. *J Chromatogr B* 2011;879:3162–8. doi:10.1016/j.jchromb.2011.06.028.
- [4] Radkov AD, Moe LA. Bacterial synthesis of D-amino acids. *Appl Microbiol Biotechnol* 2014;98:5363–74. doi:10.1007/s00253-014-5726-3.
- [5] Krebs HA. Metabolism of amino-acids: Deamination of amino-acids. *Biochem J* 1935;29:1620–44.
- [6] Vollmer W, Blanot D, De Pedro MA. Peptidoglycan structure and architecture. *FEMS Microbiol Rev* 2008;32:149–67. doi:10.1111/j.1574-6976.2007.00094.x.
- [7] Kuramitsu HK, Snoko JE. The biosynthesis of D-amino acids in *Bacillus licheniformis*. *Biochim Biophys Acta* 1962;62:114–21. doi:10.1016/0006-3002(62)90496-1.
- [8] Candela T, Fouet A. Poly-gamma-glutamate in bacteria. *Mol Microbiol* 2006;60:1091–8. doi:10.1111/j.1365-2958.2006.05179.x.
- [9] Cotter PD, O'Connor PM, Draper LA, Lawton EM, Deegan LH, Hill C, et al. Posttranslational conversion of L-serines to D-alanines is vital for optimal production and activity of the lantibiotic lactacin 3147. *Proc Natl Acad Sci U S A* 2005;102:18584–9. doi:10.1073/pnas.0509371102.
- [10] Veiga P, Piquet S, Maisons A, Furlan S, Courtin P, Chapot-Chartier M-P, et al. Identification of an essential gene responsible for d-Asp incorporation in the *Lactococcus lactis* peptidoglycan crossbridge. *Mol Microbiol* 2006;62:1713–24. doi:10.1111/j.1365-2958.2006.05474.x.
- [11] Duan X, Li Y, Du Q, Huang Q, Guo S, Xu M, et al. Mycobacterium Lysine ϵ -aminotransferase is a novel alarmone metabolism related persister gene via dysregulating the intracellular amino acid level. *Sci Rep* 2016;6:19695. doi:10.1038/srep19695.
- [12] Roberts E, Rothstein M, Baxter CF. Some Metabolic Studies of ϵ -Aminobutyric Acid. *Exp Biol Med* 1958;97:796–802. doi:10.3181/00379727-97-23883.
- [13] Pettit GR, Kamano Y, Herald CL, Tuinman AA, Boettner FE, Kizu H, et al. The isolation and structure of a remarkable marine animal antineoplastic constituent: dolastatin 10. *J Am Chem Soc* 1987;109:6883–5. doi:10.1021/ja00256a070.
- [14] Shon M, Shanmugavel R, Shin G, Mathew S, Lee S-H, Yun H. Enzymatic synthesis of chiral γ -amino acids using ω -transaminase. *Chem Commun* 2014;50:12680–3. doi:10.1039/c3cc44864a.
- [15] Li YL, Xu JH, Xu Y. Deracemization of aryl secondary alcohols via enantioselective oxidation and stereoselective reduction with tandem whole-cell biocatalysts. *J Mol Catal B Enzym* 2010;64:48–52. doi:10.1016/j.molcatb.2010.01.031.
- [16] Nutzenadel W, Scriver CR. Uptake and Metabolism of Beta-Alanine and L-Carnosine by Rat Tissues In Vitro - Role in Nutrition. *Am J Physiol* 1976;230:643–51.
- [17] Spitzer ED, Jimenez-Billini HE, Weiss B. beta-Alanine auxotrophy associated with *dfp*, a locus affecting DNA synthesis in *Escherichia coli*. *J Bacteriol* 1988;170:872–6. doi:10.1128/JB.170.2.872-876.1988.
- [18] Drozak J, Veiga-da-Cunha M, Vertommen D, Stroobant V, Van Schaftingen E. Molecular identification of carnosine synthase as ATP-grasp domain-containing protein 1 (ATPGD1). *J Biol Chem* 2010;285:9346–56. doi:10.1074/jbc.M109.095505.
- [19] Hill CA, Harris RC, Kim HJ, Harris BD, Sale C, Boobis LH, et al. Influence of β -alanine supplementation on skeletal muscle carnosine concentrations and high intensity cycling capacity. *Amino Acids* 2007;32:225–33. doi:10.1007/s00726-006-0364-4.
- [20] Kanehisa M, Sato Y, Kawashima M, Furumichi M, Tanabe M. KEGG as a reference resource for gene and protein annotation. *Nucleic Acids Res* 2016;44:D457–62. doi:10.1093/nar/gkv1070.
- [21] Kudo F, Miyayama A, Eguchi T, Huang SX, Unsin C, Tao M, et al. Biosynthesis of natural products containing β -amino acids. *Nat Prod Rep* 2014;31:1056. doi:10.1039/C4NP00007B.
- [22] You P, Qiu J, Su E, Wei D. Carica papaya lipase catalysed resolution of β -amino esters for the highly enantioselective synthesis of (*S*)-dapoxetine. *European J Org Chem* 2013:557–65. doi:10.1002/ejoc.201201055.
- [23] Yun H, Lim S, Cho B, Kim B. ω -Amino Acid: Pyruvate Transaminase from *Alcaligenes denitrificans* Y2k-2: a New Catalyst for Kinetic Resolution of β -Amino Acids and Amines -Amino Acid: Pyruvate Transaminase from *Alcaligenes denitrificans* Y2k-2: a New Catalyst for Kinetic Resolut. *Appl Environ Microbiol* 2004;70:2529–34. doi:10.1128/AEM.70.4.2529.

6) Degradation and deracemization of β -PA using different *Paraburkholderia* species

- [24] Crismaru CG, Wybenga GG, Szymanski W, Wijma HJ, Wu B, Bartsch S, et al. Biochemical Properties and Crystal Structure of a β -Phenylalanine Aminotransferase from *Variovorax paradoxus*. *Appl Environ Microbiol* 2013;79:185–95. doi:10.1128/AEM.02525-12.
- [25] Brucher B, Syltatk C, Rudat J. Mikrobielle Umsetzung von β -Phenylalanin mittels neuer Transaminasen. *Chemie Ing Tech* 2010;82:155–60. doi:10.1002/cite.200900110.
- [26] Mano J, Ogawa J, Shimizu S. Microbial Production of Optically Active β -Phenylalanine through Stereoselective Degradation of Racemic β -Phenylalanine. *Biosci Biotechnol Biochem* 2006;70:1941–6. doi:10.1271/bbb.60099.
- [27] Dold S-M. Enzymatic Synthesis and Microbial Degradation of β -Amino Acids via Transaminases. Karlsruhe Institute for Technology, 2016. doi:10.5445/IR/1000067988.
- [28] Bradford MM. A rapid and sensitive method for the quantitation of microgram quantities of protein utilizing the principle of protein-dye binding. *Anal Biochem* 1976;72:248–54. doi:10.1016/0003-2697(76)90527-3.
- [29] Brucher B, Rudat J, Syltatk C, Vielhauer O. Enantioseparation of Aromatic β^3 -Amino acid by Precolumn Derivatization with *o*-Phthaldialdehyde and *N*-Isobutryl-L-cysteine. *Chromatographia* 2010;71:1063–7. doi:10.1365/s10337-010-1578-x.
- [30] Buchholz J, Graf M, Blombach B, Takors R. Improving the carbon balance of fermentations by total carbon analyses. *Biochem Eng J* 2014;90:162–9. doi:10.1016/j.bej.2014.06.007.
- [31] Dörsam S, Fesseler J, Gorte O, Hahn T, Zibek S, Syltatk C, et al. Sustainable carbon sources for microbial organic acid production with filamentous fungi. *Biotechnol Biofuels* 2017;10:242. doi:10.1186/s13068-017-0930-x.
- [32] Wybenga GG, Crismaru CG, Janssen DB, Dijkstra BW. Structural determinants of the β -selectivity of a bacterial aminotransferase. *J Biol Chem* 2012;287:28495–502. doi:10.1074/jbc.M112.375238.
- [33] Guo F, Berglund P. Transaminase Biocatalysis: Optimization and Application. *Green Chem* 2016;333–60. doi:10.1039/C6GC02328B.
- [34] Savile CK, Janey JM, Mundorff EC, Moore JC, Tam S, Jarvis WR, et al. Biocatalytic Asymmetric Synthesis of Chiral Amines from Ketones Applied to Sitagliptin Manufacture. *Science* 2010;329:305–9.
- [35] Midelfort KS, Kumar R, Han S, Karmilowicz MJ, McConnell K, Gehlhaar DK, et al. Redesigning and characterizing the substrate specificity and activity of *Vibrio fluvialis* aminotransferase for the synthesis of imigabalin. *Protein Eng Des Sel* 2013;26:25–33. doi:10.1093/protein/gz056.
- [36] Grayson JI, Roos J, Osswald S. Development of a Commercial Process for (*S*)- β -Phenylalanine. *Org Process Res Dev* 2011;15:1201–6. doi:10.1021/op200084g.
- [37] Dold S-M, Cai L, Rudat J. One-step purification and immobilization of a β -amino acid aminotransferase using magnetic (M-PVA) beads. *Eng Life Sci* 2016;16:568–76. doi:10.1002/elsc.201600042.
- [38] Singh A, Basit A, Banerjee UC. *Burkholderia cenocepacia*: A new biocatalyst for efficient bioreduction of ezetimibe intermediate. *J Ind Microbiol Biotechnol* 2009;36:1369–74. doi:10.1007/s10295-009-0622-z.
- [39] Yamada-Onodera K, Takase Y, Tani Y. Purification and Characterization of 2-Aminoacetophenone Reductase of Newly Isolated *Burkholderia* sp. YT. *J Biosci Bioeng* 2007;104:416–9. doi:10.1263/jbb.104.416.
- [40] Donoso R, Leiva-Novoa P, Zúñiga A, Timmermann T, Recabarren-Gajardo G, González B. Biochemical and Genetic Bases of Indole-3-Acetic Acid (Auxin Phytohormone) Degradation by the Plant-Growth-Promoting Rhizobacterium *Paraburkholderia phytofirmans* PsJN. *Appl Environ Microbiol* 2017;83:e01991-16. doi:10.1128/AEM.01991-16.
- [41] Höhne M, Schätzle S, Jochens H, Robins K, Bornscheuer UT. Rational assignment of key motifs for function guides in silico enzyme identification. *Nat Chem Biol* 2010;6:807–13. doi:10.1038/nchembio.447.
- [42] Koszelewski D, Tauber K, Faber K, Kroutil W. ω -Transaminases for the synthesis of non-racemic alpha-chiral primary amines. *Trends Biotechnol* 2010;28:324–32. doi:10.1016/j.tibtech.2010.03.003.
- [43] Seo Y-M, Mathew S, Bea H-S, Khang Y-H, Lee S-H, Kim B-G, et al. Deracemization of unnatural amino acid: homoalanine using D-amino acid oxidase and ω -transaminase. *Org Biomol Chem* 2012;10:2482. doi:10.1039/c2ob07161d.
- [44] Mallin H, Höhne M, Bornscheuer UT. Immobilization of (*R*)- and (*S*)-amine transaminases on chitosan support and their application for amine synthesis using isopropylamine as donor. *J Biotechnol* 2014;191:32–7. doi:10.1016/j.jbiotec.2014.05.015.
- [45] Skalden L, Thomsen M, Höhne M, Bornscheuer UT, Hinrichs W. Structural and biochemical characterization of the dual substrate recognition of the (*R*)-selective amine transaminase from *Aspergillus fumigatus*. *FEBS J* 2015;282:407–15. doi:10.1111/febs.13149.
- [46] Mutti FG, Fuchs CS, Pressnitz D, Sattler JH, Kroutil W. Stereoselectivity of four (*R*)-selective transaminases for the asymmetric amination of ketones. *Adv Synth Catal* 2011;353:3227–33. doi:10.1002/adsc.201100558.
- [47] Jiang J, Chen X, Zhang D, Wu Q, Zhu D. Characterization of (*R*)-selective amine transaminases identified by in silico motif sequence blast. *Appl Microbiol Biotechnol* 2015;99:2613–21. doi:10.1007/s00253-014-6056-1.
- [48] Szymanski W, Wu B, Weiner B, De Wildeman S, Feringa BL, Janssen DB. Phenylalanine aminomutase-catalyzed addition of ammonia to substituted cinnamic acids: A route to enantiopure α - and β -amino acids. *J Org Chem* 2009;74:9152–7. doi:10.1021/jo901833y.
- [49] Weise NJ, Parmeggiani F, Ahmed ST, Turner NJ. The Bacterial Ammonia Lyase EncP: A Tunable Biocatalyst for the Synthesis of Unnatural Amino Acids. *J Am Chem Soc* 2015;137:12977–83. doi:10.1021/jacs.5b07326.
- [50] Bartsch S, Wybenga GG, Jansen M, Heberling MM, Wu B, Dijkstra BW, et al. Redesign of a phenylalanine aminomutase into a phenylalanine ammonia lyase. *ChemCatChem* 2013;5:1797–802. doi:10.1002/cctc.201200871.
- [51] Alexeeva M, Enright A, Dawson MJ, Mahmoudian M, Turner NJ. Deracemization of α -methylbenzylamine using an enzyme obtained by in vitro evolution. *Angew Chemie - Int Ed* 2002;41:3177–80. doi:10.1002/1521-3773(20020902)41:17.
- [52] Ghislieri D, Green AP, Pontini M, Willies SC, Rowles I, Frank A, et al. Engineering an Enantioselective Amine Oxidase for the Synthesis of Pharmaceutical Building Blocks and Alkaloid Natural Products. *J Am Chem Soc* 2013;135:10863–9. doi:10.1021/ja4051235.
- [53] Zhang D, Chen X, Zhang R, Yao P, Wu Q, Zhu D. Development of β -Amino Acid Dehydrogenase for the Synthesis of β -Amino Acids via Reductive Amination of β -Keto Acids. *ACS Catal* 2015;5:2220–4. doi:10.1021/cs5017358.
- [54] Conti E, Stachelhaus T, Marahiel MA, Brick P. Structural basis for the activation of phenylalanine in the non-ribosomal biosynthesis of gramicidin S. *EMBO J* 1997;16:4174–83. doi:10.1093/emboj/16.14.4174.
- [55] Cox BM, Bilsborrow JB, Walker KD. Enhanced Conversion of Racemic α -Arylalanines to (*R*)- β -Arylalanines by Coupled Racemase/Aminomutase Catalysis. *J Org Chem* 2009;74:6953–9.

6) Degradation and deracemization of β -PA using different Paraburkholderia species

- doi:10.1021/jo9009563.
- [56] Wu B, Szymański W, de Wildeman S, Poelarends GJ, Feringa BL, Janssen DB. Efficient Tandem Biocatalytic Process for the Kinetic Resolution of Aromatic β -Amino Acids. *Adv Synth Catal* 2010;352:1409–12. doi:10.1002/adsc.201000035.
- [57] Walter T, King Z, Walker KD. A Tyrosine Aminomutase from Rice (*Oryza sativa*) Isomerizes (*S*)- α - to (*R*)- β -Tyrosine with Unique High Enantioselectivity and Retention of Configuration. *Biochemistry* 2016;55:1–4. doi:10.1021/acs.biochem.5b01331.
- [58] Csuka P, Juhász V, Kohári S, Filip A, Varga A, Sátorhelyi P, et al. *Pseudomonas fluorescens* strain R124 encodes three different MIO-enzymes. *ChemBioChem* 2017;1–9. doi:10.1002/cbic.201700530.
- [59] Blakley ER, Simpson FJ. The microbial metabolism of cinnamic acid. *Can J Microbiol* 1964;10:175–86. doi:10.1139/m64-025.
- [60] Hillier AJ, Jericho RE, Green SM, Jago GR. Properties and Function of Fumarate Reductase (NADH) in *Streptococcus Lactis*. *Aust J Biol Sci* 1979;32:625–36. doi:10.1071/BI9790625.
- [61] Sun J, Lin Y, Shen X, Jain R, Sun X, Yuan Q, et al. Aerobic biosynthesis of hydrocinnamic acids in *Escherichia coli* with a strictly oxygen-sensitive enoate reductase. *Metab Eng* 2016;35:75–82. doi:10.1016/j.ymben.2016.02.002.
- [62] Ratnayake ND, Theisen C, Walter T, Walker KD. Whole-cell biocatalytic production of variously substituted β -aryl- and β -heteroaryl- β -amino acids. *J Biotechnol* 2016;217:12–21. doi:10.1016/j.jbiotec.2015.10.012.

7) Concluding remarks

The family of ω -TA could be the next important group of enzymes (within the enzyme class of transferases) that are important for industrial applications after hydrolases and oxidoreductases, which is also reflected as a global trend in the field of industrial biocatalysis [1]. The enzyme classes of isomerases, ligases and lyases have not been sufficiently investigated and too less enzyme engineering was performed in the past to achieve an equivalent importance of this classes compared to transferases, oxidoreductases and hydrolases. However, it is also clear that hydrolases remain the most important industrial enzyme class, as they are independent of cofactors and have already been thoroughly analyzed [2].

Transaminases have the potential to improve pharmaceutical synthesis processes and thus gain the research interest of industry and academia. This doctoral thesis therefore shows the potential of ω -transaminases as demonstrated by the exemplary synthesis of β -phenylalanine. Furthermore β -phenylalanine, and β -amino acids (esters) in general, are of particular interest for the development of new active ingredients, peptidomimetics and flavors (chapter 1) as well as drug delivering co-polymers [3,4].

Green and efficient synthesis methods have rarely been shown so far, since chiral β -amino acids are often produced using metallic-ligand based catalysts or just the racemate is synthesized. The synthesis of β -phenylalanine ester via ω -TA seems to be a green and efficient strategy, but the scientific basis for the development of processes is currently still too small. Therefore, ω -TA must first be specifically adapted for processes, as their natural variants are often not sufficiently optimized for production on a larger scale. To solve this problem, the literature data of ω -TA were analyzed in chapter 1 and 3 and functional important amino acid residues were underlined. Furthermore the diversity of the ω -transaminases family was demonstrated.

On this basis, the β -amino acid converting enzyme from *V. paradoxus* was selected as starting point. In addition, this enzyme has been thermostabilized (chapter 4) to fulfill the requirements of enzymatic processes and for enzyme engineering procedures. The improvement allowed the expansion of the long-term activity of the ω -transaminase in solution, but still the synthesis of β -phenylalanine was not possible by a one-step reaction. It could be shown that a reaction cascade consisting of lipase plus ω -TA is feasible, but neither the product yield was sufficient nor the possibility of up-scaling was given. Therefore enzyme engineering was performed (chapter 5), but it was shown that more experiments have to be performed to gain a functional *V. paradoxus* ω -transaminase. The screening of already existing engineered transaminases

7) Concluding remarks

showed, that it is possible to convert aromatic β -keto ester substrates into β -amino acid esters. Also it was highlighted, that no wildtype transaminase showed activity towards the substrate of interest. However, this is an example for modern protein engineering and underlines, how important the transformation of mutagenesis studies can be. Overall, the knowledge base of a certain enzyme class is the most important factor for successful enzyme engineering. Within this thesis, it was also shown, that this knowledge base is still not enough for engineering ω -TA into β -keto ester converting enzymes. Conversion is possible by 3FCR_4M and by ATA117_{11Rd}, but the results also suggest that both enzymes are not optimized for β -keto ester conversion and therefore more engineering has to be performed to result in an industrial enzyme. The fact that β -amino acids, although rarely free occurring in nature, can be consumed by microorganisms (Chapter 6), suggests that several β -amino acid converting enzymes (including transaminases) are still to be discovered, which might also be applicable for the synthesis of β -amino acids. The two Proteobacteria strains *Paraburkholderia* PsJN and BS115 could therefore be used as sources for new ω -TAs and other enzymes with activity against β -phenylalanine. Albeit, *in silico* mining of transaminases in databases, such as oTAED (chapter 3), is also an alternative to microbial tests, as artificial gene synthesis becomes cheaper. This represents an alternative to protein engineering.

7.1) Reaction conditions

Besides the question of identifying or generating ω -TA that can be used for the synthesis of β -amino acids (esters), the question arises how the reaction conditions can be optimized. The reaction equilibrium can be successfully shifted to the product side by removing the co-product of the transaminase reaction. This has been shown in particular for the reaction approaches with *ortho*-xylylenediamine as amino donor. *Ortho*-xylylenediamine, however, leads to polymerization products that precipitate during the reaction, but also remain partly in solution, and therefore make reaction processes more difficult. Alternative and cheaper amino donors such as 1-phenylethyl amine and isopropylamine, both of which are able to shift the chemical equilibrium in transaminase reactions, were much less equilibrium shifting than *ortho*-xylylenediamine in the reactions shown or did not even enable turnovers. But on the other hand not all ω -TA are able to accept *ortho*-xylylyenediamine as amino donor (e.g. from *V. paradoxus*). Reactions with isopropyl amine as donor would be most favorable, but this amino donor is also not accepted by the most of ω -transaminases and must also be used in high molar excess.

7.2) Outlook

The industrial application of ω -TA remains demanding, but in recent years many promising examples have already been shown that underline the possibilities. Accordingly, optimizing ω -TAs for reactions is only the first step towards an enzymatic process. It is therefore necessary to investigate how ω -transaminases can be used in a technical context, since the production of the enzymes can be associated with high costs.

Immobilization

Immobilization processes such as the LentiKats® system (encapsulation) or immobilization by magnetic beads, presented in Chapter 1, already show that these processes are realizable in smaller scales. Other immobilization methods, such as 3D-printed enzymatic flow cell reactors are also conceivable. Within the scope of this thesis and the research project Molecular Interaction Engineering (MIE), preliminary tests for 3D-printed and functionalized reaction systems were therefore performed (see appendix **Figure S14**). First tests showed that 3D functionalization of 3D-printed materials is possible to bind specifically ω -TA on the surface, but the enzymatic activity and the amount of bound transaminase remained low (data not shown). In contrast, commercially available Ni-NTA-columns proved to be significantly better transaminase reactors. Further tests and redesign of the printed 3D flow reactors must therefore be carried out.

Nevertheless, further work could show that ω -TA could be used for the synthesis of β -amino acid (esters) on a larger scale, in flow cell reactors, membrane reactors or batch reactors. Finally, after solving the mentioned challenges, ω -TA could be established as catalysts in pharmaceutical chemistry and in particular for the synthesis of β -amino acids. We will see whether ω -TA in particular and whether enzymes in general can contribute to a more efficient and greener chemical industry in the near future.

7.3) References Chapter 7

1. Buller R, Hecht K, Antonio M, Meyer H-P. An Appreciation of Biocatalysis in the Swiss Manufacturing Environment. *Biocatalysis: An Industrial Perspective*. 2017. p. 16. doi:dx.doi.org/10.1039/9781782629993-00001
2. Singh R, Kumar M, Mittal A, Mehta PK. *Microbial Enzymes: Industrial Progress in 21st Century*. 3 Biotech. Springer; 2016. p. 174. doi:10.1007/s13205-016-0485-8
3. Guo F, Berglund P. *Transaminase Biocatalysis: Optimization and Application*. *Green Chem.* Royal Society of Chemistry; 2016; 333–360. doi:10.1039/C6GC02328B
4. Langer RS, Lynn DM, Putnam DA, Amiji MM, Anderson DG. *Biodegradable Poly(beta-amino esters) and Uses Thereof*. 140-217-600-396-269. 2015; US9700627

Abbreviations and Symbols

μ_{\max}	Max growth rate
Å	Ångstrom
AB	3-Amino butyric acid
ADCL	4-Amino-4-deoxychorismate lyase
AP	Acetophenone
a_w	Water activity
BCAT	l-branched-chain aminotransferase
CRL	<i>Candida rugosa</i> lipase
DAPP	4'-Deoxy-4'-acetylamino-pyridoxal-5'-phosphate
DATA	(R)-selective d- α -transaminases
DKR	Dynamic Kinetic Resolution
<i>E. coli</i>	<i>Escherichia coli</i>
EOPP	Ethyl-3-oxo-phenylpropanoate
EtOAc	Ethyl acetate
FoldX	Empirical force field algorithm
FPLC	Fast protein liquid chromatography
GC	Gas chromatography
Hfams	Homologous families
HPLC	High performance liquid chromatography
IBLC	N-isobutyryl- L-cysteine
IPA	Isopropylamine
KG	α -Keto glutarate
KR	Kinetic resolution
L	Liter
mM	Milli-molar
MD	Molecular dynamic simulation
mg	Milli gram
ms	Milli second
ns	Nano second
ω TAED	ω -Transaminase engineering database
OXD	O-xylenylenediamine
OPA	Ortho-phthalaldehyde
PCR	Polymerase chain reaction
PEA	1-Phenylethylamine
PEEP	β -Phenylalanine ethyl ester-PLP intermediate
PLP	Pyridoxal-5-phosphate
PMP	Pyridoxamine phosphate
P-pocket	5'phosphate oriented binding pocket of PLP in ω -TA
PT	Paclitaxel
$q_{(s)}$ -PA	Specific consumption rate
$Q_{(s)}$ -PA	Volumetric consumption rate (S)- β -PA
Q-AP	Volumetric production rate AP
qPCR	Quantitative Polymerase chain reaction

REU	Rosetta Energy Units
rx	Volumetric growth rate
s	Second
ta	Doubling time (microorganism)
TLC	Thin layer chromatography
T_m	Protein melting point
OD	Spectral absorbance
<i>V. paradoxus</i>	<i>Variovorax paradoxus</i>
Y_{x/s}	Biomass yield per substrate amount
β-AA	β-Amino acid
β-KE	β-Keto ester
β-PA	β-Phenylalanine
β-PAEE	β-Phenylalanine ethyl ester
β-PAME	β-Phenylalanine methyl ester
ΔG	Change in free energy
ΔH	Enthalpy
ΔΔG	Difference in folding-energy between wild type and mutant
ω-TA	ω-Transaminase(s)
ω-VpTA	ω-TA from <i>Variovorax paradoxus</i>

List of all references

- Akasako A, Haruki M, Oobatake M, Kanaya S (1997) Conformational stabilities of *Escherichia coli* RNase HI variants with a series of amino acid substitutions at a cavity within the hydrophobic core. *J Biol Chem* 272:18686–93 . doi: 10.1074/JBC.272.30.18686
- Albuquerque L, Rainey FA, Nobre MF, da Costa MS (2008) *Elitoraea tepidiphila* gen. nov., sp. nov., a slightly thermophilic member of the Alphaproteobacteria. *Int J Syst Evol Microbiol* 58:773–778 . doi: 10.1099/ijs.0.65294-0
- Alexeeva M, Enright A, Dawson MJ, Mahmoudian M, Turner NJ (2002) Deracemization of α -methylbenzylamine using an enzyme obtained by in vitro evolution. *Angew Chemie - Int Ed* 41:3177–3180 . doi: 10.1002/1521-3773(20020902)41:17
- Alford RF, Leaver-Fay A, et. al. (2017) The Rosetta All-Atom Energy Function for Macromolecular Modeling and Design. *J Chem Theory Comput* 13:3031–3048 . doi: 10.1021/acs.jctc.7b00125
- Alibés A, Serrano L, Nadra AD (2010) Structure-based DNA-binding prediction and design. *Methods Mol Biol* 649:77–88 . doi: 10.1007/978-1-60761-753-2_4
- Alvin A, Miller KI, Neilan BA (2014) Exploring the potential of endophytes from medicinal plants as sources of antimycobacterial compounds. *Microbiol Res* 169:483–495 . doi: 10.1016/j.micres.2013.12.009
- Anbar M, Gul O, Lamed R, Sezerman UO, Bayer EA (2012) Improved thermostability of *Clostridium thermocellum* endoglucanase Cel8A by using consensus-guided mutagenesis. *Appl Environ Microbiol* 78:3458–64 . doi: 10.1128/AEM.07985-11
- Anfinsen CB (1973) Principles that Govern the Folding of Protein Chains. *Science* (80-) 181:223–230 . doi: 10.1126/science.181.4096.223
- Arabnejad H, Dal Lago M, Jekel PA, Floor RJ, Thunnissen A-MWH, Terwisscha van Scheltinga AC, Wijma HJ, Janssen DB (2016) A robust cosolvent-compatible halohydrin dehalogenase by computational library design. *Protein Eng Des Sel* 30:175–189 . doi: 10.1093/protein/gzw068
- Arvidsson PI, Frackenpohl J, Ryder NS, Liechty B, Petersen F, Zimmermann H, Camenisch GP, Woessner R, Seebach D (2001) On the antimicrobial and hemolytic activities of amphiphilic β -peptides. *Chembiochem* 2:771–773 . doi: 10.1002/1439-7633(20011001)2:10
- Ayuso-Tejedor S, Abián O, Sancho J (2011) Underexposed polar residues and protein stabilization. *Protein Eng Des Sel* 24:171–177 . doi: 10.1093/protein/gzq072
- Aziz HR, Singleton DA (2017) Concert along the Edge: Dynamics and the Nature of the Border between General and Specific Acid-Base Catalysis. *J Am Chem Soc* 139:5965–5972 . doi: 10.1021/jacs.7b02148
- Bach RD, Canepa C (1996) Electronic factors influencing the decarboxylation of β -keto acids. A model enzyme study. *J Org Chem* 61:6346–6353 . doi: 10.1021/jo960356m
- Back JF, Oakenfull D, Smith MB (1979) Increased Thermal Stability of Proteins in the Presence of Sugars and Polyols. *Biochemistry* 18:5191–5196 . doi: 10.1021/bi00590a025
- Badali H, Prenafeta-Boldo FX, Guarro J, Klaassen CH, Meis JF, De Hoog GS (2011) *Cladophialophora psammophila*, a novel species of Chaetothiales with a potential use in the bioremediation of volatile aromatic hydrocarbons. *Fungal Biol* 115:1019–1029 . doi: 10.1016/j.funbio.2011.04.005
- Bajić M, Plazl I, Stloukal R, Žnidaršič-Plazl P (2017) Development of a miniaturized packed bed reactor with α -transaminase immobilized in LentiKats®. *Process Biochem* 52:63–72 . doi: 10.1016/J.PROCBIO.2016.09.021
- Bakail M, Ochsnein F (2016) Targeting protein–protein interactions, a wide open field for drug design. *Comptes Rendus Chim* 19:19–27 . doi: 10.1016/J.CRCI.2015.12.004
- Bartsch S, Wybenga GG, Jansen M, Heberling MM, Wu B, Dijkstra BW, Janssen DB (2013) Redesign of a phenylalanine aminomutase into a phenylalanine ammonia lyase. *ChemCatChem* 5:1797–1802 . doi: 10.1002/cctc.201200871
- Bauer DC, Bodén M, Thier R, Gillam EM (2006) STAR: predicting recombination sites from amino acid sequence. *BMC Bioinformatics* 7:437 . doi: 10.1186/1471-2105-7-437
- Bava KA, Gromiha MM, Uedaira H, Kitajima K, Sarai A (2004) ProTherm, version 4.0: thermodynamic database for proteins and mutants. *Nucleic Acids Res* 32:120D–121 . doi: 10.1093/nar/gkh082
- Bednar D, Beerens K, Sebestova E, Bendl J, Khare S, Chaloupkova R, Prokop Z, Brezovsky J, Baker D, Damborsky J (2015) FireProt: Energy- and Evolution-Based Computational Design of Thermostable Multiple-Point Mutants. *PLOS Comput Biol* 11:e1004556 . doi: 10.1371/journal.pcbi.1004556
- Bedouelle H (2016) Principles and equations for measuring and interpreting protein stability: From monomer to tetramer. *Biochimie* 121:29–37 . doi: 10.1016/J.BIOCHI.2015.11.013
- Bendl J, Stourac J, Sebestova E, Vavra O, Musil M, Brezovsky J, Damborsky J (2016) HotSpot Wizard 2.0: automated design of site-specific mutations and smart libraries in protein engineering. *Nucleic Acids Res* 44:W479–W487 . doi: 10.1093/nar/gkw416
- Benedix A, Becker CM, de Groot BL, Caflisch A, Böckmann RA (2009) Predicting free energy changes using structural ensembles. *Nat Methods* 6:3–4 . doi: 10.1038/nmeth0109-3
- Benson DA, Karsch-Mizrachi I, Lipman DJ, Ostell J, Sayers EW (2011) GenBank. *Nucleic Acids Res* 39:D32–D37 . doi: 10.1093/nar/gkq1079
- Berendsen HJC, Grigera JR, Straatsma TP (1987) The missing term in effective pair potentials. *J Phys Chem* 91:6269–6271 . doi: 10.1021/j100308a038
- Betz SF (1993) Disulfide bonds and the stability of globular proteins. *Protein Sci* 2:1551–1558
- Beyer H, Walter W (1991) *Lehrbuch der Organischen Chemie*. Hirzel Verlag, Stuttgart
- Bhaskara RM, De Brevern AG, Srinivasan N (2013) Understanding the role of domain-domain linkers in the spatial orientation of domains in multi-domain proteins. *J Biomol Struct Dyn* 31:1467–1480 . doi: 10.1080/07391102.2012.743438
- Bhaskara RM, Srinivasan N (2011) Stability of domain structures in multi-domain proteins. *Sci Rep* 1:40 . doi: 10.1038/srep00040
- Bhosale SH, Rao MB, Deshpande V V (1996) Molecular and industrial aspects of glucose isomerase. *Microbiol Rev* 60:280–300
- Birch M, Challenger S, Crochard JP, Fradet D, Jackman H, Luan A, Madigan E, McDowall N, Meldrum K, Gordon CM, Widegren M, Yeo S (2011) The development of a practical multikilogram synthesis of the chiral β -amino acid imagabalin hydrochloride (PD-0332334) via asymmetric hydrogenation. *Org Process Res Dev* 15:1172–1177 . doi: 10.1021/op2001639
- Blakley ER, Simpson FJ (1964) The microbial metabolism of cinnamic acid. *Can J Microbiol* 10:175–186 . doi: 10.1139/m64-025
- Blaszczak M, Jamroz M, Kmiecik S, Kolinski A (2013) CABS-fold: Server for the de novo and consensus-based prediction of protein structure. *Nucleic Acids Res* 41:W406–W411 . doi: 10.1093/nar/gkt462
- Blomberg C, Blomberg C (2007) *The Physics of Life: Physics at Several Levels*. In: *Physics of Life*. Elsevier, pp 5–16

- Borgo B, Havranek JJ (2012) Automated selection of stabilizing mutations in designed and natural proteins. *Proc Natl Acad Sci* 109:1494–1499 . doi: 10.1073/pnas.1115172109
- Börner T, Rämisch S, Bartsch S, Vogel A, Adlercreutz P, Grey C (2017) Three in One: Temperature, Solvent and Catalytic Stability by Engineering the Cofactor-Binding Element of Amine Transaminase. *ChemBioChem*. doi: 10.1002/cbic.201700236
- Boyko KM, Stekhanova TN, Nikolaeva AY, Mardanov A V., Rakin AL, Ravin N V., Besudnova EY, Popov VO (2016) First structure of archaeal branched-chain amino acid aminotransferase from *Thermoproteus uzoniensis* specific for L-amino acids and R-amines. *Extremophiles* 20:215–225 . doi: 10.1007/s00792-016-0816-z
- Bradford MM (1976) A rapid and sensitive method for the quantitation of microgram quantities of protein utilizing the principle of protein-dye binding. *Anal Biochem* 72:248–254 . doi: 10.1016/0003-2697(76)90527-3
- Braunstein A (1973) Amino Group Transfer. In: *The Enzymes*. Academic Press, p 379
- Braunstein AE (1939) The Enzyme System of Trans-Amination, its Mode of Action and Biological Significance. *Nature* 143:609–610 . doi: 10.1038/143609a0
- Brender JR, Zhang Y, Vakser I, Kellogg E, Stephany J, Baker D (2015) Predicting the Effect of Mutations on Protein-Protein Binding Interactions through Structure-Based Interface Profiles. *PLoS Comput Biol* 11:e1004494 . doi: 10.1371/journal.pcbi.1004494
- Breslow R, Chmielewski J, Foley D, Johnson B, Kumabe N, Varney M, Mehra R (1988) Optically Active Amino Acid Synthesis by Artificial Transaminase Enzymes. *Tetrahedron* 44:5515–5524 . doi: 10.1016/S0040-4020(01)86057-9
- Bringi V, Kadkade PG, Prince CL, Roach BL (2007) Enhanced production of taxol and taxanes by cell cultures of *Taxus* species. *U.S. 48pp.*, Cont. of U.S. Ser. No. 653,036.
- Bromberg Y, et. al. (2009) Correlating protein function and stability through the analysis of single amino acid substitutions. *BMC Bioinformatics* 10:S8 . doi: 10.1186/1471-2105-10-S8-S8
- Broom A, Jacobi Z, Trainor K, Meiering EM Tradeoff between protein stability and solubility Computational tools help improve protein stability but with a solubility tradeoff. doi: 10.1074/jbc.M117.784165
- Broom A, Jacobi Z, Trainor K, Meiering EM (2017) Computational tools help improve protein stability but with a solubility tradeoff. *J Biol Chem* 292:14349–14361 . doi: 10.1074/jbc.M117.784165
- Brucher B, Rudat J, Syldatk C, Vielhauer O (2010a) Enantioseparation of Aromatic β -Amino acid by Pre-column Derivatization with *o*-Phthalaldehyde and *N*-Isobutyl-L-cysteine. *Chromatographia* 71:1063–1067 . doi: 10.1365/s10337-010-1578-x
- Brucher B, Syldatk C, Rudat J (2010b) Mikrobielle Umsetzung von β -Phenylalanin mittels neuer Transaminasen. *Chemie Ing Tech* 82:155–160 . doi: 10.1002/cite.200900110
- Brückner H, Hausch M (1989) Gas Chromatographic Detection of D-Amino Acids as Common Constituents of Fermented Foods. *Chromatographia* 28:487–492 . doi: 10.1007/BF02261066
- Bubb MR (2000) Effects of Jasplakinolide on the Kinetics of Actin Polymerization. An Explanation for Certain in Vivo Observations. *J Biol Chem* 275:5163–5170 . doi: 10.1074/jbc.275.7.5163
- Buchholz J, Graf M, Blombach B, Takors R (2014) Improving the Carbon Balance of Fermentations by Total Carbon Analyses. *Biochem Eng J* 90:162–169 . doi: 10.1016/j.bej.2014.06.007
- Buchholz PCF, Vogel C, Reusch W, Pohl M, Rother D, Spieß AC, Pleiss J (2016) BioCatNet: A Database System for the Integration of Enzyme Sequences and Biocatalytic Experiments. *ChemBioChem* 17:2093–2098 . doi: 10.1002/cbic.201600462
- Bulaj G (2005) Formation of Disulfide Bonds in Proteins and Peptides. *Biotechnol. Adv.* 23:87–92
- Buller R, Hecht K, Antonio M, Meyer H-P (2017) An Appreciation of Biocatalysis in the Swiss Manufacturing Environment. In: *Biocatalysis: An Industrial Perspective*. p 16
- Bunting KA, Cooper JB, Tickle IJ, Young DB (2002) Engineering of an Intersubunit Disulfide Bridge in the Iron-Superoxide Dismutase of *Mycobacterium tuberculosis*. *Arch Biochem Biophys* 397:69–76 . doi: 10.1006/abbi.2001.2635 S0003986101926359
- Burnett G, Yonaha K, Toyama S, Soda K, Walsh C (1980) Studies on the Kinetics and Stoichiometry of Inactivation of *Pseudomonas* omega-amino acid-pyruvate transaminase by gabaculine. *J Biol Chem* 255:428–432
- Burton AS, Stern JC, Elsilá JE, Glavin DP, Dworkin JP (2012) Understanding Prebiotic Chemistry Through the Analysis of Extraterrestrial Amino Acids and Nucleobases in Meteorites. *Chem Soc Rev* 41:5459 . doi: 10.1039/c2cs35109a
- Buß O, Buchholz PCF, Gräff M, Klausmann P, Rudat J, Pleiss J (2018) The ω -transaminase engineering database (oTAED): A navigation tool in protein sequence and structure space. *Proteins Struct Funct Bioinforma* 86:566–580 . doi: 10.1002/prot.25477
- Buß O, Jager S, Dold S-M, Zimmermann S, Hamacher K, Schmitz K, Rudat J (2016) Statistical Evaluation of HTS Assays for Enzymatic Hydrolysis of β -Keto Esters. *PLoS One* 11:e0146104 . doi: 10.1371/journal.pone.0146104
- Buß O, Müller D, Jager S, Rudat J, Rabe KS (2017) Improvement of the thermostability of a β -amino acid converting ω -transaminase using FoldX. *ChemBioChem*. doi: 10.1002/cbic.201700467
- Bussi G, Donadio D, Parrinello M (2007) Canonical sampling through velocity rescaling. *J Chem Phys* 126:14101 . doi: 10.1063/1.2408420
- Calvelage S, Dörr M, Höhne M, Bornscheuer UT (2017) A Systematic Analysis of the Substrate Scope of (*S*)- and (*R*)-Selective Amine Transaminases. *Adv Synth Catal* 359:4235–4243 . doi: 10.1002/adsc.201701079
- Campanini B, Bettati S, Di Salvo ML, Mozzarelli A, Contestabile R (2013) Asymmetry of the Active Site Loop Conformation Between Subunits of Glutamate-1-Semialdehyde Aminomutase in Solution. *Biomed Res Int* 2013:353270 . doi: 10.1155/2013/353270
- Candela T, Fouet A (2006) Poly-gamma-glutamate in bacteria. *Mol Microbiol* 60:1091–1098 . doi: 10.1111/j.1365-2958.2006.05179.x
- Capdevila J, Elez E, Macarulla T, Ramos FJ, Ruiz-Echarri M, Tabernero J (2009) Anti-epidermal growth factor receptor monoclonal antibodies in cancer treatment. *Cancer Treat. Rev.* 35:354–363
- Carninci P, Nishiyama Y, Westover a, Itoh M, Nagaoka S, Sasaki N, Okazaki Y, Muramatsu M, Hayashizaki Y (1998) Thermostabilization and Thermoactivation of Thermolabile Enzymes by Trehalose and its Application for the Synthesis of Full Length cDNA. *Proc Natl Acad Sci U S A* 95:520–4 . doi: 10.1073/pnas.95.2.520
- Cassimjee KE, Humble MS, Land H, Abedib V, Berglund P (2012) *Chromobacterium violaceum* ω -transaminase variant Trp60Cys shows increased specificity for (*S*)-1-phenylethylamine and 4'-substituted acetophenones, and follows Swain–Lupton parameterisation. *Org Biomol Chem* 10:5466–5470 . doi: 10.1039/c2ob25893e
- Cassimjee KE, Humble MS, Miceli V, Colomina CG, Berglund P (2011) Active site quantification of an ω -Transaminase by performing a half transamination reaction. *ACS Catal* 1:1051–1055 . doi: 10.1021/cs200315h
- Celniker G, Nimrod G, Ashkenazy H, Glaser F, Martz E, Mayrose I, Pupko T, Ben-Tal N (2013) ConSurf: Using Evolutionary Data to Raise Testable Hypotheses about Protein Function. *Isr. J. Chem.* 53:199–206
- Chan Joo J, Je Yoo Y, Chan Joo J, Je Yoo Y (2009) Thermostable Proteins. In: *Encyclopedia of Industrial Biotechnology*. John Wiley & Sons, Inc., Hoboken, NJ, USA
- Chen J, Yu H, Liu C, Liu J, Shen Z (2013) Improving Stability of Nitrile Hydratase by Bridging the Salt-Bridges in Specific Thermal-Sensitive Regions. *J Biotechnol* 164:354–362 . doi: 10.1016/j.jbiotec.2013.01.021

List of all references

- Chen S, Berglund P, Humble MS (2018) The Effect of Phosphate Group Binding Cup Coordination on the Stability of the Amine Transaminase from *Chromobacterium violaceum*. *Mol Catal* 446:115–123 . doi: 10.1016/j.mcat.2017.12.033
- Cheng ZQ, McFadden B a (1998) A Study of Conserved In-Loop and Out-Of-Loop Glycine Residues In the Large Subunit of Ribulose Biphosphate Carboxylase/Oxygenase By Directed Mutagenesis. *Protein Eng* 11:457–65
- Christensen NJ, Kepp KP (2012a) Accurate Stabilities of Laccase Mutants Predicted with a Modified Foldx Protocol. *J Chem Inf Model* 52:3028–3042 . doi: 10.1021/ci300398z
- Christensen NJ, Kepp KP (2013) Stability Mechanisms of Laccase Isoforms Using a Modified Foldx Protocol Applicable to Widely Different Proteins. *J Chem Theory Comput* 9:3210–3223 . doi: 10.1021/ct4002152
- Christensen NJ, Kepp KP (2012b) Accurate Stabilities of Laccase Mutants Predicted with a Modified FoldX Protocol. *J Chem Inf Model* 52:3028–3042 . doi: 10.1021/ci300398z
- Clark SM, Di Leo R, Van Cauwenbergh OR, Mullen RT, Shelp BJ (2009) Subcellular Localization and Expression of Multiple Tomato γ -Aminobutyrate Transaminases that Utilize both Pyruvate and Glyoxylate. *J Exp Bot* 60:3255 . doi: 10.1093/jxb/erp161
- Clarke J, Fersht AR (1993) Engineered Disulfide Bonds as Probes of the Folding Pathway of Barnase: Increasing The Stability of Proteins Against the Rate of Denaturation. *Biochemistry* 32:4322–4329 . doi: 10.1021/bi00067a022
- Clemente-Jiménez JM, Martínez-Rodríguez S, Rodríguez-Vico F, Heras-Vázquez FJL (2008) Optically Pure α -Amino Acids Production by the “Hydantoinase Process.” *Recent Pat Biotechnol* 2:35–46 . doi: 10.2174/187220808783330947
- Cohen M, Reichmann D, Neuvirth H, Schreiber G (2008) Similar Chemistry, but Different Bond Preferences in Inter versus Intra-Protein Interactions. *Proteins Struct Funct Genet* 72:741–753 . doi: 10.1002/prot.21960
- Cohen P (1940) Transamination with Purified Enzyme Preparations (Transaminase). *J Biol Chem* 136:565
- Conti E, Stachelhaus T, Marahiel MA, Brick P (1997) Structural Basis For the Activation of Phenylalanine in the Non-Ribosomal Biosynthesis Of Gramicidin S. *EMBO J* 16:4174–4183 . doi: 10.1093/emboj/16.14.4174
- Cotter PD, O’Connor PM, Draper LA, Lawton EM, Deegan LH, Hill C, Ross RP (2005) Posttranslational Conversion of L-Serines to D-Alanines is Vital for Optimal Production and Activity of the Lantibiotic Lactacin 3147. *Proc Natl Acad Sci U S A* 102:18584–9 . doi: 10.1073/pnas.0509371102
- Cox BM, Bilsborrow JB, Walker KD (2009) Enhanced Conversion of Racemic α -Arylalanines to (*R*)- β -Arylalanines by Coupled Racemase/Aminomutase Catalysis. *J Org Chem* 74:6953–6959 . doi: 10.1021/jo9009563
- Craig DB, Dombkowsk and AA (2013) Disulfide by Design 2.0: A Web-Based Tool for Disulfide Engineering in Proteins. *BMC Bioinformatics* 14:346
- Crawforth JM, Glossop PA, Hamper BC, Huang W, Mantell SJ, Neal BE, Olson K, Thorarensen A, Turner SR (2009) Preparation Of Nicotinamide Derivatives For The Treatment Of Allergic And Respiratory Conditions, WO 2009153721
- Crismaru CG, Wybenga GG, Szymanski W, Wijma HJ, Wu B, Bartsch S, de Wildeman S, Poelarends GJ, Feringa BL, Dijkstra BW, Janssen DB (2013) Biochemical Properties and Crystal Structure of a β -Phenylalanine Aminotransferase from *Variovorax paradoxus*. *Appl Environ Microbiol* 79:185–195 . doi: 10.1128/AEM.02525-12
- Cristen P, Metzler DE (1985) *Transaminases (Biochemistry: A Series of Monographs)*. John Wiley & Sons, Inc., New York
- Csuka P, Juhász V, Kohári S, Filip A, Varga A, Sátorhelyi P, Bencze LC, Barton HA, Paizs C, Poppe L (2017) *Pseudomonas fluorescens* strain R124 encodes three different MIO-enzymes. *ChemBioChem* 1–9 . doi: 10.1002/cbic.201700530
- Cuetos A, García-Ramos M, Fischereider E-M, Díaz-Rodríguez A, Grogan G, Gotor V, Kroutil W, Lavandera I (2016) Catalytic Promiscuity of Transaminases: Preparation of Enantioenriched β -Fluoroamines by Formal Tandem Hydrodefluorination/Deamination. *Angew Chemie Int Ed* 55:3144–3147 . doi: 10.1002/anie.201510554
- Daniel RM, Danson MJ, Eisenthal R (2001) The Temperature Optima of Enzymes: A New Perspective on an Old Phenomenon. *Trends Biochem Sci* 26:223–5
- Daniel RM, Peterson ME, Danson MJ, Price NC, Kelly SM, Monk CR, Weinberg CS, Oudshoorn ML, Lee CK (2010) The Molecular Basis of the Effect of Temperature on Enzyme Activity. *Biochem J* 425:353–360 . doi: 10.1042/BJ20091254
- Daudé D, Topham CM, Remaud-Siméon M, André I (2013) Probing Impact of Active Site Residue Mutations on Stability and Activity of *Neisseria polysaccharea* Amylosucrase. *Protein Sci* 22:1754–1765 . doi: 10.1002/pro.2375
- De Cordt S, Vanhoof K, Hu J, Maesmans G, Hendrickx M, Tobback P (1992) Thermostability of Soluble and Immobilized α -Amylase from *Bacillus licheniformis*. *Biotechnol Bioeng* 40:396–402 . doi: 10.1002/bit.260400309
- Debye P (1913) Interferenz von Röntgenstrahlen und Wärmebewegung. *Ann Phys* 348:49–92 . doi: 10.1002/andp.19133480105
- Deepankumar K, Shon M, Nadarajan SP, Shin G, Mathew S, Ayyadurai N, Kim BG, Choi SH, Lee SH, Yun H (2014) Enhancing thermostability and organic solvent tolerance of ω -transaminase through global incorporation of fluorotyrosine. *Adv Synth Catal* 356:993–998 . doi: 10.1002/adsc.201300706
- Dehnavi E, Fathi-Roudsari M, Mirzaie S, Arab SS, Ranaei Siadat SO, Khajeh K (2017) Engineering Disulfide Bonds in *Selenomonas ruminantium* β -xylosidase by Experimental and Computational Methods. *Int J Biol Macromol* 95:248–255 . doi: 10.1016/j.ijbiomac.2016.10.104
- Dehouck Y, Kwasigroch JM, Gilis D, Rooman M (2011) PoPMuSiC 2.1: A Web Server for the Estimation of Protein Stability Changes Upon Mutation and Sequence Optimality. *BMC Bioinformatics* 12:151 . doi: 10.1186/1471-2105-12-151
- Dehouck Y, Kwasigroch JM, Rooman M, Gilis D (2013) BeAtMuSiC: Prediction of Changes in Protein-Protein Binding Affinity on Mutations. *Nucleic Acids Res* 41:333–339 . doi: 10.1093/nar/gkt450
- Del Borgo MP, Kulkarni K, Aguilar MI (2017) Using β -Amino Acids and β -Peptide Templates to Create Bioactive Ligands and Biomaterials. *Curr Pharm Des* 23: . doi: 10.2174/1381612823666170616083031
- Denesyuk AI, Denessiouk KA, Korpela T, Johnson MS (2003a) Phosphate group binding “cup” of PLP-dependent and non-PLP-dependent enzymes: leitmotif and variations. *Biochim Biophys Acta - Proteins Proteomics* 1647:234–238 . doi: 10.1016/S1570-9639(03)00057-8
- Desai AA (2011) Sitagliptin Manufacture: A Compelling Tale of Green Chemistry, Process Intensification, and Industrial Asymmetric Catalysis. *Angew Chemie - Int Ed* 50:1974–1976 . doi: 10.1002/anie.201007051
- Deszcz D, Affaticati P, Ladkau N, Gegel A, Ward JM, Hailes HC, Dalby PA (2015) Single Active-Site Mutants are Sufficient to Enhance Serine:Pyruvate α -Transaminase Activity in an ω -Transaminase. *FEBS J* 282:2512–2526 . doi: 10.1111/febs.13293
- Diñçer A, Telefoncu A (2007) Improving the Stability of Cellulase by Immobilization on Modified Polyvinyl Alcohol Coated Chitosan Beads. *J Mol Catal B Enzym* 45:10–14 . doi: 10.1016/j.molcatb.2006.10.005
- Dobrev D, Hamad B, Kirkpatrick P (2010) Vernakalant. *Nat. Rev. Drug Discov* 9:915–916
- Dold S-M (2016) *Enzymatic Synthesis and Microbial Degradation of β -Amino Acids via Transaminases*. Karlsruhe Institute for Technology
- Dold S-M, Cai L, Rudat J (2016a) One-Step Purification and Immobilization of a β -Amino Acid Aminotransferase Using Magnetic (M-PVA) Beads. *Eng Life Sci* 16:568–576 . doi: 10.1002/elsc.201600042
- Dold SM, Syldatk C, Rudat J (2016b) *Transaminases and their Applications*. In: *Green Biocatalysis*. John Wiley & Sons, Inc, Hoboken, NJ, pp 715–746

- Dombkowski AA (2003a) Disulfide by Design: A Computational Method for the Rational Design of Disulfide Bonds In Proteins. *Bioinformatics* 19:1852–1853 . doi: 10.1093/bioinformatics/btg231
- Dombkowski AA, Sultana KZ, Craig DB (2014) Protein Disulfide Engineering. *FEBS Lett* 588:206–212 . doi: 10.1016/j.febslet.2013.11.024
- Donoso R, Leiva-Novoa P, Zúñiga A, Timmermann T, Recabarren-Gajardo G, González B (2017) Biochemical and Genetic Bases of Indole-3-Acetic Acid (Auxin Phytohormone) Degradation by the Plant-Growth-Promoting Rhizobacterium *Paraburkholderia phytofirmans* PsJN. *Appl Environ Microbiol* 83:e01991-16 . doi: 10.1128/AEM.01991-16
- Dörsam S, Fessler J, Gorte O, Hahn T, Zibek S, Sylđatk C, Ochsenreither K (2017) Sustainable Carbon Sources for Microbial Organic Acid Production with Filamentous Fungi. *Biotechnol Biofuels* 10:242 . doi: 10.1186/s13068-017-0930-x
- Dourado DFAR, Flores SC (2014) A Multiscale Approach to Predicting Affinity Changes in Protein-Protein Interfaces. *Proteins Struct Funct Bioinforma* 82:2681–2690 . doi: 10.1002/prot.24634
- Drozak J, Veiga-da-Cunha M, Vertommen D, Stroobant V, Van Schaftingen E (2010) Molecular Identification of Carnosine Synthase as ATP-Grasp Domain-Containing Protein 1 (ATPGD1). *J Biol Chem* 285:9346–9356 . doi: 10.1074/jbc.M109.095505
- Duan X, Li Y, Du Q, Huang Q, Guo S, Xu M, Lin Y, Liu Z, Xie J (2016) Mycobacterium Lysine ϵ -Aminotransferase is a Novel Alarmone Metabolism Related Persister Gene via Dysregulating the Intracellular Amino Acid Level. *Sci Rep* 6:19695 . doi: 10.1038/srep19695
- Dvorak P, Bednar D, Vanacek P, Balek L, Eiselleova L, Stepankova V, Sebestova E, Kunova M, Konecna Z, Mazurenko S, Kunka A, Chaloupkova R, Brezovsky J, Krejci P, Prokop Z, Dvorak P, Damborsky J (2016) Computer-Assisted Engineering of Hyperstable Fibroblast Growth Factor 2. *bioRxiv* 1–35 . doi: 10.1101/100636
- Dwivedi N, Shah J, Mishra V, Mohd Amin MCI, Iyer AK, Tekade RK, Kesharwani P (2016) Dendrimer-mediated approaches for the treatment of brain tumor. *J Biomater Sci Polym Ed* 27:557–580 . doi: 10.1080/09205063.2015.1133155
- Eddy SR (1998) Profile hidden Markov models. *Bioinformatics* 14:755–63 . doi: doi.org/10.1093/bioinformatics/14.9.755
- Edgar RC (2010) Search and clustering orders of magnitude faster than BLAST. *Bioinformatics* 26:2460–2461 . doi: 10.1093/bioinformatics/btq461
- Eijsink VGH, GÅseidnes S, Borchert T V., Van Den Burg B (2005) Directed evolution of enzyme stability. *Biomol. Eng.* 22:21–30
- Eliot AC, Kirsch JF (2004) Pyridoxal Phosphate Enzymes: Mechanistic, Structural, and Evolutionary Considerations. *Annu Rev Biochem* 73:383–415 . doi: 10.1146/annurev.biochem.73.011303.074021
- Elsila JE, Glavin DP, Dworkin JP (2009) Cometary glycine detected in samples returned by Stardust. *Meteorit Planet Sci* 44:1323–1330 . doi: 10.1111/j.1945-5100.2009.tb01224.x
- Erban R (2014) From Molecular Dynamics to Brownian Dynamics. *Proceedings Math Phys Eng Sci* 470:20140036 . doi: 10.1098/rspa.2014.0036
- Ericsson UB, Hallberg BM, DeTitta GT, Dekker N, Nordlund P (2006) Thermofluor-Based High-Throughput Stability Optimization of Proteins for Structural Studies. *Anal Biochem* 357:289–298 . doi: 10.1016/j.ab.2006.07.027
- Faber K (2011) *Biotransformations in Organic Chemistry*. Springer Berlin Heidelberg
- Famm K, Hansen L, Christ D, Winter G (2008) Thermodynamically Stable Aggregation-Resistant Antibody Domains through Directed Evolution. *J Mol Biol* 376:926–931 . doi: 10.1016/j.jmb.2007.10.075
- Fang C, Noguchi T, Yamana H (2014) Analysis of Evolutionary Conservation Patterns and their Influence on Identifying Protein Functional Sites. *J Bioinform Comput Biol* 12:1440003 . doi: 10.1142/S0219720014400034
- Farmer LJ, Clark MP, Boyd MJ, Perola E, Jones SM, Tsai A, Jacobs MD, Bandarage UK, Ledebor MW, Wang T, Deng H, Ledford B, Gu W, Duffy JP, Bethiel RS, Shannon D, Byrn RA, Leeman JR, Rijnbrand R, Bennett HB, O'Brien C, Memmott C, Nti-Addae K, Bennani YL, Charifson PS (2017) Discovery of Novel, Orally Bioavailable β -Amino Acid Azaindole Inhibitors of Influenza PB2. *ACS Med Chem Lett* 8:256–260 . doi: 10.1021/acsmchemlett.6b00486
- Feng Y, Luo Z, Sun G, Chen M, Lai J, Lin W, Goldmann S, Zhang L, Wang Z (2017) Development of an Efficient and Scalable Biocatalytic Route to (3*R*)-3-Aminoazepane: A Pharmaceutically Important Intermediate. *Org Process Res Dev* 21:648–654 . doi: 10.1021/acs.oprd.7b00074
- Fernandez-Escamilla A-M, Rousseau F, Schymkowitz J, Serrano L (2004) Prediction of Sequence-Dependent and Mutational Effects on the Aggregation of Peptides and Proteins. *Nat Biotechnol* 22:1302–1306 . doi: 10.1038/nbt1012
- Ferrandi EE, Monti D (2018) Amine Transaminases in Chiral Amines Synthesis: Recent Advances and Challenges. *World J Microbiol Biotechnol* 34: . doi: 10.1007/s11274-017-2395-2
- Ferrandi EE, Previdi A, Bassanini I, Riva S, Peng X, Monti D (2017) Novel Thermostable Amine Transferases from Hot Spring Metagenomes. *Appl. Microbiol. Biotechnol.* 101:1–17
- Fersht A (1999) *Structure and Mechanism In Protein Science. A Guide to Enzyme Catalysis and Protein Folding*. Cambridge University Press
- Finn RD, Bateman A, Clements J, Coggill P, Eberhardt RY, Eddy SR, Heger A, Hetherington K, Holm L, Mistry J, Sonnhammer ELL, Tate J, Punta M (2014) Pfam: The Protein Families Database. *Nucleic Acids Res* 42:D222–D230
- Fleming N, Kinsella B, Ing C (2016) Predicting Protein Thermostability Upon Mutation Using Molecular Dynamics Timeseries Data. *bioRxiv* 78246 . doi: 10.1101/078246
- Floor RJ, Wijma HJ, Colpa DI, Ramos-Silva A, Jekel PA, Szymański W, Feringa BL, Marrink SJ, Janssen DB (2014) Computational Library Design for Increasing Haloalkane Dehalogenase Stability. *ChemBioChem* 15:1660–1672 . doi: 10.1002/cbic.201402128
- Foit L, Morgan GJ, Kern MJ, Steimer LR, von Hacht AA, Titchmarsh J, Warriner SL, Radford SE, Bardwell JCA (2009) Optimizing Protein Stability In Vivo. *Mol Cell* 36:861–871 . doi: 10.1016/J.MOLCEL.2009.11.022
- Fortin PD, Walsh CT, Magarvey NA (2007) A Transglutaminase Homologue as a Condensation Catalyst In Antibiotic Assembly Lines. *Nature* 448:824–827 . doi: 10.1038/nature06068
- Frappier V, Chartier M, Najmanovich RJ (2015) ENCoM server: Exploring Protein Conformational Space and the Effect of Mutations on Protein Function and Stability. *Nucleic Acids Res* 43:W395–W400 . doi: 10.1093/nar/gkv343
- Fredenhagen A, Tamura SY, Kenny PTM, Komura H, Naya Y, Nakanishi K, Nishiyama K, Sugiura M, Kita H (1987) Andrimid, A New Peptide Antibiotic Produced by an Intracellular Bacterial Symbiont Isolated from a Brown Planthopper. *J Am Chem Soc* 109:4409–4411 . doi: 10.1021/ja00248a055
- Frodsham L, Golden M, Hard S, Kenworthy MN, Klauber DJ, Leslie K, Macleod C, Meadows RE, Mulholland KR, Reilly J, Squire C, Tomasi S, Watt D, Wells AS (2013) Use Of ω -Transaminase Enzyme Chemistry in the Synthesis of a JAK2 Kinase Inhibitor. *Org Process Res Dev* 17:1123–1130 . doi: 10.1021/op400133d
- Fuchs M, Koszelewski D, Tauber K, Sattler J, Banko W, Holzer AK, Pickl M, Kroutil W, Faber K (2012) Improved Chemoenzymatic Asymmetric Synthesis of (S)-Rivastigmine. In: *Tetrahedron*. Pergamon, pp 7691–7694
- Gach-Janczak K, Pieknielna-Ciesielska J, Adamska-Bartomiejczyk A, Perlikowska R, Kruszyński R, Kluczyk A, Krzywick J, Sukiennik J, Cerlesi MC, Calo G, Wasilewski A, Zielińska M, Janecka A (2017) Synthesis and Activity of Opioid Peptidomimetics with β 2- and β 3-Amino Acids. *Peptides* 95:116–123 . doi: 10.1016/j.peptides.2017.07.015
- Galman JL, Slabu I, Weise NJ, Iglesias C, Parmeggiani F, Lloyd RC, Turner NJ (2017) Biocatalytic Transamination with Near-Stoichiometric Inexpensive Amine Donors

List of all references

- Mediated by Bifunctional Mono- and Di-Amine Transaminases. *Green Chem* 19:361–366 . doi: 10.1039/C6GC02102F
- Garske AL, Kapp G, McAuliffe J (2017) Industrial Enzymes and Biocatalysis. In: Handbook of Industrial Chemistry and Biotechnology. p 1625
- Genz M, Melse O, Schmidt S, Vickers C, Dörr M, van den Bergh T, Joosten H-J, Bornscheuer UT (2016) Engineering the Amine Transaminase from *Vibrio fluvialis* towards Branched-Chain Substrates. *ChemCatChem* 8:3199–3202 . doi: 10.1002/cctc.201601007
- Genz M, Vickers C, van den Bergh T, Joosten HJ, Dörr M, Höhne M, Bornscheuer UT (2015) Alteration Of The Donor/Acceptor Spectrum of the (S)-Amine Transaminase From *Vibrio fluvialis*. *Int J Mol Sci* 16:26953–26963 . doi: 10.3390/ijms161126007
- Ghislieri D, Green AP, Pontini M, Willies SC, Rowles I, Frank A, Grogan G, Turner NJ (2013) Engineering an Enantioselective Amine Oxidase for the Synthesis of Pharmaceutical Building Blocks and Alkaloid Natural Products. *J Am Chem Soc* 135:10863–10869 . doi: 10.1021/ja4051235
- Ghislieri D, Turner NJ (2014) Biocatalytic Approaches to the Synthesis of Enantiomerically Pure Chiral Amines. *Top Catal* 57:284–300 . doi: 10.1007/s11244-013-0184-1
- Girardin M, Ouellet SG, Gauvreau D, Moore JC, Hughes G, Devine PN, O'Shea PD, Campeau LC (2013) Convergent Kilogram-Scale Synthesis of Dual Orexin Receptor Antagonist. *Org Process Res Dev* 17:61–68 . doi: 10.1021/op3002678
- Giver L, Gershenson A, Freskgard PO, Arnold FH (1998) Directed Evolution of a Thermostable Esterase. *Proc Natl Acad Sci U S A* 95:12809–13
- Glänzer BI, Faber K, Griengl H (1987) Enantioselective Hydrolyses By Baker's Yeast - III: Microbial Resolution of Alkynyl Esters Using Lyophilized Yeast. *Tetrahedron* 43:5791–5796 . doi: 10.1016/S0040-4020(01)87785-1
- Glueck DS (2008) Catalytic Asymmetric Synthesis of Chiral Phosphanes. *Chem Eur J* 14:7108–17 . doi: 10.1002/chem.200800267
- Goerigk L, Reimers JR (2013) Efficient Methods for The Quantum Chemical Treatment of Protein Structures: The Effects of London-Dispersion and Basis-Set Incompleteness on Peptide and Water-Cluster Geometries. *J Chem Theory Comput* 9:3240–3251 . doi: 10.1021/ct400321m
- Goldenzweig A, Goldsmith M, Hill SE, Gertman O, Laurino P, Ashani Y, Dym O, Unger T, Albeck S, Prilusky J, Lieberman RL, Aharoni A, Silman I, Sussman JL, Tawfik DS, Fleishman SJ (2016) Automated Structure- and Sequence-Based Design of Proteins for High Bacterial Expression and Stability. *Mol Cell* 63:337–346 . doi: 10.1016/j.molcel.2016.06.012
- Goto M, Miyahara I, Hayashi H, Kagamiyama H, Hirotsu K (2003) Crystal Structures of Branched-Chain Amino Acid Aminotransferase Complexed with Glutamate and Glutarate: True Reaction Intermediate and Double Substrate Recognition of the Enzyme. *Biochemistry* 42:3725–3733 . doi: 10.1021/bi026722f
- Grayson JJ, Roos J, Osswald S (2011) Development of a Commercial Process for (S)- β -Phenylalanine. *Org Process Res Dev* 15:1201–1206 . doi: 10.1021/op200084g
- Green AP, Turner NJ, O'Reilly E (2014) Chiral Amine Synthesis Using ω -Transaminases: An Amine Donor that Displaces Equilibria and Enables High-Throughput Screening. *Angew Chemie Int Ed* 53:10714–10717 . doi: 10.1002/anie.201406571
- Greenfield NJ (2007) Using Circular Dichroism Collected As A Function Of Temperature To Determine The Thermodynamics Of Protein Unfolding And Binding Interactions. *Nat Protoc* 1:2527–2535 . doi: 10.1038/nprot.2006.204
- Grishin N V, Phillips MA, Goldsmith EJ (1995) Modeling Of The Spatial Structure Of Eukaryotic Ornithine Decarboxylases. *Protein Sci* 4:1291–304 . doi: 10.1002/pro.5560040705
- Groger H, Trauthwein H, Buchholz S, Drauz K, Sacherer C, Godfrin S, Werner H (2004) The First Aminoacylase-Catalyzed Enantioselective Synthesis Of Aromatic β -Amino Acids. *Org Biomol Chem* 2:1977–8 . doi: 10.1039/b406380e
- Grulich M, Brezovský J, Štěpánek V, Palyzová A, Marešová H, Zahradník J, Kyslíková E, Kyslík P (2016) *In-silico* driven Engineering Of Enantioselectivity Of A Penicillin G Acylase Towards Active Pharmaceutical Ingredients. *J. Mol. Catal. B Enzym.*
- Guerois R, Nielsen JE, Serrano L (2002) Predicting Changes In The Stability Of Proteins And Protein Complexes: A Study Of More Than 1000 Mutations. *J Mol Biol* 320:369–387 . doi: 10.1016/S0022-2836(02)00442-4
- Guizzetti S, Benaglia M, Bonsignore M, Raimondi L (2011) Trichlorosilane-Mediated Stereoselective Synthesis Of β -amino Esters And Their Conversion To Highly Enantiomerically Enriched β -Lactams. *Org Biomol Chem* 9:739–743 . doi: 10.1039/c0ob00570c
- Guo F, Berglund P (2016) Transaminase Biocatalysis: Optimization and Application. *Green Chem* 333–360 . doi: 10.1039/C6GC02328B
- Hall BG, Salipante SJ, Barlow M (2003) The Metallo- β -Lactamases Fall Into Two Distinct Phylogenetic Groups. *J Mol Evol* 57:249–254 . doi: 10.1007/s00239-003-2471-0
- Han S-W, Kim J, Cho H-S, Shin J-S (2017) Active Site Engineering of ω -Transaminase Guided by Docking Orientation Analysis and Virtual Activity Screening. *ACS Catal* 7:3752–3762 . doi: 10.1021/acscatal.6b03242
- Han S-W, Shin J-S (2014) Metabolically Driven Equilibrium Shift Of Asymmetric Amination Of Ketones By ω -Transaminase Using Alanine As An Amino Donor. *Biosci Biotechnol Biochem* 78:1788–1790 . doi: 10.1080/09168451.2014.930328
- Han SW, Park ES, Dong JY, Shin JS (2015a) Active-site engineering of ω -transaminase for Production Of Unnatural Amino Acids Carrying A Side Chain Bulkier Than An Ethyl Substituent. *Appl Environ Microbiol* 81:6994–7002 . doi: 10.1128/AEM.01533-15
- Han SW, Park ES, Dong JY, Shin JS (2015b) Mechanism-Guided Engineering of ω -Transaminase to Accelerate Reductive Amination of Ketones. *Adv Synth Catal* 1732–1740 . doi: 10.1002/adsc.201500211
- Han ZL, Han SY, Zheng SP, Lin Y (2009) Enhancing thermostability of a *Rhizomucor miehei* lipase by engineering a disulfide bond and displaying on the yeast cell surface. *Appl Microbiol Biotechnol* 85:117–126 . doi: 10.1007/s00253-009-2067-8
- Hanson RW (1987) Decarboxylation of α Keto Acids. *J Chem Educ* 64:591 . doi: 10.1021/ed064p591
- Hartl FU (1996) Molecular Chaperones In Cellular Protein Folding. *Nature* 381:571–579
- Hartl FU, Bracher A, Hayer-Hartl M (2011) Molecular Chaperones In Protein Folding And Proteostasis. *Nature* 475:324–332 . doi: 10.1038/nature10317
- He Z, Mei G, Zhao C, Chen Y (2011) Potential Application of Foldx Force Field Based Protein Modeling In Zinc Finger Nucleases Design. *Sci China Life Sci* 54:442–449 . doi: 10.1007/s11427-011-4159-9
- Hermann T (2003) Industrial Production of Amino Acids by Coryneform Bacteria. *J Biotechnol* 104:155–172 . doi: 10.1016/S0168-1656(03)00149-4
- Heselpoth RD, Yin Y, Mout J, Nelson DC (2015) Increasing the Stability Of The Bacteriophage Endolysin PlyC using Rationale-Based Foldx Computational Modeling. *Protein Eng Des Sel* 28:85–92 . doi: 10.1093/protein/gzv004
- Hess B, Bekker H, Berendsen HJC, Fraaije JGEM, others (1997) LINC: A Linear Constraint Solver For Molecular Simulations. *J Comput Chem* 18:1463–1472 . doi: 10.1002/(SICI)1096-987X(199709)18:12
- Hickling D, Guenter W, Jackson ME (1990) The Effects of Dietary Methionine and Lysine on Broiler Chicken Performance and Breast Meat Yield. *Can J Anim Sci* 70:673–678 . doi: 10.4141/cjas90-079
- Hill CA, Harris RC, Kim HJ, Harris BD, Sale C, Boobis LH, Kim CK, Wise JA (2007) Influence of β -Alanine Supplementation On Skeletal Muscle Carnosine Concentrations And High Intensity Cycling Capacity. *Amino Acids* 32:225–233 . doi: 10.1007/s00726-006-0364-4

- Hillier AJ, Jericho RE, Green SM, Jago GR (1979) Properties and Function of Fumarate Reductase (NADH) in *Streptococcus lactis*. *Aust J Biol Sci* 32:625–636 . doi: 10.1071/B19790625
- Hirotsu K, Goto M, Okamoto A, Miyahara I (2005a) Dual Substrate Recognition Of Aminotransferases. *Chem Rec* 5:160–172 . doi: 10.1002/tcr.20042
- Höhne M, Bornscheuer UT (2012) Application of Transaminases. In: *Enzyme Catalysis in Organic Synthesis*. Wiley-VCH Verlag GmbH & Co. KGaA, Weinheim, Germany, pp 779–820
- Höhne M, Kühl S, Robins K, Bornscheuer UT (2008) Efficient Asymmetric Synthesis Of Chiral Amines By Combining Transaminase And Pyruvate Decarboxylase. *ChemBioChem* 9:363–365 . doi: 10.1002/cbic.200700601
- Höhne M, Schätzle S, Jochens H, Robins K, Bornscheuer UT (2010) Rational Assignment Of Key Motifs For Function Guides *In Silico* Enzyme Identification. *Nat Chem Biol* 6:807–813 . doi: 10.1038/nchembio.447
- Hoover WG (1985) Canonical dynamics: Equilibrium phase-space distributions. *Phys Rev A* 31:1695–1697 . doi: 10.1103/PhysRevA.31.1695
- Huang J, Xie D-F, Feng Y (2017) Engineering thermostable (*R*)-selective amine transaminase from *Aspergillus terreus* through in silico design employing B-factor and folding free energy calculations. *Biochem Biophys Res Commun* 483:397–402 . doi: 10.1016/j.bbrc.2016.12.131
- Huang L, Xu JH, Yu HL (2015) Significantly Improved Thermostability of a Reductase Cgkr1 from *Candida glabrata* with a Key Mutation at Asp 138 for Enhancing Bioreduction of Aromatic α -Keto Esters. *J Biotechnol* 203:54–61 . doi: 10.1016/j.jbiotec.2015.02.035
- Huang P-S, Boyken SE, Baker D (2016) The Coming Of Age Of De Novo Protein Design. *Nature* 537:320–327 . doi: 10.1038/nature19946
- Hubbard RE, Kamran Haider M (2010) Hydrogen Bonds in Proteins: Role and Strength. In: *Encyclopedia of Life Sciences*. John Wiley & Sons, Ltd, Chichester, UK
- Huisman GW, Collier SJ (2013a) On The Development Of New Biocatalytic Processes For Practical Pharmaceutical Synthesis. *Curr. Opin. Chem. Biol.* 17:284–292
- Humble MS, Cassimjee KE, Abedi V, Federsel HJ, Berglund P (2012a) Key Amino Acid Residues for Reversed or Improved Enantiospecificity of an ω -Transaminase. *ChemCatChem* 4:1167–1172 . doi: 10.1002/cctc.201100487
- Humble MS, Cassimjee KE, Håkansson M, Kimbung YR, Walse B, Abedi V, Federsel HJ, Berglund P, Logan DT (2012b) Crystal Structures of the *Chromobacterium violaceum* ω -Transaminase Reveal Major Structural Rearrangements Upon Binding of Coenzyme PLP. *FEBS J* 279:779–792 . doi: 10.1111/j.1742-4658.2012.08468.x
- Hutson S (2001) Structure And Function Of Branched Chain Aminotransferases. In: *Progress in Nucleic Acid Research and Molecular Biology*. Elsevier, pp 175–206
- Hwang B-Y, Ko S-H, Park H-Y, Seo J-H, Lee B-S, Kim B-G (2008) Identification of ω -Aminotransferase from *Caulobacter crescentus* And Site-Directed Mutagenesis To Broaden Substrate Specificity. *J Microbiol Biotechnol* 18:48–54
- Ingram CU, Bommer M, Smith MEB, Dalby PA, Ward JM, Hailes HC, Lye GJ (2007) One-Pot Synthesis of Amino-Alcohols Using a *De-Novo* Transketolase and β -Alanine:Pyruvate Transaminase Pathway in *Escherichia coli*. *Biotechnol Bioeng* 96:559–569 . doi: 10.1002/bit.21125
- Iwasaki A, Matsumoto K, Hasegawa J, Yasohara Y (2012) A novel transaminase, (*R*)-amine:Pyruvate Aminotransferase, From *Arthrobacter* Sp. KNK168 (Ferm Bp-5228): Purification, Characterization, And Gene Cloning. *Appl Microbiol Biotechnol* 93:1563–1573 . doi: 10.1007/s00253-011-3580-0
- Jacobson RH, Faber HR, Matthews BW (1992) Structure of a Stabilizing Disulfide Bridge Mutant That Closes The Active-Site Cleft Of T4 Lysozyme. *Protein Sci* 46–57
- Jager S, Schiller B, Babel P, Blumenroth M, Strufe T, Hamacher K (2017) StreAM-SST_gSS T g : Algorithms For Analyzing Coarse Grained RNA Dynamics Based On Markov Models Of Connectivity-Graphs. *Algorithms Mol Biol* 12:15 . doi: 10.1186/s13015-017-0105-0
- Janey JM (2013) Development of a Sitagliptin Transaminase. In: *Sustainable Catalysis: Challenges and Practices for the Pharmaceutical and Fine Chemical Industries*. John Wiley & Sons, Inc., Hoboken, New Jersey, pp 75–87
- Janoson JN (1998) Structure, Evolution and Action of Vitamin B6-Dependent Enzymes. *Curr Opin Struct Biol* 8:759–769 . doi: 10.1016/S0959-440X(98)80096-1
- Jensen RA, Gu W (1996) Evolutionary recruitment Of Biochemically Specialized Subdivisions Of Family I Within the Protein Superfamily of Aminotransferases. *J Bacteriol* 178:2161–2171 . doi: 10.1128/jb.178.8.2161-2171.1996
- Jia B, Jeon CO (2016) High-Throughput Recombinant Protein Expression In *Escherichia coli* : Current Status And Future Perspectives. *Open Biol* 6:160196 . doi: 10.1098/rsob.160196
- Jiang J, Chen X, Zhang D, Wu Q, Zhu D (2015) Characterization Of (*R*)-Selective Amine Transaminases Identified By In Silico Motif Sequence Blast. *Appl Microbiol Biotechnol* 99:2613–2621 . doi: 10.1007/s00253-014-6056-1
- Jiang YK (2010) Molecular Docking and 3D-QSAR Studies on β -Phenylalanine Derivatives as Dipeptidyl Peptidase IV Inhibitors. *J Mol Model* 16:1239–1249 . doi: 10.1007/s00894-009-0637-4
- Jo BH, Park TY, Park HJ, Yeon YJ, Yoo YJ, Cha HJ (2016) Engineering De Novo Disulfide Bond In Bacterial α -Type Carbonic Anhydrase For Thermostable Carbon Sequestration. *Sci Rep* 6:29322 . doi: 10.1038/srep29322
- Jones HBL, Wells SA, Prentice EJ, Kwok A, Liang LL, Arcus VL, Pudney CR (2017) A Complete Thermodynamic Analysis Of Enzyme Turnover Links The Free Energy Landscape To Enzyme Catalysis. *FEBS J* 284:2829–2842 . doi: 10.1111/febs.14152
- Jones S, Thornton JM (1995) Protein-protein interactions: A review of Protein Dimer Structures. *Prog Biophys Mol Biol* 63:31–65 . doi: 10.1016/0079-6107(94)00008-W
- Jónsdóttir LB, Ellertsson B, Invernizzi G, Magnúsdóttir M, Thorbjarnardóttir SH, Papaleo E, Kristjánsson MM (2014) The Role Of Salt Bridges On The Temperature Adaptation Of Aqualysin I, A Thermostable Subtilisin-Like Proteinase. *Biochim Biophys Acta - Proteins Proteomics* 1844:2174–2181 . doi: 10.1016/j.bbapap.2014.08.011
- Jooyoung Lee, Sitao Wu and YZ (2009) Ab Initio Protein Structure Prediction. In: *From Protein Structure to Function with Bioinformatics*. Springer Netherlands, Dordrecht, pp 3–25
- Juaristi E, Soloshonok VA (2005) Enantioselective Synthesis of β -Amino Acids. John Wiley & Sons, Inc, Hoboken, NJ, USA.
- Kabashima T, Li Y, Kanada N, Ito K, Yoshimoto T (2001) Enhancement of the thermal stability of pyroglutamyl peptidase I by introduction of an intersubunit disulfide bond. *Biochim Biophys Acta - Protein Struct Mol Enzymol* 1547:214–220 . doi: 10.1016/S0167-4838(01)00185-6
- K Korn BC, Dixon JE, Bruice TC (1973) Comparison of the Rate Constants for General Base Catalyzed Prototropy and Racemization of the Aldimine Species Formed from 3-Hydroxypyridine-4-carboxaldehyde and Alanine*. *J Biol Chem Biol Sci Anal Biochem Sci Top Phosphorus Client Nat Nat Snyder W R. Law, J Lipids Spiro R G Anna Rev Biochem Nat Methods Biochem Anal* 248:599–230
- Kanehisa M, Sato Y, Kawashima M, Furumichi M, Tanabe M (2016) KEGG as a reference resource for gene and protein annotation. *Nucleic Acids Res* 44:D457–D462 . doi: 10.1093/nar/gkv1070
- Kaneko T, Nakamura Y, Sato S, Asamizu E, Kato T, Sasamoto S, Watanabe A, Idesawa K, Ishikawa A, Kawashima K, Kimura T, Kishida Y, Kiyokawa C, Kohara M, Matsumoto M, Matsuno A, Mochizuki Y, Nakayama S, Nakazaki N, Shimpo S, Sugimoto M, Takeuchi C, Yamada M, Tabata S (2000) Complete Genome Structure of the Nitrogen-fixing Symbiotic Bacterium *Mesorhizobium loti*. *DNA Res* 7:331–338 . doi: 10.1093/dnares/7.6.331

List of all references

- Karle IL, Gopi HN, Balaran P (2001) Peptide Hybrids Containing α - and β -Amino Acids: Structure of a Decapeptide β -Hairpin with Two Facing β -Phenylalanine Residues. *Proc Natl Acad Sci U S A* 98:3716–3719 . doi: 10.1073/pnas.071050198
- Karshikoff A, Nilsson L, Ladenstein R (2015) Rigidity Versus Flexibility: The Dilemma Of Understanding Protein Thermal Stability. *FEBS J* 282:3899–3917 . doi: 10.1111/febs.13343
- Kaulmann U, Smithies K, Smith MEB, Hailes HC, Ward JM (2007) Substrate Spectrum of ω -Transaminase from *Chromobacterium violaceum* DSM30191 And Its Potential For Biocatalysis. *Enzyme Microb Technol* 41:628–637 . doi: 10.1016/j.enzmictec.2007.05.011
- Kepp KP (2015) Towards a “Golden Standard” for Computing Globin Stability: Stability and Structure Sensitivity Of Myoglobin Mutants. *Biochim Biophys Acta - Proteins Proteomics* 1854:1239–1248 . doi: 10.1016/j.bbapap.2015.06.002
- Kepp KP (2014) Computing Stability Effects of Mutations in Human Superoxide Dismutase 1. *J Phys Chem B* 118:1799–1812 . doi: 10.1021/jp4119138
- Khan S, Vihinen M (2010) Performance of Protein Stability Predictors. *Hum Mutat* 31:675–684 . doi: 10.1002/humu.21242
- Kim J, Grate JW, Wang P (2006) Nanostructures for Enzyme Stabilization. *Chem. Eng. Sci.* 61:1017–1026
- Kim J, Kyung D, Yun H, Cho BK, Seo JH, Cha M, Kim BG (2007) Cloning and Characterization of a Novel β -transaminase from *Mesorhizobium* sp. strain LUK: A New Biocatalyst for the Synthesis of Enantiomerically Pure β -Amino acids. *Appl Environ Microbiol* 73:1772–1782 . doi: 10.1128/AEM.02119-06
- Kirsch JF, Eichele G, Ford GC, Vincent MG, Jansonius JN, Gehring H, Christen P (1984) Mechanism Of Action Of Aspartate Aminotransferase Proposed On The Basis Of Its Spatial Structure. *J Mol Biol* 174:497–525 . doi: 10.1016/0022-2836(84)90333-4
- Kiss L, Mándity IM, Fülöp F (2017) Highly functionalized cyclic β -amino Acid Moieties As Promising Scaffolds In Peptide Research And Drug Design. *Amino Acids* 49:1441–1455 . doi: 10.1007/s00726-017-2439-9
- Klausmann P (2017) Disulfide-bond Engineering of an (*S*)-selective ω -Transaminase to Enhance its Thermostability (Master Thesis). Karlsruhe Institut of Technology
- Klein-Marcuschamer D, Oleskowicz-Popiel P, Simmons BA, Blanch HW (2012) The Challenge Of Enzyme Cost In The Production Of Lignocellulosic Biofuels. *Biotechnol Bioeng* 109:1083–1087 . doi: 10.1002/bit.24370
- Kohlstaedt M, Von Der Hocht I, Hilbers F, Thielmann Y, Michel H (2015) Development of a Thermofluor assay for stability determination of membrane proteins using the Na⁺/H⁺ antiporter NhaA and cytochrome c oxidase. *Acta Crystallogr Sect D Biol Crystallogr* 71:1112–1122 . doi: 10.1107/S1399004715004058
- Kometani T, Morita Y, Yoshii H, Kiyama Y, Matsun02 R (1995) Oxidative Resolution with Bakers’ Yeast for Large-Scale of Chiral 1,2-Alkanediols Production. *J Ferment BIOENGINEERING* 80:180–184
- Komor RS, Romero PA, Xie CB, Arnold FH (2012a) Highly thermostable fungal cellobiohydrolase I (Cel7A) engineered using predictive methods. *Protein Eng Des Sel* 25:827–833 . doi: 10.1093/protein/gzs058
- Korkegian A, Black ME, Baker D, Stoddard BL (2005) Computational Thermostabilization of an Enzyme. *Science (80-)* 308:857–860 . doi: 10.1126/science.1107387
- Koszelewski D, Clay D, Faber K, Kroutil W (2009a) Synthesis of 4-phenylpyrrolidin-2-one via dynamic kinetic resolution catalyzed by ω -transaminases. *J Mol Catal B Enzym* 60:191–194 . doi: 10.1016/j.molcatb.2009.05.006
- Koszelewski D, Lavandera I, Clay D, Rozzell D, Kroutil W (2008) Asymmetric synthesis of optically pure pharmacologically relevant amines employing ω -transaminases. *Adv Synth Catal* 350:2761–2766 . doi: 10.1002/adsc.200800496
- Koszelewski D, Pressnitz D, Clay D, Kroutil W (2009b) Deracemization of Mexiletine Biocatalyzed by ω -Transaminases. *Org Lett* 11:4810–4812 . doi: 10.1021/ol901834x
- Koszelewski D, Tauber K, Faber K, Kroutil W (2010) ω -Transaminases for the synthesis of non-racemic α -chiral primary amines. *Trends Biotechnol* 28:324–32 . doi: 10.1016/j.tibtech.2010.03.003
- Kothiwale S, Mendenhall JL, Meiler J (2015) BCL::Conf: Small Molecule Conformational Sampling Using A Knowledge Based Rotamer Library. *J Cheminform* 7:47 . doi: 10.1186/s13321-015-0095-1
- Krebs HA (1935) Metabolism of Amino-Acids: Deamination of Amino-Acids. *Biochem J* 29:1620–1644
- Kritzmann Mg (1939) The Enzyme System Transferring the Amino-Group of Aspartic Acid. *Nature* 143:603–604 . doi: 10.1038/143603a0
- Kudo F, Miyanaga A, Eguchi T, Huang SX, Unsin C, Tao M, Coughlin JM, Shen B, Salas JA, Ullrich C, Stein T, Leenders F, Vater J, Poelarends GJ (2014) Biosynthesis of natural products containing β -amino acids. *Nat Prod Rep* 31:1056 . doi: 10.1039/C4NP00007B
- Kumar V, Rahman S, Choudhry H, Zamzami MA, Sarwar Jamal M, Islam A, Ahmad F, Hassan MI (2017) Computing Disease-Linked SOD1 Mutations: Deciphering Protein Stability And Patient-Phenotype Relations. *Sci Rep* 7:4678 . doi: 10.1038/s41598-017-04950-9
- Kundu S, Jha S, Ghosh B (2017) Metabolic Engineering for Improving Production of Taxol. In: *Reference Series in Phytochemistry*. Springer International Publishing, pp 463–484
- Kuramitsu HK, Snoko JE (1962) The biosynthesis of D-amino acids in *Bacillus licheniformis*. *Biochim Biophys Acta* 62:114–121 . doi: 10.1016/0006-3002(62)90496-1
- Laemmli U (1979) Slab Gel Electrophoresis: SDS–PAGE with Discontinuous Buffers. *Nature* 227:680–685
- Laidler KJ, Peterman BF (1979) Temperature Effects in Enzyme Kinetics. *Methods Enzymol* 63:234–57
- Landau M, Mayrose I, Rosenberg Y, Glaser F, Martz E, Pupko T, Ben-Tal N (2005) ConSurf 2005: The projection of evolutionary conservation scores of residues on protein structures. *Nucleic Acids Res* 33:W299–W302 . doi: 10.1093/nar/gki370
- Langer Rs, Lynn Dm, Putnam Da, Amiji Mm, Anderson Dg (2015) Biodegradable poly (β -amino esters) and uses thereof. *US8287849B2*
- Lauchli R, Rabe KS, Kalbarczyk KZ, Tata A, Heel T, Kitto RZ, Arnold FH (2013) High-Throughput Screening for Terpene-Synthase-Cyclization Activity and Directed Evolution of a Terpene Synthase. *Angew Chemie Int Ed* 52:5571–5574 . doi: 10.1002/anie.201301362
- Leaver-Fay A et al. (2011) ROSETTA3: An Object-Oriented Software Suite for the Simulation and Design of Macromolecules. *Methods Enzymol* 487:545–74 . doi: 10.1016/B978-0-12-381270-4.00019-6
- Lee GM, Palsson BO (1990) Immobilization Can Improve The Stability Of Hybridoma Antibody Productivity In Serum-Free Media. *Biotechnol Bioeng* 36:1049–1055 . doi: 10.1002/bit.260361010
- Lee TM (2014a) Computationally-Guided Thermostabilization of the Primary Endoglucanase from *Hypocrea jecorina* for Cellulosic Biofuel Production Thesis by. Thesis 2014: . doi: 10.7907/Z9S180G0
- Leflemme N, Freret T, Boulouard M, Dallemagne P, Rault S (2005) Synthesis and Preliminary In Vivo Evaluation of New 2-Aryl-6-Methyl-1,2-Dihydro-1H-Pyridin-4-Ones and 2-Aryl-6-Methylpiperidin-4-Ols, as Potential Anti-Amnesiac Agents. *J Enzyme Inhib Med Chem* 20:551–556 . doi: 10.1080/14756360500212266
- Lehmann M, Wyss M (2001) Engineering Proteins for Thermostability: The Use Of Sequence Alignments Versus Rational Design And Directed Evolution. *Curr. Opin. Biotechnol.* 12:371–375
- Li D, Cheng S, Wei D, Ren Y, Zhang D (2007a) Production of Enantiomerically Pure (*S*)- β -phenylalanine and (*R*)- β -Phenylalanine by Penicillin G Acylase from *Escherichia*

- coli* in Aqueous Medium. *Biotechnol Lett* 29:1825–1830 . doi: 10.1007/s10529-007-9480-9
- Li D, He Q, Cui Y, Duan L, Li J (2007b) Immobilization of Glucose Oxidase Onto Gold Nanoparticles With Enhanced Thermostability. *Biochem Biophys Res Commun* 355:488–493 . doi: 10.1016/j.bbrc.2007.01.183
- Li M, Simonetti FL, Goncarenco A, Panchenko AR (2016a) MutaBind Estimates And Interprets The Effects Of Sequence Variants On Protein-Protein Interactions. *Nucleic Acids Res* 44:W494–W501 . doi: 10.1093/nar/gkw374
- Li M, Zhang ZJ, Kong XD, Yu HL, Zhou J, Xu JH (2017) Engineering *Streptomyces coelicolor* Carbonyl Reductase For Efficient Atorvastatin Precursor Synthesis. *Appl Environ Microbiol* 83:1081–1091 . doi: 10.1128/AEM.00603-17
- Li S, Fu C, Zhang M, Zhang Y, Xie S, Yu L (2012) Enhancing Taxol Biosynthesis by Overexpressing a 9-Cis-Epoxycarotenoid Dioxygenase Gene in Transgenic Cell Lines of *Taxus chinensis*. *Plant Mol Biol Report* 30:1125–1130 . doi: 10.1007/s11105-012-0436-4
- Li Y, Wang S, Umarov R, Xie B, Fan M, Li L, Gao X (2016b) DEEPRe: Sequence-Based Enzyme EC number Prediction By Deep Learning. *Bioinformatics* 0:1–9 . doi: 10.1093/bioinformatics/btx680
- Li YL, Xu JH, Xu Y (2010) Deracemization of Aryl Secondary Alcohols Via Enantioselective Oxidation And Stereoselective Reduction With Tandem Whole-Cell Biocatalysts. *J Mol Catal B Enzym* 64:48–52 . doi: 10.1016/j.molcatb.2010.01.031
- Lienhard GE (2004) Transition State Analogs as Enzyme Inhibitors. *Annu Rep Med Chem* 7:1–19 . doi: 10.1016/S0065-7743(08)60818-0
- Liljeblad A, Kanerva LT (2006) Biocatalysis as a Profound Tool In the Preparation of Highly Enantiopure β -Amino Acids. *Tetrahedron* 62:5831–5854
- Limanto J, Ashley ER, Yin J, Beutner GL, Grau BT, Kassim AM, Kim MM, Klapars A, Liu Z, Strotman HR, Truppo MD (2014) A Highly Efficient Asymmetric Synthesis Of Vernakalant. *Org Lett* 16:2716–2719 . doi: 10.1021/o501002a
- Liu BL, Jong CH, Tzeng YM (1999) Effect of Immobilization on Ph and Thermal Stability of *Aspergillus ficuum* phytase. *Enzyme Microb Technol* 25:517–521 . doi: 10.1016/S0141-0229(99)00076-9
- Liu H, Zhu L, Bocola M, Chen N, Spiess AC, Schwaneberg U (2013) Directed Laccase Evolution For Improved Ionic Liquid Resistance. *Green Chem* 15:1348 . doi: 10.1039/c3gc36899h
- Liu Y, Kuhlman B (2006) RosettaDesign Server for Protein Design. *Nucleic Acids Res* 34:W235–W238 . doi: 10.1093/nar/gkl1163
- Lobstein J, Emrich CA, Jeans C, Faulkner M, Riggs P, Berkmen M (2012) SHuffle, a Novel *Escherichia coli* Protein Expression Strain Capable of Correctly Folding Disulfide Bonded Proteins In Its Cytoplasm. *Microb Cell Fact* 11:753 . doi: 10.1186/1475-2859-11-56
- Logue MW, Pollack RM, Vitullo VP (1975a) Nature of The Transition State For The Decarboxylation Of Beta-Keto Acids. *J Am Chem Soc* 97:6868–6869 . doi: 10.1021/ja00856a047
- Loksha I V., Maiolo JR, Hong CW, Ng A, Snow CD (2009) SHARPEN-Systematic Hierarchical Algorithms for Rotamers and Proteins on an Extended Network. *J Comput Chem* 30:999–1005 . doi: 10.1002/jcc.21204
- Lu J, Lin Q, Li Z, Rohani S (2012) Solubility of L-Phenylalanine Anhydrous And Monohydrate Forms: Experimental Measurements And Predictions. *J Chem Eng Data* 57:1492–1498 . doi: 10.1021/jc201354k
- Lueck JD, Fromm HJ (1973) Analysis Of Exchange Rates For The Ping Pong Bi Bi Mechanism And The Concept Of Substrate Synergism. *FEBS Lett* 32:184–186 . doi: 10.1016/0014-5793(73)80767-7
- Lülsdorf N, Vojcic L, Hellmuth H, Weber TT, Mußmann N, Martinez R, Schwaneberg U (2015) A First Continuous 4-Aminoantipyrine (4-AAP)-Based Screening System For Directed Esterase Evolution. *Appl Microbiol Biotechnol* 99:5237–5246 . doi: 10.1007/s00253-015-6612-3
- Luo XJ, Zhao J, Li CX, Bai YP, Reetz MT, Yu HL, Xu JH (2016) Combinatorial Evolution Of Phosphotriesterase Toward A Robust Malathion Degradator By Hierarchical Iteration Mutagenesis. *Biotechnol Bioeng* 113:2350–2357 . doi: 10.1002/bit.26012
- Lyskov S, Chou FC, Conchúir SÓ, Der BS, Drew K, Kuroda D, Xu J, Weitzner BD, Renfrew PD, Sripakdeevong P, Borgo B, Havranek JJ, Kuhlman B, Kortemme T, Bonneau R, Gray JJ, Das R (2013) Serverification of Molecular Modeling Applications: The Rosetta Online Server That Includes Everyone (ROSIE). *PLoS One* 8:e63906 . doi: 10.1371/journal.pone.0063906
- Lyskowski A, Gruber C, Steinkellner G, Schürmann M, Schwab H, Gruber K, Steiner K (2014) Crystal structure of an (*R*)-selective ω -Transaminase from *Aspergillus terreus*. *PLoS One* 9:e87350 . doi: 10.1371/journal.pone.0087350
- Mackay DJC (2003) Inference, and Learning Algorithms. Cambridge University Press
- Malik MS, Park ES, Shin JS (2012a) Features and Technical Applications of ω -Transaminases. *Appl. Microbiol. Biotechnol.* 94:1163–1171
- Malik S, Cusidó RM, Mirjalili MH, Moyano E, Palazón J, Bonfill M (2011) Production of the Anticancer Drug Taxol in *Taxus baccata* Suspension Cultures: A review. *Process Biochem.* 46:23–34
- Mallin H, Höhne M, Bornscheuer UT (2014) Immobilization of (*R*)- and (*S*)-Amine Transaminases on Chitosan Support and Their Application for Amine Synthesis Using Isopropylamine as Donor. *J Biotechnol* 191:32–37 . doi: 10.1016/j.jbiotec.2014.05.015
- Malz RE (1996) Catalysis of Organic Reactions. CRC Press
- Mandelstam J (1958) The Free Amino Acids In Growing And Non-Growing Population Of *Escherichia coli*. *Biochem J* 89:103–110
- Mano J, Ogawa J, Shimizu S (2006) Microbial Production of Optically Active β -Phenylalanine through Stereoselective Degradation of Racemic β -Phenylalanine. *Biosci Biotechnol Biochem* 70:1941–1946 . doi: 10.1271/bbb.60099
- Manta B, Cassimjee KE, Himo F (2017) Quantum Chemical Study of Dual-Substrate Recognition in ω -Transaminase. *ACS Omega* 2:890–898 . doi: 10.1021/acsomega.6b00376
- Markova M, Peneff C, Hewlins MJE, Schirmer T, John RA (2005) Determinants of Substrate Specificity In ω -Aminotransferases. *J Biol Chem* 280:36409–16 . doi: 10.1074/jbc.M506977200
- Marshall S a, Morgan CS, Mayo SL (2002) Electrostatics significantly Affect The Stability Of Designed Homeodomain Variants. *J Mol Biol* 316:189–99 . doi: 10.1006/jmbi.2001.5326
- Martin AR, DiSanto R, Plotnikov I, Kamat S, Shonnard D, Pannuri S (2007) Improved Activity and Thermostability Of (*S*)-Aminotransferase By Error-Prone Polymerase Chain Reaction For The Production Of A Chiral Amine. *Biochem Eng J* 37:246–255 . doi: 10.1016/j.bej.2007.05.001
- Martin OA, Vila JA, Scheraga HA (2012) CheShift-2: Graphic validation of protein structures. *Bioinformatics* 28:1538–1539 . doi: 10.1093/bioinformatics/bts179
- Martinez del Pozo A, van Ophem PW, Ringe D, Petsko G, Soda K, Manning JM (1996) Interaction of Pyridoxal 5'-Phosphate with Tryptophan-139 at The Subunit Interface of Dimeric D-Amino Acid Transaminase. *Biochemistry* 35:2112–2116 . doi: 10.1021/bi9522211
- Masso M, Vaisman II (2010) AUTO-MUTE: Web-based Tools for Predicting Stability Changes In Proteins Due to Single Amino Acid Replacements. *Protein Eng Des Sel* 23:683–687 . doi: 10.1093/protein/gzq042
- Mathew S, Bea H, Nadarajan SP, Chung T, Yun H (2015) Production of Chiral β -Amino Acids Using ω -Transaminase from *Burkholderia graminis*. *J Biotechnol* 196–197:1–8 . doi: 10.1016/j.jbiotec.2015.01.011

List of all references

- Mathew S, Deepankumar K, Shin G, Hong EY, Kim B-G, Chung T, Yun H (2016a) Identification of Novel Thermostable ω -Transaminase and its Application for Enzymatic Synthesis of Chiral Amines at High Temperature. *RSC Adv* 6:69257–69260 . doi: 10.1039/C6RA15110H
- Mathew S, Deepankumar K, Shin G, Hong EY, Kim B-G, Chung T, Yun H, Yun H, Lee SH, Yun H, Devine PN, Hmauin GW, Hughes GJ (2016b) Identification of Novel Thermostable ω -Transaminase and its Application for Enzymatic Synthesis of Chiral Amines at High Temperature. *RSC Adv* 6:69257–69260 . doi: 10.1039/C6RA15110H
- Mathew S, Jeong SS, Chung T, Lee SH, Yun H (2016c) Asymmetric synthesis of aromatic β -amino acids using ω -transaminase: Optimizing the lipase concentration to obtain thermodynamically unstable β -keto acids. *Biotechnol J* 11:185–190 . doi: 10.1002/biot.201500181
- Mathew S, Nadarajan SP, Chung T, Park HH, Yun H (2016d) Biochemical Characterization of Thermostable ω -Transaminase from *Sphaerobacter thermophilus* and its Application for Producing Aromatic β - and γ -Amino Acids. *Enzyme Microb Technol*. doi: 10.1016/j.enzmictec.2016.02.013
- Mathew S, Nadarajan SP, Sundaramoorthy U, Jeon H, Chung T, Yun H (2016e) Biotransformation of β -keto nitriles to chiral (*S*)- β -Amino Acids Using Nitrilase and ω -Transaminase. *Biotechnol Lett*. doi: 10.1007/s10529-016-2271-4
- Matsumoto M, Ohashi K (2003) Effect of Immobilization On Thermostability Of Lipase From *Candida rugosa*. *Biochem Eng J* 14:75–77 . doi: 10.1016/S1369-703X(02)00138-9
- Matsumura K, Saito T (2004) Asymmetric reductive amination of keto acid derivatives for producing amino acid derivatives. EP2100875B1
- Matsumura M, Becktel WJ, Levitt M, Matthews BW (1989a) Stabilization of phage T4 lysozyme by engineered disulfide bonds. *Proc Natl Acad Sci* 86:6562–6566 . doi: 10.1073/pnas.86.17.6562
- Matsumura M, Becktel WJ, Levitt M, Matthews BW (1989b) Stabilization of Phage T4 Lysozyme By Engineered Disulfide Bonds. *Proc Natl Acad Sci* 86:6562–6566 . doi: 10.1073/pnas.86.17.6562
- Matsumura M, Signor G, Matthews BW (1989c) Substantial Increase Of Protein Stability By Multiple Disulphide Bonds. *Nature* 342:291–293 . doi: 10.1038/342291a0
- Matsumura M, Becktel WJ, Levitt M, Matthews BW (1989) Stabilization of Phage T4 Lysozyme By Engineered Disulfide Bonds (Thermostability/Lysozyme/Protein Structure). *Biochemistry* 86:6562–6566 . doi: 10.1073/pnas.86.17.6562
- Mayer S, Junne S, Ukkonen K, Glazyrina J, Glauche F, Neubauer P, Vasala A (2014) Lactose Autoinduction With Enzymatic Glucose Release: Characterization Of The Cultivation System In Bioreactor. *Protein Expr Purif* 94:67–72 . doi: 10.1016/j.pep.2013.10.024
- McDonald IK, Thornton JM (1994) Satisfying Hydrogen Bonding Potential in Proteins. *J Mol Biol* 238:777–793 . doi: 10.1006/jmbi.1994.1334
- Mehta PK, Hale TI, Christen P (1993a) Aminotransferases: demonstration of homology and division into evolutionary subgroups. *Eur J Biochem* 214:549–561 . doi: 10.1111/j.1432-1033.1993.tb17953.x
- Midelfort KS, Kumar R, Han S, Karmilowicz MJ, McConnell K, Gehlhaar DK, Mistry A, Chang JS, Anderson M, Villalobos A, Minshull J, Govindarajan S, Wong JW (2013a) Redesigning and characterizing the substrate specificity and activity of *Vibrio fluvialis* aminotransferase for the synthesis of imigabalin. *Protein Eng Des Sel* 26:25–33 . doi: 10.1093/protein/gzso65
- Mittal S, Kaur H, Gautam N, Mantha AK (2017) Biosensors for Breast Cancer Diagnosis: A Review Of Bioreceptors, Biotransducers And Signal Amplification Strategies. *Biosens Bioelectron* 88:217–231 . doi: 10.1016/j.bios.2016.08.028
- Mittendorf J, Kunisch F, Matzke M, Militzer H, Schmidt A, Scho W (2003) Novel Antifungal -Amino Acids : Synthesis and Activity Against *Candida albicans*. *Bioorg Med Chem Lett* 13:433–436 . doi: 10.1016/S0960-894X(02)00958-7
- Miyazaki K, Arnold FH (1999) Exploring Nonnatural Evolutionary Pathways By Saturation Mutagenesis: Rapid Improvement Of Protein Function. *J Mol Evol* 49:716–720 . doi: 10.1007/PL00006593
- Miyazaki K, Wintrod PL, Grayling RA, Rubingh DN, Arnold FH (2000) Directed Evolution Study Of Temperature Adaptation In A Psychrophilic Enzyme. *J Mol Biol* 297:1015–26 . doi: 10.1006/jmbi.2000.3612
- Modarres HP, Mofrad MR, Sanati-Nezhad A (2016) Protein Thermostability Engineering. *RSC Adv* 6:115252–115270 . doi: 10.1039/C6RA16992A
- Modarres P (2015) Modeling and Engineering Proteins Thermostability. *Ecole Polytechnique Federale de Lausanne*
- Molinaro C, Bulger PG, Lee EE, Kosjek B, Lau S, Gauvreau D, Howard ME, Wallace DJ, O’Shea PD (2012) CRTH2 Antagonist MK-7246: A Synthetic Evolution from Discovery through Development. *J Org Chem* 77:2299–2309 . doi: 10.1021/jo202620r
- Morrow JK, Zhang S (2012) Computational Prediction of Protein Hot Spot Residues. *Curr Pharm Des* 18:1255–12565 . doi: 10.2174/138920012799362909
- Mugford PF, Wagner UG, Jiang Y, Faber K, Kazlauskas RJ (2008) Enantiocomplementary Enzymes: Classification, Molecular Basis for Their Enantioselectivity, and Prospects for Mirror-Image Biotransformations. *Angew Chemie Int Ed* 47:8782–8793 . doi: 10.1002/anie.200705159
- Musil M, Stourac J, Bendl J, Brezovsky J, Prokop Z, Zendulka J, Martinek T, Bednar D, Damborsky J (2017) FireProt: Web Server For Automated Design Of Thermostable Proteins. *Nucleic Acids Res* 45:W393–W399 . doi: 10.1093/nar/gkx285
- Mutti FG, Fuchs CS, Pressnitz D, Sattler JH, Kroutil W (2011a) Stereoselectivity of Four (*R*)-Selective Transaminases for the Asymmetric Amination of Ketones. *Adv Synth Catal* 353:3227–3233 . doi: 10.1002/adsc.201100558
- Mutti FG, Kroutil W (2012) Asymmetric Bio-amination of Ketones in Organic Solvents. *Adv Synth Catal* 354:3409–3413 . doi: 10.1002/adsc.201200900
- Nakai T, Okada K, Akutsu S, Miyahara I, Kawaguchi S, Kato R, Kuramitsu S, Hirotsu K (1999) Structure of *Thermus thermophilus* HB8 Aspartate Aminotransferase and Its Complex with Maleate. *Biochemistry* 38:2413–2424 . doi: 10.1021/b9981988i
- Needham DM (1930) A Quantitative Study Of Succinic Acid In Muscle. Glutamic and aspartic acids as precursors. *Biochem J* 24:208–227
- Needham TE (1970) The Solubility Of Amino Acids In Various Solvent Systems. *Open Access Diss* 1–95
- Newman JD, Turner APF (2005) Home Blood Glucose Biosensors: A Commercial Perspective. *Biosens. Bioelectron*. 20:2435–2453
- Nielsen S V., Stein A, Dinitzen AB, Papaleo E, Tatham MH, Poulsen EG, Kassem MM, Rasmussen LJ, Lindorff-Larsen K, Hartmann-Petersen R (2017) Predicting the impact of Lynch syndrome-causing missense mutations from structural calculations. *PLoS Genet* 13:1–26 . doi: 10.1371/journal.pgen.1006739
- Niesen FH, Berglund H, Vedadi M (2007) The Use Of Differential Scanning Fluorimetry To Detect Ligand Interactions That Promote Protein Stability. *Nat Protoc* 2:2212–2221 . doi: 10.1038/nprot.2007.321
- Nobili A, Steffen-Munzberg F, Kohls H, Trentin I, Schulzke C, Höhne M, Bornscheuer UT (2015) Engineering the Active Site of the Amine Transaminase from *Vibrio fluvialis* for the Asymmetric Synthesis of Aryl-Alkyl Amines and Amino Alcohols. *ChemCatChem* 7:757–760 . doi: 10.1002/cctc.201403010
- Nohira H, Sakai K (2004) Optical resolution by means of crystallization. In: *Enantiomer separation: Fundamentals and practical methods*. Springer Netherlands, Dordrecht, pp 165–191
- Nosé S (1984) A Molecular Dynamics Method For Simulations In The Canonical Ensemble. *Mol Phys* 52:255–268 . doi: 10.1080/00268978400101201

- Nugent TC, El-Shazly M (2010) Chiral Amine Synthesis - Recent Developments And Trends For Enamide Reduction, Reductive Amination, And Imine Reduction. *Adv Synth Catal* 352:753–819
- Núñez-Toldrà R, Dosta P, Montori S, Ramos V, Atari M, Borrós S (2016) Improvement of Osteogenesis In Dental Pulp Pluripotent-Like Stem Cells By Oligopeptide-Modified Poly(B-Amino Ester)S. *Acta Biomater* 53:152–164
- Nutzenadel W, Scriver CR (1976) Uptake and Metabolism of β -Alanine and L-Carnosine by Rat Tissues In Vitro - Role in Nutrition. *Am J Physiol* 230:643–651
- O'Rourke PEF, Eadsforth TC, Fyfe PK, Shepherd SM, Hunter WN (2011) *Pseudomonas aeruginosa* 4-Amino-4-Deoxychorismate Lyase: Spatial Conservation of an Active Site Tyrosine and Classification of Two Types of Enzyme. *PLoS One* 6:e24158 . doi: 10.1371/journal.pone.0024158
- Ogawa J, Mano J, Shimizu S (2006) Microbial production of optically active β -phenylalanine ethyl ester through stereoselective hydrolysis of racemic β -phenylalanine ethyl ester. *Appl Microbiol Biotechnol* 70:663–669 . doi: 10.1007/s00253-005-0141-4
- Ohide H, Miyoshi Y, Maruyama R, Hamase K, Konno R (2011) D-Amino Acid Metabolism in Mammals: Biosynthesis, Degradation and Analytical Aspects of the Metabolic Study. *J Chromatogr B* 879:3162–3168 . doi: 10.1016/j.jchromb.2011.06.028
- Otte KB, Hauer B (2015) Enzyme Engineering in The Context of Novel Pathways and Products. *Curr Opin Biotechnol* 35:16–22
- Ouzounis C, Sander C (1993) Homology of the NifS family of Proteins To A New Class Of Pyridoxal Phosphate-Dependent Enzymes. *FEBS Lett* 322:159–164 . doi: 10.1016/0014-5793(93)81559-1
- Pace CN, Fu H, Fryar KL, Landua J, Trevino SR, Shirley BA, Hendricks MN, Iimura S, Gajiwala K, Scholtz JM, Grimsley GR (2011) Contribution Of Hydrophobic Interactions To Protein Stability. *J Mol Biol* 408:514–528 . doi: 10.1016/j.jmb.2011.02.053
- Pal D, Chakrabarti P (2001) Non-hydrogen Bond Interactions Involving the Methionine Sulfur Atom. *J Biomol Struct Dyn* 19:115–128 . doi: 10.1080/07391102.2001.10506725
- Panigrahi P, Sule M, Ghanate A, Ramasamy S, Suresh CG (2015) Engineering Proteins for Thermostability with iRDP Web Server. *PLoS One* 10:1–20 . doi: 10.1371/journal.pone.0139486
- Pannuri S, Kamat SV, Garcia ARM (2010) Thermostable Omega-Transaminases. *EP1819825*
- Park E-S, Dong J-Y, Shin J-S (2013) ω -Transaminase-Catalyzed Asymmetric Synthesis Of Unnatural Amino Acids Using Isopropylamine As An Amino Donor. *Org Biomol Chem* 11:6929 . doi: 10.1039/c3ob40495a
- Park E-S, Kim M, Shin J-S (2012) Molecular Determinants For Substrate Selectivity of ω -Transaminases. *Appl Microbiol Biotechnol* 93:2425–2435 . doi: 10.1007/s00253-011-3584-9
- Park ES, Park SR, Han SW, Dong JY, Shin JS (2014a) Structural Determinants For The Non-Canonical Substrate Specificity of the ω -Transaminase from *Paracoccus denitrificans*. *Adv Synth Catal* 356:212–220 . doi: 10.1002/adsc.201300786
- Park SH, Kim HU, Kim TY, Park JS, Kim S-S, Lee SY (2014b) Metabolic engineering of *Corynebacterium glutamicum* for L-arginine production. *Nat Commun* 5:4618 . doi: 10.1038/ncomms5618
- Parker AS, Zheng W, Griswold KE, Bailey-Kellogg C (2010) Optimization Algorithms For Functional Deimmunization Of Therapeutic Proteins. *BMC Bioinformatics* 11:180 . doi: 10.1186/1471-2105-11-180
- Parrinello M, Rahman A (1981a) Polymorphic transitions in single crystals: A new molecular dynamics method. *J Appl Phys* 52:7182–7190 . doi: 10.1063/1.328693
- Parthiban V, Gromiha MM, Schomburg D (2006) CUPSAT: prediction of protein stability upon point mutations. *Nucleic Acids Res* 34:W239–W242 . doi: 10.1093/nar/gkl190
- Parween S, Misra A, Ramakumar S, Chauhan VS (2014) Self-assembled dipeptide nanotubes constituted by flexible β -phenylalanine and conformationally constrained α,β -dehydrophenylalanine residues as drug delivery system. *J Mater Chem B* 2:3096–3106 . doi: 10.1039/c3tb21856b
- Pavkov-Keller T, Strohmeier GA, Diepold M, Peeters W, Smeets N, Schürmann M, Gruber K, Schwab H, Steiner K (2016a) Discovery And Structural Characterisation Of New Fold Type IV-Transaminases Exemplify The Diversity Of This Enzyme Fold. *Sci Rep* 6:38183 . doi: 10.1038/srep38183
- Pavlidis I V., Weiß MS, Genz M, Spurr P, Hanlon SP, Wirz B, Iding H, Bornscheuer UT (2016) Identification of (*S*)-Selective Transaminases For The Asymmetric Synthesis Of Bulky Chiral Amines. *Nat Chem* 8:1–7 . doi: 10.1038/NCHEM.2578
- Pedragosa-Moreau S, Le Flohic A, Thienpondt V, Lefoulon F, Petit AM, Ros-Lombarda N, Mors F, Gonzalez-Sabn J (2017) Exploiting the Biocatalytic Toolbox for the Asymmetric Synthesis of the Heart-Rate Reducing Agent Ivabradine. *Adv Synth Catal* 359:485–493 . doi: 10.1002/adsc.201601222
- Percudani R, Peracchi A (2009) The B6 database: A Tool For The Description And Classification Of Vitamin B6-Dependent Enzymatic Activities and of the corresponding protein families. *BMC Bioinformatics* 10:273 . doi: 10.1186/1471-2105-10-273
- Peterson ME, Daniel RM, Danson MJ, Eysenhard R (2007) The dependence of Enzyme Activity On Temperature: Determination And Validation Of Parameters. *Biochem J* 402:331–337 . doi: 10.1042/BJ20061143
- Petersen EF, Goddard TD, Huang CC, Couch GS, Greenblatt DM, Meng EC, Ferrin TE (2004a) UCSF Chimera - A visualization System For Exploratory Research And Analysis. *J Comput Chem* 25:1605–1612 . doi: 10.1002/jcc.20084
- Pettit GR, Kamano Y, Herald CL, Tuinman AA, Boettner FE, Kizu H, Schmidt JM, Baczynskij L, Tomer KB, Bontems RJ (1987) The Isolation And Structure Of A Remarkable Marine Animal Antineoplastic Constituent: Dolastatin 10. *J Am Chem Soc* 109:6883–6885 . doi: 10.1021/ja00256a070
- Petukhov M, Cregut D, Soares CM, Serrano L (1999) Local water bridges and protein conformational stability. *Protein Sci* 8:1982–9 . doi: 10.1110/ps.8.10.1982
- Pey AL, Stricher F, Serrano L, Martinez A (2007) Predicted Effects of Missense Mutations on Native-State Stability Account for Phenotypic Outcome in Phenylketonuria, a Paradigm of Misfolding Diseases. *Am J Hum Genet* 81:1006–1024 . doi: 10.1086/521879
- Plessl T, Bürer C, Lutz S, Yue WW, Baumgartner MR, Froese DS (2017) Protein Destabilization And Loss Of Protein-Protein Interaction Are Fundamental Mechanisms In Cbla-Type Methylmalonic Aciduria. *Hum Mutat* 38:988–1001 . doi: 10.1002/humu.23251
- Pokala N, Handel TM (2005) Energy Functions For Protein Design: Adjustment With Protein-Protein Complex Affinities, Models For The Unfolded State, And Negative Design Of Solubility And Specificity. *J Mol Biol* 347:203–227 . doi: 10.1016/j.jmb.2004.12.019
- Polizzi KM, Chaparro-Riggers JF, Vazquez-Figueroa E, Bommarius AS (2006) Structure-Guided Consensus Approach To Create A More Thermostable Penicillin G Acylase. *Biotechnol J* 1:531–536 . doi: 10.1002/biot.200600029
- Pollard DJ, Woodley JM (2007) Biocatalysis for Pharmaceutical Intermediates: The Future Is Now. *Trends Biotechnol* 25:66–73 . doi: 10.1016/j.tibtech.2006.12.005
- Potapov V, Cohen M, Schreiber G (2009) Assessing Computational Methods For Predicting Protein Stability Upon Mutation: Good On Average But Not In The Details. *Protein Eng Des Sel* 22:553–560 . doi: 10.1093/protein/gzp030
- Prasain JK, Stefanowicz P, Kiyota T, Habeichi F, Konishi Y (2001) Taxines from the needles of *Taxus wallichiana*. *Phytochemistry* 58:1167–1170 . doi: 10.1016/S0031-9422(01)00305-3
- Pucci F, Bourgeas R, Rooman M (2016) Predicting protein thermal stability changes upon point mutations using statistical potentials: Introducing HoTMuSiC. *Sci Rep* 6:23257 . doi: 10.1038/srep23257

List of all references

- Purich DL, Purich DL (2010) Active Sites and their Chemical Properties. In: Enzyme Kinetics: Catalysis & Control. Elsevier, pp 53–169
- Radadia AD, Stavits CJ, Carr R, Zeng H, King WP, Carlisle JA, Aksimentiev A, Hamers RJ, Bashir R (2011) Control of Nanoscale Environment to Improve Stability of Immobilized Proteins on Diamond Surfaces. *Adv Funct Mater* 21:1040–1050 . doi: 10.1002/adfm.201002251
- Radivojac P et al. (2013) A large-scale evaluation of computational protein function prediction. *Nat Methods* 10:221–227 . doi: 10.1038/nmeth.2340
- Radkov AD, Moe LA (2014) Bacterial synthesis of D-amino acids. *Appl Microbiol Biotechnol* 98:5363–5374 . doi: 10.1007/s00253-014-5726-3
- Rahman RNZRA, Zakaria II, Salleh AB, Basri M (2012) Enzymatic Properties And Mutational Studies Of Chalcone Synthase From *Physcomitrella patens*. *Int J Mol Sci* 13:9673–9691 . doi: 10.3390/ijms13089673
- Ramakrishnan V, Srinivasan SP, Salem SM, Matthews SJ, Colón W, Zaki M, Bystroff C (2012) Geofold: Topology-based Protein Unfolding Pathways Capture The Effects Of Engineered Disulfides On Kinetic Stability. *Proteins Struct Funct Bioinforma* 80:920–934 . doi: 10.1002/prot.23249
- Ratnayake ND, Theisen C, Walter T, Walker KD (2016) Whole-cell Biocatalytic Production of Various Substituted β -aryl- and β -heteroaryl- β -Amino Acids. *J Biotechnol* 217:12–21 . doi: 10.1016/j.jbiotec.2015.10.012
- Rausch C, Lerchner A, Schiefner A, Skerra A (2013) Crystal Structure of the ω -Aminotransferase from *Paracoccus denitrificans* and its Phylogenetic Relationship with Other class III Amino-Transferases that have Biotechnological Potential. *Proteins Struct Funct Bioinforma* 81:774–787 . doi: 10.1002/prot.24233
- Reetz MT, Carballeira JD, Vogel A (2006) Iterative saturation mutagenesis on the basis of b factors as a strategy for increasing protein thermostability. *Angew Chemie - Int Ed* 45:7745–7751 . doi: 10.1002/anie.200602795
- Rehdorf J, Zimmer CL, Bornscheuer UT (2009) Cloning, expression, characterization, and biocatalytic investigation of the 4-hydroxyacetophenone monooxygenase from *Pseudomonas putida* JD1. *Appl Environ Microbiol* 75:3106–14 . doi: 10.1128/AEM.02707-08
- Rejasse B, Maugard T, Legoy MD (2003) Enzymatic procedures for the synthesis of water-soluble retinol derivatives in organic media. *Enzyme Microb Technol* 32:312–320 . doi: 10.1016/S0141-0229(02)00289-2
- Reyes BA, Pendergast JS, Yamazaki S (2008) Mammalian peripheral circadian oscillators are temperature compensated. *J Biol Rhythms* 23:95–98
- Rice P, Longden I, Bleasby A (2000) EMBOSS: the European Molecular Biology Open Software Suite. *Trends Genet* 16:276–7 . doi: doi.org/10.1016/S0168-9525(00)02024-2
- Richard JP, Amyes TL, Crujeiras J, Rios A (2009) Pyridoxal 5'-phosphate: electrophilic catalyst extraordinaire. *Curr Opin Chem Biol* 13:475–483 . doi: 10.1016/j.cbpa.2009.06.023
- Richter N, Simon RC, Kroutil W, Ward JM, Hailes HC (2014) Synthesis of pharmaceutically relevant 17- α -amino steroids using an ω -transaminase. *Chem Commun* 50:6098–6100 . doi: 10.1039/C3CC49080G
- Roberts E, Ayengar P, Posner I (1953) Transamination of gamma-aminobutyric acid and beta-alanine in microorganisms. *J Biol Chem* 203:195–204
- Roberts E, Rothstein M, Baxter CF (1958) Some Metabolic Studies of γ -Aminobutyric Acid. *Exp Biol Med* 97:796–802 . doi: 10.3181/00379727-97-23883
- Rodríguez-Mata M, García-Urdiales E, Gotor-Fernández V, Gotor V (2010) Stereoselective Chemoenzymatic Preparation Of β -Amino Esters: Molecular Modelling Considerations In Lipase-Mediated Processes And Application To The Synthesis Of (S)-dapoxetine. *Adv Synth Catal* 352:395–406 . doi: 10.1002/adsc.200900676
- Roland Barth, Kathrin HÖFERL-PRANTZ, Frank Richter GS (2015) Novel Route of Synthesis for the Preparation of Suvorexant
- Rose PW, Beran B, Bi C, Bluhm WF, Dimitropoulos D, Goodsell DS, Prlić A, Quesada M, Quinn GB, Westbrook JD, Young J, Yukich B, Zardecki C, Berman HM, Bourne PE (2011) The RCSB Protein Data Bank: Redesigned web site and web services. *Nucleic Acids Res* 39:D392–D401 . doi: 10.1093/nar/gkq1021
- Roy A, Kucukural A, Zhang Y (2010) I-TASSER: A unified platform for automated protein structure and function prediction. *Nat Protoc* 5:725–738 . doi: 10.1038/nprot.2010.5
- Rozzell JD (1984) Production of L-amino acids by transamination. *EP* 0135846 A2
- Rudat J, Brucher BR, Syldatk C (2012a) Transaminases for the Synthesis of Enantiopure β -Amino Acids. *AMB Express* 2:11 . doi: 10.1186/2191-0855-2-11
- Rui Y, Quiñones G, Green JJ (2017) Biodegradable and Bioreducible poly(beta-amino ester) Nanoparticles for Intracellular Delivery to Treat Brain Cancer. *AIChE J* 63:1470–1482 . doi: 10.1002/aic.15698
- Russell RB, Barton GJ (1992) Multiple Protein Sequence Alignment From Tertiary Structure Comparison: Assignment Of Global And Residue Confidence Levels. *Proteins Struct Funct Genet* 14:309–323 . doi: 10.1002/prot.340140216
- Salazar O, Cirino PC, Arnold FH (2003) Thermostabilization of a Cytochrome P450 Peroxygenase. *ChemBioChem* 4:891–893 . doi: 10.1002/cbic.200300660
- Salihu A, Alam MZ (2015) Solvent Tolerant Lipases: A review. *Process Biochem* 50:86–96
- Sánchez IE, Beltrao P, Stricher F, Schymkowitz J, Ferkinghoff-Borg J, Rousseau F, Serrano L (2008) Genome-Wide Prediction of SH2 Domain Targets Using Structural Information and the FoldX Algorithm. *PLoS Comput Biol* 4:e1000052 . doi: 10.1371/journal.pcbi.1000052
- Sánchez IE, Tejero J, Gómez-Moreno C, Medina M, Serrano L (2006) Point Mutations in Protein Globular Domains: Contributions from Function, Stability and Misfolding. *J Mol Biol* 363:422–432 . doi: 10.1016/j.jmb.2006.08.020
- Sanda F, Endo T (1999) Syntheses and functions of polymers based on amino acids. *Macromol Chem Phys* 200:2651–2661 . doi: 10.1002/(sici)1521-3935(19991201)200:12
- Saraf MC, Moore GL, Goodey NM, Cao VY, Benkovic SJ, Maranas CD (2006) IPRO: An Iterative Computational Protein Library Redesign and Optimization Procedure. *Biophys J* 90:4167–4180 . doi: 10.1529/biophysj.105.079277
- Sato S, Morita T, Fukuoka T, Kitamoto D, Habe H (2015) Microbial resolution of DL-glyceric acid for L-glyceric acid production with newly isolated bacterial strains. *J Biosci Bioeng* 119:554–557 . doi: 10.1016/j.jbiosc.2014.10.016
- Satola B, Wübbeler JH, Steinbüchel A (2013) Metabolic Characteristics of the Species *Variovorax paradoxus*. *Appl Microbiol Biotechnol* 97:541–560 . doi: 10.1007/s00253-012-4585-z
- Savile CK, Janey JM, Mundorff EC, Moore JC, Tam S, Jarvis WR, Colbeck JC, Krebber A, Fleitz FJ, Brands J, Devine PN, Huisman GW, Hughes GJ (2010a) Biocatalytic Asymmetric Synthesis of Chiral Amines from Ketones Applied to Sitagliptin Manufacture. *Science* 329:305–309 . doi: 10.1126/science.1188934
- Sayer C, Isupov MN, Westlake A, Littlechild JA (2013) Structural studies of *Pseudomonas* and *Chromobacterium* ω -aminotransferases provide insights into their differing substrate specificity. *Acta Crystallogr Sect D Biol Crystallogr* 69:564–576 . doi: 10.1107/S0907444912051670
- Sayer C, Martínez-Torres RJ, Richter N, Isupov MN, Hailes HC, Littlechild JA, Ward JM (2014) The substrate specificity, enantioselectivity and structure of the (R)-selective amine : pyruvate transaminase from *Nectria haematococca*. *FEBS J* 281:2240–2253 . doi: 10.1111/febs.12778
- Schätzle S, Höhne M, Redestad E, Robins K, Bornscheuer UT (2009) Rapid and Sensitive Kinetic Assay for Characterization of ω -Transaminases. *Anal Chem* 81:8244–8248 . doi: 10.1021/ac901640q

- Scheraga HA, Khalili M, Liwo A (2007) Protein-Folding Dynamics: Overview of Molecular Simulation Techniques. *Annu Rev Phys Chem* 58:57–83 . doi: 10.1146/annurev.physchem.58.032806.104614
- Schiller B, Jager S, Hamacher K, Strufe T (2015) StreaM - A stream-based algorithm for counting motifs in dynamic graphs. In: *Lecture Notes in Computer Science (including subseries Lecture Notes in Artificial Intelligence and Lecture Notes in Bioinformatics)*. Springer, Cham, pp 53–67
- Schneider G, Käck H, Lindqvist Y (2000) The manifold of vitamin B6 dependent enzymes. *Structure* 8:1–6 . doi: 10.1016/S0969-2126(00)00085-X
- Schubert B, Schärfe C, Dönnies P, Hopf T, Marks D, Kohlbacher O (2017) Population-specific design of de-immunized protein biotherapeutics. arXiv 1706.09083:
- Schymkowitz J, Borg J, Stricher F, Nys R, Rousseau F, Serrano L (2005a) The FoldX web server: an online force field. *Nucleic Acids Res* 33:W382–W388 . doi: 10.1093/nar/gki387
- Seebach D, Matthews J (1997) β -Peptides: a Surprise at Every Turn. *Chem Commun* 2015–2022
- Sehl T, Hailes HC, Ward JM, Menyes U, Pohl M, Rother D (2014) Efficient 2-step biocatalytic strategies for the synthesis of all nor(pseudo)ephedrine isomers. *Green Chem* 16:3341–3348 . doi: 10.1039/C4GC00100A
- Sehl T, Hailes HC, Ward JM, Wardenga R, von Lieres E, Offermann H, Westphal R, Pohl M, Rother D (2013) Two Steps in One Pot: Enzyme Cascade for the Synthesis of Nor(pseudo)ephedrine from Inexpensive Starting Materials. *Angew Chemie Int Ed* 52:6772–6775 . doi: 10.1002/anie.201300718
- Seo Y-M, Mathew S, Bea H-S, Khang Y-H, Lee S-H, Kim B-G, Yun H (2012) Deracemization of unnatural amino acid: homoalanine using D-amino acid oxidase and ω -transaminase. *Org Biomol Chem* 10:2482 . doi: 10.1039/c2ob07161d
- Sergio Sanchez, Romina Rodríguez-Sanoja AR& ALD (2017) Our microbes not only produce antibiotics, they also overproduce amino acids. *J Antibiot (Tokyo)*. doi: 10.1038/ja.2017.142
- Serrano L, Horovitz A, Avron B, Bycroft M, Fersht AR (1990) Estimating the Contribution of Engineered Surface Electrostatic Interactions to Protein Stability by Using Double-Mutant Cycles. *Biochemistry* 29:9343–9352 . doi: 10.1021/bi00492a006
- Sheldon RA, van Pelt S (2013) Enzyme immobilisation in biocatalysis: why, what and how. *Chem Soc Rev* 42:6223–6235 . doi: 10.1039/C3CS60075K
- Shin J-S, Yun H, Jang J-W, Park I, Kim B-G (2003) Purification, characterization, and molecular cloning of a novel amine:pyruvate transaminase from *Vibrio fluvialis* JS17. *Appl Microbiol Biotechnol* 61:463–471 . doi: 10.1007/s00253-003-1250-6
- Shin JS, Kim BG (1998) Kinetic modeling of ω -transamination for enzymatic kinetic resolution of α -methylbenzylamine. *Biotechnol Bioeng* 60:534–540 . doi: 10.1002/(SICI)1097-0290(19981205)60:5
- Shin JS, Kim BG (1999) Asymmetric Synthesis of Chiral Amines with ω -Transaminase. *Biotechnol Bioeng* 65:206–211 . doi: 10.1002/(SICI)1097-0290(19991020)65:2
- Shiono Y, Tsuchinari M, Shimanuki K, Miyajima T, Murayama T, Koseki T, Laatsch H, Funakoshi T, Takanami K, Suzuki K (2007) Fusaristatins A and B, Two New Cyclic Lipopeptides from an Endophytic *Fusarium* sp. *J Antibiot (Tokyo)* 60:309–316 . doi: 10.1038/ja.2007.39
- Shon M, Shanmugavel R, Shin G, Mathew S, Lee S-H, Yun H (2014) Enzymatic Synthesis of Chiral γ -Amino Acids Using ω -Transaminase. *Chem Commun (Camb)* 50:12680–3 . doi: 10.1039/c3cc44864a
- Sievers F, Wilm A, Dineen D, Gibson TJ, Karplus K, Li W, Lopez R, McWilliam H, Remmert M, Söding J, Thompson JD, Higgins DG (2011) Fast, scalable generation of high-quality protein multiple sequence alignments using Clustal Omega. *Mol Syst Biol* 7:539 . doi: 10.1038/msb.2011.75
- Simon RC, Grischek B, Zepeck F, Steinreiber A, Belaj F, Kroutil W (2012) Regio- and stereoselective monoamination of diketones without protecting groups. *Angew Chemie - Int Ed* 51:6713–6716 . doi: 10.1002/anie.201202375
- Sin ML, Mach KE, Wong PK, Liao JC (2014) Advances and Challenges in Biosensor-Based Diagnosis Of Infectious Diseases. *Expert Rev Mol Diagn* 14:225–244 . doi: 10.1586/14737159.2014.888313
- Singh A, Basit A, Banerjee UC (2009) Burkholderia cenocepacia: A new biocatalyst for efficient bioreduction of ezetimibe intermediate. *J Ind Microbiol Biotechnol* 36:1369–1374 . doi: 10.1007/s10295-009-0622-z
- Singh R, Kumar M, Mittal A, Mehta PK (2016) Microbial enzymes: industrial progress in 21st century. *3 Biotech* 6:174
- Skalden L, Thomsen M, Höhne M, Bornscheuer UT, Hinrichs W (2015a) Structural and biochemical characterization of the dual substrate recognition of the (*R*)-selective amine transaminase from *Aspergillus fumigatus*. *FEBS J* 282:407–415 . doi: 10.1111/febs.13149
- Slabu I, Galman JL, Iglesias C, Weise NJ, Lloyd RC, Turner NJ (2016) n-Butylamine as an alternative amine donor for the stereoselective biocatalytic transamination of ketones. *Catal. Today*
- Slomka C, Späth GP, Lemke P, Skoupi M, Niemeyer CM, Syltatk C, Rudat J (2017) Toward a Cell-Free Hydantoinase Process: Screening For Expression Optimization And One-Step Purification As Well As Immobilization Of Hydantoinase And Carbamoylase. *AMB Express* 7:122 . doi: 10.1186/s13568-017-0420-3
- Slomka C, Zhong S, Fellinger A, Engel U, Syltatk C, Bräse S, Rudat J (2015) Chemical Synthesis And Enzymatic , Stereoselective Hydrolysis of a Functionalized Dihydropyrimidine for the Synthesis Of β -Amino Acids. *AMB Express* 5:1–8 . doi: 10.1186/s13568-015-0174-8
- Smith CA, Kortemme T (2010) Structure-Based Prediction Of The Peptide Sequence Space Recognized By Natural And Synthetic PDZ Domains. *J Mol Biol* 402:460–474 . doi: 10.1016/j.jmb.2010.07.032
- Smith CA, Kortemme T (2011) Predicting the Tolerated Sequences For Proteins And Protein Interfaces Using RosettaBackrub Flexible Backbone Design. *PLoS One* 6:e20451 . doi: 10.1371/journal.pone.0020451
- Smith DK, Radivojac P, Obradovic Z, Dunker AK, Zhu G (2003) Improved Amino Acid Flexibility Parameters. *Protein Sci* 12:1060–1072 . doi: 10.1110/ps.0236203
- Smith LJ, Daura X, van Gunsteren WF (2002) Assessing Equilibration And Convergence In Biomolecular Simulations. *Proteins Struct Funct Genet* 48:487–496 . doi: 10.1002/prot.10144
- Söhngen C, Bunk B, Podstawka A, Gleim D, Overmann J (2014) BacDive—the Bacterial Diversity Metadatabase. *Nucleic Acids Res* 42:D592–D599 . doi: 10.1093/nar/gkt1058
- Song X, Wang Y, Shu Z, Hong J, Li T, Yao L (2013) Engineering a More Thermostable Blue Light Photo Receptor *Bacillus subtilis* YtvA LOV Domain by a Computer Aided Rational Design Method. *PLoS Comput Biol* 9: . doi: 10.1371/journal.pcbi.1003129
- Spitzer ED, Jimenez-Billini HE, Weiss B (1988) beta-Alanine auxotrophy associated with dfp, a locus affecting DNA synthesis in *Escherichia coli*. *J Bacteriol* 170:872–876 . doi: 10.1128/JB.170.2.872-876.1988
- Steffen-Munsberg F, Vickers C, Kohls H, Land H, Mallin H, Nobili A, Skalden L, van den Bergh T, Joosten HJ, Berglund P, Höhne M, Bornscheuer UT (2015) Bioinformatic analysis of a PLP-dependent enzyme superfamily suitable for biocatalytic applications. *Biotechnol Adv* 33:566–604 . doi: 10.1016/j.biotechadv.2014.12.012
- Steffen-Munsberg F, Vickers C, Thontowi A, Schätzle S, Meinhardt T, Svedendahl M, Land H, Berglund P, Bornscheuer UT, Höhne M (2013) Revealing the Structural Basis of Promiscuous Amine Transaminase Activity. *ChemCatChem* 5:154–157 . doi: 10.1002/cctc.201200545

List of all references

- Steinberg TH, Jones LJ, Haugland RP, Singer VL (1996) SYPRO orange and SYPRO red protein gel stains: One-step fluorescent staining of denaturing gels for detection of nanogram levels of protein. *Anal Biochem* 239:223–237 . doi: 10.1006/abio.1996.0319
- Steipe B, Schiller B, Plückthun A, Steinbacher S (1994) Sequence Statistics Reliably Predict Stabilizing Mutations in a Protein Domain. *J Mol Biol* 240:188–192 . doi: 10.1006/jmbi.1994.1434
- Stekhanova TN, Rakitin AL, Mardanov A V., Bezsudnova EY, Popov VO (2017) A Novel highly thermostable branched-chain amino acid aminotransferase from the crenarchaeon *Vulcanisaeta moutnovskia*. *Enzyme Microb Technol* 96:127–134 . doi: 10.1016/j.enzmictec.2016.10.002
- Stloukal R, Watzková J, Turková K (2018) Biocatalysis: An Industrial Perspective. The Royal Society of Chemistry
- Strecker A (1850) Über die künstliche Bildung der Milchsäure und einen neuen, dem Glycocoll homologen Körper. *Justus Liebigs Ann Chem* 75:27–45 . doi: 10.1002/jlac.18500750103
- Struvay C, Feller G (2012) Optimization to Low Temperature Activity in Psychrophilic Enzymes. *Int J Mol Sci* 13:11643–11665 . doi: 10.3390/ijms130911643
- Studier FW (2005) Protein production by auto-induction in high-density shaking cultures. *Protein Expr Purif* 41:207–234 . doi: 10.1016/j.pep.2005.01.016
- Suárez M, Tortosa P, Jaramillo A (2008) PROTDES: CHARMM toolbox for Computational Protein Design. *Syst Synth Biol* 2:105–113 . doi: 10.1007/s11693-009-9026-7
- Sugawara T, Tanaka A, Tanaka K, Nagai K, Suzuki K, Suzuki T, Change IM (1998) YM-170320, a Novel Lipopeptide Antibiotic Inducing Morphological Change of Colonies in a Mutant of *Candida tropicalis* pK233. *J Antibiot (Tokyo)* 51:435–438 . doi: http://dx.doi.org/10.7164/antibiotics.51.435
- Sugio S, Petsko GA, Manning JM, Soda K, Ringe D (1995) Crystal Structure of a D-Amino Acid Aminotransferase: How the Protein Controls Stereoselectivity. *Biochemistry* 34:9661–9669 . doi: 10.1021/bi00030a002
- Sulkowska JI, Morcos F, Weigt M, Hwa T, Onuchic JN (2012) Genomics-aided structure prediction. *Proc Natl Acad Sci* 109:10340–10345 . doi: 10.1073/pnas.1207864109
- Sullivan BJ, Nguyen T, Durani V, Mathur D, Rojas S, Thomas M, Syu T, Magliery TJ (2012) Stabilizing proteins from sequence statistics: The interplay of conservation and correlation in triosephosphate isomerase stability. *J Mol Biol* 420:384–399 . doi: 10.1016/j.jmb.2012.04.025
- Sun J, Lin Y, Shen X, Jain R, Sun X, Yuan Q, Yan Y (2016) Aerobic Biosynthesis of Hydrocinnamic Acids in *Escherichia coli* with a Strictly Oxygen-Sensitive Enolate Reductase. *Metab Eng* 35:75–82 . doi: 10.1016/j.mben.2016.02.002
- Suzek BE, Wang Y, Huang H, McGarvey PB, Wu CH (2015) UniRef clusters: A Comprehensive And Scalable Alternative For Improving Sequence Similarity Searches. *Bioinformatics* 31:926–932 . doi: 10.1093/bioinformatics/btu739
- Suzuki K, Nagao K, Monnai Y, Yagi A, Uyeda M (1998) Topostatin, a Novel Inhibitor Of Topoisomerases I And II Produced By *Thermomonospora Alba* Strain No. 1520. I. Taxonomy, Fermentation, Isolation And Biological Activities. *J Antibiot (Tokyo)* 51:991–8
- Svedendahl M, Branneby C, Lindberg L, Berglund P (2010) Reversed Enantioselectivity of an ω -Transaminase by a Single-Point Mutation. *ChemCatChem* 2:976–980 . doi: 10.1002/cctc.201000107
- Swain BK, Johri TS (2000) Effect of Supplemental Methionine, Choline And Their Combinations On The Performance And Immune Response Of Broilers. *Br Poult Sci* 41:83–88 . doi: 10.1080/00071660086457
- Szcepek M, Brondani V, Büchel J, Serrano L, Segal DJ, Cathomen T (2007) Structure-based redesign of the dimerization interface reduces the toxicity of zinc-finger nucleases. *Nat Biotechnol* 25:786–793 . doi: 10.1038/nbt1317
- Szymanski W, Wu B, Weiner B, De Wildeman S, Feringa BL, Janssen DB (2009) Phenylalanine aminomutase-catalyzed addition of ammonia to substituted cinnamic acids: A route to enantiopure α - and β -amino acids. *J Org Chem* 74:9152–9157 . doi: 10.1021/jo901833y
- Tabata H (2004) Paclitaxel Production by Plant-Cell-Culture Technology. Springer, Berlin, Heidelberg, pp 1–23
- Takagi H, Takahashi T, Momose H, Inouye M, Maeda Y, Matsuzawa H, Ohta T (1990) Enhancement of the thermostability of subtilisin E by introduction of a disulfide bond engineered on the basis of structural comparison with a thermophilic serine protease. *J Biol Chem* 265:6874–6878
- Takayama T, Shibata T, Shiozawa F, Kawabe K, Shimizu Y, Hamada M, Hiratae A, Takahashi M, Ushiyama F, Oi T, Shirasaki Y, Matsuda D, Koizumi C, Kato S, Tetsu S (2014) Preparation of partially saturated nitrogen-containing heterocyclic compounds, and PHD2 inhibitors, EPO formation promoters, and anti-anemic agents containing the heterocyclic compounds. WO 2014021281 A1
- Talebi M, Ghassempour A, Talebpour Z, Rassouli A, Dolatyari L (2004) Optimization of the extraction of paclitaxel from *Taxus baccata* L. by the use of microwave energy. *J Sep Sci* 27:1130–1136 . doi: 10.1002/jssc.200401754
- Tanghe M, Danneels B, Last M, Beerens K, Stals I, Desmet T (2017) Disulfide bridges as essential elements for the thermostability of lytic polysaccharide monoxygenase LPMO10C from *Streptomyces coelicolor*. *Protein Eng Des Sel* 30:401–408 . doi: 10.1093/protein/gzx014
- Tanizawa K, Masu Y, Asano S, Tanaka H, Soda K (1989) Thermostable D-amino acid aminotransferase from a thermophilic *Bacillus* species. Purification, characterization, and active site sequence determination. *J Biol Chem* 264:2445–2449
- Tauber K, Fuchs M, Sattler JH, Pitzer J, Pressnitz D, Koszelewski D, Faber K, Pfeiffer J, Haas T, Kroutil W (2013) Artificial Multi-Enzyme Networks for the Asymmetric Amination of sec -Alcohols. *Chem - A Eur J* 19:4030–4035 . doi: 10.1002/chem.201202666
- Taylor PP, Pantaleone DP, Senkpeil RF, Fotheringham IG (1998) Novel biosynthetic approaches to the production of unnatural amino acids using transaminases. *Trends Biotechnol* 16:412–418 . doi: 10.1016/S0167-7799(98)01240-2
- Thiltgen G, Goldstein RA (2012) Assessing Predictors of Changes in Protein Stability upon Mutation Using Self-Consistency. *PLoS One* 7: . doi: 10.1371/journal.pone.0046084
- Thomsen M, et al. (2014) Crystallographic Characterization of the (*R*)-selective Amine Transaminase from *Aspergillus fumigatus*. *Acta Crystallogr Sect D Biol Crystallogr* 70:1086–1093 . doi: 10.1107/S1399004714001084
- Thornburg CK, Walter T, Walker KD (2017) Biocatalysis of a Paclitaxel Analogue: Conversion of Baccatin III to N -Debenzoyl- N -(2-furoyl)paclitaxel and Characterization of an Amino Phenylpropanoyl CoA Transferase. *Biochemistry* 56:acs.biochem.7b00912 . doi: 10.1021/acs.biochem.7b00912
- Tian J, Wu N, Chu X, Fan Y (2010) Predicting changes in protein thermostability brought about by single- or multi-site mutations. *BMC Bioinformatics* 11:370 . doi: 10.1186/1471-2105-11-370
- Timucin E, Sezerman OU (2013) The conserved lid tryptophan, w211, potentiates thermostability and thermoactivity in bacterial thermoalkalophilic lipases. *PLoS One* 8:1–17 . doi: 10.1371/journal.pone.0085186
- Tokuriki N, Stricher F, Schymkowitz J, Serrano L, Tawfik DS (2007) The Stability Effects of Protein Mutations Appear to be Universally Distributed. *J Mol Biol* 369:1318–1332 . doi: 10.1016/j.jmb.2007.03.069
- Tokuriki N, Stricher F, Serrano L, Tawfik DS (2008) How protein stability and new functions trade off. *PLoS Comput Biol* 4:35–37 . doi: 10.1371/journal.pcbi.1000002
- Truppo MD, David Rozzell J, Turner NJ (2010) Efficient production of enantiomerically pure chiral amines at concentrations of 50 g/L using transaminases. *Org Process Res Dev* 14:234–237 . doi: 10.1021/op900303q

- Truppo MD, Rozzell JD, Moore JC, Turner NJ (2009) Rapid screening and scale-up of transaminase catalysed reactions. *Org Biomol Chem* 7:395–398 . doi: 10.1039/B817730A
- Tufvesson P, Lima-Ramos J, Jensen JS, Al-Haque N, Neto W, Woodley JM (2011) Process considerations for the asymmetric synthesis of chiral amines using transaminases. *Biotechnol. Bioeng.* 108:1479–1493
- Vachal P, Raheem I, Guo Z, Hartingh Tj (2017) Antiviral Beta-Amino Acid Ester Phosphodiamide Compounds. *WO/2017/027434*
- Valentine JS, Doucette PA, Zittin Potter S (2005) Copper-Zinc Superoxide Dismutase And Amyotrophic Lateral Sclerosis. *Annu Rev Biochem* 74:563–593 . doi: 10.1146/annurev.biochem.72.121801.161647
- Van Durme J, Delgado J, Stricher F, Serrano L, Schymkowitz J, Rousseau F (2011) A graphical interface for the FoldX forcefield. *Bioinformatics* 27:1711–1712 . doi: 10.1093/bioinformatics/btr254
- van Oosterwijk N, Willies S, Hekelaar J, Terwisscha van Scheltinga AC, Turner NJ, Dijkstra BW (2016) Structural Basis of the Substrate Range and Enantioselectivity of Two (*S*)-Selective ω -Transaminases. *Biochemistry* 55:4422–4431 . doi: 10.1021/acs.biochem.6b00370
- Veiga-da-Cunha M, Hadi F, Balligand T, Stroobant V, Van Schaftingen E (2012) Molecular identification of hydroxylysine kinase and of ammoniophosphorylases acting on 5-phosphohydroxy-L-lysine and phosphoethanolamine. *J Biol Chem* 287:7246–7255 . doi: 10.1074/jbc.M111.323485
- Veiga P, Piquet S, Maisons A, Furlan S, Courtin P, Chapot-Chartier M-P, Kulakauskas S (2006) Identification of an essential gene responsible for D-Asp incorporation in the *Lactococcus lactis* peptidoglycan crossbridge. *Mol Microbiol* 62:1713–1724 . doi: 10.1111/j.1365-2958.2006.05474.x
- Vieille C, Zeikus GJ (2001) Hyperthermophilic enzymes: sources, uses, and molecular mechanisms for thermostability. *Microbiol Mol Biol Rev* 65:1–43 . doi: 10.1128/MMBR.65.1.1-43.2001
- Villafranca JE, Howell EE, Oatley SJ, Xuong NH, Kraul J (1987) An Engineered Disulfide Bond in Dihydrofolate Reductase. *Biochemistry* 26:2182–2189 . doi: 10.1021/bi00382a017
- Vlasi M, Cesareni G, Kokkinidis M (1999) A correlation between the loss of hydrophobic core packing interactions and protein stability 1 | Edited by A. R. Fersht. *J Mol Biol* 285:817–827 . doi: 10.1006/jmbi.1998.2342
- Voeltz VA, Bowman GR, Beauchamp K, Pande VS (2010) Molecular simulation of ab initio protein folding for a millisecond folder NTL9(1-39). *J Am Chem Soc* 132:1526–1528 . doi: 10.1021/ja9090353
- Voet D, Voet JG (2011) *Biochemistry*. Wiley
- Vogel A, Schmiedel R, Hofmann U, Gruber K, Zangger K (2014) Converting aspartase into a β -amino acid lyase by cluster screening. *ChemCatChem* 6:965–968 . doi: 10.1002/cctc.201300986
- Vogel C, Widmann M, Pohl M, Pleiss J (2012) A standard numbering scheme for thiamine diphosphate-dependent decarboxylases. *BMC Biochem* 13:24 . doi: 10.1186/1471-2091-13-24
- Vollmer W, Blanot D, De Pedro MA (2008) Peptidoglycan structure and architecture. *FEMS Microbiol Rev* 32:149–167 . doi: 10.1111/j.1574-6976.2007.00094.x
- Vriend G (1990) WHAT IF: A molecular modeling and drug design program. *J Mol Graph* 8:52–56 . doi: 10.1016/0263-7855(90)80070-V
- Wahab RA, Basri M, Rahman MBA, Rahman RNZRA, Salleh AB, Chor LT (2012a) Engineering catalytic efficiency of thermophilic lipase from *Geobacillus zalihae* by hydrophobic residue mutation near the catalytic pocket. *Adv Biosci Biotechnol* 3:158–167 . doi: 10.4236/abb.2012.32024
- Wahab RA, Basri M, Rahman RNZRA, Salleh AB, Rahman MBA, Chor LT (2012b) Manipulation of the Conformation and Enzymatic Properties of T1 Lipase by Site-Directed Mutagenesis of the Protein Core. *Appl Biochem Biotechnol* 167:612–620 . doi: 10.1007/s12010-012-9728-2
- Waller I (1923) Zur Frage der Einwirkung der Wärmebewegung auf die Interferenz von Röntgenstrahlen. *Zeitschrift für Phys* 17:398–408 . doi: 10.1007/BF01328696
- Walter T, King Z, Walker KD (2016) A Tyrosine Aminomutase from Rice (*Oryza sativa*) Isomerizes (*S*)- α - to (*R*)- β -Tyrosine with Unique High Enantioselectivity and Retention of Configuration. *Biochemistry* 55:1–4 . doi: 10.1021/acs.biochem.5b01331
- Wang B, Land H, Berglund P (2013) An efficient single-enzymatic cascade for asymmetric synthesis of chiral amines catalyzed by ω -transaminase. *Chem Commun* 49:161–163 . doi: 10.1039/C2CC37232K
- Wang Q, Buckle AM, Foster NW, Johnson CM, Fersht AR (1999) Design of highly stable functional GroEL minichaperones. *Protein Sci* 8:2186–2193 . doi: 10.1110/ps.8.10.2186
- Wang S, Liu M, Zeng D, Qiu W, Ma P, Yu Y, Chang H, Sun ZW (2014) Increasing stability of antibody via antibody engineering: Stability engineering on an anti-hVEGF. *Proteins Struct Funct Bioinforma* 82:2620–2630 . doi: 10.1002/prot.24626
- Wani MC, Taylor HL, Wall ME, Coggon P, McPhail AT (1971) Plant antitumor agents. VI. The isolation and structure of taxol, a novel antileukemic and antitumor agent from *Taxus brevifolia*. *J Am Chem Soc* 93:2325–7
- Wani NA, Gurpreet Singh, Shankar S, Sharma A, Katoch M, Rai R (2017) Short hybrid peptides incorporating β - and γ -amino acids as antimicrobial agents. *Peptides* 97:46–53 . doi: 10.1016/J.PEPTIDES.2017.09.016
- Watanabe K, Hata Y, Kizaki H, Katsube Y, Suzuki Y (1997) The refined crystal structure of *Bacillus cereus* oligo-1,6-glucosidase at 2.0 Å resolution: structural characterization of proline-substitution sites for protein thermostabilization. *J Mol Biol* 269:142–153 . doi: 10.1006/jmbi.1997.1018
- Weber N, Gorwa-Grauslund M, Carlquist M (2014) Exploiting cell metabolism for biocatalytic whole-cell transamination by recombinant *Saccharomyces cerevisiae*. *Appl Microbiol Biotechnol* 98:4615–4624 . doi: 10.1007/s00253-014-5576-z
- Weiner B (2009) New Methods towards the Synthesis of β -Amino Acids. *Rijksuniversiteit Groningen*
- Weiner SJ, Kollman PA, Case DA, Singh UC, Ghio C, Alagona G, Profeta S, Weiner P (1984) A new force field for molecular mechanical simulation of nucleic acids and proteins. *[J]-[A]m [C]hem [S]oc* 106:765–784
- Weise NJ, Ahmed ST, Parmeggiani F, Turner NJ (2017) Kinetic Resolution of Aromatic β -Amino Acids Using a Combination of Phenylalanine Ammonia Lyase and Aminomutase Biocatalysts. *Adv Synth Catal* 359:1570–1576 . doi: 10.1002/adsc.201600894
- Weise NJ, Parmeggiani F, Ahmed ST, Turner NJ (2015) The Bacterial Ammonia Lyase EncP: A Tunable Biocatalyst for the Synthesis of Unnatural Amino Acids. *J Am Chem Soc* 137:12977–12983 . doi: 10.1021/jacs.5b07326
- Weiß MS, Pavlidis I V., Spurr P, Hanlon SP, Wirz B, Iding H, Bornscheuer UT (2016a) Protein-engineering of an amine transaminase for the stereoselective synthesis of a pharmaceutically relevant bicyclic amine. *Org Biomol Chem* 14:10249–10254 . doi: 10.1039/C6OB02139E
- Wheeler TJ, Clements J, Finn RD (2014) Skyline: A tool for creating informative, interactive logos representing sequence alignments and profile hidden Markov models. *BMC Bioinformatics* 15:7 . doi: 10.1186/1471-2105-15-7
- Widmann M, Pleiss J, Samland AK (2012) Computational Tools For Rational Protein Engineering Of Aldolases. *Comput Struct Biotechnol J* 2:e201209016 . doi: 10.5936/csbi.201209016

List of all references

- Wijma HJ, Floor RJ, Jekel PA, Baker D, Marrink SJ, Janssen DB (2014a) Computationally designed libraries for rapid enzyme stabilization. *Protein Eng Des Sel* 27:49–58 . doi: 10.1093/protein/gzt061
- Wilding M, Peat TS, Newman J, Scott C (2016) A β -Alanine Catabolism Pathway Containing a Highly Promiscuous ω -Transaminase in the 12-Aminododecanate-Degrading *Pseudomonas* sp. Strain AAC. *Appl Environ Microbiol* 82:3846–56 . doi: 10.1128/AEM.00665-16
- Willuda J, Honegger A, Waibel R, Schubiger PA, Stahel R, Zangemeister-Wittke U, Plückthun A (1999) High Thermal Stability Is Essential for Tumor Targeting of Antibody Fragments. *Cancer Res* 59:
- Witherup KM, Look SA, Stasko MW, Ghiorzi TJ, Muschik GM, Cragg GM (1990) *Taxus* spp. Needles contain amounts of Taxol comparable to the bark of *Taxus brevifolia*: Analysis and isolation. *J Nat Prod* 53:1249–1255 . doi: 10.1021/np50071a017
- Wolfenden R (1976) Transition State Analog Inhibitors and Enzyme Catalysis. *Annu Rev Biophys Bioeng* 5:271–306 . doi: 10.1146/annurev.bb.05.060176.001415
- Wolfenden R, Snider M, Ridgway C, Miller B (1999) The temperature dependence of enzyme rate enhancements. *J. Am. Chem. Soc.* 121:7419–7420
- Wong TS, Roccatano D, Zacharias M, Schwaneberg U (2006) A statistical analysis of random mutagenesis methods used for directed protein evolution. *J Mol Biol* 355:858–871 . doi: 10.1016/j.jmb.2005.10.082
- Woodley JM (2013) Protein engineering of enzymes for process applications. *Curr Opin Chem Biol* 17:310–316 . doi: 10.1016/j.cbpa.2013.03.017
- Wörn A, Plückthun A (2001) Stability engineering of antibody single-chain Fv fragments. *J Mol Biol* 305:989–1010 . doi: 10.1006/jmbi.2000.4265
- Wu B, Szymański W, de Wildeman S, Poelarends GJ, Feringa BL, Janssen DB (2010) Efficient Tandem Biocatalytic Process for the Kinetic Resolution of Aromatic β -Amino Acids. *Adv Synth Catal* 352:1409–1412 . doi: 10.1002/adsc.201000035
- Wu B, Wijma HJ, Song L, Rozeboom HJ, Poloni C, Tian Y, Arif MI, Nuijens T, Quaedflieg PJLM, Szymanski W, Feringa BL, Janssen DB (2016) Versatile Peptide C-Terminal Functionalization via a Computationally Engineered Peptide Amidase. *ACS Catal* 6:5405–5414 . doi: 10.1021/acscatal.6b01062
- Wu H-L, Zhang J-D, Zhang C-F, Fan X-J, Chang H-H, Wei W-L (2017) Characterization of Four New Distinct ω -Transaminases from *Pseudomonas putida* NBRC 14164 for Kinetic Resolution of Racemic Amines and Amino Alcohols. *Appl Biochem Biotechnol* 181:972–985 . doi: 10.1007/s12010-016-2263-9
- Wu I (2013) Engineering Thermostable Fungal Cellobiohydrolases. California Institute of Technology
- Wybenga GG, Crismaru CG, Janssen DB, Dijkstra BW (2012a) Structural determinants of the β -selectivity of a bacterial aminotransferase. *J Biol Chem* 287:28495–28502 . doi: 10.1074/jbc.M112.375238
- Wybenga GG, Crismaru CG, Janssen DB, Dijkstra BW (2012b) Structural determinants of the β -selectivity of a bacterial Aminotransferase. *J Biol Chem* 287:28495–28502 . doi: 10.1074/jbc.M112.375238
- Xie DF, Fang H, Mei JQ, Gong JY, Wang HP, Shen XY, Huang J, Mei LH (2017) Improving thermostability of (R)-selective amine transaminase from *Aspergillus terreus* through introduction of disulfide bonds. *Biotechnol. Appl. Biochem.*
- Xiong Y, Luo Y, Li Z (2013) Method for preparing aminophenylpropanoic acid-terminated polyoxyethylene acid or activated ester, and application thereof
- Yamada-Onodera K, Takase Y, Tani Y (2007) Purification and Characterization of 2-Aminoacetophenone Reductase of Newly Isolated *Burkholderia* sp. YT. *J Biosci Bioeng* 104:416–419 . doi: 10.1263/jbb.104.416
- Yamamoto C, Okamoto Y (2004) Resolution of enantiomers by High-Performance Liquid Chromatography. In: *Enantiomer Separation: Fundamentals and Practical Methods*. Springer Netherlands, Dordrecht, pp 301–322
- Yan BX, Sun Qing Y (1997) Glycine residues provide flexibility for enzyme active sites. *J Biol Chem* 272:3190–3194 . doi: 10.1074/jbc.272.6.3190
- Yang AS, Honig B (1994) Structural origins of pH and ionic strength effects on protein stability. *Acid denaturation of sperm whale apomyoglobin*. *J. Mol. Biol.* 237:602–14
- Yang J, Yan R, Roy A, Xu D, Poisson J, Zhang Y (2015) The I-TASSER Suite: protein structure and function prediction. *Nat Methods* 12:7–8 . doi: 10.1038/nmeth.3213
- Yazbeck DR, Martinez CA, Hu S, Tao J (2004) Challenges in the development of an efficient enzymatic process in the pharmaceutical industry. *Tetrahedron Asymmetry* 15:2757–2763
- Yonaha K, Suzuki K, Minei H, Toyama S (1983a) Distribution of omega-amino acid: Pyruvate transaminase and aminobutyrate: a-ketoglutarate transaminase in microorganisms. *Agric Biol Chem* 47:2257–2265 . doi: 10.1080/00021369.1983.10865941
- Yonaha K, Toyama S, Kagamiyama H (1983b) Properties of the bound coenzyme and subunit structure of omega-amino acid:pyruvate aminotransferase. *J Biol Chem* 258:2260–2265
- Yonaha K, Toyama S, Yasuda M, Soda K (1976) Purification and crystallization of bacterial ω -amino acid-pyruvate aminotransferase. *FEBS Lett* 71:21–24 . doi: 10.1016/0014-5793(76)80889-7
- Yonaha K, Toyama S, Yasuda M, Soda K (1977) Properties of crystalline (ν -amino acid: Pyruvate aminotransferase of *Pseudomonas* sp. f-126. *Agric Biol Chem* 41:1701–1706 . doi: 10.1080/00021369.1977.10862739
- Yoo E-H, Lee S-Y (2010) Glucose Biosensors: An Overview of Use in Clinical Practice. *Sensors* 10:4558–4576 . doi: 10.3390/s100504558
- Yoo YJ, Feng Y, Kim Y-H, Yagonia CFJ (2017) *Fundamentals of Enzyme Engineering*. Springer Berlin Heidelberg
- You P, Qiu J, Su E, Wei D (2013) Carica papaya lipase catalysed resolution of β -amino esters for the highly enantioselective synthesis of (*S*)-dapoxetine. *European J Org Chem* 557–565 . doi: 10.1002/ejoc.201201055
- Yue WW (2016) From structural biology to designing therapy for inborn errors of metabolism. *J Inherit Metab Dis* 39:489–498 . doi: 10.1007/s10545-016-9923-3
- Yun H, Cho BK, Kim BG (2004a) Kinetic resolution of (*R,S*)-sec-butylamine using omega-transaminase from *Vibrio fluvialis* JS17 under reduced pressure. *Biotechnol Bioeng* 87:772–778 . doi: 10.1002/bit.20186
- Yun H, Lim S, Cho B-K, Kim B-G (2004b) omega-Amino acid:pyruvate transaminase from *Alcaligenes denitrificans* Y2k-2: a new catalyst for kinetic resolution of beta-amino acids and amines. *Appl Environ Microbiol* 70:2529–34 . doi: 10.1128/AEM.70.4.2529-2534.2004
- Yun H, Lim S, Cho B, Kim B (2004c) ω -Amino Acid: Pyruvate Transaminase from *Alcaligenes denitrificans* Y2k-2: a New Catalyst for Kinetic Resolution of β -Amino Acids and Amines -Amino Acid: Pyruvate Transaminase from *Alcaligenes denitrificans* Y2k-2: a New Catalyst for Kinetic Resolut. *Appl Environ Microbiol* 70:2529–2534 . doi: 10.1128/AEM.70.4.2529
- Yusuf S, Camm AJ (2003) Sinus tachyarrhythmias and the specific bradycardic agents: a marriage made in heaven? *J Cardiovasc Pharmacol Ther* 8:89–105 . doi: 10.1177/107424840300800202
- Yvon M, Chambellon E, Bolotin A, Roudot-Algaron F (2000) Characterization and Role of the Branched-Chain Aminotransferase (BcaT) Isolated from *Lactococcus lactis* subsp. cremoris NCDO 763. *Appl Environ Microbiol* 66:571–577 . doi: 10.1128/AEM.66.2.571-577.2000
- Zapun A, Bardwell JC, Creighton TE (1993) The reactive and destabilizing disulfide bond of DsbA, a protein required for protein disulfide bond formation *in vivo*. *Biochemistry* 32:5083–92

- Zhan Z, Gupta D, Khan AA (1992) Kinetics and mechanism of decarboxylation of aspartic acid with ninhydrin. *Int J Chem Kinet* 24:481–487 . doi: 10.1002/kin.550240508
- Zhang D, Chen X, Zhang R, Yao P, Wu Q, Zhu D (2015a) Development of β -amino acid dehydrogenase for the synthesis of β -amino acids via reductive amination of β -ketoacids. *ACS Catal* 5:2220–2224 . doi: 10.1021/cs5017358
- Zhang D, Chen X, Zhang R, Yao P, Wu Q, Zhu D (2015b) Development of β -Amino Acid Dehydrogenase for the Synthesis of β -Amino Acids via Reductive Amination of β -Keto Acids. *ACS Catal* 5:2220–2224 . doi: 10.1021/cs5017358
- Zhang J, Yang JR (2015) Determinants of the rate of protein sequence evolution. *Nat. Rev. Genet.* 16:409–420
- Zhang ZJ, Cai RF, Xu JH (2018) Characterization of a new nitrilase from *Hoeflea phototrophica* DFL-43 for a two-step one-pot synthesis of (S)- β -amino acids. *Appl. Microbiol. Biotechnol.* 1–10
- Zhong F, Yao W, Dou X, Lu Y (2012) Enantioselective Construction of 3-Hydroxy Oxindoles via Decarboxylative Addition of β -Ketoacids to Isatins. *Org Lett* 14:4018–4021 . doi: 10.1021/ol301855w
- Zhou C, Ye J, Xue Y, Ma Y (2015) Directed evolution and structural analysis of alkaline pectate lyase from the alkaliphilic bacterium *Bacillus* sp. strain N16-5 to improve its thermostability for efficient ramie degumming. *Appl Environ Microbiol* 81:5714–5723 . doi: 10.1128/AEM.01017-15
- Zhou NE, Kay CM, Hodges RS (1993) Disulphide bond contribution to protein stability: positional effects of substitution in the hydrophobic core of the two stranded alpha-helical coiled-coil. *Biochemistry* 32:3178–3187
- Ziegelbauer K, Babczinski P, Schönfeld W (1998) Molecular mode of action of the antifungal beta-amino acid BAY 10-8888. *Antimicrob Agents Chemother* 42:2197–205
- Zor T, Selinger Z (1996) Linearization of the Bradford Protein Assay Increases Its Sensitivity: Theoretical and Experimental Studies. *Anal Biochem* 236:302–308 . doi: 10.1006/abio.1996.0171

Appendices

Chapter 4)

Codon optimized gene-sequence of ω -VpTA for *E. coli* BL21-expression.

```
ATGACCCATGCAGCAATTGATCAGGCACTGGCAGATGCATATCGTCGTTTTACCG
ATGCAAATCCGGCAAGCCAGCGTCAGTTTGAAGCACAGGCACGTTATATGCCTGG
TGCAAATAGCCGTAGCGTTCTGTTTTATGCACCGTTTCCGCTGACCATTGCACGTG
GTGAAGGTGCAGCACTGTGGGATGCAGATGGTCATCGTTATGCAGATTTTATTGC
AGAGTATACCGCAGGCGTTTATGGTCATAGCGCACCGGAAATTCGTGATGCAGTT
ATTGAAGCAATGCAGGGTGGTATTAATCTGACAGGTCATAATCTGCTGGAAGGTC
GTCTGGCACGTCTGATTTGTGAACGTTTTCCGCAGATTGAACAGCTGCGTTTTACC
AATAGCGGCACCGAAGCAAATCTGATGGCACTGACCGCAGCACTGCATTTTACCG
GTCGTCGTAAAATTGTTGTTTTTAGCGGTGGTTATCATGGTGGTGTCTGGGTTTT
GGTGCACGTCCGAGCCCGACCACCGTTCCGTTTGATTTTCTGGTTCTGCCGTATAA
TGATGCACAGACCGCACGTGCACAGATCGAACGTCATGGTCCGGAAATTGCAGTT
GTTCTGGTTGAACCTATGCAAGGTGCAAGCGGTTGTATTCCGGGTCAGCCGGATT
TTCTGCAGGCACTGCGTGAAAGCGCAACCCAGGTTGGTGCACCTGCTGGTTTTTGA
TGAAGTTATGACCAGTCGCCTGGCACCGCATGGTCTGGCAAATAAACTGGGTATT
CGTAGCGATCTGACCACCCTGGGCAAATATATCGGTGGTGGTATGAGCTTTGGTG
CATTGTTGGTGGTTCGTGCAGATGTTATGGCACTGTTTGATCCGCGTACCGGTCCGCTG
GCACATAGCGGTACATTTAACAATAATGTGATGACCATGGCAGCCGGTTATGCAG
GTCTGACCAAACCTGTTTACACCGGAAGCAGCCGGTGCACCTGGCCGAACGCGGTG
AAGCTCTGCGTGCCCGTCTGAATGCACTGTGTGCAAATGAAGGTGTTGCAATGCA
GTTTACCGGCATTGGTAGCCTGATGAATGCACATTTTGTTCAGGGTGATGTTTCGTA
GCAGCGAAGATCTGGCAGCAGTTGATGGTCGTCTGCGTCAGCTGCTGTTTTTTCAT
CTGCTGAATGAAGATATCTATAGCAGTCCGCGTGGTTTTGTTGTTCTGAGCCTGCC
GCTGACCGATGCCGATATTGATCGTTATGTGGCAGCGATTGGTAGCTTTATTGGT
GGTCATGGTGCCCTGCTGCCTCGTGCCAATTAA
```

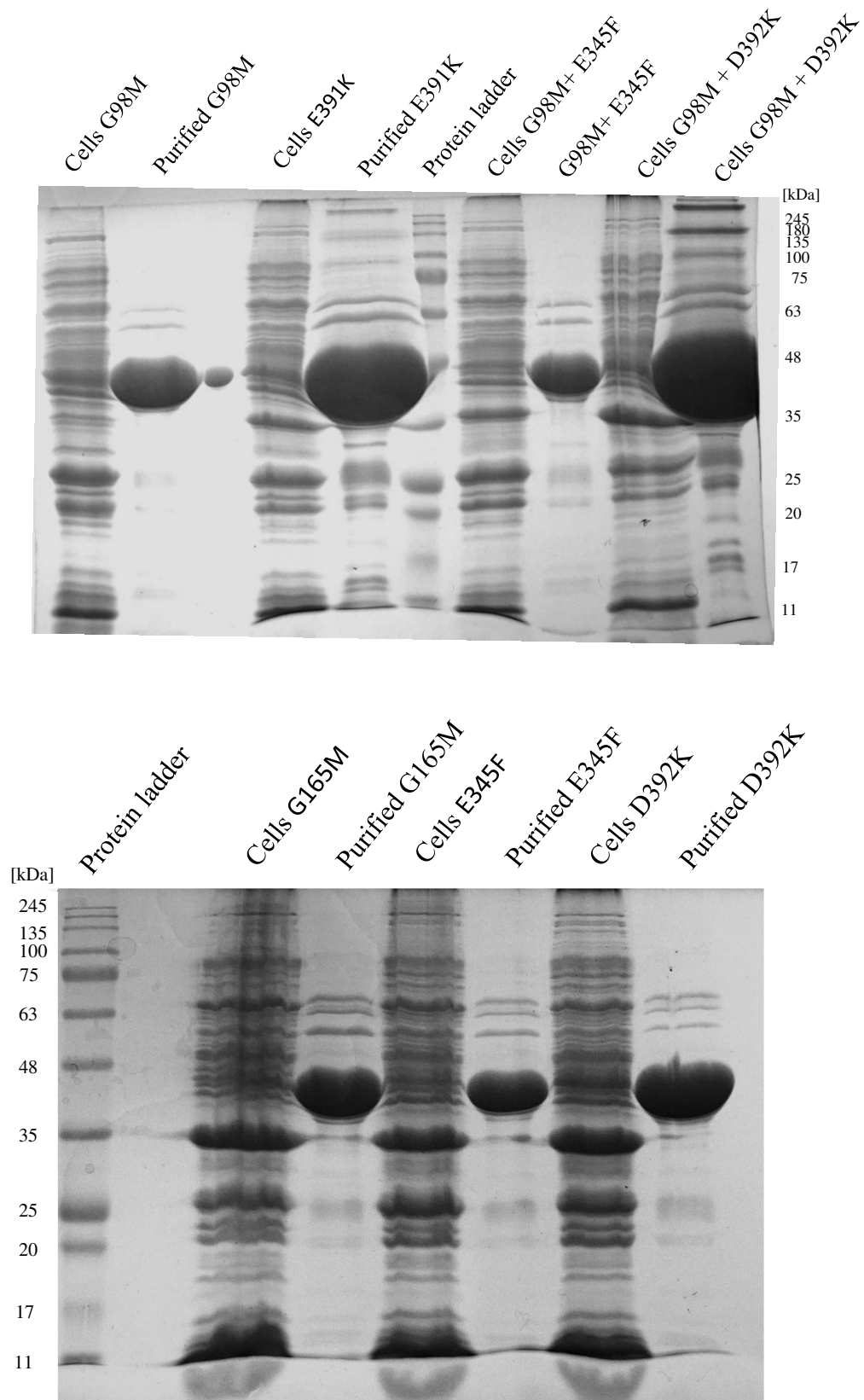


Figure S1 SDS-PAGE analysis of the purification of the wild type ω -VpTA and mutant enzyme variants by Ni-NTA affinity chromatography. Comparison of whole cells expressing the variants ω -VpTA G98M, E391K, G98M+E345F, G98M+392K, G165M, E345F, D392K along with the corresponding purified enzymes.

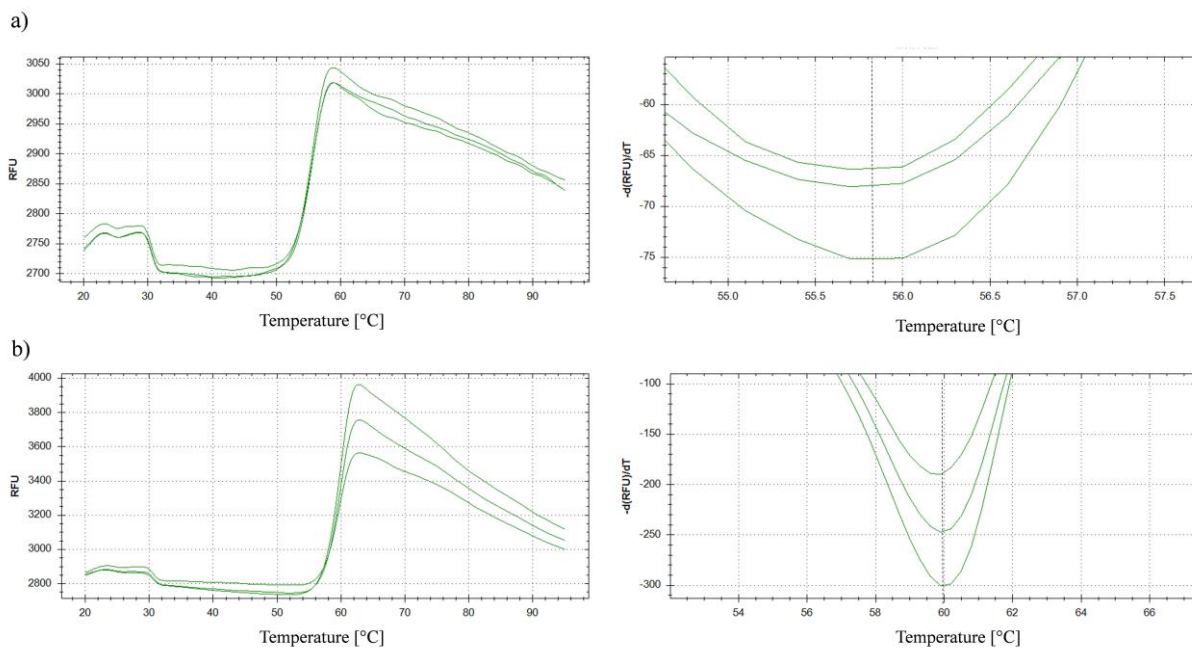


Figure S2 Thermal-shift assay for determination of exemplary melting curves and melting points of the wild type ω -VpTA (a) and of variant G98M+D392K (b). The inflection point of the melting curve function marks the T_m (protein melting point). The melting point was determined by triple measurement. Protein expression was performed twice for the final determination of the protein melting point. For each determination 5 μM of Ni-NTA purified ω -VpTA were utilized.

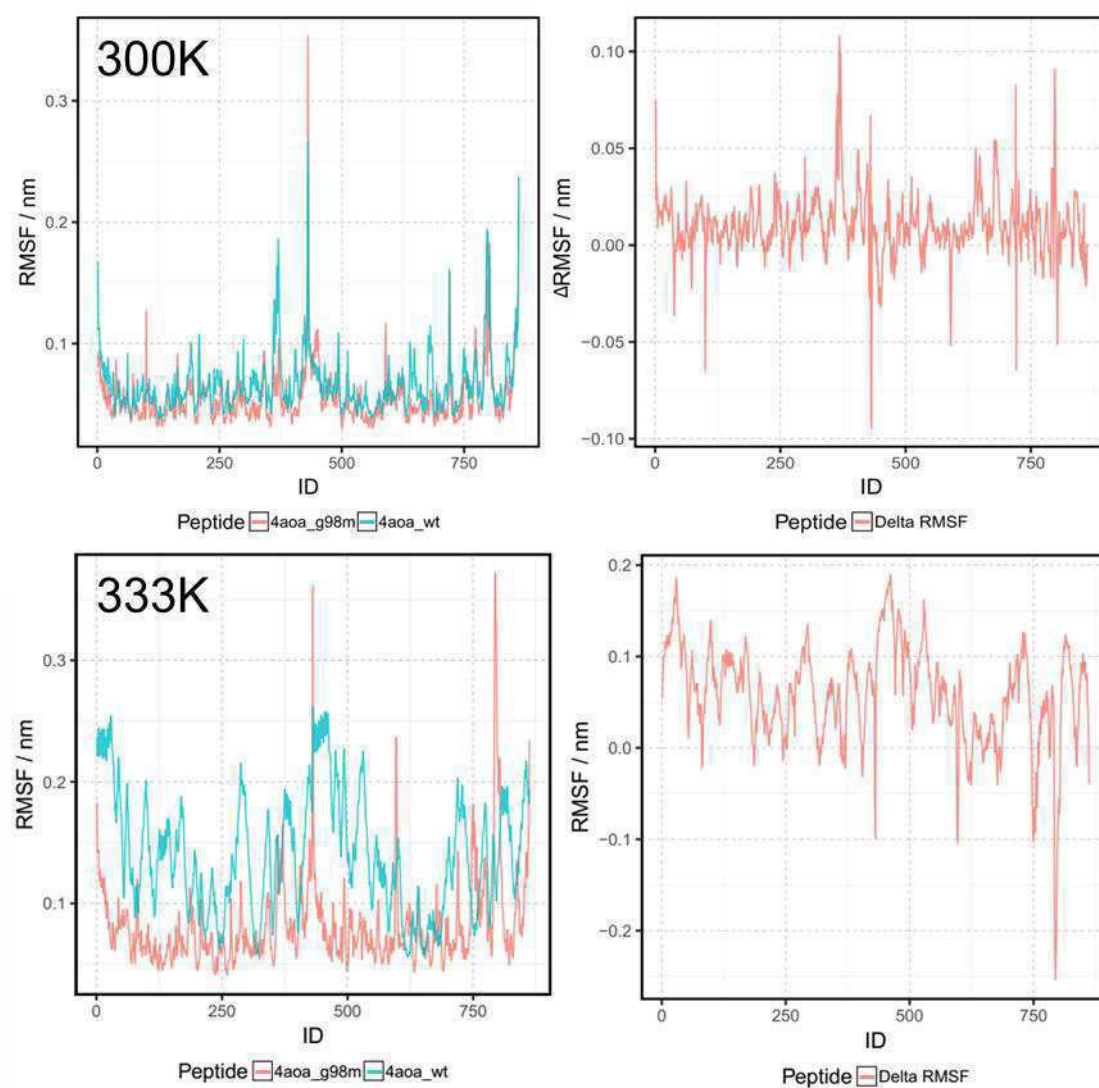


Figure S3 Influence of the G98M mutation on the protein flexibility. The amino acid position of dimer A and B is numbered consecutively. The MD-Simulation was performed over a time period of 100 ns in 40 mM sodium phosphate buffer at 300 K and 333 K. (Left) MD-Simulation data for the wild type is shown in blue, G98M is shown in red. The backbone flexibility is indicated by RMSF-value. (Right) The Δ RMSF-values of every position of the wildtype in relation to G98M highlighting the differences in flexibility. Note that at 333 K the behavior of the G98M mutant remains largely unchanged (compare the red curves in the left images) in comparison to the simulation at 300 K, whereas the wild type clearly shows less thermostability (compare the blue curves in the left images).

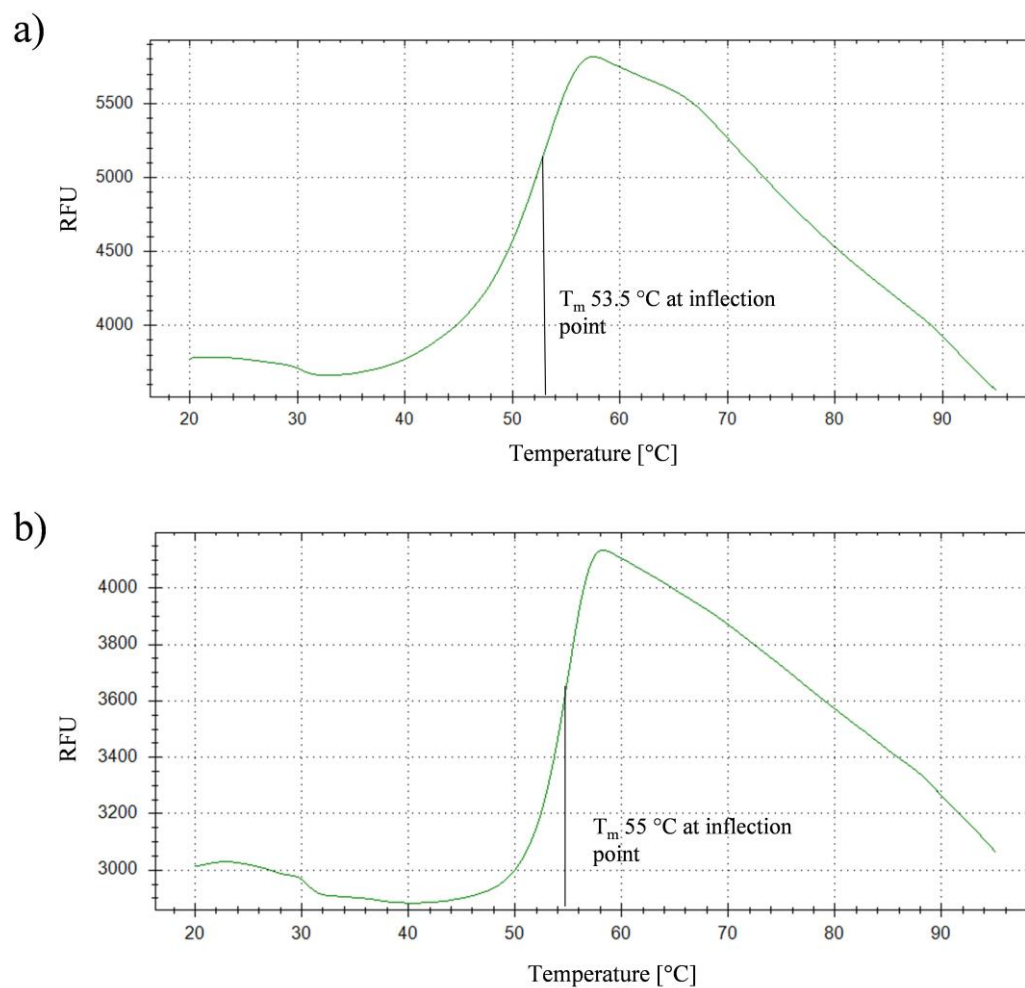


Figure S4 Melting curve of disulfide variants of ω -VpTA. a) Variant 125C showed a melting point of only 53.5°C, this is 2°C less than known for wild type. b) Variant 5C+429C showed no significant difference compared to the wild type. The variants were expressed using *E. coli* SHuffle and purified using Ni-NTA.

Chapter 5)

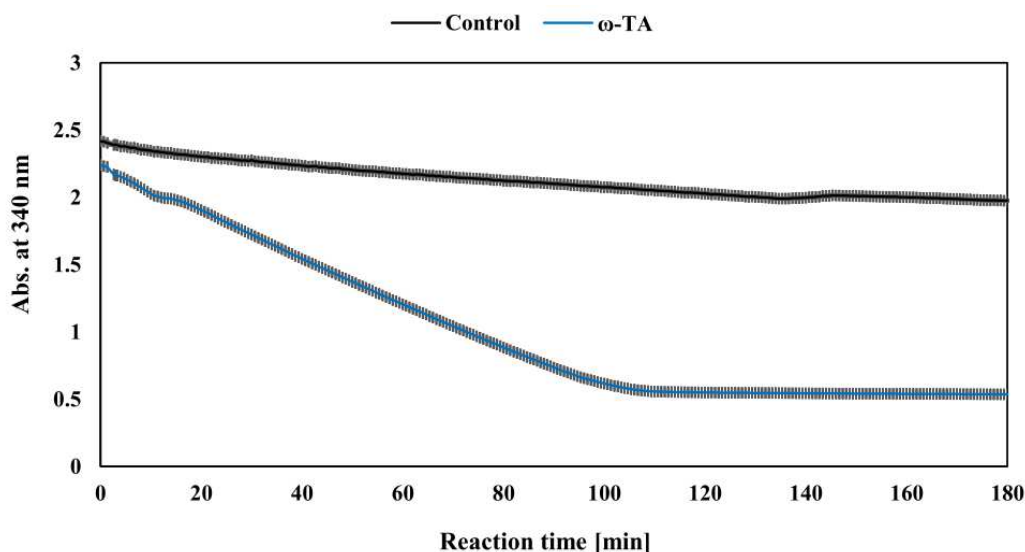


Figure S5 Alanine conversion by ω -VpTA using α -ketoglutarate as acceptor. For reaction 4 μ M of ω -TA were utilized in 100 mM sodium phosphate buffer at pH 7.2 with 0.2 mM of PLP, 50 mM α -ketoglutarate and 250 mM of *rac*-alanine. For removal of pyruvate 1 U mL⁻¹ lactate dehydrogenase was utilized, which oxidizes NADH to NAD⁺. The reaction was observed at 340 nm in Tecan-plate reader in a scale of 200 μ L. The temperature was set to 35°C. The control was performed without α -ketoglutarate. The reaction was performed in threefold determination. The standard deviation is shown as grey bars.

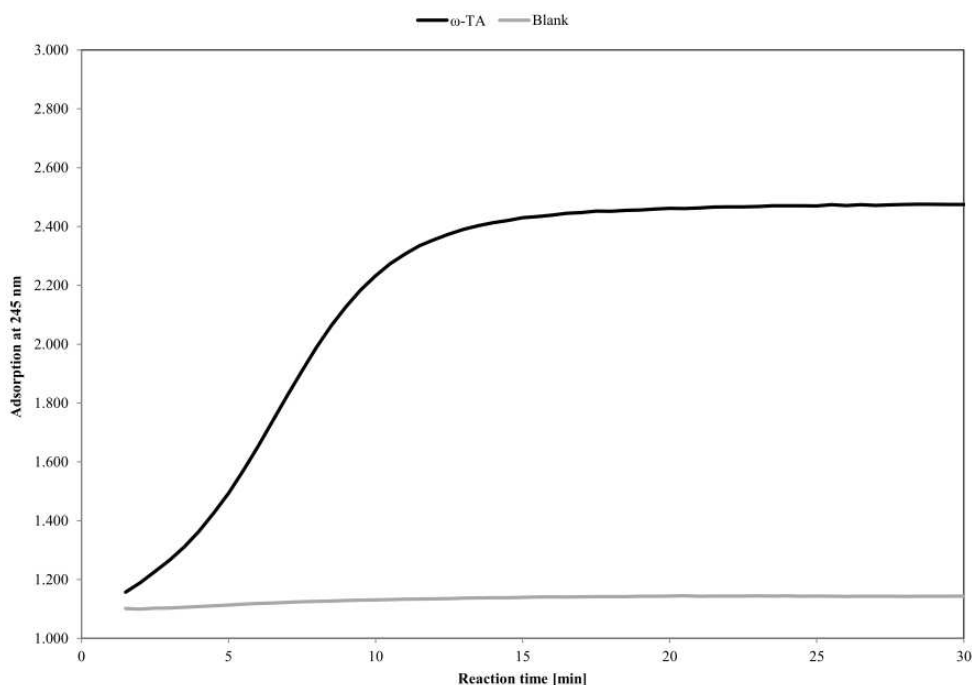


Figure S6 ω -VpTA showing activity towards (*S*)-PEA. 0.5 μ M of ω -TA was utilized in 400 μ L of reaction buffer at 45°C. The reaction mixture consisted of: 100 mM α -MBA, 15 mM α -ketoglutarate, 0.1 mM PLP and 40 mM of sodium phosphate buffer (pH 7.2). The reaction was started by addition of enzyme solution. The control was performed without α -ketoglutarate.

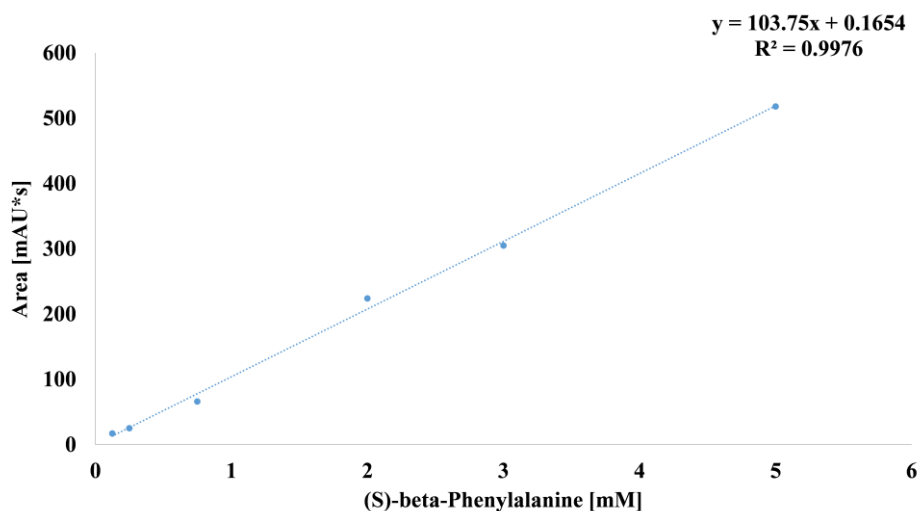


Figure S7. Calibration of (S)-β-phenylalanine concentration with peak area for quantitative HPLC analysis of the transaminase reaction. The standard solutions were diluted and treated identically to the reaction samples.

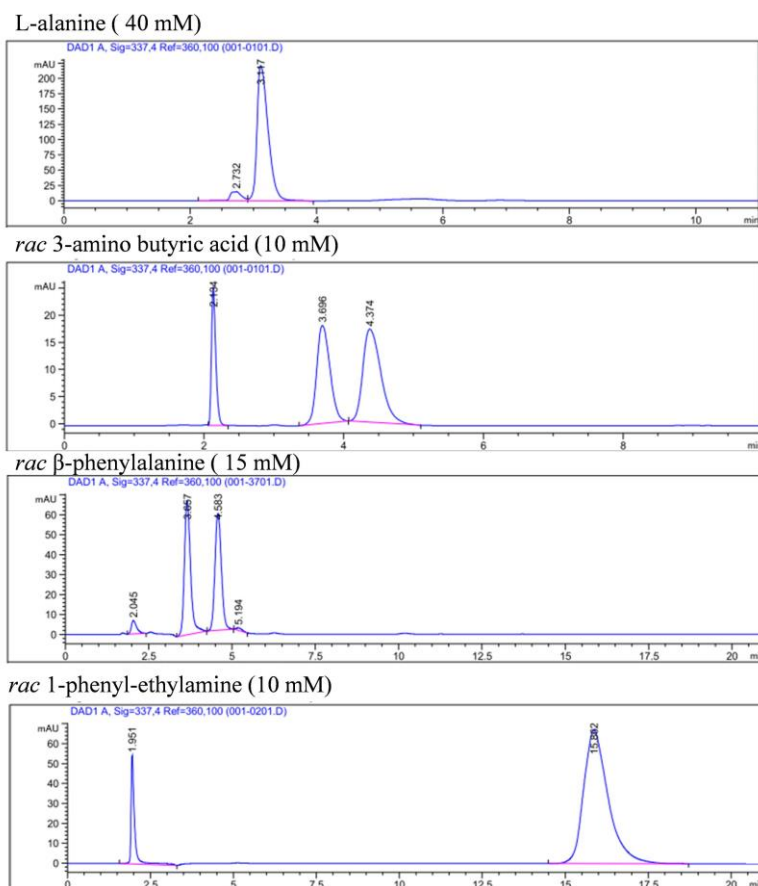


Figure S8 Analysis of different amino acids (amines) by reversed phase chromatography and IBLC-OPA derivatization. Concentrations were used which typically represent the initial situations of enzymatic reactions. The method is described in **Chapter 4**.

Table S1 Standard numbering of VpTA (PDB ID 4AOA). The standard numbering (S.N.) was created using the oTAED standard numbering tool.

S.N.	AA	S.N.	AA	S.N.	AA	S.N.	A	S.N.	A	S.N.	A	S.N.	A	S.N.	A	S.N.	A
0.1	M	0.5 1	L	50	N	100	K	150	I	200	G	251	F	301	F	346.6	V
0.2	T	0.5 2	T	51	L	101	I	151	A	201	L	252	N	302	T	346.7	V
0.3	H	2	I	52	T	102	V	152	V	202	A	253	N	303	G	346.8	L
0.4	A	3	A	53	G	103	V	153	V	203	N	254	N	304	I	346.9	S
0.5	A	4	R	54	H	104	F	154	L	204	K	255	V	305	G	346.1	L
0.6	I	5	G	55	N	105	S	155	V	205	L	256	M	306	S	346.1 1	P
0.7	D	6	E	56	L	106	G	156	E	206	G	257	T	307	L	346.1 2	L
0.8	Q	7	G	57	L	107	G	157	P	207	I	258	M	308	M	346.1 3	T
0.9	A	8	A	58	E	108	Y	158	M	208	R	259	A	309	N	346.1 4	D
0.1	L	9	A	59	G	109	H	159	Q	209	S	260	A	310	A	346.1 5	A
0.1 1	A	10	L	60	R	110	G	160	G	210	D	261	G	311	H	346.1 6	D
0.1 2	D	11	W	61	L	111	G	161	A	211	L	262	Y	312	F	346.1 7	I
0.1 3	A	12	D	62	A	112	V	162	S	212	T	263	A	313	V	346.1 8	D
0.1 4	Y	13	A	63	R	113	L	163	G	213	T	264	G	314	Q	346.1 9	R
0.1 5	R	14	D	64	L	114	G	164	C	214	L	265	L	315	G	346.2	Y
0.1 6	R	15	G	65	I	115	F	165	I	215	G	266	T	316	D	346.2 1	V
0.1 7	F	16	H	66	C	118. 4	G	166	P	216	K	267	K	317	V	346.2 2	A
0.1 8	T	17	R	67	E	118. 5	A	167	G	217	Y	268	L	318	R	346.2 3	A
0.1 9	D	18	Y	68	R	118. 6	R	168	Q	218	I	269	F	319	S	346.2 4	I
0.2	A	19	A	69	F	119	P	169	P	219	G	270	T	320	S	346.2 5	G
0.2 1	N	20	D	70	P	120	S	170	D	220	G	271	P	321	E	346.2 6	S
0.2 2	P	21	F	71	Q	121	P	171	F	221	G	272	E	322	D	346.2 7	F
0.2 3	A	22	I	72	I	122	T	172	L	222	M	273	A	323	L	346.2 8	I
0.2 4	S	23	A	73	E	123	T	173	Q	223	S	274	A	324	A	346.2 9	G
0.2 5	Q	24	E	74	Q	124	V	174	A	224	F	275	G	325	A	346.3	G

0.2	R	25	Y	75	L	125	P	175	L	22	G	27	A	326	V	346.3	H
6										5		6				1	
0.2	Q	26	T	76	R	126	F	176	R	22	A	27	L	327	D	346.3	G
7										6		7				2	
0.2	F	27	A	77	F	127	D	177	E	22	F	27	A	328	G	346.3	A
8										7		8				3	
0.2	E	28	G	78	T	128	F	178	S	22	G	27	E	329	R	346.3	L
9										8		9				4	
0.3	A	29	V	79	N	129	L	179	A	22	G	28	R	330	L	346.3	L
										9		0				5	
0.3	Q	30	Y	80	S	130	V	180	T	23	R	28	G	331	R	346.3	P
1										0		1				6	
0.3	A	31	G	81	G	131	L	181	Q	23	A	28	E	332	Q	346.3	R
2										1		2				7	
0.3	R	32	H	82	T	132	P	182	V	23	D	28	A	333	L	346.3	A
3										2		3				8	
0.3	Y	33	S	83	E	133	Y	183	G	23	V	28	L	334	L	346.3	N
4										3		4				9	
0.3	M	34	A	84	A	134	N	184	A	23	M	28	R	335	F		
5										4		5					
0.3	P	35	P	85	N	135	D	185	L	23	A	28	A	336	F		
6										5		6					
0.3	G	36	E	86	L	136	A	186	L	23	L	28	R	337	H		
7										6		7					
0.3	A	37	I	87	M	137	Q	187	V	23	F	28	L	338	L		
8										7		8					
0.3	N	38	R	88	A	138	T	188	F	23	D	28	N	339	L		
9										8		9					
0.4	S	39	D	89	L	139	A	189	D	23	P	29	A	340	N		
										9		0					
0.4	R	40	A	90	T	140	R	190	E	24	R	29	L	341	E		
1										1		1					
0.4	S	41	V	91	A	141	A	191	V	24	T	29	C	342	D		
2										2		2					
0.4	V	42	I	92	A	142	Q	192	M	24	G	29	A	343	I		
3										3		3					
0.4	L	43	E	93	L	143	I	193	T	24	P	29	N	344	Y		
4										4		4					
0.4	F	44	A	94	H	144	E	194	S	24	L	29	E	345	S		
5										5		5					
0.4	Y	45	M	95	F	145	R	195	R	24	A	29	G	346.	S		
6										6		6		1			
0.4	A	46	Q	96	T	146	H	196	L	24	H	29	V	346.	P		
7										7		7		2			
0.4	P	47	G	97	G	147	G	197	A	24	S	29	A	346.	R		
8										8		8		3			
0.4	F	48	G	98	R	148	P	198	P	24	G	29	M	346.	G		
9										9		9		4			
0.5	P	49	I	99	R	149	E	199	H	25	T	30	Q	346.	F		
										0		0		5			

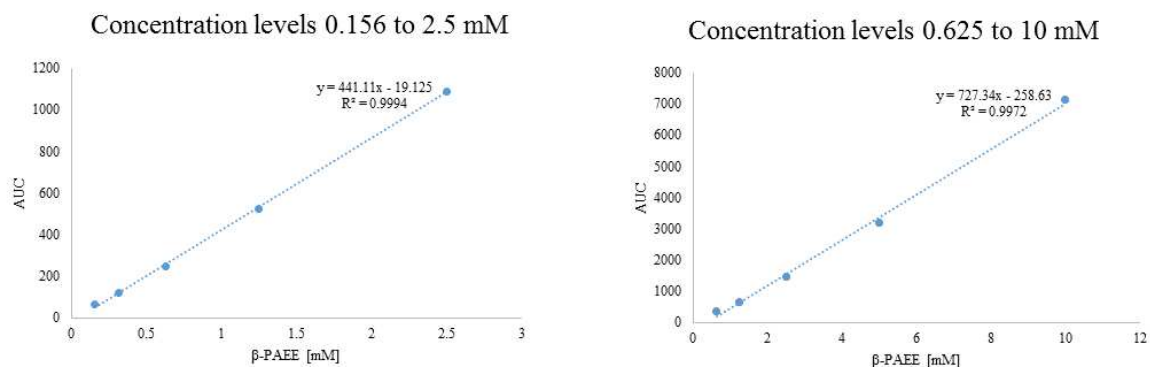


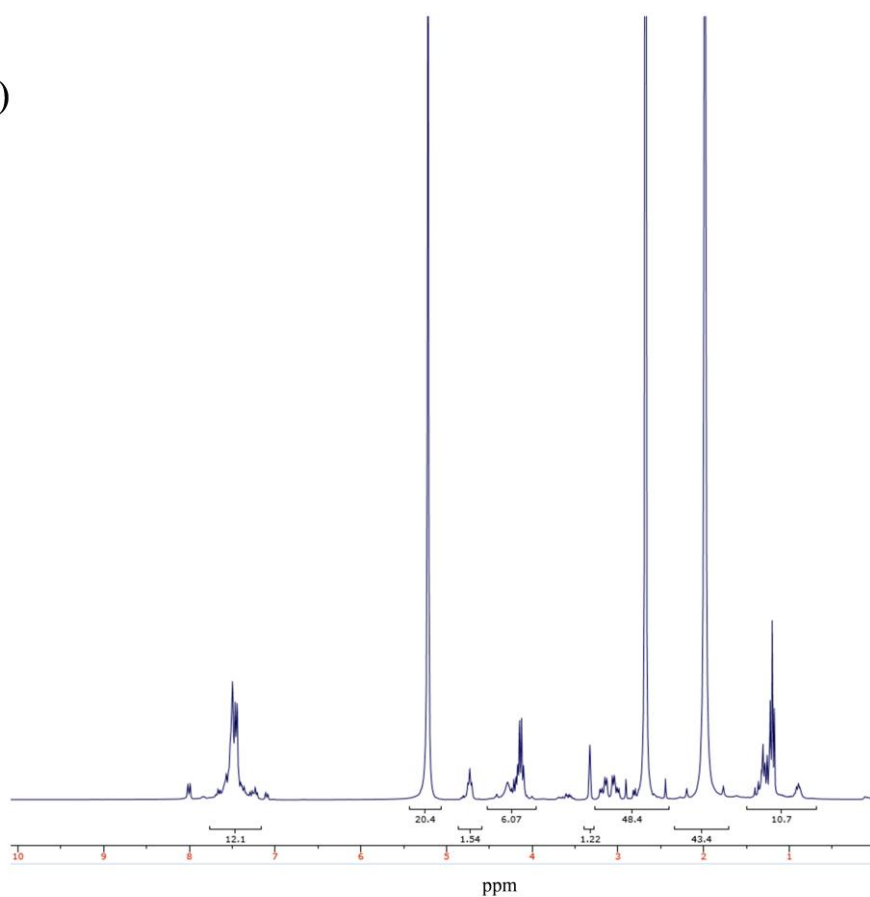
Figure S9 Gas chromatography for detection of β -PAEE. The calibration solution were mixed in EtOAc. The resulting peak area under the curve (AUC) at 28.9 min, detected by FID, was utilized for linear calibration.

Table S2 ω -TA gene-sources for β -PAEE screening. Therefore different Fold type I and IV ω -TA were expressed in *E. coli* BL21 and tested in OXD-screening.

Source	Abbr.	Vector	Resistance	Induction	Fold type	PDB code or protein ID (NCBI)
<i>Ruegeria pomeroyi</i>	3HMU	pET22b	Amp	IPTG	I	3HMU
) <i>Ruegeria sp.</i> TM1040	3FCR	pET22b	Amp	IPTG	I	3FCR
<i>Mesorhizobium loti</i>	3GJU	pET22b	Amp	IPTG	I	3GJU
<i>Rhodobacter sphaeroides</i> KD131	3I5T	pET22b	Amp	IPTG	I	3I5T
<i>Vibrio fluvialis</i>	VibFlu	pET24b	Kan	IPTG	I	3NUI
<i>Mesorhizobium sp.</i> LUK	2YKY	pET28b	Kan	IPTG	I	2YKY
<i>Chromobacterium violaceum</i>	Cvi	pET28a	Kan	IPTG	I	4BA5
<i>Aspergillus oryzae</i>	AspOry	pGASTON	Amp	Rhamnose	IV	(16976819)
<i>Aspergillus terreus</i>	AspTer	pGASTON	Amp	Rhamnose	IV	4CE5
<i>Mycobacterium vanbaalenii</i>	MycVan	pGASTON	Amp	Rhamnose	IV	(120405468)

<i>Penicillium chrysogenum</i>	PenChr	pGASTON	Amp	Rhamnose	IV	(211591081)
<i>Burkholderia sp.</i>	BurSp	pGASTON	Amp	Rhamnose	IV	(78059900)
<i>Rhizobium etli</i>	RhiEtl	pGASTON	Amp	Rhamnose	IV	(190895112)
<i>Hyphomonas neptunium</i>	HypNep	pGASTON	Amp	Rhamnose	IV	(114797240)
<i>Gamma proteobacterium</i>	GamPro	pGASTON	Amp	Rhamnose	IV	(219677744)
<i>Labrenzia alexandrii</i>	LabAle	pGASTON	Amp	Rhamnose	IV	(EEE43073)
<i>Marimonas sp.</i>	MarSp	pGASTON	Amp	Rhamnose	IV	(8712265)
<i>Nocardia farcinica</i>	NocFar	pGASTON	Amp	Rhamnose	IV	(unpublished)
<i>Rhodoferax ferrireducens</i>	RhoFer	pGASTON	Amp	Rhamnose	IV	(89899273)
<i>Bacillus sp.</i>	D-AlaTA	pGASTON	Amp	Rhamnose	IV	(ecDATA)
<i>Aspergillus fumigatus</i>	AspFum	pET22b	Amp	IPTG	IV	(70986662)
<i>Gibberella zeae</i>	GibZea	pET22b	Amp	IPTG	IV	(4610976)
<i>Neosartorya fischeri</i>	NeoFis	pET22b	Amp	IPTG	IV	(119483224)
<i>Rhodobacter sphaeroides</i>	RhoSph	pET22b	Amp	IPTG	I	3I5T
<i>Jannaschia sp.</i>	JanSp	pET22b	Amp	IPTG	IV	8905361
<i>Mesorhizobium loti</i>	MesLoti	pET22b	Amp	IPTG	IV	1347158
<i>Roseobacter sp.</i>	RosSp	pET22b	Amp	IPTG	IV	8613754
<i>Arthrobacter sp.</i> KNK168	ATA117	pET22b	Amp	IPTG	IV	3WWH
<i>Arthrobacter sp.</i> KNK168 (mut)	ATA117 27rd	pET22b	Amp	IPTG	IV	5FR9

a)



b)

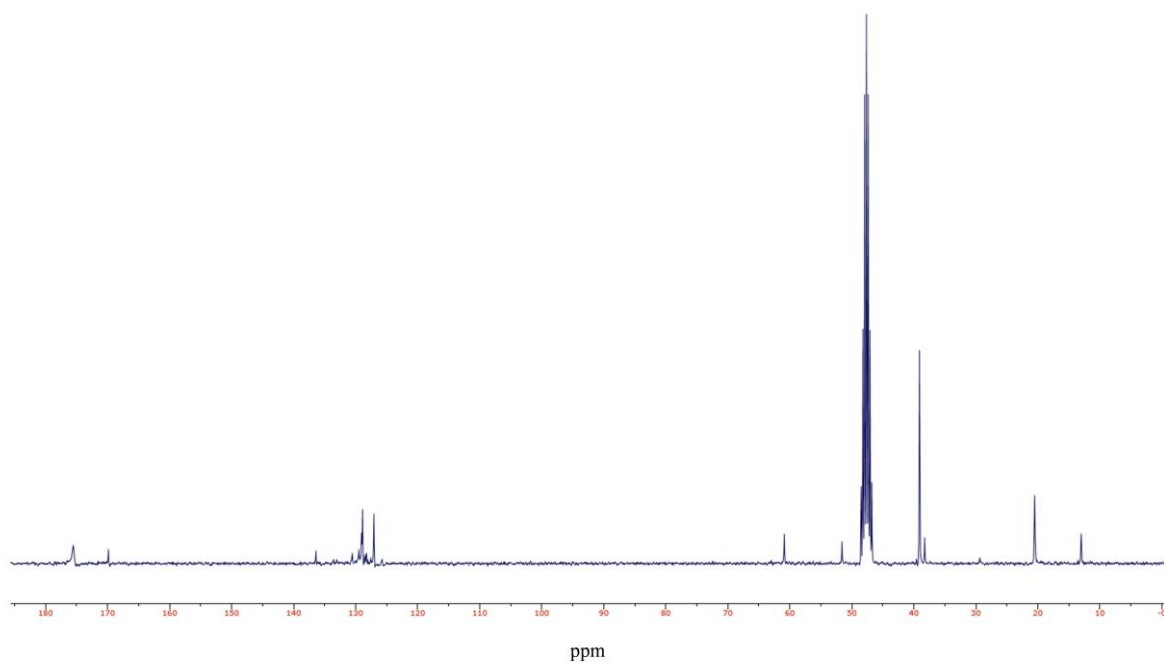


Figure S10 ^1H (a) and ^{13}C (b) – NMR-spectra of the purified β -PAEE product. Besides the product, acetic acid could also be determined. H/C-NMR was determined at 500 MHz.

Chapter 6)

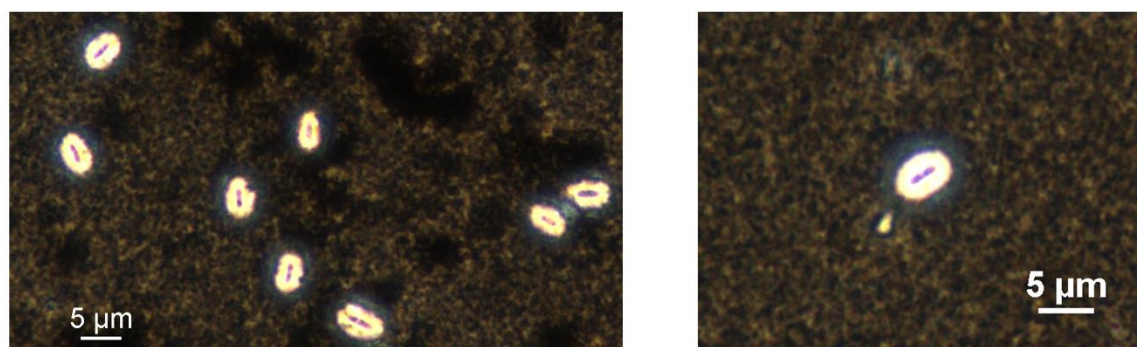


Figure S11 Negative contrasting of *Paraburkholderia* BS115 cells after growing on β -phenylalanine using Chinese ink. Figures were captured by J. Rudat.

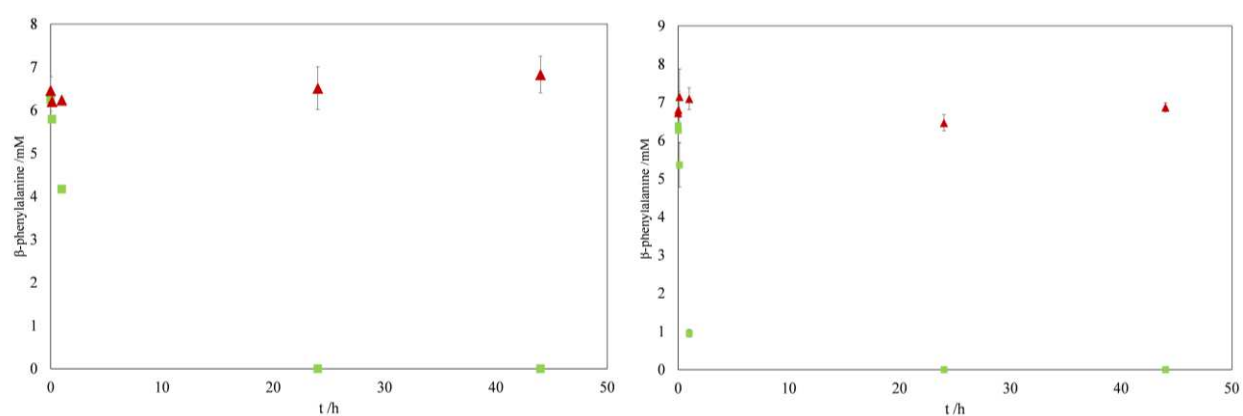


Figure S12 Activity of cell free lysate of BS115 and PsJN. In red triangles: (*R*)- β -PA; in green triangles (*S*)- β -PA. The reaction was performed at 30°C in reaction mixture.

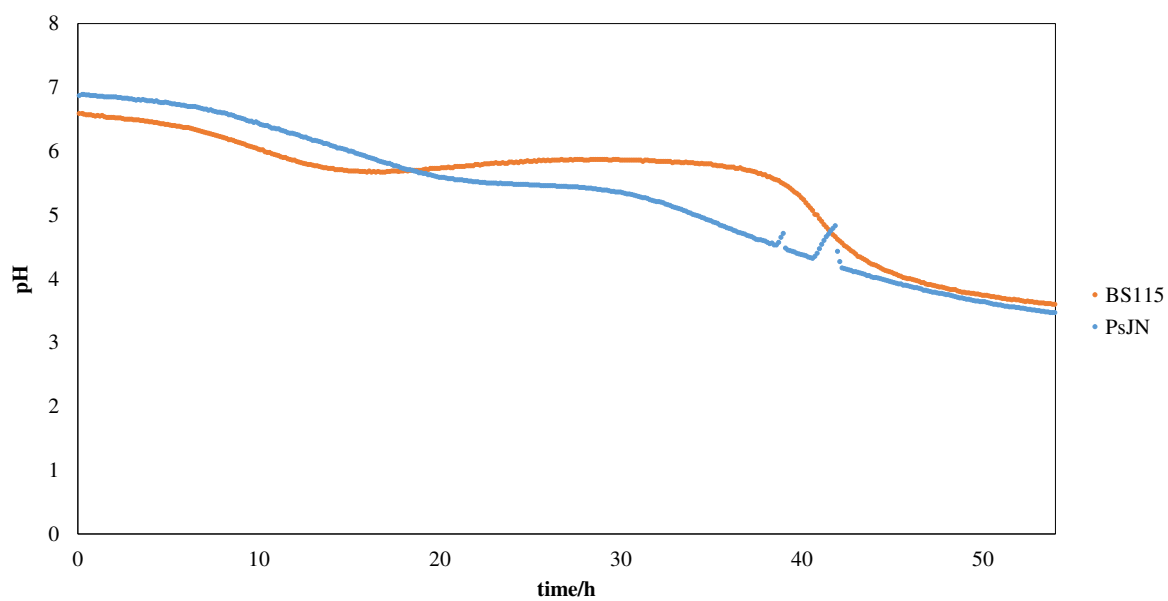


Figure S13. Change in pH during fermentation of *Paraburkholderia* BS115 and PsJN in 2.5 L bioreactor systems using minimal medium.

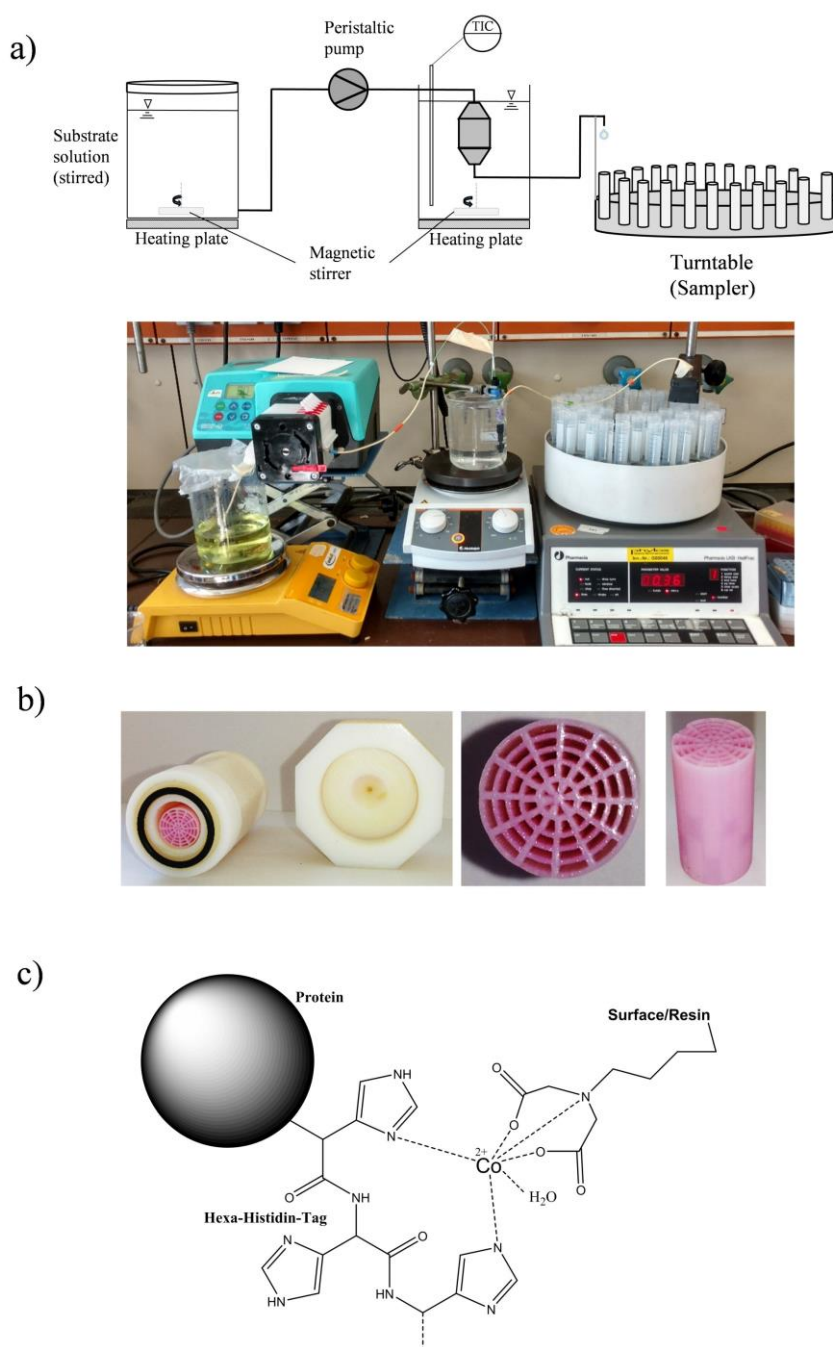


Figure S14 3D-printed flow cell reactor for immobilization of ω -TAs via metal affinity binding. The 3D-printed material was functionalized with IDA (c) to ensure the coordination of a two-valued metal atom, like cobalt (produced by group of Prof. Franzreb). To test the flow-cell device, IDA-cylinder (b) were incubated with protein solution contain 3FCR_4M (with Hexa-his-Tag). For enzymatic reactions, the substrate solution (10 mM PEA, 10 mM pyruvate, 50 mM HEPES (pH 7.5) was preheated to 40°C, passed via a persistaltic pump (flow rate approx. 100 $\mu\text{L min}^{-1}$) into the 40°C tempered enzyme reactor. Samples were collected in an auto sampler and analyzed by TLC and HPLC. The system was compared with a Ni-NTA-column (Thermofischer) as a reference for a functional flow cell system. It turned out that only small amounts of enzyme could be bound specifically. Therefore, both the IDA functionalization and the nature of the enzyme carrier have to be improved.

Keyword index

3

3-Aminobutyric acid	13
3FCR	IV, IX, 60, 63, 68, 206, 209, 211, 214, 215, 216, 217, 219, 220, 221, 264, 268
3-Oxo-3-phenylpropanoic acid	21

4

4AOA	21, 63, 68, 73, 81, 130, 141, 150, 151, 152, 153, 180, 183, 184, 185, 186, 187, 188, 189, 190, 191, 192, 193, 198, 201, 262
------	---

A

Acetophenone	10, 14, 25, 176, 178, 212, 214, 242, 245
Aldimine	21
Amino acid racemases	20
Amino sugar	17
Amino sugars	17
Amino-sugar transaminases	18
Andrimid	5
<i>Arthrobacter citreus</i>	59, 128
Aspartate aminotransferase	19
<i>Aspergillus terreus</i>	35, 63, 65, 73, 74, 84, 96, 101, 115, 129, 151, 162, 168, 169, 171
ATA117	VII, XII, 25, 33, 206, 211, 212, 213, 215, 216, 217, 218, 219, 220, 221, 265
Auto-induction medium	141

B

BAY 10-8888	4
BCA-assay	23
BCAT	69, 76, 77, 78, 88, 89, 90, 91, 94
B-factor	101, 109, 115, 129, 151, 153, 168, 169, 171

C

Cadaverine	68
------------	----

Cascade reaction	IV, 12, 13, 32, 175, 178, 212
<i>Chromobacterium violaceum</i>	35, 59, 68, 78, 91, 99, 101
L-branched-chain aminotransferase	69
BCAT	69
<i>Corynebacterium glutamicum</i>	3

D

Debye–Waller factor	151
Decarboxylation	14
D-Glucose	24
disulfide bond	156
Disulfide bridge	45, 155
DKR	27, 28
Docetaxel	6
Dynamic kinetic resolution	27

E

<i>E. coli</i> BL21	13
Enzyme engineering	IV, 1, 16, 32, 36, 46, 58, 59, 61, 69, 92, 107, 128, 129, 139, 155, 205, 222
Epimerase	18
Ethyl benzoylacetate	10, 13

F

Flavor enhancer	2
Fold type	18
Fold types I and IV	60
FoldX	VI, XI, XVI, 38, 42, 44, 101, 105, 107, 108, 109, 110, 111, 112, 114, 115, 116, 117, 118, 119, 120, 121, 122, 124, 125, 126, 130, 131, 139, 140, 143, 148, 149, 151, 153, 154, 162, 166, 167, 168, 170, 201
Free energy change	138

G

Glucose-dehydrogenase	24
Glutamate-1-semialdehyde transaminases	18

H

Half-reaction	20
HoTMuSiC	145

I

Icofugipen	4
Imagabalin	8, 34, 35, 205, 206
Imine	21, 22, 31
Immobilized metal ion affinity chromatography	
IMAC	135, 141
IPA	25, 26, 35, 85, 212, 214
Isopropylamine	25, 102
Ivabradine	28, 33

J

Jasplakinolid	6
---------------	---

K

Ketoglutaric acid	16
Kinetic stability	41

L

Lactate dehydrogenase	24
L-Alanine	24, 26, 27
L-Arginine	2
LentiKats	24
L-Erythro-3,5-diaminohexanoate dehydrogenase	31
L-glutamate	2, 42
L-Glutamate	22
Lipase	13
Lipopeptides	6
L-lysine	2
L-threonine	2
L-tryptophan	2
Lysine 2,3 aminomutases	20
L- α -amino	2

M

Melting curves	161
Melting point	43, 44, 45, 156, 158, 159, 160, 257, 259
<i>Mesorhizobium loti</i>	187
Methionine	2

N

<i>n</i> -Butylamine	17
Ninhydrin	22
Nitrilase	13

O

Ornithine decarboxylases	20
Oryzoxymicin	4
<i>o</i> TAED	IV, XVI, 56, 57, 62, 65, 66, 67, 68, 69, 76, 85, 87, 89, 92, 187, 192, 221, 262
Oxaloacetic acid	16
OXD	25, 27, 200, 202, 206, 209, 211, 212, 213, 214, 215, 216, 221
Oxetin	4
<i>o</i> -xylylenediamine	25, 200, 206, 207, 211, 212

P

Paclitaxel	IX, 6
PEA13	15, 25, 28, 29, 35, 68, 81, 82, 181, 196, 197, 198, 199, 212, 213, 214, 215, 268
Peptidomimectis	5
Pfam	60
PLP	16, 17, 18, 19, 20, 21, 22, 23, 24, 27, 58, 60, 62, 70, 71, 72, 74, 75, 78, 79, 81, 85, 87, 92, 101, 102
PMP	22
Polyamines	17
PoPMuSiC	122
Protein melting point	43
<i>Pseudomonas aeruginosa</i>	68
<i>Pseudomonas putida</i>	63, 65, 79, 91, 102
Putrescine	58
Pyridoxal-5-phosphate	16

Keyword index

R

Racemase	18, 27, 31
Reaction equilibrium	24
Root-mean-square deviation	
RMSD	120

S

<i>Saccharomyces cerevisiae</i>	29
Sitagliptin	16, 25, 33, 34, 97
Spermidine	68
<i>Sphaerobacter thermophilus</i>	13, 79, 92, 97
Standard numbering	62
Sulfofpyruvic acid	16

T

<i>Taxus baccata</i>	6
<i>Taxus brevifolia</i>	6
<i>Taxus wallchiana</i>	6
Thermodynamic stability	41
Thermostability	40, 92, 101, 104, 128, 166, 169, 171
Tilidin	4
T _m	43
Transaminases	16
Tryptophan synthases	20

U

Umaminierung	16
Unfolding	41

V

<i>V. paradoxus</i>	179
Van-der-Waals interaction	42
<i>Variovorax paradoxus</i>	54
Vernakalant	28, 33
<i>Vibrio fluvialis</i>	30, 35, 59, 60, 65, 79, 91, 97, 98, 99, 101, 187, 205, 223
Vitamin B ₆	16

Y

YM-170320	6
-----------	---

β

β-Amino acid dehydrogenase	31
β-Amino acid lyase	31, 32
β-amino acids	4
β-keto acid	14
β-Lactam antibiotic	5
β-phenylalanine	IV, V, VII, VIII, XVI, 1, 5, 7, 9, 10, 13, 15, 20, 21, 32, 35, 54, 58, 79, 88, 136, 137, 144, 170, 177, 178, 179, 180, 183, 184, 185, 186, 192, 193, 194, 196, 198, 205, 206, 208, 211, 213, 219, 220, 226, 227, 229, 230, 231, 235, 239, 261, 267

ω

ω-Transaminase	16
----------------	----

